Root Cell-Type Specific Expression of Multiple Salinity Tolerance Genes to Alter Plant Shoot Sodium Accumulation

By
Gordon Bertram Wellman

A thesis submitted for the degree of
Doctor of Philosophy

University of Adelaide
School of Agriculture, Food and Wine
and
Australian Centre for Plant Functional Genomics

THE UNIVERSITY
of ADELAIDE

February 2016

Table of Contents

Acknowledgments

Firstly, I would like to thank my supervisors, Dr. Andrew Jacobs and Dr. Stuart Roy, and my advisors, Dr. Matthew Gilliham and Prof. Mark Tester. Your guidance, ideas and support has made my candidature enjoyable, stimulating and character building. It was an honour to work with you all.

I here acknowledge the University of Adelaide (UofA), the Australian Centre for Plant Functional Genomics Pty. Ltd. (ACPFG), the Australian Government Department of Education and Training and the International Workshop on Plant Membrane Biology (IWPMB) for their financial support during my studies and for assisting conference travel.

I extend my sincere thanks to Dr. Mahima Krishnan, Dr. Gehan Safwat El-Hussieny, Dr. Inge Møller and Dr. Sam Henderson who started sections of this work and provided me with plant material for use and analysis.

To all my many colleagues and friends, almost too many to mention, that I have made at the UofA, the ACPFG and the Waite agriculture postgraduate student society (AgPOGS) I give my warmest thanks for all your work and friendship.

I would like to give special mention to the Salt Group at the ACPFG as I knew it; Dr. Aurelie Everard, Dr. Rhiannon Schilling, Dr. Monique Shearer, Dr. Damien Lightfoot, Dr. Sandra Schmöeckel, Dr. Li Bo, Ms. Jessica Bovill, Dr. Nawar Shamaya, Dr. Wenmian Huang, Dr. Aris Hairmansis and Ms. Melissa Pickering. Honorary ‘Salties’; Mr. Shane Waters, Dr. Yagnesh Nagarajan, Mr. Jayachandra Rongala and Dr. Laura Blake. We survived and remain the best of friends.

I would like to thank family; firstly my parents, Guy and Deirdre and my ‘little’ brother Robert for always being there and putting up with me throughout my studies over the years. Special mention to my grandfather Albert Wellman for his words of inspiration to complete my studies, ‘When is the graduation?’ and ‘Do you have a real job yet?’

I would also like to thank Samantha Thorpe for her support throughout my PhD. I’m sorry for the toll this work took on us and that we could not make it work in the end.

Abstract

Increasing soil salinity of agricultural land is of growing concern world-wide as excessive soil salinity has a detrimental effect on growth and yield of many plant species of agricultural importance. The accumulation of sodium ions (Na^+) from saline soils into the shoots of crop plants contributes to the negative effect salinity has on plant growth in cereals. In recent years, many molecular targets involved in Na^+ transport in plants have been identified in a number of species. Genetic modification (GM) utilising these genes may enable manipulation of Na^+ transport with an aim of reducing Na^+ accumulation in the shoot. Constitutive and/or tissue-specific over-expression (OX) of such genes in transgenic plants can prove beneficial in reducing Na^+ shoot accumulation and improve plant salinity tolerance in some cases. However, further reductions could be made by fine tuning Na^+ transport through the plant by co-expressing multiple salinity tolerance associated genes of interest (GOI) in specific root-cell types. To date, this has proved difficult.

Previously generated barley (*Hordeum vulgare* c.v Golden Promise) lines with putative cell-type specific OX of salinity tolerance associated GOIs, *High Affinity K^+-Transporter 1;5* (*HvHKT1;5*) and *vacuolar H^+-pyrophosphatase 1* (*HvHVP1*), were screened in saline hydroponics to assess for improvements in salinity tolerance. Lines with the simultaneous root-cell-type specific OX of both *HvHKT1;5* and *HvHVP1* were developed through hybridisation and assessed for improved salinity tolerance. Although no significant improvements were identified in both the single- or dual-GOI transgenic lines, this approach could be used for other transgenic lines with cell-type specific OX of other GOIs combinations.

The role of *vacuolar H^+-pyrophosphatase 1* (*AtAVP1*) was re-examined when over-expressed in the root-epidermal and –cortical cell types in the model plant species *Arabidopsis thaliana*. OX of *AtAVP1* in these cell-types was thought to improve Na^+ sequestration and there-by improve salinity tolerance. However, saline hydroponics assays of lines with root-epidermal and/or –cortical OX of *AtAVP1* failed to identify improvements in plant salt tolerance or Na^+ uptake, suggesting that *AtAVP1* contributes little to Na^+ sequestration in these cell-types.

Finally, a system that would allow the cell-type specific over-expression of different GOIs in different root cell-types was developed. Such a system would allow the trialling

different gene combinations to identify combinations that would allow more targeted manipulation of Na^+ transport throughout a plant and alter salinity tolerance. This work was carried out in the model plant species, *Arabidopsis thaliana*, and cell-type expression was enabled through the use of dual *GAL4* and *HAP1* enhancer-trap systems and trans-activation constructs. Lines and constructs were developed to allow the cell-type specific OX of selected GOIs, however testing of dual salinity tolerance GOI lines was not achievable during the timeframe of this project.

Declaration

I certify that this work contains no material which has been accepted for the award of any other degree or diploma in any university or other tertiary institution and, to the best of my knowledge and belief, contains no material previously published or written by another person, except where due reference has been made in the text. In addition, I certify that no part of this work will, in the future, be used in a submission for any other degree or diploma in any university or other tertiary institution without prior approval of the University of Adelaide and where applicable, any partner institution responsible for the joint-award of this degree.

I give my consent to this copy of my thesis, when deposited in the University Library, being made available for loan and photocopying, subject to the provisions of the Copyright Act 1968.

I also give permission for the digital version of my thesis to be made available on the web, via the University's digital research repository, the Library catalogue and also through web search engines, unless permission has been granted by the University to restrict access for a period of time.

Signed

…….

Gordon B. Wellman

Date

……

List of Figures

List of Tables

List of Publications, Presentations and Conference Posters

General Publications

Gordon Wellman, (2013, March 30) Stranger than fiction: Food crops for a future, *Adelaide Advertiser.*

Radio Interviews

Gordon Wellman (Guest) & Sarah Martin (Presenter) (2015, October, 21), Taking Plant Genomics from Adelaide to Saudi Arabia [Radio broadcast]. In Sarah Martin (Producer), *The Sound of Science.* Adelaide, Australia, Radio Adelaide

Conference Posters

Gordon Wellman, Mahima Krishnan, Stuart Roy and Andrew Jacobs "*Cell-type Specific Expression of Multiple Salt Tolerance Genes to Improve Plant Salinity Tolerance*" International Workshop in Plant Membrane Biology (IWPMB) 2013, Kurashiki, Japan, March 2013

Gordon Wellman, Mahima Krishnan, Stuart Roy & Andrew Jacobs "*Cell-type Specific Expression of Multiple Salt Tolerance Genes to Improve Plant Salinity Tolerance*" ComBio 2012, Adelaide, Australia, September 2012

Oral Presentations

Gordon Wellman, Mahima Krishnan, Stuart Roy and Andrew Jacobs "*Cell-type Specific Expression of Multiple Salt Tolerance Genes to Improve Plant Salinity Tolerance*", ACPFG Joint Research meeting, Adelaide, Australia, November 2014

Gordon Wellman, Mahima Krishnan, Stuart Roy and Andrew Jacobs "*Cell-type Specific Expression of Multiple Salt Tolerance Genes to Improve Plant Salinity Tolerance*", Shinozaki Lab, RIKEN, Tsukuba, Japan, March 2013

Gordon Wellman, Mahima Krishnan, Stuart Roy and Andrew Jacobs "*Cell-type Specific Expression of Multiple Salt Tolerance Genes to Improve Plant Salinity Tolerance*" ACPFG Joint Research meeting, Adelaide, Australia, November 2012

Gordon Wellman, Mahima Krishnan, Stuart Roy and Andrew Jacobs "*Cell-type Specific Expression of Multiple Salt Tolerance Genes to Improve Plant Salinity Tolerance*" ACPFG Joint Research meeting, Adelaide, Australia, November 2012

Gordon Wellman, Mahima Krishnan, Stuart Roy and Andrew Jacobs "*Cell-type Specific Expression of Multiple Salt Tolerance Genes to Improve Plant Salinity Tolerance*" University of Adelaide Post Graduate Symposium, Adelaide, Australia, September 2012

Abbreviations

#	number
%	percentage
[element]	concentration of element. e.g. [Na^+], [K^+]
≈	approximately
×	times
°C	degrees Celsius
µg	microgram(s)
µL	microlitre(s)
µm	micrometre(s)
µM	micromolar
µmol	micromole(s)
3′-	three prime, of nucleic acid sequence. End of a coding sequence
5′-	five prime, of nucleic acid sequence. Start of a coding sequence
A	adenine
aa	amino acid
ABARE	Australian Bureau of Agricultural and Resource Economics
ABS	Australian Bureau of Statistics
ACPFG	Australian Centre for Plant Functional Genomics
AGRF	Australian Genome Research Facility
Agrobacterium	*Agrobacterium tumefaciens*
ANOVA	Analysis of variance
Arabidopsis	*Arabidopsis thaliana*
At	*Arabidopsis thaliana*. Prefix for Arabidopsis genes
AtAVP1	*Vacuolar pyrophatase 1* from *Arabidopsis thaliana*
ATP	adenosine 5′-triphosphate
ATPase	adenosine 5′-triphosphatase
Barley	*Hordeum vulgare*
BLAST	Basic local alignment search tool
bp	base pairs, of nucleic acid
BSA	bovine serum albumin
C	cytosine
C-	carboxyl (COOH) - terminus of a peptide
C24	Arabidopsis ecotype C24
Ca / Ca^{2+}	calcium / calcium cation
$CaCl_2$	calcium chloride
CaMV	cauliflower mosaic virus
Cat. No:	catalogue number
ccdB	cytotoxic coupled cell division
cDNA	complimentary deoxyribonucleic acid
CFP	Cyan Flourescent Protein
Cl / Cl^-	chloride / chloride anion
cm	centimetre(s) (1 cm = 1×10^{-2} m)
Col-0	Arabidopsis ecotype Columbia-0
CSIRO	Commonwealth Scientific and Industrial Research Organisation
cv.	cultivar
d	day(s)
dATP	deoxyadenosine triphosphate
dCTP	deoxycytidine triphosphate

dGTP	deoxyguanosine triphosphate
dH_2O	deionised/distilled water
DNA	deoxyribonucleic acid
dNTP	deoxynucleotide triphosphate
dNTPs	mixture of equal equivalents of deoxynucleotide triphosphates (dATP, dTTP, dCTP and dGTP)
dTTP	deoxythymine triphosphate
dS	deciSiemens
DW	dry weight (of plant material)
EDTA	ethylene diamine tetraacetate acid
ER	endoplasmic reticulum
EST	expressed sequence tag
FACS	fluorescence-activated cell sorting
FAO	Food and Agricultural Organization of the United Nations
FW	fresh weight (of plant material)
F_y	Progeny resulting from a hybridisation event - y refers to generation from hybridisation F_1 – plants resulting from hybridisation, F_2 – progeny of F_1 plants… etc.
g	gravity
g	gram(s)
G	guanine
GAPdh	*glyceraldehydes- 3- phosphate dehydrogenase*
gDNA	genomic deoxyribonucleic acid
GFP	green fluorescent protein
GOI	gene of interest
GSS	genome survey sequence
GUS	β-glucuronidase protein/assay
H^+	hydrogen ion/proton
H^+-ATPase	proton translocating ATPase
H^+-PPase	proton translocating pyrophosphatase
H_2O	dihydrogen monoxide
H2B	Histone 2B
Ha	hectare (1 ha = 1×10^4 m^2)
HA	haemagglutinin
HCl	hydrochloric acid
HKT	High-affinity potassium transport
Hr	hour(s)
Hv	*Hordeum vulgare,* Barley. Prefix for barley genes
HvHVP1	*Vacuolar H^+-Pryrophosphatase 1* from *Hordeum vulgare*
Hyg	hygromycin B
ICP-AES	inductively coupled plasma atomic emission spectrometry
IMVS	Institute of Medical & Veterinary Science
IPTG	isopropyl-β-D-thiogalactopyranoside
IRRI	International Rice Research Institute
K / K^+	potassium / potassium cation
KAc	potassium acetate
Kan	kanamycin
kbp	kilo base pairs, of nucleic acid
KCl	potassium chloride

kg	kilogram(s)
km	kilometre(s)
KOH	potassium hydroxide
L	litre(s)
LB	left border, of T-DNA sequence
LB media	Luria and Bertani medium
M	molar
m	metre(s)
max.	maximum
mg	milligram(s)
mL	millilitre(s)
mm	millimetre(s)
mM	millimolar
Mha	megahectares (1 ha = 1×10^4 m^2)
MPa	megapascal
Mg / Mg^{2+}	magnesium / magnesium cation
$MgCl_2$	magnesium chloride
Milli-Q H_2O	ultra-pure water
min	minute(s)
miRNA	micro ribonucleic acid
Mn	manganese
Mol	mole(s)
MPM	transmembrane segment, pore, transmembrane segment domain
MPSS	massively parallel signature sequence
mRNA	messenger ribonucleic acid
MS	Murashige and Skoog medium
n	sample size
ng	nanogram(s)
nL	nanolitre(s)
nm	nanometre(s)
nM	nanomolar
nA	nanoampere
N-	amino (NH_2) - terminus of a peptide
N/A	not applicable
N_2	nitrogen
Na / Na^+	sodium / sodium cation
NaCl	sodium chloride
NaOH	sodium hydroxide
NCBI	National Center for Biotechnology Information
NH_4	ammonium
NHX1	Na^+/H^+ exchanger 1
No.	number
nos	nopaline synthase gene
nosT	*nopaline synthase* polyA terminator sequence
NSCC	non-selective cation channel
O/N	overnight
Os	*Oryza sativa*. Prefix for rice (*Oryza sativa*) genes
P	Probability
P	phosphorus
pg	picogram(s)

pmol	picomole(s)
pat	*phosphinotricin acetyl transferase* conferring BASTA resistance.
PCR	polymerase chain reaction
pCR8	entry vector pCR™8/GW/TOPO Gateway®
P_i	inorganic orthophosphate
PI	propidium iodide
PP_i	inorganic pyrophosphate
pro	promoter
qPCR	quantitative real-time polymerase chain reaction
qRT-PCR	quantitative reverse transcription polymerase chain reaction
RACE	rapid amplification of cDNA ends
RB	right border, of T-DNA sequence
Rice	*Oryza sativa*
RNA	ribonucleic acid
RNAi	RNA interference
RO	reverse osmosis
rpm	revolutions per minute
RT	room temperature
RT-PCR	reverse transcription polymerase chain reaction
S	sulphur
S	second(s)
S.E.M	standard error of the mean
SARDI	South Australian Research & Development Institute
Sc	*Saccharomyces cerevisiae* (yeast). Prefix for yeast genes
SDS	sodium dodecyl sulphate
Sec	second(s)
siRNA	short interfering ribonucleic acid
SNP	single nucleotide polymorphism(s)
SOB	Super Optimal Broth
SOS1	Salt Overly Sensitive 1
T	thymine
Ta	*Triticum aestivum* (wheat). Prefix for wheat genes.
TAE	tris base, acetic acid and EDTA
TAIL-PCR	thermal asymmetric interlaced polymerase chain reaction
TAIR	The Arabidopsis Information Resource
T-DNA	transfer deoxyribonucleic acid
TE	tris-EDTA
TF	transcription factor
T_m	melting temperature, of primers
TPM	transcripts per million
Tris	tris(hydroxymethyl)aminomethane
T_x	Progeny of transformation event - x refers to generation from transformation Barley: T_0 – initial transformants, T_1 – progeny of T_0 plants… etc. Arabidopsis: T_1 – initial transformants, T_2 – progeny of T_1 plants… etc.
T_xF_y	Progeny resulting from hybridised transformants. See T_x and F_y. T_3F_1 – plants resulting from hybridisation of T_2 lines T_4F_2 – progeny of T_3F_1 plants… etc.
U	units

UAS	upstream activation sequence
UAS_{GAL4}	upstream activating sequence of *GAL4*
UAS_{HAP1}	upstream activating sequence of *HAP1*
uidA	β-glucuronidase gene
USDA	U.S. Department of Agriculture
UTR	untranslated region
UV	ultraviolet
V	Volts
v/v	volume per volume
w/w	weight per weight
wk	week(s)
X-Gal	5-bromo-4-chloro-3-indoyl-β-D-galactopyranoside
X-Gluc	5-bromo-4-chloro-3-indolyl β-D-glucuronide
Xp	xylem parenchyma
Xy	Xylem

Chapter 1

Literature Review and Research Aims

Chapter 1 - Review of the Literature and Research Aims

1.1. Soil salinisation

Soil salinisation is the process of accumulation of water-soluble salts in soils to levels in which plant and microbial life is affected. Although many different salts are present in soils (such as potassium chloride (KCl) or magnesium chloride ($MgCl_2$)), the major contributor to salinisation is sodium chloride (NaCl). This is of no great surprise as NaCl is by far the most abundant water-soluble salt on earth; present in sea water at concentrations of 30 g/L (≈ 500 mM NaCl) (Flowers, 2004) and is naturally occurring in varying extents in soils especially those of marine origins and areas subject to inundation by sea water (Szabolcs, 1989). Further natural deposition of NaCl in soils can be attributed to rainwater, containing 6 to 50 mg/L of NaCl (reviewed in Munns & Tester, 2008) and to a lesser extent, from salt spray from ocean winds and run-off from weathering of parental rocks (Rengasamy, 2002).

In arid and semi-arid areas, where rainfall levels and natural leaching of water-soluble salts out of soils is low, NaCl levels can accumulate to significant concentrations (Rengasamy, 2006). Ground-water can also contain significant levels of dissolved salts which normally remain well below the root zone of most plants but can be mobilised and brought to the soil surface due to human activities such as irrigation and land clearing (Ghassemi *et al.*, 1995). For agricultural purposes, soils are generally considered saline when the soil saturation extract has an electrical conductivity greater than 4 dSm^{-1} (Rengasamy, 2006), equivalent to approximately 40 mM of NaCl, depending on soil type, with an osmotic pressure of 0.2 MP (Munns & Tester, 2008). At this level, the majority of commercially important crop species suffer severe penalties in both growth and yield (Katerji *et al.*, 2003; Quarrie & Mahmood, 1993).

Globally, approximately 190 Mha of land are classified as “solonchaks” or naturally occurring saline-effected soils by the Food and Agricultural Organisation of the United Nation (FAO, 2000) affecting more than 100 countries world-wide (Rengasamy, 2006). In Australia alone, approximately 30% of the landmass is affected by various forms of salinisation, affecting 16% of land currently used for agriculture with 67% having a potential to develop transient salinity (Rengasamy, 2002). While it is difficult to estimate the direct cost of salinity on the Australian economy, it is believed to be somewhere in the range of AUD$130 M to AUD$300 M per annum (Rengasamy, 2002).

1.1.1. Plant growth in saline soils: Stress and Tolerance

Excessive soil salinity imposes significant stress on plants reducing growth, development and, most importantly from an agronomic view, yield. The ability to maintain growth and yield under saline conditions, comparable to non-stressed plants is, for the purpose of the thesis, termed as salinity tolerance. The presence of naturally occurring saline soils, differing in extent and severity, has led to the evolution of a range of mechanisms for plant species to tolerate soil salinity and significant variation in salinity tolerance between species is present (see Figure 1.1). Some plant species, termed halophytes, are highly adapted to saline soils, requiring some soil salinity for optimal growth. One such halophytic species is Australian saltbush (*Atriplex amnicola*) which grows better when moderate levels of NaCl are present (Aslam *et al.*, 1986). However, the majority of plant species (glycophytes), including most commercial crop species such as rice, wheat and barley, require relatively non-saline soils (< 40 mM NaCl or < 4 dSm^{-1}) for optimal growth.

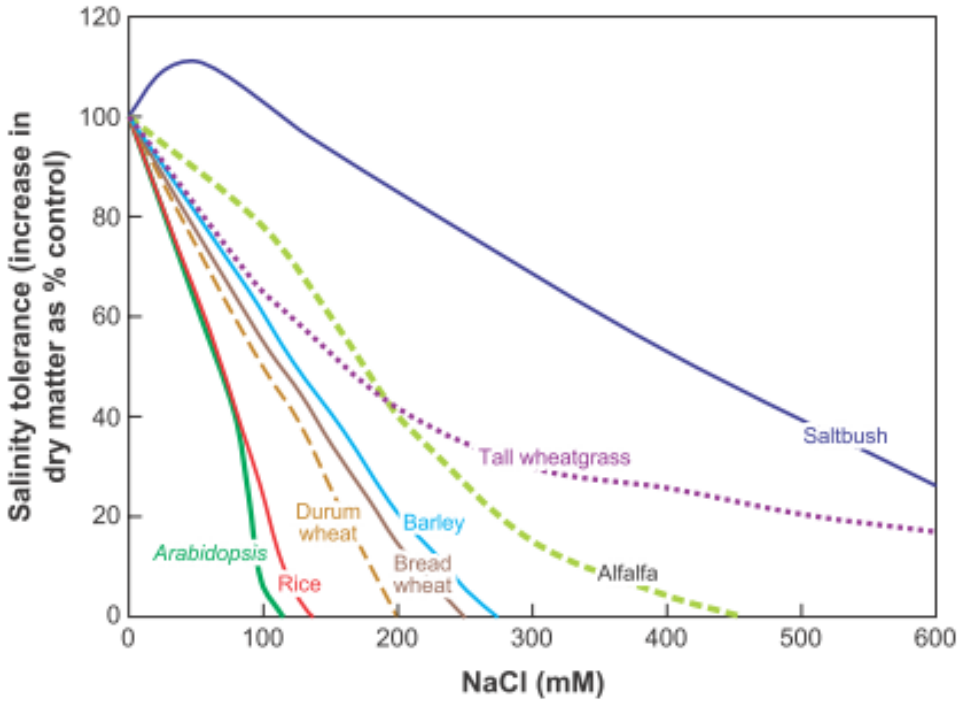

Figure 1.1: Variations in salinity tolerance of different plants.
The relative salinity tolerance of a number of common glycophytes and the halophyte saltbush (*Atriplex amnicola*) as measured by comparing shoot biomass when grown in soil containing NaCl compared to controls grown in soil without NaCl (From Munns & Tester, 2008).

The effect of soil salinity on plant health can be broadly divided into two categories; ionic and non-ionic stress (Roy *et al.*, 2014 and references within). The first of these, ionic stress, which will be the focus of this thesis, is the slow accumulation of toxic ions, primarily sodium (Na^+) or chloride (Cl^-) in plant tissues to damaging levels. Non-ionic stress, otherwise known as shoot sodium-independent stress (Roy *et al.*, 2014) and previously considered as osmotic stress (Munns & Tester, 2008), relates, in part, to the osmotic imbalance between the soil and the cells of the plant root but also to the rapid reduction in plant growth by unknown mechanisms prior to any significant accumulation of ions in the plant shoot.

The different natures of these two stresses require different tolerance mechanisms. A detailed description of these two important stresses and some tolerance mechanism to each follows. An overview of these two stresses and tolerance mechanisms is presented in Table 1.1.

Table 1.1: Summary of the effects of salinity stress on plants
Information included; the two major stresses induced by salinity, the speed of onset, site of effect and adaptations to tolerate high soil salinity (adapted from Munns & Tester, 2008)

Stress	***Non-ionic ('Osmotic')***	***Ionic Stress (high Na^+/Cl^-)***
Speed of Onset	Rapid	Slow
Primary site of effect	Decreased new shoot growth	Increased senescence of older leaves
Tolerance mechanisms	**Osmotic tolerance** - Restore osmotic balance - Synthesis of compatible solutes - Reduce further water loss through stomatal closure and reduced growth. - Ability to maintain growth through mechanisms yet to be identified	**Tissue tolerance** - Intracellular partitioning of toxic ions - Synthesis of compatible solutes **Ion exclusion** - Controlling influx/efflux of toxic ions into the roots from soil - Minimise transport of toxic ions to shoot via reducing loading of or increasing retrieval from xylem vessels

1.1.2. Non-ionic 'Osmotic' stress

When exposed to high salinity levels, greater than 40 mM NaCl for the majority of crop species, plant growth and development, such as leaf expansion, elongation and tillering, are slowed almost immediately after exposure to soil salts. (reviewed in Greenway & Munns, 1983; Munns & Gilliham, 2015; Munns & Tester, 2008; Roy *et al.*, 2014). The increased external osmotic pressure outside the root, due to the presence of the salts, initially causes dehydration and loss of cell turgor. However, this initial dehydration is only transient as the plant undergoes osmotic adjustment to restore the balance in favour of water up-take. The continued presence of soil salts makes it more difficult to extract water from the soil and this reduced water availability coincides with the reduced shoot growth (Greenway & Munns, 1980) and inhibited root growth (Munns, 2002; Munns *et al.*, 2000) often attributed to osmotic stress (reviewed in Munns & Tester, 2008). The rapid onset of these effects however suggests the initial reduction in growth may be a response to the sensing of salt rather than as an impact of soil salinity directly (Roy *et al.*, 2014). Although, some osmotic imbalance is likely present which may negatively impact plant growth.

1.1.2.1. Non-ionic 'Osmotic' stress tolerance

Non-ionic stress tolerance in plants is evidenced by the ability to maintain cell turgor and continued production of new shoots and leaves (reviewed in Munns & Tester, 2008). The reduced water availability due to osmotic stress is similar to that imposed by drought stress and there is most likely some overlap in the mechanisms involved in both tolerances. However many of these mechanisms controlling non-ionic stress tolerance are still relatively unknown. Currently known mechanisms are involved in maintaining the water status of the plant through a combination of promoting water uptake from the soil and reducing further water loss, either via transpiration or the osmotic balance in the root/soil interface (Munns & Tester, 2008; Tester & Davenport, 2003). Restoration of the osmotic balance in favour of water uptake often occurs via the synthesis of compatible solutes such as proline and mannitol, which can be energetically expensive, or by the uptake of soil osmolytes such as Cl^- or Na^+ (Tester & Davenport, 2003). Meanwhile, reductions in water loss are thought to be made by controlling rates of transpiration and photosynthesis as a reduction in stomatal aperture is often seen in response to salinity stress, although the exact mechanism controlling this processes is unknown (Munns & Tester, 2008). Other mechanisms presumably exist to down-regulate leaf expansion and

shoot growth to prevent further water loss. However, it is difficult to determine if the reduction in shoot growth seen in response to non-ionic stress is in fact a response to or is caused by soil salinity. The relatively limited knowledge of non-ionic stress tolerance mechanisms, while potentially an important component of overall salinity tolerance, will not be a focus of this thesis. Instead, we have focused on the ionic stress component where there currently is a greater understanding of the molecular basis behind the ionic stress tolerance mechanisms.

1.1.3. Ionic stress

Continued exposure to high soil salinity leads to ionic stress, namely the accumulation of ions to toxic levels within the cytoplasm of plant tissues, particularly photosynthetic tissues. The toxicity of Na^+ is due to the fact that Na^+ competes with the essential element Potassium (K^+). Potassium is the dominant counter-ion to balance the negative charge on proteins and DNA and is involved in many enzymatic reactions including pyruvate synthesis (Maathuis & Amtmann, 1999) and protein synthesis (Blaha *et al.*, 2000). Na^+ has similar physio-chemical properties to K^+ and excess intracellular Na^+ competes with K^+ leading to disruption of cellular processes regulated by K^+ (Maathuis & Amtmann, 1999).

Ionic stress is first evidenced by increased senescence of mature leaves (Munns, 2002) leading to a drop in photosynthetic capability resulting in an overall reduction in growth rates and ultimately yield (Munns & Tester, 2008). In the majority of plant species, including important cereals such as wheat, rice and barley, Na^+ is the toxic ion (Munns & Tester, 2008). This is doubly troublesome not only due to the prevalence of Na^+ in saline soils but also that uptake of Na^+ into the roots is energetically favoured by voltage and concentration gradients across the cell membrane (Apse & Blumwald, 2007; Tester & Davenport, 2003). Under non-saline conditions, most plant cells maintain a membrane potential of approximately -150 mV across the cell membrane (Lunde *et al.*, 2007) and intracellular Na^+ concentrations of 10 – 30 mM (Carden *et al.*, 2003). However, in saline environments, the external Na^+ concentration can be much higher, promoting uptake of Na^+ into root cells.

While the plasma membrane of plant cells are effectively impermeable to Na^+, the electrical and chemical gradient allows passive influx of Na^+ into the cell through a number of yet unidentified non-selective cation channels (NSCC) (Davenport & Tester,

2000; Demidchik & Tester, 2002; Tester & Davenport, 2003). Species lacking the ability to effectively exclude or efflux Na^+ from the root will therefore accumulate high levels of cytoplasmic Na^+ within the root which the majority of which will be transported to the shoot via the transpiration stream, resulting in accumulation of Na^+ in the shoot and leaves (see Figure 1.3) (reviewed in Apse & Blumwald, 2007; Munns & Tester, 2008). This slow accumulation of Na^+ in leaves results in increased senescence observed in the mature leaves of salt stressed plants (Munns, 2002).

Plants commonly maintain a high cellular K^+:Na^+ ratio (approx. 100-200 mM K^+ versus 1-30 mM Na^+) (Apse & Blumwald, 2007; Munns & Tester, 2008) and it has been suggested that this balance may be more important than absolute Na^+ levels (Dubcovsky *et al.*, 1996; Maathuis & Amtmann, 1999). Interestingly, there appears to be little evidence for improved resistance to Na^+ inhibition of enzymes in halophytic species (Tester & Davenport, 2003), and many halophytic species maintain higher Na^+ and Cl^- levels in leaf tissues than many glycophytes (reviewed in Munns & Gilliham, 2015) suggesting that controlling the Na^+/K^+ balance may underlie many of the tolerance mechanisms to ionic stress.

Tolerance mechanisms for ionic stress can fall into two separate mechanisms, tolerance to high intracellular Na^+ concentration and exclusion of Na^+ from the shoot (for review see Munns & Tester, 2008).

1.1.3.1. Tissue tolerance to Na^+

Tissue tolerance to high cellular Na^+ seems to be the simplest of the potential tolerance mechanisms to toxic Na^+ accumulation. However, as mentioned earlier there appears to be little evidence for improved resistance to Na^+ inhibition of enzymes in halophytic species despite many halophytic species maintaining increased Na^+ and Cl^- in leaf tissues (Munns & Gilliham, 2015; Tester & Davenport, 2003). Instead, intracellular compartmentalisation is thought to be the main mechanism supporting tissue tolerance. Sequestration of Na^+ within the cell vacuole lowers the cytoplasmic Na^+ concentration preventing Na^+ from reaching levels that result in inhibition of K^+-requiring processes (Munns & Gilliham, 2015; Munns & Tester, 2008). However, as Na^+ is sequestered into the vacuole, there needs to be synthesis of compatible solutes to maintain the osmotic balance across the tonoplast, without inhibiting biological processes (Munns & Tester, 2008). Often these solutes are similar to those involved in restoring the osmotic

imbalance initially caused by the osmotic stress, such as proline and mannitol, and again these are energetically expensive to synthesise.

1.1.3.2. Molecular basis of tissue Na^+ tolerance

Salinity tolerance has been extensively studied in the model species *Arabidopsis thaliana*, especially in relation to tissue tolerance (Møller & Tester, 2007) and several molecular targets suggested to be involved in vacuolar sequestration of Na^+ have been identified. One of these is the Arabidopsis *Na^+/H^+ Exchanger 1* (*AtNHX1* - At5g27150) (Gaxiola *et al.*, 1999) which encodes a vacuolar Na^+/H^+ antiporter initially thought to be responsible for translocating Na^+ in to the vacuole in exchange for a proton (H^+) (Blumwald *et al.*, 2000). New research suggests that *NHX1* may play a role in vacuolar K^+ uptake instead and also play a role in turgor regulation and stomata function (Barragán *et al.*, 2012). *AtNHX1* is expressed in all tissues except for the root tip and is regulated in response to NaCl supporting its role in Na^+ response (Shi & Zhu, 2002). Constitutive over-expression of *AtNXH1* has been shown to improve salinity tolerance in a range of species, Arabidopsis (Apse *et al.*, 1999), tomato (Zhang & Blumwald, 2001) and cotton (He *et al.*, 2005) while expression of orthologous cereal *NHX* genes have been used to improve salinity tolerance in rice (Fukuda *et al.*, 2004b), wheat (Xue *et al.*, 2004) and barley (Fukuda *et al.*, 2004a).

In order to drive Na^+ translocation, a proton gradient is established across the tonoplast by various vacuolar *H^+-adenosine triphosphatases* (*H^+-ATPases*) and *H^+-pyrophosphatases* (*H^+-PPases*) (Gaxiola *et al.*, 2001). A second gene often associated linked to tissue tolerance in Arabidopsis is *Arabidopsis vacuolar hydrogen-translocating pyrophosphatase 1* (*AtAVP1* –, At1g15690) which encodes a vacuolar *H^+-PPase*, thought to be involved in generating the proton gradient across the vacuole tonoplast (Sarafian *et al.*, 1992). To do so, AtAVP1 reduces pyrophosphate (PPi) and the energy released is used to pump protons into the lumen of the vacuole establishing the proton gradient (Blumwald *et al.*, 2000). While most likely not the major contributor to the proton gradient, *AtAVP1* has been of great interest to salinity research due to its small size, consisting of a single subunit (rather than 26 subunits for most H^+-ATPases), making it more suitable for transgenic studies (Gaxiola *et al.*, 2002). Similar to *AtNHX1*, over-expression of *AtAVP1* has been shown improve salinity tolerance in Arabidopsis (Gaxiola *et al.*, 2001), cotton (Pasapula *et al.*, 2011), tomato (Park *et al.*, 2005), alfalfa (Bao *et al.*, 2009) and barley (Schilling, 2014, 2010; Schilling *et al.*, 2014). Additionally, increased

expression of native *H*$^+$*-PPases* in Arabidopsis and barley have been associated with increase salinity tolerance (Fukuda *et al.*, 2004a; Jha *et al.*, 2010).

Since the onset of this project, new hypotheses as to the function of vacuolar *H*$^+$*-PPases*, have been put forward, with possible roles in cytoplasmic PPi cycling (Ferjani *et al.*, 2011), promoting cell proliferation and final leaf size (Vercruyssen *et al.*, 2011), or sucrose transport (Paez-Valencia *et al.*, 2011). A recent model suggests *AtAVP1* acts in the sieve element-companion cells of plant vasculature and plays a role in PPi homeostasis important for phloem loading and sucrose transport (Pizzio *et al.*, 2015).

The actions of *AtAVP1* and *AtNHX1* are possibly linked in response to salinity stress. In barley, homologues of both *AtNHX1* and *AtAVP1* are both up-regulated in response to salt stress (Fukuda *et al.*, 2004a). While simultaneous over expression of homologues of both *AtAVP1* and *AtNHX1* has been shown to increase salinity tolerance in both Arabidopsis (Brini *et al.*, 2007) and rice (Zhao *et al.*, 2006). These results suggest the importance of these genes in the tissue tolerance to Na^+ via the compartmentalisation of Na^+ in the vacuole. A possible model for *AtNHX1* and *AtAVP1* working in conjunction to assist with Na^+ sequestration is presented below in Figure 1.2.

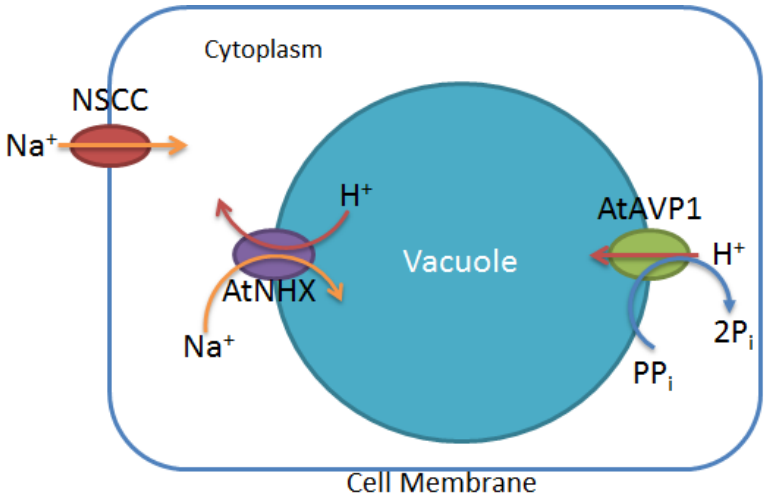

Figure 1.2 Model of sequestration of Na^+ into the plant cell vacuole by the combined action of AtNHX1 and AtAVP1
Na^+ enters from the cell via the non-specific cation channels (NSCC – red oval) present in the cell membrane, raising the cytoplasmic Na^+ concentration. In order reduce the effective cytoplasmic Na^+ level, Na^+ is sequestered into the vacuole by the combined action of the vacuolar H^+-pyrophosphatases 1 (AtAVP1 – green oval) and Na^+/H^+ exchanger 1 (AtNHX1 – purple oval). AtAVP1 reduces pyrophosphate (PPi) to inorganic phosphate (2Pi) and the energy released is used to pump protons (H^+) into the vacuole to establish the proton gradient. AtNHX1 then uses the proton gradient to drive Na^+ translocation into the vacuole thereby reducing the effective Na^+ concentration in the cytoplasm. See section 1.1.3.1 Tissue tolerance to Na+.

1.1.3.3. Na^+ exclusion from shoot and leaves

The second tolerance mechanism to the ionic component of salinity stress is exclusion of Na^+ from the plant shoot and leaves. It has been noted that plants, especially those of agricultural importance such as wheat and barley, that are more able to exclude Na^+ from the shoot are often more salt tolerant and that the salinity tolerance is inversely proportional to shoot Na^+ concentration (Munns & James, 2003). This is contrasting to halophilic species which often accumulate Na^+ and Cl^- to high levels in leaf tissues (Flowers *et al.*, 2015; Munns & Gilliham, 2015).

While uptake of Na^+ is favoured by voltage and concentration gradients, physical barriers exist to reduce Na^+ influx. The roots of most vascular plants possess an endodermis with a Casparian band separating the root cortex from the vascular bundle (Enstone *et al.*, 2002). The presence of this layer reduces the apoplastic leakage of Na^+ directly into the root vasculature which presumably contributes to salinity tolerance. Halophytes appear to have additional thickening of the Casparian band compared to glycophytes (Peng *et al.*, 2004) while apoplastic leakage appears to be main site of entry of Na^+ in relatively salt-sensitive Rice (Yeo *et al.*, 1987).

In most species then, Na^+ is taken up mainly by the root epidermal and cortical cells (Tester & Leigh, 2001; White & Broadley, 2001) through a range of ion channels including the yet unidentified NSCCs previously mentioned (for review see Plett & Møller, 2010). Once inside the epidermal and cortical cells Na^+ is then free to move through the symplast to the stele where it may be loaded into the xylem (see Figure 1.3). Under normal conditions, the potential difference between the xylem parenchyma (the cells bordering the xylem) and the xylem is approximately 100 mV in favour of the xylem parenchyma (De Boer, 1999; Wegner *et al.*, 1999). This electrical gradient suggests active transport may be required for xylem loading of Na^+, although this process may be passive at high external Na^+ concentrations (Shi *et al.*, 2002) such as experienced during salt stress. Once inside the xylem, Na^+ can then be transported to the shoot and leaves via the transpiration flow (Apse & Blumwald, 2007) where it accumulates in the cytoplasm of leaf and shoot cells, leading to the observed toxic effect (Munns, 2002).

With an understanding of how Na^+ reaches the shoot and leaves, it is now possible to determine a number of ways in which plants can prevent Na^+ from being transported to

the shoot thereby preventing accumulation. These processes include (reviewed in Tester & Davenport, 2003):

- Maximise efflux of Na^+ from the root back into the soil.
- Minimising initial influx Na^+ into the root from the soil.
- Minimise xylem loading of Na^+ to prevent transport to the shoot.
- Maximising retrieval of Na^+ from the xylem vessels.

1.1.3.4. Molecular basis of Na^+ exclusion from the shoot

In recent years, a number of molecular targets involved in the Na^+ efflux from the root have been identified. One such target is the Arabidopsis plasma membrane Na^+/H^+ antiporter; *Salt Overly Sensitive 1* (*AtSOS1*– At2g01980) (Shi *et al.*, 2000; Shi & Zhu, 2002; Wu *et al.*, 1996) which is NaCl inducible (Shi *et al.*, 2000) and expressed specifically in the root epidermis (Shi *et al.*, 2003). Knockout mutants of *AtSOS1* over accumulate Na^+ in the shoot (Shi *et al.*, 2000) while over expression leads to reduced shoot and xylem Na^+ levels suggesting a role in efflux of Na^+ from the root (Shi *et al.*, 2003). Interestingly, *AtSOS1* also appears to be expressed in the vascular tissues (Shi *et al.*, 2000) suggesting it may also be involved in loading or retrieval of Na^+ from the xylem in low salt conditions (reviewed in Apse & Blumwald, 2007; Shi *et al.*, 2002) (see Figure 1.3).

Vascular plants also utilise retrieval of Na^+ from the xylem as an important mechanism for reducing Na^+ in the shoot (Tester & Davenport, 2003). Research in recent years has identified a number of members of the group 1 high-affinity K^+-transporters (HKT1) family that are involved in regulation of Na^+ and K^+ transport and contribute to salinity tolerance in a number of species (Byrt *et al.*, 2014; Horie *et al.*, 2009; Munns *et al.*, 2012; Platten *et al.*, 2006). One such member, isolated from Arabidopsis is *AtHKT1;1* (At4g10310) (Uozumi *et al.*, 2000). *AtHKT1;1* is expressed specifically in vascular tissues (Berthomieu *et al.*, 2003; Maser *et al.*, 2002) and is localised to the plasma membrane (Sunarpi *et al.*, 2005). While *AtHKT1;1* was originally thought to be involved in Na^+ influx (Rus *et al.*, 2001) or phloem loading (Berthomieu *et al.*, 2003) recent work has shown it to be involved specifically in unloading of Na^+ from the xylem (Davenport *et al.*, 2007)(see Figure 1.3). Evidence for a similar role of Class 1 HKTs exists in other species such as *Triticum monococcum* (*TaHKT1;5*) (Munns *et al.*, 2012), bread wheat (*TaHKT1;5*)(Byrt *et al.*, 2014) and rice (*OsHKT1;5*)(Ren *et al.*, 2005)

In support of its role in xylem unloading and salinity tolerance, tissue specific expression of *AtHKT1;1* in root stelar cells decreases shoot Na^+ concentration and increases salinity tolerance in Arabidopsis (Møller *et al.*, 2009). Furthermore, along with the reduced shoot Na^+, Møller and colleagues (2009) also noticed increased Na^+ in the root cortical cells of hydroponically grown plants, indicating that as Na^+ was retrieved from the xylem it was being sequestered in these cell types (Møller *et al.*, 2009), presumably into the vacuole similar to the mechanism described in section 1.1.3.1. Interestingly, over-expression of *AtHKT1;1* in the epidermal and cortical layers of the roots in both Arabidopsis and rice also leads to decreased shoot Na^+ (Plett *et al.*, 2010b). While these results appear contrary to the role in xylem unloading, it appears the native rice homologue *OsHKT1;5* is up-regulated in response to the mis-expression of *AtHKT1;1* (Plett *et al.*, 2010b) which may account for the improved salinity tolerance in these plants, although the exact process through which this occurs is still unknown.

A number of other processes exist for controlling shoot Na^+ concentration, including recirculation of Na^+ in the phloem and secretion of Na^+ from the leaf surface such as in certain halophytes. However, the contribution of these processes to salinity tolerance in agriculturally important species and the molecular basis behind these processes are still debated and will not be discussed in this introduction (for review see Tester & Davenport, 2003).

1.1.3.5. Gene candidates from other species to improve plant salinity tolerance

Although Na^+ efflux from the roots directly, such as by *AtSOS1* (section 1.1.3.3), appears to be a powerful way to control Na^+ accumulation, vascular plants appear to lack dedicated efflux Na^+-ATPases (ENA-type Na^+-ATPases) common to many soil fungi and some mosses (Benito *et al.*, 2002; Benito & Rodriguez-Navarro, 2003). One such Na^+-ATPase, isolated from the bryophyte *Physcomitrella patens*, *PpENA1* (PHYPADRAFT_105562) (Benito *et al.*, 2002) has been shown to act as a Na^+ efflux pump contributing to salinity tolerance in *P. patens* (Jacobs *et al.*, 2011; Lunde *et al.*, 2007). While the reason why ENA-type Na^+-ATPases, such as *PpENA1*, have been lost from vascular plants remains unknown, the identification of *PpENA1* allows the potential use of this gene to improve salinity tolerance of agriculturally important species (Jacobs *et al.*, 2007), especially when combined with cell-type specific expression (Plett & Møller, 2010) (see Figure 1.3).

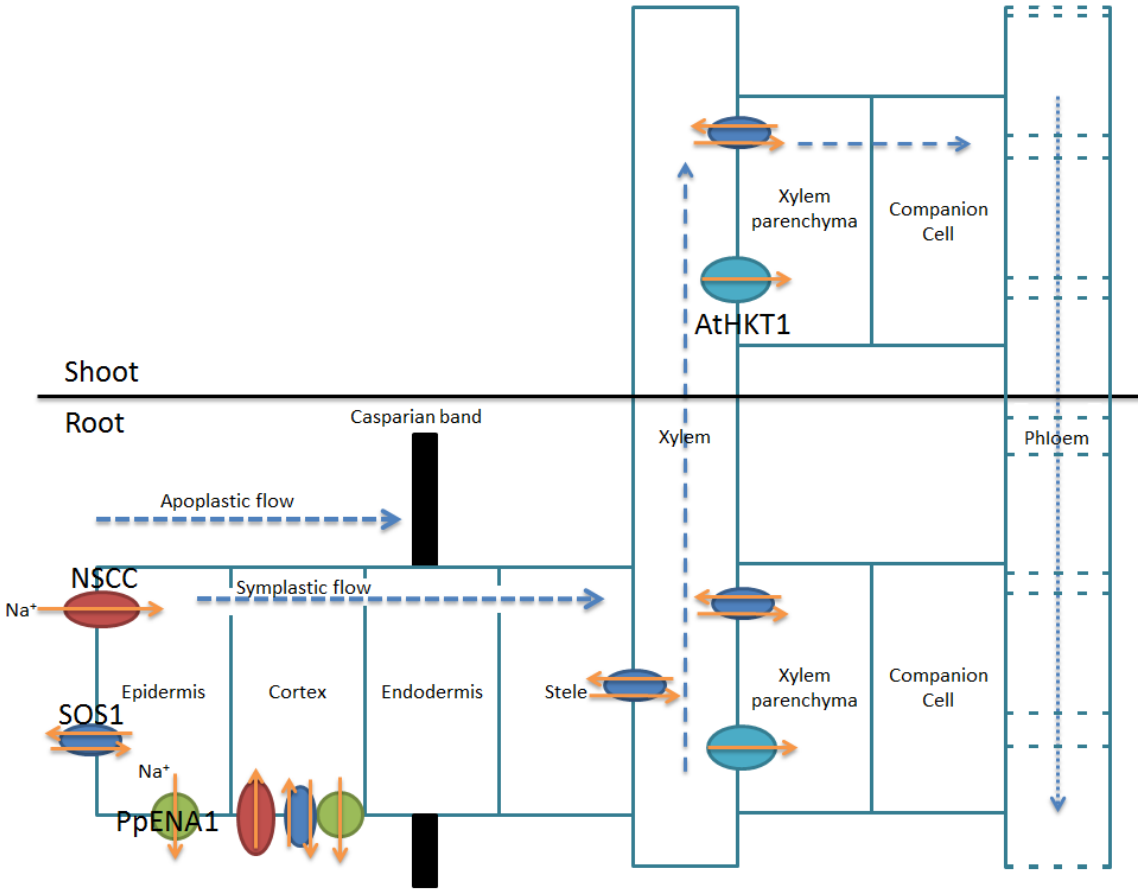

Figure 1.3: A model of Na^+ transport throughout plants.
This figure illustrates the key stages in transport of Na^+ from the soil, through the different root cell types (via apoplastic and symplastic flow) and its eventual accumulation in the shoot (as indicated by the blue dashed arrows). The extent of phloem recirculation of Na^+ from the shoot to the root is still debated and is indicated by the blue dotted arrow. Several of the proteins known to be involved in the control of Na^+ movement throughout the plant have been added and are indicated in their proposed tissue-specific locations by the coloured ovals. These include: the proposed NSCC (red) which facilitates Na^+ entry into the epidermal/cortical cells; AtSOS1 (blue), involved in Na^+ transport in many different cell types, possibly involved in efflux or xylem loading; and HKT1;1 (light blue) involved in retrieval of Na^+ from the xylem. While PpENA1 (green) is not native to vascular plants, it has been included in this diagram in the epidermal and cortical cell types where, when introduced through genetic modification, it may be used for Na^+ efflux back out to the soil. The orange arrows super-imposed on each of the proteins indicate the proposed direction of Na^+ movement mediated by these transporters/channels (Adapted from Apse & Blumwald, 2007)

1.2. Controlling Na^+ transport to improve salinity tolerance

Control of Na^+ transport throughout the plant to reduce shoot Na^+ concentrations is a powerful way to improve salinity tolerance, especially in agriculturally important species such as wheat, rice and barley. With the current knowledge regarding the molecular basis behind such transport, several strategies can be employed to improve salinity tolerance in agriculturally important species. These include;

(1) reducing influx of Na^+ into the root;
(2) minimise loading of Na^+ into the xylem;
(3) and sequestration of Na^+ into vacuoles (reviewed in Tester & Davenport, 2003).

While constitutive over-expression of salinity tolerance genes has proven successful in some cases (for examples see; Bao *et al.*, 2009; Jacobs *et al.*, 2011; Pasapula *et al.*, 2011) spatially and temporally controlled expression of such genes allows finer control of Na^+ transport to further improve salinity tolerance (demonstrated with the cell-specific expression of AtHKT1;1; Møller *et al.*, 2009; Plett *et al.*, 2010b), while avoiding potential pleiotropic effects.

Beyond single genes, being able to utilise multiple salinity tolerance genes in different cell types may provide greater gains in salinity tolerance by allowing further fine tuning Na^+ transport. For example, coordinated over-expression of *HKTs* to root stele, to promoter xylem Na^+ retrieval, and *H^+-PPases* in the root cortex, to promote Na^+ sequestration, may provide a greater reduction in shoot Na^+ accumulations than either expressed singly.

1.2.1. Control of cell-type specific expression of transgenes

Such cell-specific expression of genes of interest (GOIs) can be performed using specific promoters, however these can be difficult to identify and characterise especially in species where genomic resources are limited like many crop species.

One way around the requirement for cell-type specific promoters is through the use of enhancer-traps. The enhancer-trap concept was originally developed for use in *Drosophila* developmental research (Brand & Perrimon, 1993) to monitor gene expression and cell-fate and has since been modified for use in *Arabidopsis* and rice, and integrated by *Agrobacterium*-mediated transformation (Engineer *et al.*, 2005; Haseloff, 1999; Klimyuk *et al.*, 1995; Sundaresan *et al.*, 1995) (see Figure 1.4). The enhancer-trap system has been successfully used *in planta* in numerous instances for cell-type specific

expression of transgenes (for examples see: Gardner *et al.*, 2009; Johnson *et al.*, 2005; Kiegle *et al.*, 2000; Laplaze *et al.*, 2005) and was the technique used for the cell-type specific expression of *AtHKT1;1* in Arabidopsis and rice previously mentioned (Møller *et al.*, 2009; Plett *et al.*, 2010b).

Several different enhancer-trap systems exist for use in Arabidopsis but these generally consist of a DNA construct with *Agrobacterium tumefaciens* T-DNA cassette containing a number of components:

(1) a minimal promoter, such as a 35S Cauliflower Mosaic Virus promoter (*CaMV35S*), upstream (5′) of (2);
(2) a protein coding sequence (CDS) encoding a transcriptional activator,
(3) an *in planta* selectable marker CDS (such as *neomycin phosphotransferase II* (*nptII)*) for selection of T-DNA transformants,
(4) an upstream activation sequence (*UAS*) to which the transcriptional activator binds,
(5) and a reporter gene CDS (such as *green fluorescent protein* (*GFP*)) for visualisation of expression patterns.

In order to drive cell-type specific expression of *mGFP5-ER*, the *GAL4-VP16* enhancer-trap is transformed into Arabidopsis using *Agrobacterium tumefaciens* and integrated randomly into the genome (Figure 1.4, a). As the *GAL4-VP16* gene has only a minimal *CaMV35S* promoter (-45 35S) a native upstream enhancer is required for expression of the *GAL4-VP16* transcriptional activator. In instances where the enhancer trap is integrated into the Arabidopsis genome downstream of a tissue-specific enhancer, *GAL4-VP16* is expressed and translated. GAL4-VP16 (Figure 1.4, a, blue triangles) then bind to the UAS_{GAL4} sequences activating transcription of *mGFP5-ER* (Figure 1.4, a, red arrow 1). mGFP5-ER (Figure 1.4, a, green stars) is targeted to the endoplasmic reticulum allowing identification of the specific cell type by visualisation using confocal microscopy. To express a *GOI* in the identified cell-type, the enhancer-trap line is re-transformed with the GOI expression cassette. As *GAL4-VP16* is expressed from the enhance-trap in the specific cell-type, GAL4-VP16 (Figure 1.4, a, blue triangles) can also bind to UAS_{GAL4} present in the *GOI* expression cassette (Figure 1.4, b, red arrow 2), activating expression of the *GOI*.

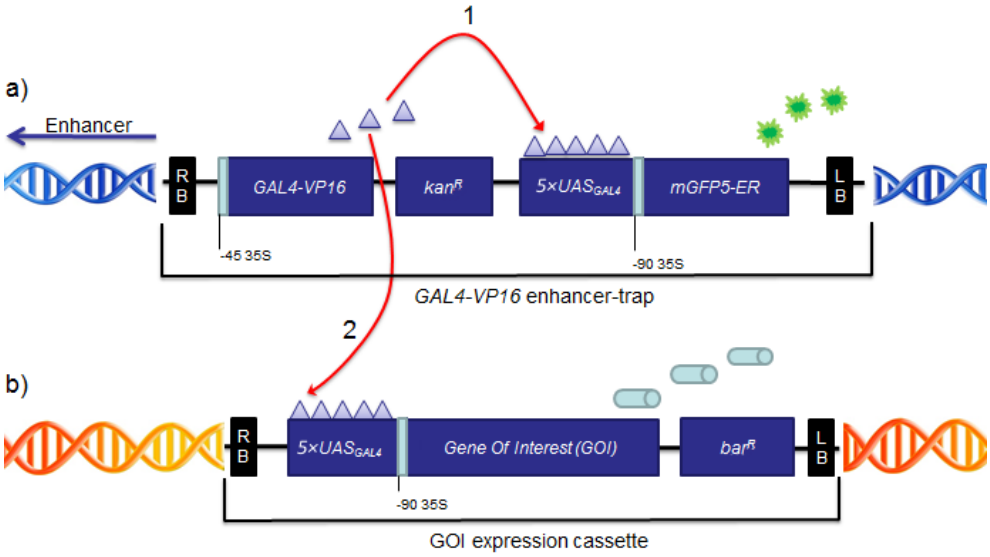

Figure 1.4: Overview of the *GAL4-VP16* enhancer-trap & GOI expression cassette for cell-type expression of genes of interest.
a) The *GAL4-VP16* enhancer-trap integrated into the Arabidopsis genome: From the right border (RB): A minimal CaMV35S minimal promoter (-45 35S); *GAL4-VP16* transcriptional activator fusion gene (*GAL4-VP16)*; Kanamycin resistance gene (kan^R) for *in planta* selection; five tandem repeats of the *GAL4* binding site upstream activation sequence ($5\times UAS_{GAL4}$); a secondary minimal *CaMV35S* promoter (-90 35S); the reporter gene, endoplasmic reticulum targeted green fluorescent protein (*mGFP5-ER*); left border (LB).
b) The *gene of interest* (*GOI*) expression cassette: From the right border (RB): five tandem repeats of the *GAL4* binding site upstream activation sequence ($5\times UAS_{GAL4}$); a minimal *CaMV35S* promoter (-90 35S); selected *gene of interest* (*GOI)* CDS; bialophos (BASTA) resistance gene (bar^R) for BASTA *in planta* selection; left border (LB). (adapted from Møller *et al.*, 2009)

The major variations between enhancer-trap systems are the transcriptional activator used. The transcription activator use in the GAL4 enhancer-trap system is composed of a DNA-binding domain, GAL4 from *Saccharomyces cerevisiae*, fused to the *Herpes simplex* virus virion-protein-16 transcriptional activator (VP16) and is capable of promoting transcription in plants. This DNA-binding domain binds to specific DNA sequences termed Upstream Activation sequences (UAS) allowing the VP16 transcriptional activator to recruit RNA polymerase II promoting transcription of downstream genes (Engineer *et al.*, 2005). The use of a DNA-binding domain from yeast also reduces the likelihood of the enhancer-trap transcriptional activator binding to promoter elements in plants which would result in mis-activation of the enhancer-trap.

1.2.2. Cell-type specific expression of multiple genes

In order to drive the expression of a second GOI in a different cell-type, again promoters may be used, or through the use of a secondary enhancer-trap such as the *HAP1-VP16* enhancer-trap (Haseloff *et al.*, 2005). The *HAP1-VP16* enhancer-trap is modelled on the *GAL4-VP16* enhancer-trap (see Figure 1.4) but uses a modified version of the yeast transcription factor HAP1 (Hon *et al.*, 1999; Lan *et al.*, 2004), *HAP1-VP16*, and replaces the GAL4 UAS (UAS_{GAL4}) with the HAP1 UAS binding site (UAS_{HAP1}). Additionally, a different marker, nucleus localised cyan fluorescent protein (*H2B::mCFP*) encoded by the the *HAP1-VP16* enhancer-trap allows the distinction of patterns of expression for both enhancer-traps.

1.3. Project aims and research questions

A greater understanding of the molecular basis behind Na^+ transport and shoot exclusion will further allow the development of agricultural crops with improved salinity tolerance, whether by conventional breeding or genetic modification. Over- and/or mis-expression of native genes, or the introduction of novel genes from other species, has already been demonstrated to improve salinity tolerance with a number of genes previously described.

In this project, we assess ways to manipulate Na^+ transport processes in the root thereby reduce Na^+ accumulation in the shoot, increasing overall plant salinity tolerance. To do this we targeted the following processes and molecular targets:

1) Increasing the potential for Na^+ sequestration in the root cortex, by the root cortex cell-type specific over-expression of *H^+-PPases* in both the model organism Arabidopsis and a commercially important crop, barley.
2) Increasing the xylem Na^+ retrieval in barley, by root stele cell-type specific over-expression of the barley class I HKT Na^+ transporter *HvHKT1;5*. The role of *HvHKT1;5* and the importance of Na^+ retrieval in barley was also to be examined.
3) Examine the effect of the root cell-type over-expression of both *HvHVP1* and *HvHKT1;5* simultaneously in barley to see if enhancing both Na^+ sequestration and xylem retrieval results in greater Na^+ tolerance than expressing either of these genes individually.

Finally, the major goal of this project was to develop a system that would allow the cell-type specific expression of multiple salinity tolerance genes in specific but different cell-types to more accurately control transport of Na^+ through the plant. This may provide

greater improvement in salinity tolerance than expression of single salinity tolerance genes. With the recently gained knowledge regarding the molecular basis of Na^+ transport and the development of new tools for cell-specific expression of transgenes (via the *GAL4-VP16* and *HAP1-VP16* enhancer-traps) it has become possible to test this approach. To our knowledge, the use dual enhancer-traps (such as combined *GAL4-VP16* and *HAP1-VP16* enhancer-trap systems) have not been previously developed and used to express multiple GOIs.

1.4. Thesis outline

The remainder of this thesis is divided into 6 chapters:

Chapter 2- General Methods and Materials, outlines general materials and methods used throughout different components of this thesis.

Chapter 3- Development and characterisation of transgenic barley lines with co-ordinated root cell-type specific expression of salinity tolerance genes, *HvHVP1* and *HvHKT1;5*, examines the benefit of root cell-type over-expression of salinity tolerance genes in lines with dual expression of vacuolar H^+-PPase I (*HvHVP1*) and Na^+ transporter (*HvHKT1;5*).

Chapter 4- Evaluating the effect of root cell-type over-expression of the Arabidopsis vacuolar H+-pyrophosphatase, *AtAVP1*, on plant salinity tolerance, carries on from previous work investigating the role of the vacuolar *H^+-PPase*, *AtAVP1*, when over-expressed specifically in root cortex.

Chapter 5- Characterisation and development of Arabidopsis dual enhancer-trap lines to express genes of interest in two specific cell-types, describes the characterisation of enhancer trap lines selected for root cell-type specific expression patterns and the development of dual enhancer-trap lines.

Chapter 6- Vector construction for cell-type specific expression of multiple GOIs, details the development of trans-activation constructs to drive the cell-type specific expression of GOIs in enhancer trap lines.

Chapter 7- General Discussion and Future Directions, summarises the results of this research project and discuss the importance of the various strategies trailed. Future prospects for various molecular tools and plant material generated by this study are also discussed.

Finally, several appendices with supplementary data, figures and references are included.

Chapter 2

General Methods and Materials

Chapter 2 - General Methods and Materials

2.1. Introduction

This chapter provides general methods and materials used in various experiments throughout other chapters of this thesis. Specific conditions have been provided where possible, however experiment-specific conditions and modifications have been detailed in full in their relevant chapters. This chapter also makes extensive reference to **Appendix IV: Media, Solutions and Equipment** where relevant solutions have been detailed.

2.2. General Molecular Methods

2.2.1. *In silico* DNA manipulation: sequence analysis, vector and primer design

All *in silico* DNA manipulation, including sequence selection, vector and primer design was carried out using the Invitrogen™ Vector NTI Advance® 11.5.2 software suite (2012, Invitrogen™ Corporation, Carlsbad, California, USA). Further testing of designed primers was conducted using Primer3 (Rozen & Skaletsky, 1999). Chromatograms from sequencing experiments were processed to remove poor quality base reads and final contiguous sequences (contigs) were assembled using ContigExpress (2012, Invitrogen™ Corporation, Carlsbad, California, USA). AlignX (2012, Invitrogen™ Corporation, Carlsbad, California, USA) and the Basic Local Alignment Search Tool (BLAST v. 2.2.23 http://blast.ncbi.nlm.nih.gov/Blast.cgi) were used to verify consensus between cloned and expected DNA sequences.

2.2.2. Amplification of DNA by polymerase chain reaction (PCR)

Primers were sourced from Geneworks Pty. Ltd. (Thebarton, South Australia) or Sigma-Aldrich Pty. Ltd (Castle Hill, NSW) and re-suspended in autoclaved Milli-Q H_2O to a stock concentration of 100 mM. Working primer concentration was 10 mM in Milli-Q H_2O. Several different DNA polymerases and reactions conditions were used for different experimental techniques and are outlined in Table 2.1. Primer sequences, annealing temperatures and extension times are given for each are in relevant chapters. PCR cycling was conducted using a DNA-engine Tetrad® 2 Peltier Thermo-cycler (Bio-Rad Laboratories Pty. Ltd. Gladesville, New South Wales, Australia, Model No: AU500165) fitted with 48 and 96 well heating blocks. Cycling conditions PCR products were separated and visualized using agarose gel electrophoresis (section 2.2.4).

Cloning PCR (Table 2.1) was used for cloning DNA from cDNA or plasmids for vector assembly where a low copy-error rate is essential. For these reactions, the proof-reading DNA polymerase Invitrogen® Platinum® *Taq* DNA Polymerase High Fidelity (Invitrogen Australia Pty. Ltd., Mount Waverley, Victoria, Australia. Cat. No: 11304-011) was used.

A-tailing PCR (Table 2.1) was used for the addition 3′-deoxyadenosine to blunt-ended DNA fragments for use in A-tail cloning (section 2.2.7). Invitrogen® Platinum® *Taq* DNA polymerase (Invitrogen Australia Pty. Ltd., Mount Waverley, Victoria, Australia. Cat. No: 10966-026), which has non-template–dependent terminal transferase activity to adds 3′ deoxyadenosine to product ends, was used.

Colony PCR (Table 2.1) was used for screening of *Agrobacterium* and *E. coli* colonies following transformation for the presence of specific DNA vectors, prior to use for plant transformation or DNA extraction. Invitrogen® Platinum® *Taq* DNA Polymerase was used.

Plant genotyping PCR (Table 2.1) was used for large-scale PCR screening of gDNA extracted from transgenic plants for the presence or absence of transgene constructs. OneTaq® DNA Polymerase (NEB, Genesearch Pty. Ltd. Arundel, Qld, Australia, Cat. No: M0840L) was used as it proved more cost-effective.

Finally, RT-PCR was conducted using cDNA (section 2.2.22) synthesised from RNA extracted from transgenic plant tissues (section 2.2.21) to determine transgene expression (presence or absence). Again, lab standard Invitrogen® Platinum® *Taq* DNA Polymerase was used.

Table 2.1: PCR conditions for various PCR-based techniques

Information includes; DNA polymerase, reaction components and reaction conditions used for the 5 different PCR based techniques throughout this thesis: Cloning, A-tailing, Colony, Plant Genotyping PCRs and RT-PCR. Annealing temperature (X °C) differs based on the primer pair used and are specified in relevant experimental chapters. Extension time based on final PCR product size (Kbps).

Reaction Components	**Technique**									
	Cloning PCR		*A-tailing PCR*		*Colony PCR*		*Plant Genotyping*		*RT-PCR*	
DNA polymerase (kit)	Invitrogen® Platinum® *Taq* High Fidelity		Invitrogen® Platinum® *Taq*		Invitrogen® Platinum® *Taq*		OneTaq® DNA Polymerase		Invitrogen® Platinum® *Taq*	
Buffer (kit supplied)	1× High Fidelity PCR Buffer		1× PCR Buffer		1× PCR Buffer		1× PCR Buffer		1× PCR Buffer	
50 mM $MgCl_2$	2 mM		1.5 mM		1.5 mM		1.5 mM		1.5 mM	
dNTPs (of each)	0.2 mM		0.2 mM		0.2 mM		0.2 mM		0.2 mM	
Forward Primer	0.2 µM		0.2 µM		0.2 µM		0.2 µM		0.2 µM	
Reverse Primer	0.2 µM		0.2 µM		0.2 µM		0.2 µM		0.2 µM	
DNA polymerase	0.5 - 1 U		0.5 U		0.2 U		0.2 U		0.2 U	
Template DNA	1 µL (≈ 100 ng)		1 µL (≈ 100 ng)		colony inoculation		2 µL (100 - 200 ng)		1 µL (≈ 100 ng)	
Milli-Q H_2O	to 25 or 50 µL		to 25 µL		to 15 µL		to 15 µL		to 25 µL	
PCR Conditions										
Initial denaturation	94°C for 2 mins		94°C for 2 mins		94°C for 2 mins		94°C for 2 mins		94°C for 2 mins	
Denaturation	94 °C for 30 secs	Repeat for 25 – 30 cycles	94 °C, 30 secs	35 cycles	94 °C 30 secs	30 cycles	94 °C 30 secs	30 cycles	94 °C, 30 secs	25 - 35 cycles
Annealing	X °C for 30 secs		X °C, 30 secs		X °C, 30 secs		X °C, 30 secs		X °C, 30 secs	
Extension	1 min/Kbp		30 sec/Kbp		30 sec/Kbp		30 sec/Kbp		30 sec/Kbp	
Final extension	68 °C for 10 mins		68 °C for 10 mins		N/A		N/A		N/A	

2.2.3. Restriction enzyme digest of plasmid DNA

All restriction enzymes (REs) were sourced via New England Biolabs (NEB) (Genesearch Pty. Ltd. Arundel, Qld, Australia) and manufacturer recommended buffers, incubation temperatures and durations were used unless otherwise indicated. RE digests were incubated in a thermo-cycler (DNA Engine Tetrad® 2, Bio-Rad Laboratories Pty. Ltd. Gladesville, NSW, Australia). Where possible, heat inactivation of REs were carried out by additional incubation at 65 °C for 20 minutes.

Cloning digest reactions (Table 2.2) were used to linearize plasmid DNA for vector construction and were optimised for minimal non-specific cutting and to maintain over-hangs to allow improved ligation efficiency for vector construction. In cases where multiple RE are used in a single reaction, equal volumes of each restriction enzyme were used for a total of 1 unit (U). If heat inactivation of REs was not possible, gel electrophoresis (section 2.2.4) was used to separate enzymes and DNA fragments prior to extraction (section 2.2.5) and use in ligation (section 2.2.6).

Colony digest reactions (Table 2.2) were used to linearize plasmid DNA extracted from overnight cell-cultures (section 2.2.12) as a rough diagnostic prior to selection of plasmids for sequencing (section 2.2.13)

Table 2.2: Reaction components and conditions for RE digests
Information included; reaction components and proportions for the two experimental techniques, cloning digest and colony digest; and reaction conditions.

	Technique	
Reaction Components	*Cloning digest*	*Colony Digest*
NEB RE Buffer 4	1 ×	1×
RE Enzyme	1 U	0.25 U
Milli-Q H_2O	to 50 µL	to 15 µL
Reaction conditions		
Incubation temperature	37 °C	37 °C
Incubation time	1 hr	1 hr – O/N
Heat inactivation	60 °C for 15 minutes	N/A

2.2.4. Separation of DNA fragments using agarose gel electrophoresis

Separation for DNA fragments for analysis or isolation following PCR or restriction enzyme digestion was conducted using agarose gel electrophoresis using a Sub-Cell® GT Cell (Bio-Rad Laboratories Pty. Ltd. Gladesville, New South Wales, Australia. Cat. No. 170-4401) and PowerPac Basic™ Power Supply (Bio-Rad Laboratories Pty. Ltd. Gladesville, New South Wales, Australia. Cat. No. 164-5050).

Expected Fragments larger than 300 bp were separated on a 1 % w/v agarose gel, while smaller products utilised a 2 % w/v gel to aid separation between small molecular weight fragments. The required amount of powdered agarose (Bioline Pty. Ltd., Alexandria, NSW, Australia. Cat. No. BIO-41026) was added to 1 × TAE (40 mM TRIS-acetate pH 8.0, 1 mM Na_2EDTA see Appendix IV: 50 × Tris base, acetic acid and EDTA (TAE) Buffer Stock) and heated gently using a microwave to dissolve. Once cooled to approx. 60 °C, 0.005 % v/v (5 µL per 100 mL of agarose gel) SYBR® Safe DNA gel stain (Life Technologies™ Pty. Ltd., Mulgrave, Victoria, Australia. Cat. No. S33102) was added to allow visualisation of DNA under ultraviolet light excitation. From our experience, SYBR® Safe performs similarly to the standard ethidium bromide stain in this role, but is a less hazardous alternative.

10 × Sucrose or 6 × Orange G loading dye (See Appendix IV: Loading Dyes) was added to samples prior to loading into the wells of an agarose gel. Five µL of HyperLadder™ I/1Kbp (Bioline Pty. Ltd., Alexandria, NSW, Australia. Cat. No. BIO-33026) or Hyperladder™ II/100bp (Bioline Pty. Ltd., Alexandria, NSW, Australia. Cat. No. BIO-33030) was used as a molecular weight marker to allow size determination of the fragments.

Separation of DNA fragments via gel electrophoresis was carried out at 90 Volts for approximately 30 minutes. DNA was then visualised using a GeneFlash UV transilluminator (MEDOS Pty. Ltd., Adelaide, South Australia, Australia) and images taken using Geneflash Syngene bio-imaging booth (MEDOS Pty. Ltd., Adelaide, South Australia, Australia).

DNA fragments required for downstream cloning applications were extracted from agarose gel as per section 2.2.5.

2.2.5. DNA extraction and purification following PCR or restriction enzyme digest.

2.2.5.1. DNA extraction from agarose gel

Following DNA separation by agarose gel electrophoresis, target DNA fragments were extracted for downstream applications such as cloning into pCR8/GW-TOPO (section 2.2.7) or joined to other fragments using DNA ligation (section 2.2.6). DNA bands on the agarose gel stained with SYBR® Safe DNA gel stain were visualised using a UV-transilluminator (Spectroline® Model TR-302/F, Spectronics Corp., Westbury, New

York, USA) and were quickly excised from the gel using a razor blade. Time under UV was kept to a minimum to reduce exposure and damage to the DNA by the high energy UV radiation.

Excised gel was weighed, maximum 300 mg per fragment, and transferred to a 2 mL Safe-lock Eppendorf® microfuge tube (Eppendorf South Pacific Pty. Ltd., North Ryde, NSW, Australia, Cat. No. 0030-120.094). DNA was purified using an ISOLATE® PCR and Gel Kit (Bioline Pty. Ltd., Alexandria, NSW, Australia, Cat. No. BIO-52030) as per the manual for DNA extraction from agarose gel.

In brief, 650 µL of kit supplied Gel Solubiliser Buffer was added to the excised gel fragment and incubated at 50 °C for approximately 10 minutes until the gel had dissolved. Inverting the samples several times assists this process. 50 µL of kit supplied Binding Optimiser Buffer was then added to each of the samples before transferring the sample to the supplied spin column containing a silica membrane. The two buffers contain chaotropic salts which assist in dissolving the agarose gel, denaturing DNA and altering the pH of the solution to 5.0 – 6.0 which facilitates binding of the DNA to the silica membrane. Samples on silica membranes were then centrifuged at 10,000 *g* for 1 minute in a mini centrifuge (Eppendorf™ 5415-D, BioLab Australia, Pty. Ltd., Mulgrave, Victoria, Australia) and filtrate was discarded. A washing step involving the addition of 700 µL of kit supplied Wash Buffer A to the spin column and centrifugation at 10,000 *g* was repeated twice to remove excess salts and PCR components such as spare nucleotides and primers. Filtrate was again discarded.

20 µL kit supplied elution buffer, preheated to 50 °C, was added to each of the spin columns and allowed to incubate at room temperature for 1 minute to allow the disassociation of the DNA from the silica membrane. Samples were then centrifuged for 1 minute at 10,000 *g* to elute DNA. The eluate was re-run through the spin column at 10,000 *g* a second time to increase the DNA recovered from the silica membrane. Eluted DNA in 20 µL of kit supplied Elution buffer can be used directly for downstream applications such as pCR8 cloning or ligation reactions.

2.2.5.2. Direct DNA extraction from PCR

For some samples with little non-specific PCR product or primer-dimer formation, DNA can be extracted directly from the reaction mix using an ISOLATE® PCR and Gel Kit (Bioline Pty. Ltd., Alexandria, NSW, Australia. Cat. No. BIO-52030) as per the manual.

In brief, up to 50 µL of DNA containing sample for isolation was added to a kit supplied spin column containing a silica membrane. 500 µL of kit supplied Binding Buffer A was added to the spin column and mixed by pipetting. Binding buffer A contains chaotropic salts which assist to denature DNA and alters the pH of the solution to 5.0 – 6.0 facilitating binding of the DNA to the silica membrane. Samples were centrifuged for 1 minute at 10,000 *g* and filtrate was discarded. Following this, 10 µL kit supplied elution buffer, preheated to 50 °C, was added to each of the spin columns and allowed to incubate at room temperature for 1 minute to allow the disassociation of the DNA from the silica membrane. Samples were then centrifuged for 1 minute at 6,000 *g* to elute DNA. Eluted DNA in 10 µL of kit supplied Elution buffer can be used directly for downstream applications such as pCR8 cloning (section 2.2.7) or ligation reactions.

2.2.6. Ligation of restriction enzyme digestion products

Assembly of constructs from restriction enzyme digest products were joined by T4 DNA ligase (Invitrogen Australia Pty. Ltd., Mount Waverley, Victoria, Australia. Cat. No: 15224-025). DNA concentration of both insert (smaller fragment) and vector (larger fragment) fragments were estimated with the use of a Nanodrop® DNA/RNA Spectrophotometer (Biolab Australia Pty. Ltd. Mulgrave, Vic, Australia, Model No: ND-1000). Insert and Vector DNA fragments were combined in 0.25 mL microfuge tube in a 3:1 molar ratio, i.e smaller fragment at 3× higher concentration than larger to improve ligation efficiency. Reactions components were added and incubated in a DNA-engine Tetrad® 2 Peltier Thermo-cycler (Bio-Rad Laboratories Pty. Ltd. Gladesville, New South Wales, Australia, Model No: AU500165) as outlined in Table 2.3 which details changes to protocol required depending on the nature of the fragment ends requiring joining.

Table 2.3: Reaction components and conditions for the ligation of RE digest products using T4 DNA ligase.
Information included; Reaction components and conditions for ligation of either Cohesive- or Blunt-ended DNA fragments with T4 DNA ligase

	Technique	
Reaction Components	*Cohesive End Joining*	*Blunt End Joining*
5 × Ligase reaction Buffer	1×	1×
Insert:Vector Molar Ratio	3:1	3:1
Total DNA	50 - 100 ng	200-1000 ng
T4 DNA Ligase	0.1 U	1 U
autoclaved Milli-Q H_2O	To 20 µL	to 20 µL
Reaction Conditions		
Incubation temperature	25 °C	15 °C
Incubation time	1 hr	16 hrs or O/N

2.2.7. Cloning of DNA into pCR8/GW-TOPO TA Gateway® entry vectors

For sequencing and further manipulation, DNA fragments were cloned into pCR8/GW/TOPO-TA vector (Invitrogen Australia Pty. Ltd., Mount Waverley, Victoria, Australia. Cat. No: K2500-20) (Figure 2.1) which utilises a 3′A overhang for ligation requiring final extension step outlined in Cloning PCR, section 2.2.2, Table 2.1. Additionally, some restriction enzymes used (section 2.2.3) produce blunt-ended fragments that required an A-Tailing PCR to be conducted (section 2.2.2) to add 3′ A overhang.

Approximately 100 ng of 3′ A overhang DNA extracted as per section 2.2.4 (generally 1 - 2 µL) was added to 0.5 µL of pCR8/GW-TOPO TA Gateway® entry vector, 1 µL of kit supplied Salt solution and autoclaved Milli-Q H_2O to a final volume of 6 µL. Reactions were briefly mixed by pipetting and spun in a microfuge to collect contents. Following overnight incubation at 4 °C, 1-2 µL of reaction mix was used for transformation into E. coli strain TOP-10™ or DH5α (section 2.2.11). This modified protocol uses 50 % less entry vector then the recommended protocol, however results are comparable and produce a large number of successfully transformed colonies following transformation.

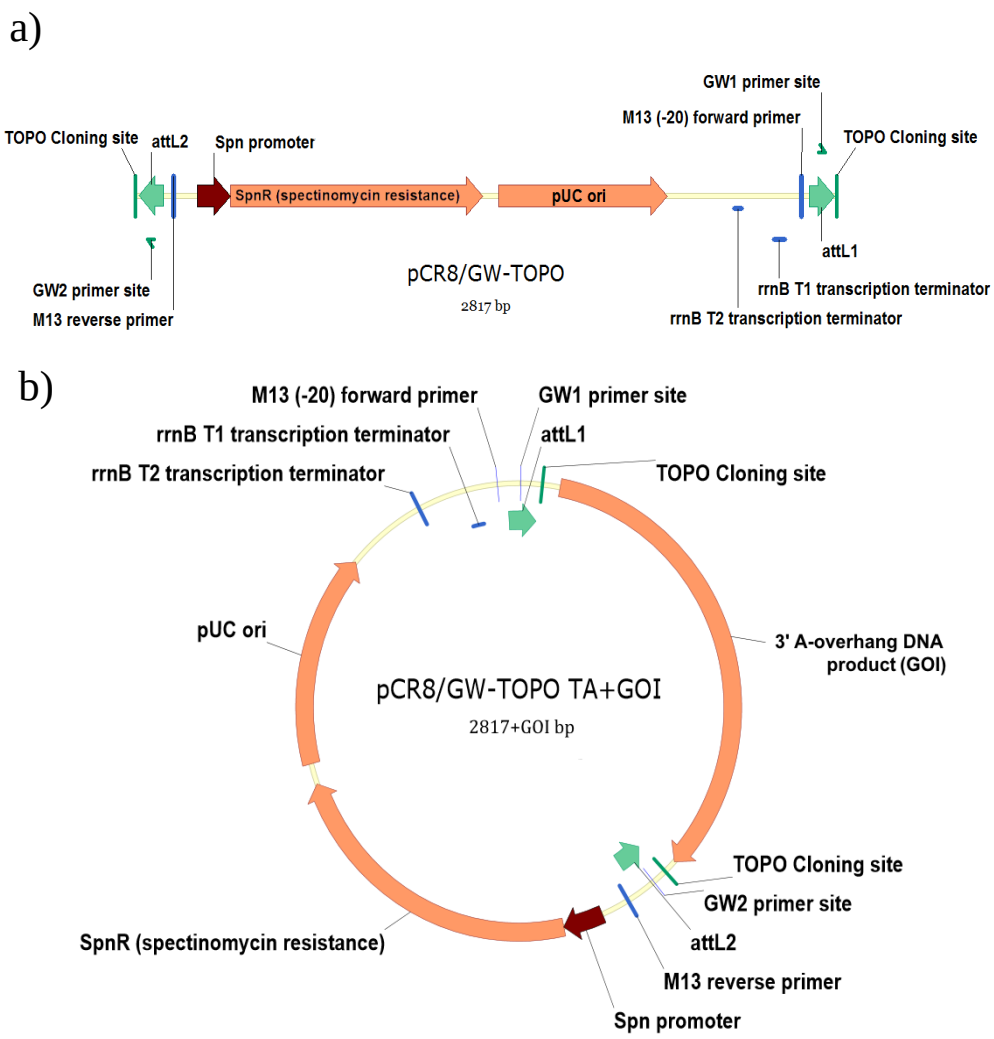

Figure 2.1: Overview of the pCR8/GW-TOPO TA Gateway® entry vector used to clone DNA fragments.
The pCR8/GW-TOPO Gateway® entry vector is supplied in linearised form (a). Following an overnight ligation reaction with 3′ A-overhanging PCR amplified or A-tailed products, the plasmid become circularised and contains the A-tailed DNA product between the TOPO cloning sites. Cloned products are flanked by Gateway® recombination sites *attL1* and *attL2* to enable Gateway®-enabled destination vectors (section 2.2.8). The vector also contains the pUC origin of replication (pUC ori) and a spectinomycin resistance gene (Spn promoter and SpnR) allowing for specintomycin selection in *E. Coli* harbouring the circularised plasmid.

2.2.8. Recombination of entry and destination vectors to produce expression vectors for plant transformation

The use of Invitrogen® Gateway® LR recombination system (Curtis & Grossniklaus, 2003) allowed the directional transfer of DNA sequences from TOPO Gateway® entry vectors (pCR8/GW/TOPO-TA, pENTR-D-TOPO) into Gateway®-enabled destination

vectors to produce expression vectors for plant transformation in a single reaction. DNA sequences between the *attL* motifs of the Gateway® entry vector are recombined with the region between the *attR* motifs of the Gateway® destination vector with the use of Invitrogen® Gateway® LR Clonase II Enzyme Kit (Invitrogen Australia Pty. Ltd., Mount Waverley, Victoria, Australia, Cat. No: 11791). LR reactions prepared as per Table 2.4 and incubated over night at 25 °C in a thermo-cycler (DNA Engine Tetrad® 2, Bio-Rad Laboratories Pty. Ltd. Gladesville, NSW, Australia).

Table 2.4: Reaction components and conditions for LR clonase reactions
Information included; reaction components, proportions and conditions

Reaction Components	*LR Recombination reaction*
5 × LR Buffer	2 µL
Entry Clone	100 – 200 ng (1 – 2 µL)
Destination Clone	100 – 200 ng (1 – 2 µL)
TE buffer pH 8.0	4 µL
LR Clonase enzyme	2 µLs
Reaction Conditions	
Incubation temperature	25 °C
Incubation time	16 hrs – O/N

2.2.9. Preparation of chemically competent *E. coli* for cloning

For cloning of plasmids not requiring highly chemically competent *E. coli*, such as for re-transformations and for transformation with pCR8 ligation reactions, $CaCl_2$ chemically competent *E. coli* (strains DH5α, DB3.1 and Top-10®) were produced in-house based on a protocol adapted from (Seidman *et al.*, 2001). Strains were kept in -80 °C in 25 % Glycerol stocks (section 2.2.10) for long term storage. Sterile 2 mL O/N cultures without antibiotics were grown as per section 2.2.12. 100 mL of LB medium was inoculated with 1mL of O/N culture and incubated with vigorous shaking at 37 °C for approximately 2 hours, until OD600 reached 0.3 as measured by spectrophotometry (Shimadzu Corporation, Rydalmere, NSW, Australia, Model No: UV-160A). The cell culture was then cooled on ice for 15 minutes before centrifugation at 3300 *g* (Hettich GmBH & Co.KG., Tuttlingen, Germany, Model No: Rotanta 460-R), for 10 minutes at 4 °C. The supernatant was decanted and the cell pellet was gently resuspended in 30 mL of 0.1M $CaCl_2$ pre-cooled on ice, by pipetting. Cells were incubated on ice for 30 minutes before another centrifugation at 3300 *g* for 10 minutes at 4 °C. Supernatant was again discarded and cells were resuspended in 6 mL of pre-cooled 0.1M $CaCl_2$ with 15 %

autoclaved sterile glycerol. 200 µL aliquots of cell culture were transferred to pre-cooled autoclaved sterile micro-centrifuge tubes before being snap frozen in liquid nitrogen and stored at -80 °C for use.

2.2.10. Glycerol stocks for long term storage of bacterial cultures.

Both *E. coli* and *A. tumefaciens* cell cultures were kept at -80 °C for long term storage in a 25 % glycerol solution to prevent cell lysis during freezing. 1 mL of overnight bacterial culture (generally LB and appropriate selective antibiotics) was added to 1 mL of a 50 % Glycerol solution in a 2 mL microfuge tube and mixed by vortexing briefly. Cultures were snap-frozen in liquid nitrogen prior to being stored at -80 °C. Cultures were re-grown from frozen glycerol stocks by scraping an autoclave sterile 200 µL pipette tip across the still frozen stock and then placing the pipette tip in LB medium with appropriate antibiotics before O/N incubation as per section 2.2.12.

2.2.11. Transformation of *E. coli* via heat-shock method

LR and pCR8 ligation reactions were transformed into commercially chemically competent Invitrogen™ TOP10 *E. coli* cells (Invitrogen Australia Pty. Ltd., Mount Waverley, Victoria, Australia. Cat. No. C4040-10) or in-house made chemically competent cells as per section 2.2.9. Commercially competent Invitrogen™ TOP10 *E. coli* are supplied in 50 µL aliquots and in most cases a 10 µL aliquot of competent cells into pre-cooled microfuge tubes is sufficient for efficient transformation. For in-house made competent cells the full 200 µL aliquot was used for efficient transformation.

Following thawing of competent cells from -80 °C on ice for approximately 10 minutes, competent cells were transferred to a pre-cooled 1.5 mL microfuge tube containing 2 µL of ligation reaction. Samples were gently flicked to ensure mixing and were incubated on ice for approximately 10 minutes before being transferred to a 42 °C water bath (Gesellschaft für Labortechnik (GFL), Model: 1012) for 30 seconds to heat-shock. Samples were returned to ice for 5 mins before the addition of 250 µL of LB media to each sample. Samples were then incubated in a 37 °C orbital mixer incubator with agitation at 200 rpm (Ratek Instruments Pty. Ltd., Boronia, Victoria, Australia) for 45 minutes to allow the transformed cells to recover. For selection of transformed cells, a 100 µL aliquot of each reaction, was spread onto 90 x 14 mm petri dishes (Techno Plas Pty. Ltd., St Marys, SA, Australia. Cat. No: 10603001) containing 20 mL of Luria Broth Agar (see Appendix IV: Luria Broth Agar (LBA)) with 100 $\mu g.mL^{-1}$ of appropriate

antibiotic (kanamycin, ampicillin and/or chloramphenicol depending on construct used for transformation) and incubated overnight at 37°C.

2.2.12. Overnight growth of *E. coli* and *A. tumefaciens* cultures

Overnight growth of E. coli cultures was conducted in autoclave sterile 10 mL glass culture tubes containing Luria Broth (see Appendix IV: Luria Broth (LB medium)), plus 100 $\mu g.mL^{-1}$ of suitable antibiotics if required (kanamycin, ampicillin, and/or chloramphenicol depending on construct transformed), and incubated in an orbital mixer incubator (Ratek Instruments Pty. Ltd., Boronia, Victoria, Australia) at 37 °C with agitation at 200 rpm to ensure vigorous growth.

2.2.13. DNA sequencing of plasmids and PCR products

DNA sequencing of plasmids and PCR products was conducted using the PCR based BigDye® Terminator V3.1 Cycle Sequencing system (Applied Biosystems Pty. Ltd., Mulgrave, Vic, Australia, Cat. #433745). Reactions were performed in 0.5 mL microfuge tubes with 200 ng of DNA. Generally 1 µL from plasmid extractions performed as in section 2.2.18, or 1 µL of PCR product extractions from section 2.2.5 was used for sequencing. Reactions were prepared and incubated as specified in Table 2.5 and PCR cycling was conducted using a DNA-engine Tetrad® 2 Peltier Thermo-cycler (Bio-Rad Laboratories Pty. Ltd. Gladesville, New South Wales, Australia, Model No: AU500165)

Table 2.5: Reaction components and conditions of BigDye® Terminator V3.1 Cycle Sequencing Reaction.
Information included; reaction components and reaction conditions

Reaction Components	*BigDye® V3.1 sequencing reaction*	
BigDye® Buffer	3.5 µL	
10 µM Primer	0.32 µL	
Template DNA	100 – 200 ng	
Milli-Q H_2O	to 10 µL	
Reaction conditions		
Initial Denaturation	96 °C for 2 minutes	
Denaturation	96 °C for 10 seconds	Repeat for 30 cycles
Annealing	50 °C for 5 seconds	
Elongation	60 °C for 4 minutes	
Hold until clean-up	4 °C	

2.2.13.1. Isopropanol and Magnesium sulphate ($MgSO_4$) post-sequencing clean-up

BigDye® Terminator V3.1 sequencing reaction samples require a clean-up reaction to remove excess fluorophores and reaction components. In brief, protecting from light wherever possible, reactions were warmed to room temperature and transferred to 1.5 mL micro tube containing 75 µL of room temperature 0.2 mM $MgSO_4$ in 70 % ethanol (see Appendix IV: Sequencing Reaction clean-up) and incubated at room temperature for 15 minutes protected from light. Samples were then centrifuged at 15,000 *g* for 15 minutes to precipitate DNA and supernatant was removed using a pipette. 75 µL of 70 % Ethanol was added to samples, vortexed briefly (1 to 2 seconds), followed by another round of centrifugation at 15,000 *g* for 15 minutes. Supernatant was decanted and disposed of and samples were inverted onto a paper towel and allowed to air dry for approximately 15 minutes or incubated at 37°C upright to dry the DNA in both cases samples were protected from light. Samples were sealed and sent for sequencing.

2.2.13.2. DNA sequencing and analysis

The DNA sequences of samples was determined using Fluorescent DNA capillary separation using an AB3730xl 96-capillary sequencer (Life Technologies, ThermoFisher Scientific Inc., Waltham, WA, USA, Model No: AB3730xl) operated by Australian Genome Research Facility Pty. Ltd. (AGRF), Adelaide Node, Urrbrae, South Australia.

Sequencing reads were analysed using ContigExpres, a component of Vector NTI Advance® 11.5.2 software suite (2012, Invitrogen™ Corporation, Carlsbad, California, USA,). Poor quality bases sequencing reads at the ends of the reads where removed

automatically. Generally, reads were 600 – 900 bps in length following quality trimming and removal of plasmid derived sequences. AlignX, another component of Vector NTI Advance® 11.5.2 software, was used to assemble multiple sequencing reads across cloned fragments to identify potential SNPs and to verify cloning and ligation events.

2.2.14. Preparation of chemically competent *A. tumefaciens* AGL-1

Chemically competent *A. tumefaciens* strain AGL-1 suitable for transformation using the freeze/thaw protocol (section 2.2.15) were prepared in-house using a protocol modified from (Höfgen & Willmitzer, 1988). 200 mL of LB media with of 50 $\mu g.mL^{-1}$ of both carbenicillin and 50 µg.mL-1 of rifampicin was inoculated with 1 mL of O/N culture of *A. tumefaciens* prepared as per section 2.2.12. The cultures were then incubated in an orbital mixer incubator (Ratek Instruments Pty. Ltd., Boronia, Victoria, Australia) at 28 °C with agitation at 200 rpm for approximately 16 hours until OD600 reached 0.8. The cell culture was then cooled on ice for 15 minutes before centrifugation at 3000 *g* (Hettich GmBH & Co.KG., Tuttlingen, Germany, Model No: Rotanta 460 R), for 15 minutes at 4 °C. The supernatant was decanted and the cell pellet was washed with 20 mL of room temperature 1× TE buffer (10 mM Tris-HCl, 1 mM EDTA, pH 8.0) and vortexed briefly. Cells were resuspended in 20 mL of LB without antibiotics by gently pipetting and 250 µL aliquots of cell culture were transferred to pre-cooled autoclave sterile 1.5 mL micro-centrifuge tubes before being snap frozen in liquid nitrogen and stored at -80 °C before use.

2.2.15. Transformation of *A. tumefaciens* via freeze-thaw protocol

Approximately 100 – 200 ng of DNA (2 µL from standard E. coli plasmid DNA extraction protocol) was added to 250 µl of chemically competent *A. tumefaciens* strain AGL-1 prepared as described in section 2.2.14 in 2 mL tubes. Tubes were flicked gently to stir contents and allowed to incubate on ice for 10 minutes. Tubes were then immersed in liquid nitrogen and left to incubate in liquid nitrogen for 5 minutes to ensure complete freezing. Tubes where transferred directly into a 42 °C water bath (Gesellschaft für Labortechnik (GFL), Burgwedel, Germany, Model No: 1012) for 5 minutes. One mL of LB media (without antibiotics) was added to the samples and incubated at 28 °C in an orbital mixer incubator for 4 hours to allow the cells to recover from transformation.

Samples were centrifuged at 6,000 *g* for 3 minutes to pellet cells. Supernatant was decanted and cells were resuspended in 200 µL of LB media. The full 200 µL was plated

onto LBA containing petri dishes with appropriate plasmid selection antibiotic in addition to 50 µg.mL^{-1} carbenicillin and 50 µg.mL^{-1} rifampicin for selection of *A. tumefaciens* strains. Plates were protected from light by wrapping in aluminium foil and incubated at 28 °C for 3 days until colonies were visible. Colony PCR was performed to confirm successful transformation events as per section 2.2.2.

2.2.16. Growth of small *A. tumefaciens* cultures

Growth of small scale *A. tumefaciens* cultures was conducted in autoclave sterile 10 mL glass culture tubes, with addition of 50 µg.mL^{-1} of carbenicillin for Ti Plasmid selection and 50 µg.mL^{-1} of rifampicin for Chromosomal/Agrobacterium selection. Additional antibiotics for selection of the plant transformation vector, generally 50 µg.mL^{-1} kanamycin, was added if required. The cultures were incubated in an orbital mixer incubator (Ratek Instruments Pty. Ltd., Boronia, Victoria, Australia) at 28 °C with agitation at 200 rpm for approximately 2 days until reaching stationary phase or OD600 at 0.3.

2.2.17. Isolation of plasmid DNA from *E. coli* – Standard protocol

Two mL overnight E. coli cultures (section 2.2.12) were centrifuged at 16,100 *g* for 1 minute centrifuge (BioLab Australia, Pty. Ltd., Mulgrave, Victoria, Australia. Model No: Eppendorf™ 5415-D) to pellet cells and supernatant was decanted. Bacterial cells were resuspended in 100 µL of alkaline extraction solution I (Appendix IV: Media, Solutions, Appendix IV: Alkaline Lysis extraction) by briefly vortexed. 200 µL of alkaline extraction II and 150 µL of alkaline extraction solution III were added and tubes sealed and inverted 5-10 times to mix and allow cell lysis. Lysed cells were then centrifuged at 16,100 *g* for 15 minute to pellet chromosomal DNA and cell contents. The supernatant, containing plasmid DNA was transferred to a new microfuge tube containing 750 µL of 100 % Isopropanol to precipitate DNA and incubated overnight at -20 °C. Following incubation, samples were spun again at 16,100 *g* for 15 minute to pellet plasmid DNA and supernatant was aspirated by pipette. The plasmid DNA containing pellet was washed with 0.5 mL of 70 % v/v Ethanol and briefly vortexed before centrifugation at 16,100 *g* for 1 minute. The ethanol was aspirated and tube inverted to allow the pellet to air dry. The pellet was then be resuspended in 20 µL of 40 ug.mL^{-1} RNase A in 1× TE buffer and incubated at 37 °C for 10 minutes to remove RNA prior to use.

2.2.18. Isolation of plasmid DNA from *E. coli* – High purity DNA protocol

For techniques requiring high quality DNA, such as RE digests for cloning or prior to LR ligation reaction, DNA was extracted from E. coli using ISOLATE® PCR and Gel Kit (Bioline Pty. Ltd., Alexandria, NSW, Australia, Cat. No. 52029). This product is chemically similar to the alkaline extraction described in section 2.2.17, however the commercial kit utilises a silica membrane to bind plasmid DNA allowing further washing and improved removal of bacterial cell contaminates.

Selected colonies were cultured overnight in 2 mL of LB medium including appropriate antibiotics. Cultures were pelleted by centrifugation at 16,100 *g* for 1 minute in a 2 mL microfuge tube and supernatant decanted. Pellets were resuspended in 250 µL of kit supplied re-suspension buffer followed by addition of 350 µL of kit supplied Lysis Buffer P and mixed by inverting. 350 µL of kit supplied Neutralisation buffer was added and samples centrifuged at 16,100 *g* for 10 minutes to pellet cell debris. The supernatant was transferred to a kit supplied spin column containing a silica membrane and centrifuged at 10,000 *g* for 1 minute and filtrate discarded. The silica membrane was washed by the addition of 500 µL of kit supplied wash buffer AP and centrifuged at 10,000 *g* for 1 minute. Eluate was disposed of and 700 µL of wash buffer B added directly to the spin column and centrifuged at 10,000 *g* for 1 minute. The silica membrane was dried by centrifugation at 16,100 *g* for 2 minutes. Samples were eluted by the addition 30 µL of kit supplied elution buffer, preheated to 50 °C, directly to the silica membrane in the spin columns and allowed to incubate at room temperature for 1 minute to allow the disassociation of the DNA from the silica membrane. Samples were then centrifuged for 1 minute at 10,000 *g* to elute DNA. Isolated DNA can then be used directly or stored at -20 °C for several months.

2.2.19. Genomic DNA extraction protocol - Freeze dry protocol

Genomic DNA (gDNA) was extracted from transgenic plant material as described in Shavrukov *et al.* (2012). Although this protocol was used designed for wheat and barley DNA extraction, it works adequately with Arabidopsis leaf material. Young leaf samples were harvested from Arabidopsis or barley and stored on ice during collection into 1 mL strip tubes. Collected leaf samples were freeze-dried for 16 hrs (over-night) at 0.1 mBar and -20 °C (John Morris Scientific Pty. Ltd., Willoughby, NSW, Australia, Model No: Alpha 1-2L Dplus). Two 4 mm ball bearings (cleaned with 70 % v/v Ethanol) were added to the tubes and the samples were transferred to -20 °C as quickly as possible to minimise

degradation of DNA prior to grinding. Samples were ground for 3 cycles of 40 seconds at 1200 RPM with the use of a Retch-mill (MEP Instruments Pty. Ltd. North Ryde, NSW, Australia. Model No: MM-300). Plates were allowed to warm to room temperature before the addition of 600 µL of Freeze Dry Extraction Buffer (Appendix IV: Plant DNA Extraction). Tubes sealed and mixed thoroughly by inversion. Samples were incubated at 65 °C for 30 minutes then allowed to cool to room temperature. 300 µL of 4 °C cooled 6 M ammonium acetate ($NH_4C_2H_3O_2$) was added to each sample, mixed by inversion and incubated at 4 °C for 15 minutes. Samples were centrifuged at 4000 *g* (Hettich GmBH & Co.KG., Tuttlingen, Germany, Model No: Rotanta 460 R) to precipitate plant cell material. 600 µL of supernatant was transfer to new tubes with the addition of 360 µL of 100 % isopropanol before samples were allowed to incubate overnight at -20°C to precipice DNA. The following day, ball bearings were removed from strip tubes with a hand-held electro-magnet developed during this project for this purpose (Appendix IV: Electromagnet for extraction of ball-bearings). Samples were centrifuged at 4000 *g* to pellet DNA before decanting the supernatant. The pellets were washed in 300 µL of 70 % ethanol and mixed by inverting and centrifuged at 4000 *g* to re-pellet DNA. All traces of ethanol were aspirated off by pipette and samples resuspended in 100 µL of Milli-Q H_2O for general PCR.

2.2.20. DNA extraction protocol – Edwards extraction protocol

For small scale DNA extractions, young leaf samples harvested from Arabidopsis or barley were snap frozen in liquid nitrogen in 2 mL microfuge tubes and stored at -80°C prior to extraction. Frozen samples were first ground by adding two 4 mm ball bearings (cleaned with 70 % Ethanol) to the tubes and vortexed until the sample had been ground to a fine powder. 400 µL of Edwards extraction Buffer (0.2 M Tris-HCl pH 8.0, 0.25 M NaCl, 0.0025 M EDTA, 5% SDS) (Edwards *et al.*, 1991) was added to each tube and vortexed for 5 seconds. Samples were allowed to incubate at room temperature for approximately 2 hours for extraction to take place. Samples were centrifuged at 16,100 *g* for 1 minute in a mini-centrifuge (BioLab Australia, Pty. Ltd., Mulgrave, Victoria, Australia. Model No: Eppendorf™ 5415-D) to pellet cell material. Supernatant was transferred to a new 1.5 mL microfuge tube with the addition of 300 µL of 100 % Isopropanol. Samples were allowed to incubate at room temperature for 20 minutes or at -20 °C overnight to precipitate DNA followed by centrifugation at 16,100 *g* for 5 minutes to pellet DNA. Isopropanol was then aspirated using a pipette and the pellet air dried and

protected from light. Samples were then be re-suspended in 100 µL of Milli-Q H_2O for use in PCR.

2.2.21. Extraction of RNA from Root and Leaf Tissue

Total RNA was extracted from Arabidopsis and barley root and leaf samples using the Direct-zol™ RNA purification kit (Zymo Research Corp., Irvine, USA, Cat no: R2052). Approximately, 200 mg of leaf or root samples were harvested from plants and placed in 2 mL microfuge tubes containing two 4mm stainless steel ball bearings and snap frozen in liquid nitrogen prior to RNA extraction. Samples selected for RNA extraction were transferred in liquid nitrogen and ground for 30 seconds at 1,000 RPM in a SPEX SamplePrep Geno/grinder 2010 (Metuchen, NJ, USA). Samples were suspended in 500 µL of TRIzol-like reagent (Invitrogen Australia Pty. Ltd., Mount Waverley, Victoria, Australia. Cat no: 15596-026) and centrifuged for 1 min at 12,000 g. The supernatant was transferred into a kit-supplied Zymo-Spin™ ICC column and centrifuged for 1 min at 10,000 *g* to remove cell-contents. An in-column DNase I digestion was preformed to remove bound DNA by first washing the spin columns with 400 µL of RNA wash buffer and centrifuged for 30 s at 10,000 g. 80 µL of DNase I Reaction Mix (kit supplied: 5 µL/5U lyophilized DNAse I (E1009), 8 µL 10X DNase I reaction buffer, 3 µL DNase/RNase-free water, 64 µL of RNA wash buffer) was added directly to the column of each sample and incubated at room temperature for 15 mins then centrifuged for 30 secs at 10,000 g. Following, 400 µL of Direct-zol™ RNA pre-wash was added to each column and centrifuged for 1 minute at 10,000 g. Supernatant was discarded and this step repeated. Spin columns were then washed with 700 µL of RNA wash buffer and centrifuged for 1 minute and flow-through discarded. Columns were then spun for 2 minutes at 16,000 *g* to remove excess wash buffer. Finally, 25 µL of DNase/RNase-free water was added to each column, allowed to incubate for 1 minute at room temperature, and then centrifuged at 10,000 *g* for 1 minute to elute RNA. RNA concentration was quantified by use of a Nanodrop® DNA/RNA Spectrophotometer (Biolab Australia Pty. Ltd. Mulgrave, Vic, Australia, Model No: ND-1000) and quality visually inspected by gel-electrophoresis (section 2.2.4) on a 1 % agarose gel. RNA samples were stored at -80°C until required.

2.2.22. Synthesis of cDNA from RNA extracted from root and leaf tissue.

cDNA was synthesised from total RNA extracted as previously described (section 2.2.21) using the SuperScript® III First-strand Synthesis Kit Invitrogen Australia Pty. Ltd.,

Mount Waverley, Victoria, Australia. Cat no: 18080-5051) with oligo(dT)20 primer to specifically synthesise poly(A)+-mRNAs. One µg of RNA was mixed with 1 µL of 50 µM oligo(dT)20 primer, 1 µL of 10 mM dNTP and miliQ-H2O to a total volume of 10 µL. Samples were incubated at 65 °C for 5 minutes with a dry block heater (Ratek Instruments Pty. Ltd., Model No: DBH30). Samples were then transferred onto ice for one minute before addition of 10 uL of cDNA synthesis mix (2 µL of 10X RT buffer, 4 µL 25 mM MgCL2, 2 µL of 0.1 M DTT, 1 µL of RNaseOUT™ and 1 µL of SuperScript® III Reverse Transcriptase) to each tube. Samples were briefly vortexed and centrifuged to collect tube contents then incubated for 50 minutes at 50 °C in a DNA-engine Tetrad® 2 Peltier Thermo-cycler (Bio-Rad Laboratories Pty. Ltd. Gladesville, New South Wales, Australia, Model #:AU500165). The synthesis reaction was terminated by a programed increase in the incubation temperature to 85 °C for 5 minutes before being transferred onto ice. Samples were collected by brief centrifugation and 1 µL of kit supplied RNase H added to each tube and incubated at 37 °C for 20 minutes to remove any remaining RNA. cDNA samples were stored at -20 °C before use.

2.3. *Arabidopsis thaliana* experiments

2.3.1. Arabidopsis growth in controlled environment chambers

Growth of Arabidopsis ecotypes C24 and Col-0, in soil, on petri dishes and in mini-hydroponics was carried out in separate controlled environment growth chambers located at the University of Adelaide, Waite Campus, Urrbrae, ACPFG PC2 greenhouse facilities. One chamber was set to short day light conditions, 10/14 hr light/dark cycle, and the other to long day light conditions, 16/8 light/dark cycle with lighting provided by florescent globes with an irradiance of approximately 120 µmol $m^{-2}.s^{-1}$. Both rooms were maintained at approximately 23-24 °C with refrigerative cooling with a relative humidity between 50 – 70 %.

To monitor growth-room temperature in real-time, a system was developed during the course of this project via the use of an internet connected laptop PC (ACER Inc., San Jose, CA, USA, Model: ACER Aspire One ZG5) running Windows XP installed inside of the growth-room. Temperature was measured using a USB sensor with external wired temperature probe (RDing Technology Ltd. Co., Shenzhen, Guangdong, PRC, Model No: TEMPer1) and logged using ThermoHID® (V2.0.1.27 release 16 Dec, 2012, Steve Timms, 2012) (Timms) designed for use with this hardware. The use of the ThermoHID

software allowed prompt reporting of over-heating events via e-mail and ensured plants were not exposed to excessive heat stress.

2.3.2. Surface sterilisation of Arabidopsis seeds

Seeds for selection or for growth on vertical plates were surface sterilised in 2 mL microfuge tubes (or 10 mL tubes if a large volume of seeds was being sterilised) by gentle rocking in 70 % (v/v) ethanol for 2 minutes, in bleach solution (50 % v/v Domestos (JohnsonDiversey Pty. Ltd., Australia. Active ingredients: 49.9 g/L Sodium hypochlorite, 12.0 g/L Sodium hydroxide, 0.5 g/L Alkaline salts) for 5 minutes, followed by approximately 5 to 8 washes in autoclaved Milli-Q water until bleach is removed. Rinsed seeds imbibed overnight at 4 °C in Milli-Q H_2O to improve germination, before being positioned individually using a 2 µL pipette onto selection media (section 2.3.7).

To spread a larger quantity of seeds evenly over selection media plates, as much of the water from the final Milli-Q water rinse was removed and a final rinse in 95% v/v ethanol was performed for 30 seconds. Seeds were spread over autoclaved Whatman™ filter paper and allowed to dry inside a laminar flow for approximately 1 hour, seeds were then distributed evenly over selection media (section 2.3.7).

2.3.3. Plant growth on MS medium in vertical petri dishes

Sterilised seeds were sown onto Murashige & Skoog 'MS' media containing 0.5× Murashige & Skoog Basal Salts mixture (Sigma-Aldrich Co. Llc., Castle Hill, NSW, Australia. Cat. No. M5524-1L), 0.3 % w/v Gelrite® Gellan Gum gelling agent (PhytoTechnologies Laboratories, LLC. Shawnee Mission, KS, USA. Cat. No: G469) supplemented with 0.5% w/v sucrose and buffered to pH 5.7 using KOH in 100×100×20 mm Square petri dishes (SARSTEDT Australia Pty. Ltd., Ingle Farm, SA, Australia. Cat. No. 82.9923.422). Seeds were positioned individually following sterilisation as per 2.3.2 using a 2 µL pipette. Petri dishes were sealed with micropore tape and protected from light using aluminium foil and kept for 2 days at 4 °C to allow for stratification of the seeds. Following this, plates were placed vertically in the short day growth chamber (section 2.3.1) for a maximum growing period of 4 weeks.

2.3.4. Arabidopsis growth on soil

Soil for Arabidopsis growth was prepared and supplied by SARDI (Waite Campus, Urrbrae, Australia) and was composed of equal parts (v/v) sand, perlite, peatmoss and vermiculite with the addition of: 100 g agricultural lime, 40 g hydrated lime, 200 g

dolomite, 50 g gypsum, 100 g iron sulphate and 300 g Osmocote Plus (Scotts, Australia) per 100 L of soil mix. pH of the soil mix following addition of all components was between 5.7 - 5.9.

2.3.4.1. Growth of Arabidopsis from Seed on soil

Before sowing, seeds were imbibed in water for 2 days at 4 °C and protected from light. Soil for Arabidopsis growth was prepared one day prior to sowing in small free-draining pots (8 cm depth × 6 cm diameter, Berry Plastics Corporation, Evansville, IN, USA) and allowed to soak standing in a tray (16 pots per tray) containing a mixture of reverse osmosis (RO) water and biological insecticide, VectorBac (Valent BioSciences Pty. Ltd., Australia), at a recommended rate of 0.5 mL per 1 L. The following day once the soil was moist, excess water was drained off and seeds were pipetted directly onto the soil surface. To maintain humidity and aid germination, a mini greenhouse (Yates Australia Pty. Ltd., Padstow, NSW, Australia) with adjustable air holes was placed over the pots. After germination, the adjustable air holes were opened to allow seedlings to adapt to the relatively low humidity of the growth chambers. The mini greenhouse was removed after approximately 2 weeks once the seedlings were established. Seedlings were thinned if necessary at this time. Plants were kept in the short-day growth chamber for approximately 5 weeks to allow for extra growth before being transferred to the long day growth chamber to promote flowering. Plants were watered approximately every three days by allowing pots to stand in tap water for approximately 1 hr or until soil was saturated.

2.3.4.2. Transfer of Arabidopsis from MS plates to soil

Plants recovered from selective media (section 2.3.3) or transferred from vertical plates (section 2.3.7) were gently washed in Milli-Q H_2O to remove excess media before being transferred into peat-pellets (Jiffy International AS, Kristiansand, Norway, Cat. No: Jiffy-7) pre-soaked in a mixture of reverse osmosis (RO) water and VectorBac at a recommended rate of 0.5 mL per 1 L. A mini greenhouse (Yates Australia Pty. Ltd., Padstow, NSW, Australia) with adjustable air holes was placed over the tray containing the transferred seedlings to maintain humidity. After 1 week growth, the peat-pellets were cut and plants transferred to soil pots prepared as in section 2.3.4.1 and grown normally until seed set.

2.3.4.3. Harvest of seed from mature plants

On flowering, plants were placed inside crispy loaf bags and watering was reduced to allow the plants to complete seed set and dry, process taking approximately 2 weeks. Siliques were collected and dried in paper bags at 37°C in an incubator for one week. Following drying, seeds were separated from siliques and were transferred to either 2 mL or 15 mL microfuge tubes (depending on seed quantity) and stored at 4°C protected from light.

2.3.5. Hybridisation of Arabidopsis lines

Arabidopsis plants of selected lines for crossing were grown in soil as described in section 2.3.4, under short day light conditions for approximately 5 weeks or until on onset of flowering. The initial inflorescence stem was cut to promote development of secondary inflorescences. Several of the largest unopened florets were selected for emasculation. In the ecotype used in this study for crossing, C24, if there is any visible petal emerged, fertilisation is likely to have already occurred and is not suitable. Using needle-nosed forceps, sepals and petals were plucked away to expose the carpel and the six stamen. All six stamen were removed and the emasculated floret was placed inside an uncapped 1.5 mL microfuge tube to maintain humidity and allowed to develop overnight.

The following day, newly opened flowers with visible viable pollen from plants selected for crossing were selected and using needle-nosed forceps, the stamen were collected and used to pollinate the emasculated carpels. Pollinated florets were kept in the 1.5 mL microfuge tube to maintain humidity while the siliques developed. After approximately 10 days, the siliques became yellow as seed matured and were harvested into 1.5 mL microfuge tubes and were incubated at 37 °C for 1 week uncapped to allow seeds to dry and release from siliques. Harvested seeds were stored at 4 °C and protected from light for minimum of 2 weeks to allow seeds to stratify.

2.3.6. Transformation of Arabidopsis with binary vectors

2.3.6.1. Preparation of *A. tumefaciens* culture for transformation

4 mL of a small *A. tumefaciens* AGL-1 culture (section 2.2.16) transformed and confirmed positive for the presence of a selected expression vector via colony PCR (section 2.2.2) was used to inoculate 250 ml LB media with appropriate antibiotics (50 µg/mL Rifampicin, 50 µg/mL Carbenicillin plus expression vector selection, generally 50 µg/mL of Kanamycin) and incubated in an orbital mixer incubator (Ratek Instruments

Pty. Ltd., Boronia, Victoria, Australia) at 28 °C with agitation at 200 rpm overnight or until cloudy (OD600 approximately 0.8). Cultures were transfer to 50 mL screw capped tubes (SARSTEDT Australia Pty. Ltd., Ingle Farm, SA, Australia. Cat. No. 62.547.254) and centrifuged at 3000 *g* for 15 minutes at 4 °C. Supernatant was poured off and cells resuspended in 50 mL of 5 % w/v sucrose in Milli-Q H_2O with the use of pipette. 0.01% (25 µL) of Silwet L-77 (Lehle Seeds, Round Rock, TX, USA, Cat. No: Vac-In-Stuff® VIS-01) was added to each 50 mL culture and stored at 4 °C before use.

2.3.6.2. Transformation of Arabidopsis by floral dipping and/or floral spraying

For Arabidopsis transformation the floral dip method (similar to Clough & Bent, 1998) was used. Arabidopsis plants were grown on soil as per 2.3.4, under short day light conditions for approximately 4 weeks or until on onset of flowering. The initial inflorescence stem was cut to promote development of secondary inflorescences and after 2 days, when secondary inflorescences start to show floret opening, plants were ready for transformation. Several different techniques for applying the agrobacterium solution, prepared in section 2.3.6.1, to the florets were trialled to increase transformation efficiency. For most transformations, plants were inverted and dipped into trays containing the *Agrobacterium* solution and swirled for 30 seconds to allow the Agrobacterium to enter the floret or with the use of a small spray bottle to mist the opening florets until wet. Where multiple transformation events per plant were required, droplets of *Agrobacteria* solution was applied to individual florets with either a 200 µL pipette or with the use of a small paintbrush. Plants were then protected from light and covered with a plastic mini-glasshouse to maintain humidity and allowed to rest overnight. Plants were returned to normal growing conditions the next morning and grown onto maturity and seeds harvested.

2.3.7. Selection of Arabidopsis transformants on selective media

Arabidopsis primary (T_1) and later generation transformants were identified by selection on media containing antibiotics (Hygromycin B or Kanamycin) or the herbicide, Glufosinate ammonium (BASTA), depending on which resistance genes were present in the transformed constructs, as outlined in Weigel and Glazebrook (2002).

Several different selection mediums were trialled during the course of this project. All selective media contained 0.5 × MS Murashige and Skoog Basal Salt Mixture. 0.5 % w/v

sucrose was required to be added to promote the germination of the Arabidopsis C24 ecotype lines. Initial transformation selection was conducted using 0.3 % w/v Phytagel® gelling agent (Sigma-Aldrich Co. Llc., Castle Hill, NSW, Australia. Cat. No. P8169) or 0.9 % w/v Difco™ granulated Agar (DB Co. Australia, North Ryde, NSW, Australia. Cat. No: 214530) as solidifying agents. However, the Australian Department of Agriculture & Biosecurity (AQIS) imposed post-import restriction on these gelling agents for in planta use (AQIS, 2012) which limited the use of these media for Arabidopsis selection. 0.3 % w/v Gelrite® gellum gum gelling agent was used as a compromise with limited success.

For constructs conferring Kanamycin resistance (*nptI* or *nptII*) (see Appendix II: Vectors Maps) selection media was supplemented with 50 $mg.mL^{-1}$ Kanamycin (Appendix IV: Antibiotics and selective agents). For constructs conferring Hygromycin B resistance (hpt) selection media was supplemented with 40 $mg.mL^{-1}$ Hygromycin B. For constructs conferring BASTA resistance (*bar* or *pat*), selection media was supplemented with 12 mg.mL-1 Glufosinate ammonium (Sigma-Aldrich Co. Llc., Castle Hill, NSW, Australia. Cat. No. G4670). For selective media for selection of T_1 seed, 100 $mg.mL^{-1}$ Cefotaxime was added to inhibit growth of *Agrobacterium* potentially surviving following transformation (section 2.3.6.2).

Seeds for selection were surface sterilised as per section 2.3.2, and sown onto low profile Square Bio-assay Dishes (Corning Inc., Corning, NY, USA. Cat. No: 431301) containing 150 mL of appropriate selective media and sealed with 3M™ micropore™ microporus surgical tape (3M Australia, North Ryde, NSW, Australia). Plates were incubated at 4°C for two days before transfer to the short day growth chamber (section 2.3.1). Plants grown for 2 – 3 weeks and growth observed. Excess moisture was removed by opening the plates in a sterile laminar flow station poured off or aspirated by pipet. Plants susceptible to Kanamycin or Glufosinate ammonium, either failed to germinate or became chlorotic within ≈1 week of germination (Weigel & Glazebrook, 2002) .

Hygromycin B resistant plants were more difficult to identify as this antibiotic only slows growth and untransformed plants remain green (Harrison *et al.*, 2006). Successfully transformed individuals were larger and had increased root growth compared to untransformed plants.

Additional genotyping was conducted to confirm transformants by extracting gDNA from leaf tissue of possible transformants per section 2.2.20 and performing genotyping PCR as per 2.2.2 with construct specific primers.

Several other selection techniques were trial such as selection on sand (Davis *et al.*, 2009) and selection in liquid culture (Nichols *et al.*, 1997) and are discussed in Chapter 5.

2.3.8. Arabidopsis growth in mini-hydroponics

Selected Arabidopsis lines were grown in mini-hydroponics similar to as described in Conn *et al.* (2013) and Shearer (2013) .

All hydroponic equipment was sterilised by washing with RO water and Domestos bleach (JohnsonDiversey Pty. Ltd., Australia) followed by exposure to UV light inside a laminar flow for 15 minutes to reduce the build-up of algal growth. Approximately, 0.04 g (60 µL) of dried seeds were imbibed in cooled autoclaved sterile 0.1 % w/v Agarose in Milli-Q H_2O overnight at 4 °C. The lids of 1.5 mL microcentrifuge tubes (Astral Scientific Pty. Ltd, Gymea, NSW, Australia. Cat. No: B74010) were removed and a 4 mm hole was made into the centre of the lid. The lids were then placed upside down and were filled 150 µL of liquid autoclaved 1/2 x MS + 0.9% (w/v) M-type Agar (pH 5.6 with KOH) and allowed to set, forming an agarose plug. Lids were then placed plug-side-down into a germination tray, capable of supporting ≈ 400 seedlings (Figure 2.2, a), and filled with 2 L of 0.25× MS solution (pH 5.6 with KOH) so that the agarose plugs were in contact with the nutrient solution. Individual seeds were then pipetted onto the exposed agar on the top of microfuge tube lids with a 2 µL pipette. Trays were transferred to PC2 growth chambers and grown under short day growth conditions outlined in section 2.3.1 and covered with cling film (Clorox Australia Pty Ltd, Unley, SA, Australia) at a height of 5 cm to maintain humidity to assist germination and to prevent contamination of the agar plugs.

Germination of seed took approximately 5 days and after nutrient solution was changed every 7 days. Cling film was removed after 2 weeks growth and poor growing plants were removed and remaining plants positioned so all had equal access to light and that the base of the agar plugs were kept in contact with nutrient solution. Plants were ready for transfer to mini-hydroponics tanks after approximately 20 days growth or when at stage 1.05, with 5 rosette leaves are greater than 1 mm in length (as outlined in https://www.arabidopsis.org/portals/education/growth.jsp) (Figure 2.2, b, c).

For each mini-hydroponic, three independent mini-hydroponic systems were used to screen Arabidopsis under different salinity treatments. Each mini-hydroponic system consisted of a 12 L tub (40 × 10 × 13 cm) capable of supporting 48 Arabidopsis plants until rosette growth is completed (Figure 2.2, d,e). Small 3W 160L/hr aquarium air pumps (Aqua One® Kong's (Aust) Pty. Ltd., Ingleburn NSW, Australia, Model No. Precision 2500 Air Pump) were used to aerate the hydroponics solution constantly through two stone bubblers located at each end of the tubs. The tubs were filled with 10 L of Arabidopsis basal nutrient solution. pH was adjusted to 5.9 with 1 M KOH. Hydroponics solutions were changed weekly. Plants were exposed to under three different salinity treatments (+0 mM, +50 mM or +100 mM additional NaCl) for 7 days prior to harvest (Figure 2.2, e,f)

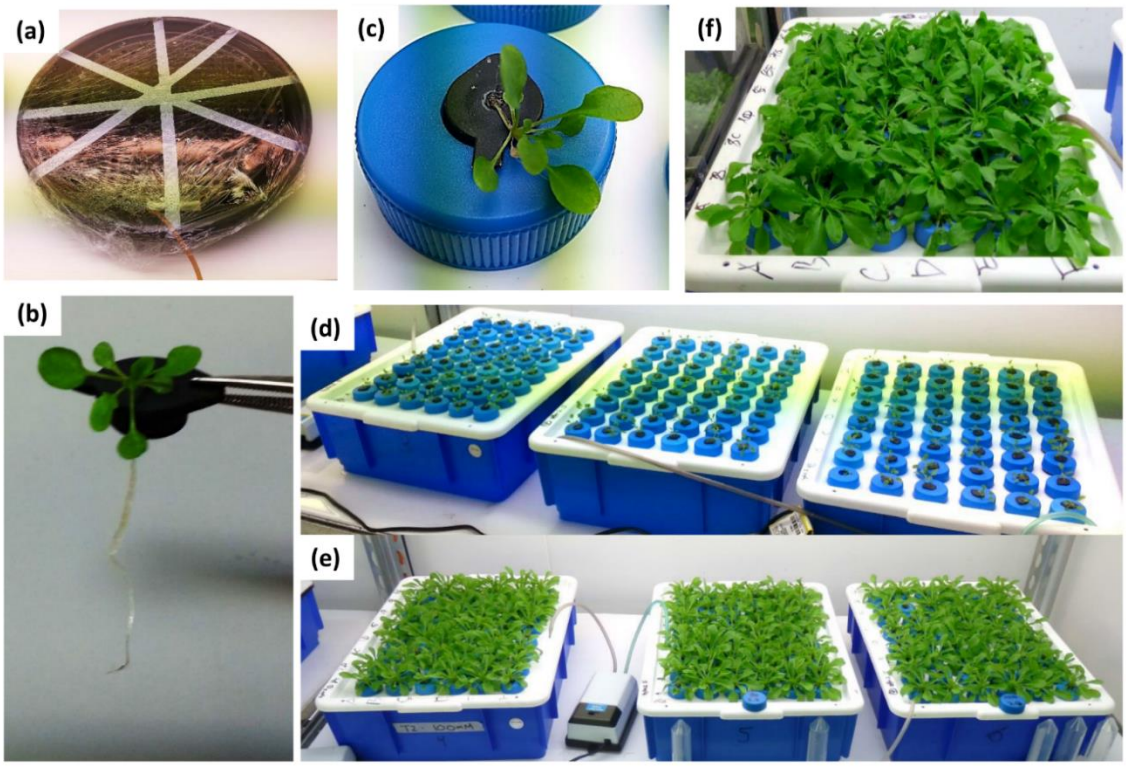

Figure 2.2: Overview of the Arabidopsis mini-hydroponics setup used for salinity (NaCl) tolerance exeperiments
Arabidopsis seeds sown on agar containing plugs and grown in germination tray for two weeks (a), until reaching appropriate size (b) for transfer to hydroponics setup (c & d). Plants grown and exposed to three different NaCl concentrations (+0 mM, +50 mM or +100 mM additional NaCl) for one week, prior to harvest (f).

2.4. *Hordeum vulgare* (barley) experiments

2.4.1. Barley growth in glasshouse conditions.

All barley growth experiments for crossing and hydroponics were conducted at the University of Adelaide, Waite Campus, Urrbrae, ACPFG PC2 glasshouse facility. Day/Night temperature was maintained at approximately 22/18 °C respectively by evaporative air-conditioning with a relative humidity of between 30 - 50 %. Plants were exposed to natural long day (13/11 hrs day/night) lighting conditions or supplemented with artificial lighting to maintain 13/11 hrs light/dark lighting conditions where specified.

2.4.2. Germination and growth of barley cv. Golden Promise

2.4.2.1. Surface sterilisation of barley seeds UV light.

To reduce fungal growth during germination, barley seeds were surface sterilised by exposure to ultraviolet (UV) light for 5 minutes inside a laminar flow workstation (Gelman Sciences Pty. Ltd, Cheltenham, VIC, Australia). Seeds were turned after 2 ½ minutes with forceps to ensure even sterilisation. Seeds were then placed on autoclaved paper towelling (Scott® Brand, Kimberly-Clark Professional Inc., Milsons Point, NSW, Australia, Cat. No. 01980) cut to fit inside sterile 145 × 20 mm diameter Petri-dishes (Interpath Services Pty. Ltd., Heidelberg West, VIC, Australia, Cat. No. 639161) and moisten with 12 mL of autoclaved Milli-Q H_2O. Petri-dishes were then sealed inside polyethylene autoclave bags and wrapped in aluminium foil to protect from light. Seeds there then incubated at 4°C for 2 days to ensure even germination.

2.4.2.2. Surface sterilisation of barley seeds using bleach

More stringent sterilisation for barley seeds was required for both β-glucuronidase (GUS) and Green Florescent protein (GFP) assay experiments, as fungal contamination of plants on germination plates and seedlings interferes with visualisation. Sterilisation of seeds was conducted in 50 mL screw cap tubes, by first washing for 3 minutes with 70 % v/v Ethanol followed by incubation in 30 % v/v Domestos (Unilever Australia, Ltd., Sydney, NSW, Australia) with gentle rocking on a platform rocker (Bioline Pty. Ltd., Alexandria, NSW, Australia. Model No. BIO-8040) for 10 minutes. Seeds were rinsed with autoclaved Milli-Q H_2O five times to remove excess traces of bleach and placed onto autoclaved paper towelling pre-moistened with Milli-Q H_2O in Petri dishes as described in section 2.4.2.1.

2.4.2.3. Germination of barley seedlings

Following 2 days imbibing at 4°C in the dark, the aluminium foil was removed and seeds in Petri dishes and sealed in polyethylene bags were exposed to light and allowed to germinate. This was done on the lab beach at approximately 22°C under a combination of fluorescent lighting and natural light. Where seed quality was an issue, seeds that had failed to swell after imbibing were removed with forceps in a laminar flow and disposed of as per PC2 regulations.

After approximately 2 days, germinating seedlings were transported to the ACPFG PC2 glasshouse described in section 2.4.1 and incubated at approximately 28°C day/18°C night under natural daylight conditions for approximately 2 days until they reached a suitable size (coleoptiles 5-10 mm in length), for use in hydroponics (sections 2.4.3 and 2.4.4) or for transplantation into soil (section 2.4.2.4).

2.4.2.4. Barley growth in soil and seed production

Individual seedlings were transplanted directly into free-draining pots (0.55 L volume, Masrac Pty. Ltd., Dry Creek, SA, Australia, Cat. No: MK1 punnet pot) filled with modified University of California (UC) mixture (Nauer *et al.*, 1967). Soil was prepared and supplied by SARDI (Waite Campus, Urrbrae, Australia) and was composed ⅔ (v/v) coco-peat and ⅓ (v/v) sand with the addition of: 75 g dolomite lime, 250 g agricultural lime, 100 g hydrated lime, 75 g gypsum, 75 g superphosphate, 187.5 g iron sulphate, 12.5 g iron chelate, 187.5 g Calcium nitrate, 75 g Micromax® micro-nutrient fertiliser (Scotts Australia Pty. Ltd., Bella Vista, NSW, Australia) and 200 g Osmocote Plus® slow-release fertiliser (Scotts Australia Pty. Ltd., Bella Vista, NSW, Australia) per 100 L of soil mix. Final pH of the soil mix was between 6 – 6.5. Plants were grown in greenhouse conditions (as per section 2.4.1) and watered with RO water until seed set (≈ 3 months). Mature seed was harvested from mature plants following ≈ 1 month drying in the greenhouse and hand-threshed before use.

2.4.3. Mini-hydroponics for salt stress treatments

For short-term (< 30 days) salinity tolerance screens, a mini-hydroponics setup as describe below was used.

2.4.3.1. Setup of mini-hydroponics system

Transgenic barley plants were grown in a mini-hydroponics system similar to that described in Shavrukov *et al.* (2012). All hydroponic equipment was sterilised by

washing with RO water and Domestos bleach (JohnsonDiversey Pty. Ltd., Australia) followed by exposure to UV light inside a laminar flow for 15 minutes to reduce the build-up of algal growth.

For each mini-hydroponic experiment, four independent mini-hydroponic systems (2 tanks per treatment) were used. Each mini-hydroponic system consisted of a 12 L (40 cm length × 10 cm depth × 13 cm width) tub capable of supporting 48 barley seeding up until the 5th leaf stage, approximately 30 days post germination (Figure 2.3, a). Small 3W 160L/hr aquarium air pumps (Aqua One® Kong's (Aust) Pty. Ltd., Ingleburn NSW, Australia, Model No. Precision 2500 Air Pump) were used to aerate the hydroponics solution constantly through two stone bubblers located at each end of the tanks. The tanks were filled with 5 L of RO H_2O before addition of 50 mL of each macro-nutrient, and 10 mL of micro-nutrient stock solutions in order. A precipitate forms by mixing undiluted stock solutions, particularly between (macro-nutrient #5) $Na_2Si_3O_7$ and (micro-nutrient #1) NaFe(III)EDTA, so the measuring cylinder was rinsed with RO water between each stock solution to prevent this. The total volume was then brought up to 10 L with additional RO H_2O, stirred and then pH was adjusted to 6.5 with the addition of 3.2 % v/v HCl. Plants in pilot hydroponics experiments suffered from visible boron toxicity due to high boron levels in the RO water supply used. To compensate, no additional H_3BO_3 was added to micronutrient stocks for all experiments in this project.

2.4.3.2. Germination and transfer of barley seedlings into mini-hydroponics systems

Barley seeds of selected lines were surface sterilised using UV and germinated as described in (section 2.4.2.1). Four-day old seedlings (2 days at dark/4°C and 4 days at natural-light/21°C) of each line examined were divided equally between each of the hydroponic tanks. Shoots of germinating seedlings were approximately 1 cm long and seminal roots were approximately 2 cm long. Larger seedlings are prone to root damage if transferred when too large. Selected seedlings then were transferred with forceps into 1.5mL microfuge tubes which had that bottom 5 mm cut off so the roots could be in contact with the hydroponic nutrient solution (Figure 2.3, b). Plants were inspected daily throughout the experiment to maintain hydroponic solution levels and pH at 6.5.

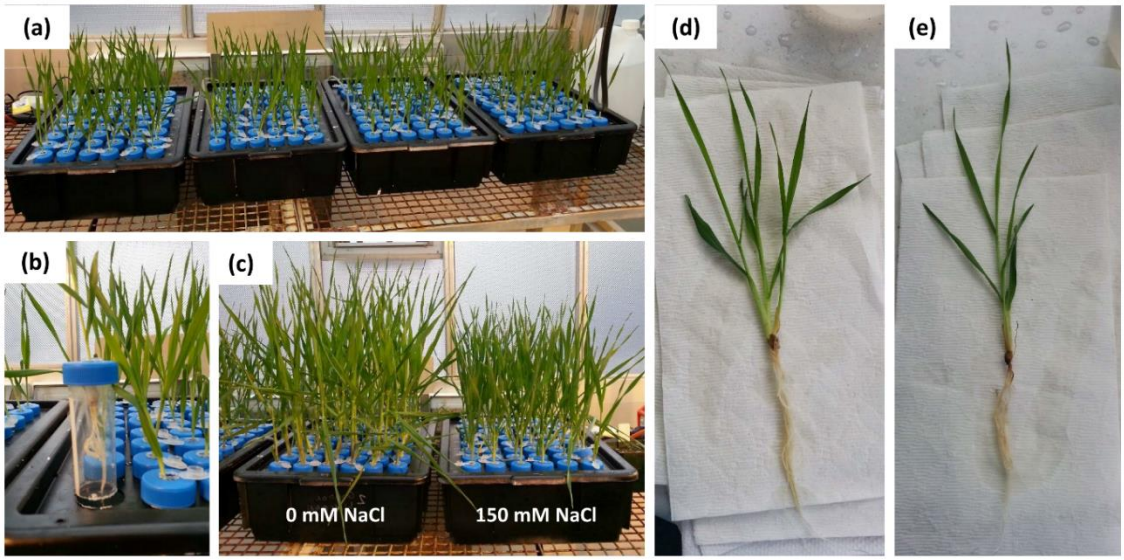

Figure 2.3: Overview of Barley cv. Golden Promise growth and salinity screening in mini-hydroponics
Overall hydroponic setup (a). Barley seedlings germinated and placed into 1.5 mL microcentrifuge (b) and exposed to differing NaCl concentrations (c). Representative difference in plant grown observed after 10 days post reaching final salt concentration (c). Individual plants under control - 0mM, (d) and salt stressed - 150 mM, (e) conditions.

2.4.3.3. Salt stress treatment in mini-hydroponics system

At 10 days post transfer (16 days after germination, approximately 3rd leaf stage) the nutrient solution for all tanks were changed and pH adjusted to 6.5 by the addition of 1 M HCl acid.

For tanks selected for salt treatment every 12 hours (at 6:00 am and 6:00 pm) over the course of 3 days, an additional 25 mM of NaCl (supplemented with 0.35 mM $CaCl_2$ to maintain Ca^{2+} activity) was added to reach a final NaCl concentration of 150 mM (first mini hydroponics experiment) or 200 mM (second mini hydroponic experiment and supported hydroponics experiment). Both control and salt treated barley plants were grown for a further 10 days. (Figure 2.3, b)

2.4.3.4. Tissue collection following salt stress treatment in mini-hydroponics

At 10 days post treatment (29 days after germination) barley plants were removed from the mini-hydroponic tanks. The roots were quickly rinsed in a 10 mM $CaCl_2$ solution to remove excess NaCl from the hydroponic growth solution and patted dry with paper towel. Latex examination gloves were worn to reduce contamination and washed with 70 % ethanol between samples. The seedling fresh weight (g) was measured for both control and salt treated plants to determine the reduced growth due to salt application.

For destructive analysis, both control and salt treated plants were cut at the crown (junction between root and shoot) and additional measurements were made for the fresh root weight (g) and the fresh shoot weight (g). In the preliminary mini-hydroponic experiment, control plants were left intact for transplantation into soil (see section 2.4.2.4) to obtain seed for additional rounds of hydroponics.

Five tissue samples were harvested from both control and salt treated plants; (1) the 4th leaf which expanded under salt stress for leaf ion content, two sections of the youngest emerged leaf for (2) genotyping and (3) RNA extraction, root tissue for (4) ion content and root tissue for (5) RNA extraction.

Samples designated for ion content measurements (1 and 4) were placed into sterile 50 mL screw capped tubes (SARSTEDT Australia Pty. Ltd., Ingle Farm, SA, Australia. Cat. No. 62.547.254) prior to drying and flame photometry and chloride analysis (section 2.4.4.1).

Samples designated for RNA (3 and 5) extraction were placed into pre-cooled sterile 10 mL screw capped tubes (SARSTEDT Pty. Ltd., Mawson Lakes, SA, Australia. Cat. No. 62.9924.284) and snap frozen in liquid nitrogen and stored at -80°C prior to grinding and RNA extraction.

Samples designated for DNA extraction (2) were placed directly into pre-cooled 1.1 mL micro tubes (ADELAB Scientific Pty. Ltd., Thebarton, SA, Australia, Cat. No. N946-08B) on ice prior to DNA extraction by Freeze-dry method (section 2.2.19). For small scale experiments, leaf samples were place into 2 mL microfuge tubes and snap frozen in liquid nitrogen and stored at -80 °C prior to extraction using the Edwards extraction Method (section 2.2.20).

2.4.3.5. Plant fresh and dry weight measurements

Fresh weights of all root and leaf tissue harvested for flame photometry, chloride analysis, DNA and RNA extractions were measured using a semi-micro balance (Shimadzu Corporation, Rydalmere, NSW, Australia, Model No. UniBloc® AUW220D). Shoot dry weight was determined followed drying of sectioned shoot material in paper bags incubated at 65°C for 7 days in a drying oven (Contherm Scientific Pty. Ltd., Petone, New Zealand, Model No: Contherm® 8150). Dry weights of both root and 4th leaf samples taken for ion content were measured following incubation at 65 °C for 2 day.

2.4.4. Supported Hydroponics for Barley growth and salinity screening.

For long-term (> 30 days until flowering) salt stress treatment experiments, a 80 L flood-drain hydroponics system was used (similar to Shavrukov *et al.*, 2012).

2.4.4.1. Setup of Supported hydroponics system

For each supported hydroponic experiment, 2 independent hydroponic systems were used (one per treatment) were used. Each supported-hydroponic system consisted of a trolley supporting two 20 L tubs (Figure 2.4, a) capable of supporting 42 barley seedlings up until tillering, approximately 45 days post germination. Plants were grown in separate PVC tubes (280 mm long × 45 mm in diameter) containing 3 mm black polycarbonate plastic beads (Plastics Granulating Services, Adelaide, SA, Australia) to provide support (Figure 2.4 b, c). 110 L tanks mounted below the growing tubs were filled with 80 L of RO H_2O with the use of a flow meter (Timec Pty. Lty., Taren Point NSW, Australia. Model No: Trimec RT12 Rate Totaliser) and made up to standard ACPFG nutrient solution (Appendix IV: Barley hydroponics growth solutions). Nutrient solution pH was adjusted to 6.5 - 7 with 3.2 % v/v HCl. Submersion pumps (flowrate = 160 L/hr) in the tanks circulated the nutrient solution into the growing tubs above on a 30 minute flood-drain cycle. Overflow from the growing tubs was recirculated back into the tanks underneath to complete the cycle.

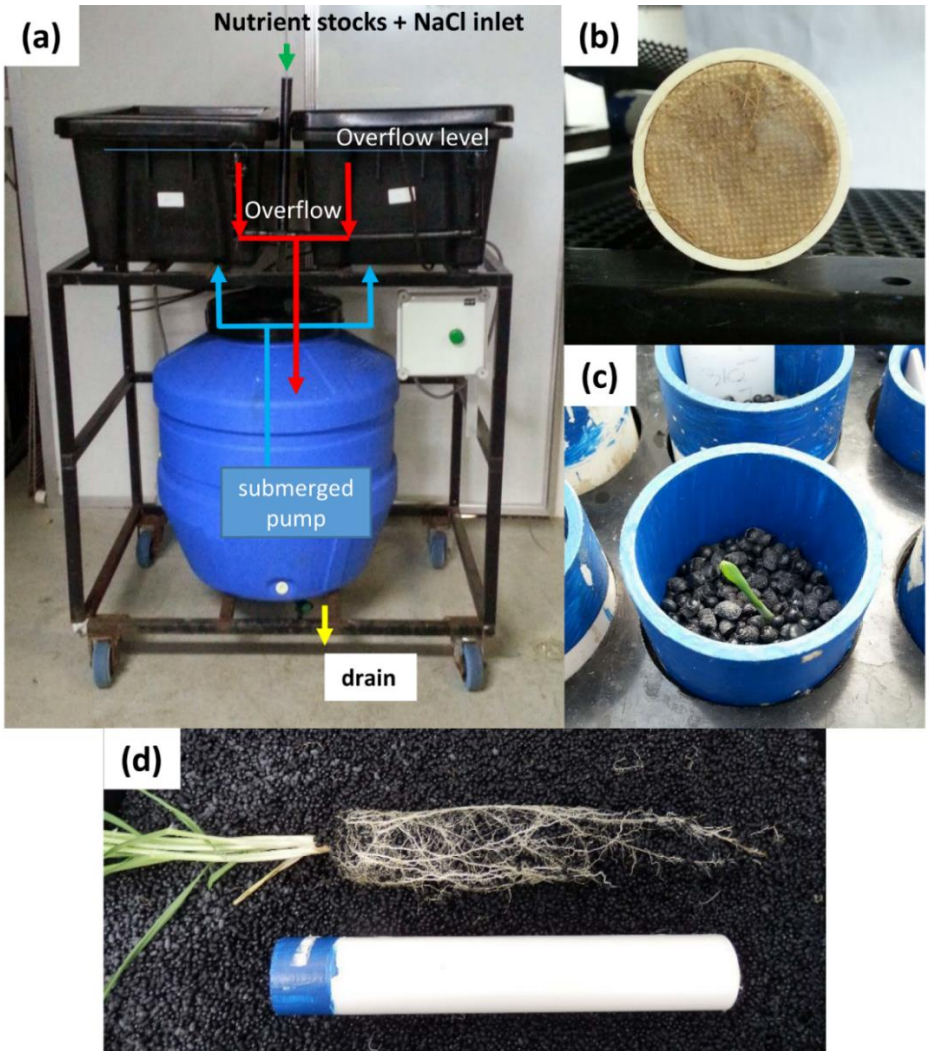

Figure 2.4: Diagram of supported hydroponics used for salinity screening of barley transgenics

Overview (a) of the supported hydroponics setup developed at the ACPFG. PVC tubing with mesh base (b) holding polycarbonate plastic beads provide support for germinated barley seedlings (c) during the hydroponics experiment. Representative root growth at the conclusion of 45 days in hydroponics under control conditions (d).

2.4.4.1. Germination and transfer of barley seedlings into supported hydroponics system

Barley seeds of selected lines were surface sterilised using UV and germinated as described in (section 2.4.2.1). 5-day old seedlings (2 days at dark/4°C and 5 days at natural-light/21°C) of each line were divided equally between each of the hydroponic set-up. Shoots of germinating seedlings were approximately 5 cm long and seminal roots were approximately 3 cm long before transplantation into the supported hydroponics system. Seedlings from each line were assigned a location randomly and were placed into separate PVC tubes partially filled with polycarbonate beads (Figure 2.4 c, Figure 2.5, a). Additional polycarbonate beads were added to provide support and to maintain the position of the seedling so that the roots were in contact with the nutrient solution, while the crown remained above the level of the nutrient solution when the tanks were at maximum capacity.

2.4.4.2. Salt stress treatment in supported hydroponics system

At emergence of the 3rd leaf on the majority of transgenic plants, approximately 10 days after transfer to the hydroponics setup, the nutrient solution of both trolleys were changed and pH maintained at 6.5 – 7 with 3.2 % v/v HCl. Salt stress was applied at the emergence of the 3rd leaf through increments of 25 mM NaCl plus 0.35 mM of $CaCl_2$ (in the form of $CaCl_2.2H_2O$), every 12 hours until the final concentration of 200 mM was reached (Figure 2.5, b).

2.4.4.3. Tissue collection following salt stress treatment in supported hydroponics

At 21 days post treatment (approx.45 after germination) (Figure 2.5, c) barley plants were removed from the hydroponic tanks. The roots were quickly rinsed in a 10 mM $CaCl_2$ solution to remove excess NaCl from the hydroponic growth solution and patted dry with paper towel. Latex examination gloves were worn to reduce contamination and washed with 70 % ethanol between samples. The plant fresh weight (g) was measured for both control and salt treated plants to determine the reduced growth due to salt application. For destructive analysis, both control and salt treated plants were cut at the crown (junction between root and shoot) and additional measurements were made for the fresh root weight (g) and the fresh shoot weight (g) as per section 2.4.3.5. Five tissue samples were harvested from both control and salt treated plants; (1) the 4th leaf which expanded under salt stress for leaf ion content, two sections of the youngest emerged leaf for (2)

genotyping and (3) RNA extraction, root tissue for (4) ion content and root tissue for (5) RNA extraction. Samples designated for ion content measurements (1 and 4) were placed into sterile 50 mL screw capped tubes (SARSTEDT Australia Pty. Ltd., Ingle Farm, SA, Australia. Cat. No. 62.547.254) prior to drying and flame photometry and chloride analysis (section 2.4.4.1). Samples designated for RNA (3 and 5) extraction were placed into pre-cooled sterile 10 mL screw capped tubes (SARSTEDT Pty. Ltd., Mawson Lakes, SA, Australia. Cat. No. 62.9924.284) and snap frozen in liquid nitrogen and stored at -80°C prior to grinding and RNA extraction. Samples designated for DNA extraction (2) were placed directly into pre-cooled 1.1 mL micro tubes (ADELAB Scientific Pty. Ltd., Thebarton, SA, Australia, Cat. No. N946-08B) on ice prior to DNA extraction by Freeze-dry method (section 2.2.19).

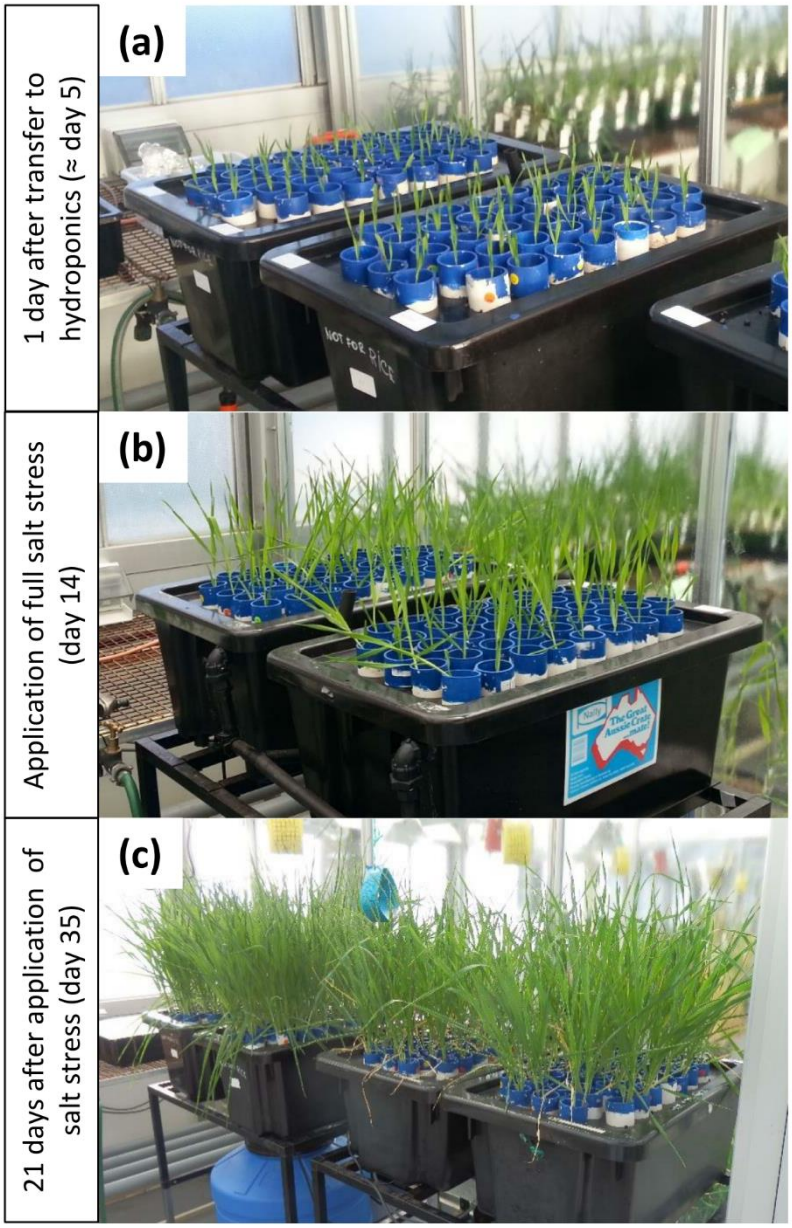

Figure 2.5: Representative images of barley plant growth in the supported hydroponics setup used for salinity screening.
Plant size one day after transfer to hydroponics (approximately 5 day old seedlings) (a); at application of full salt stress (day 14) (b) and after three weeks growth under control (left) or salt (200 mM NaCl) stress (right), prior to harvest (c)

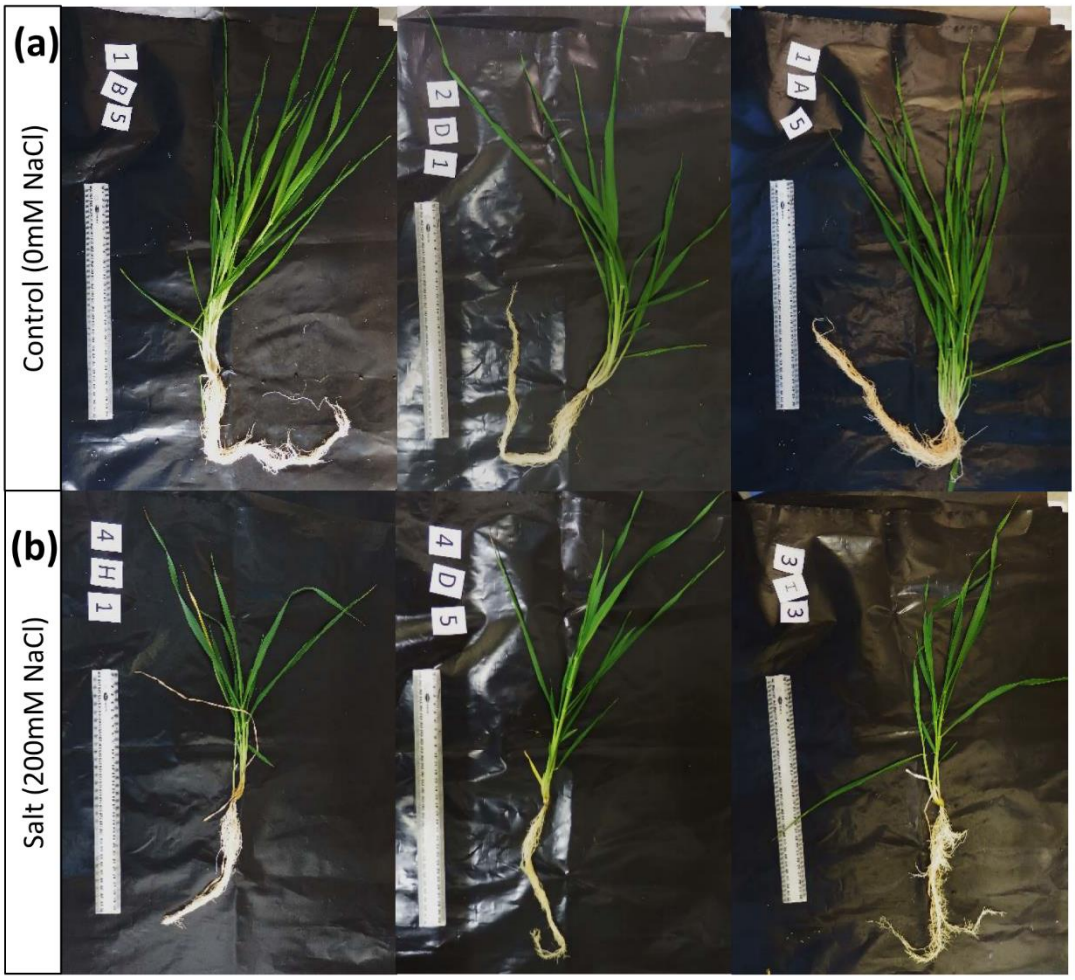

Figure 2.6: Plant biomass after 35 days in supported hydroponics under control and salinity stress conditions
Representative images of approx. 40 day old plants grown in supported hydroponics and treated with 0 mM or 200 mM NaCl for 21 days post 3rd leaf emergence. Reduction in overall plant biomass and tillering can be observed between the two treatments.

2.5. Determination of tissue Na^+, K^+ and Cl^- concentration

Both Na^+ and K^+ tissue concentrations were measured through the use of Flame photometry. Cl^- tissue concentration was measured via a digital Chloride analyser, based on silver nitrate titration method and the formation of insoluble silver chloride salt. Prior to measurement, samples were treated with a hot nitric acid (HNO_3) digest detailed below, with modification to allow for different tissue types and weights.

2.5.1. Arabidopsis tissue digest

Following harvest of root and leaf tissue from Arabidopsis mini-hydroponics experiments. Root samples were placed into uncapped 10 mL tubes (Brand information) and leaf samples were placed into uncapped 2 mL microfuge tubes (Brand information) and dried at 65 °C for 2 days in a drying oven (Contherm Scientific Pty. Ltd., Petone,

New Zealand, Model No: Contherm 8150). Dry weights were measured on a semi-micro balance (Shimadzu Corporation, Rydalmere, NSW, Australia, Model No: UniBloc® AUW220D) and recorded.

For digestion, 2 mL of 1 %v/v Nitric acid (HNO_3 in Milli-Q H_2O) was added to each sample root and leaf sample and tubes were capped and shaken to ensure all material was submerged. Samples were incubated at 65 °C (Contherm Scientific Pty. Ltd., Petone, New Zealand, Model No: Contherm 8150 drying oven) with intermittent inverting every 30 minutes for 4 hours before being left at 65 °C over-night.

2.5.2. Barley tissue digest

Following harvest of root and 4th leaf tissue from the mini- and supported hydroponics experiments fresh weight of both root and leaf tissue was measured using semi-micro balance (Shimadzu Corporation, Rydalmere, NSW, Australia, UniBloc® AUW220D) and recorded. Samples were placed in uncapped 50 mL screw cap tubes (SARSTEDT Australia Pty. Ltd., Ingle Farm, SA, Australia. Cat. No. 62.547.254) and dried at 65 °C for 4 days in a drying oven (Contherm Scientific Pty. Ltd., Petone, New Zealand, Model No: Contherm 8150). Dry weights were measured on the same semi-micro balance and recorded.

Dried leaf and root samples were digested in 10 mL of 1 %v/v Nitric acid (HNO_3 in Milli-Q H_2O) for 4 hours at 85 °C using a heating block (Environmental Express Inc., Charleston, SC, USA, Model No: HotBlock™ SC100-240,) with shaking every hour to ensure all material was submerged. Tube caps were kept loose to prevent pressure build up.

2.5.3. Flame Photometry to measure Na^+ and K^+

Sodium [Na^+] and potassium [K^+] concentrations in the roots and 4th leaf samples were measured using a Flame Photometer (Sherwood® Flame Photometer 420, Sherwood Scientific Ltd., Cambridge, UK). In brief, 200 µl of nitric acid digested samples was diluted into 1800 µl of Milli-Q H_2O before analysis. 3 technical replicates for each digested sample were measured on the flame photometer and final values used for calculating [Na^+] and [K^+] was based on the mean of the technical repeats. Different concentrations of the Na^+ and K^+ standards and sample dilutions were used to ensure the photometer readings were within the photometer limits for plants from different treatments. The concentration of Na^+ or K^+ per gram dry weight of tissue (µmoles.g^{-1}

DW) or in tissue water (mM) can then be calculated with Equation 1 and Equation 2 below respectively.

2.5.3.1. Sodium [Na^+] and Potassium [K^+] concentration calculations:

Equation 1 – Calculations of [Na^+] per gram of dry material (mol.g^{-1})

$$\left[Na^+\right] \text{ mol.g}^{-1} \text{ Dry Weight} = \frac{Na^+\text{reading}_{\text{flame photometer (units)}} . \text{coefficient}}{\text{Sample Dry Weight (g)}}$$

Equation 2 – Calculation of [Na^+] per L of tissue water (mol.mL^{-1})

$$[Na^+] \text{ Fresh Weight } (\text{mol. mL}^{-1}) = \frac{Na^+\text{reading}_{\text{flame photometer (units)}} . \text{standard coefficent}}{(\text{Sample Fresh Weight (g)} - \text{Sample Dry Weight (g)})}$$

Where:

$$\text{Dilution Factor} = \frac{V_{\text{total dilution volume (µL)}}}{V_{\text{sample volume (µL)}}}$$

$$\text{standard coefficient} = \frac{[Na^+\text{standard}] \text{ (M)}}{100} . \text{Dilution Factor. Sample Digest Volume (L)}$$

* [K^+] concentrations can be similarly worked out by substituting the photometer Na^+ reading (for photometer K^+ reading) and in both equations and substituting the [Na^+ standard] (for [K^+ standard]) in the coefficient.

2.5.4. Chloride analysis to measure tissue [Cl^-]

Chloride concentrations in the roots and leaf samples of barley and Arabidopsis plants were measured using a Chloride Analyser (Sherwood® Chloride Analyser 926, Sherwood Scientific Ltd., Cambridge, UK). In brief, 1000 µl of nitric acid digested samples was added to the combined acid buffer (Appendix IV: Chloride analysis solutions) and then titrated to estimate Cl^- concentration. As the chloride analyser assumes a sample size of 100 µL and the digested samples are relatively dilute a dilution factor calculation is required. The concentration of Cl^- per gram dry weight of tissue (µmol.g^{-1}) or in tissue water (mM) can then be calculated with Equation 3 and Equation 4 below respectively.

2.5.4.1. Chloride [Cl^-] concentration calculations:

Equation 3 – Calculations of [Cl^-] per gram of dry material (mmol.g^{-1})

$$[Cl^-]\ \text{mmol.}\ g^{-1}\text{Dry Weight} = \frac{(\text{Reading}_{\text{Cloride Meter}}.\ \text{Dilution Factor})}{\text{Sample Dry Weight (g)}}$$

Equation 4 – Calculation of [Cl^-] per L of tissue water (mM)

$$[\mathbf{Cl^-}]\ \mathbf{Fresh\ Weight\ (mM)} = \frac{(\mathbf{Reading_{Cloride\ Meter}}.\ \mathbf{Dilution\ Factor})}{(\mathbf{Sample\ Fresh\ Weight\ (g) - Sample\ Dry\ Weight\ (g)})}$$

Where:

$$\text{Dilution Factor}^* = \frac{100}{V_{\text{volume of digest added for measurement (µL)}}}.\ V_{\text{total sample digest volume (L)}}$$

* The chloride meter reading (in mmol/L) is based on an assumed sample volume of 100 µL. We routinely use 1 mL for accurate measurements in the plant tissues sampled. This dilution factor is required to normalise readings with the volume used for measurement.

2.6. Epifluorescence stereo and confocal microscopy for imaging plant tissues

A range of microscopic techniques and devices were used for imaging and screening of plant material during the course of this project. Barley sectioned root and shoot material was screened for GUS staining or presence of mGFP5/6 under an epifluorescence-capable stereomicroscope (Leica Microsystems GmbH, Wetzlar, Germany. Model No: MZFLIII). mGFP5/6 (excitation max: 489 nm, emission max: 509 nm) was visualised using a GFP2 filter (480/40 nm barrier filter, 510 nm long pass filter). Plant material was either imaged directly, or suspended in Milli-Q H_2O. Digital images were captured with attached digital camera (Leica Microsystems GmbH, Heerbrugg, Switzerland, Model No: Leica DC300F digital camera) and processed with IM50 software package (Leica Microsystems GmbH, Wetzlar, Germany, version 1.2). Images displayed are representative of at least three biological replicates, unless otherwise stated.

Arabidopsis root and shoot material examined for GUS staining and mGFP(5 or 6)-ER expression patterns was imaged similarly. For plants grown in mini-hydroponics or GUS stained samples, plants were suspended in Milli-Q H_2O prior for imaging. For plants grown on vertical 0.5× MS Agar plates, plants were imaged directly on the growing media. GFP2 filter was again used for mGFP5/6 visualisation and all images captured. H2B::CFP (Excitation max: 434 nm, Emission max: 477 nm) could also be detected

faintly using the long pass GFP2 filter, no suitable CFP filter was available. Images displayed are representative of at least three biological replicates, unless otherwise stated.

Confocal laser scanning microscopy was used for fine examination of Arabidopsis roots, grown either hydroponically or on vertical 0.5 × MS Agar plates. To visualise cell walls, whole plants or root material was submerged in 10 µg/ml propidium iodide (Sigma-Aldrich Pty. Ltd., Sydney, NSW, Australia, Cat. No: 287075) in Milli-Q H_2O for 10 minutes. Excess propidium iodide was then removed by placing samples in Milli-Q H_2O for an additional 10 minutes before mounting onto glass slides in Milli-Q H_2O. Samples were then examined using a Zeiss Axioskop 2 MOT Plus LSM5 PASCAL laser scanning microscope, equipped with an argon and neon lasers (Carl Zeiss AG., Jena, Germany). Propidium iodide (excitation max: 535 nm, emission max: 617 nm) was detected with excitation wavelength of 543 nm and a 560 nm long pass emission filter. mGFP5/6 was detected with an excitation wavelength of 488 nm and a 505-530 nm band pass emission filter. H2B::CFP was detected with a excitation wavelength of 458 nm and a 475-525 nm band pass emission filter.

Focal depth was increased for H2B::CFP images to ≥2µm to capture entire nuclei and improve fluorescence detection. Transmitted light was also captured. PI and mGFP5/6 could be imaged simultaneously. However, spectral overlapping between mGFP5/6 and H2B::CFP required these fluorophores to be imaged sequentially. All images captured in greyscale and false coloured with PI (red), mGFP5/6 (green), H2B::CFP (blue) and transmitted light (grey). Images displayed are representative of at least three biological replicates, unless otherwise stated.

2.7. Data management

All plant measurements (root and shoot dry and fresh weights, tiller number, Na^+, K^+ and Cl^- concentrations etc.) were collated using Microsoft® Office® 2013 Excel (Version 15.0.4569.1504(64-bit), Microsoft). Statistical analysis where required was conducted in either GenStat 16th Edition (Version 16.2.0.11713(64-bit edition), VSN International Ltd., Hemel Hempstead, UK) or Microsoft® Excel. Significance was determined with one- or two-way ANOVAs, those with significance ($P \leq 0.05$) were subjected to Tukey-Kramer post-hoc HSD analysis. Graphs were generated in Microsoft® Office® Excel 2013 with additional formatting using Microsoft® Office® PowerPoint® 2013

Chapter 3

Development and characterisation of transgenic barley lines with co-ordinated root-cell type expression of HvHKT1;5 and HvHVP1

Chapter 3 - Development and characterisation of transgenic barley lines with co-ordinated root cell-type specific expression of salinity tolerance genes, *HvHVP1* and *HvHKT1;5*

3.1. Introduction

3.1.1. Increasing salinity tolerance in barley

Barley is the most salt tolerant of the commonly grown cereals and is often grown in preference to wheat on salt-affected soils (Colmer *et al.*, 2005), despite barley fetching a lower financial return on unaffected soils (ABARES, 2015). High soil salinity however still causes substantial reduction in grain yield and quality in barley and further improvement in salt tolerance would be of benefit to growers to improve yields on currently cropped land, or allow better usage of land unsuitable for cropping.

Barley can also be used as a 'model' organism to trial GM approaches to improve salt tolerance in the more salt susceptible wheat. The relatively genetic closeness of wheat and barley, and similar dryland farming practice makes barley a more suitable choice than other more commonly used model species such as rice and Arabidopsis. Additionally, barley is more amenable to *Agrobacterium* transformation than wheat. The barley cultivar, Golden Promise, used in this study, has been widely used in transgenic studies because of its high transformation efficiency (Finnie *et al.*, 2004).

3.1.2. Use of native barley genes to improve salinity tolerance in barley

For this project, a 'cis-genic' rather than a 'trans-genic' approach was taken (Holme *et al.*, 2013). That is, native barley genes were over-expressed in barley (termed 'cis-genes'), rather than using orthologous genes from other species such as Arabidopsis or rice (termed 'transgenes').

Previous work has shown that cell-type specific over-expression of *AtHKT1;1* can be used to improve plant salinity tolerance in rice and Arabidopsis (Plett & Møller, 2010; Plett *et al.*, 2010b) and strong evidence for a similar role for other Class 1 HKTs exists in other species such as *Triticum monococcum* (*TaHKT1;5*) (Munns *et al.*, 2012), bread wheat (*TaHKT1;5D*) (Byrt *et al.*, 2014) and rice (*OsHKT1;5*)(Ren *et al.*, 2005). Similarly, *AtAVP1* has been shown to improve salinity tolerance in a number of species including Arabidopsis (Gaxiola *et al.*, 2001), cotton (Pasapula *et al.*, 2011), tomato (Park *et al.*), alfalfa (Bao *et al.*, 2009) and barley (Schilling, 2014, 2010; Schilling *et al.*, 2014).

Barley orthologues of both these genes are known and there is little reason to suggest that the native barley genes would act in any way significantly differently from their orthologues in other species when over-expressed. The barley *HKT* homologue *HvHKT1;5* has been show to mediate Na^+ uptake similar to other Class I HKTs (Banuelos *et al.*, 2008; Haro *et al.*, 2005). While the barley *H^+-PPase* orthologues, *HvHVP1* and *HvHVP10*, share significant homology with *AtHVP1* both increasing expression levels under salinity stress (Fukuda *et al.*, 2004a; Shavrukov *et al.*, 2013), however there is little research of their affect *in planta* when over-expressed in barley (Krishnan, 2013; Jessica Bovil, ACPFG, unpublished)

The use of cis-genes, over trans-genes from other species, may have the benefit of allowing interactions with species-specific regulatory networks, involving processes such as post-translational modifications, which may enhance the effect of over-expression of a cis-gene over that of a transgene. Additionally, the use cis-genes genes may also potentially reduce regulatory complications when integrating GM material into conventional breeding programs, fast tracking these varieties to agronomic use.

3.1.3. Previous development of tissue-type specific barley lines expressing salinity tolerance genes *HvHVP1* and *HvHKT1;5*

In order to drive tissue-type specific expression of these genes in barley, tissue-type specific promoters were required. Previous work carried out by Dr Mahima Krishnan (2013) at the Australian Centre for Plant Functional Genomics (ACPFG, University of Adelaide) identified several potential root-stele and root-cortex tissue-specific promoters from a DuPont™ Pioneer massively parallel signature sequencing (MPSS) dataset produced from the maize cultivar B73. This dataset consisted of the relative abundance of 16 - 20 bp mRNA sequence tags isolated from different maize tissue types, including root-stele and root-cortex (Brenner *et al.*, 2000). This allowed the identification of potentially root-stele and root-cortex specific MPSS tags which were subsequently verified for tissue-specificity via semi-quantitative PCR in Maize (cv. B73) tissues. Due to little genomic sequence information being available for barley at the time of this preliminary research (c. 2008), putative promoter sequences, ≈ 2 Kbp fragments 5′ of the identified genes, were cloned from either maize (cv. B73) or from orthologous genes in rice (cv. Nipponbare). These putative promoter sequences were then used to drive the expression of transgenes in barley in a tissue-type specific manner. The rice promoter

sequences were preferred, as rice is more closely related to barley than is Maize, which may reduce difficulties when using promoter sequences from different species.

The promoters were subsequently trialled in barley cv. Golden Promise, by using them to drive the expression reporter genes, *mGFP6* and *uidA*. Initial screening of the T_0 and T_1 *promoter*:*reporter* (*mGFP6* and *uidA*) lines proved inconclusive. However, only 10 day old seedlings grown in petri-dishes, were screened and RT-PCR was not conducted to verify the expression of reporter transgenes in the correct tissues. Potentially, the expression of reporter genes under these promoters may be under additional temporal control and/or only expressed at certain developmental stages and so may have been missed during these early screens. Additionally, the tissue-type specificity may have made it difficult to effectively view their expression patterns.

A number of these promoters were also used to drive the over expression of several barley GOIs, including Na^+ transporter *HvHKT1;5* (DQ912169.1) and vacuolar *H^+-PPase HvHVP1* (AB032829.1) in specific root cell-types (root stele and root cortex respectively) and assessed for improved salinity tolerance. Preliminary data from initial screening of T_1 lines of the *promoter*::GOI (*HvHVP1* or *HvHKT1;5*) grown in mini-hydroponics and exposed to 100 mM NaCl stress suggested a trend towards increased salinity tolerance (Krishnan, 2013).

Lines expressing *HvHKT1;5* under the control of the rice putative root-stele specific promoter, *proS147*, had a trend towards reduced [Na^+] in the 4^{th} leaf sap under saline conditions compared to null segregants and as well as a greater 4^{th} leaf sap K^+/Na^+ ratio (Figure 3.1). Although, neither result was statistically significant. The reduction in shoot Na^+ is potentially as a result of reduced root to shoot translocation of Na^+ by *HvHKT1;5* as seen similarly in Arabidopsis and rice when *AtHKT1;1* is over expressed in the root stele (Møller *et al.*, 2009; Plett *et al.*, 2010a)

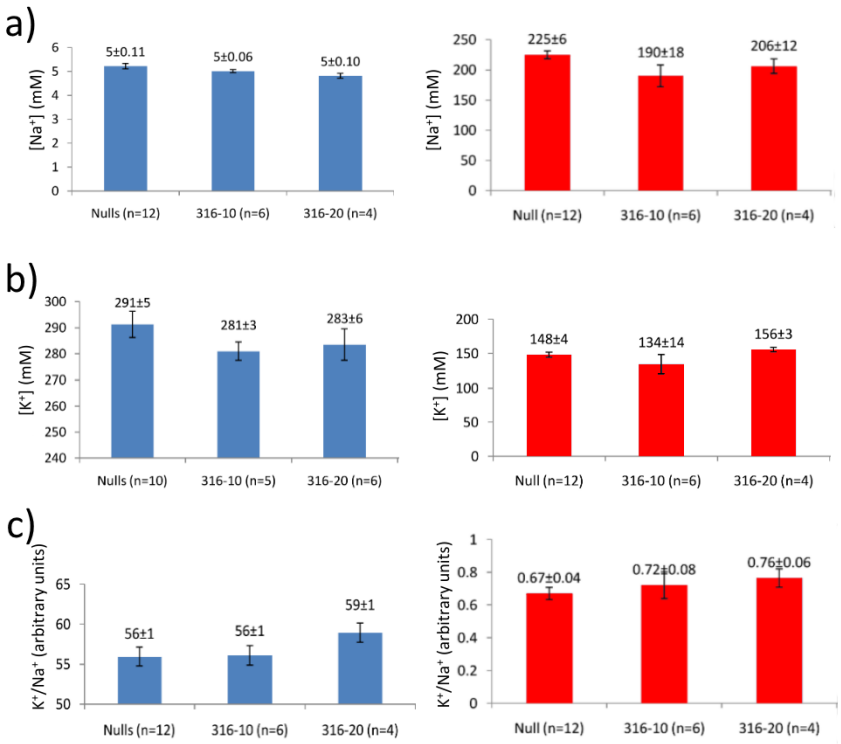

Figure 3.1: Potential for reduced 4th leaf Na^+ in two independent T_1 *proS147*:*HvHVP1* lines (316-10, 316-20) when grown in mini-hydroponics under control and 100 mM NaCl salt stress

Concentrations of Na^+ (a), K^+ (b) in the 4th leaf sap and K^+/Na^+ ratio (c) of the two T_1 *proS147*:*HvHKT1*;5 lines (316.10 and 316.20) selected for use in this study. Plants were grown in mini-hydroponics with standard hydroponics nutrient solution (control – blue) or hydroponics nutrient solution + 100 mM NaCl + 3 mM $CaCl_2$ (salt – red). Error bars represent standard deviation. Values shown are mean ± S.D., n = number of replicates. Figure reproduced and adapted from Krishnan (2013)

Conversely, lines expressing *HvHVP1* under the control of putative root-cortex specific promoter, *proC34*, had increased [Na^+] in the 4th leaf sap, under both control and 100 mM NaCl salt stress conditions, when compared to null segregants, although not signicantly. This was presumed to be due to the role of HvHVP1 in energising the tonoplast, leading to increased Na^+ sequestration in the vacuole by native Na^+ transporters (Figure 3.2). These results may have been indicative of increased Na^+ sequestration throughout the plant, rather than just root cortex specific sequestration as RT-PCR of *proC34:HvHVP1* lines detected occasional ectopic expression *HvHVP1* in leaf tissues (Krishnan, 2013)

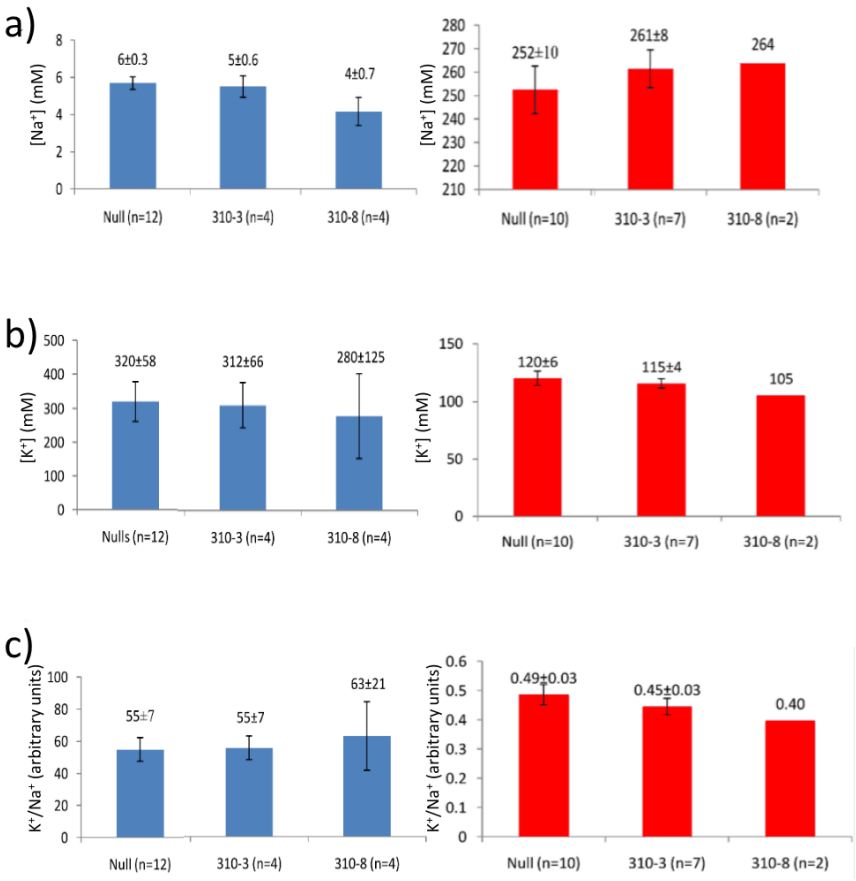

Figure 3.2: Potential for increased 4th leaf Na^+ in two independent T_1 *proC34*:*HvHVP1* lines (310-3, 310-8) in mini-hydroponics under control or 100 mM NaCl salt stress + 3 mM $CaCl_2$

Concentrations of Na^+ (a), K^+ (b) in the 4th leaf sap and K^+/Na^+ ratio (c) of the two T_1 *proC34*:*HvHVP1* lines (310.3 and 310.8) selected for use in this study. Plants were grown in mini-hydroponics with standard hydroponics nutrient solution (control – blue) or hydroponics nutrient solution plus 100 mM NaCl + 3 mM $CaCl_2$ (salt – red). Error bars represent standard deviation. Values shown are mean ± S.D., n = number of replicates. Figure reproduced and adapted from Krishnan (2013)

As both these T_1 material was still segregating, these initial results were quite limited (n= 2 - 7) and additional measurements of root and shoot biomass were not presented. The relatively small changes in Na^+ concentration in leaf sap suggested that the expression of the transgenes *HvHKT1;5* and *HvHVP1* with tissue-specific promoters could influence Na^+ transport *in planta*. Rigorous testing on advanced transgenic lines was required to confirm these phenotypes, and assess their impact on plant salinity tolerance. Therefore, screening of T_3 lines was performed during the course of this project.

3.1.4. Combining multiple salinity tolerance genes to improve salinity tolerance

Despite significant effort to improve salt tolerance in cereals through conventional breeding and transgenic approaches, the complex nature of salinity tolerance has made

the progress towards salt tolerance crops slow (Colmer *et al.*, 2005). Like many other abiotic stresses, soil salinity is often associated with other stresses (waterlogging, low pH, etc.) and there are also several different mechanisms for tolerance (reviewed in Munns & Tester, 2008). There is also a growing understanding of the large number of genes involved in each of the mechanisms of salt tolerance so it is increasingly unlikely that a single gene, integrated through GM or conventional breeding techniques, will effectively solve salinity tolerance in all cases. There has been extensive work conducted to demonstrate that manipulation of individual genes can have a positive effect on salinity tolerance (reviewed in Roy *et al.*, 2014), however, the possibility of combining multiple transgenes to target and improve multiple tolerance mechanisms would be of great benefit. This idea will also be explored in Arabidopsis (Chapters 5 and 6), however, migrating this preliminary work into a commercially relevant monocot species, barley selected for this study, is perhaps of greater importance.

To trial this, the potential Na^+ sequestration activity of in the root cortex by *HvHVP1,* with the Na^+ xylem retrieval activity of *HvHKT1;5* were combined through the hybridisation of the tissue-type specific lines also characterised in this chapter. This combination shows promise, as in a previous study, the over-expression of *AtHKT1;1* in rice, lead to increased expression of rice Class I *HKTs* (*OsHKT1;5*) and *H^+-PPases* (*OsOVPs)*, resulting in lower shoot [Na^+] and increase root cortex [Na^+] (Plett *et al.*, 2010b). These results suggest cooperation between xylem Na^+ retrieval and Na^+ sequestration mechanisms and potentially, the combined action of these two genes (*HvHVP1* and *HvHKT1;5)* in a cell-type specific manner will further enhance salinity tolerance over the either gene expressed individually.

3.1.5. Research aims

This aims of the work described in this chapter was to:

1) Assess the specificity of the root-stele and -cortex promoters, *proS147* and *proC34* by further examining the *uidA* and *mGFP6* reporter lines and the use of current bioinformatics data.
2) Screen T_3 lines with potential root cell-specific over-expression of *HvHKT1;5* and *HvHVP1* to further the previous work (Krishnan, 2013) indicating a potential altered leaf [Na^+] phenotype and/or improved plant salinity tolerance.
3) Develop transgenic lines with tissue-type specific over-expression of both *HvHVP1* and *HvHKT1;5* through crossing of selected *proC34:HvHVP1* and *proS147:HvHKT1;5* transgenic lines.
4) Screen these dual *HvHVP1* and *HvHKT1;5* over-expressing lines for altered root or shoot [Na^+] and for improved salinity tolerance over singly transformed lines and null lines.

3.2. Methods and Materials

3.2.1. Putative cell-type specific promoters

Two different putative tissue-type specific promoters were used in this study (Table 3.1). These promoters were originally identified, cloned and assessed by Dr Mahima Krishnan (ACPFG) (Krishnan, 2013).

Table 3.1: Putative tissue-type specific promoters used in this study
Information included; promoter name, genomic loci, putative tissue-specific expression, size of promoter cloned (sequences in Appendix V: Promoter Sequences).

Putative promoter	Genomic loci	Putative tissue expression	Size (bp)	Source
proC34	LOC_Os12g36240[1]	root-cortex	2468	*Oryza sativa* cv. Nipponbare
proS147	LOC_Os04g52720[2]	root-stele	2000	*Oryza sativa* cv. Nipponbare

[1] http://rice.plantbiology.msu.edu/cgi-bin/ORF_infopage.cgi?orf=LOC_Os12g36240
[2] http://rice.plantbiology.msu.edu/cgi-bin/ORF_infopage.cgi?orf=LOC_Os04g52720

3.2.2. Genomic sequences and expression profile databases

Further assessment of tissue-type specificity of these promoters was carried out by comparison to expression profile data available at the rice, maize and barley eFP browser (http://bar.utoronto.ca/welcome.htm - Patel *et al.* (2012)) as well as The Rice Expression Profile Database (RiceXPro) (http://ricexpro.dna.affrc.go.jp/ Sato *et al.* (2013)).

Rice loci and promoter sequences were identified from the Rice Genome Annotation Project (Rice cv. Nipponbare) reference genome MSU Osa1 Release 7 - http://rice.plantbiology.msu.edu, Ouyang *et al.* (2007)) and the plant promoter database (PPDB - http://ppdb.agr.gifu-u.ac.jp/ppdb/cgi-bin/index.cgi - Yamamoto and Obokata (2008)). Maize loci and promoter sequences were identified from the Gramene Database (Maize cv. B73 reference genome v 3.4 - http://ensembl.gramene.org/ - Monaco *et al.* (2014)).

3.2.3. Plant material

3.2.3.1. Transgenic lines expressing salinity tolerance GOIs

T_2 transgenic barley (*Hordeum vulgare* cv. Golden Promise) lines transformed with cDNA of *HvHVP1* (AB032829.1) or *HvHKT1;5* (DQ912169.1) and driven by the putative cell-type specific promoters *proC34* and *proS147* respectively were developed in a previous PhD project and kindly provided by Dr Mahima Krishnan (ACPFG) (Krishnan, 2013). A summary of the lines selected is presented in Table 3.2. These lines have previously been shown to be single T-DNA lines and have shown a potential for an altered 4th leaf sodium phenotype when grown in mini-hydroponics and exposed to 100 mM NaCl (Krishnan, 2013) (see also Figure 3.2 and Figure 3.1).

Table 3.2: Summary of transgenic barley (cv. Golden Promise) T_2 lines selected for crossing and screened for altered salinity tolerance in hydroponics.
Information included; T_2 Line identification, Name of expression vector transformed via *Agrobacterium*, containing included promoter and gene of interest (GOI)

Line ID	Expression Vector	Promoter	GOI
310.3	*pTOOL36-MK15*	*proC34*	*HvHVP1*
310.8	*pTOOL36-MK15*	*proC34*	*HvHVP1*
316.10	*pTOOL36-MK25*	*proS147*	*HvHKT1;5*
316.20	*pTOOL36-MK25*	*proS147*	*HvHKT1;5*

3.2.3.2. Transgenic lines expressing reporter genes for assessing tissue-type specificity

Additionally, several lines containing *promoter*:*reporter* (*mGFP5* or *uidA*) constructs were selected to assess the cell-type specificity of the promoters used in these lines. The lines selected for testing are outlined in Table 3.3. Three independent lines were selected per transformed construct and were kindly provided by Dr Mahima Krishnan (ACPFG) (Krishnan, 2013)

In all experiments, Golden Promise was used a negative control. In the β-glucuronidase assays, a T_2 line of *Oryza sativa* cv. Nipponbare expressing *uidA* under the control of the seeding specific promoter of *OsPRPI-11* (Os03g0130300) previously characterised by Kovalchuk *et al.* (2010) was used as a positive control. No suitable barley lines expressing *mGFP6* were available for a control.

Table 3.3: Summary of transgenic barley (cv. Golden Promise) T_2 lines screened for tissue-type specific expression of reporter genes (*mGFP6* or *uidA*)
Information included; T_2 Line identification, Name of destination vector containing promoter and reporter gene transformed via *Agrobacterium* and expected tissue-type specific expression pattern

Line ID	Destination vector	Promoter	Reporter Gene	Expected expression pattern
G300.1 **G300.5** **G300.10**	*pMDC107*	Rice (Nipponbare) *proC34*	*mGFP6*	Putative root cortex specific
G301.1 **G301.2** **G301.3**	*pMDC164*		*uidA (β-glucuronidase)*	
G304.3 **G304.4** **G304.7**	*pMDC107*	Rice (Nipponbare) *proS147*	*mGFP6*	Putative root stele specific
G305.1 **G305.3** **G305.7**	*pMDC164*		*uidA (β-glucuronidase)*	

3.2.4. DNA extraction and genotyping

Genotyping of individual transgenic lines and crosses was performed by extraction of genomic DNA (gDNA) from approximately 40 mg of young leaf material (3 – 4 cm of leaf tip) of selected plants using the Edwards extraction method as per section 2.2.20. For gDNA extractions from a large number of plants, the freeze-dry gDNA extraction method was used as per section 2.2.19. gDNA extraction quality was checked via PCR to amplify native gene *VRT2* (AK356695) (Primers: Table 3.4: VRT2_F and VRT2_R).

For genotyping of *uidA*, *mGFP6* or single transgene plants, a genotyping PCR was conducted as per section 2.2.2, on gDNA with primers designed to amplify a 815 bp fragment of the Hygromycin B antibiotic resistance gene (*hpt*) used as the plant selectable marker common to all barley transgenic constructs used (Primers: Table 3.4: Hyg1 and Hyg2).

For genotyping of crossed lines, PCR was performed on gDNA to amplify a unique ≈400 bp region between the putative cell-type promoters and transgenes of constructs MK15 (*proC34:HvHVP1*) (Primers: Table 3.4: gtMK15F and gtMK15R) and MK25 (*proS147:HvHKT1;5*) (Primers: Table 3.4: gtMK25F and gtMK25R). This allowed the detection of each construct separately and did not amplify the native *HvHKT1;5* or *HvHVP1* genes.

Table 3.4: PCR primers for genotyping and RT-PCR of transgenic barley lines.
Information included: Primer name, length; sequence, PCR conditions for use in genotyping PCR (section 2.2.2), amplicon size and intended purpose. Primer pairs are shaded.

Primer Name	Length (bp)	Sequence (5′ → 3′)	PCR conditions	Product size (bp)	Intended purpose
gtMK15F	20	GCACTTGAGGACGACGTTGT	Anneal: 57°C Extension: 30 s	498	Genotyping for MK15 construct presence of (*proC34:HvHVP1*)
gtMK15R	23	TGAACGACTGATCGAGAGCA			
gtMK25_F	20	GTGGGCATGTTGGTCTTCAT	Anneal: 57°C Extension: 30 s	368	Genotyping for MK25 construct (*proS147:HvHKT1;5)*
gtMK25_R	25	GGAGTAGTAGTGGAATGCAGTGA			
GUSiF	20	GGCACAGCACATCAAAGAGA	Anneal: 56°C Extension: 45 s	735	*uidA* RT-PCR
GUSiR	20	CTGATAGCGCGTGACAAAAA			
HvHVP1_SF3	19	ACGACCGTTGATGTCCTGA	Anneal: 57°C Extension: 45 s	685	RT-PCR of ectopic *HvHVP1* expression
NOS_R	25	CATCGCAAGACCGGCAACAGGATTC			
HvHKT15_SF2	16	CGGCTACGACCACCTC	Anneal: 57°C Extension: 45 s	749	RT-PCR of ectopic *HvHKT1;5* expression
NOS_R	25	CATCGCAAGACCGGCAACAGGATTC			
VRT2_F	24	CCGAATGTACTGCCGTCATCACAG	Anneal: 63°C Extension: 30 s	129	genomic DNA quality check
VRT2_R	27	TGGCAGAGGAAAATATGCGCTTGA			
HYG1	20	GTCGATCGACAGATCCGGTC	Anneal: 60°C Extension: 45 s	815	*hpt* Genotyping PCR
HYG2	20	GGGAGTTTAGCGAGAGCCTG			
HvGAP-R	22	TGGTGCAGCTAGCATTTGAGAC	Anneal: 60°C Extension: 30 s	685	cDNA quality check
HvGAP-F	21	GTGAGGCTGGTGCTGATTACG			
GFPiF	20	TCAAGGAGGACGGAAACATC	Anneal: 55°C Extension: 30 s	234	*mGFP6* RT-PCR
GFPiR	20	AAAGGGCAGATTGTGTGGAC			

3.2.5. Total root and leaf RNA extraction and reverse transcriptase-PCR

To detect ectopic expression of transgenes, total RNA was extracted from root and leaf tissue as per section 2.2.21 and used for cDNA synthesis as per section 2.2.22.

RT-PCR was then carried out using cDNA and appropriate primers to detect transgene expression: *uidA* (Primers: Table 3.4: GUSiF and GUSiR), *mGFP6* (Primers: Table 3.4: GFPiF and GFPiR), *HvHKT1;5* (Primers: Table 3.4: HvHKT15_SF2 and NOS_R) and *HvHVP1* (Primers: Table 3.4: HvHVP1_SF3 and NOS_R).

3.2.6. Screening promoter tissue specificity under salt stress in mini-hydroponics system

In order to assess the tissue specificity of the promoter activity in developing barley plants under salt stress, T_2 transgenic *promoter::reporter* lines outlined Table 3.2, grown in mini-hydroponic and exposed to mild-salinity stress. On average, 16 plants (8 per treatment) of each line were germinated and grown in mini-hydroponics as per section 2.4.3. After approximately 10 days in the mini-hydroponics set-up, at 3rd leaf emergence, plants in the salt treatment tanks were challenged with 150 mM NaCl, applied in 25 mM increments at 12 hour intervals, 6 AM and 6 PM, with the addition of 0.3 mM $CaCl_2$ (in the form of $CaCl_2.2H_2O$) per 25 mM NaCl to maintain free-Ca^{2+} activity.

Three time points were selected to assess developmental expression differences for each reporter (1) five day old seedlings on transfer to mini-hydroponics, (2) At emergence of 3rd leaf (day 14) and onset of 150 mM NaCl treatment, and (3) at five days post salt treatment.

3.2.6.1. Screening for GFP fluorescence in *promoter:mGFP6* expressing barley transgenic lines.

To assess promoter activity in the barley *promoter:mGFP6* transgenic lines (Table 3.3) under control and 150 mM NaCl, transformed lines were screened in two rounds of mini-hydroponics as described above. To visualise mGFP6, seedlings collected at the above time points (section 3.2.6) were rinsed briefly in Milli-Q H_2O and examined using a stereo dissecting microscope as per section 2.6. Sectioning was carried out to examine the shoot and roots of selected plants, however, most plants were left intact until the end of the experiment before sectioning. Plants were genotyped for the presence of the *mGFP6* containing constructs by PCR as per section 3.2.4, prior to salt application and examination.

3.2.7. Histochemical staining of transgenic *β-glucuronidase* (*uidA*) expressing barley seedlings.

To assess promoter activity in barley *promoter:uidA* transgenic lines (Table 3.3) under control and salt-stress conditions in mini-hydroponics, histochemical *β-glucuronidase* (GUS) staining was carried out. Transgenic plants from lines outlined in Table 3.3 were surface sterilised with bleach as per section 2.4.2.2 and germinated as per section 2.4.2.3. Plants were transferred into the mini-hydroponics set-up detailed in section 2.4.3. Three time points were selected to assess developmental expression differences; 5 day-old seedlings on transfer to mini-hydroponics, 15 day old plants before onset of 100 mM NaCl treatment (as per section 2.4.3.3) and at 5-days post salt treatment. DNA from all plants transferred to mini-hydroponics was extracted by the freeze-dry method (section 2.2.19) and plants were genotyped for the presence of *uidA* transgene of by PCR (section 2.2.2).

Five day old seedling were sectioned with the root and shoot and stained as below. For larger plants grown in mini-hydroponics (salt and control conditions), roots of salt treated and control plants were washed in 10 mM $CaSO_4$ briefly before being patted dry with paper towelling. Plants were sectioned at the junction between stem and roots with scissors. Samples taken from the stem, the crown, 3 cm lengths of both new and mature leaves and 3 cm of stem. 5 cm lengths sections of the root tip, mature root, lateral root and seminal roots were also taken. Root and leaf samples were also taken, RNA was extracted (as per section 2.2.21) and cDNA synthesised (as per 2.2.22) to assess transgene expression via RT-PCR (section 2.2.2) with primers specific to *uidA*.

Tissue samples were grouped by plant, submerged into 25 mL of GUS staining solution (Appendix IV: GUS Staining Buffer) in 50 mL falcon tubes and vacuum infiltrated at room temperature at approximately 700 mbar for 30 minutes (Thermo Fisher Scientific Inc., Waltham, MA, USA. Model No: Napco® 5831 Vacuum oven – Edwards Inc., Singapore, Model No: E2M5 Vacuum Pump). Samples were then transferred to an oven and incubated at 37 °C protected from light. Samples were inspected every 30 minutes for 4 hours for staining and then at 16, 24 and 48 hours.

Stained samples were drained of GUS staining solution, then incubated at room temperature in 25 % v/v ethanol for 1 hour, and then in 50 % v/v ethanol for 1 hour. Plants were stored in 70 % v/v ethanol at 4 °C and protected from light by wrapping in

aluminium foil before imaging. Chlorophyll was removed from shoot tissue by incubation for 1 week in 70 % v/v ethanol at 4 °C.

Stained samples were transferred to Petri dishes containing 70 % v/v ethanol and inspected using a stereo dissecting Microscope (Leica Microsystems GmbH, Heerbrugg, Switzerland, Model No: Leica MZ FLIII), digitally imaged (Leica Microsystems GmbH, Heerbrugg, Switzerland, Model No: Leica DC300F digital camera) and analysed using the Leica Microsystems IM50 Image Manager (Leica Microsystems GmbH, v1.2).

As the mini-hydroponics system used is non-sterile, there is the possibility of contamination by native uidA-containing microorganisms leading to spurious GUS staining. Wild-type barley cv. Golden Promise was grown alongside transgenic plants in the mini-hydroponics set-up to act as a negative control and stained.

As a positive control for GUS staining in transgenic plants, seeds of T_2 *Oryza sativa* cv. Nipponbare transgenic line expressing *uidA* under the control of a seeding specific promoter of *OsPRPI-11* (Os03g0130300) (Kovalchuk *et al.*, 2010), were surface sterilised as per section 2.4.2.1, germinated on filter paper and incubated at 28 °C. Ten-day old seedlings were sectioned at the junction between root and shoot and stained alongside the barley samples as above.

3.2.8. Growth of barley plants in soil

Routine bulking up barley plants was carried out in soil under greenhouse conditions specified as per section 2.4.1. Hydroponically growth plants were also able to be transplanted and successfully grown onto maturity and seed set in soil as above.

3.2.9. Hybridisation of T_2 barley transgenic lines

To hybridise T_2 transgenic *proC34*:*HVP1* and *proS147*:*HvHKT1;5* lines (Table 3.2), seed from T_1 plants were UV sterilised as per section 2.4.2.1 and germinated as per section 2.4.2.3. As seed from T_1 material was scarce, the seed used was from plants grown in a control mini-hydroponics and transplanted to soil at the conclusion of the experiment and grown until seed set. Twelve of the most uniform seedlings from each line were transplanted to soil as per section 3.2.8. Plants were genotyped for the presence of the transgene construct, as per section 3.2.4 prior to flowering. For each positive transgenic plant, 1 spike was bagged to allow self-pollination, 1 spike was emasculated as per section 3.2.9.1 and used for hybridisation and 1-2 spikes were kept for pollen production

where possible. Nulls were segregated and bagged to prevent cross pollination. For comparison in later experiments, wild-type Golden Promise was grown in the same conditions to produce seed.

3.2.9.1. Emasculation and crossing of barley cv. Golden Promise

With Golden Promise, immature ears were at the correct stage for emasculation when the awns were protruding approximately 1-2 cm out of the boot, approximately 70 days after germination. As pollination often occurs within the boot, care was taken to ensure pollination has not occurred before crossing. All tools (forceps, scissors, etc.) and gloves were sterilised with 70 % v/v Ethanol between each emasculation to prevent accidental pollination and fungal contamination. The boot of the developing spike was opened with small dissection scissors to expose the spike. Awns were trimmed and needle forceps were used to fold back the lamma to expose the anthers and all 3 anthers were removed. Approximately, 20 florets were emasculated per spike (only one floret per spikelet). As spikelets mature from mid spike, underdeveloped spikelets at the either end of the spike that were not suitable for emasculation were removed. The emasculated ear was then bagged to maintain humidity and to prevent cross pollination. After approximately 5 days following emasculation, emasculated florets had developed and the stigma was exposed ready for pollination. Pollination was conducted at sunrise, as this is when pollen quality is best, giving best pollination results. Anthers from non-emasculated plants were inspected and anthers with viable pollen were removed similarly to above and used to pollinate emasculated florets. For each plant, where possible, 1 spike was used for emasculation and crossing, 1 for self-pollination and 2 spikes kept for pollination. All pollenated ears, crossed or selfed, were bagged to prevent cross pollination and plants were grown onto maturity and seeds harvested.

3.2.10. Bromocresol Purple rhizosphere acidification assay

To assess potential increased rhizosphere acidification of transgenic *HVP1* over-expressing barley lines, the pH sensitive bromocresol purple dye (Sigma-Aldrich Pty. Ltd., Sydney, NSW, Australia, Cat. No: 29F3712) was used in a protocol originally from Heckman and Strick (1996) and further refined by Dr Rhiannon Schilling (Schilling, 2014).

Seedlings of Golden Promise and transgenic *HVP1* lines germinated and grown in control (no additional NaCl) mini-hydroponics, as described in section 2.4.3. After five days

growth, seedlings were removed from growth solution, gently patted dry with paper towelling to remove excess water and transferred into 7.2 cm^2 white PVC trays (SARSTEDT Australia Pty. Ltd., Ingle Farm, SA, Australia. Cat. No. 71.9923.212). Care was taken not to damage the roots as this may cause leakage of cell contents resulting in an erroneous pH drop. 25 mL of liquid bromocresol purple agarose solution (Appendix IV: Bromocresol purple pH indicator gel), cooled to 30 °C, was poured over the roots of the seedlings to a depth of approximately 3 mm and allowed to solidify. Plants were incubated at room temperature for 4 hrs under fluorescent lighting and digitally photographed (Olympus Imagining Corp., Tokyo, Japan, Model No: SZ-30MR)

3.2.11. Barley growth in mini-hydroponics

For short-term (approximately 3 weeks) salt stress treatments, barley plants were grown in mini-hydroponics setup described in section 2.4.3.

3.2.12. Barley growth in supported hydroponics

For longer salt stress treatment experiments, a 80 L flood-drain hydroponics system was used, as described in section 2.4.4 (similar to Shavrukov *et al.*, 2012).

3.2.13. Statistical analysis

All data collected from hydroponics experiments was analysed in Microsoft Excel 2013 with significant differences between transgenic and null lines and between treatments were determined by one- or two-way ANOVAs. Analyses with significance ($P \leq 0.05$) were subjected to Tukey-Kramer HSD post-hoc analysis.

3.3. Results and Discussion

3.3.1. Expression of reporter genes, *mGFP6* and *uidA*, under the control of putative tissue-type specific promoters, *proC34* and *proS147*.

3.3.1.1. GFP fluorescence was not detected in *promoter:mGFP6* lines grown under 150 mM NaCl in mini-hydroponics

Three independent T_2 lines of transgenic barley cv. Golden Promise expressing *mGFP6* under the control of putative tissue-type specific promoters: *proC34* or *proS147* were screened in mini-hydroponics and exposed to 150 mM NaCl, added at 25 mM increments every 12 hrs on the emergence of the 3rd leaf. Plants were sampled and imaged after 7 days growth at 150 mM NaCl.

RT-PCR on cDNA synthesised from RNA extracted from root and leaf material indicated that the *mGFP6* transcript was present in the roots of all *proC34:mGFP6* plants and occasionally in the shoots when a high numbers of cycles was used (35 cycles) under both control and 150 mM NaCl stress conditions. The *mGFP6* transcript was detectable in both roots and shoots of most *proS147:mGFP6* plants, however, only at high cycle numbers (35 cycles). A subset of these results are presented in Figure 3.3.

Wild-type and transgenic lines appeared similar in growth in mini-hydroponics under control conditions and similar reduction in growth was observed when challenged with 150 mM NaCl.

Despite detecting *GFP* transcript, no GFP fluorescence could be observed in any *promoter:mGFP6* lines in both control and salt treatments when compared to wild-type plants (Figure 3.4). Increased auto-fluorescence was observed in mature tissues and in salt treated plants due to increased senescence.

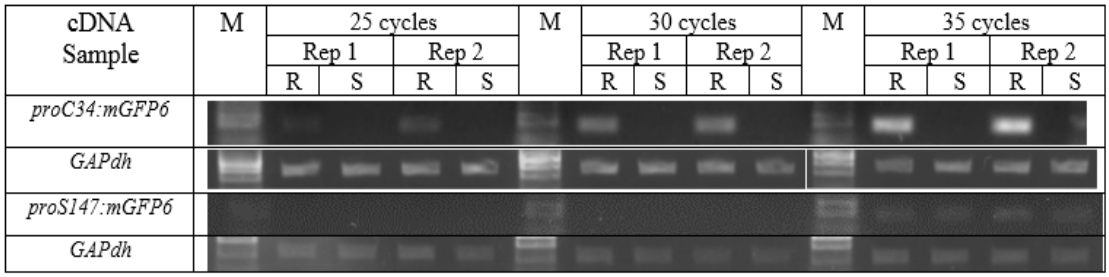

Figure 3.3: Expression of *mGFP6* under the control of root-specific promoters, *proC34* and *proS147* in selected barley lines under 150mM NaCl confirmed by RT-PCR
Semi-quantitative RT-PCR performed on RNA extracted from 21-day old salt stressed (150 mM NaCl) roots and shoots of 2 independent biological reps from lines *proC34:mGFP6* and *proS147:mGFP6*, with increasing number of PCR cycles. R = root sample, S = shoot samples, M = 100 bp molecular marker.

Wt Golden Promise		**Assorted *promoter:mGFP6* lines**	
Bright field	GFP2 filter	Bright field	GFP2 filter

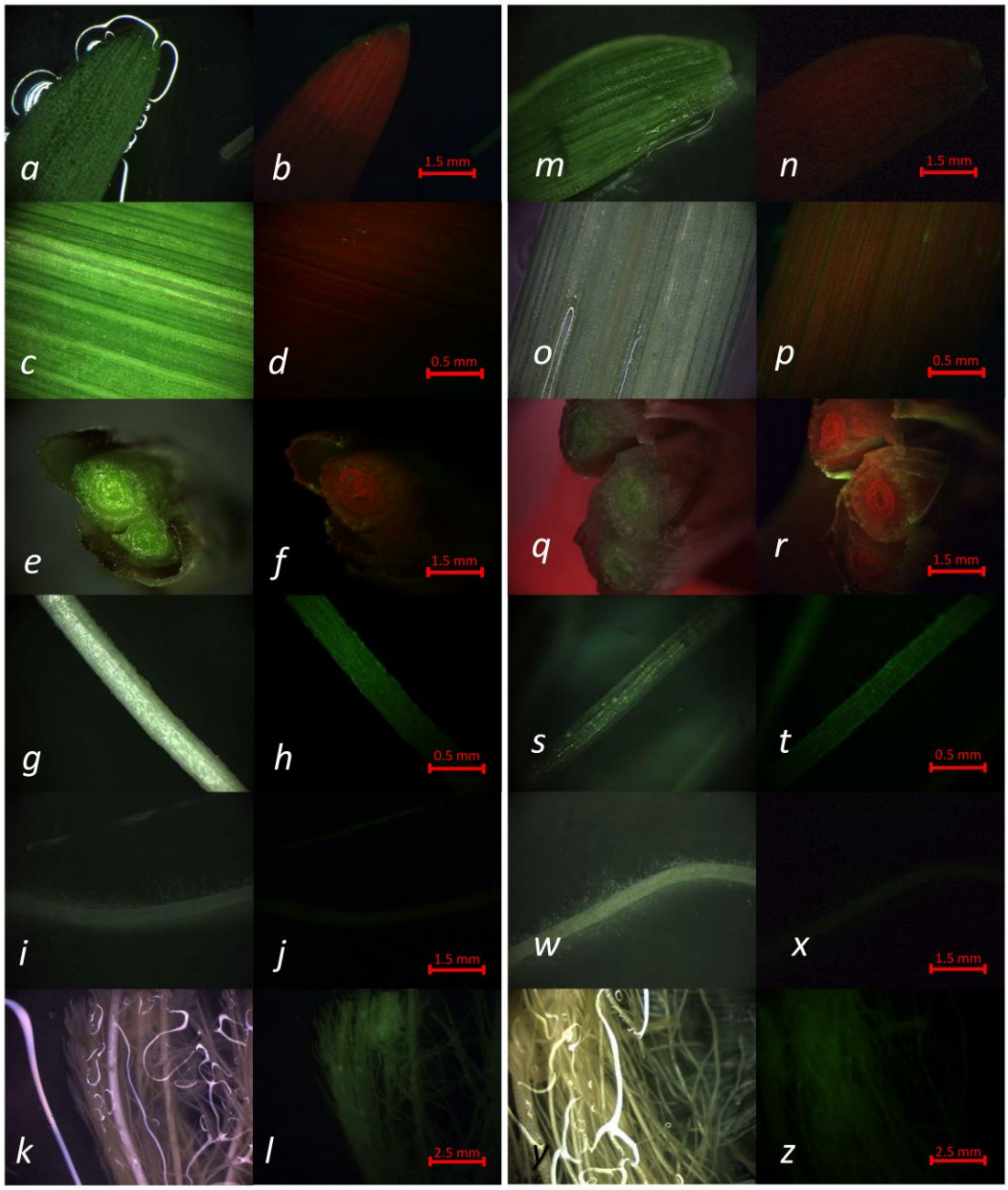

Figure 3.4: Images of plant tissue used in screening for GFP fluorescence in Golden Promise barley and assorted *proC34:mGFP6* and *proS147:mGFP6* lines.
Representative fluorescence stereo-microscopy images of various tissues of 21 day-old WT Golden Promise (a-l) and assorted *promoter:mGFP6* lines (m-z) grown under 150 mM NaCl for 7 days. Approximately 3 plants per line, per treatment, examined. A Leica GFP2 filter (510 nm Long Pass) was used to examine for GFP fluorescence (477 nm excitation, peak emission 509 nm).

3.3.1.2. GUS staining was not detected in *promoter:uidA* lines grown under 0 mM or 150 mM NaCl in mini-hydroponics

Three independent T_2 lines of transgenic barley cv. Golden Promise expressing *uidA* under the control of putative tissue-type specific promoters *proC34* or *proS147* (Table 3.3) were grown in mini-hydroponics and exposed to either a 0 mM (control) or 150 mM NaCl treatment. Plants were sampled and stained at four time points: Five day old seedlings on transfer to hydroponics, day 14 at onset of 150 mM NaCl treatment and 7 days following NaCl treatment. Approximately three plants identified as having the *uidA*, by genotyping PCR (section 3.2.4), were GUS stained at each time point and examined by stereo-microscopy.

RNA was extracted from root and leaf material of plants following 7 days NaCl treatment (0 mM NaCl or 150 mM NaCl) at the completion of the salt stress treatment. RT-PCR was conducted to detect the presence of *uidA* transcript in root or leaf material (Figure 3.8).

For the three independent T_2 lines expressing *uidA* under the control of a putative rice root-cortex specific promoter, *proC34*, *uidA* was detected primarily in the roots (Figure 3.8, A and B), with occasional ectopic expression. For the three independent T_2 lines expressing *uidA* under the control of putative rice root-stele specific promoter, *proS147*, *uidA* was detected in both the roots and leaf material (Figure 3.8, C and D), similar to the *promoter*:*mGFP6* results (section 3.3.1.1) and previously in Krishnan (2013).

GUS activity was not detected in leaf material (Figure 3.7) of both control Golden Promise or in transgenic lines following 4 to 24 hours incubation in GUS solution. Extended incubation (48 – 120 hours) was undertaken in the roots for potential low level expression of the promoters in root tissue, similarly no GUS activity was detected in either *proC34:uidA* (or roots (Figure 3.5) or *proS147:uidA* (Figure 3.6) lines. GUS staining was however detectable in concurrently stained *uidA* expressing Arabidopsis or 10 day old T_1 rice seedlings which acted as a positive control for the GUS staining solution within 30 minutes of incubation (not shown).

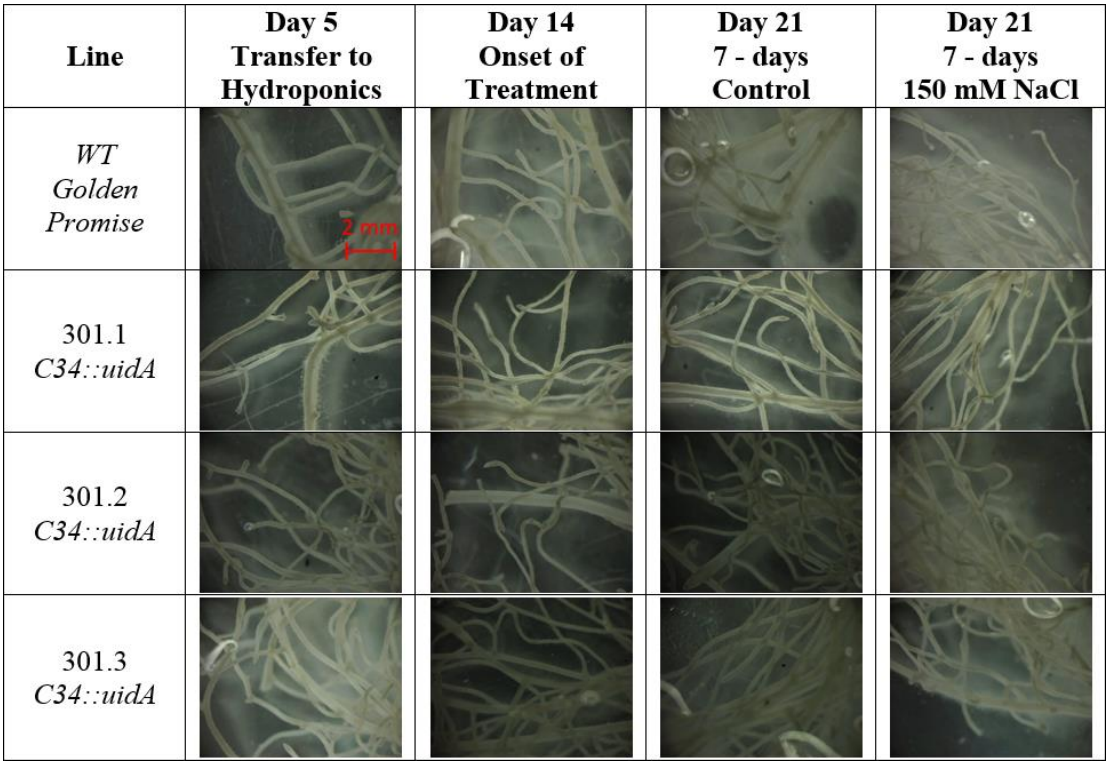

Figure 3.5: Images of roots used for histochemical GUS staining of roots of Golden Promise and *proC34:uidA* lines in mini-hydroponics

Representative images of sectioned roots. Golden Promise (row 1) and three independent transgenic barley *proC34:uidA* lines (301.1 row 2, 301.2 row 3, 301.3 row 4) grown in mini-hydroponics. Roots harvested at 3 time points. Day 5, after transfer to mini-hydroponics (column 1), Day 14 on onset of NaCl treatment (column 2), and after 7 d after either 0 mM NaCl (Control – column 3) or 150 mM NaCl (column 4). Whole root samples sectioned to approximately 3 cm lengths and stained by vacuum infiltrated with GUS staining solution for 30 minutes and incubated at 37°C for 48 hours. β-glucuronidase activity was visualised by stereo-microscopy. Three to five plants per line, per treatment, were inspected. All images captured at 140× magnification. No GUS activity was distinguishable in the roots of the transgenic *proC34:uidA* lines or wild-type plants. GUS activity was observed in co-currently stained *uidA* expressing Arabidopsis and rice material controls (not shown).

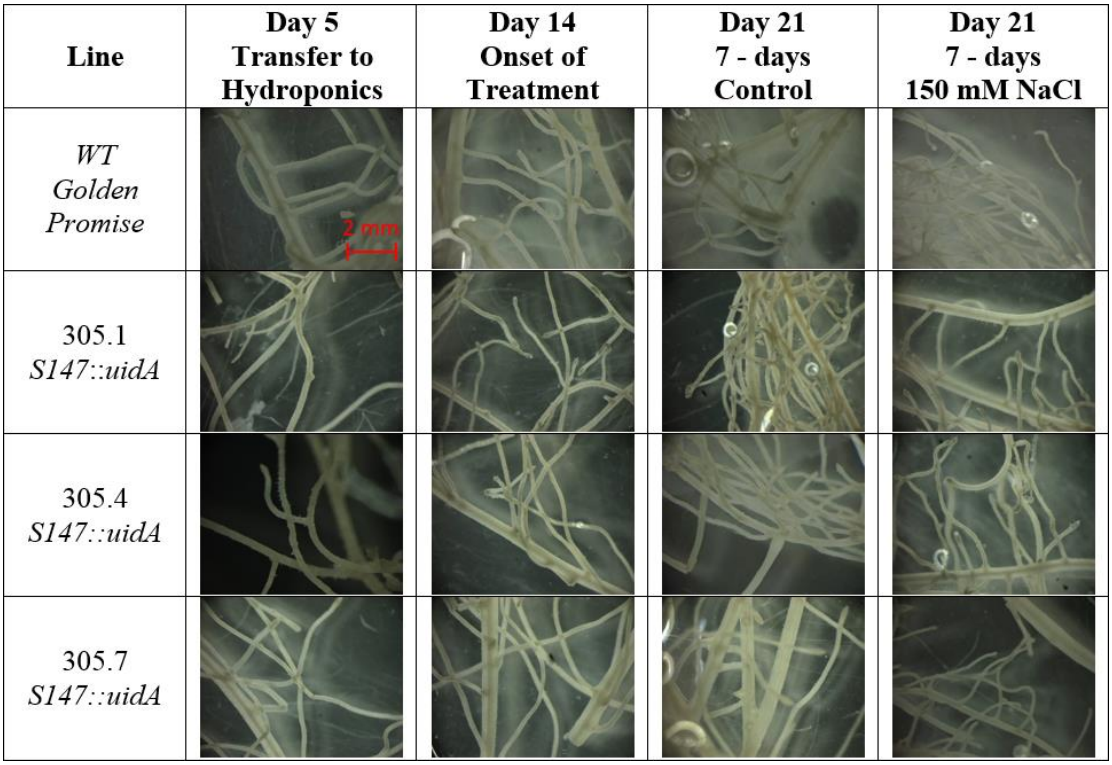

Figure 3.6: Images of roots used for histochemical GUS staining of roots of Golden Promise and *proS147:uidA* lines in mini-hydroponics

Representative images of sectioned roots: Golden Promise (row 1) and three independent transgenic barley *proS147:uidA* lines (305.1 row 2, 305.4 row 3, 305.7 row 4) grown in mini-hydroponics. Roots harvested at 3 time points. Day 5, after transfer to mini-hydroponics (column 1), Day 14 on onset of NaCl treatment (column 2), and after 7 d after either 0 mM NaCl (Control – column 3) or 150 mM NaCl (column 4). Whole root samples sectioned to approximately 3 cm lengths and stained by vacuum infiltrated with GUS staining solution for 30 minutes and incubated at 37°C for 48 hours. β-glucuronidase activity was visualised by stereo-microscopy. Three to five plants per line, per treatment, were inspected. All images captured at 140× magnification. No GUS activity was distinguishable in the roots of the transgenic *proS147:uidA* lines or wild-type plants. GUS activity was observed in co-currently stained *uidA* expressing Arabidopsis and rice material controls (not shown).

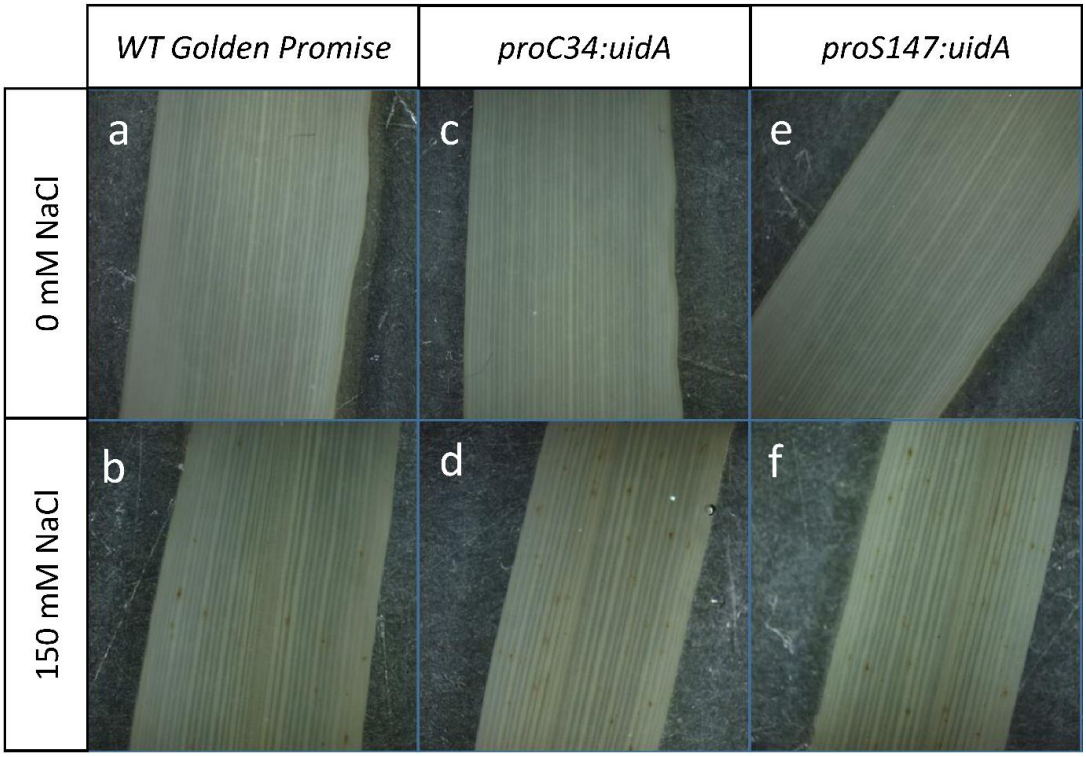

Figure 3.7: Images of leaves used for histochemical GUS staining of leaves of Golden Promise and *proC34:uidA* and *proS147:uidA* lines in mini-hydroponics.
Representative images of leaves of 21 day-old Golden Promise (a & b) and transgenic *promoter:uidA* lines (c-g) grown in mini-hydroponics and subjected to 0 mM (a,c,e) or 150 mM NaCl (b,d,f) treatment for a 7-day. Samples were vacuum infiltrated with GUS staining solution for 30 minutes and incubated at 37°C for 48 hours. Leaves were cleared of chlorophyll by incubating at 4 °C in 70 % ethanol for two weeks. *β-glucuronidase* activity was visualised by stereo-microscopy. Three to five plants per line, per treatment were inspected. All images captured at 160× magnification. No distinctive GUS activity was distinguishable in the transgenic promoter::uidA lines or wild-type plants. GUS activity was observed in co-currently stained *uidA* expressing Arabidopsis and rice material (not shown).

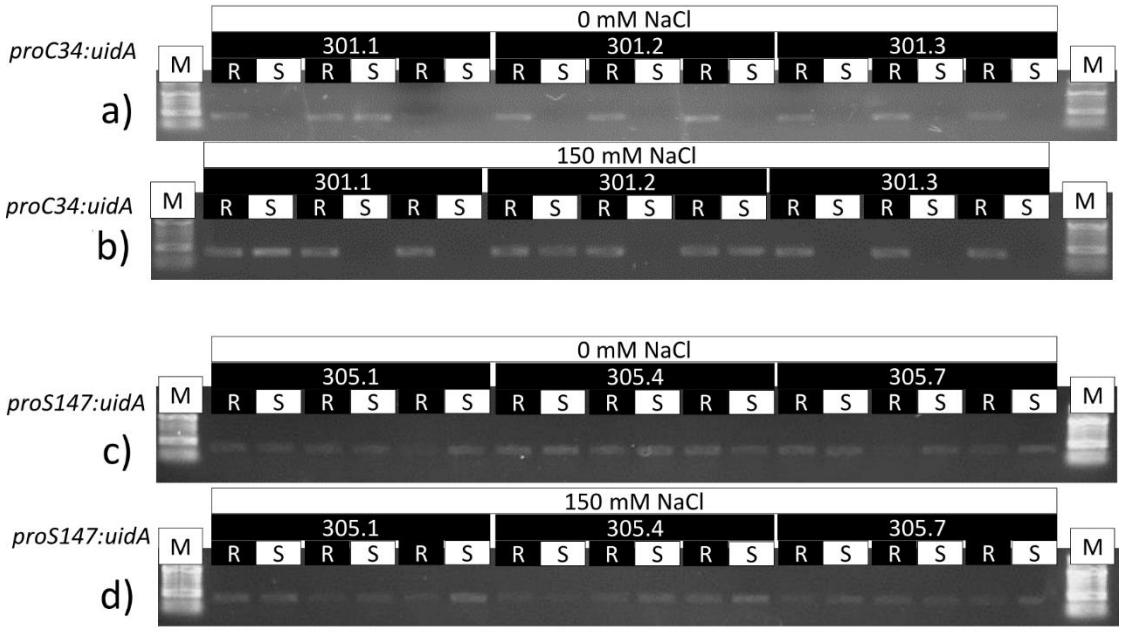

Figure 3.8: Images of gels shows Expression of *uidA* under the control of putative root cell-type specific promoters *proC34* and *proS147* in selected barley lines under control or 150 mM NaCl
RT-PCR (35 cycles) performed on cDNA synthesised from RNA extracted from roots and shoots of 21-day old control (0 mM Nacl) or salt stressed (150 mM NaCl) plants. Three independent biological replicates from three independent lines of: *proC34:uidA* (a and b), *proS147:uidA* (c and d). R = root sample, S = shoot samples, M = 100 bp molecular marker.

3.3.2. Evaluating the salinity tolerance of lines expressing *HvHVP1* or *HvHKT1;5* in supported hydroponics

To further assess the salinity tolerance of transgenic barley lines transformed with *HvHVP1* and *HvHKT1*;5 under the control of the putative root cell-type specific promoters *proC34* and *proS147* respectively, T_3 plants were grown in flood-drain supported hydroponics (section 2.4.4) and exposed to 200 mM NaCl at the emergence of the 3rd leaf and grown for an additional 21 days.

3.3.2.1. *HvHKT1;5* and *HvHVP1* transgenes are expressed in roots of hydroponically grown T_3 plants under 0 mM and 200 mM NaCl treatments.

Genotyping PCR confirmed the presence of either the *proS147:HvHKT1;5* (MK25) or *proC34:HvHVP1* (MK15) constructs in the respective lines and was not detected in the nulls lines (not shown). RT-PCR was performed (as per section 3.2.5) with on subset of samples to verified that *HvHVP1:nosT* (Figure 3.9) and *HvHVP1:nosT* (Figure 3.10) transcript was expressed in root tissues under control (0 mM) and 200 mM NaCl treatments.

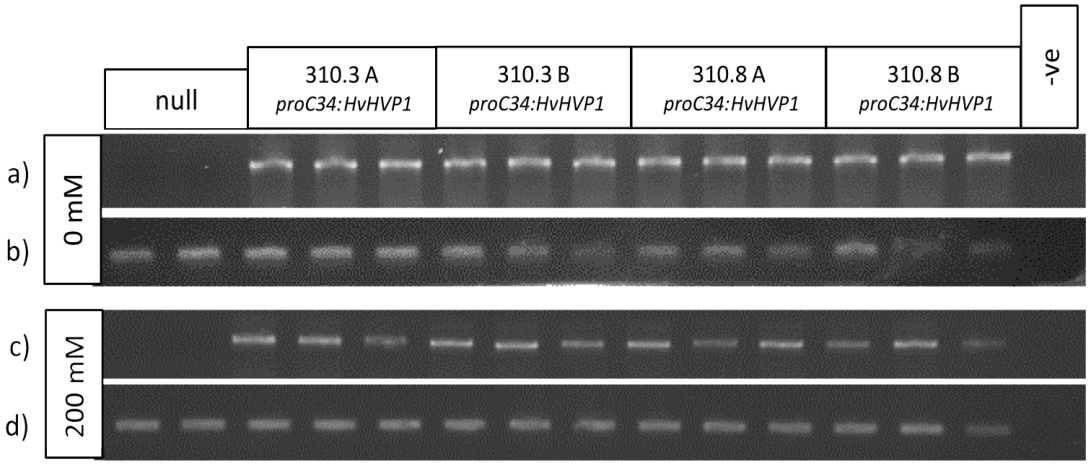

Figure 3.9: Images of gels showing *HvHVP1:nosT* transcript present in root tissues of selected lines grown in supported hydroponics under 0 or 200 mM NaCl .
RT-PCR (35 cycles) for *HvHVP1:nosT* (a,c) and *HvGAPDH* (b,d) performed on cDNA synthesised from RNA extracted from roots of subset of plants following 21 days salt treatment (0 mM or 200 mM NaCl). Three independent biological replicates from the two T_2 sibling lines (A and B) from two independent lines transformed with *proC34:HvHVP1* (310.3 and 310.8) plus, two selected nulls lines and a water negative (-ve) control. Rows (a & c) presence/absence of *HvHVP1:nosT* under 0 mM or 200 mM NaCl. Rows (b & d) presence/absence of *HvGAPDH* in same samples to check cDNA quality.

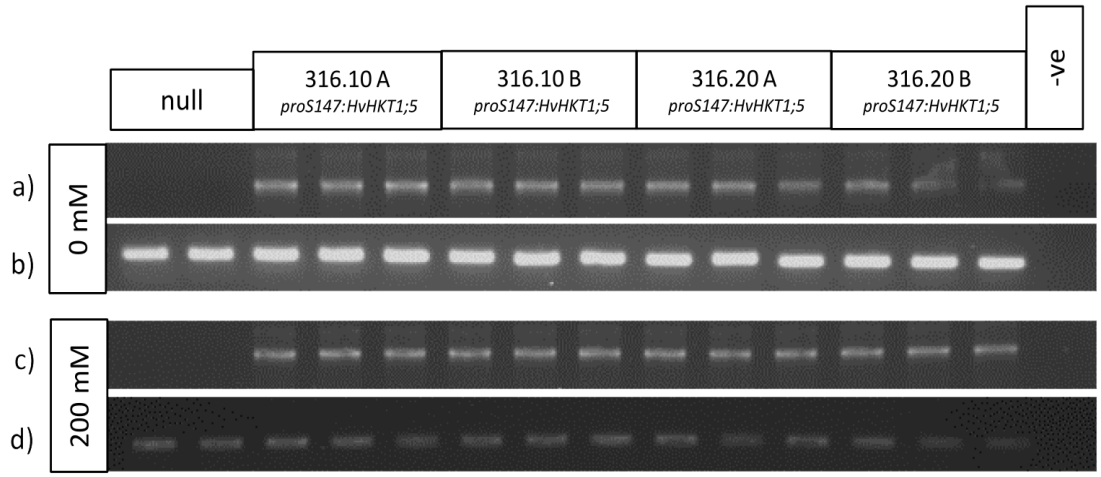

Figure 3.10: Images of gels showing *HvHKT1;5:nosT* transcript present in root tissues of selected lines grown in supported hydroponics under 0 or 200 mM NaCl . RT-PCR (35 cycles) for *HvHKT1;5:nosT* (a,c) and *HvGAPDH* (b,d) performed on cDNA synthesised from RNA extracted from roots of subset of plants following 21 days salt treatment (0 mM or 200 mM NaCl). Three independent biological replicates from the two T_2 sibling lines (A and B) from two independent lines transformed with *proS147:HvHKT1;5* (316.10 and 316.20) plus, two selected nulls lines and a water negative (-ve) control. Rows (a & c) presence/absence of *HvHVP1:nosT* under 0 mM or 200 mM NaCl. Rows (b & d) presence/absence of *HvGAPDH* in same samples to check cDNA quality.

3.3.2.2. Root and Shoot Biomass (fresh and dry weight) and number of tillers in all transgenic lines are similar to null segregants

Shoot (Figure 3.11, a) and root (Figure 3.11, b) fresh weight biomass is not significantly different in control or 150 mM NaCl treatments in the majority of the transgenic lines when compared to null segregants. A significant difference was observed in one of the *proC34::HvHVP1 lines* (310.3-B) with overall reduced shoot (≈ -30%) and root fresh weight (≈ -30%) - compared to nulls or the other lines. Another independent line, *proC34:HvHVP1* 310.8 A also had a significant reduction in root fresh weight (≈ -17%) compared to nulls in the 150 mM NaCl treatment only. In both cases, however, their respective sibling lines (310.3-A and 310.8-B) are not significantly different. A significant treatment affect was observed with a general reduction in shoot FW biomass of ≈ 50 % and root FW biomass of ≈ 25 %, leading to a 36% increase in the root to shoot ratio (Figure 3.11, c) in all lines. A similar trend can be seen in the dry weight biomass measurements (Figure 3.12). The number of tillers was also measured (Figure 3.11, d), with a trend for a reduction in tillers in the *proC34*::*HvHVP1* lines. However, as there was little tillering overall and only the absolute number of tillers measured rather than the mean tiller weight, little significance should be placed on this.

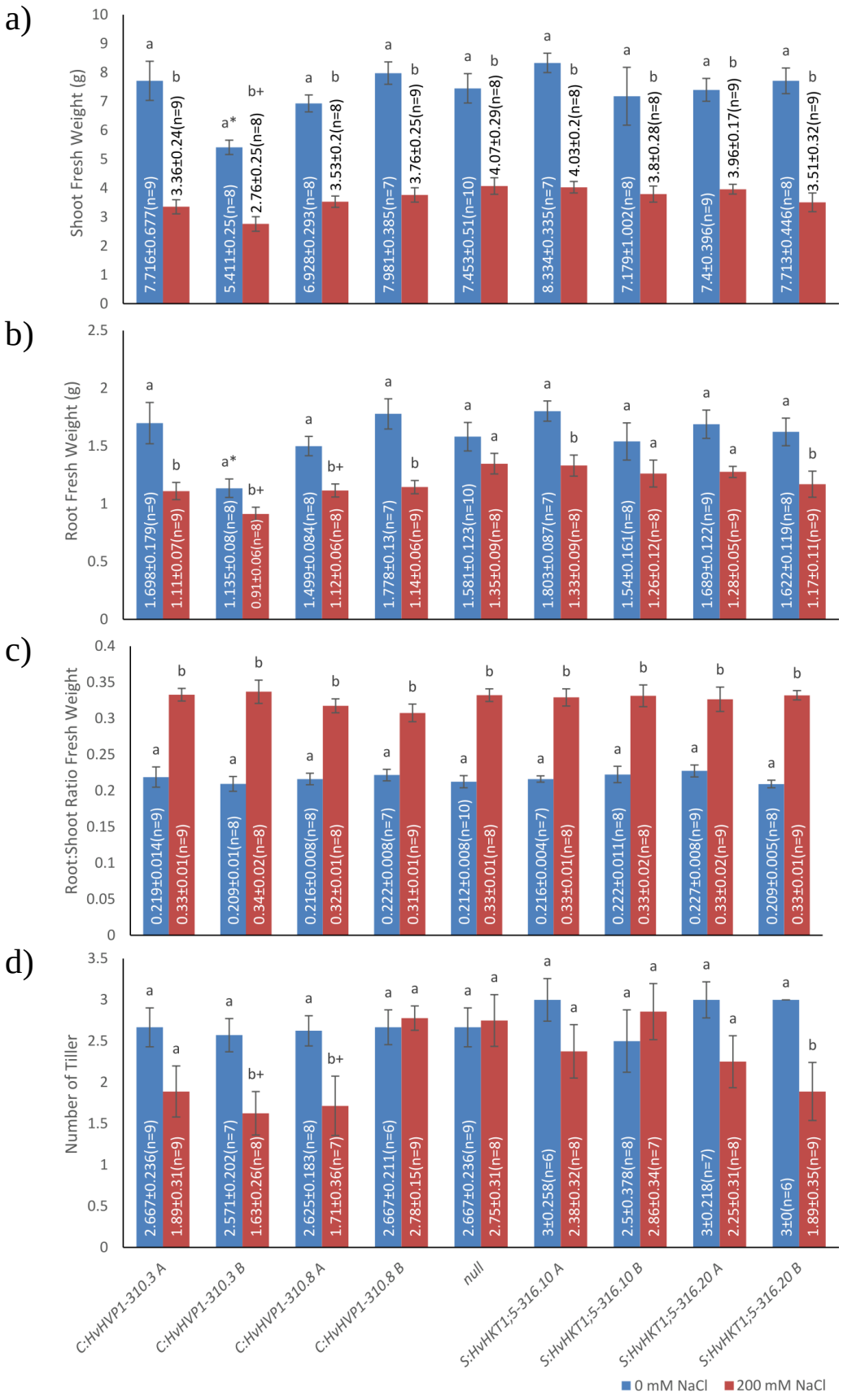
a)
Shoot Fresh Weight (g)
7.716±0.677(n=9)
3.36±0.24(n=9)
5.411±0.25(n=8)
2.76±0.25(n=8)
6.928±0.293(n=8)
3.53±0.2(n=8)
7.981±0.385(n=7)
3.76±0.25(n=9)
7.453±0.51(n=10)
4.07±0.29(n=8)
8.334±0.335(n=7)
4.03±0.2(n=8)
7.179±1.002(n=8)
3.8±0.28(n=8)
7.4±0.396(n=9)
3.96±0.17(n=9)
7.713±0.446(n=8)
3.51±0.32(n=9)
b)
Root Fresh Weight (g)
1.698±0.179(n=9)
1.11±0.07(n=9)
1.135±0.08(n=8)
0.91±0.06(n=8)
1.499±0.084(n=8)
1.12±0.06(n=8)
1.778±0.13(n=7)
1.14±0.06(n=9)
1.581±0.123(n=10)
1.35±0.09(n=8)
1.803±0.087(n=7)
1.33±0.09(n=8)
1.54±0.161(n=8)
1.26±0.12(n=8)
1.689±0.122(n=9)
1.28±0.05(n=9)
1.622±0.119(n=8)
1.17±0.11(n=9)
c)
Root:Shoot Ratio Fresh Weight
0.219±0.014(n=9)
0.33±0.01(n=9)
0.209±0.01(n=8)
0.34±0.02(n=8)
0.216±0.008(n=8)
0.32±0.01(n=8)
0.222±0.008(n=7)
0.31±0.01(n=9)
0.212±0.008(n=10)
0.33±0.01(n=8)
0.216±0.004(n=7)
0.33±0.01(n=8)
0.222±0.011(n=8)
0.33±0.02(n=8)
0.227±0.008(n=9)
0.33±0.02(n=9)
0.209±0.005(n=8)
0.33±0.01(n=9)
d)
Number of Tiller
2.667±0.236(n=9)
1.89±0.31(n=9)
2.571±0.202(n=7)
1.63±0.26(n=8)
2.625±0.183(n=8)
1.71±0.36(n=7)
2.667±0.211(n=6)
2.78±0.15(n=9)
2.667±0.236(n=9)
2.75±0.31(n=8)
3±0.258(n=6)
2.38±0.32(n=8)
2.5±0.378(n=8)
2.86±0.34(n=7)
3±0.218(n=7)
2.25±0.31(n=8)
3±0(n=6)
1.89±0.35(n=9)
C:HvHVP1-310.3 A
C:HvHVP1-310.3 B
C:HvHVP1-310.8 A
C:HvHVP1-310.8 B
null
S:HvHKT1;5-316.10 A
S:HvHKT1;5-316.10 B
S:HvHKT1;5-316.20 A
S:HvHKT1;5-316.20 B
0 mM NaCl
200 mM NaCl

Figure 3.11: Root and shoot biomass of T_3 transgenic barley lines expressing *HvHVP1* or *HvHKT1;5* under the control of putative cell-type specific promoters were similar to null segregants.
Mean shoot (a) and root (b) fresh weight measurements, fresh weight root-shoot ratio (c) and tiller number (d) of selected lines grown in supported hydroponics. Two sibling lines from each of four independent transgenic lines expressing either; *HvHVP1* under the putative root-cortex specific promoter *proC34* (*C:HvHVP1-310.3* A & B and *C:HvHVP1-310.8* A & B); or *HvHKT1;5* driven by the putative root-stele specific promoter *proS147* (*S:HKT1;5-316.10* A & B and *S:HKT1;5-316.20* A & B); and null segregants. Plants were grown in supported hydroponics and exposed to either 0 or 200 mM NaCl for 21 days before harvest. Values plotted are means ± SEM (shown on graph). Letters represent significant differences within lines but between treatments (one-way ANOVA, Tukey-Kramer, $P \leq 0.05$). * and + represent significant difference from null segregants grown in either control conditions or 150 mM NaCl respectively (one-way ANOVA, Tukey-Kramer, $P \leq 0.05$)

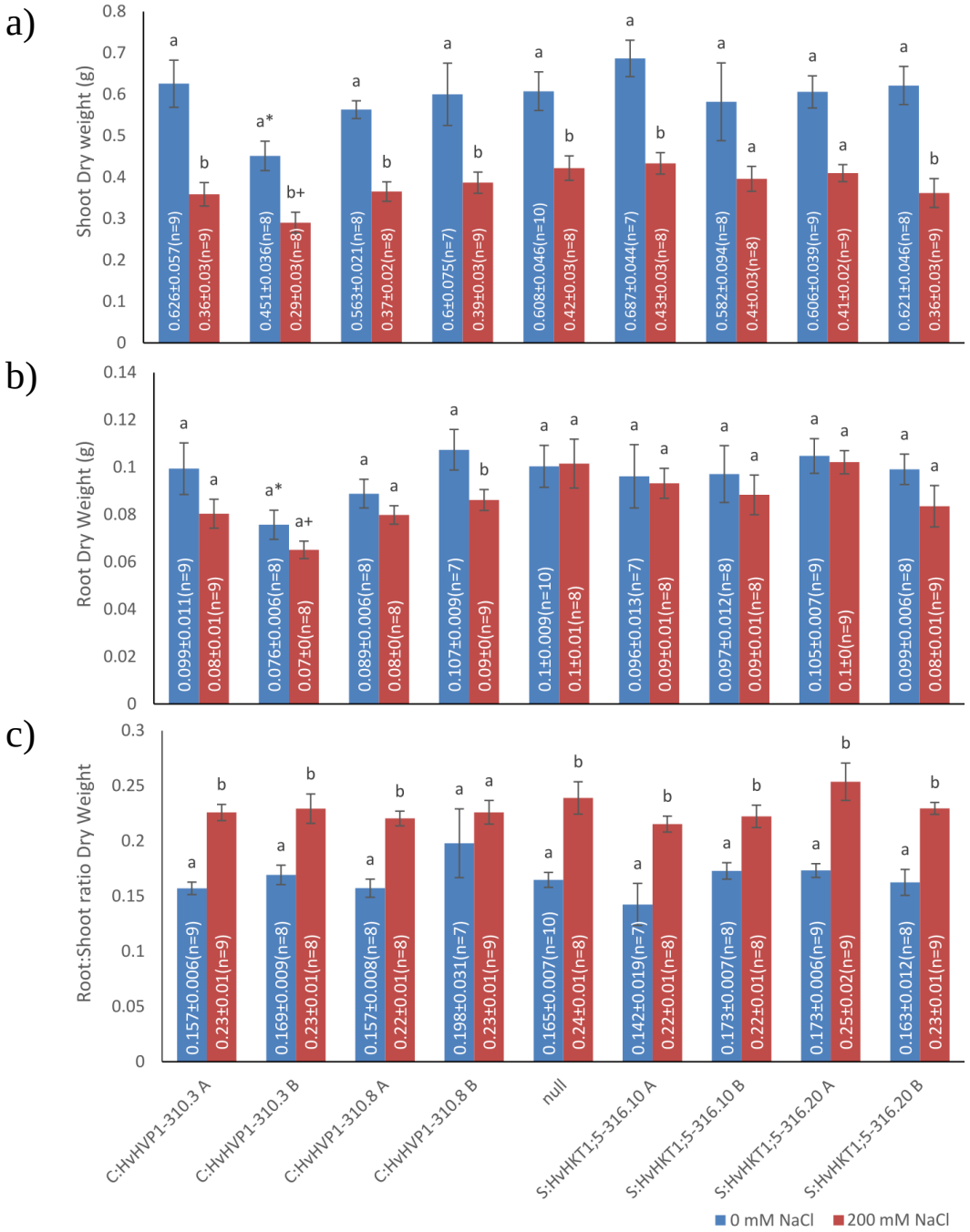

Figure 3.12: Root and shoot dry weight biomass of T_3 transgenic barley lines expressing *HvHVP1* or *HvHKT1*;5 under the control of putative cell-type specific promoters were similar to that of null segregants.

Mean shoot (a) and root (b) dry weight measurements and root-shoot ratio (c) of selected lines in supported hydroponics. Two sibling lines from each of four independent transgenic lines expressing either; *HvHVP1* under the putative root-cortex specific promoter *proC34* (C:HvHVP1-310.3 A & B and C:HvHVP1-310.8 A & B); or *HvHKT1*;5 driven by the putative root-stele specific promoter *proS147* (S:HKT1;5-316.10 A & B and S:HKT1;5-316.20 A & B); and null segregants. Plants were grown in supported hydroponics and exposed to either 0 or 200 mM NaCl for 21 days before harvest. Values plotted are means ± SEM (shown on graph) letters representing significant difference (one-way ANOVA, Tukey-Kramer, $P \leq 0.05$).

3.3.2.3. Ion concentration (Na^+, K^+ and Cl^-) in 4th leaf and roots of all transgenic lines are similar to null segregants

Significant increases in shoot [Na^+] and [Cl^-] and a significant decrease in shoot [K^+] were observed when all plants were grown in 200 mM NaCl (Figure 3.13, a, b & c). A similar trend was also observed in root tissues (Figure 3.14, a, b, c). There was little difference in ion accumulation between the transgenic and null lines. Only one line (310.3B) showed a significant reduction in 4th leaf Na^+ from the null segregants under 200 mM NaCl however it is to be noted that this line was smaller overall compared to null lines (Figure 3.11, a) and a similar phenotype was not observed in its sibling line 310.3 A.

No significant difference was observed between transgenic and the null segregants for 4th leaf Cl^- content (Figure 3.13, c). Although not significant, line 310.3 B displayed a trend towards lower Cl^- content, again possibly due to this line's overall reduced biomass as seen for Na^+ content. Under 200 mM NaCl conditions, the 310.3 A line had significantly higher root [Cl^-] (+26 %) than null segregants, while the sibling line 310.3 B was also trending higher although not significantly.

Interestingly, all *proS147*:*HvHKT1;5* lines (316.10 A & B, 316.20 A & B) tended to have on average a 25% increase in 4th leaf [K^+] compared to nulls under 200 mM NaCl leading to slightly decreased 4th leaf [Na^+]:[K^+] (Figure 3.13, d) although this was not statistically significant (one-way ANOVA, Tukey-Kramer, $P \leq 0.05$). Conversely, these lines also had slightly increased root [Na^+] leading to slight, but not significant, increase in root [Na^+]:[K^+] (Figure 3.14, d).

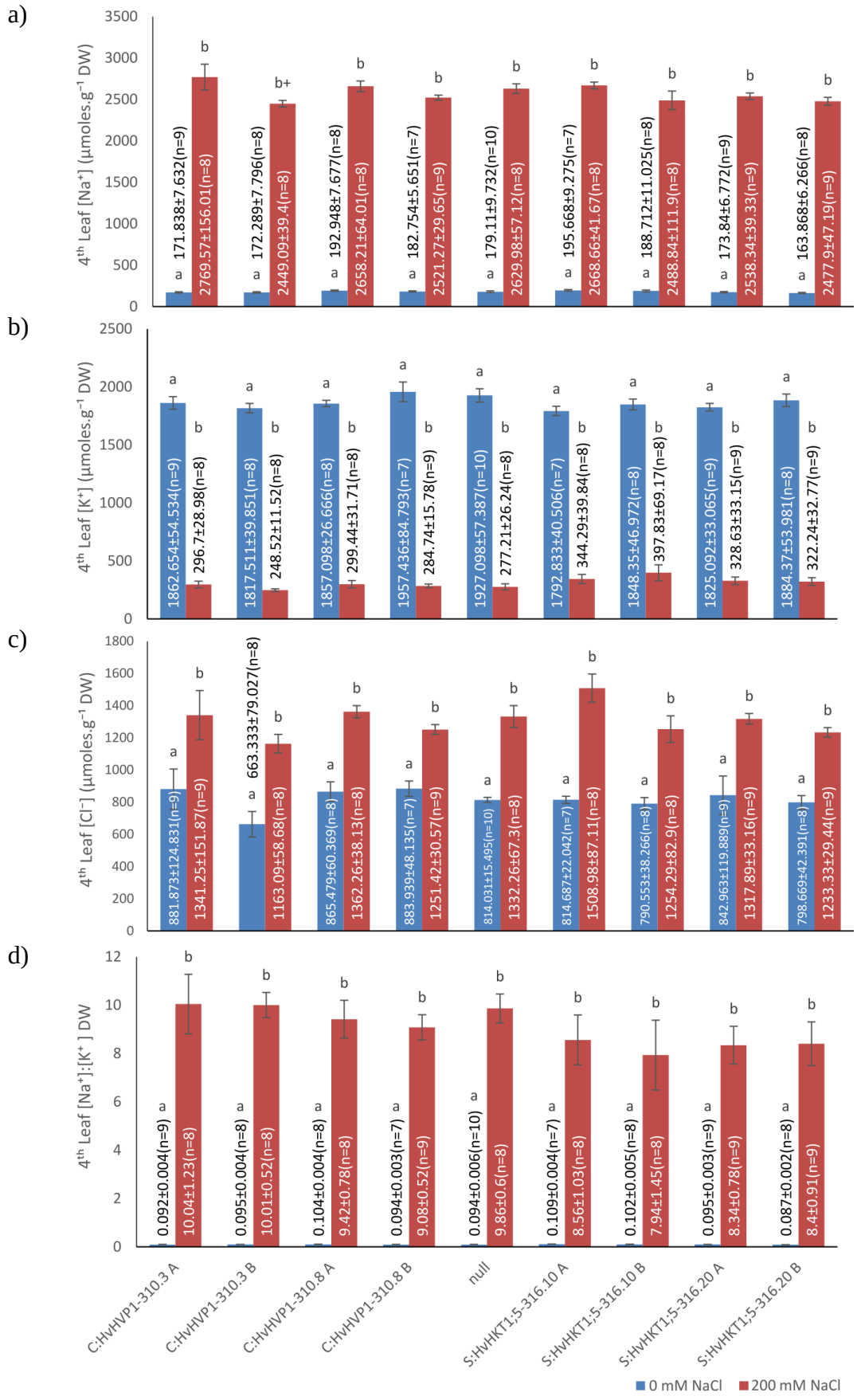
a)
4th Leaf [Na+] (µmoles.g-1 DW)
171.838±7.632(n=9)
2769.57±156.01(n=8)
172.289±7.796(n=8)
2449.09±39.4(n=8)
192.948±7.677(n=8)
2658.21±64.01(n=8)
182.754±5.651(n=7)
2521.27±29.65(n=9)
179.11±9.732(n=10)
2629.98±57.12(n=8)
195.668±9.275(n=7)
2668.66±41.67(n=8)
188.712±11.025(n=8)
2488.84±111.9(n=8)
173.84±6.772(n=9)
2538.34±39.33(n=9)
163.868±6.266(n=8)
2477.9±47.19(n=9)
b)
4th Leaf [K+] (µmoles.g-1 DW)
1862.654±54.534(n=9)
296.7±28.98(n=8)
1817.511±39.851(n=8)
248.52±11.52(n=8)
1857.098±26.666(n=8)
299.44±31.71(n=8)
1957.436±84.793(n=7)
284.74±15.78(n=9)
1927.098±57.387(n=10)
277.21±26.24(n=8)
1792.833±40.506(n=7)
344.29±39.84(n=8)
1848.35±46.972(n=8)
397.83±69.17(n=8)
1825.092±33.065(n=9)
328.63±33.15(n=9)
1884.37±53.981(n=8)
322.24±32.77(n=9)
c)
4th Leaf [Cl-] (µmoles.g-1 DW)
881.873±124.831(n=9)
1341.25±151.87(n=9)
663.333±79.027(n=8)
1163.09±58.68(n=8)
865.479±60.369(n=8)
1362.26±38.13(n=8)
883.939±48.135(n=7)
1251.42±30.57(n=9)
814.031±15.495(n=10)
1332.26±67.3(n=8)
814.687±22.042(n=7)
1508.98±87.11(n=8)
790.553±38.266(n=8)
1254.29±82.9(n=8)
842.963±119.889(n=9)
1317.89±33.16(n=9)
798.669±42.391(n=8)
1233.33±29.44(n=9)
d)
4th Leaf [Na+]:[K+] DW
0.092±0.004(n=9)
10.04±1.23(n=8)
0.095±0.004(n=8)
10.01±0.52(n=8)
0.104±0.004(n=8)
9.42±0.78(n=8)
0.094±0.003(n=7)
9.08±0.52(n=9)
0.094±0.006(n=10)
9.86±0.6(n=8)
0.109±0.004(n=7)
8.56±1.03(n=8)
0.102±0.005(n=8)
7.94±1.45(n=8)
0.095±0.003(n=9)
8.34±0.78(n=9)
0.087±0.002(n=8)
8.4±0.91(n=9)
C:HvHVP1-310.3 A
C:HvHVP1-310.3 B
C:HvHVP1-310.8 A
C:HvHVP1-310.8 B
null
S:HvHKT1;5-316.10 A
S:HvHKT1;5-316.10 B
S:HvHKT1;5-316.20 A
S:HvHKT1;5-316.20 B
0 mM NaCl
200 mM NaCl

Figure 3.13: 4th leaf ion (Na^+, K^+ and Cl^-) content of T_3 transgenic barley lines expressing *HvHVP1* or *HvHKT1;5* under the control of putative cell-type specific promoters were similar to null segregants.
Mean 4th leaf DW [Na^+] (a), [K^+] (b) and [Cl^-] (c) measurements and 4th leaf [Na^+]:[K^+] ratio (d) of selected lines in supported hydroponics. Two T_3 sibling lines from each of four independent transgenic lines expressing either; *HvHVP1* under the putative root-cortex specific promoter *proC34* (C:HvHVP1-310.3 A & B and C:HvHVP1-310.8 A & B); or *HvHKT1;5* driven by the putative root-stele specific promoter *proS147* (S:HKT1;5-316.10 A & B and S:HKT1;5-316.20 A & B); and null segregants. Plants were grown in supported hydroponics and exposed to either 0 or 200 mM NaCl for 21 days before harvest. Values plotted are means ± SEM (shown on graph) letters representing significant difference (one-way ANOVA, Tukey-Kramer, $P \leq 0.05$).

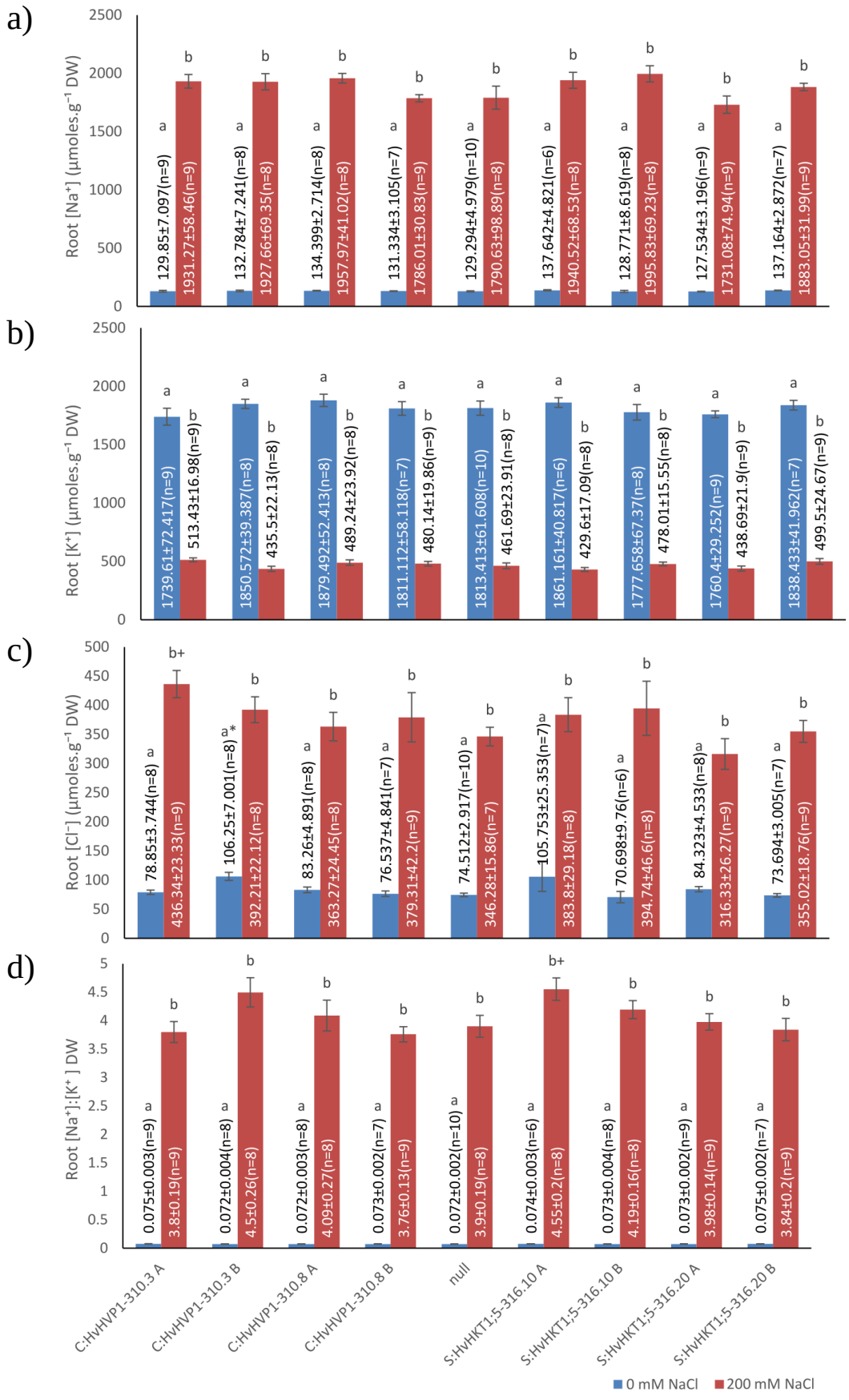
a)
Root [Na+] (µmoles.g-1 DW)
2500
2000
1500
1000
500
0
129.85±7.097(n=9)
1931.27±58.46(n=9)
132.784±7.241(n=8)
1927.66±69.35(n=8)
134.399±2.714(n=8)
1957.97±41.02(n=8)
131.334±3.105(n=7)
1786.01±30.83(n=9)
129.294±4.979(n=10)
1790.63±98.89(n=8)
137.642±4.821(n=6)
1940.52±68.53(n=8)
128.771±8.619(n=8)
1995.83±69.23(n=8)
127.534±3.196(n=9)
1731.08±74.94(n=9)
137.164±2.872(n=7)
1883.05±31.99(n=9)
b)
Root [K+] (µmoles.g-1 DW)
1739.61±72.417(n=9)
513.43±16.98(n=9)
1850.572±39.387(n=8)
435.5±22.13(n=8)
1879.492±52.413(n=8)
489.24±23.92(n=8)
1811.112±58.118(n=7)
480.14±19.86(n=9)
1813.413±61.608(n=10)
461.69±23.91(n=8)
1861.161±40.817(n=6)
429.6±17.09(n=8)
1777.658±67.37(n=8)
478.01±15.55(n=8)
1760.4±29.252(n=9)
438.69±21.9(n=9)
1838.433±41.962(n=7)
499.5±24.67(n=9)
c)
Root [Cl-] (µmoles.g-1 DW)
500
450
400
350
300
250
200
150
100
50
0
78.85±3.744(n=8)
436.34±23.33(n=9)
106.25±7.001(n=8)
392.21±22.12(n=8)
83.26±4.891(n=8)
363.27±24.45(n=8)
76.537±4.841(n=7)
379.31±42.2(n=9)
74.512±2.917(n=10)
346.28±15.86(n=7)
105.753±25.353(n=7)
383.8±29.18(n=8)
70.698±9.76(n=6)
394.74±46.6(n=8)
84.323±4.533(n=8)
316.33±26.27(n=9)
73.694±3.005(n=7)
355.02±18.76(n=9)
d)
Root [Na+]:[K+] DW
5
4.5
4
3.5
3
2.5
2
1.5
1
0.5
0
0.075±0.003(n=9)
3.8±0.19(n=9)
0.072±0.004(n=8)
4.5±0.26(n=8)
0.072±0.003(n=8)
4.09±0.27(n=8)
0.073±0.002(n=7)
3.76±0.13(n=9)
0.072±0.002(n=10)
3.9±0.19(n=8)
0.074±0.003(n=6)
4.55±0.2(n=8)
0.073±0.004(n=8)
4.19±0.16(n=8)
0.073±0.002(n=9)
3.98±0.14(n=9)
0.075±0.002(n=7)
3.84±0.2(n=9)
C:HvHVP1-310.3 A
C:HvHVP1-310.3 B
C:HvHVP1-310.8 A
C:HvHVP1-310.8 B
null
S:HvHKT1;5-316.10 A
S:HvHKT1;5-316.10 B
S:HvHKT1;5-316.20 A
S:HvHKT1;5-316.20 B
0 mM NaCl
200 mM NaCl

Figure 3.14: Root ion (Na^+, K^+ and Cl^-) content of T_3 transgenic barley lines expressing *HvHVP1* or *HvHKT1;5* under the control of putative cell-type specific promoters were similar to null segregants

Mean root DW [Na^+] (a), [K^+] (b) and [Cl^-] (c) measurements and 4th leaf [Na^+]:[K^+] ratio (d) of selected lines in supported hydroponics. Two sibling lines from each of four independent transgenic lines expressing either; *HvHVP1* under the putative root-cortex specific promoter *proC34* (C:HvHVP1-310.3 A & B and C:HvHVP1-310.8 A & B); or *HvHKT1;5* driven by the putative root-stele specific promoter *proS147* (S:HKT1;5-316.10 A & B and S:HKT1;5-316.20 A & B); and null segregants. Plants were grown in supported hydroponics and exposed to either 0 or 200 mM NaCl for 21 days before harvest. Values plotted are means ± SEM (shown on graph) letters representing significant difference (one-way ANOVA, Tukey-Kramer, $P \leq 0.05$).

3.3.2.4. Assessing rhizosphere acidification potential of *HvHVP1* when expressed under the putative root-cortex specific promoter *proC34* in barley

To assess potential enhanced rhizosphere acidification in the transgenic barley line over-expressing *HvHVP1* driven by the putative root-cortex specific promoter *proC34*, T_3 transgenic lines, examined in the previous supported hydroponics experiment (section 3.3.2), were germinated and 7-day old seedlings transferred into trays containing solidifying bromocresol media (as per section 3.2.10). At four hours following transfer, while all lines showed rhizosphere acidification by a pH-induced colour change in the media surrounding the root zone, no conclusive difference in colour or acidified area was distinguishable between transgenic lines (Figure 3.15, b, c, f, g, n = 4), wild-type plants (a,e) or the respective null lines (d, h). Some increased acidification around the seed of two seedlings in (b, tray 4) and (f, tray 1) is likely due to cytoplasmic leakage when roots are damaged during transfer. There may be increased rhizosphere acidification compared to wild-type plants, however, differences between transgenic and selected null lines suggest this result may be an artefact of the assay.

Further optimisation of the assay to improve repeatability and visualisation could have been attempted. However, as there is little evidence to support improved plant growth or salinity tolerance in the initial hydroponics experiments, or evidence to suggest high over-expression of transgenes under the *proC34* promoter based in the *GFP* or *uidA* assays (section 3.3.1) it is unlikely that *HvHVP1* expressed under the control of *proC34*, is resulting in increased rhizosphere acidification.

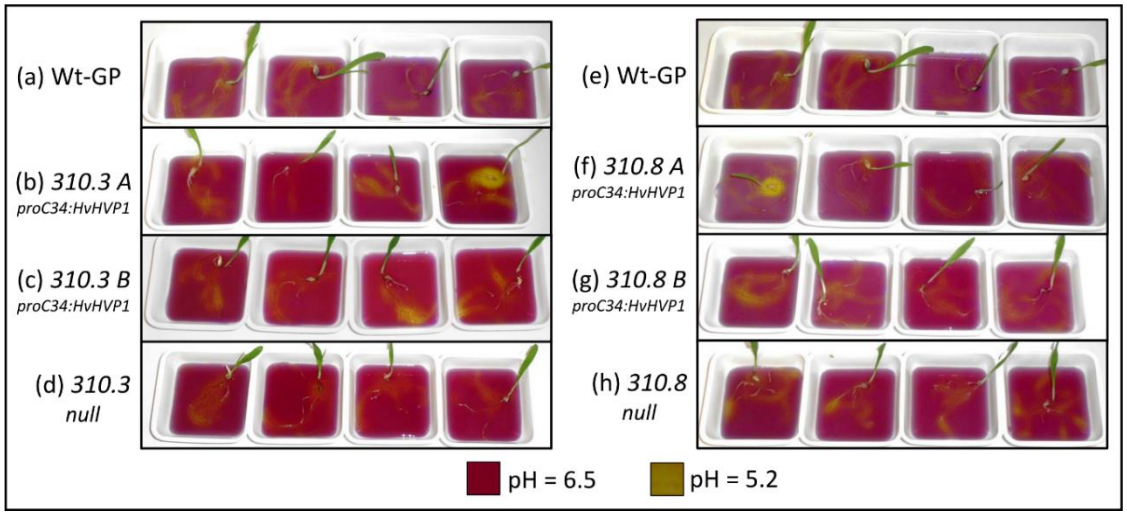

Figure 3.15: Rhizosphere acidification of 7-day old seedlings expressing *HvHVP1* under the control of putative root-cortex specific promoter *proC34*
Representative images of 7 d-old seedlings of Golden Promise (a, e – Wt-GP), two T3 sibling line from 2 independent *proC34:HvHVP1* over-expressing lines (310.3 A (b) & 310.3 B (c) and 310.8 A (f) & B (g)) and respective null segregants (d, h). Images taken 4 h after solidification of the bromocresol purple media at pH 6.5. All lines show rhizosphere acidification by colour change in the media from purple (pH ≈ 6.5) to yellow (pH ≈ 5.2). No conclusive difference is area acidified or greater colour change was observable between Wild-type plants, transgenic lines, or their respective nulls.

3.3.3. Development of transgenic barley lines over-expressing *HvHVP1* and *HvHKT1;5* in different root cell-types.

To develop lines with over-expression of *HvHVP1* in the root cortex and *HvHKT1;5* in the root stele, two independent T_2 lines expressing *HvHVP1* under the control putative root-cortex specific promoter *proC34* (*proC34:HvHVP1* - 310.3 and 310.8) and two independent T_2 lines expressing *HvHKT1;5* under the control of putative root-stele specific promoter *proS147* (*proS147:HvHKT1;5* - 316.10 and 316.20) were selected for crossing. A delay in flowering of the *proC34:HvHVP1* line (310.3) prevented the use of this line for crossing, while poor seed set in the *proS147:HvHKT1;5* line (316.20) prevented the recovery of F_1 progeny. Several reciprocal crossing events were successfully conducted between *proC34:HvHVP1* line 310.8 and *proS147:HvHKT1;1* line 316.10 and produced viable T_3F_1 progeny.

Resultant progeny were grown in soil and selected for the presence of both *proC34:HvHVP1* and *proS147:HvHKT1;5* constructs by PCR. Subsequent T_4F_2 progeny were trialled in a mini-hydroponics experiment (0 or 150 mM NaCl treatments) and lines for further testing were identified (not shown). In total, four T_5F_3 lines positive for both the *proC34:HvHVP1* and *proS147:HvHKT1;1* constructs (A, B, C, D) were selected for further testing in mini-hydroponics (section 3.3.4) and later in flood-drain supported

hydroponics (section 3.3.5). Consecutively grown, T_5 parental lines and nulls were also selected for analysis and are outlined in Table 3.5.

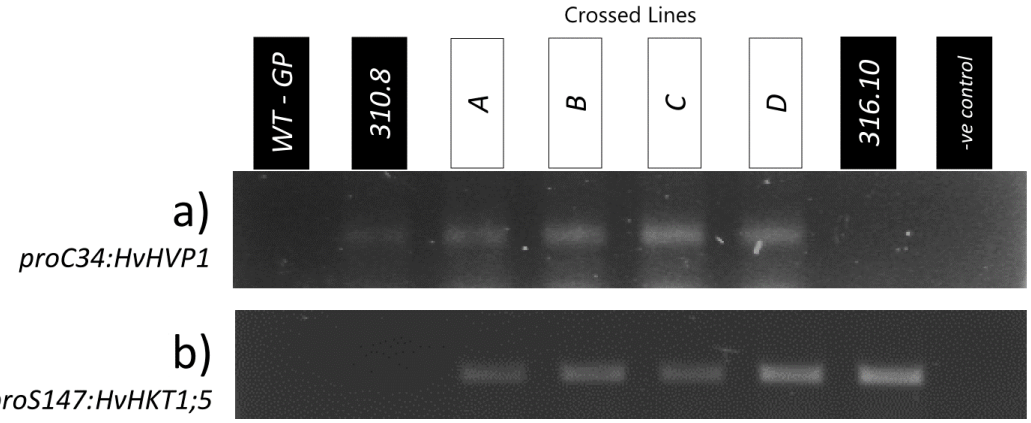

Figure 3.16: Presence of *proC34:HvHVP1* and *proS147:HvHKT1;5* constructs in leaf determined by genotyping PCR in T_5 (310.8 and 316.10) and T_5F_4 (A, B, C & D) lines selected for salinity screening in supported hydroponics.
Genotyping PCR on gDNA extracted from leaf material of selected T_5 (310.8 and 316.10) and T_5F_4 crossed lines (A, B, C & D) for the presence of *proC34:HvHVP1* (a) and *proS147::HvHKT1;5* (b) constructs. Negative (water) and wild-type Golden Promise (WT-GP) included as controls.

Table 3.5: T_5 and crossed T_5F_3 barley cv. Golden Promise lines, expressing *proS147:HvHKT1;5* and/or *proC34:HvHVP1* selected for analysis in later experiments.
Information included; Line identification, presence of transgene constructs and parents

Line	Transgenes	Parent ♀	Parent ♂
T_5F_3 A	*proS147:HvHKT1;5* + *proC34:HvHVP1*	*proS147:HvHKT1;5* 316.10	*proC34:HvHVP1* *310.8*
T_5F_3 B	*proS147:HvHKT1;5* + *proC34:HvHVP1*	*proS147:HvHKT1;5* 316.10	*proC34:HvHVP1* 310.8
T_5F_3 C	*proC34:HvHVP1* + *proS147:HvHKT1;5*	*proC34:HvHVP1* 310.8	*proS147:HvHKT1;5* 316.10
T_5F_3 D	*proC34:HvHVP1* + *proS147:HvHKT1;5*	*proC34:HvHVP1* 310.8	*proS147:HvHKT1;5* 316.10
T_5 316.10 null	*Null*	316.10 null	
T_5 316.10	*proS147:HvHKT1;5*	316.10 – selfed	
T_5 310.8 null	*Null*	310.8 null	
T_5 310.8	*proC34:HvHVP1*	310.8 – selfed	
GP	WT control - barley cv. Golden Promise		

3.3.4. Evaluating the salinity tolerance of lines over-expressing both *HvHVP1* and *HvHKT1;5* in mini-hydroponics

A mini-hydroponics experiment was carried out to screen the salinity tolerance of the T_5 parental, T_5F_3 crosses and segregants containing *proC34:HvHVP1* (MK15) and/or *proS147:HvHKT1;5* (MK25) lines outlined in Table 3.5.

Plants were germinated and grown in mini-hydroponics as per section 3.2.11. Plants were divided into two groups to which either 0 mM NaCl (control) or 150 mM NaCl (salinity treatment) was applied on the emergence of the 3rd leaf.

3.3.4.1. Expression of transgenes in the roots and shoots of transgenic plants

The presence of both the *proS147:HvHKT1;5* (MK25) and *proC34:HvHVP1* (MK15) constructs detected by PCR in genomic DNA their respective lines and lacking from the nulls lines. RT-PCR verified that the transgenic *HvHVP1* was expressed in the roots in the majority of samples, with some occasional low level of expression in leaf material. RT-PCR verified that transgenic *HvHKT1;5* was expressed at low levels in both root and leaf material of transgenic plants as seen previously.

3.3.4.2. Root and Shoot biomass of T_5F_3 plants is similar to segregants

As in the previous supported hydroponics experiment (section 3.3.2) conducted with parental lines containing either *proC34:HvHVP1* or *proS147:HvHKT1;5*, the T_5F_3 crosses and segregants did not have significantly altered shoot (Figure 3.17, a) or root biomass (Figure 3.17, b) compared to null segregants or Golden Promise . A significant reduction (≈-19%) in shoot biomass was observed in one of the parental T_5 lines 316.10 compared to null segregants, under control conditions for unknown reasons. Although not significantly different, the parental T_5 *proC34:HvHVP1* line 310.8 also had reduced growth compared to null segregants. These results are possibly due to the previous generation (T_4) of the parental lines being grown under slightly different glasshouse conditions from the T_5F_3 crosses which, although grown concurrently, were segregated in the glasshouse then genotyped.

The T_5F_3 segregants possessing only *proS147:HvHKT1;5* construct (T_5F_3 *HvHKT1;5/null*) or *proC34:HvHVP1* (T_5F_3 *HvHVP1/null*) however had similar root and shoot biomass to both null segregants and the 4 reciprocal crossed lines containing both *proC34:HvHVP1* and *proS147:HvHKT1;5* (T_5F_3 *HvHKT1;5/HvHVP1* A & B and T_5F_3 *HvHVP1/HvHKT1;5* C & D)

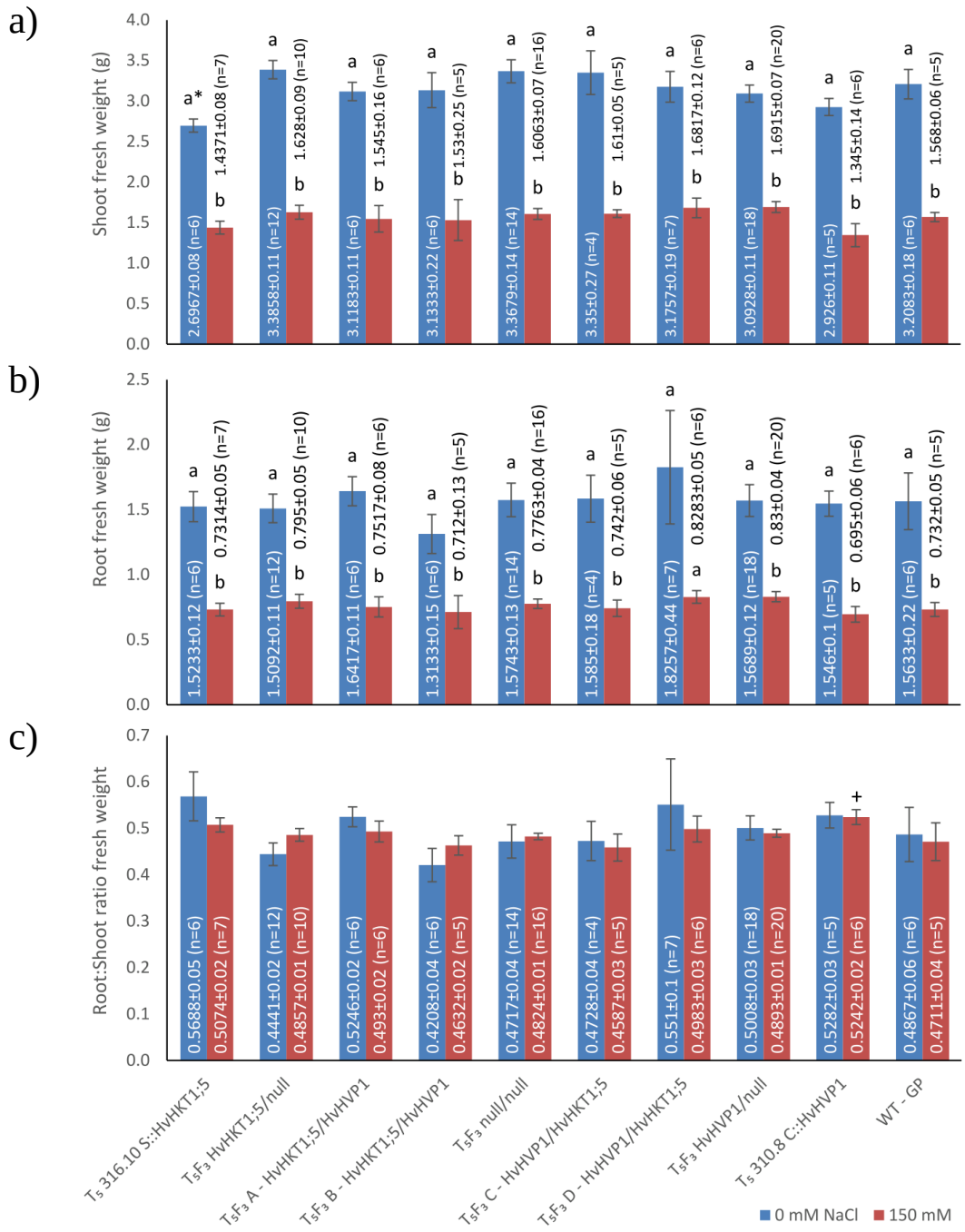
a)
Shoot fresh weight (g)
4.0
3.5
3.0
2.5
2.0
1.5
1.0
0.5
0.0
a*
b
1.4371±0.08 (n=7)
2.6967±0.08 (n=6)
a
b
1.628±0.09 (n=10)
3.3858±0.11 (n=12)
a
b
1.545±0.16 (n=6)
3.1183±0.11 (n=6)
a
b
1.53±0.25 (n=5)
3.1333±0.22 (n=6)
a
b
1.6063±0.07 (n=16)
3.3679±0.14 (n=14)
a
b
1.61±0.05 (n=5)
3.35±0.27 (n=4)
a
b
1.6817±0.12 (n=6)
3.1757±0.19 (n=7)
a
b
1.6915±0.07 (n=20)
3.0928±0.11 (n=18)
a
b
1.345±0.14 (n=6)
2.926±0.11 (n=5)
a
b
1.568±0.06 (n=5)
3.2083±0.18 (n=6)
b)
Root fresh weight (g)
2.5
2.0
1.5
1.0
0.5
0.0
a
b
0.7314±0.05 (n=7)
1.5233±0.12 (n=6)
a
b
0.795±0.05 (n=10)
1.5092±0.11 (n=12)
a
b
0.7517±0.08 (n=6)
1.6417±0.11 (n=6)
a
b
0.712±0.13 (n=5)
1.3133±0.15 (n=6)
a
b
0.7763±0.04 (n=16)
1.5743±0.13 (n=14)
a
b
0.742±0.06 (n=5)
1.585±0.18 (n=4)
a
a
0.8283±0.05 (n=6)
1.8257±0.44 (n=7)
a
b
0.83±0.04 (n=20)
1.5689±0.12 (n=18)
a
b
0.695±0.06 (n=6)
1.546±0.1 (n=5)
a
b
0.732±0.05 (n=5)
1.5633±0.22 (n=6)
c)
Root:Shoot ratio fresh weight
0.7
0.6
0.5
0.4
0.3
0.2
0.1
0.0
0.5688±0.05 (n=6)
0.5074±0.02 (n=7)
0.4441±0.02 (n=12)
0.4857±0.01 (n=10)
0.5246±0.02 (n=6)
0.493±0.02 (n=6)
0.4208±0.04 (n=6)
0.4632±0.02 (n=5)
0.4717±0.04 (n=14)
0.4824±0.01 (n=16)
0.4728±0.04 (n=4)
0.4587±0.03 (n=5)
0.551±0.1 (n=7)
0.4983±0.03 (n=6)
0.5008±0.03 (n=18)
0.4893±0.01 (n=20)
0.5282±0.03 (n=5)
+
0.5242±0.02 (n=6)
0.4867±0.06 (n=6)
0.4711±0.04 (n=5)
T5 316.10 S::HvHKT1;5
T5F3 HvHKT1;5/null
T5F3 A - HvHKT1;5/HvHVP1
T5F3 B - HvHKT1;5/HvHVP1
T5F3 null/null
T5F3 C - HvHVP1/HvHKT1;5
T5F3 D - HvHVP1/HvHKT1;5
T5F3 HvHVP1/null
T5 310.8 C::HvHVP1
WT - GP
0 mM NaCl
150 mM

Figure 3.17: Root and shoot biomass of nulls and T_5F_3 transgenic barley lines expressing *HvHVP1* and/or *HvHKT1;5* under the control of putative cell-type specific promoters are similar to null segregants and parental lines.
Mean shoot (a) and root (b) fresh weight measurements and root-shoot ratio (c) of selected lines: Four T_5F_3 lines (A, B, C, D) expressing both *HvHVP1* under the putative root-cortex specific promoter *proC34* (*proC34:HvHVP1*) and *HvHKT1;5* driven by the putative root-stele specific promoter *proS147* (*proC34:HvHVP1*). Segregants were grouped into Null segregants (T_5F_3 *null/null)* or segregants containing only *proC34:HvHVP1* or *proS147:HvHKT1;5* constructs (T_5F_3 *proC34:HvHVP1/null* or T_5F_3 *proS147:HvHKT1;5/null*). Two parental uncrossed T_5 lines (T_5 *316.10-S:HKT1;5* and T_5 310.8 C*:HvHVP1*) and wild-type Golden Promise were included for comparison. Plants were grown in mini-hydroponics and exposed to either 0 or 150 mM NaCl and grown for a further 14 days before harvest. Values plotted are means ± SEM (shown on graph). Letters represent significant differences within lines but between treatments (one-way ANOVA, Tukey-Kramer, $P \leq 0.05$). * and + represent significant difference from null segregants grown in either control conditions or 150 mM NaCl respectively (one-way ANOVA, Tukey-Kramer, $P \leq 0.05$)

3.3.4.3. Ion concentrations (Na^+, K^+ and Cl^-) in 4th leaf and roots of T_5F_3 transgenic lines are similar to segregants under control and 150 mM NaCl.

A significant treatment effect on the accumulation of the ions examined in this study (Na^+, K^+ and Cl^-) was observed between control plants and those grown at 150 mM NaCl in 4th leaf (Figure 3.18) and root tissue (Figure 3.19). However, there were no significant differences observed between the transgenic lines, segregants and the Golden Promise control. A slight decrease was observed in root and leaf Na^+ in the 4th leaf of both T_5 parental lines, 310.8 and 316.10 under control and 150 mM NaCl treatments (Figure 3.18, a), likely related to these plants overall reduced shoot biomass (Figure 3.17, a).

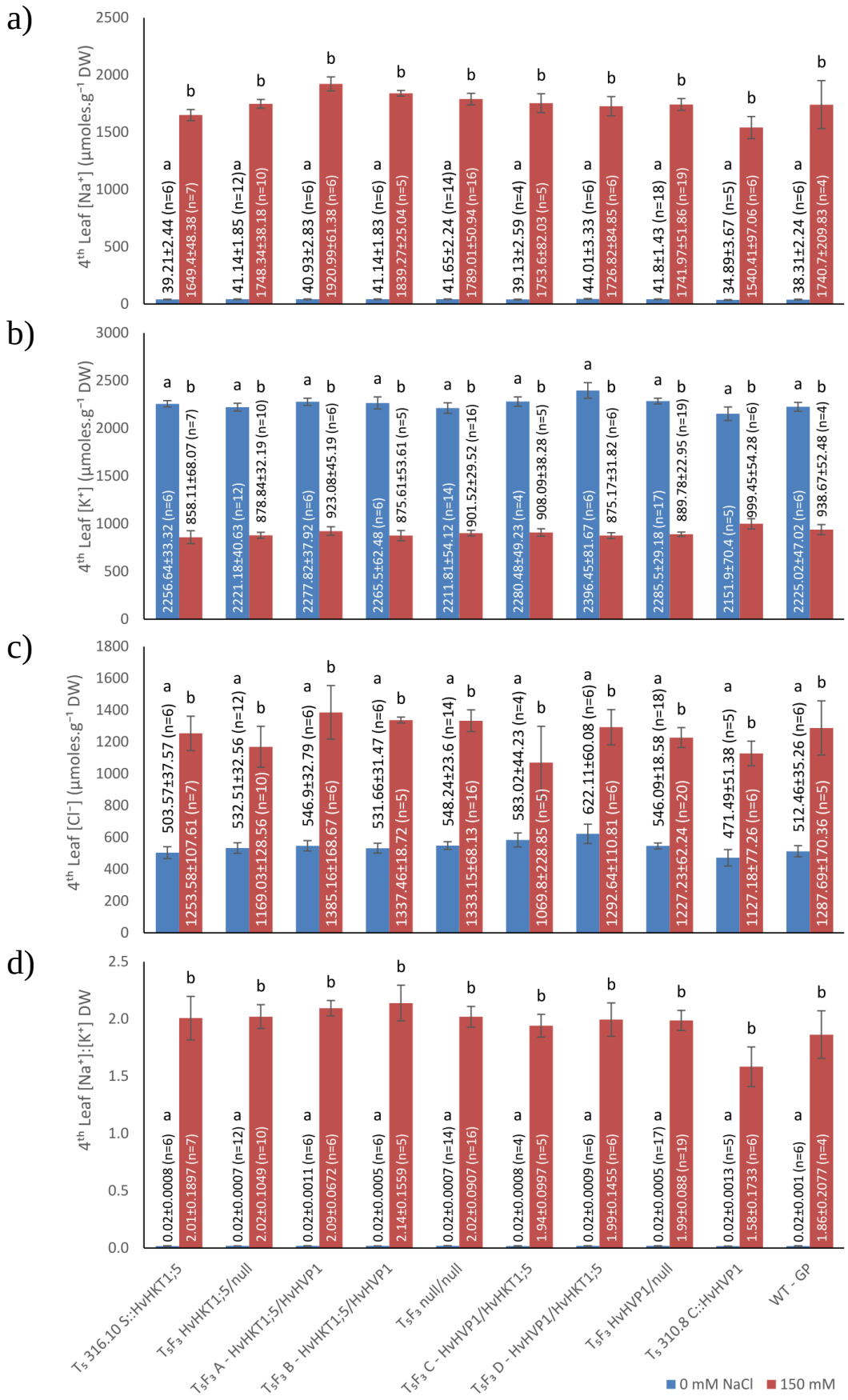
a)
4th Leaf [Na+] (µmoles.g-1 DW)
39.21±2.44 (n=6)
1649.4±48.38 (n=7)
41.14±1.85 (n=12)
1748.34±38.18 (n=10)
40.93±2.83 (n=6)
1920.99±61.38 (n=6)
41.14±1.83 (n=6)
1839.27±25.04 (n=5)
41.65±2.24 (n=14)
1789.01±50.94 (n=16)
39.13±2.59 (n=4)
1753.6±82.03 (n=5)
44.01±3.33 (n=6)
1726.82±84.85 (n=6)
41.8±1.43 (n=18)
1741.97±51.86 (n=19)
34.89±3.67 (n=5)
1540.41±97.06 (n=6)
38.31±2.24 (n=6)
1740.7±209.83 (n=4)
b)
4th Leaf [K+] (µmoles.g-1 DW)
2256.64±33.32 (n=6)
858.11±68.07 (n=7)
2221.18±40.63 (n=12)
878.84±32.19 (n=10)
2277.82±37.92 (n=6)
923.08±45.19 (n=6)
2265.5±62.48 (n=6)
875.61±53.61 (n=5)
2211.81±54.12 (n=14)
901.52±29.52 (n=16)
2280.48±49.23 (n=4)
908.09±38.28 (n=5)
2396.45±81.67 (n=6)
875.17±31.82 (n=6)
2285.5±29.18 (n=17)
889.78±22.95 (n=19)
2151.9±70.4 (n=5)
999.45±54.28 (n=6)
2225.02±47.02 (n=6)
938.67±52.48 (n=4)
c)
4th Leaf [Cl-] (µmoles.g-1 DW)
503.57±37.57 (n=6)
1253.58±107.61 (n=7)
532.51±32.56 (n=12)
1169.03±128.56 (n=10)
546.9±32.79 (n=6)
1385.16±168.67 (n=6)
531.66±31.47 (n=6)
1337.46±18.72 (n=5)
548.24±23.6 (n=14)
1333.15±68.13 (n=16)
583.02±44.23 (n=4)
1069.8±228.85 (n=5)
622.11±60.08 (n=6)
1292.64±110.81 (n=6)
546.09±18.58 (n=18)
1227.23±62.24 (n=20)
471.49±51.38 (n=5)
1127.18±77.26 (n=6)
512.46±35.26 (n=6)
1287.69±170.36 (n=5)
d)
4th Leaf [Na+]:[K+] DW
0.02±0.0008 (n=6)
2.01±0.1897 (n=7)
0.02±0.0007 (n=12)
2.02±0.1049 (n=10)
0.02±0.0011 (n=6)
2.09±0.0672 (n=6)
0.02±0.0005 (n=6)
2.14±0.1559 (n=5)
0.02±0.0007 (n=14)
2.02±0.0907 (n=16)
0.02±0.0008 (n=4)
1.94±0.0997 (n=5)
0.02±0.0009 (n=6)
1.99±0.1455 (n=6)
0.02±0.0005 (n=17)
1.99±0.088 (n=19)
0.02±0.0013 (n=5)
1.58±0.1733 (n=6)
0.02±0.001 (n=6)
1.86±0.2077 (n=4)
T5 316.10 S::HvHKT1;5
T5F3 HvHKT1;5/null
T5F3 A - HvHKT1;5/HvHVP1
T5F3 B - HvHKT1;5/HvHVP1
T5F3 null/null
T5F3 C - HvHVP1/HvHKT1;5
T5F3 D - HvHVP1/HvHKT1;5
T5F3 HvHVP1/null
T5 310.8 C::HvHVP1
WT - GP
0 mM NaCl
150 mM

Figure 3.18: 4th leaf ion (Na^+, K^+ and Cl^-) content of T_5F_3 transgenic barley lines expressing *HvHVP1* and/or *HvHKT1;5* under the control of putative cell-type specific promoters are similar to null segregants.
Mean 4th leaf DW [Na^+] (a), [K^+] (b) and [Cl^-] (c) measurements and 4th leaf [Na^+]:[K^+] ratio (d) of selected lines: Four T_5F_3 lines (A, B, C, D) expressing both *HvHVP1* under the putative root-cortex specific promoter *proC34* (*proC34:HvHVP1*) and *HvHKT1;5* driven by the putative root-stele specific promoter *proS147* (*proC34:HvHVP1*). Segregants were grouped into Null segregants (T_5F_3 *null/null)* or segregants containing only *proC34:HvHVP1* or *proS147:HvHKT1;5* constructs (T_5F_3 *proC34:HvHVP1/null* or T_5F_3 *proS147:HvHKT1;5/null*). Two parental uncrossed T_5 lines (T_5 *316.10-S:HKT1;5* and T_5 310.8 C*:HvHVP1*) and wild-type Golden Promise were included for comparison. Plants were grown in mini-hydroponics and exposed to either 0 or 150 mM NaCl and grown for a further 14 days before harvest. Values plotted are means ± SEM (shown on graph). Letters represent significant differences within lines but between treatments (one-way ANOVA, Tukey-Kramer, $P \leq 0.05$). * and + represent significant difference from null segregants grown in either control conditions or 150 mM NaCl respectively (one-way ANOVA, Tukey-Kramer, $P \leq 0.05$)

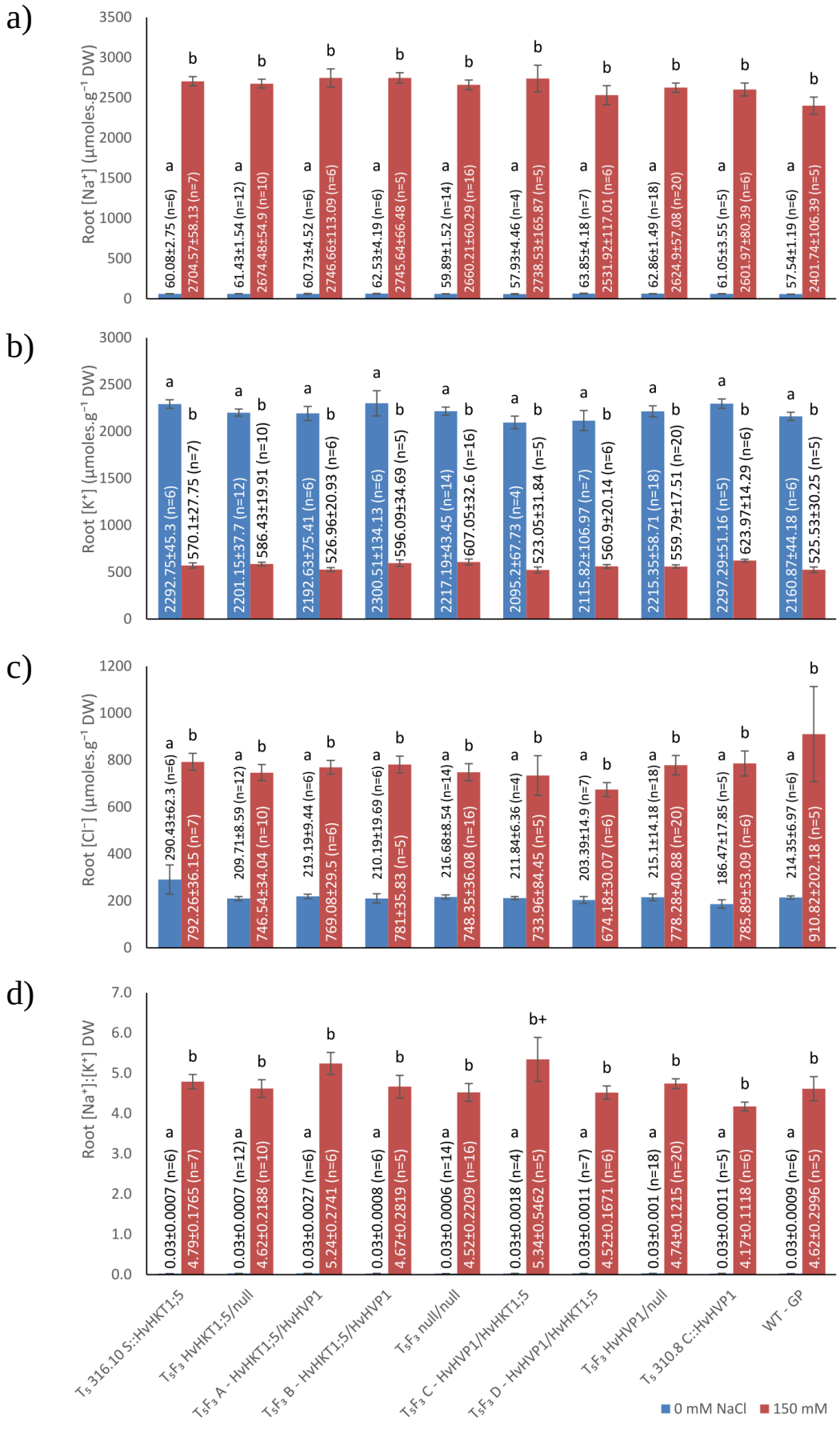
a)
Root [Na+] (µmoles.g-1 DW)
60.08±2.75 (n=6)
2704.57±58.13 (n=7)
61.43±1.54 (n=12)
2674.48±54.9 (n=10)
60.73±4.52 (n=6)
2746.66±113.09 (n=6)
62.53±4.19 (n=6)
2745.64±66.48 (n=5)
59.89±1.52 (n=14)
2660.21±60.29 (n=16)
57.93±4.46 (n=4)
2738.53±165.87 (n=5)
63.85±4.18 (n=7)
2531.92±117.01 (n=6)
62.86±1.49 (n=18)
2624.9±57.08 (n=20)
61.05±3.55 (n=5)
2601.97±80.39 (n=6)
57.54±1.19 (n=6)
2401.74±106.39 (n=5)
b)
Root [K+] (µmoles.g-1 DW)
2292.75±45.3 (n=6)
570.1±27.75 (n=7)
2201.15±37.7 (n=12)
586.43±19.91 (n=10)
2192.63±75.41 (n=6)
526.96±20.93 (n=6)
2300.51±134.13 (n=6)
596.09±34.69 (n=5)
2217.19±43.45 (n=14)
607.05±32.6 (n=16)
2095.2±67.73 (n=4)
523.05±31.84 (n=5)
2115.82±106.97 (n=7)
560.9±20.14 (n=6)
2215.35±58.71 (n=18)
559.79±17.51 (n=20)
2297.29±51.16 (n=5)
623.97±14.29 (n=6)
2160.87±44.18 (n=6)
525.53±30.25 (n=5)
c)
Root [Cl-] (µmoles.g-1 DW)
290.43±62.3 (n=6)
792.26±36.15 (n=7)
209.71±8.59 (n=12)
746.54±34.04 (n=10)
219.19±9.44 (n=6)
769.08±29.5 (n=6)
210.19±19.69 (n=6)
781±35.83 (n=5)
216.68±8.54 (n=14)
748.35±36.08 (n=16)
211.84±6.36 (n=4)
733.96±84.45 (n=5)
203.39±14.9 (n=7)
674.18±30.07 (n=6)
215.1±14.18 (n=18)
778.28±40.88 (n=20)
186.47±17.85 (n=5)
785.89±53.09 (n=6)
214.35±6.97 (n=6)
910.82±202.18 (n=5)
d)
Root [Na+]:[K+] DW
0.03±0.0007 (n=6)
4.79±0.1765 (n=7)
0.03±0.0007 (n=12)
4.62±0.2188 (n=10)
0.03±0.0027 (n=6)
5.24±0.2741 (n=6)
0.03±0.0008 (n=6)
4.67±0.2819 (n=5)
0.03±0.0006 (n=14)
4.52±0.2209 (n=16)
0.03±0.0018 (n=4)
5.34±0.5462 (n=5)
0.03±0.0011 (n=7)
4.52±0.1671 (n=6)
0.03±0.001 (n=18)
4.74±0.1215 (n=20)
0.03±0.0011 (n=5)
4.17±0.1118 (n=6)
0.03±0.0009 (n=6)
4.62±0.2996 (n=5)
T5 316.10 S::HvHKT1;5
T5F3 HvHKT1;5/null
T5F3 A - HvHKT1;5/HvHVP1
T5F3 B - HvHKT1;5/HvHVP1
T5F3 null/null
T5F3 C - HvHVP1/HvHKT1;5
T5F3 D - HvHVP1/HvHKT1;5
T5F3 HvHVP1/null
T5 310.8 C::HvHVP1
WT - GP
0 mM NaCl
150 mM

Figure 3.19: Root ion (Na^+, K^+ and Cl^-) content of nulls and T_3 transgenic barley lines expressing *HvHVP1* or *HvHKT1;5* under the control of putative cell-type specific promoters.
Mean root DW [Na^+] (a), [K^+] (b) and [Cl^-] (c) measurements and 4th leaf [Na^+]:[K^+] ratio (d) of selected lines: Four T_5F_3 lines (A, B, C, D) expressing both *HvHVP1* under the putative root-cortex specific promoter *proC34* (*proC34:HvHVP1*) and *HvHKT1;5* driven by the putative root-stele specific promoter *proS147* (*proC34:HvHVP1*). Segregants were grouped into Null segregants (T_5F_3 null/null*)* or segregants containing only *proC34:HvHVP1* or *proS147:HvHKT1;5* constructs (T_5F_3 proC34:HvHVP1/null or T_5F_3 proS147:HvHKT1;5/null). Two parental uncrossed T_5 lines (T_5 *316.10-S:*HKT1;5 and T_5 310.8 C*:*HvHVP1) and wild-type Golden Promise were included for comparison. Plants were grown in mini-hydroponics and exposed to either 0 or 150 mM NaCl and grown for a further 14 days before harvest. Values plotted are means ± SEM (shown on graph). Letters represent significant differences within lines but between treatments (one-way ANOVA, Tukey-Kramer, $P \leq 0.05$). * and + represent significant difference from null segregants grown in either control conditions or 150 mM NaCl respectively (one-way ANOVA, Tukey-Kramer, $P \leq 0.05$)

3.3.4.4. Summary of mini-hydroponics experiment

Although the mini-hydroponics experiment did not detect any significant differences between the lines co-expressing *HvHVP1* and *HvHKTl;5* and segregants or parental lines, possible improvements may have been obscured by the use of the mini-hydroponics set up. The salt stress (150 mM) may have not been severe enough or the treatment length (14 days) may have been too short for differences to be become apparent. Additionally, crowding and shading by neighbouring plants may have affected plant growth reducing transpiration and uptake of Na^+.

3.3.5. Evaluating the salinity tolerance of lines co-expressing *HvHVP1* and *HvHKT1;5* in supported hydroponics

T_6F_4 seed was collected from selected T_5F_3 individuals grown in control conditions in the previous mini-hydroponic experiment. Seed was selected by weight (43.0±0.5 mg) in an attempt to reduce possible variation due to seed quality. T_6F_4 seeds were germinated and assessed for salinity tolerance in supported hydroponics as per section 3.2.12 and treated with 0 or 200 mM NaCl.

3.3.5.1. Expression of transgenes in the roots and shoots of transgenic plants

The presence of both the *proS147:HvHKT1;5* and *proC34:HvHVP1* constructs was detected by PCR in the respective lines and was lacking in null lines. RT-PCR verified that the transgenic *HvHVP1* was expressed in the roots in the majority of samples, with some occasional low level of expression in leaf material. RT-PCR verified that transgenic *HvHKT1;5* was expressed at low levels in both root and leaf material of transgenic plants.

3.3.5.2. Root and shoot biomass may be improved in lines expressing both *HvHKT1;5* and *HvHVP1* under control conditions

As is the previous supported hydroponics experiment, there was a significant treatment effect on both root and shoot biomass between control and 200 mM NaCl treatments. Overall shoot FW biomass was reduced by ≈60 % (-35 % shoot DW biomass) and root FW biomass was reduced by ≈35 % (-23 % root DW biomass). Two of the T_6F_4 lines (*HvHKT1;5/HvHVP1* A, *HvHVP1/HvHKT1;5* C) showed significantly higher mean shoot (+42 % and +35 %) and root FW biomass (+34 % and +43 %) under control conditions when compared to null segregants. This increase was also maintained in the 200 mM treatment. The T_6 parental line 310.3 was also significantly larger under control and 200 mM NaCl treatments. The larger plant size of line *HvHKT1;5/HvHVP1* A and *HvHVP1/HvHKT1;5* C was also translated into a significant increase number of tillers over the null segregants lines in the control treatment.

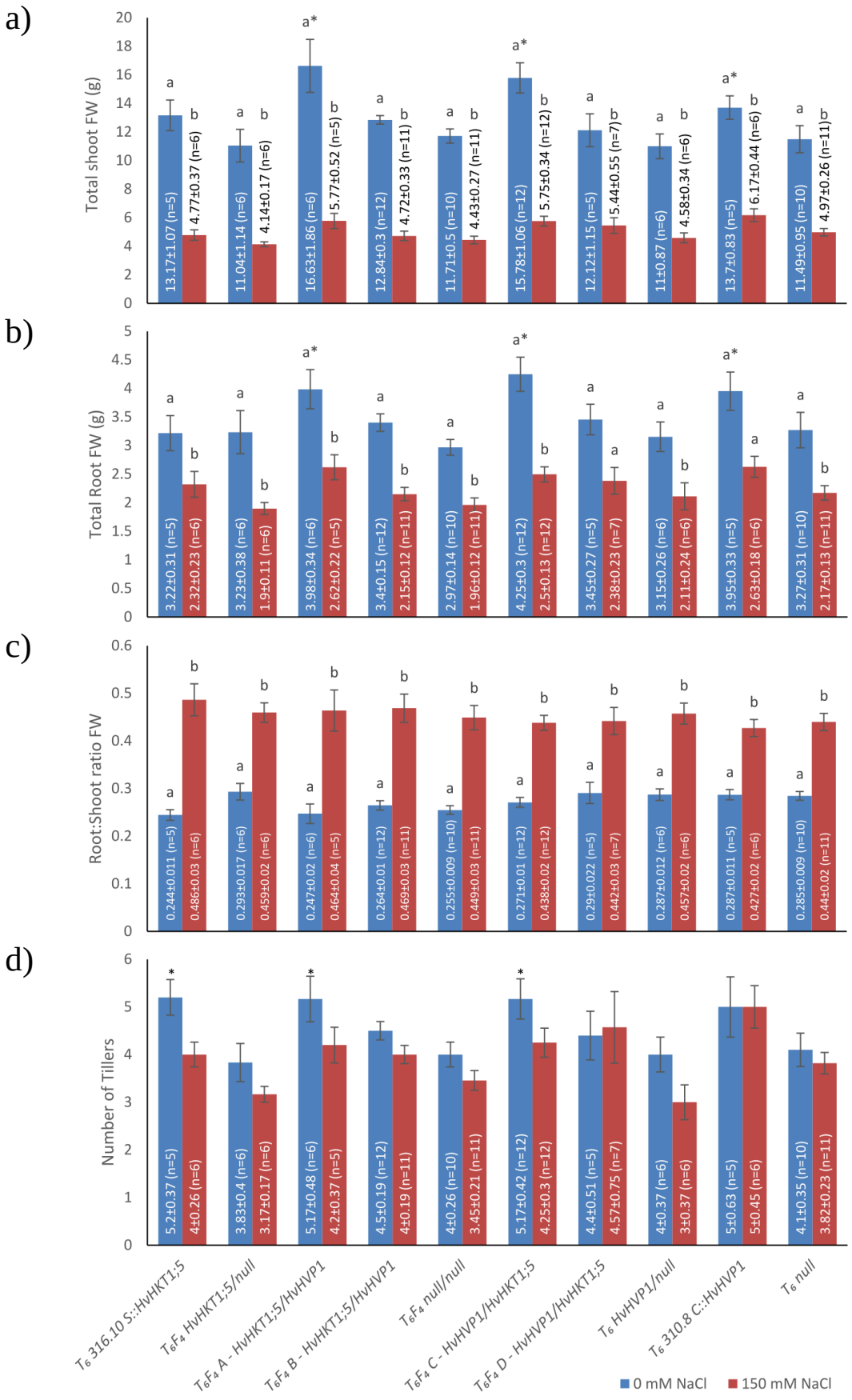
a)
Total shoot FW (g)
13.17±1.07 (n=5)
4.77±0.37 (n=6)
11.04±1.14 (n=6)
4.14±0.17 (n=6)
16.63±1.86 (n=6)
5.77±0.52 (n=5)
12.84±0.3 (n=12)
4.72±0.33 (n=11)
11.71±0.5 (n=10)
4.43±0.27 (n=11)
15.78±1.06 (n=12)
5.75±0.34 (n=12)
12.12±1.15 (n=5)
5.44±0.55 (n=7)
11±0.87 (n=6)
4.58±0.34 (n=6)
13.7±0.83 (n=5)
6.17±0.44 (n=6)
11.49±0.95 (n=10)
4.97±0.26 (n=11)
b)
Total Root FW (g)
3.22±0.31 (n=5)
2.32±0.23 (n=6)
3.23±0.38 (n=6)
1.9±0.11 (n=6)
3.98±0.34 (n=6)
2.62±0.22 (n=5)
3.4±0.15 (n=12)
2.15±0.12 (n=11)
2.97±0.14 (n=10)
1.96±0.12 (n=11)
4.25±0.3 (n=12)
2.5±0.13 (n=12)
3.45±0.27 (n=5)
2.38±0.23 (n=7)
3.15±0.26 (n=6)
2.11±0.24 (n=6)
3.95±0.33 (n=5)
2.63±0.18 (n=6)
3.27±0.31 (n=10)
2.17±0.13 (n=11)
c)
Root:Shoot ratio FW
0.244±0.011 (n=5)
0.486±0.03 (n=6)
0.293±0.017 (n=6)
0.459±0.02 (n=6)
0.247±0.02 (n=6)
0.464±0.04 (n=5)
0.264±0.01 (n=12)
0.469±0.03 (n=11)
0.255±0.009 (n=10)
0.449±0.03 (n=11)
0.271±0.01 (n=12)
0.438±0.02 (n=12)
0.29±0.022 (n=5)
0.442±0.03 (n=7)
0.287±0.012 (n=6)
0.457±0.02 (n=6)
0.287±0.011 (n=5)
0.427±0.02 (n=6)
0.285±0.009 (n=10)
0.44±0.02 (n=11)
d)
Number of Tillers
5.2±0.37 (n=5)
4±0.26 (n=6)
3.83±0.4 (n=6)
3.17±0.17 (n=6)
5.17±0.48 (n=6)
4.2±0.37 (n=5)
4.5±0.19 (n=12)
4±0.19 (n=11)
4±0.26 (n=10)
3.45±0.21 (n=11)
5.17±0.42 (n=12)
4.25±0.3 (n=12)
4.4±0.51 (n=5)
4.57±0.75 (n=7)
4±0.37 (n=6)
3±0.37 (n=6)
5±0.63 (n=5)
5±0.45 (n=6)
4.1±0.35 (n=10)
3.82±0.23 (n=11)
T6 316.10 S::HvHKT1;5
T6F4 HvHKT1;5/null
T6F4 A - HvHKT1;5/HvHVP1
T6F4 B - HvHKT1;5/HvHVP1
T6F4 null/null
T6F4 C - HvHVP1/HvHKT1;5
T6F4 D - HvHVP1/HvHKT1;5
T6 HvHVP1/null
T6 310.8 C::HvHVP1
T6 null
0 mM NaCl
150 mM NaCl

Figure 3.20: Root and shoot biomass of nulls and T_6F_4 transgenic barley lines expressing *HvHVP1* and/or *HvHKT1;5* under the control of putative cell-type specific promoters are similar to null segregants and parental lines.
Mean shoot (a) and root (b) fresh weight measurements, root-shoot ratio (c) and Tiller number (d) of selected lines: Four T_6F_4 lines (A, B, C, D) expressing both *HvHVP1* under the putative root-cortex specific promoter *proC34* (*proC34:HvHVP1*) and *HvHKT1;5* driven by the putative root-stele specific promoter *proS147* (*proC34:HvHVP1*). Segregants were grouped into Null segregants (T_6F_4 *null/null)* or segregants containing only *proC34:HvHVP1* or *proS147:HvHKT1;5* constructs (T_6F_4 *proC34:HvHVP1/null* or T_6F_4 *proS147:HvHKT1;5/null*). Two parental uncrossed T_6 lines (T_6 *316.10-S:HKT1;5* and T_6 310.8 C*:HvHVP1*). Plants were grown in supported hydroponics and exposed to either 0 or 200 mM NaCl and grown for a further 21 days before harvest. Values plotted are means ± SEM (shown on graph). Letters represent significant differences within lines, between treatments (one-way ANOVA, Tukey-Kramer, $P \leq 0.05$). * and + represent significant difference from null segregants grown in either control conditions or 200 mM NaCl respectively (one-way ANOVA, Tukey-Kramer, $P \leq 0.05$)

3.3.5.3. Ion (Na^+, K^+, Cl^-) accumulation in the 4th leaf of hydroponically grown plants may be altered when compared to NaCl

As previously seen, a significant treatment effect on the accumulation of the ions examined in this study (Na^+, K^+ and Cl^-) was observed between control plants and those grown at 200 mM NaCl in both 4th leaf (Figure 3.21) and root tissue (Figure 3.22).

A very slight decrease in 4th leaf [Na^+] of several lines (Figure 3.21, a) under control (0 mM NaCl) conditions compared to null segregants although not significant. No significant trends where observed for other lines or in relation to the other ions examined; [K^+] (Figure 3.21, a) or [Cl^-] (Figure 3.21, c), or 4th leave [Na^+:K^+] (Figure 3.21, d), under control or 200 mM salt conditions.

Similarly, there were no significant differences in root ion accumulation (Figure 3.22) under control or 200 mM salt conditions observed between the transgenic lines and null segregants. A slight decrease in root [Na^+] (Figure 3.22, a) and associated increase in root [K^+] (Figure 3.22, b) in the uncrossed T_6 *proC34:HvHVP1* parental lines was observed.

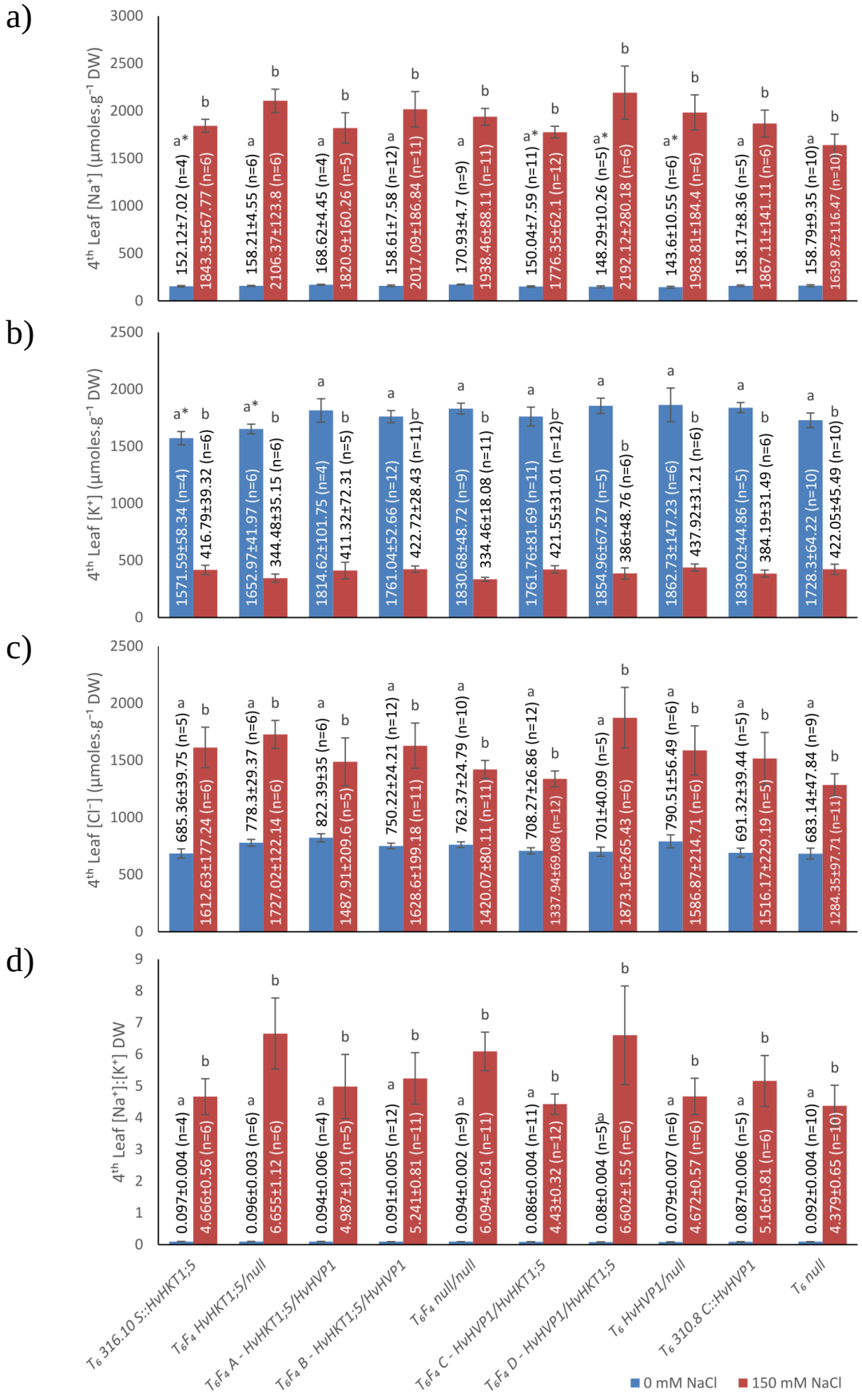
a)
4th Leaf [Na+] (µmoles.g-1 DW)
152.12±7.02 (n=4)
1843.35±67.77 (n=6)
158.21±4.55 (n=6)
2106.37±123.8 (n=6)
168.62±4.45 (n=4)
1820.9±160.26 (n=5)
158.61±7.58 (n=12)
2017.09±186.84 (n=11)
170.93±4.7 (n=9)
1938.46±88.11 (n=11)
150.04±7.59 (n=11)
1776.35±62.1 (n=12)
148.29±10.26 (n=5)
2192.12±280.18 (n=6)
143.6±10.55 (n=6)
1983.81±184.4 (n=6)
158.17±8.36 (n=5)
1867.11±141.11 (n=6)
158.79±9.35 (n=10)
1639.87±116.47 (n=10)
b)
4th Leaf [K+] (µmoles.g-1 DW)
1571.59±58.34 (n=4)
416.79±39.32 (n=6)
1652.97±41.97 (n=6)
344.48±35.15 (n=6)
1814.62±101.75 (n=4)
411.32±72.31 (n=5)
1761.04±52.66 (n=12)
422.72±28.43 (n=11)
1830.68±48.72 (n=9)
334.46±18.08 (n=11)
1761.76±81.69 (n=11)
421.55±31.01 (n=12)
1854.96±67.27 (n=5)
386±48.76 (n=6)
1862.73±147.23 (n=6)
437.92±31.21 (n=6)
1839.02±44.86 (n=5)
384.19±31.49 (n=6)
1728.3±64.22 (n=10)
422.05±45.49 (n=10)
c)
4th Leaf [Cl-] (µmoles.g-1 DW)
685.36±39.75 (n=5)
1612.63±177.24 (n=6)
778.3±29.37 (n=6)
1727.02±122.14 (n=6)
822.39±35 (n=6)
1487.91±209.6 (n=5)
750.22±24.21 (n=12)
1628.6±199.18 (n=11)
762.37±24.79 (n=10)
1420.07±80.11 (n=11)
708.27±26.86 (n=12)
1337.94±69.08 (n=12)
701±40.09 (n=5)
1873.16±265.43 (n=6)
790.51±56.49 (n=6)
1586.87±214.71 (n=6)
691.32±39.44 (n=5)
1516.17±229.19 (n=5)
683.14±47.84 (n=9)
1284.35±97.71 (n=11)
d)
4th Leaf [Na+]:[K+] DW
0.097±0.004 (n=4)
4.666±0.56 (n=6)
0.096±0.003 (n=6)
6.655±1.12 (n=6)
0.094±0.006 (n=4)
4.987±1.01 (n=5)
0.091±0.005 (n=12)
5.241±0.81 (n=11)
0.094±0.002 (n=9)
6.094±0.61 (n=11)
0.086±0.004 (n=11)
4.43±0.32 (n=12)
0.08±0.004 (n=5)
6.602±1.55 (n=6)
0.079±0.007 (n=6)
4.672±0.57 (n=6)
0.087±0.006 (n=5)
5.16±0.81 (n=6)
0.092±0.004 (n=10)
4.379±0.65 (n=10)
T6 316.10 S::HvHKT1;5
T6F4 HvHKT1;5/null
T6F4 A - HvHKT1;5/HvHVP1
T6F4 B - HvHKT1;5/HvHVP1
T6F4 null/null
T6F4 C - HvHVP1/HvHKT1;5
T6F4 D - HvHVP1/HvHKT1;5
T6 HvHVP1/null
T6 310.8 C::HvHVP1
T6 null
0 mM NaCl
150 mM NaCl

Figure 3.21: 4th leaf ion (Na^+, K^+ and Cl^-) content of T_6F_4 transgenic barley lines expressing *HvHVP1* and/or *HvHKT1;5* under the control of putative cell-type specific promoters may be improved compared to null segregants.
Mean 4th leaf DW [Na^+] (a), [K^+] (b) and [Cl^-] (c) measurements and 4th leaf [Na^+]:[K^+] ratio (d) of selected lines: Four T_6F_4 lines (A, B, C, D) expressing both *HvHVP1* under the putative root-cortex specific promoter *proC34* (*proC34:HvHVP1*) and *HvHKT1;5* driven by the putative root-stele specific promoter *proS147* (*proC34:HvHVP1*). Segregants were grouped into Null segregants (T_6F_4 *null/null)* or segregants containing only *proC34:HvHVP1* or *proS147:HvHKT1;5* constructs (T_6F_4 *proC34:HvHVP1/null* or T_6F_4 *proS147:HvHKT1;5/null*). Two parental uncrossed T_6 lines (T_6 *316.10-S:HKT1;5* and T_6 310.8 C*:HvHVP1*) were included for comparison. Plants were grown in supported hydroponics and exposed to either 0 or 200 mM NaCl and grown for a further 21 days before harvest. Values plotted are means ± SEM (shown on graph). Letters represent significant differences within lines but between treatments (one-way ANOVA, Tukey-Kramer, $P \leq 0.05$). * and + represent significant difference from null segregants grown in either control conditions or 200 mM NaCl respectively (one-way ANOVA, Tukey-Kramer, $P \leq 0.05$)

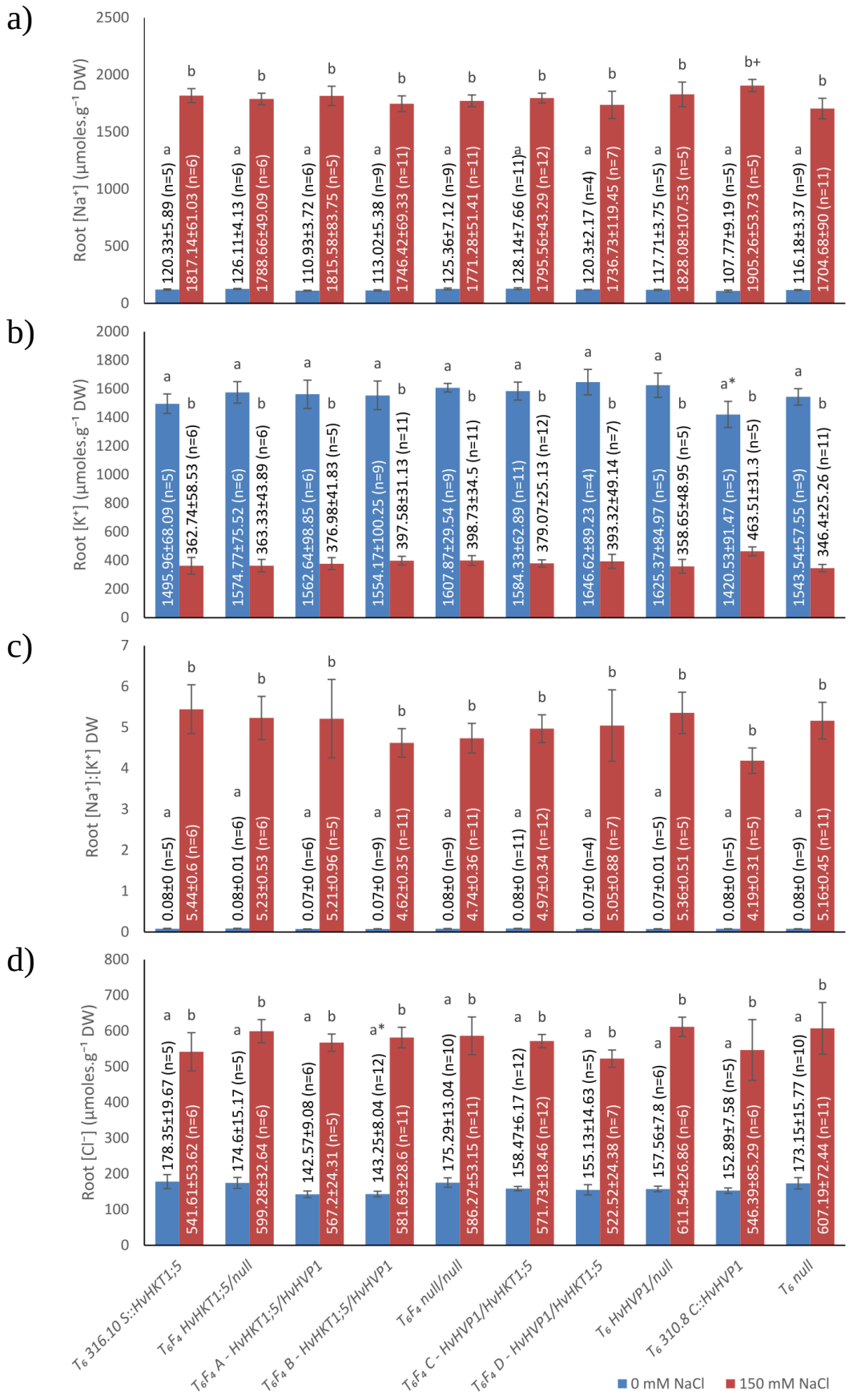
a)
Root [Na+] (µmoles.g-1 DW)
b)
Root [K+] (µmoles.g-1 DW)
c)
Root [Na+]:[K+] DW
d)
Root [Cl-] (µmoles.g-1 DW)
T6 316.10 S::HvHKT1;5
T6F4 HvHKT1;5/null
T6F4 A - HvHKT1;5/HvHVP1
T6F4 B - HvHKT1;5/HvHVP1
T6F4 null/null
T6F4 C - HvHVP1/HvHKT1;5
T6F4 D - HvHVP1/HvHKT1;5
T6 HvHVP1/null
T6 310.8 C::HvHVP1
T6 null
0 mM NaCl
150 mM NaCl

Figure 3.22 Root Ion (Na^+, K^+ and Cl^-) content of T_6F_4 transgenic barley lines expressing *HvHVP1* and/or *HvHKT1;5* under the control of putative cell-type specific promoters may be improved compared to null segregants
Mean root DW [Na^+] (a), [K^+] (b) and [Cl^-] (c) measurements and root [Na^+]:[K^+] ratio (d) of selected lines: Four T_6F_4 lines (A, B, C, D) expressing both *HvHVP1* under the putative root-cortex specific promoter *proC34* (*proC34:HvHVP1*) and *HvHKT1;5* driven by the putative root-stele specific promoter *proS147* (*proC34:HvHVP1*). Segregants were grouped into Null segregants (T_6F_4 *null/null)* or segregants containing only *proC34:HvHVP1* or *proS147:HvHKT1;5* constructs (T_6F_4 *proC34:HvHVP1/null* or T_6F_4 *proS147:HvHKT1;5/null*). Two parental uncrossed T_6 lines (T_6 *316.10-S:HKT1;5* and T_6 310.8 C*:HvHVP1*) were included for comparison. Plants were grown in supported hydroponics and exposed to either 0 or 200 mM NaCl and grown for a further 21 days before harvest. Values plotted are means ± SEM (shown on graph). Letters represent significant differences within lines but between treatments (one-way ANOVA, Tukey-Kramer, $P \leq 0.05$). * and + represent significant difference from null segregants grown in either control conditions or 200 mM NaCl respectively (one-way ANOVA, Tukey-Kramer, $P \leq 0.05$)

3.3.6. Bioinformatics review of promoters used for driving cell-type specific expression in barley (cv. Golden Promise)

In light of the above results, the rice putative root cell-type specific promoters, *proC34* and *proS147,* utilised in this study to drive the expression of both reporter genes (*mGFP6* and *uidA*) and salinity tolerance genes *HvHKT1;5* and *HvHVP1* were re-examined with more recent bioinformatics resources to verify their suitability to drive tissue-type specific expression of transgenes.

3.3.6.1. Putative root-cortex specific promoter *proC34*: Rice (cv. Nipponbare) LOC_Os12g36240

The 2468 bp putative root-cortex specific promoter, *proC34*, was cloned from the 5′ of LOC_Os12g36240 from rice (cv. Nipponbare) genomic DNA. According to the latest rice loci annotations (MSU Osa1 Release 7, 2014 -http://rice.plantbiology.msu.edu Ouyang *et al.* (2007)), the coding sequence at LOC_Os12g36240 consisting of two exons, is predicted to encode a small (86 a.a.), putatively expressed, proteinase inhibitor family 1 protein. No additional experimental data into the function of this gene is currently available. The current *proC34* putative promoter sequence used in this study includes the predicted first exon (Figure 3.23) and partial first intron of the coding region. While previous RT-PCR experiments examining the expression of reporter genes (section 3.3.1) and *HvHVP1* (section 3.3.2) indicate that transgenes can be expressed under this promoter, if the gene annotation is correct, the inclusion of the first exon and partial first intron would result in a mis-translated CDS and non-functional protein. This may explain

the lack of detectable GUS staining in *proC34*:*uidA* experiments (section 3.3.1) and potentially the lack of a significant phenotype in later experiments using this promoter to drive the expression of *HvHVP1*.

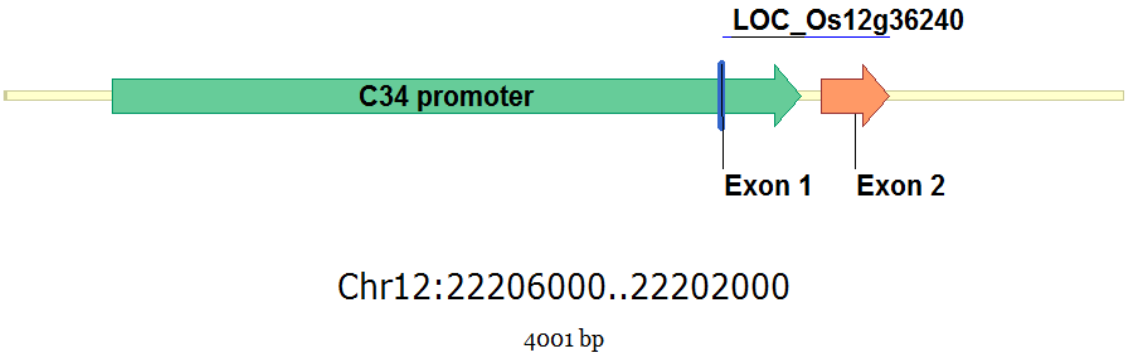

Figure 3.23: Genomic position of the *proC34* promoter sequence relative to LOC_Os12g36240
The cloned promoter sequence (green), *proC34*, relative to the genomic position of LOC_Os12g36240 on rice cv. Nipponbare Chromosome 12, illustrating the potential inclusion of the predicted first exon of LOC_Os12g36240 in the promoter sequence. Sequence and gene annotation obtained from Ouyang *et al.* (2007) (MSU Osa1 Release 7, 2014 -http://rice.plantbiology.msu.edu)

Expression of LOC_Os12g36240 in Rice

Since the initial work carried out to identify the root-cortex specific expression of the *proC34* promoter, additional datasets have become available allowing *in silico* comparison of promoter sequences and gene expression. To verify the tissue specificity in rice to the original maize MPSS data set, several databases were screened for expression data for the CDS encoded at LOC_Os12g36240. From eFP browser microarray data (Patel *et al.*, 2012) of the tissue-type expression (Figure 3.24, a) and the expression changes in 7 day seedling in response to several abiotic stresses (drought, salt, cold) (Figure 3.24, b) the loci *Os12g36240* shows highest expression in the seedling root as well as in the stage 3 inflorencese (Figure 3.24, a). Additionally, there is an increase in expression in the 7-day old seedling under salt stress (Figure 3.24, b). Although the 7-day old seeding data may not be overly biologically relevant, due to the stress conditions used in the original study (7 d old seedlings transferred to 200 mM NaCl for 3 hrs) (Jain *et al.*, 2007).

Additional microarray gene expression data from dissected rice roots (Figure 3.25) shows the highest expression in root tissues with some expression in the developing embryos (Figure 3.25, a). Expression data from laser micro-dissected roots support root-cortex

specific expression in elongation and early maturation zones, however, expression is significantly reduced in late stage maturation zone (V) (Figure 3.25, b and c).

LOC_Os12g36240 – *proC34*	
a) Global tissue expression	b) Abiotic stress response - 7d seeding
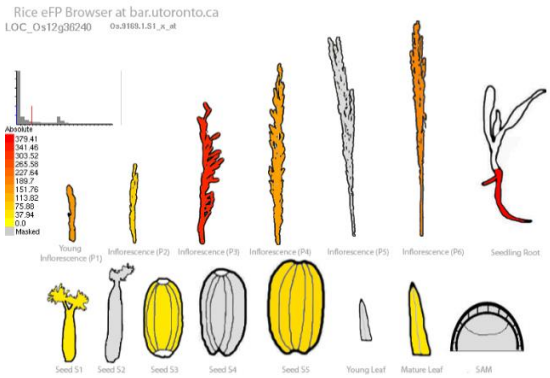	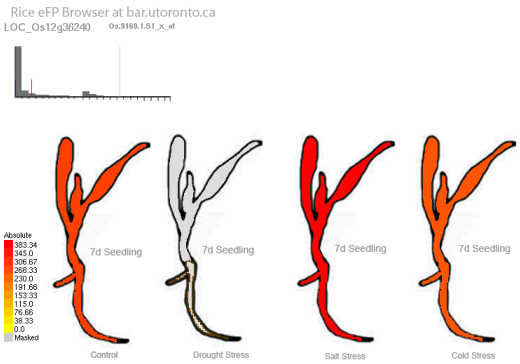

Figure 3.24: Expression of LOC_Os12g36240 (source of *proC34*) in seedling roots supported by Rice eFP micro-array datasets

Rice eFP output for (a) tissue expression (rice_mas dataset) and (b) 7d seedling abiotic stress response (ricestress_mas dataset) of LOC_Os12g36240. Shading from yellow to red indicates increasing expression Standard deviation filtering of samples was applied and samples with S.D. > 50% of expression value were masked (greyed). Raw values tabled in appendix (cross ref) ± S.D. eFP by (Patel *et al.*, 2012) http://bar.utoronto.ca/efprice/cgi-bin/efpWeb.cgi Drawings by R. Patel adapted from images by Dr D. Brar as well as images contained within (Jain *et al.*, 2007). Data from same paper, normalised by MAS 5.0 method (TGT=100, n=3)

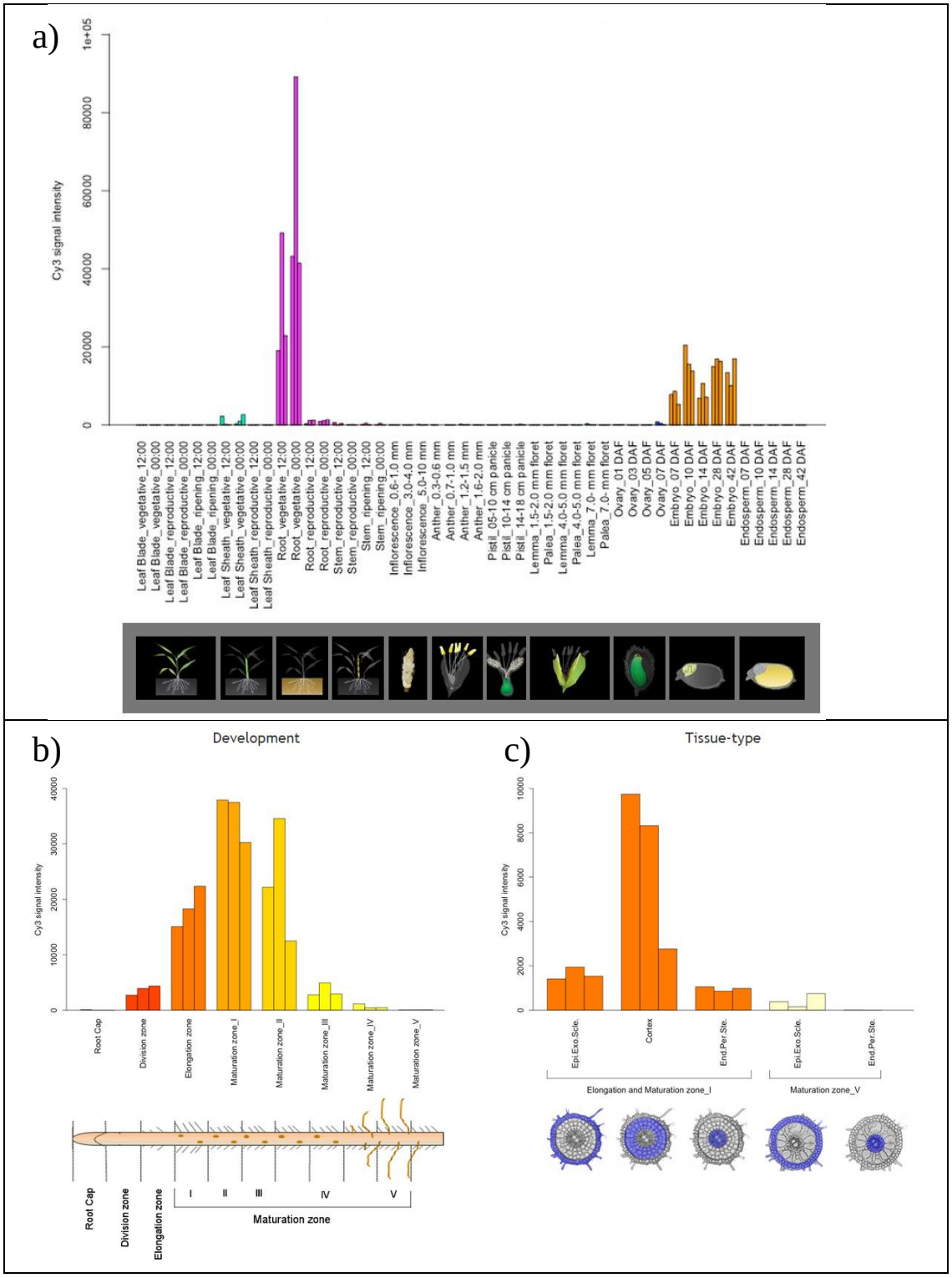
a)
Cy3 signal intensity
0
20000
40000
60000
80000
1e+05
Leaf Blade_vegetative_12:00
Leaf Blade_vegetative_00:00
Leaf Blade_reproductive_12:00
Leaf Blade_reproductive_00:00
Leaf Blade_ripening_12:00
Leaf Blade_ripening_00:00
Leaf Sheath_vegetative_12:00
Leaf Sheath_vegetative_00:00
Leaf Sheath_reproductive_12:00
Leaf Sheath_reproductive_00:00
Root_vegetative_12:00
Root_vegetative_00:00
Root_reproductive_12:00
Root_reproductive_00:00
Stem_reproductive_12:00
Stem_reproductive_00:00
Stem_ripening_12:00
Stem_ripening_00:00
Inflorescence_0.6-1.0 mm
Inflorescence_3.0-4.0 mm
Inflorescence_5.0-10 mm
Anther_0.3-0.6 mm
Anther_0.7-1.0 mm
Anther_1.2-1.5 mm
Anther_1.6-2.0 mm
Pistil_05-10 cm panicle
Pistil_10-14 cm panicle
Pistil_14-18 cm panicle
Lemma_1.5-2.0 mm floret
Palea_1.5-2.0 mm floret
Lemma_4.0-5.0 mm floret
Palea_4.0-5.0 mm floret
Lemma_7.0- mm floret
Palea_7.0- mm floret
Ovary_01 DAF
Ovary_03 DAF
Ovary_05 DAF
Ovary_07 DAF
Embryo_07 DAF
Embryo_10 DAF
Embryo_14 DAF
Embryo_28 DAF
Embryo_42 DAF
Endosperm_07 DAF
Endosperm_10 DAF
Endosperm_14 DAF
Endosperm_28 DAF
Endosperm_42 DAF
b)
Development
Cy3 signal intensity
0
10000
20000
30000
40000
Root Cap
Division zone
Elongation zone
Maturation zone_I
Maturation zone_II
Maturation zone_III
Maturation zone_IV
Maturation zone_V
Root Cap
Division zone
Elongation zone
I
II
III
IV
V
Maturation zone
c)
Tissue-type
Cy3 signal intensity
0
2000
4000
6000
8000
10000
Epi.Exo.Scle.
Cortex
End.Per.Ste.
Epi.Exo.Scle.
End.Per.Ste.
Elongation and Maturation zone_I
Maturation zone_V

Figure 3.25: Spatiotemporal gene expression profile of LOC_Os12g36240 (source of *proC34*) in rice (cv. Nipponbare) roots supports root-cortex specific expression. Expression of LOC_Os12g36240 (database reference Os12g0548700) across organs and tissues of various developmental stages (a), across root development zones (b) and radial root zones (c).All graphs were downloaded from the Rice Expression Profile Database(RiceXPro, http://ricexpro.dna.affrc.go.jp/). Microarray of (a) organ and tissue performed on paddy grown rice cv. Nipponbare. Root sampling point points vegetative_12:00, vegetative _00:00, reproductive_12:00, reproductive_00:00 collected at 27, 28, 76 and 77 d after transplant to field respectively. Embryo sample points, Embro_07, _10, _28 and _48 DAF collected at 7, 10, 28 and 48 d after flowering. Further details of dataset and diagram features available at http://ricexpro.dna.affrc.go.jp/GGEP/sample-list.php. Expression data from root development zone and radial root zones was based on RNA extracted from the crown root of 10 day old seedlings divided by laser micro-dissection into 8 developmental zones laterally (b) and 3 radial root zone regions (epidermis, cortex and vascular bundle) in the elongation and final root maturation zones (c). Further details of the dataset and diagram features available at http://ricexpro.dna.affrc.go.jp/RXP_4001/index.php. Data graphed is the raw hybridisation signal intensity of Agilent one-colour (Cy3) microarray system performed in triplicate.

Comparison of expression of LOC_Os12g36240 (proC34) to identified salinity tolerance genes OsOVP1, 2 and 3 in rice.

Although the previous microarray data (Figure 3.24 and Figure 3.25) of LOC_Os12g3624 supports root-cortex specific expression, the level of expression is also important for its use to drive transgenes. When compared to the 3 rice homologues of *HvHVP1, OsOVP(1,2* and *3),* LOC_Os12g3624 is expressed at increased levels in the root elongation and early maturation zones (Figure 3.26, a) and the epidermis of late maturation zone roots (Figure 3.26, b).

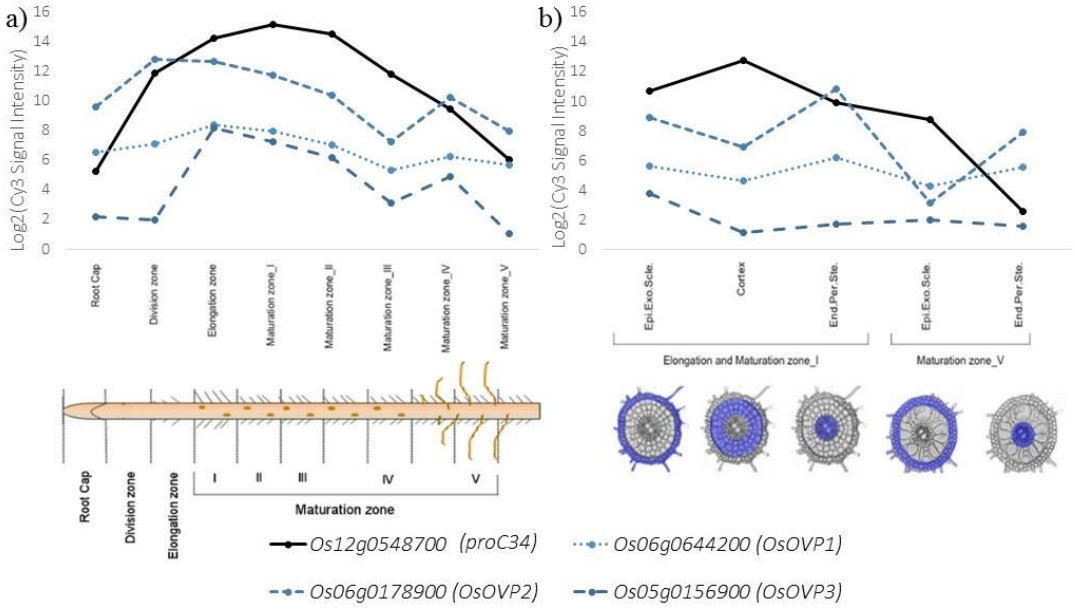

Figure 3.26: Comparison of the spatiotemporal gene expression profile of LOC_Os12g36240 (*proC34*) to in rice (cv. Nipponbare) roots to salinity tolerance genes *OsOVP1,2* & *3*.
Expression of LOC_Os12g36240 (*proC34*) (database reference Os12g0548700), *OsOVP1* (OsO6g0644200), *OsOVP2* (Os06g0178900) and *OsOVP3* (Os05g0156900) across root development zones (a) and radial root zones (c).All graphs were downloaded from the Rice Expression Profile Database(RiceXPro, http://ricexpro.dna.affrc.go.jp/). Expression data from root development zone and radial root zones was based on RNA extracted from the crown root of 10 day old seedlings divided by laser micro-dissection into 8 developmental zones laterally (a) and 3 radial root zone regions (epidermis, cortex and vascular bundle) in the elongation and final root maturation zones (b). Further details of the dataset and diagram features available at http://ricexpro.dna.affrc.go.jp/RXP_4001/index.php. Data graphed as log2 of the raw hybridisation signal intensity of Agilent one-colour (Cy3) microarray system performed in triplicate.

3.3.6.2. Putative root-stele specific promoter proS147: Rice (Nipponbare) LOC_Os04g52720

According to the latest rice loci annotations (http://rice.plantbiology.msu.edu, 2014 - MSU Osa1 Release 7 Ouyang *et al.* (2007) the loci at LOC_Os04g52720 is predicted to encode a 2 exon, 255 a.a. expressed, cupin domain contain protein of unknown function. The cloned two Kbp putative promoter fragment lies 5′ of the CDS show in Figure 3.27. A secondary neighbouring loci, LOC_OsO452720, is also predicted to overlap LOC_OsO4g52720, however the CDS is predicted to be transcribed in the opposite direction.

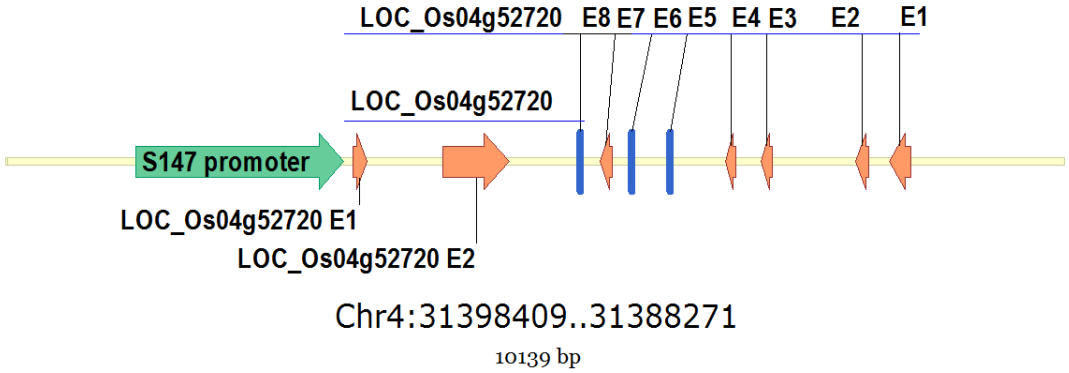

Figure 3.27: Genomic position of the *proS147* promoter sequence relative to LOC_Os04g52720 and neighbouring loci LOC_Os04g52720.
The cloned promoter sequence, *proS147*, relative to the genomic position of LOC_ Os04g52720 on rice cv. Nipponbare Chromosome 4. Sequence and gene annotation obtained from Ouyang *et al.* (2007) (MSU Osa1 Release 7, 2014 - http://rice.plantbiology.msu.edu)

Expression of LOC_Os04g52720 in Rice

Similar to the previous *proC34* promoter, the tissue specificity of the promoter *proS147*, originally determined by the maize MPSS data set (Krishnan, 2013), was re-examined from several more recent micro-array datasets. From eFP browser microarray data (Patel *et al.*, 2012) of the tissue-type expression (Figure 3.28, a) and the expression changes in 7 day seedling in response to several abiotic stresses (drought, salt, cold) (Figure 3.28, b) the loci *Os04g52720* shows highest expression in the seedling root as expected (Figure 3.28, a). Interestingly, there is a decrease in expression in salt stress seedlings compared to seedlings under control conditions (Figure 3.28, b). Although the 7-day old seeding data may not be overly biologically relevant, due to the stress conditions used in the original study (7 d old seedlings transferred to 200 mM NaCl for 3 hrs) (Jain *et al.*, 2007).

Additional microarray gene expression data from dissected rice roots (Figure 3.29) shows the highest expression in vegetative root tissues (Figure 3.29, a). However, expression data from laser micro-dissected roots does not support root-stele specific expression and is expressed at similarly levels in all root samples examined (Figure 3.30, b, c) and at very low levels.

LOC_Os04g52720 - *proS147*	
a) Global tissue expression	b) Abiotic stress response - 7d seeding

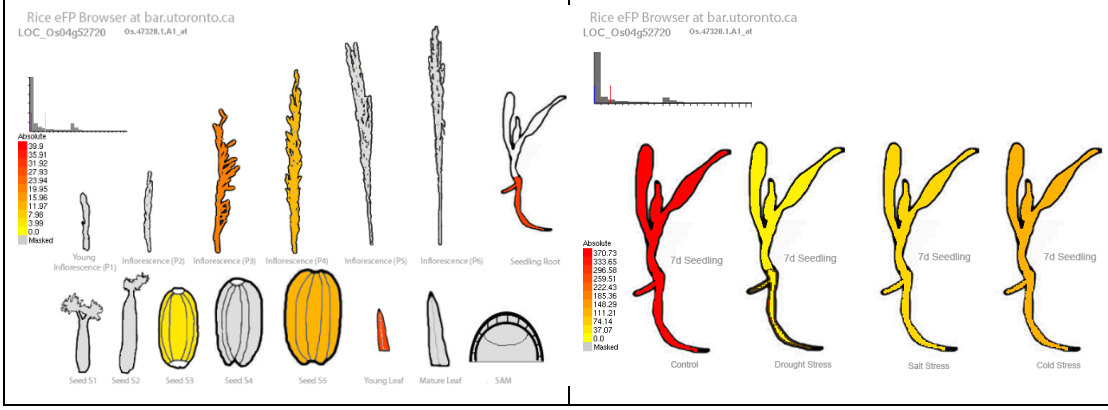

Figure 3.28: Expression of LOC_Os04g52720 by Rice eFP

Rice eFP output for (a) tissue expression (rice_mas dataset) and (b) 7d seedling abiotic stress response (ricestress_mas dataset) of LOC_ Os04g52720. Shading from yellow to red indicates increasing expression Standard deviation filtering of samples was applied and samples with S.D. > 50% of expression value were masked (greyed). Raw values tabled below ± S.D. eFP by Patel *et al.* (2012) (http://bar.utoronto.ca/efprice/cgi-bin/efpWeb.cgi). Drawings by R. Patel adapted from images by Dr D. Brar as well as images contained within Jain *et al.* (2007). Data from same paper, normalised by MAS 5.0 method (TGT=100, n=3)

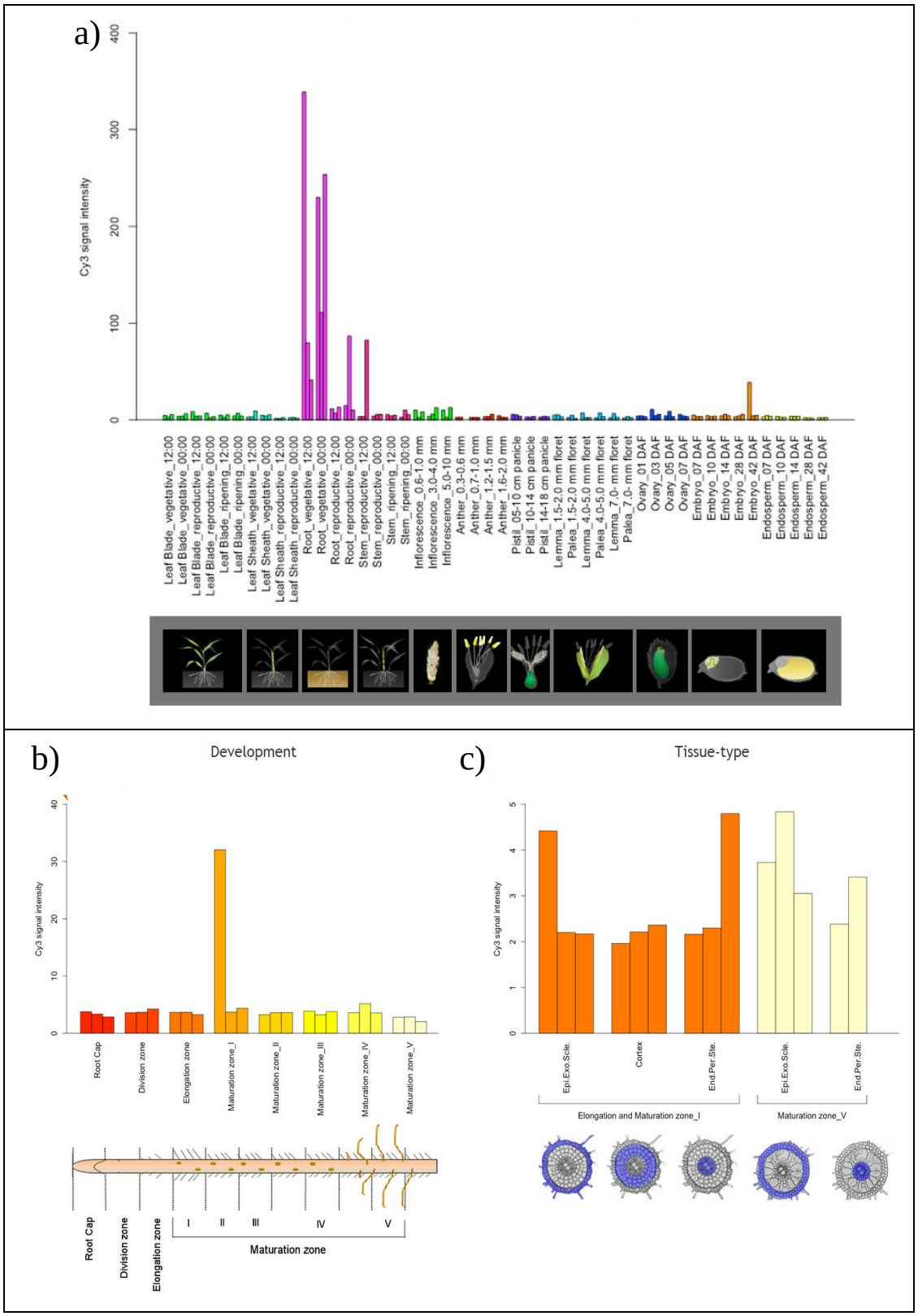
a)
Cy3 signal intensity
0
100
200
300
400
Leaf Blade_vegetative_12:00
Leaf Blade_vegetative_00:00
Leaf Blade_reproductive_12:00
Leaf Blade_reproductive_00:00
Leaf Blade_ripening_12:00
Leaf Blade_ripening_00:00
Leaf Sheath_vegetative_12:00
Leaf Sheath_vegetative_00:00
Leaf Sheath_reproductive_12:00
Leaf Sheath_reproductive_00:00
Root_vegetative_12:00
Root_vegetative_00:00
Root_reproductive_12:00
Root_reproductive_00:00
Stem_reproductive_12:00
Stem_reproductive_00:00
Stem_ripening_12:00
Stem_ripening_00:00
Inflorescence_0.6-1.0 mm
Inflorescence_3.0-4.0 mm
Inflorescence_5.0-10 mm
Anther_0.3-0.6 mm
Anther_0.7-1.0 mm
Anther_1.2-1.5 mm
Anther_1.6-2.0 mm
Pistil_05-10 cm panicle
Pistil_10-14 cm panicle
Pistil_14-18 cm panicle
Lemma_1.5-2.0 mm floret
Palea_1.5-2.0 mm floret
Lemma_4.0-5.0 mm floret
Palea_4.0-5.0 mm floret
Lemma_7.0- mm floret
Palea_7.0- mm floret
Ovary_01 DAF
Ovary_03 DAF
Ovary_05 DAF
Ovary_07 DAF
Embryo_07 DAF
Embryo_10 DAF
Embryo_14 DAF
Embryo_28 DAF
Embryo_42 DAF
Endosperm_07 DAF
Endosperm_10 DAF
Endosperm_14 DAF
Endosperm_28 DAF
Endosperm_42 DAF
b)
Development
Cy3 signal intensity
0
10
20
30
40
Root Cap
Division zone
Elongation zone
Maturation zone_I
Maturation zone_II
Maturation zone_III
Maturation zone_IV
Maturation zone_V
Root Cap
Division zone
Elongation zone
I
II
III
IV
V
Maturation zone
c)
Tissue-type
Cy3 signal intensity
0
1
2
3
4
5
Epi.Exo.Scle.
Cortex
End.Per.Ste.
Epi.Exo.Scle.
End.Per.Ste.
Elongation and Maturation zone_I
Maturation zone_V

Figure 3.29: Spatiotemporal gene expression profile of LOC_Os04g52720 (*proS147*) in rice (cv. Nipponbare) roots.
Expression of LOC_Os04g52720 (database reference Os04g0617900) across organs and tissues of various developmental stages (a), across root development zones (b) and radial root zones (c). All graphs were downloaded from the Rice Expression Profile Database (RiceXPro, http://ricexpro.dna.affrc.go.jp/). Microarray of (a) organ and tissue performed on paddy grown rice cv. Nipponbare. Root sampling point points vegetative_12:00, vegetative _00:00, reproductive_12:00, reproductive_00:00 collected at 27, 28, 76 and 77 d after transplant to field respectively. Embryo sample points, Embro_07,_10,_28 and _48 DAF collected at 7, 10, 28 and 48 d after flowering. Further details of dataset and diagram features available at http://ricexpro.dna.affrc.go.jp/GGEP/sample-list.php. Expression data from root development zone and radial root zones was based on RNA extracted from the crown root of 10 day old seedlings divided by laser micro-dissection into 8 developmental zones laterally (b) and 3 radial root zone regions (epidermis, cortex and vascular bundle) in the elongation and final root maturation zones (c). Further details of the dataset and diagram features available at http://ricexpro.dna.affrc.go.jp/RXP_4001/index.php. Data graphed is the raw hybridisation signal intensity of Agilent one-colour (Cy3) microarray system performed in triplicate.

Comparison of expression of LOC_Os04g52720 (proS147) to salinity tolerance gene OsHKT1;5 in rice

Although it would be expected that root-stele specific genes would be expressed at low levels, due to the dilution effect when whole root samples are taken, the relative expression of LOC_Os04g52720 (*proS147*) was compared to the expression of the rice homologue of *HvHKT1;5*, *OsHKT1;5* (Figure 3.30). LOC_Os04g52720 was expressed at similar levels throughout all root tissues sampled, with a slight increase in early root maturation zone (Figure 3.30, a). However, expression of *OsHKT1;5* was significantly (300-fold) increased in the maturation zone root stele cells compared to LOC_Os04g52720 (*proS147*) (Figure 3.30, b). The apparent low level of expression of LOC_Os04g52720 (Figure 3.29) may impact the usefulness of transgenes expressed using the cloned promoter *proS147* such as reporter gene *uidA* (section 3.3.1) or *HvHKT1;5* (section 3.3.2).

While previous RT-PCR experiments examining the expression of reporter genes (section 3.3.1) and *HvHKT1;5* (section 3.3.2) indicate that transgenes can be expressed under the *proS147* promoter. The requirement for high cycle number suggests low expression levels, potentially due to the native low level of expression of the cloned *proS147* promoter. This may explain the lack of detectable GUS staining in *proS147*:*uidA*

experiments and the lack of a significant salinity tolerance phenotype for lines expressing *proS147:HvHKT1;5.*

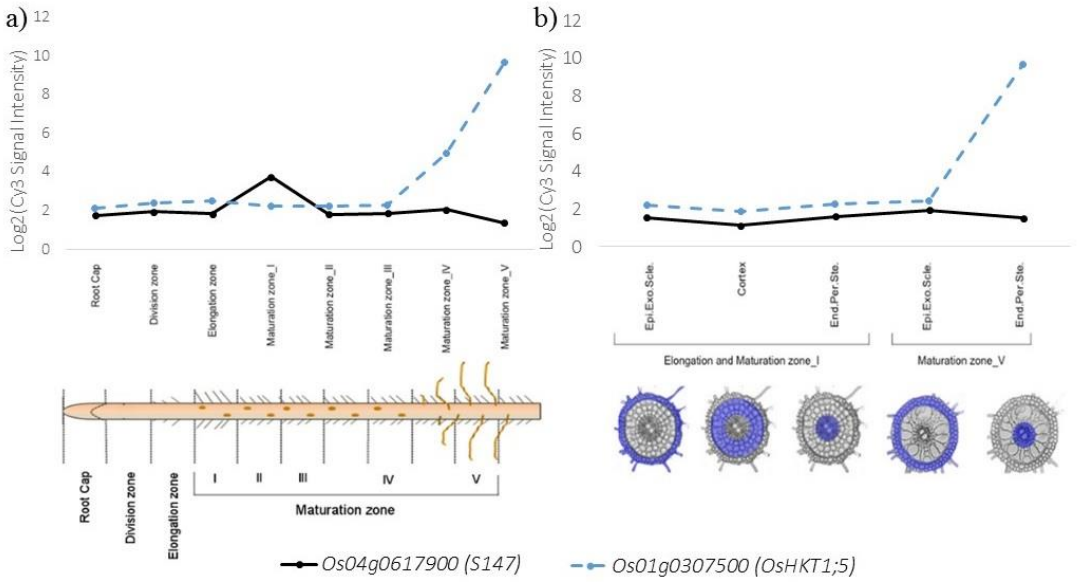

Figure 3.30: Spatiotemporal gene expression profile of LOC_Os04g52720 (*proS147*) in rice (cv. Nipponbare) roots compared to Os01g0307500 (*OsHKT1;5*) .
Expression of LOC_Os04g52720 (database reference Os04g0617900) and *OsHKT1;5* (Os01g037500) across root development zones (a) and radial root zones (b). Data obtained from Rice Expression Profile Database (RiceXPro, http://ricexpro.dna.affrc.go.jp/). Expression data from root development zone and radial root zones was based on RNA extracted from the crown root of 10 day old seedlings divided by laser micro-dissection into 8 developmental zones laterally (a) and 3 radial root zone regions (epidermis, cortex and vascular bundle) in the elongation and final root maturation zones (b). Further details of the dataset and diagram features available at http://ricexpro.dna.affrc.go.jp/RXP_4001/index.php. Data graphed is log2 scaled hybridisation signal intensity of Agilent one-colour (Cy3) microarray system performed in triplicate.

3.4. General Discussion

3.4.1. Summary of findings

Overall, the results of the experiments in this chapter indicate that:

3.4.1.1. Expression of *HvHVP1* under the control of the rice putative root cortex specific promoter, *proC34* does not improve plant salinity tolerance barley.

In previous preliminary experiments with T_1 material (Krishnan, 2013), the expression of *HvHVP1* under the control of rice putative root-cortex specific promoter, *proC34*, resulted in increased [Na^+] in the 4th leaf sap, under both control and 100 mM NaCl salt stress conditions, when compared to null segregants when grown in mini-hydroponics (Figure 3.2).

Re-examination of two advanced (T_3) lines in supported hydroponics under 200 mM NaCl (section 3.3.2) did show that while transcript was present (3.3.2.1), root and shoot biomass (section 3.3.2.2), as well as root and shoot, Na^+, K^+ and Cl^- accumulation (section 3.3.2.3) was similar to null segregants and wild-type Golden Promise. Furthermore, examination of potential increased root zone acidification was inconclusive (section 3.3.2.4). Later experiments, with T_5 (section 3.3.4) and T_6 (section 3.3.5) progeny of one of these lines, also supported the similarity of these lines to null segregants and wild-type plants under control and salt stress conditions, in both supported and mini-hydroponics.

The recent expression and bioinformatics data obtained for the original loci from which *proC34* promoter was cloned (section 3.3.6.1) indicates that while the initial root-specificity of the promoter predicted by the earlier Maize MPSS dataset (Krishnan, 2013), the potential inclusion of the first exon and partial intron sequence into the cloned promoter may explain the lack of significant phenotype for the transgenic line, as well as the lack of a distinguishable GUS staining in *proC34:uidA* experiments (section 3.3.1). To test this, full-length sequencing of the expressed *uidA* transcript could be carried out to detect if the first exon and partial intron sequences are present.

3.4.1.2. Expression of *HvHKT1;5* with the rice putative root-stele specific promoter, *proS147*, does not significantly improve plant salinity tolerance in barley.

Preliminary screening of T_1 lines expressing *HvHKT1;5*, under the control of *proS147*, grown in mini-hydroponics and exposed to 100 mM NaCl stress suggested a trend towards increased salinity tolerance (Krishnan, 2013). Lines had a trend towards reduced

[Na^+] in the 4th leaf sap compared to null segregants and as well as a greater 4th leaf sap K^+/Na^+ ratio (Figure 3.1). Re-examination of two advanced (T_3) lines in supported hydroponics under 200 mM NaCl (section 3.3.2) did show that while transcript was present (3.3.2.1), root and shoot biomass (section 3.3.2.2), as well as root and shoot, Na^+, K^+ and Cl^- accumulation (section 3.3.2.3) was similar to null segregants and wild-type Golden Promise.

The recent expression and bioinformatics data obtained for the original loci from which *proS147* promoter was cloned (section 3.3.6.2) indicates that while the initial root-specificity of the promoter predicted by the earlier Maize MPSS dataset (Krishnan, 2013), the relative expression levels was relatively low in all root cell-types and significantly reduced compared to the root-stele expressed OsHKT1;5. This low level of expression may be responsible for the lack of significant phenotype for the transgenic line, as well as the lack of a distinguishable GUS staining in *proS147:uidA* experiments (section 3.3.1).

3.4.1.3. Co-expression of *HvHKT1;5* and *HvHVP1* under the control of root cell-type specific promoters does not significantly improve plant salinity tolerance in barley.

During the course of this research, several lines with co-expression of *HvHKT1;5* and *HvHVP1* by the root cell-type specific promoters discussed above were developed through hybridisation of the previously examined lines (section 3.3.3). Preliminary screening for salinity stress tolerance of these lines in both mini-hydroponics (section 3.3.4) and supported hydroponics (section 3.3.5) did not show significant increases in root or shoot biomass or altered Na^+, K^+ or Cl^- accumulation compared to null segregants or parental lines. Some improvement in shoot biomass was seen under control conditions (section 3.3.5) however this was not supported by sibling lines. Ultimately, the co-expression of these *HvHVP1* and *HvHKT1;5* under the control of the root cell-type promoters previously characterised does not significantly improve salinity tolerance under salt stress conditions in hydroponics in barley. However, it is worth testing this approach in wheat and other Na^+ excluding plants.

3.4.2. Future work

The work presented here illustrates the need for through characterisation of cloned promoters before their use to drive GOIs. Understandably, this is not always possible with relatively short projects timeframes, especially in studies focusing on species with

more complex genomes and/or relatively slow transformation protocols such as wheat and barley compared other model species such as rice or Arabidopsis.

The use of reporter gene assays (such as *uidA* and GFP) to examine the cell-type specific expression of cloned promoters *in planta* is of value to verify expression patterns. However, the use of appropriate reporter genes is paramount. The auto-florescence of senescing tissues observed when screening for GFP florescence in the relatively young hydroponically grown plants, both under control and salinity tolerance, examined in this study requires the appropriate controls to be examined to avoid mis-identification. Furthermore, GFP florescence is not suitable for lowly expressed, or cell-type specific expressed promoters, (Mantis & Tague, 2000), especially in tissues such as the root cortex where cell size is small and sectioning is required for proper visualisation.

The *β-glucuronidase* staining assay overcomes these problem, as the enzymatic reaction does not require extensive staining and sectioning can be carried out to examine otherwise hidden anatomical structures such as the root vasculature. Further staining and section of roots of the *promoter:uidA* lines examined in this study, (similar to Hairmansis, 2014) may be able to verify the cell-type specificity of the putative stele specific promoter *proS147,* even with the very low expression levels suggested by the recent expression data presented (section 3.3.6.2).

Although the RT-PCR experiments in this chapter show that the transgenes were transcribed by the putative rice promoters in the barley lines examined, further dissection and potentially Q-PCR, could have been used to verify the expression levels of the transgenes in specific root cell-types. Similar, the inclusion of the first exon in the *proC34* promoter leading to a mis-spliced or mis-translated product could have been confirmed by immuno-localisation (Abe *et al.*, 2011) of mGFP6 of in the *proC34:mGFP6* lines. Similar methods could have been used to examine the abundance of mGFP6 in the *proS147:mGFP6* lines to support that the *proS147* promoter results in very low level of protein, suggested by the expression profile of this promoter.

However, continuation of experiments with this material was deemed not constructive, in light of the *promoter:reporter* (*uidA* and *mGFP6*) assays performed, the new bioinformatics data and the lack of a noticeable phenotype in the *promoter:GOIs* (*HvHKT1;5* and *HvHVP1*) hydroponics salinity tolerance assays. In hindsight, continued development of the dual *HvHKT1;5* and *HvHVP1* root cell-type specific expression lines

(section 3.3.3) should have followed further confirmation of the improved salinity tolerance. However, due to the research timeframe for this PhD project, development of these lines was initiated prior to the completion of the original T_1 study (Krishnan, 2013).

In future work with cell-type specific expression of abiotic stress tolerance genes, careful consideration should be given, not only to the cell-type specificity, but also to the relative expression of promoters used and to confirm the responsiveness under stress conditions, especially when taking promoter elements from different species as has been done in this chapter.

The increased access to species specific sequencing data, especially in monocots of commercial relevance such as wheat and barley, as well as greater tissue-type specific expression data (through micro-arrays or RNA-seq) will make the identification of tissue-type specific promoters easier and allow the fine-tuning of promoters elements to enable expression of transgenes in desired cell-types.

3.4.3. Conclusion

The preliminary results of the T_1 *promoter:GOIs* (*HvHKT1;5* and *HvHVP1*) mini-hydroponic salinity tolerance assays (Krishnan, 2013) showing altered shoot Na^+ phenotypes were not supported by later experiments with more advanced material in supported hydroponics. Although, the hybridisation of these was successful, similarly there was no significant alteration in Na^+ phenotypes compared to null for lines generated with putative cell-type specific over-expression of *HvHKT1;5* and *HvHVP1*. The use of cell-type specific promoters to drive the expression of potential salinity tolerance genes such as *HvHKT1;5* and *HvHVP1*, individually or in combination, still has promise, despite the difficulties in obtaining cell-type specific promoters demonstrated in this study.

Chapter 4

Evaluating the effect of root cell-type specific over-expression of AtAVP1

Chapter 4 - Evaluating the effect of root cell-type over-expression of the Arabidopsis vacuolar H^+-pyrophosphatase, *AtAVP1*, on plant salinity tolerance

4.1. Introduction

4.1.1. Arabidopsis *vacuolar H^+-pyrophosphatase, AtAVP1,* and its use for improving plant salinity tolerance

The Arabidopsis *vacuolar H^+-pyrophosphatase* (*H^+-PPase*) *AtAVP1* (At1g15690) is a small, single subunit H^+-PPase which functions to reduce inorganic pyrophosphate (PP_i) to two orthophosphates (Sarafian *et al.*, 1992). The energy released by this reaction is used by *AtAVP1* to move a proton to assist in establishment of a proton gradient across membranes, such as the tonoplast (Blumwald *et al.*, 2000). This proton gradient was thought to be used by other transporters to translocate ions, such Na^+ by *AtNHX1* (*Na^+/H^+ Exchanger 1* - At5g27150) (Gaxiola *et al.*, 1999), which may improve Na^+ sequestration and salinity tolerance (Blumwald *et al.*, 2000). More recently, alternative hypotheses regarding the native role of *AtAVP1* have been put forward, potentially functioning in cytoplasmic PP_i cycling (Ferjani *et al.*, 2011) or sucrose transport (Paez-Valencia *et al.*, 2011) to improve heterotrophic plant growth, possibly dependant on the tissue in which *AtAVP1* is expressed. During the preparation of this thesis, new hypotheses have been put forward for the role of *AtAVP1* functioning in the sieve element companion cells playing a critical for phloem function, sucrose transport and PP_i homeostasis (Pizzio *et al.*, 2015).

AtAVP1 has been of interest to abiotic stress research due to its small size, consisting of a single subunit (rather than 26 subunits for most H^+-ATPases), making it more suitable for transgenic studies manipulating tonoplast transport (Gaxiola *et al.*, 2002). Constitutive over-expression of *AtAVP1* has previously been shown to positively impact multiple abiotic stresses, including salt tolerance, (Bao *et al.*, 2009; Gaxiola *et al.*, 2001; Kim *et al.*, 2014; Li *et al.*, 2010; Park *et al.*; Pasapula *et al.*, 2011), nitrogen use (Paez-Valencia *et al.*, 2013; Yang *et al.*, 2007) and phosphorous deficiency (Gaxiola *et al.*, 2012). There is also compelling evidence that plant biomass can also be increased under non-stress conditions in barley (Schilling *et al.*, 2014). Over-expression and ectopic expression of this gene in transgenic lines may also result in mistrafficing of the H^+-PPase to the plasma membrane and lead to novel functions (Gaxiola *et al.*, 2012; Li *et al.*, 2005).

4.1.2. Root cortical cell-type over-expression of *H*$^+$*-PPases* to improve plant N$^+$ tolerance

When this study was started *AtAVP1* was hypothesised to enhance the vacuolar proton gradient and thereby increase Na^+ sequestration, resulting in overall improved salinity tolerance. Root cortex cell-type specific over-expression of *AtAVP1* could allow the safe vacuolar sequestration of Na^+ in these cell-types due to the relatively large size of these cells. Increased Na^+ concentration in these cell-types would hypothetically reduce the Na^+ gradient between soil and root cells, preventing the further Na^+ uptake and thereby reducing overall translocation of Na^+ to the shoot.

In the previous chapter (Chapter 3), this hypothesis was tested in barley with root cortex cell-type over-expression of the barley orthologue *HvHVP1* driven by putative cell-type specific promoters. However, no significant effect on overall plant Na^+ accumulation was observed, although this result may have been due to the use of an inappropriate promoter. To further test the role of *H*$^+$*-Ppases* in the root cortex for Na^+ sequestration and improvement of salinity tolerance, we examined the effect of the root cortex cell-type expression of *AtAVP1* in Arabidopsis, carrying on from work started by a previous PhD student, Dr Gehan El-Hussieny (2006).

Rather than relying on cell-type specific promoters, Arabidopsis *GAL4-VP16* enhancer trap lines, originally developed by J. Haseloff (1999), with root cortex and root epidermal specific expression were used. *AtAVP1* was over expressed in these cell-types by introduction of the *pGOF-UAS$_{GAL4}$:AtAVP1* trans-activation construct (Figure 4.1) by *Agrobacterium* floral dip transformation. The *pGOF-UAS$_{GAL4}$:AtAVP1* construct contains the full-length *AtAVP1* cDNA sequence, downstream of a secondary *UAS$_{GAL4}$* sequence which promotes expression of *AtAVP1* in the identified cell types, in this case, root-epidermal and -cortical cells.

This experimental approach has since been validated by the over-expression of the Na^+ transporter *AtHKT1;1* in the root stele of both Arabidopsis (Møller *et al.*, 2009) where significant reduction in shoot Na^+ translocation has been observed.

Preliminary Q-PCR data from T_1 material by El-Hussieny (2006), has indicated that *AtAVP1* can be over-expressed in the root through the use of the *GAL4-VP16* enhancer trap system and the *pGOF-UAS$_{GAL4}$:AtAVP1* transactivation cassette (Figure 4.2),

although significant variation in expression levels of *AtAVP1* between different transgenic lines is apparent.

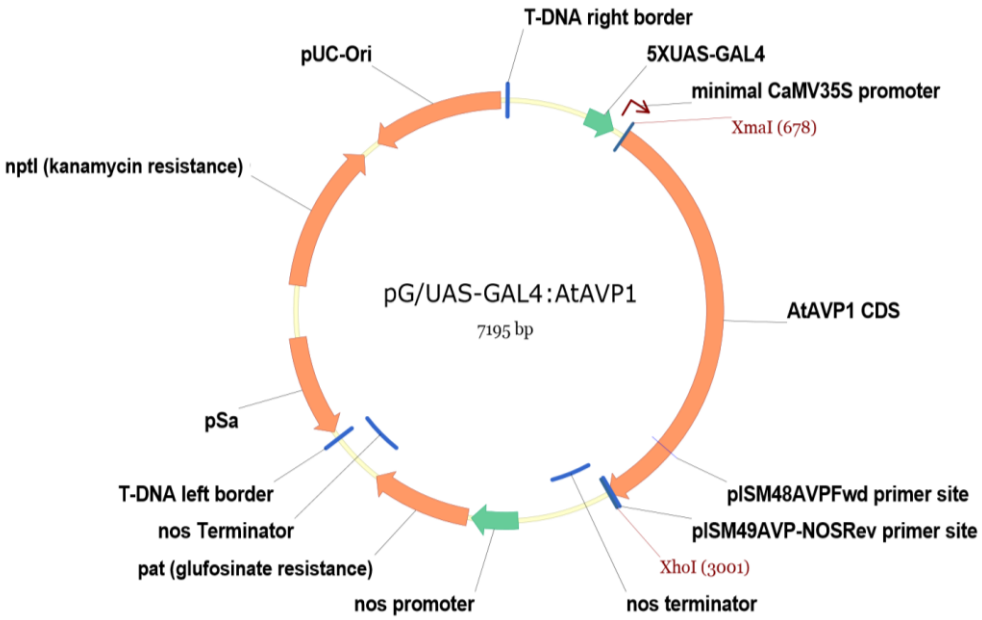

Figure 4.1: Schematic diagram of the expression vector *pGOF-UAS$_{GAL4}$:AtAVP1* used to drive the cell-type specific expression of *AtAVP1* in Arabidopsis *GAL4-VP16* enhancer trap-lines, J1551 and J1422.
From the T-DNA right border (clockwise) to the T-DNA left border: the T-DNA cassette contains [5 repeats of the *GAL4* upstream activation sequence (*5×UAS$_{GAL4}$*); a minimal *CaMV35S* promoter; *AtAVP1* CDS from Arabidopsis ecotype Col-0 (inserted via restriction enzyme sites, XmaI and XhoI); bacterial *nopaline synthase* (*nos*) terminator; bacterial *nopaline synthase* (*nos*) promoter; *phosphinothricin acetyltransferase* (*pat*) gene (Glufosinate resistance for Basta in planta selection); *nos* terminator, T-DNA left border sequence]. The remaining vector consists of the pSa replication origin (requiring the *Agrobacterium* strain for transformation to be co-transformed with the pSoup helper plasmid for successful replication in *Agrobacterium*), *neomycin phosphotransferase* (*nptI*) gene (Kanamycin resistance for bacterial selection) and the pUC replication origin (*pUC-Ori*) for *E. coli* replication. The primer binding sites for detecting the expression of *AtAVP1* by RT-PCR (pISM48AVPFwd & pISM48AVP-NOSRev) are also displayed.

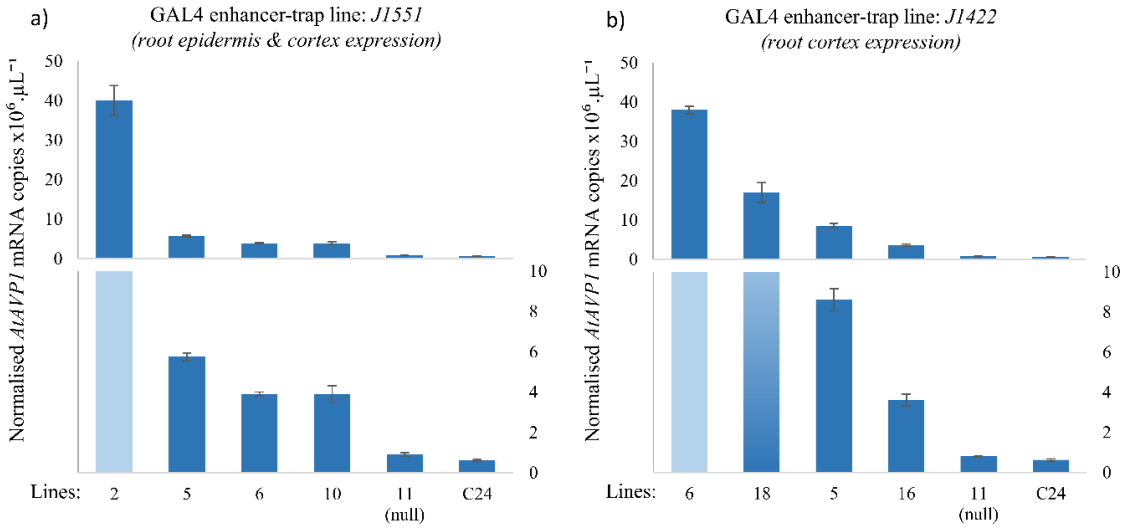

Figure 4.2: *AtAVP1* transcript level is increased in root tissues of selected 5 week-old T1 *pGOF-UAS$_{GAL4}$:AtAVP1* plants.
Normalised *AtAVP1* mRNA levels (both native *AtAVP1* and transgenic UAS$_{GAL4}$::*AtAVP1*) in root tissues of selected individual 5 week-old soil grown T_1 *A. thaliana* ecotype C24, enhancer-trap lines: (a) J1551 lines: 2, 5, 6, 10 and 11, and (b) J1422 lines: 6, 18, 5, 16 and 11) transformed with pGOF-UAS$_{GAL4}$::*AtAVP1* and Wild-type *A. thaliana* ecotype C24. *AtAVP1* mRNA levels determined by Q-PCR. Most transgenic lines show higher levels of *AtAVP1* mRNA transcript in the roots compared to Wild-type control likely due to the transgenic *AtAVP1* expression. Null segregant lines, J1551-11 and J1422-11, show similar expression levels to wild-type C24. Errors bars represent S.D. of four technical repeats. Q-PCR primers were not specific to transgene UASGAL4::*AtAVP1* but also hybridise to the native *AtAVP1*. Figure reproduced and adapted from El-Hussieny (2006), figure 4.13.

The over-expression of *AtAVP1* in the root cortex also appeared to drastically alter leaf elemental profiles in a number of the T_1 lines examined when plants were grown in soil and treated with a very mild (10 mM NaCl) salt stress. Reductions in leaf Na^+ content of between 50 – 80 % were observed in a number of lines, along with smaller reductions in Ca^{2+} and Mg^{2+} (Figure 4.3). Although, these results are from preliminary experiments using T_1 material, and as such should be interpreted carefully, such a significant reduction in shoot Na^+ is worth examining.

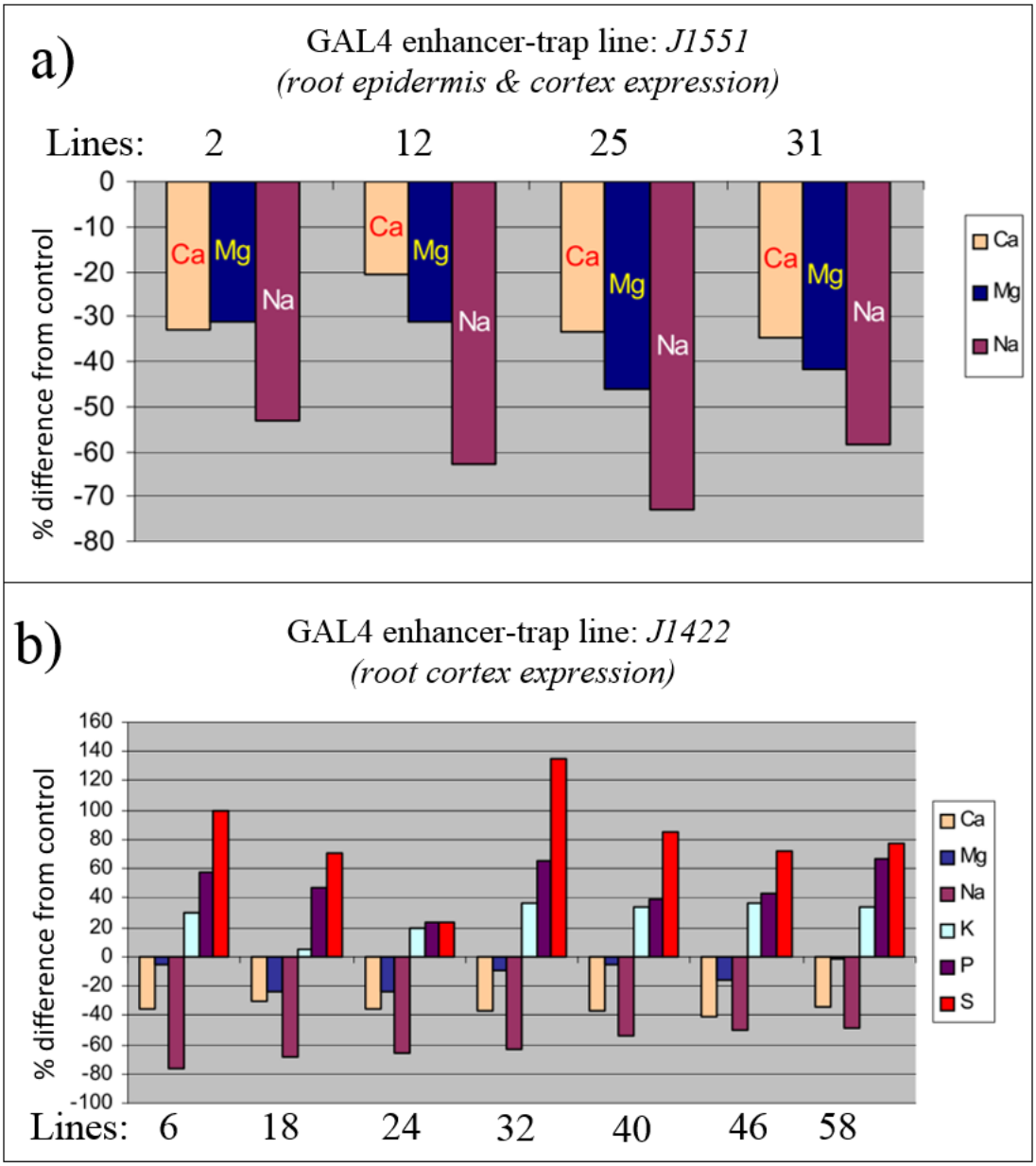

Figure 4.3: Selected individual soil grown T_1 pGOF-UAS_{GAL4}:*AtAVP1* plants show an altered leaf elemental profile.
Altered leaf elemental content (elements Ca, Mg, Na, K, P and S), expressed as a change in percentage from wild-type A. thaliana (ecotype. C24), of selected individual (n=1) T_1 *A. thaliana* (ecotype. C24, enhancer-trap lines: (a) J1551 and (b) J1422) transformed with *pGOF-UAS_{GAL4}:AtAVP1*. Elemental composition (ppm) of leaves from soil grown 6 week-old plants determined by ICP-OES. This graph shows several transformed lines with large alterations in several elements. A potential decrease in leaf Na^+ content (≈ 50 – 70 %) was observed in several T_1 lines with *UAS_{GAL4}* driven *AtAVP1* expression in both the J1551 and J1422 enhancer-trap backgrounds. Figure adapted from El-Hussieny (2006), figure 4.18.

4.1.3. Aims of this study

The work described in this chapter carries on from a preliminary study (El-Hussieny, 2006) in which Arabidopsis ecotype C24 showed altered shoot concentration of several

key elements (Na^+, Ca^{2+}, Mg^{2+}, S^- and P^-) when over-expressing *AtAVP1* in the root epidermis and/or root cortex through the use of *GAL4-VP16* enhancer trap lines. Several transgenic lines were selected for analysis based on previous Q-PCR data showing high level of root *AtAVP1* mRNA expression, presumably due to the expression of transgenic *AtAVP1* driven by the *GAL4-VP16* enhancer-trap and the *pGOF-UAS$_{GAL4}$:AtAVP1* transactivation construct and where ICP-OES elemental composition showing a phenotype was available. Screening of these lines for altered root/leaf Na^+ or K^+ accumulation and/or altered plant biomass was carried out in mini-hydroponics under a range of NaCl concentrations. To-date, the effect of root-cortex cell-type specific expression of *AtAVP1* has not been reported outside of the previous unpublished preliminary study by El-Hussieny (2006).

4.2. Methods and Materials

4.2.1. Plant material

T_2 seed of several lines of Arabidopsis ecotype C24 *GAL4-VP16* enhancer-trap lines J1551 (root epidermis and cortex expression) and J1422 (root cortex specific expression) transformed with *pGOF-UAS$_{GAL4}$:AtAVP1* were selected for analysis. Lines were selected based on previous ICP-OES elemental data (Figure 4.3), *AtAVP1* mRNA expression level (Figure 4.2) and seed availability. Seed were obtained from the ACPFG (Adelaide), stocks prepared by Dr. El-Hussieny (2006) in the original study kept at 4°C since circa. 2006.

T_2 seeds from each selected line were sown on vertical 0.5 × MS BASTA selection plates as per section 2.3.7 to select for the presence of *pGOF-UAS$_{GAL4}$:AtAVP1* construct. Surviving two week-old plants were inspected for the presence of GFP via stereo microscopy (section 2.6) to ensure similar GFP pattern to the parental enhancer-trap lines, J1551 or J1422 prior to being transferred to soil as per section 2.3.4.2 and grown until maturity. Several lines were grown until T_3 to ensure uniform growth and genotyped for the presence of *GAL4-VP16* enhancer-trap and the *pGOF- UAS$_{GAL4}$:AtAVP1* construct via PCR. T_4 seed of transgenic and null lines (Table 4.1) were used for salt stress screening in mini-hydroponics.

Table 4.1: Lines selected for salinity-stress screening
Information included; Line background and Line number for transformants selected for analysis

Background	Lines
Arabidopsis ecotype C24 *GAL4-VP16* Enhancer trap line: J1551 (root-epidermis and -cortex specific expression)	T_4 *pGOF-UAS$_{GAL4}$:AtAVP1* – 2
	T_4 *pGOF-UAS$_{GAL4}$:AtAVP1* – 5
	T_4 *pGOF-UAS$_{GAL4}$:AtAVP1* – 6
	T_4 *pGOF-UAS$_{GAL4}$:AtAVP1* – 10
	T_4 selected null line (A11)
	untransformed J1551
Arabidopsis ecotype C24 GAL4-Enhancer trap line: J1422 (root-cortex specific expression)	T_4 *pGOF-UAS$_{GAL4}$:AtAVP1* – 6
	T_4 *pGOF-UAS$_{GAL4}$:AtAVP1* – 18
	T_4 *pGOF-UAS$_{GAL4}$:AtAVP1* – 5
	T_4 *pGOF-UAS$_{GAL4}$:AtAVP1* – 16
	T_4 selected null line (B11)
	untransformed J1422
Wild-type Arabidopsis ecotype C24	untransformed wild-type C24

4.2.2. Salinity screening of root specific *AtAVP1* over-expressing Arabidopsis plants in mini-hydroponics

T_4 transgenic and control lines (Table 4.1) were grown in mini-hydroponics set-up described as in section 2.3.8 under short-day growth conditions in the growth chambers specified in section 2.3.1. Plants were transferred after two weeks growth (5 rosette leaf stage) to the mini-hydroponics setup and grown for an additional two weeks before onset of three salinity treatments, control (0 mM additional NaCl), mid (50 mM additional NaCl) or high (100 mM additional NaCl). Treatment was applied by 25 mM NaCl (+ 0.35 mM CaCl2) increments every 12 hours (7 AM and 7 PM). Plants were harvested after 7 days from the onset of salinity treatment. Root and shoot fresh weight was recorded for all plants, root material and youngest fully expanded leaf were collected for tissue Na^+ and K^+ accumulation by flame photometry (section 2.5.3). Root and leaf material was collected and snap-frozen in liquid N_2 for RNA extraction and transgene expression analysis (section 4.2.4). Leaf material was harvested for gDNA extraction and plant genotyping (section 4.2.3).

4.2.3. Genotyping of plants for the presence of *pGOF-UAS$_{GAL4}$:AtAVP1* constructs and *GAL4-VP16* enhancer-trap

Genomic DNA (gDNA) was extracted from leaf material of soil or hydroponically grown plants by the freeze-dry method (section 2.2.19) and genotyping PCR (section 2.2.2) was conducted to determine the presence of the *GAL4-VP16* enhancer-trap via the presence

of reporter gene *mGFP-ER* (primers: Table 4.2 - GFPiF and GFPiR) and *pGOF-UAS$_{GAL4}$:AtAVP1* construct via the presence of BASTA selectable marker (primers: Table 4.2 - Basta_F and Basta_R). Genomic DNA quality was checked by PCR with native gene *AtActin2* (At3g18780) (primers: Table 4.2 - pISM42AtAct2Fwd and pISM43AtAct2Rev). Genomic DNA from wild-type C24, and parental *GAL4-VP16* enhancer trap lines, J1551 and J1422, plus a no-template (H_2O) control were included for all experiments.

4.2.4. Extraction of RNA, cDNA synthesis and transgene expression by RT-PCR

Total RNA was extracted from the leaf and root material of selected plants as per 2.2.21 and cDNA synthesized as per section 2.2.22. Expression of transgenic *AtAVP1* was verified by reverse transcription (RT) PCR (section 2.2.2) with primers specific to *AtAVP1* and transcribed *nos* terminator (primers: Table 4.2 - pISM48AVPFwd and pISM49AVP-NOSRev). Expression of the *GAL4-VP16* transcriptional activator was determined by RT-PCR with synthesized cDNA with primers specific to enhancer-trap reporter gene *mGFP5-ER* (primers: Table 4.2 - GFPiF and GFPiR). cDNA quality was checked by RT-PCR of housekeeping gene *AtActin2* (At3g18780), (primers: Table 4.2 - pISM42AtAct2Fwd and pISM43AtAct2Rev). cDNA from wild-type C24 and parental GAL4-VP16 enhancer trap lines, J1551 and J1422, plus a no-template control were included for all experiments.

4.2.5. Statistical analysis

All data collected from hydroponics experiments was analysed in Microsoft Excel 2013 with significant differences between transgenic and null lines and between treatments were determined by one- or two-way ANOVAs. Analyses with significance ($P \leq 0.05$) were subjected to Tukey-Kramer HSD post-hoc analysis.

Table 4.2: Primers for genotyping and RT-PCR of *Arabidopsis AtAVP1OX* lines.
Information included; primer name, length, sequence, expected amplicon length and PCR conditions for either genotyping PCR or RT-PCR. Genotyping and RT PCRs conducted as per section 2.2.2 with specified PCR conditions, 35 cycles.

Primer	Length (bp)	Sequence (5′ - 3′)	Amplicon Size (bp)	PCR conditions	Purpose
GFPiF	20	TCAAGGAGGACGGAAACATC	234	Anneal: 55 °C Extension: 30s	Genotyping & RT-PCR for presence/expression of *GAL4-VP16* enhancer- trap
GFPiR	20	AAAGGGCAGATTGTGTGGAC			
Basta_F	20	GACTTCAGCAGGTGGGTGTA	377	Anneal: 62 °C Extension: 30s	Genotyping for presence of *pGOF-UAS$_{GAL4}$:AtAVP1 (bar* gene)
Basta_R	17	AAATCTCGGTGACGGGC			
pISM42AtAct2Fwd	20	GCCCAGAAGTCTTGTTCCAG	297	Anneal: 53 °C Extension: 30s	gDNA RT-PCR cDNA quality check
pISM43AtAct2Rev	20	ACATCTGCTGGAATGTGCTG			
pISM48AVPFwd	21	GATGCTTCCATCAAGGAAATG	405	Anneal: 60 °C Extension: 30s	RT-PCR for AtAVP1:nosT expression via *pGOF-UAS$_{GAL4}$:AtAVP1*
pISM49AVP-NOSRev	24	CCCCTCGAGTTAGAAGTACTTGAA			

4.3. Results and Discussion

4.3.1. Obtaining T_4 transgenic lines and difficulties encountered during screening of Arabidopsis growth in mini-hydroponics.

Difficulties were encountered in obtaining T_4 *AtAVP1* over-expressing lines due to their long storage before use in this project. Selection and additional screening of plant material was required which allowed the development 4 homozygous T_4 lines from each of the two enhancer-trap lines, J1551 and J1442 (Table 4.1) with consistent expression of both *AtAVP1:nosT* by RT-PCR.

In total, 7 rounds of mini-hydroponics were conducted with these lines, two of which were successfully completed and discussed below. The five preliminary rounds were terminated early in trials to ensure correct staging and salt stress application, or due to inconstancies of growth between lines or breakdown of the growth facilities. Care must be taken in interpreting the results as significant variation between hydroponics experiments exists, primarily due to growth chamber conditions, despite careful positioning and monitoring of growth conditions. Figure 4.4 illustrates the significant variation between two hydroponics setups (3 tanks per setup), grown concurrently but in different bays within the growth chambers. The two enhancer trap-lines J1551 and J1422 show significantly different root and shoot biomass (≈20%), which may have been explained by their separate transformation events. However, the inclusion of a single line of wild-type C24 plants, germinated concurrently and transferred into both mini-hydroponics setups, displays an almost 50 % difference in shoot and root FW biomass between hydroponic setups. For this reason, the hydroponics experiments are considered independently, however, with such variation between experiments it is unlikely that significant differences could be detected with any certainty.

a)

b)

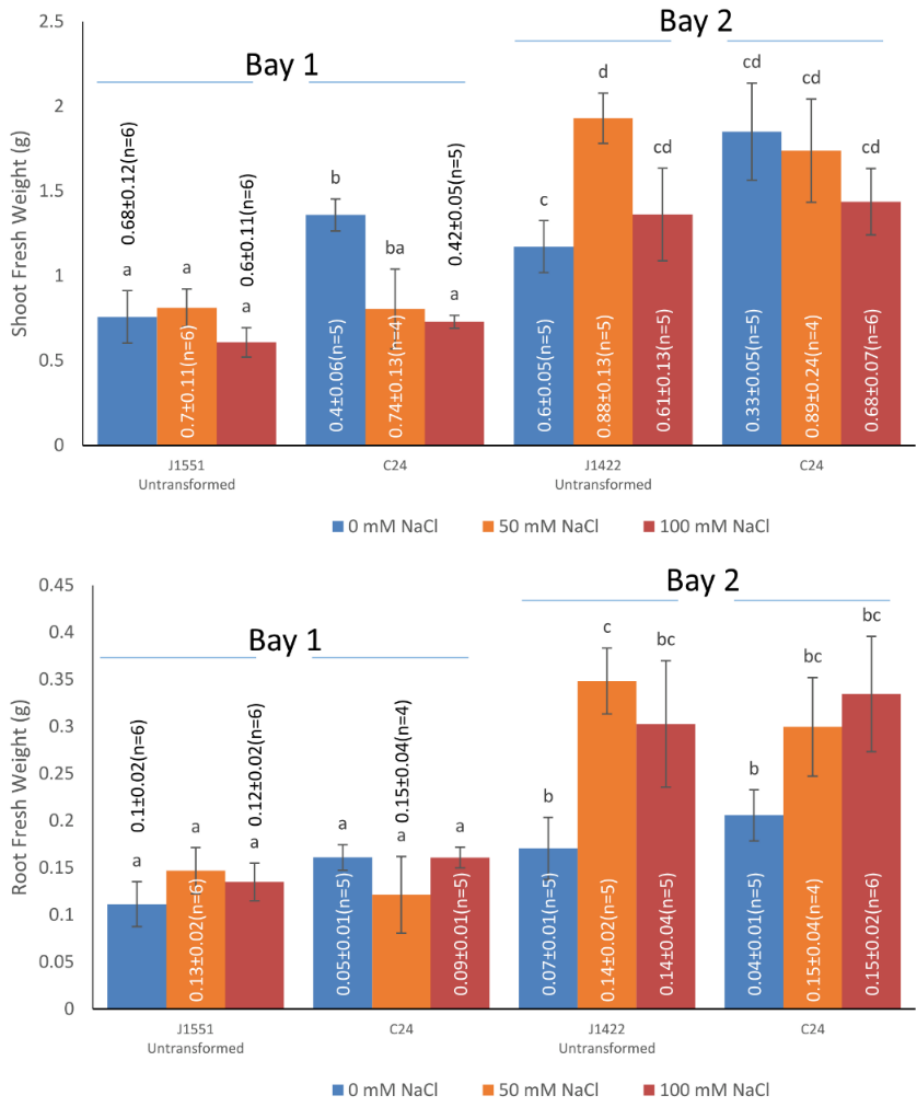

Figure 4.4: Position of Arabidopsis hydroponics in growth chambers can have a significant effect on plant growth.

Two rounds of mini-hydroponics were grown consecutively in separate bays (bay 1 or bay 2) within the growth chambers. Plants were grown in mini-hydroponics for five weeks before the application of three levels of NaCl stress. 0 mM NaCl (+ 0 mM $CaCl_2$) (blue bars), 50 mM NaCl (+ 0.7 mM $CaCl_2$) (orange bars) or 100 mM NaCl (+ 1.4 mM $CaCl_2$) (red bars) added in 25 mM NaCl (+ 0.35 mM $CaCl_2$) increments every 12 hours until the final concentration was reached. Plants were harvested after 1 week at the final NaCl concentration. Significant differences between means of different lines under same treatments (0, 50 or 100 mM NaCl) were determined by one-way ANOVA, followed by Tukey-Kramer HSD test ($P \leq 0.05$), letters represent significant differences.

4.3.2. Assessing the salinity tolerance of Arabidopsis enhancer trap line J1551 Over-expression of *AtAVP1* in the root-cortex and -epidermis.

Four independent T_4 lines with root-cortex and -epidermis over-expression of *AtAVP1* via the *pGOF- UAS_{GAL4}:AtAVP1* transactivation construct (Figure 4.5) in the *GAL4-VP16* enhancer-trap line, J1551, were screened under 3 salinity treatments (control – 0 mM NaCl, medium – 50 mM additional NaCl, or high – 100 mM additional NaCl). A null segregant line and the untransformed parental enhancer-trap line (J1551) were included as controls. The complete tabulated data is available in Appendix III: Arabidopsis hydroponics experiment #2 - tabulated data. The results of a primary round in which wild-type C24 plants were also included are tabulated in Appendix III: Arabidopsis hydroponics experiment #1 - tabulated data, however will not be discussed as the inclusion of an additional line reduced the overall number of replicates and is less statistically significant.

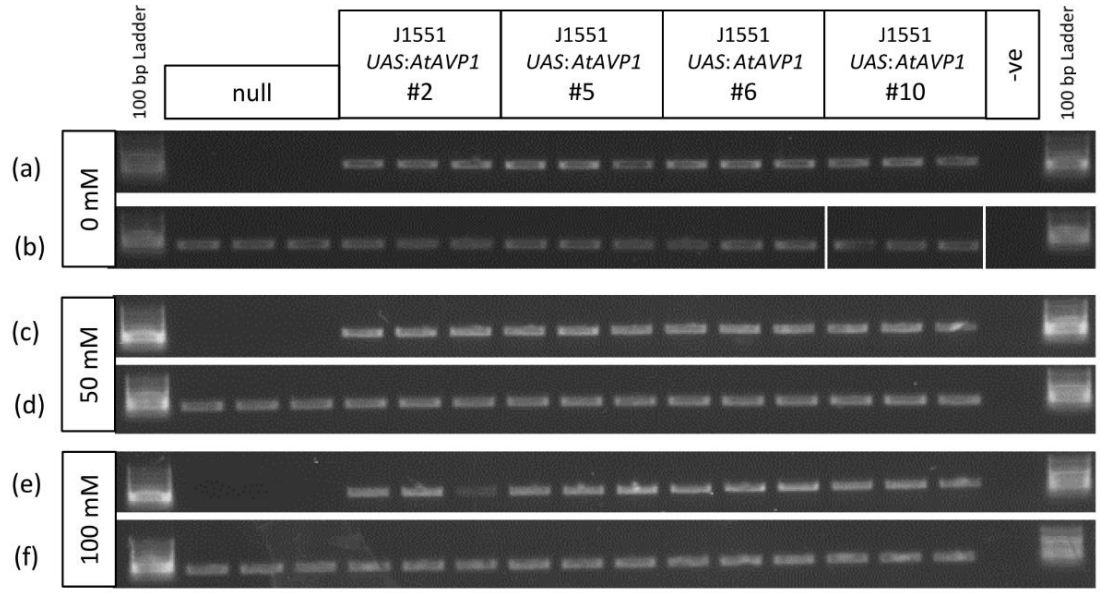

Figure 4.5: *AtAVP1:nosT* transcript was detected in root material of *J1551* lines transformed with the p*GOF-UAS_{GAL4}:AtAVP1* trans-activation construct.
Representative electrophoresis gel showing the presences of *AtAVP1:nosT* transcript in cDNA synthesised from root extracted RNA via RT-PCR. T_4 lines, 2, 5, 6 and 10 all showed expression of the *AtAVP1:nosT* transcript under 0 mM (a), 50 mM (c) and 100 mM (e) NaCl, but missing from the null line and water negative (-ve) control. Expression of *Actin2* (b, d, f) was detected in all corresponding cDNA samples.

4.3.2.1. Root to shoot biomass is not significantly affected under medium (50mM) and high (100mM) NaCl. Root to shoot ratio increases under increasing NaCl.

No significant difference was seen in root or shoot biomass between the root specific *AtAVP1* over-expressing (OX) transgenic lines and null segregants line when grown in either 50 or 100 mM NaCl treatments **(**Figure 4.6**)**. Three of the four (lines 2, 6 and 10) had a significant ($P \leq 0.05$) decrease in shoot fresh weight biomass (≈30 %) compared to null and the untransformed parental line J1551 in control (+ 0 mM additional NaCl) conditions (Figure 4.6**,** a). Root FW biomass increased in all lines in response of increase salinity treatments (Figure 4.6, b) leading to increased root-shoot biomass ratio (Figure 4.6, c).

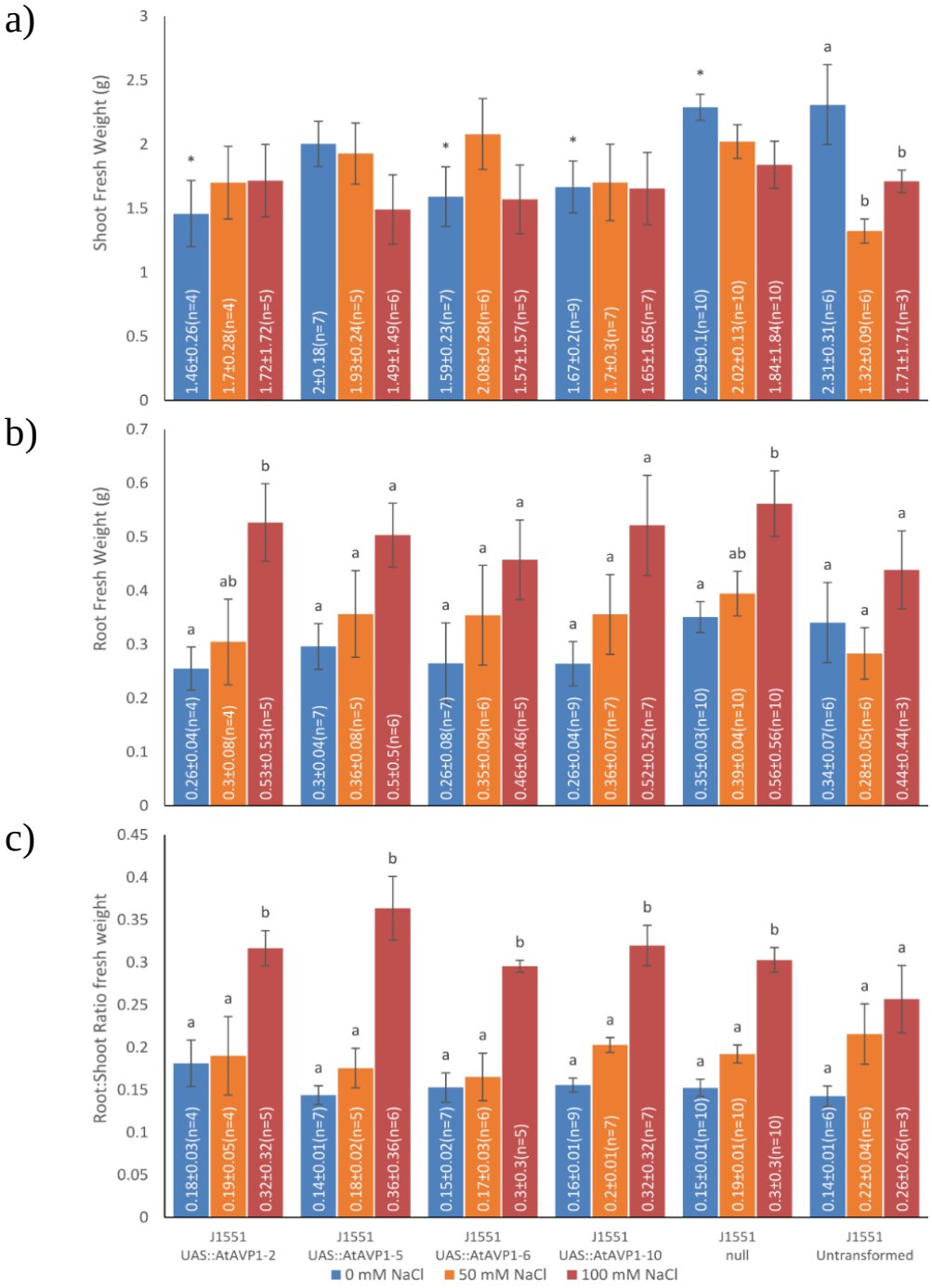

Figure 4.6: Shoot and Root FW biomass of hydroponically grown T_4 enhancer-trap J1551 plants with root-specific over-expression of *AtAVP1* under increasing salinity treatments.

Mean shoot (a) and root (b) fresh weight measurements and root-shoot ratio (c) of four T_4 enhancer-trap J1551 lines with root-specific over-expression of *AtAVP1*, null line and untransformed parental line (J1551) for comparison. Plants were harvested after 7 d of NaCl treatment (blue – 0 mM additional NaCl, orange – 50 mM additional NaCl, red – 100 mM additional NaCl). Values shown are mean ± S.E.M (n = number of replicates). Letters indicate significant differences between treatments ($P \leq 0.05$). Asterisks (*) indicate significant difference ($P \leq 0.05$), between control (0 mM NaCl) grown transgenic plants and the null line. Tabulated data is presented in Arabidopsis hydroponics experiment #2 - tabulated data.

4.3.2.2. Over-expression of *AtAVP1* in the root-cortex and root epidermis of Arabidopsis enhancer trap line J1551 may alter leaf Na^+ or K^+ accumulation under high salinity treatments

A significant treatment affect was seen in the leaf Na^+ and K^+ content. Leaf [Na^+] increased with increasing salinity treatments (≈150 µmoles.g^{-1} DW under 0 mM NaCl, ≈1300 µmoles.g^{-1} DW under 50 mM, and ≈2700 µmoles.g^{-1} DW under 100 mM NaCl) (Figure 4.7, a). Leaf [K^+] decreased with increasing salinity treatments (≈1650 µmoles.g^{-1} DW under 0 mM NaCl, ≈680 µmoles.g^{-1} DW under 50 mM, and ≈520 µmoles.g^{-1} DW under 100 mM NaCl) (Figure 4.7, b). Two of the *AtAVP1* OX lines (lines 2 and 6) show significantly higher leaf [Na^+] (≈30% increase) compared to the null line under 100 mM NaCl, while one line (line 2) shows a significantly higher leaf [Na^+] (≈30% increase) compared to the null line under control conditions. Leaf [K^+] is not significantly altered compared to the null line under any treatment.

4.3.2.3. Over-expression of *AtAVP1* in the root-cortex and root epidermis of Arabidopsis enhancer trap line J1551 does not significantly alter root Na^+ or K^+ accumulation

A similar treatment affect was observed on Na^+ content in the roots (Figure 4.8, a), with increasing [Na^+] with increasing salinity treatment (≈30 µmoles.g^{-1} DW under 0 mM NaCl, ≈500 µmoles.g^{-1} DW under 50 mM, and ≈700 µmoles.g^{-1} DW under 100 mM NaCl). Interestingly, total root [Na^+] content is less than that in the leaves, indicating the majority of Na^+ taken up via the root is transported to the shoot. No significant difference in [Na^+] was observed between transgenic and the null line.

In contrast, root [K^+] is not significantly altered by increasing salinity treatments (Figure 4.8, b) maintaining at ≈2100 µmoles.g^{-1} DW under all NaCl treatments levels. Only one line (line 6) showed a significant, though small, increase in root [K^+] compared to the null line under control conditions.

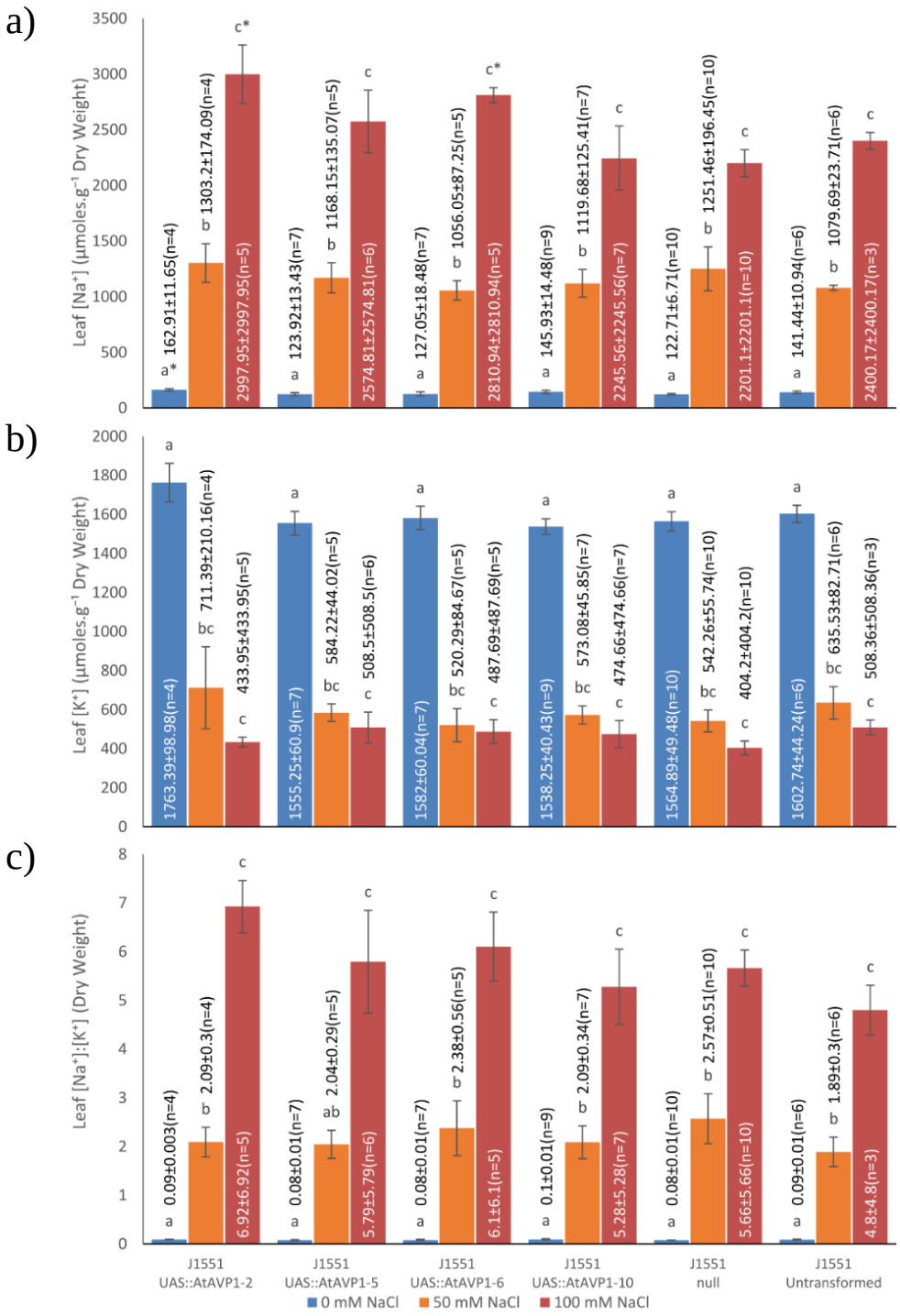

Figure 4.7: Leaf Na^+, K^+ concentration of hydroponically grown T_4 enhancer-trap J1551 plants with root-specific over-expression of *AtAVP1* under increasing salinity treatments

Mean leaf Na^+ (a) and K^+ (b) content (µmoles.g^{-1} DW) and [Na^+]:[K^+] ratio (c) of 5 week old four T_4 enhancer-trap J1551 lines with root-specific over-expression of *AtAVP1*, null line and untransformed parental line (J1551) for comparison. Plants were harvested after 7 days of NaCl treatment (blue – 0 mM additional NaCl, orange – 50 mM additional NaCl, red – 100 mM additional NaCl). Values shown are mean ± S.E.M (n=number of replicates).Letters indicate significant differences between treatments ($P \leq 0.05$). Asterisks (*) indicate significant difference ($P \leq 0.05$), between 100 mM NaCl grown transgenic plants and the J1551 null line.

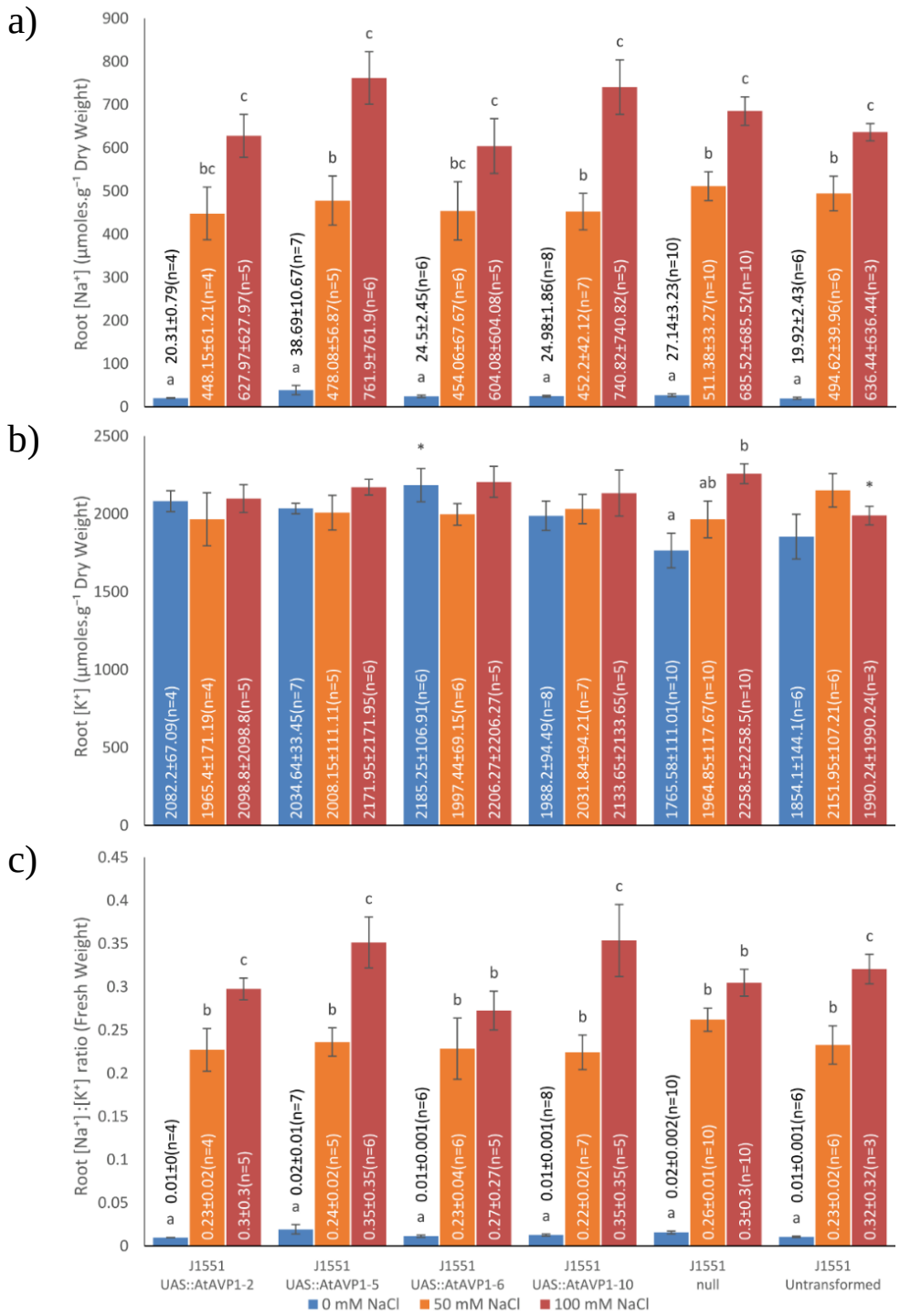

Figure 4.8: Root Na^+, K^+ concentration of hydroponically grown T_4 enhancer-trap J1551 plants with root-specific over-expression of *AtAVP1* under increasing salinity treatments.

Mean root Na^+ (a) and K^+ (b) content (µmoles.g^{-1} DW) and [Na^+]:[K^+] ratio (c) of 5 w old four T_4 enhancer-trap J1551 lines with root-specific over-expression of *AtAVP1* with null line and untransformed parental J1551 line for comparison. Plants were harvested after 7 d of NaCl treatment (blue – 0 mM additional NaCl, orange – + 50 mM additional NaCl, red – + 100 mM additional NaCl). Values shown are mean ± S.E.M (n=number of replicates). Letters indicate significant differences between treatments ($P \leq 0.05$). Asterisks (*) indicate significant difference ($P \leq 0.05$), between control (0 mM NaCl) grown transgenic plants and the J1551 null line.

4.3.3. Assessing the salinity tolerance of Arabidopsis enhancer trap line J1422 over-expressing *AtAVP1* specifically in the root-cortex.

Four independent T_4 lines with root-cortex specific over-expression of *AtAVP1* (Figure 4.9) via the *pGOF-UAS$_{GAL4}$:AtAVP1* transactivation construct in the *GAL4-VP16* enhancer-trap line, J1422, were screened under 3 salinity treatments (control - 1.5 mM NaCl, medium – 50 mM additional NaCl, or high - 100 mM additional NaCl). A null segregate line and the untransformed parental enhancer-trap line (J1422) were included as controls. The complete tabulated data is available in Appendix III: Arabidopsis hydroponics experiment #2 - tabulated data. The results of a primary round in which wild-type C24 plants were also included are tabulated in Appendix III: Arabidopsis hydroponics experiment #1 - tabulated data, however will not be discussed as the inclusion of an additional line reduced the overall number of replicates and is less statistically significant

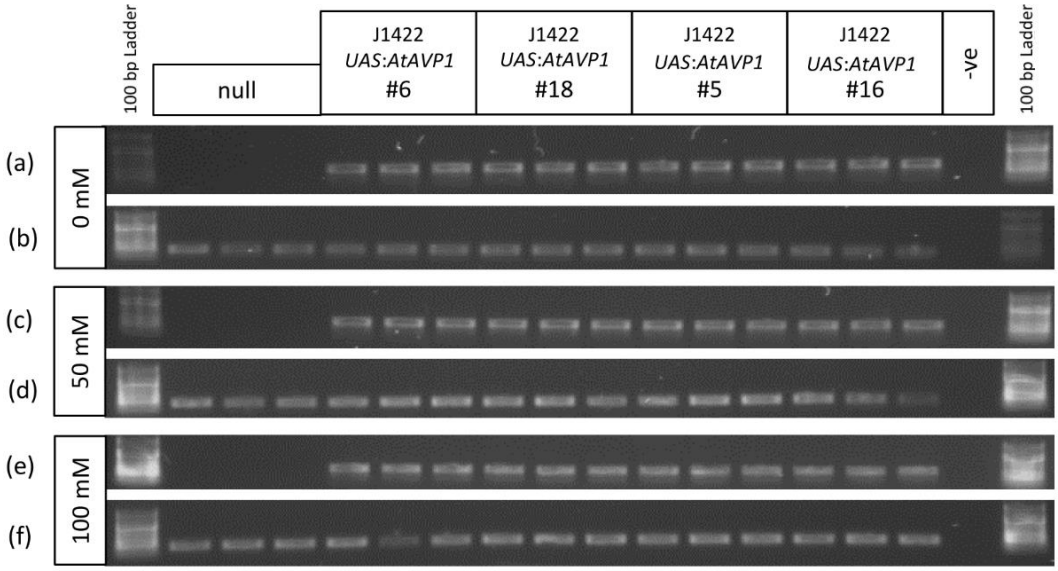

Figure 4.9: *AtAVP1:nosT* transcript was detected in root material of *J1422* lines transformed with the *pGOF-UAS$_{GAL4}$:AtAVP1* trans-activation construct.
Representative electrophoresis gel showing the presences of *AtAVP1:nosT* transcript in cDNA synthesised from root extracted RNA via RT-PCR. T_4 lines, 6, 18, 5 and 16 all showed expression of the *AtAVP1:nosT* transcript under 0 mM (a), 50 mM (c) and 100 mM (e) NaCl, but missing from the null line and water negative (-ve) control. Expression of *Actin2* (b, d, f) was detected in all corresponding cDNA samples.

4.3.3.1. Root to shoot biomass is not significantly affected under increasing salinity treatments. Root to shoot ratio increases under increasing NaCl.

Similar to the results of *AtAVP1* cell-type specific expression in the J1551 lines (section 4.3.2), there was no significant difference seen in root or shoot biomass between the root

specific *AtAVP1* over-expressing J1422 lines and null segregants line when grown in any NaCl treatment (Figure 4.10). Shoot FW biomass was not significantly affected by increasing salinity treatments (Figure 4.10, a) while root FW biomass increased in all lines in response to increased salinity treatments (Figure 4.10, b) again leading to increased root-shoot biomass ratio (Figure 4.10, c).

4.3.3.2. Over-expression of *AtAVP1* in the root-cortex and root epidermis of Arabidopsis enhancer trap line J1422 does not alter leaf Na^+ or K^+ accumulation.

A significant treatment affect was seen in the leaf Na^+ and K^+ content of all lines (Figure 4.11). Leaf [Na^+] increased with increasing salinity treatments (≈90 µmoles.g-1 DW under 0mM NaCl, ≈1750 µmoles.g-1 DW under 50 mM, and ≈3700 µmoles.g^{-1} DW under 100 mM NaCl) (Figure 4.11, a). Leaf [K^+] decreased with increasing salinity treatments (≈1650 µmoles.g^{-1} DW under 0mM NaCl, ≈900 µmoles.g^{-1} DW under 50 mM, and ≈580 µmoles.g^{-1} DW under 100 mM NaCl) (Figure 4.11, a). Only two significant differences were found between transgenic plants and the null line, with line 16, accumulating more Na^+ under control conditions (≈25% increase), and line 5, accumulating more [K^+] (≈35% increase) under the 50 mM NaCl treatment. Root [Na^+] and [K^+] was not significantly altered in other conditions.

4.3.3.3. Over-expression of *AtAVP1* in the root-cortex and root epidermis of Arabidopsis enhancer trap line J1422 does not significantly alter root Na^+ -or K^+ accumulation

A significant treatment effect was observed on Na^+ content in the roots (Figure 4.12, a), similar to that seen in the J1551 lines (section 4.3.2.3). Root [Na^+] increased with increasing salinity treatment (≈30 µmoles.g^{-1} DW under 0mM NaCl, ≈500 µmoles.g^{-1} DW under 50 mM, and ≈700 µmoles.g^{-1} DW under 100 mM NaCl). Two *AtAVP1* OX lines had significantly greater [Na^+] content (≈40 %) under 50 mM NaCl treatment compared to the null line. No other significant difference in [Na^+] was observed between *AtAVP1* OX lines and the null line. Although there is a trend for reduced [Na^+] in the roots of *AtAVP1* OX lines under 100 mM NaCl, compared to the null line. However the root [Na^+] is comparable to that in the untransformed J1422 line.

In contrast, root [K^+] is not significantly altered by increasing salinity treatments (Figure 4.12, b), maintaining at ≈2000 µmoles.g^{-1} DW under all NaCl treatments levels. Only one line (line 18) showed a significant decrease in root [K^+] (≈10 %) compared to the null line under control conditions.

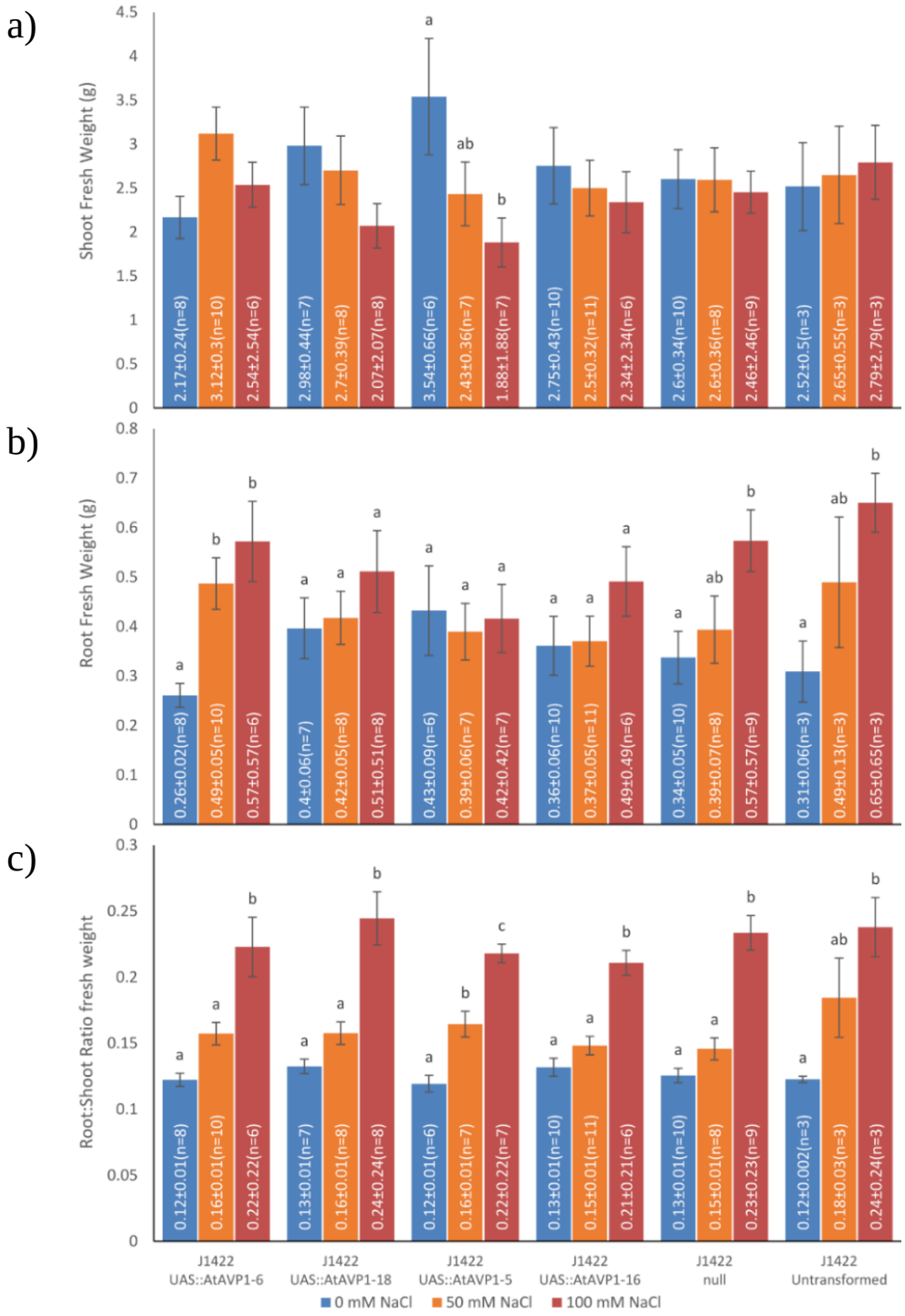

Figure 4.10: Shoot and Root FW biomass of hydroponically grown T_4 enhancer-trap J1422 plants with root-specific over-expression of *AtAVP1* under increasing salinity treatments.

Mean shoot (a) and root (b) fresh weight measurements and root-shoot ratio of 5 w old four T_4 enhancer-trap J1422 lines with root-specific over-expression of *AtAVP1* with null line and untransformed parental J1422 line for comparison. Plants were harvested after 7 d of NaCl treatment (blue – 0 mM additional NaCl, orange – 50 mM additional NaCl, red – 100 mM additional NaCl). Values shown are mean ± S.E.M (n = number of replicates). Letters indicate significant differences between treatments ($P \leq 0.05$).

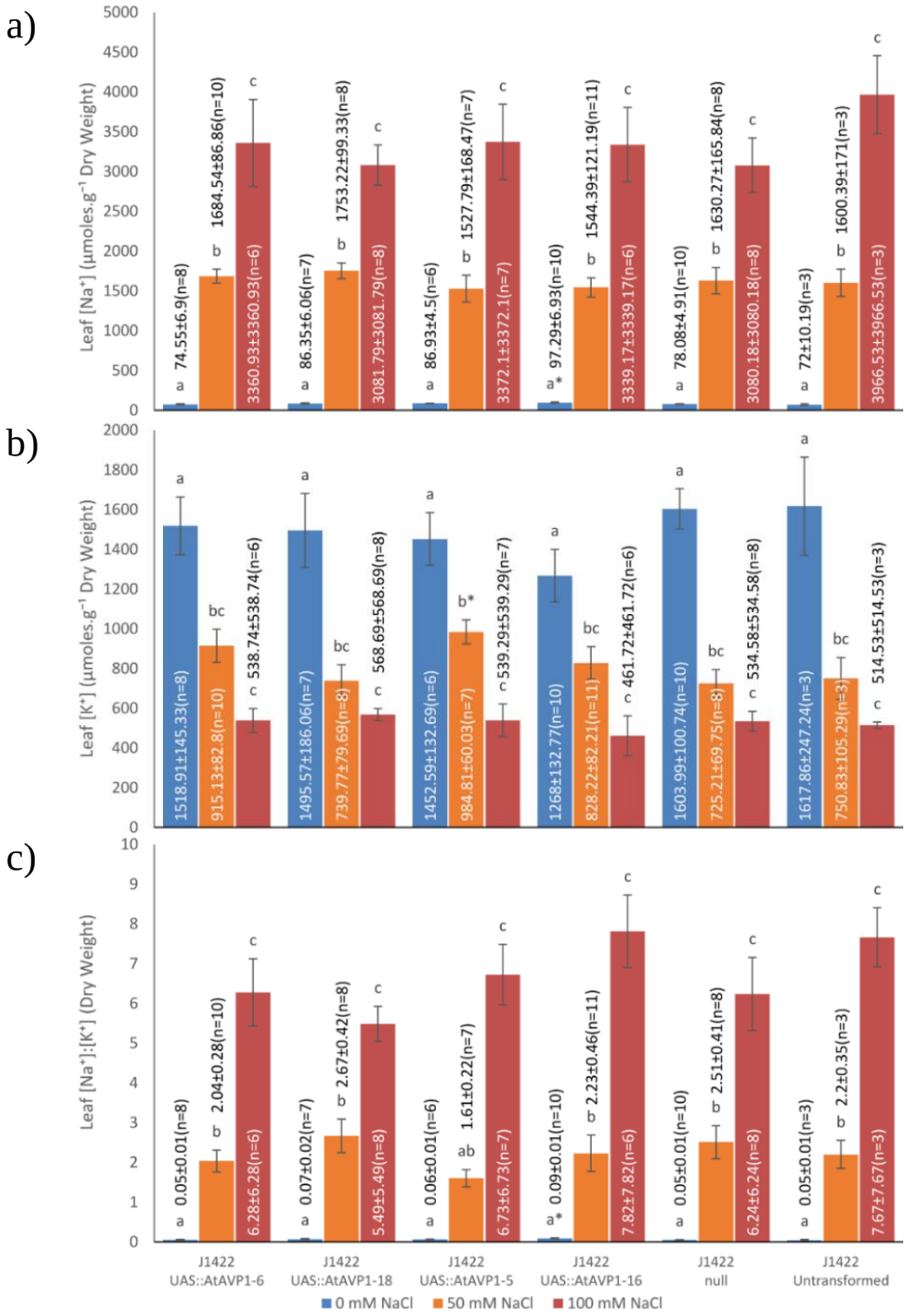

Figure 4.11: Leaf Na^+, K^+ concentration of hydroponically grown T_4 enhancer-trap J1422 plants with root-specific over-expression of *AtAVP1* under increasing salinity treatments

Mean leaf Na^+ (a) and K^+ (b) content (µmoles.g^{-1} DW) and [Na^+]:[K^+] ratio (c) of 5 w old four T_4 enhancer-trap J1422 lines with root-specific over-expression of *AtAVP1* with null line and untransformed parental J1422 line for comparison. Plants were harvested after 7 d of NaCl treatment (blue – 0 mM additional NaCl, orange – 50 mM additional NaCl, red – 100 mM additional NaCl). Values shown are mean ± S.E.M (n = number of replicates). Letters indicate significant differences between treatments ($P \leq 0.05$). No significant differences were observed between transgenic and null lines.

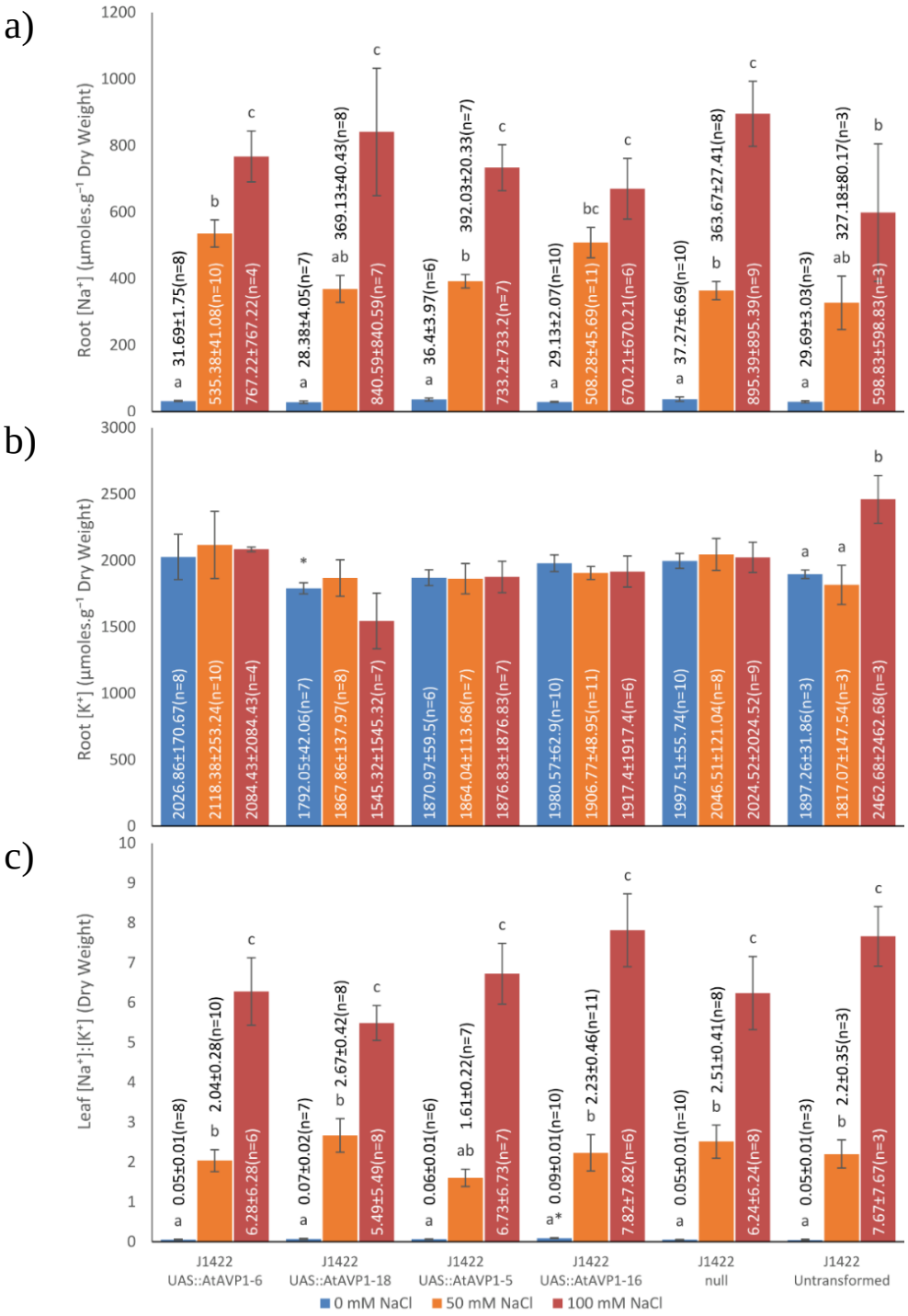

Figure 4.12: Root Na^+, K^+ concentration of hydroponically grown T_4 enhancer-trap J1422 plants with root-specific over-expression of *AtAVP1* under increasing salinity treatments

Mean root Na^+ (a) and K^+ (b) content (µmoles.g^{-1} DW) and [Na^+]:[K^+] ratio (c) of 5 w old four T_4 enhancer-trap J1422 lines with root-specific over-expression of *AtAVP1* with null line and untransformed parental J1422 line for comparison. Plants were harvested after 7 d of NaCl treatment (blue – 0 mM additional NaCl, orange – 50 mM additional NaCl, red – 100 mM additional NaCl). Values shown are mean ± S.E.M (n = number of replicates). Letters indicate significant differences between treatments ($P \leq 0.05$). Asterisks (*) indicate significant difference ($P \leq 0.05$), between control (0 mM NaCl) grown transgenic plants and the J1422 null line.

4.4. General Discussion

4.4.1. Summary of the findings

In summary, no significant and consistent differences were observed in root or shoot Na^+ and K^+ accumulations between the trialled *AtAVP1 OX* lines and respective null line or parental untransformed enhancer-trap lines. Neither was any significant differences in root or shoot biomass observed. While significant variation exists and there are some concerns about the reliability of the data due to plant growth conditions, overall, the results of the hydroponics experiments carried out in this chapter do not support previous preliminary work (El-Hussieny, 2006) which had shown that the over-expression of the vacuolar *H^+-PPase, AtAVP1*, in Arabidopsis root cortex and epidermis through the use of the *GAL4-VP16* enhancer-trap resulted in significant decreased leaf Na^+ accumulation. A trend for reduced root [Na^+] in the J1422 *AtAVP1* OX lines may be worth examining (section 4.3.3.3), by additional hydroponics experiments with increased number of replicates.

4.4.2. Comparison of these experiments to previous preliminary experiments

The preliminary experiments (showing a reduction in leaf Na^+ of between 50 – 80 % for some plants - Figure 4.3) from which this work was based (El-Hussieny, 2006) should be treated with a degree of caution. Although the expression of *AtAVP1::nosT* transcript was confirmed in the root of the T_4 lines examined, the experimental technique used to assess leaf ion content was limited due to its reliance on T_1 material. The altered leaf ion profiles was determined by ICPS of leaf material from individual T_1 plants, following selection and transplantation, and compared to the mean of ion content of wild-type (i.e. non enhancer-trap lines) C24 plants (n =3). This initial screen was also conducted with soil grown plants and treated with a very mild salinity (10 mM NaCl) compared to experiments carried out in hydroponics with much higher salinity levels (50 – 100 mM NaCl) in this study which may have led to a different effect on Na^+ accumulation.

Additionally, the long delay between the initial research (2006) and its continuation in this study, added additional complications, particularly in relation to selection of lines and issues with seed germination. In hindsight, re-transformation and selection of new lines, rather than using lines kept since 2006 would have simplified line selection.

4.4.3. The role of *AtAVP1* in root cortex of Arabidopsis

The Arabidopsis ecotype used in this study, C24, was primarily selected due to the availability of the Arabidopsis enhancer-traps and the expression patterns displayed. Interestingly, C24 behaves significantly differently from the other commonly used ectoype Columbia (Col-0) when exposed to salt stress. Under high salinity in soil and hydroponics, C24 appears less stressed compared to Col-0 despite accumulating greater shoot Na^+. C24 is also effectively able to maintain root K^+ content under increasing Na^+ concentrations (Jha *et al.*, 2010; Munns & Tester, 2008). This is also seen in the transgenic and wild-type C24 lines examined in this study.

This ecotype difference may be of importance, as the majority of the *AtAVP1* work in Arabidopsis has been carried out in the Col-0 ecotype (Ferjani *et al.*, 2011; Gonzalez *et al.*, 2010; Paez-Valencia *et al.*, 2011; Pizzio *et al.*, 2015; Vercruyssen *et al.*, 2011) and the positive effects of *AtAVP1* over-expression has yet to been reported in the C24 ecotype. Potentially, the differences between the ways Col-0 and C24 treat salinity stress and Na^+ uptake may be masking the effect of root cell-type over-expression of *AtAVP1*. If available, an interesting comparison for future experiments would be test Arabidopsis ecotype C24 constitutive over-expressing *AtAVP1* to see if the improved growth phenotype is observed in this ecotype.

Additionally, as the bulk of previous work showing improvement in abiotic stress tolerance has used constitutive over-expression of transgenes. Potentially the expression of *AtAVP1* in the root-epidermis and root cortex with the use of the *GAL4-VP16* lines used in this study may have missed the tissues in which *AtAVP1* has a beneficial effect. Alternative hypotheses regarding the native role of *AtAVP1* functioning in cytoplasmic PPi cycling (Ferjani *et al.*, 2011), promoting cell proliferation and final leaf size (Vercruyssen *et al.*, 2011), sucrose transport (Paez-Valencia *et al.*, 2011) and phloem function (Pizzio *et al.*, 2015) have been put forward. Potentially over-expression of *AtAVP1* in rapidly dividing cells such as root and shoot meristems or in vascular tissues may prove beneficial compared to root-cortex or -epidermal expression as done in this study.

Expression of *AtAVP1* in barley has also been linked with early plant vigour (Schilling, 2010; Schilling *et al.*, 2014) with increased plant biomass during early development, leading to overall increased growth and salinity tolerance, but no reduction in Na^+

accumulation. Potentially, examining plants under a late (5 weeks post germination) stress treatment as conducted in this study, any early growth improvement may have masked by extended growth in mini-hydroponics.

4.4.4. Further work

Further experimentation with the T_4 lines developed in this chapter and subsequent generations, may be warranted to investigate the other altered shoot ions phenotypes observed in these lines in the original study (decreased [Ca^{2+}], [Mg^{2+}] in both J1422 and J1551 lines, increased [P^{3-}] [S^{-}] in J1422 lines) by additional rounds of mini-hydroponics.

Replication of these experiments in soil and applying NaCl stress by watering with different concentrations with NaCl, similar to the original study is also possible (Conn *et al.*, 2013; Weigel & Glazebrook, 2002) and may also give a different response than observed in mini-hydroponics used in this study. Additionally, screening of these lines on agar plates, with or without various NaCl concentrations, for enhanced early seeding biomass or altered ion content would also be an interesting avenue of research. However, this technique prevents adequate transpiration which may influence ion distribution throughout the plant which makes it less desirable for screening lines with altered shoot ion content (Møller, 2008).

Arguably, screening for NaCl tolerance in soil-grown plants would be preferable to the use of hydroponics or MS plates as it is closer to normal growth conditions (i.e. longer growth times and allowing transpiration). However, mini-hydroponics has twin benefits of ease of ensuring uniformity and the ease of application of salt stress making phenotyping in mini-hydroponics the only practical choice in this case. The use of mini-hydroponics, as in this study, should be considered first for screening any future experiments with an aim for manipulating ion content of plants under salinity stress.

While all lines examined in this study had detectable *AtAVP1::nosT* expression, Q-PCR could be carried out to quantify the exact levels of expression of the transgene in the root. Potentially, ectopic and over-expression *AtAVP1* in the roots may influence the expression of the native *AtAVP1* and other salinity tolerance genes. A similar effect has been seen when over-expressing the *AtHKT1;1* in Rice (Plett *et al.*, 2010b).

Further experimental work to verify that *AtAVP1* is in-fact correctly expressed and processed in the cell-types could be done by *in situ* PCR (Byrt *et al.*; Haase *et al.*, 1990). Furthermore, experiments may be done to test that the transcribed gene forms a functional

H^+-PPase through immuno-localisation (Holwerda *et al.*, 1990; Sauer & Friml, 2010) or via FACS of root protoplasts (Evrard, 2012) and ELISA analysis or Western Blot. Repetition of the hydroponics experiments may be warranted, however further optimisation of the Arabidopsis growth conditions will be required before this could be effectively done and was not achievable during the time frame of this project.

The role of *AtAVP1* expression in the Arabidopsis ectype C24 should also be examined further, by initially trialling constitutive over-expression of *AtAVP1* and examining knock-out or knock-down mutants to see if similar phenotypes seen in Col-0 are present. *AtAVP1* over-expression in the other cell-types, both in Col-0 and C24, through the use of the GAL4-VP16 and transactivation construct

4.4.5. Conclusion

The work carried out in this chapter demonstrates that, at least in the selected lines screened in mini-hydroponics system, the root-cortex and/or root-epidermal specific expression of *AtAVP1* via the *GAL4-VP16* enhancer-trap and the *pGOF-UAS_{GAL4}:AtAVP1* trans-activation system does not result in significant differences in the Na^+ or K^+ accumulation profile of the roots or leaves compared to null segregants. Additionally, biomass production under control or saline growth conditions is not significantly affected. A number of possible reasons for the lack of detectable phenotype have been discussed and additional work may be done to further confirm these results. However, as the over-arching theme of the thesis was to investigate methods for manipulating Na^+ transport throughout plants, through cell-type specific expression of salinity tolerance genes, such as *AtAVP1*, without a strong, detectable and consistent, altered shoot or root ion phenotype in these lines, it was decided that other research avenues may prove beneficial.

These results and the recent hypotheses regarding the native role of *H^+-PPases* in phloem function (Pizzio *et al.*, 2015) suggests that the over-expression of *H^+-PPases* in the root cortex does not promote Na^+ sequestration in these cell-types by itself. Potentially, over-expression of other genes responsible for direct Na^+ transport are required to promote sequestration. Potential candidates include Class I HKTs (as trialled previously in Chapter 3) or vacuolar Na^+/H^+ exchangers (NHXs), such as *AtNHX1* (Gaxiola *et al.*, 1999), which have been shown to improve Na^+ tolerance when homologues of *AtAVP1* and *AtNHX1* are over-expressed in in Arabidopsis (Brini *et al.*, 2007) and rice (Zhao *et*

al., 2006). A system for the cell-type specific over-expression of such gene combinations, without the use of cell-type specific promoters which may have caused issues previously in Chapter 3, is therefore required. The development of such as system and preliminary experiments are described in Chapters 5 and 6.

Chapter 5

Characterisation and development of Arabidopsis dual enhancer-trap lines to express genes of interest in two cell-types

Chapter 5 - Characterisation and development of Arabidopsis dual enhancer-trap lines to express genes of interest in two specific cell-types

5.1. Introduction

The overall aim of this thesis was to investigate ways to improve plant salt tolerance by manipulating root to shoot Na^+ transport. Control of Na^+ transport throughout plants is controlled by a significant number of genes, some of which have been described (section 1.1.3.4), while others are yet to be discovered. Adjusting the plants ability to regulate Na^+ transport in one cell type is likely to influence Na^+ levels in other cell types. For example, cell type specific expression of *AtHKT1;1* in Arabidopsis root stelar cells resulted in increased root cortical cell accumulation of Na^+ (Møller *et al.*, 2009), with similar results observed in rice (Plett *et al.*, 2010b). Increased cortical Na^+ could be detrimental to root growth and metabolism, unless the Na^+ was either removed from the root back into the soil or compartmentalised in the vacuole of cortical cells. It may be necessary to adjust the ability to regulate ion transport in other cells simultaneously, by altering the expression of multiple genes in difference cells types, to obtain the best phenotype.

The trialling of potential gene combinations to alter transport of Na^+, and potentially other ions or solutes, requires a system that would allow consistent cell-type specific expression of a variety of transgenes in specific cell-types to be developed. While the use of cell-type specific promoters to drive transgene expression would be ideal, development and thorough characterisation of candidate promoters can be time consuming. Although many of the regulatory elements are located primarily within the first ≈2kbp upstream (5′) of the protein coding region of genes such as TATA and CAAT box motifs and other *cis*-acting regulatory elements, other more distal elements (enhancers) can have a significant impact on gene expression and tissue specificity (Clark *et al.*, 2006; De Laat & Grosveld, 2003; Porto *et al.*, 2014). It is not always a straightforward process to identify cell-type specific promoters for research purposes as extensive work is be required to characterise the expression patterns, at different developmental stages and under stress conditions, before they could be effectively used as seen and discussed in Chapter 3.

Additionally, differences in expression levels of transgenes due to the location of T-DNA integration (van Leeuwen *et al.*, 2001) in different transgenic events requires multiple lines per construct to be examined to select lines with suitable expression. Excessive or

ectopic transgene expression may lead to undesirable pleiotrophic effects (Karakas *et al.*, 1997; Tarczynski *et al.*, 1992), while transcriptional transgene silencing (Schubert *et al.*, 2004) may suppress phenotypes. These issues would provide additional complications when expressing multiple transgenes in multiple tissues making comparison of lines complex.

One method to overcome these issues is through the use of enhancer-trapping systems. The Arabidopsis *GAL4-VP16* enhancer-trap and the *pGOF-UAS$_{GAL4}$* trans-activation construct (described in section 1.2.1) has been previously used to drive the expression of Na^+ tolerance genes (El-Hussieny, 2006; Møller, 2008) and successfully modify Na^+ transport in Arabidopsis (Møller *et al.*, 2009) and has been used to drive the expression of *AtAVP1* in Arabidopsis root cells in this thesis (Chapter 4). To drive a second transgene, a secondary enhancer-trap system could be used, such as *HAP1-VP16* (Figure 5.1) (Haseloff *et al.*, 2005). To our knowledge, the development of dual *GAL4-VP16* and *HAP1-VP16* enhancer- traps has yet to be developed to drive multiple GOIs.

5.1.1. Cell-type specific expression of multiple genes

In order to drive the expression of a second GOI in a different cell-type, again promoters may be used, or through the use of a secondary enhancer-trap such as the *HAP1-VP16* enhancer-trap (Haseloff *et al.*, 2005). The *HAP1-VP16* enhancer-trap is modelled on the *GAL4-VP16* enhancer-trap (see Figure 1.4 and Figure 5.1) but uses a modified version of the yeast transcription factor HAP1 (Hon *et al.*, 1999; Lan *et al.*, 2004), *HAP1-VP16*, and replaces the *GAL4 UAS* (*UAS$_{GAL4}$*) with the *HAP1 UAS* binding site (*UAS$_{HAP1}$*). Additionally, a different marker, nucleus localised *cyan fluorescent protein* (H2B::mCFP) encoded by the *HAP1-VP16* enhancer-trap allows the distinction of patterns of expression for both enhancer-traps. Despite these differences, there is still significant sequence similarity between the two enhancer-trap systems and also a small degree of conservation between the *GAL4* and *HAP1* UAS motifs (see Appendix V: Promoter Sequences) and this could lead to cross-activation of the enhancer-trap systems in dual enhancer-trap lines. To our knowledge, cross-activation of *GAL4-VP16* and *HAP1-VP16* enhancer-traps has not been examined *in planta* and remains to be trialled.

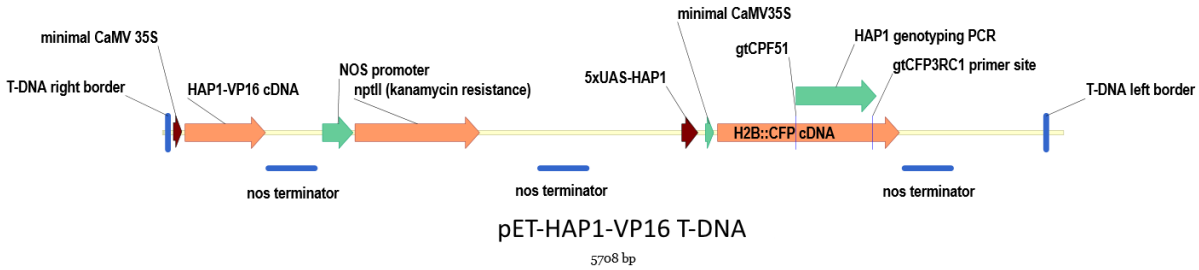

Figure 5.1: Outline of the *HAP1-VP16* enhancer trap (*pET-HAP1*) T-DNA
From left to right: T-DNA right border, minimal Cauliflower Mosaic Virus 35S (*CaMV35S*) promoter, *HAP1-VP16* transcriptional activator coding sequence followed by a bacterial nopaline synthase (*nos*) terminator; a bacterial nopaline synthase (*nos*) promoter driving *neomycin phosphotransferase* (*nptII*) gene (kanamycin resistance for *in planta* selection) followed by a secondary *nos* terminator; 5 repeats HAP1 upstream activation sequence (5×UAS-HAP1) fused to a minimal *CaMV35S* promoter driving the expression of nucleus localised *cyan fluorescent protein* (H2B::mCFP), final *nos* terminator sequence, and T-DNA left border. Primer binding sites used for plant genotyping (primers: Table 5.1 - Basta_F and Basta_R) have also been included.

5.1.2. Aims of this study

The aim of this chapter was to characterise selected Arabidopsis *GAL4-VP16* and *HAP1-VP16* enhancer-trap lines with suitable expression patterns in root-stele and -cortical cells for further experiments. The enhancer-traps were screened under both control and salt stress conditions in order to determine the stability and cell-type specificity of the reporter gene expression.

These lines were then be hybridised to develop lines with both *GAL4-VP16* and *HAP1-VP16* enhancer-traps and expression patterns. Developed dual enhancer-trap lines will be assessed to ensure the cell-type specificity of both parental lines is maintained. To our knowledge, the development of dual *GAL4-VP16* and *HAP1-VP16* enhancer- traps has yet to be developed to drive multiple GOIs. The dual enhancer-trap lines developed were then to be used to enable the simultaneous expression two or more selected GOIs using the trans-activation constructs developed in Chapter 6.

5.2. Methods and Materials

5.2.1. Plant material

The *GAL4-VP16* and *HAP1-VP16* enhancer-trap lines were originally developed by Dr. J. Haseloff (University of Cambridge) (Haseloff, 1999); Haseloff *et al.* (2003). Selected lines are described in sections 5.2.1.1 and 5.2.1.2. Although the *GAL4-VP16* enhancer-trap system has been transformed into the Arabidopsis ecotypes Col-0 and C24, the lines obtained for the *HAP1-VP16* enhancer trap lines were only available into the C24

ecotype. As Col-0 are known to have different response to salinity and to avoid difficulties with inter-ecotype crosses, only C24 ecotype *GAL4-VP16* enhancer-trap lines were selected for crossing. Additionally, the Arabidopsis ecotype C24 was used as wild-type for comparison in this study. Seeds for these ecotypes were originally sourced from the Nottingham Arabidopsis Stock Centre and have been maintained in the laboratory for several generations (ACPFG, University of Adelaide, Waite Campus).

5.2.1.1. Root-stele and root-parenchyma cell-type specific expression lines

The Arabidopsis ecotype C24 *GAL4-VP16* enhancer trap line J2371*C identified for stelar specific expression was originally developed by Dr. J. Haseloff (University of Cambridge). Further characterisation and development of the homozygous single T-DNA insert line (J2371*C) through backcrossing was conducted by Dr. I. Møller (2008). These lines contain the *GAL4-VP16* enhancer trap construct and as such are kanamycin resistant, conferred by the resistance gene *nptII*, and express the reporter gene *mGFP5-ER*; an endoplasmic reticulum (ER) localised green florescent protein (GFP) optimised for plant expression (Haseloff, 1999).

Additionally, several T_4 lines of the J2371*C line transformed with the *pGOF-UAS$_{GAL4}$:AtHKT1;1* trans-activation construct (Appendix Figure 4) by Dr. I. Møller (ACPFG) were obtained. These lines with over-expression of *AtHKT1;1* in the root stele showed reduced shoot Na^+ levels (Møller *et al.*, 2009), and were included in this study to reduce the number of additional transformations required during this project.

5.2.1.2. Root cortex and epidermis cell-type

For root-epidermis and -cortex cell-type specific expression, two Arabidopsis ecotype C24 *HAP1-VP16* enhancer trap lines, HAP1C (original ID: H009180) and HAP1D (original ID: H000810) were selected. These lines were originally developed by Dr. J. Haseloff (University of Cambridge) and were sourced from Dr. M. Gilliham (University of Adelaide, Waite Campus). Preliminary screening of these lines was carried out by Dr. S. Henderson and Mr. M. Yew (University of Adelaide, Waite Campus).

5.2.2. Arabidopsis growth and imaging

To screen for the presence mGFP5-ER and H2B::CFP fluorescence in the enhancer-trap lines; seeds were sown on vertical 0.5 × MS 0.3 % w/v gellum gum plates as described in section 2.3.3 and grown in short day growth chamber conditions described in section

2.3.1 Seedlings were allowed to grow until approximately 2 - 3 weeks (3 - 5 rosette leaves) before imaging by stereo and confocal microscopy as per section 2.6.

5.2.3. Hybridisation and selection of dual enhancer-trap Arabidopsis lines

Parental enhancer trap-lines (section 5.2.1) selected for crossing were grown in soil as per section 2.3.4 under short day growth chamber conditions (section 2.3.1) for ≈ 5 weeks until flowering. Reciprocal crosses were conducted between parental *GAL4-VP16* and *HAP1-VP16* lines as per section 2.3.5. Progeny were sown onto vertical 0.5 × MS plates (section 2.3.3) and screened for mGFP5-ER and H2B::CFP fluorescence (section 2.6) to identify successfully crossed progeny, before being transfer to soil (section 2.3.4.2) for seed production. Selected lines were carried through and screened for the presence of the *GAL-VP16* and *HAP1-VP16* enhancer traps by mGFP-ER and H2B::CFP fluorescence as above, and by genotyping PCR (as per section 5.2.4), until generation F_4 to identify homologous lines with consistent expression of both reporter genes.

5.2.4. Genotyping of plants for the presence of *pGOF-UAS$_{GAL4}$:AtHKT1;1* constructs and *GAL4-VP16, HAP1-VP16* enhancer-traps

Genomic DNA (gDNA) was extracted from leaf material of soil or hydroponically grown plants by the freeze-dry method (section 2.2.19). Genotyping PCR (section 2.2.2) was conducted to determine the presence of the *GAL4-VP16* enhancer-trap by detection of the reporter gene *mGFP-ER* (primers: Table 5.1 - GFPiF and GFPiR); the presence of the *HAP1-VP16* enhancer-trap by the presence of the reporter gene *H2B::CFP* (primers: Table 5.1 - CFP51 and CFP3RC1) and the presence of the *pG/UAS$_{GAL4}$:AtHTK1;1* construct by the BASTA selectable marker (primers: Table 5.1 - Basta_F and Basta_R). Genomic DNA quality was checked by PCR with a native gene *AtActin2* (At3g18780) (primers: Table 5.1 - pISM42AtAct2Fwd and pISM43AtAct2Rev). Genomic DNA from wild-type C24 plus a no-template (H_2O) control were included for all experiments.

Table 5.1: Primers for genotyping Arabidopsis *GAL4-VP16, HAP1-VP16* and transgenic lines.
Information included; primer name, length, sequence, expected amplicon length and PCR conditions for either genotyping PCR or RT-PCR. Genotyping and RT PCRs conducted as per section 2.2.2 with specified PCR conditions, 35 cycles.

Primer	Length (bp)	Sequence (5′ - 3′)	Amplicon size (bp)	PCR conditions	Purpose
GFPiF	20	TCAAGGAGGACGGAAACATC	234	Anneal: 55 °C Extension: 30s	Genotyping & RT-PCR for presence of *GAL4-VP16* enhancer- trap
GFPiR	20	AAAGGGCAGATTGTGTGGAC			
Basta_F	20	GACTTCAGCAGGTGGGTGTA	377	Anneal: 62 °C Extension: 30s	Genotyping for presence of *pGOF-UAS$_{GAL4}$:AtHKT1;1 (bar* gene)
Basta_R	17	AAATCTCGGTGACGGGC			
CFP51	22	TCGAGCTGGACGGCGACGTAAA	502	Anneal: 62 °C Extension: 30s	Genotyping & RT-PCR for presence of *HAP1-VP16* enhancer- trap
CFP3RC1	22	TCCTGCTGGTAGTGGTCGGCGA			
pISM42AtAct2Fwd	20	GCCCAGAAGTCTTGTTCCAG	297	Anneal: 53 °C Extension: 30s	gDNA RT-PCR cDNA quality check
pISM43AtAct2Rev	20	ACATCTGCTGGAATGTGCTG			

5.2.5. Salinity screening of parental and crossed lines in mini-hydroponics system

To screen parental enhancer-trap lines and selected T_6F_4 dual enhancer-trap lines for reporter gene expression under salinity stress, plants were grown in the mini-hydroponics setup as described in section 2.3.8 under short-day growth conditions in the growth chambers specified in section 2.3.1.Plants were transferred after two weeks growth (5 rosette leaf stage) to a mini-hydroponics setup and grown for an additional two weeks before onset of three salinity treatments, control (0 mM NaCl), mid (50 mM NaCl) or high (100 mM NaCl). Treatment was applied in 25 mM NaCl (+ 0.35 mM $CaCl_2$) increments every 12 hours (7 AM and 7 PM). Plants were harvested after 7 days from the onset of salinity treatment. Root and shoot fresh weight was recorded for all plants, root material and youngest fully expanded leaf were collected for determination of tissue Na^+ and K^+ accumulation by flame photometry (section 2.5.3). Root and leaf material was collected and snap-frozen in liquid N_2 for RNA extraction and transgene expression analysis (section 2.2.21). Leaf material was harvested for gDNA extraction and plant genotyping (section 5.2.4). Selected plants were also screened by confocal microscopy (section 2.6) to confirm enhancer-trap expression patterns under salinity stress and in mini-hydroponics.

5.2.6. Statistical analysis

All data collected from hydroponics experiments was analysed in Microsoft Excel 2013 with significant differences between transgenic and null lines and between treatments determined by one- or two-way ANOVAs. Analyses with significance ($P \leq 0.05$) were subjected to Tukey-Kramer HSD post-hoc analysis.

5.3. Results

5.3.1. Root cell-type expression patterns in selected enhancer trap lines

Prior to hybridisation, *HAP1-VP16* lines, HAP1C and HAP1D, and *GAL4-VP16* enhancer-trap line, J2371*C, were grown on vertical 0.5 × MS plants as per section 2.3.3 and screened for both the presence of mGFP5-ER and H2B::CFP with epifluorescence stereo and confocal microscopy as per section 2.6 to determine the enhancer-trap expression patterns.

5.3.1.1. mGFP-ER present in the in *GAL4-VP16* enhancer-trap line J2371*C root stele/pericycle cells

H2B::CFP was not detected in the J2371*C plants (not shown). mGFP-ER fluorescence was detected in the roots by epifluorescence stereo microscopy (Figure 5.2) as previously seen in (Møller, 2008). However, mGFP-ER fluorescence was also detected in leaf vasculature, not previously reported (Møller, 2008) (Figure 5.2 a). Confocal microscopy confirmed that mGFP-ER fluorescence was in the root, primarily in the root pericycle cells (Figure 5.10, a), in the root maturation zone and mature roots, (Figure 5.3, a) and lateral root junctions, (Figure 5.3, b), but not in the root tips (Figure 5.3, c), of both primary and lateral roots.

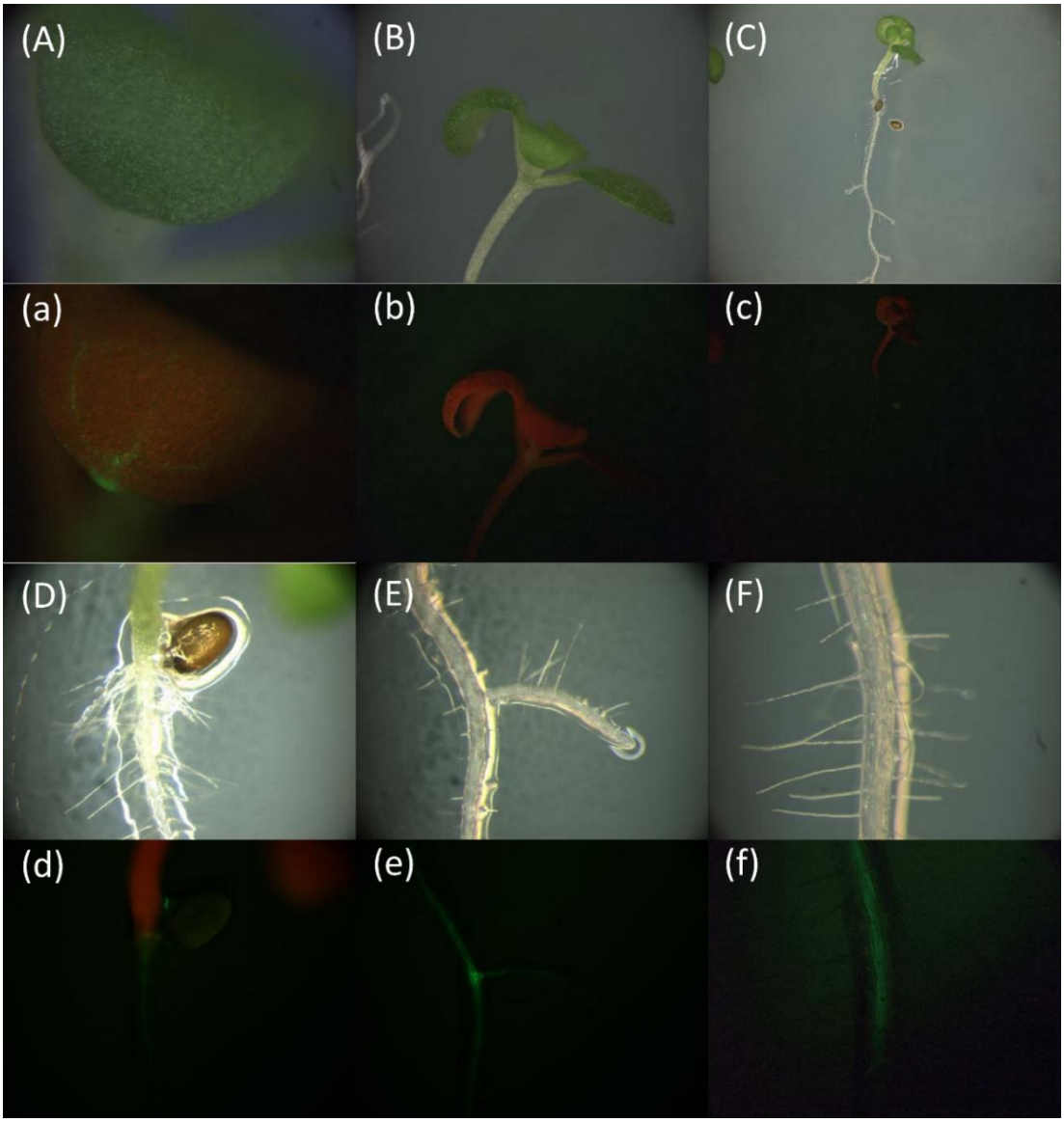

Figure 5.2: J2371*C Epifluorescence stereo micrographs of root and shoots of *GAL4-VP16* enhancer-trap line J2371*C for mGFP5-ER fluorescence
Representative images of 3 week old seedlings of *GAL4-VP16* enhancer-trap line J2371*C, grown on vertical MS plates (as per section 2.3.3) and imaged for mGFP-ER florescence by epifluorescence stereo microscopy (as per section 2.6). Images taken under bright field (A-F) and GFP2 (a-f) filters under a range of focal distances, examining shoots (A-C) and roots (D-F). Approximately 10 seedlings screened per line. GFP fluorescence was detected in leaf vasculature (a) and mature roots (e,f).

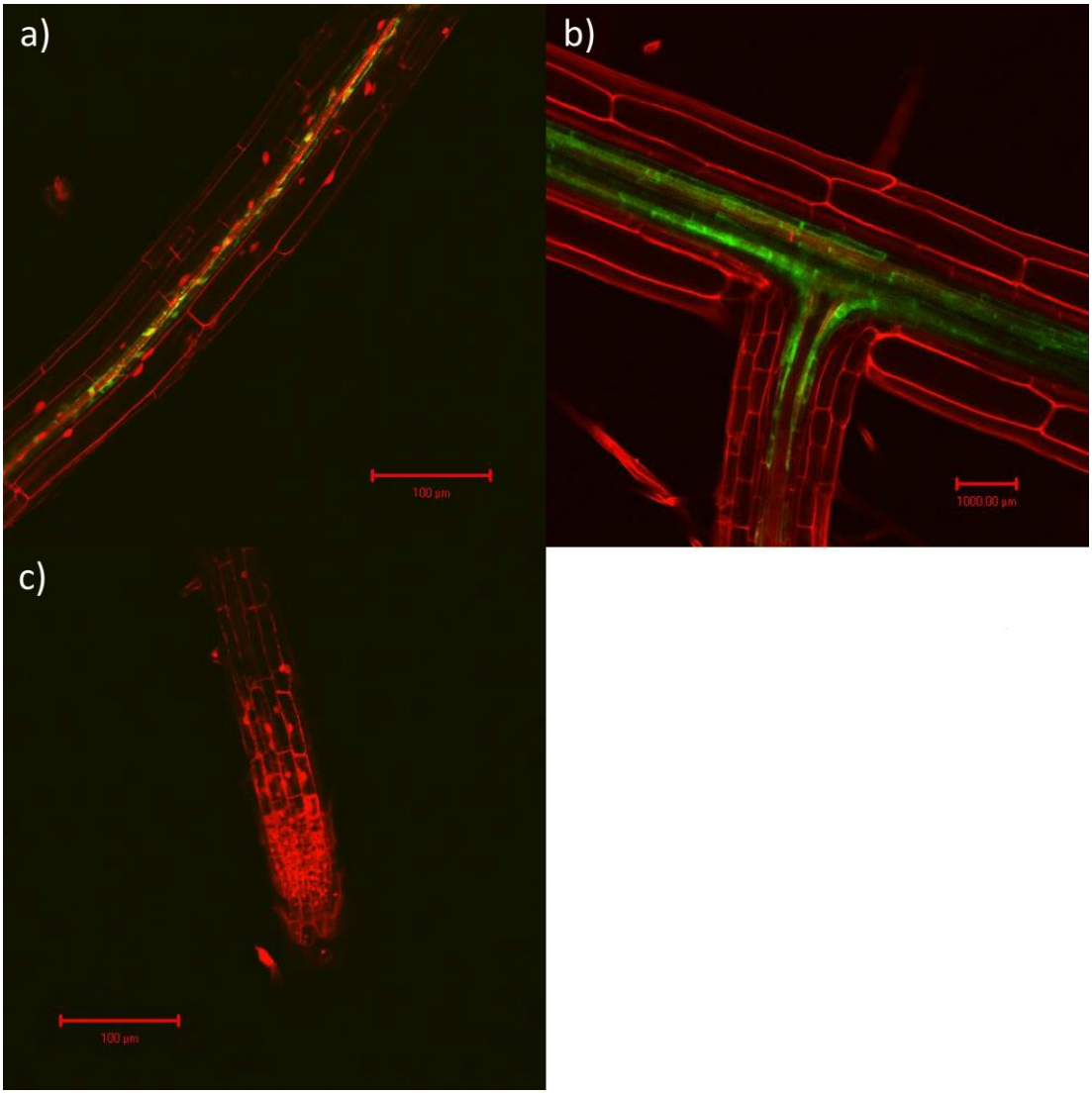

Figure 5.3: Confocal micrographs of roots of *GAL4-VP16* enhancer-trap line J2371*C shows the presence of mGFP-ER fluorescence in the root vasculature
Representative confocal images of 3 week old seedlings of *GAL4-VP16* enhancer-trap line, J2371*C, grown on vertical MS plates (as per section 2.3.3) and imaged by confocal microscopy (as per section 2.6). Cells walls stained with propidium iodine appear red, Endoplasmic reticulum localised mGFP-ER fluorescence appears green. Images taken under a range of focal distances (scale bars shown), examining root maturation zone (a), lateral root junctions (b) and root tip (c). Approximately 10 seedlings screened per line. GFP fluorescence (via mGFP5-ER) was detected primarily in root vasculature.

5.3.1.2. H2B::CFP confirmed to be present in the in *HAP1-VP16* enhancer-trap line HAP1C root cortical cells

mGFP-ER was not detected in the roots or shoots of HAP1C plants by epifluorescence stereo microscopy (see Appendix figure 21). H2B::CFP was detected (Figure 5.4) primarily in the nucleus of cortical cells (Figure 5.10, b) in the root maturation zone, (Figure 5.4, a) mature roots (Figure 5.4, b), as well as in root elongation zone behind the root tip (Figure 5.4, c) in both primary and lateral roots.

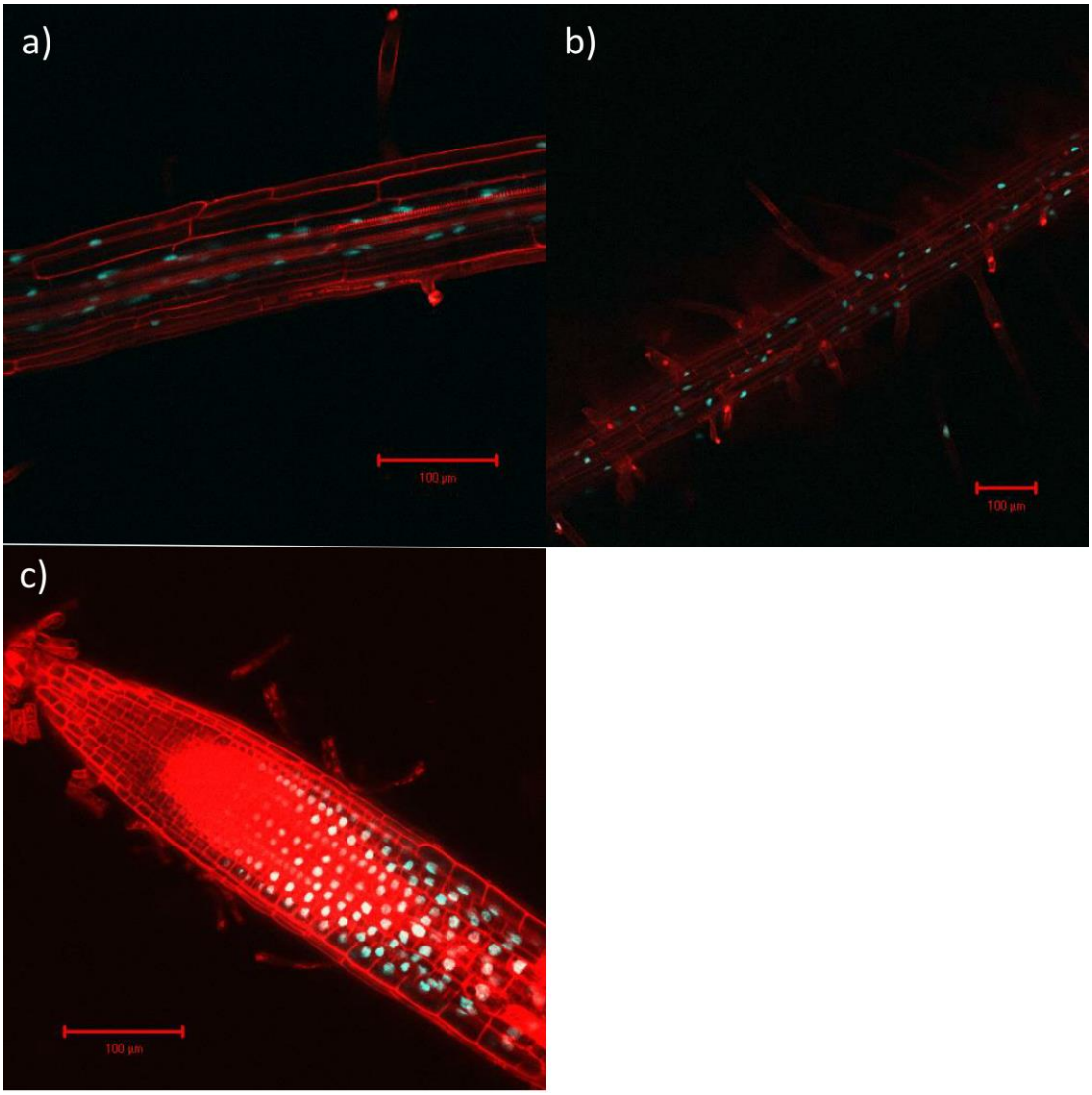

Figure 5.4: Confocal micrographs of roots of *HAP1-VP16* enhancer-trap line HAP1C shows the presence of CFP fluorescence in the root cortex
Representative confocal images of 3 week old seedlings of *HAP1-VP16* enhancer-trap line, grown on vertical MS plates (as per section 2.3.3) and imaged by confocal microscopy (as per section 2.6). Cells walls stained with propidium iodine appear red, nuclear localised H2B::CFP fluorescence appear blue. Images taken under a range of focal distances (scale bars shown), examining root maturation zone (a) and mature roots (b) and root tip (c). Approximately 10 seedlings screened per line. CFP fluorescence (via H2B::CFP) was detected primarily in root-cortex.

5.3.1.3. H2B::CFP confirmed to be present in the in *HAP1-VP16* enhancer-trap line HAP1D root cortical cells

mGFP-ER was not detected in in the roots or shoots of HAP1D plants by epifluorescence stereo microscopy (see Appendix figure 22). CFP was detected (Figure 5.5) primarily in the nucleus of root epidermal cells (Figure 5.10, c) in the root maturation zone, (Figure 5.5, a) mature roots (Figure 5.5, b and c), as well as in root tip (Figure 5.5, d) in both primary and lateral roots.

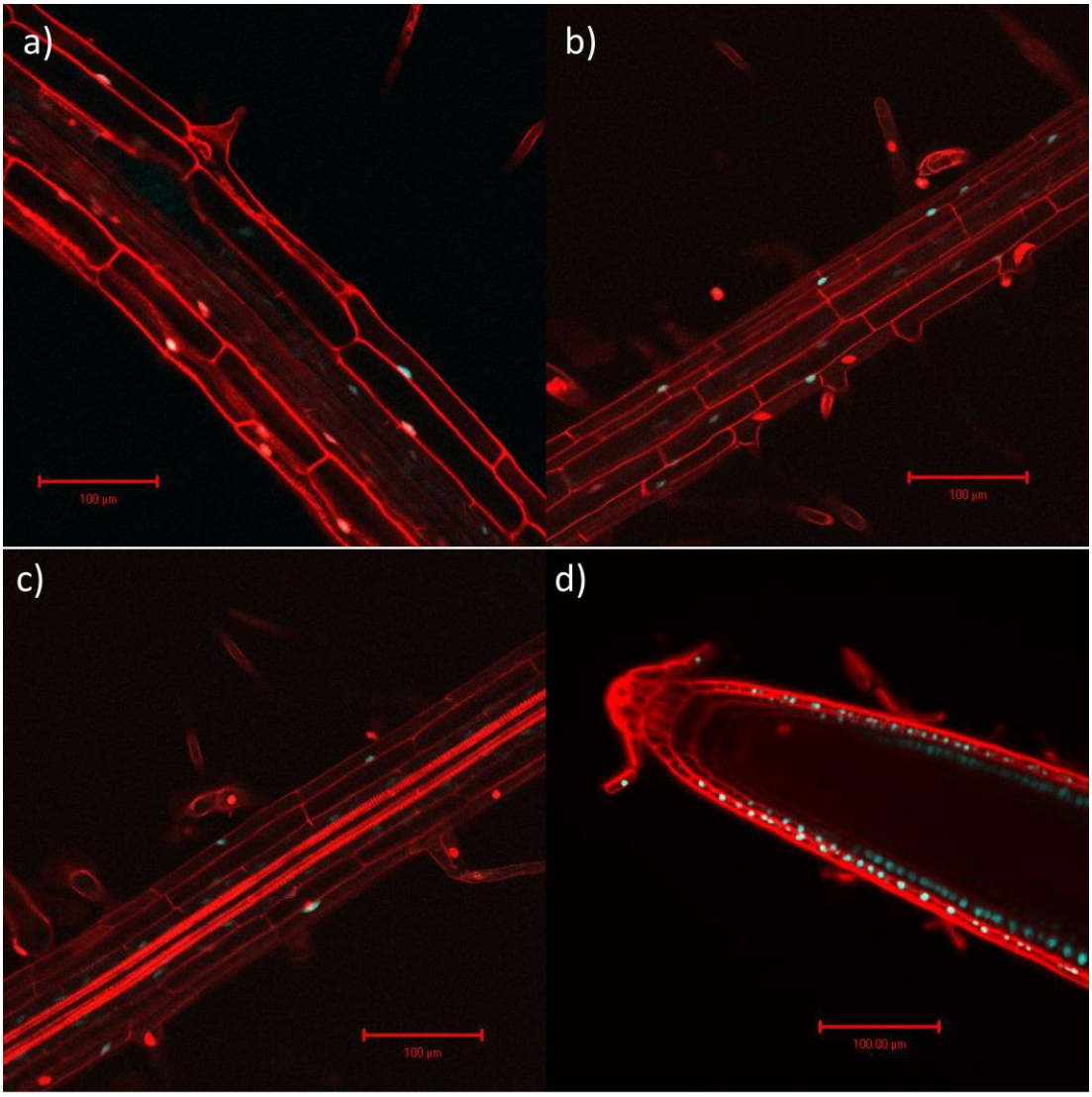

Figure 5.5: Confocal micrographs of roots of *HAP1-VP16* enhancer-trap line HAP1D shows the presence of CFP fluorescence in the root epidermis
Representative confocal images of 3 week old seedlings of *HAP1-VP16* enhancer-trap line HAP1D, grown on vertical MS plates (as per section 2.3.3) and imaged by confocal microscopy (as per section 2.6). Cells walls stained with propidium iodine appear red, nuclear localised H2B::CFP fluorescence appear blue. Images taken under a range of focal distances (scale bars shown), examining root maturation zone (a), inner (a) and outer (b) mature roots and root tip (d). Approximately 10 seedlings screened per line. CFP fluorescence (via H2B::CFP) was detected primarily in root epidermis.

5.3.1.4. The *GAL4-VP16* and *HAP1-VP16* expression patterns were unaffected by salinity stress in examined enhancer-trap lines: J2371*C, HAP1C, HAP1D.

To assess if expression of *GAL4-VP16* and *HAP1-VP16* is altered under salinity stress, plants were grown for 2 weeks on 0.5 × MS vertical plates (section 2.3.3) supplemented with 0, 50 or 100 mM NaCl. (Figure 5.6) show mGFP5-ER patterns in the *GAL4-VP16* J2371*C line (Figure 5.6, a) was consistent at higher salinity levels, as previously shown by (Møller, 2008). H2B::CFP fluorescence patterns were consistent for both *HAP1-VP16* enhancer trap lines (Figure 5.6, b and c) under both 50 and 100 mM NaCl. However, there was increased collapse of epidermal and cortical cells and deformation of root-tips at high salinity which made visualisation difficult. Similar patterns were seen in 5 week old hydroponically grown plants under same NaCl concentrations (examined in section 5.3.2), however, imaging was difficult due to increased auto-fluorescence (images not presented).

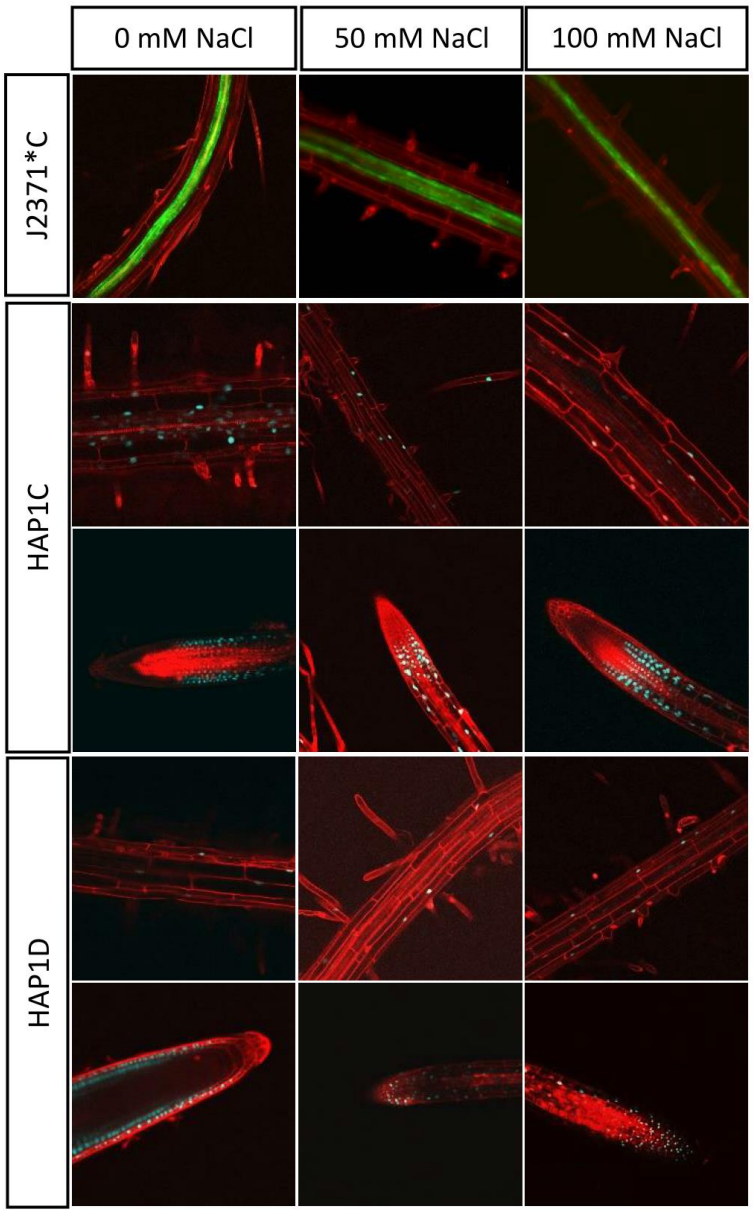

Figure 5.6: Reporter gene fluorescence was stable in parental enhancer trap lines, J2371*C, HAP1C and HAP1D, under salinity stress on plates.
Representative confocal micrographs of selected lines grown on vertical 0.5 × MS plates supplemented with 0, 50 or 100 mM NaCl. mGFP5 was visualised in root pericycle cells in the roots of J2371*C plants and not altered under increase salinity as seen previously (Møller, 2008). CFP observed in the HAP1C and HAP1D lines was confined to root-cortex and -epidermis respectively in both mature roots and root tips and not altered by increasing NaCl. Approximately, 10 plants per line screened.

5.3.2. Successful hybridisation and development of dual *GAL4-VP16* and *HAP1-VP16* enhancer-trap lines

Through several rounds of crossing between *HAP1-VP16* enhancer-trap lines (HAP1D or HAP1C) and *GAL4-VP16* enhancer-trap line J2371*C or T_4 lines of J2371*C+*pG/UAS$_{GAL4}$:AtHKT1;1*, a number of individuals were successfully recovered and grown until F_3 generation. Developed lines are outlined below in Table 5.2.

Genotyping for the presence of the *HAP1-VP16* and *GAL4-VP16* constructs, as well as the *pG/UAS$_{GAL4}$:AtHKT1;1*, also confirmed successful crossing (Figure 5.7). Selected lines show the presence of both reporters, mGFP5 and CFP, when grown on vertical 0.5 × MS plates and screened by confocal microscopy (Figure 5.8; HAP1C-J2731*C) and (Figure 5.9; HAP1D-J2731*C). Fluorescent patterns of both reporters are consistent with those of the parental lines (Figure 5.10, d and e), which indicates no cross-activation of the enhancer-trap systems.

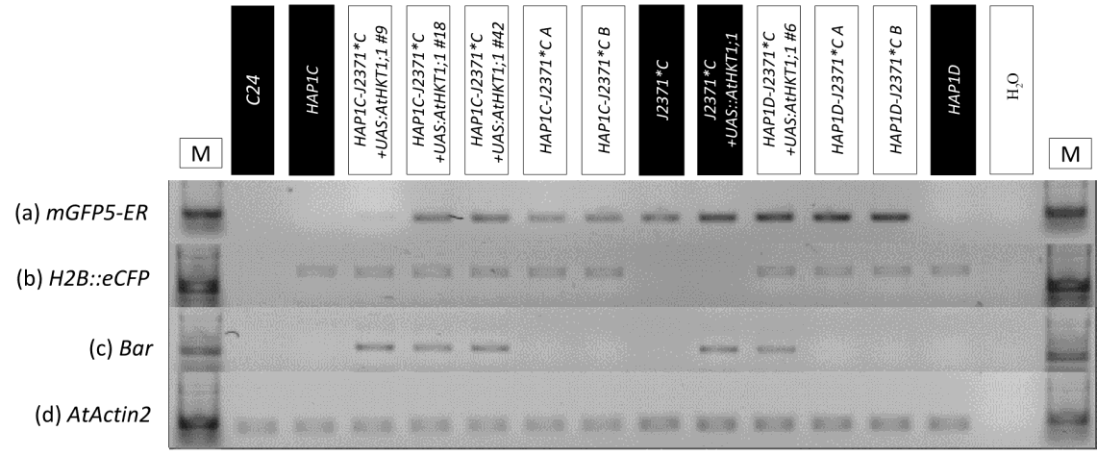

Figure 5.7: Genotyping PCRs on selected T_7 parental lines and selected T_7F_3 dual enhancer-trap lines show the presence for both *GAL4-VP16* and *HAP1-VP16* constructs

Electrophoresis gel showing the presence of (a) *mGFP5-ER* (GAL4-VP16 enhancer trap), (b) *H2B::CFP* (HAP1-VP16 enhancer trap), *bar* (*pGOF-UAS$_{GAL4}$-AtHKT1;1*) and DNA positive control gene (d) *AtActin2* in PCR products amplified from gDNA extracted from selected T_7 parental and T_7F_3 dual enhancer-trap lines. Negative controls: gDNA from wild-type C24 plants or H_2O.

Table 5.2: Parental lines and dual enhancer-trap lines developed and observed fluorescent reporter patterns
Information included; line identification, presence of selected constructs and observed GFP/CFP patterns

Line ID	Construct presence			Fluorescent Reporter Pattern
	HAP1-VP16	*GAL4-VP16*	*UAS_{GAL4}:AtHTK1;1*	
HAP1C	✓	N/A	✓	H2B::CFP – Root cortex Figure 5.4
HAP1D	✓	N/A	✓	H2B::CFP – Root epidermis Figure 5.5
J2371*C	N/A	✓	N/A	mGFP-ER – Root Stele Figure 5.2 and Figure 5.3
T_7 J2371*C+pG/UASGAL4:AtHKT1;1	N/A	✓	✓	GFP – Root Stele
T_7F_3 HAP1C-J2371*C+*UAS_{GAL4}:AtHKT1;1* #9	✓	✓	✓	mGFP-ER – Root stele H2B::CFP – Root cortex
$T_{7F}3$ HAP1C-J2371*C+*UAS_{GAL4}:AtHKT1;1* #18	✓	✓	✓	
T_7F_3 HAP1C-J2371*C+*UAS_{GAL4}:AtHKT1;1* #42	✓	✓	✓	
F_3 HAP1C-J2371*C A	✓	✓	N/A	mGFP-ER – Root stele H2B::CFP – Root cortex Figure 5.8
F_3 HAP1C-J2371*C B	✓	✓	N/A	
T_7F_3 HAP1D-J2371*C+*UAS_{GAL4}:AtHKT1;1* #6	✓	✓	✓	mGFP-ER - Root stele H2B::CFP – Root epidermis
F_3 HAP1D-J2371*C A	✓	✓	N/A	mGFP-ER - Root stele H2B::CFP – Root epidermis Figure 5.9
F_3 HAP1D-J2371*C B	✓	✓	N/A	
✓: Present		N/A: Not applicable		
mGFP-ER – ER-targeted Green florescent protein		H2B::CFP – nuclear localised Cyan florescent protein		

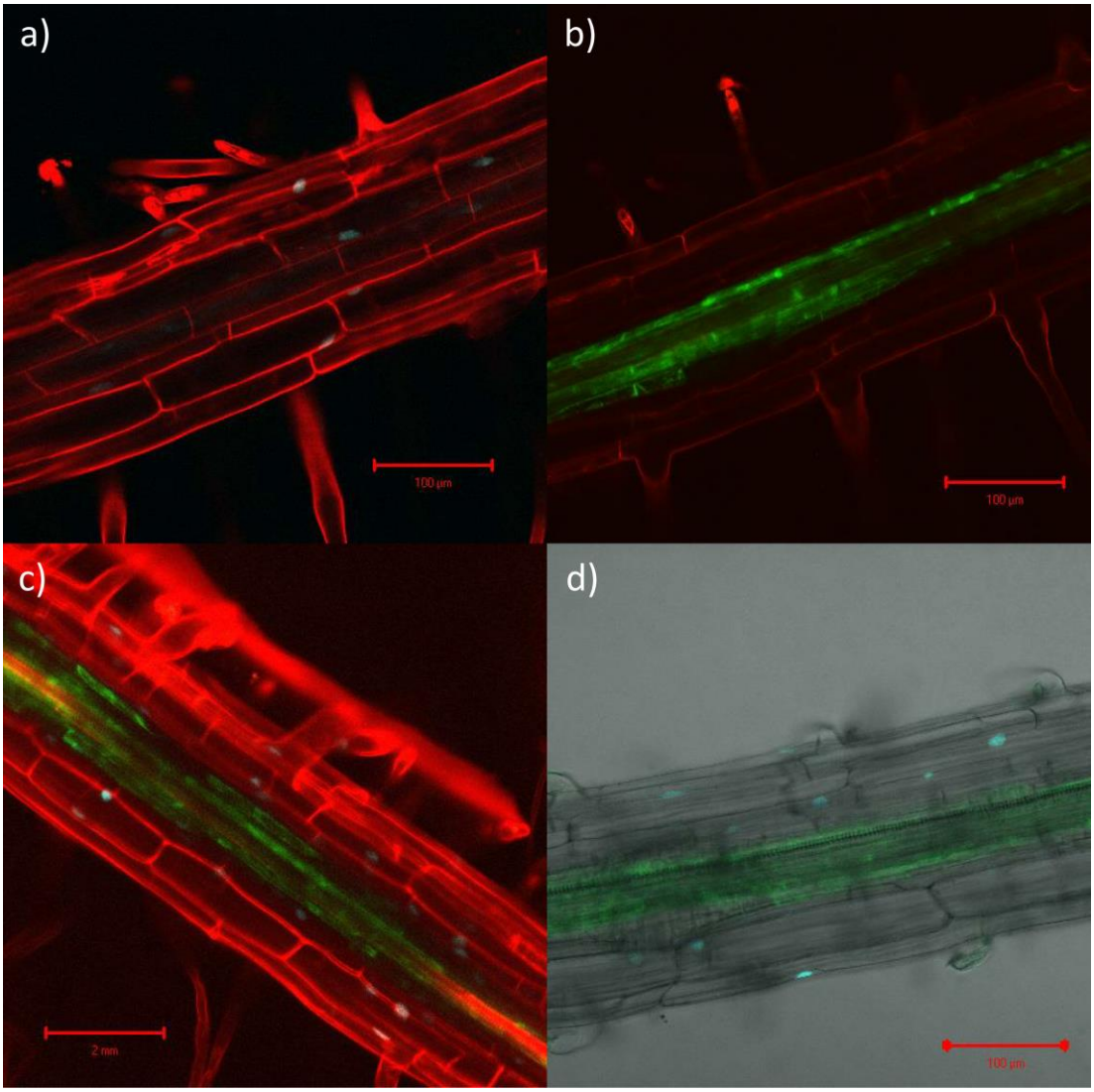

Figure 5.8: mGFP-ER and H2B::CFP detected in HAP1C-J2371*C A/B lines detected by confocal microscopy

Representative multi-layer confocal micrographs of propidium iodine (red) stained HAP1C-J2371*C A/B plants grown on vertical 0.5 × MS plates. H2B::CFP (blue) was observed in the outer root (a) (root-cortex and –epidermis) and mGFP5 observed in inner root (b) (root pericycle) of individual plants similar to parental lines. mGFP-ER and H2B::CFP can be visualised together in mature roots (c) and (d – bright field and no PI). Approximately, 10 plants per line screened. Additional micrographs, Appendix figure 12.

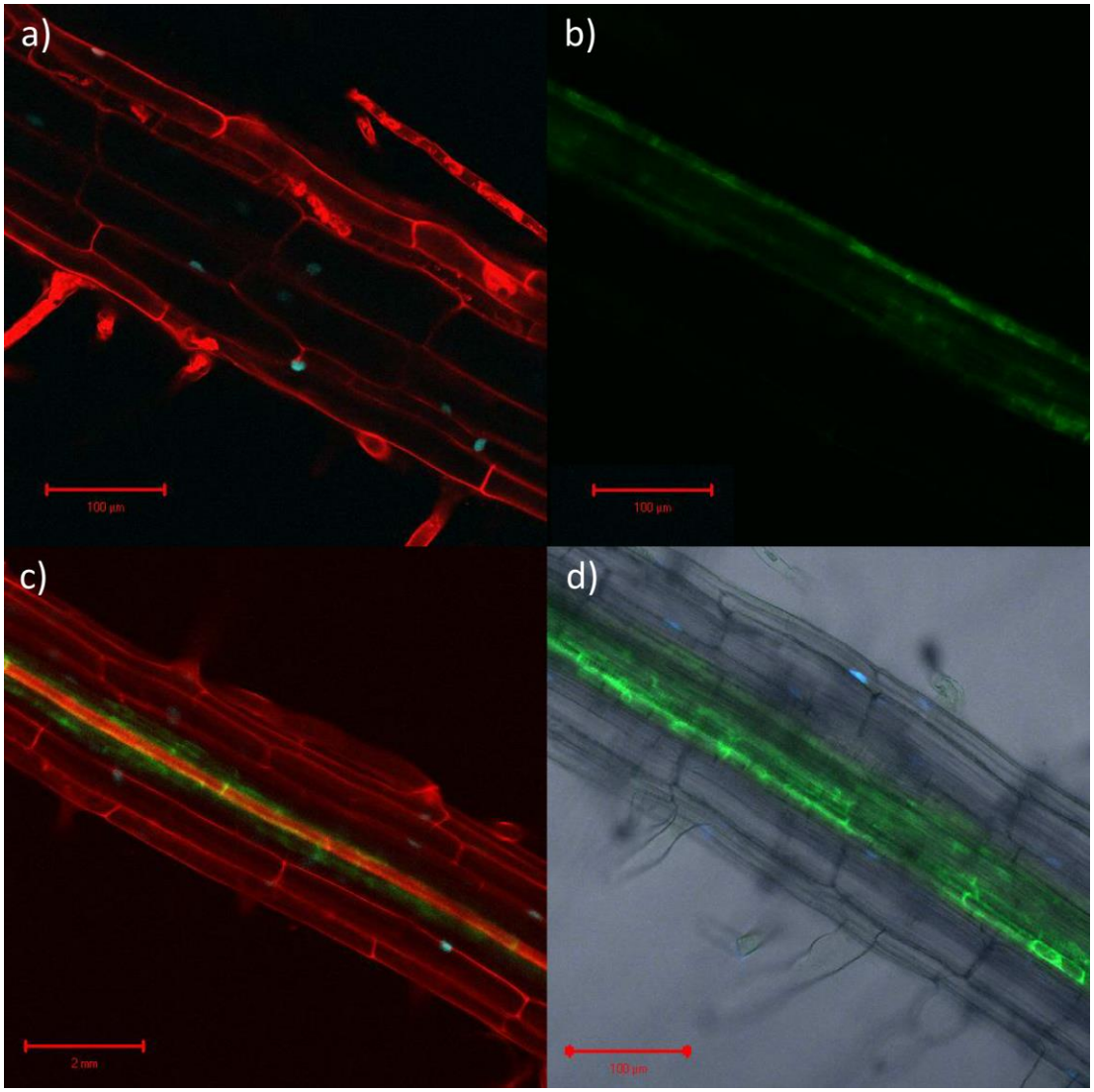

Figure 5.9: mGFP-ER and H2B::CFP detected in HAP1D-J2371*C A/B lines detected by confocal microscopy

Representative multilayer confocal micrographs of propidium iodine (PI) (red) stained HAP1D-J2371*C A/B plants grown on vertical 0.5 × MS plates. H2B::CFP (blue) was observed in the outer root (a) (root-epidermis) and mGFP5-ER observed in inner root (b) (root pericycle) of individual plants similar to parental lines. mGFP-ER and H2B::CFP can be observed together in mature roots (c) and (d – bright field and no PI). Approximately, 10 plants per line screened. Approximately, 10 plants per line screened. Additional micrographs, Appendix figure 13.

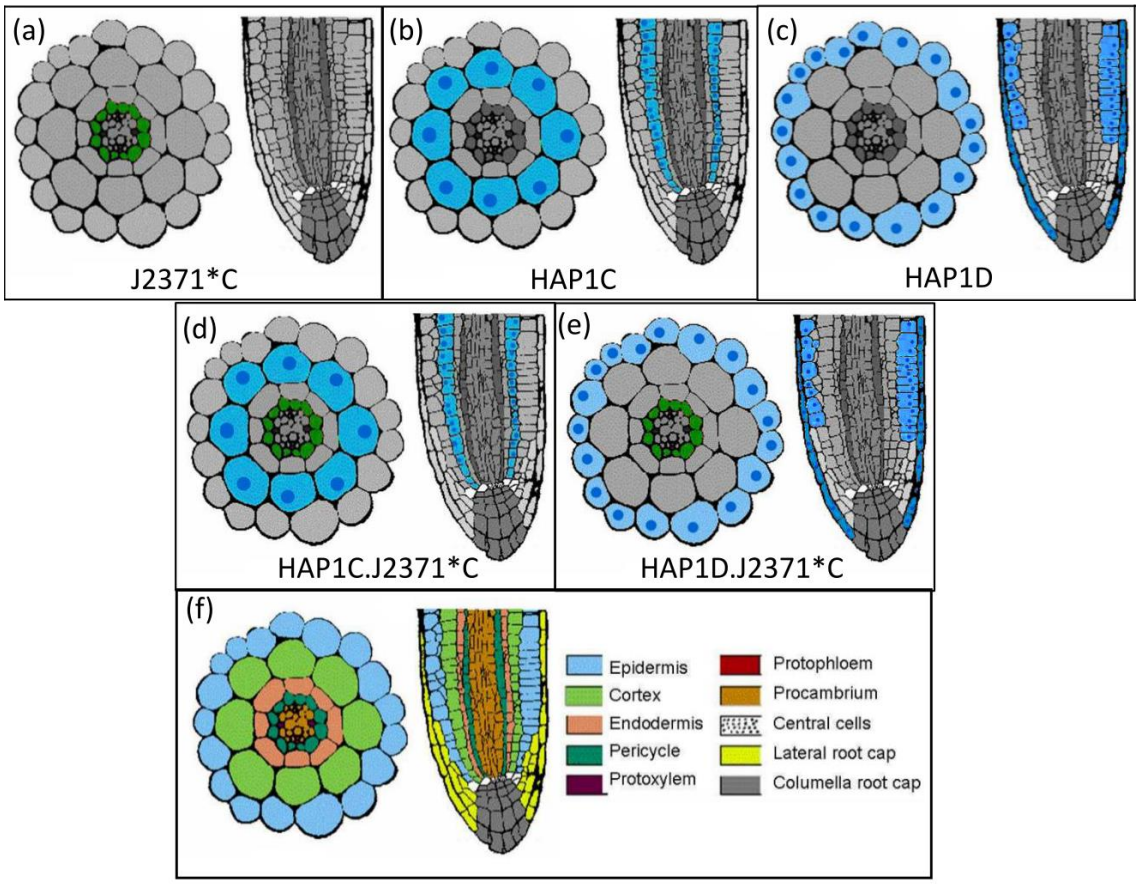

Figure 5.10: Schematic diagram of reporter gene expression patterns in the root cell-types of enhancer trap-lines used and developed in this study.
Overview of the *GAL4-VP16* (green) and *HAP1-VP16* (blue) enhancer-trap expression patterns in lines J2371*C (a), HAP1C (b), HAP1D (c) and dual enhancer trap lines, HAP1C-J2371*C A (d) and HAP1D-J2371*C A (e), in the root and root tip. Colour-coded transverse and longitudinal Root architecture and cell-type for comparison (f). Figure adapted from (Dolan *et al.*, 1993)

5.3.3. Parental and dual enhancer-trap lines perform similarly under control and salinity stress conditions

To assess the performance of parental enhancer-trap lines and selected dual enhancer-trap lines under salinity stress, seeds of T_7 parental lines (HAP1C, HAP1D and J2371*c) and T_7F_3 dual enhancer-trap lines (HAP1C-J2371*C A and HAP1D-J2371*C A - Table 5.2) lines were germinated and grown in a mini-hydroponics system outlined in section 2.3.8. Plants were exposed to three different salinity treatments (0 mM, 50 mM and 100 mM additional NaCl - with additional $CaCl_2$ to maintain Ca^{2+} activity) after 4 weeks growth and harvested after 1 week after onset of salinity stress. Plant root and shoot fresh weight biomass was measured (section 5.3.3.1) and root and shoot [Na^+] (section 5.3.3.2) and [K^+] (section 5.3.3.3) were measured as per section 5.2.5.

5.3.3.1. Root and shoot fresh weight of dual-enhancer trap lines are similar parental lines

No significant difference was observed in root and shoot biomass between the parental and dual enhancer-trap lines grown in either 50 or 100 mM NaCl treatments (Figure 5.11 a, b). Shoot FW biomass remained relatively constant, with a trend to decreasing under high (100 mM NaCl) (Figure 5.11 a). Root FW biomass increased in all lines in response to increasing salinity treatments (Figure 5.11 b) leading to an increased root to shoot biomass ratio (Figure 5.11 c).

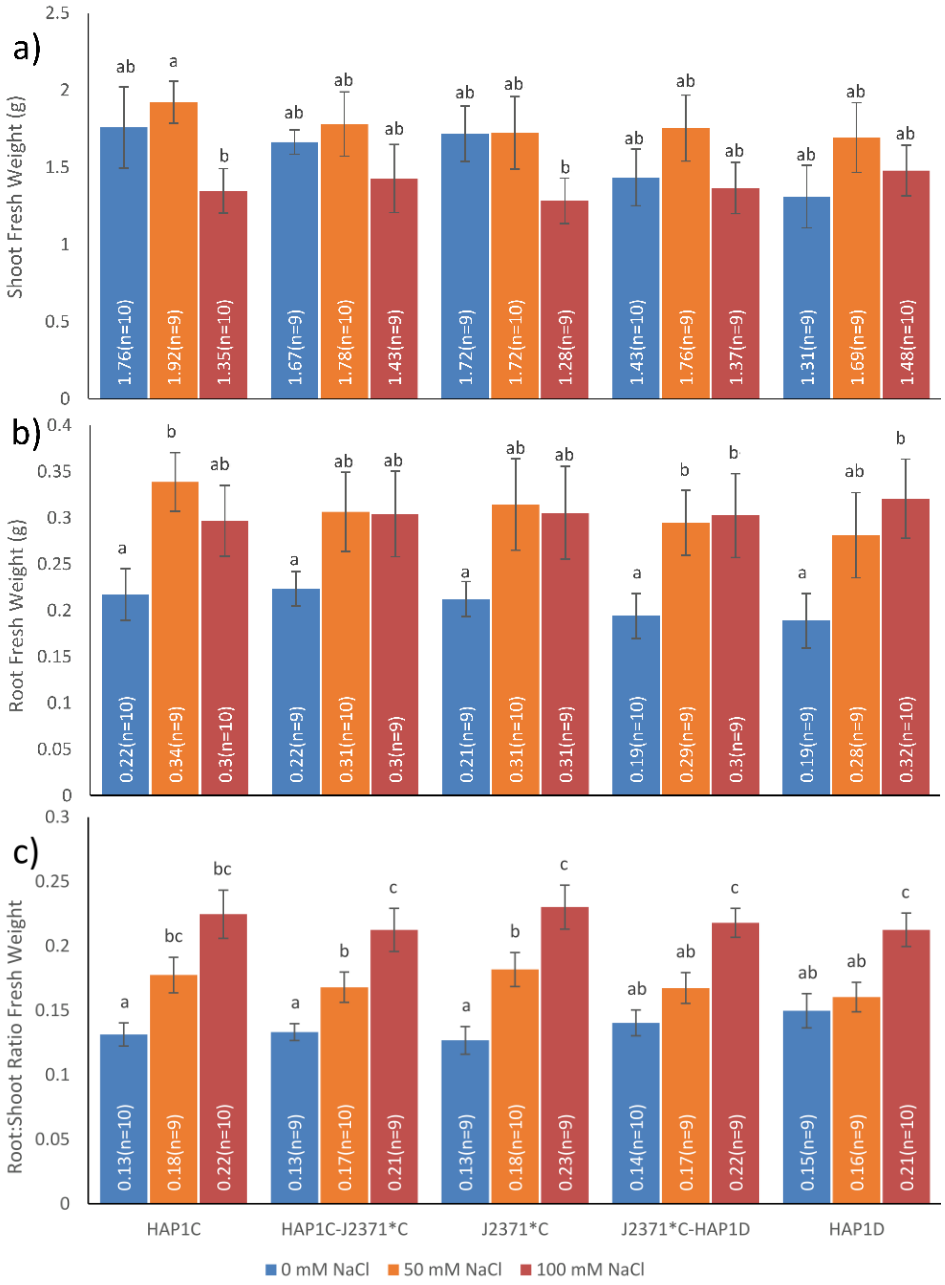

Figure 5.11: Shoot and root fresh weight of dual enhancer-trap lines is consistent with parental lines.

Data shown are mean shoot (a) and root (b) fresh weight and root to shoot fresh weight ratio (c) of the parental enhancer-trap lines (*GAL4-VP16* or *HAP1-VP16*: HAP1C, J2371*C, HAP1D) and two dual enhancer-trap lines (*GAL4-VP16* and *HAP1-VP16*: HAP1C-J2371*C A and J2371*C-HAP1D A). Plants were grown for 4 w in mini-hydroponics then treated with an additional 0, 50 or 100 mM NaCl for 1 week before harvest. Values are means ± SEM (n=9-10) with letters indicating significant differences between treatments. Significance between lines within-treatments or within lines between treatments determined by one- or two-way ANOVA, Tukey-Kramer HSD ($P \leq 0.05$).

5.3.3.2. Root and Leaf [Na^+] of dual enhancer-trap lines is similar to that parental enhancer-trap lines

A significant treatment affect was observed in the leaf Na^+ content in both parental and dual enhancer-trap lines as expected. Leaf [Na^+] increased with increasing salinity treatments (≈100 µmoles.g^{-1} DW under 0 mM NaCl, ≈1500 µmoles.g^{-1} DW under 50 mM, and ≈2200 µmoles.g^{-1} DW under 100 mM NaCl) (Figure 5.12, a). Root [Na^+] was similarly affected in all lines examined (≈25 µmoles.g^{-1} DW under 0 mM NaCl, ≈215 µmoles.g^{-1} DW under 50 mM, and ≈570 µmoles.g^{-1} DW under 100 mM NaCl) (Figure 5.12, b). No significant difference between parental lines and dual enhancer-trap lines in root or leaf Na^+ accumulation was observed.

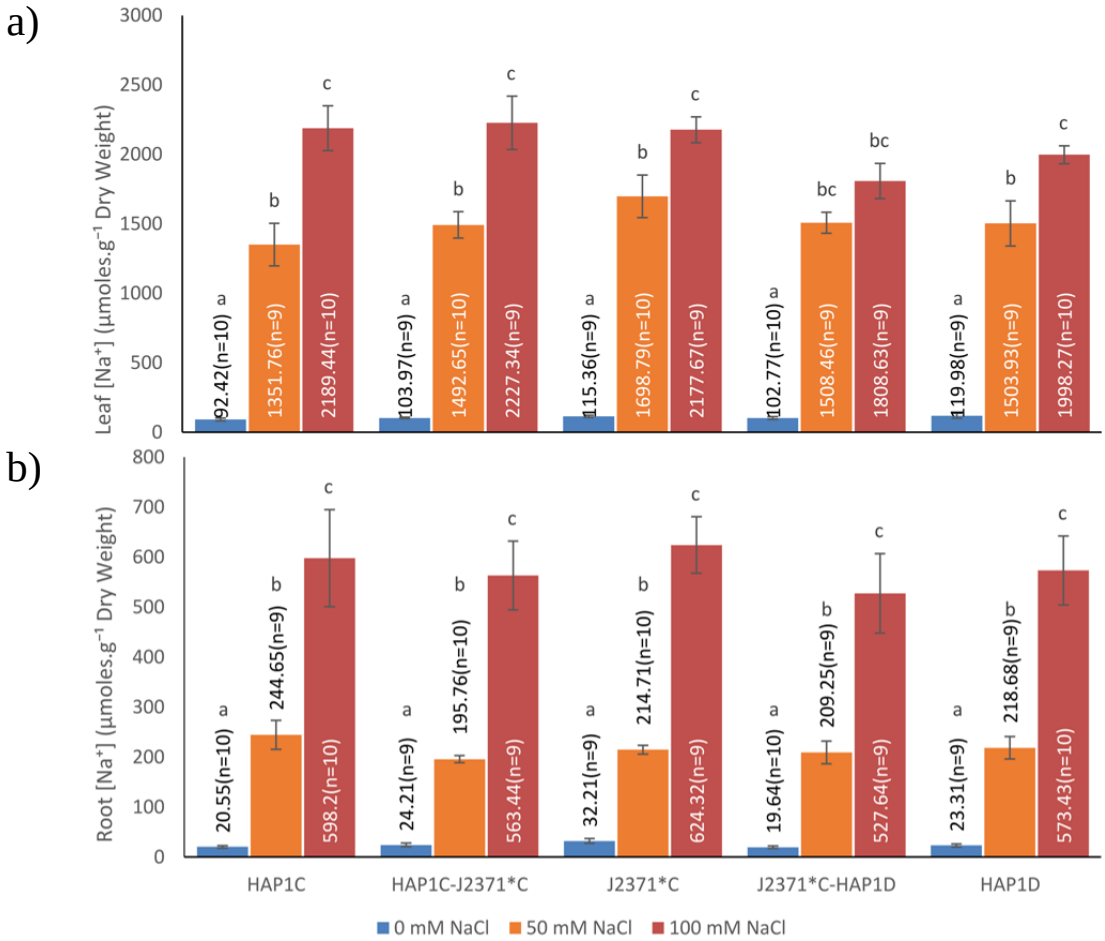

Figure 5.12: Leaf and root Na^+ content of dual enhancer-trap lines is similar to parental enhancer-trap lines.

Data shown are mean leaf (a) and root (b) dry weight Na^+ content of parental enhancer-trap lines (*GAL4-VP16* or *HAP1-VP16*: HAP1C, J2371*C, HAP1D) and two dual enhancer-trap lines (*GAL4-VP16* and *HAP1-VP16*: HAP1C-J2371*C A and J2371*C-HAP1D A). Plants were grown for 4 weeks in mini-hydroponics for then treated with an additional 0, 50 or 100 mM NaCl for 1 week before harvest. Values are means ± SEM (n=9-10) with letters indicating significant differences between treatments. Significance between lines within-treatments or within lines between treatments determined by one- or two-way ANOVA, Tukey-Kramer HSD ($P \leq 0.05$). Significant differences were observed between treatments. No significant differences were observed between lines parental or crossed line within treatments.

5.3.3.3. Root and leaf [K^+] of dual enhancer-trap lines is similar to that parental lines

A significant treatment affect was seen in the leaf K^+ content in both parental and dual-enhancer trap lines as expected. Leaf [K^+] decreased with increasing salinity treatments (≈1500 µmoles $K^+.g^{-1}$ DW under 0 mM NaCl, ≈700 µmoles.g^{-1} DW under 50 mM, and ≈500 µmoles.g^{-1} DW under 100 mM NaCl) (Figure 5.13, a). Root [K^+] was not significantly altered by increasing salinity treatments in the majority of lines (Figure 5.13, b). A slight trend for increased root [K^+] under increased NaCl was observed and was significant in the HAP1D and HAP1D-J2371*C A lines. The ability to maintain root [K^+] has been seen in previous Arabidopsis hydroponics experiments with the C24 ecotype (see section 4.3).

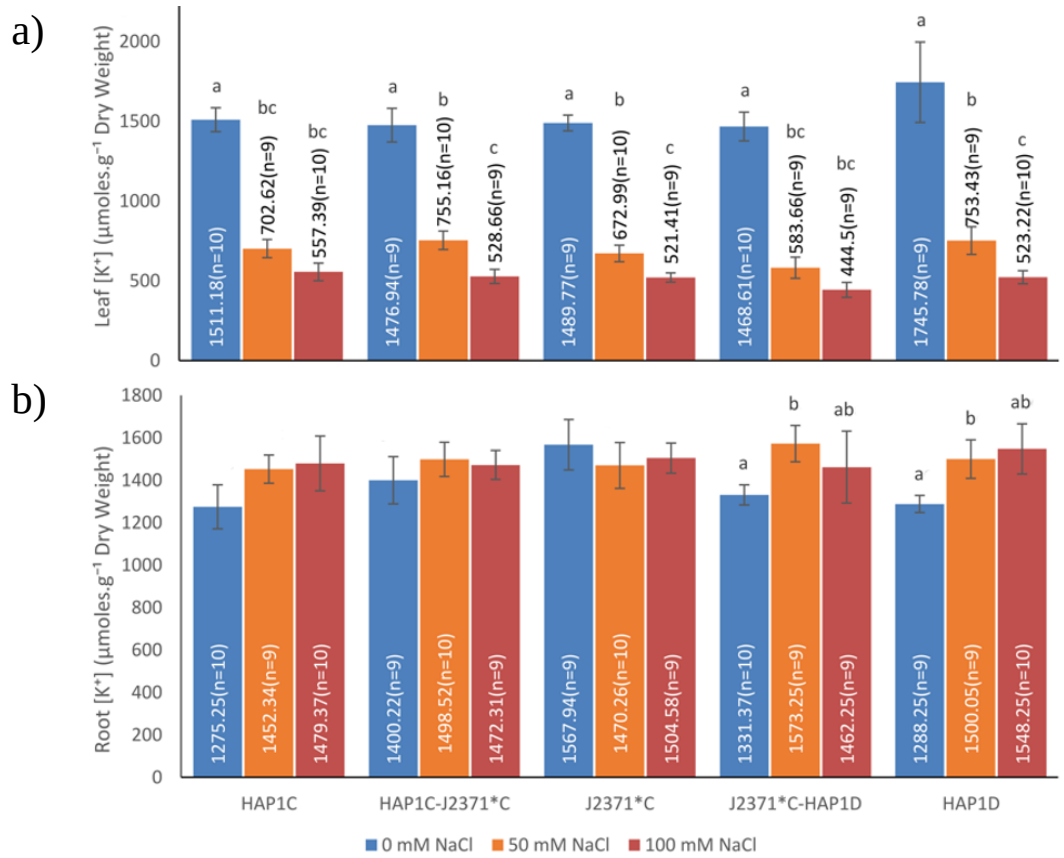

Figure 5.13: Leaf and root K^+ content of dual enhancer-trap lines is similar to parental enhancer-trap lines.

Data shown are mean leaf (a) and root (b) dry weight K^+ content of parental enhancer-trap lines (*GAL4-VP16* or *HAP1-VP16*: HAP1C, J2371*C, HAP1D) and two dual enhancer-trap lines (*GAL4-VP16* and *HAP1-VP16*: HAP1C-J2371*C A and J2371*C-HAP1D A). Plants were grown for 4 w in mini-hydroponics then treated with an additional 0, 50 or 100 mM NaCl for 1 week before harvest. Values are means ± SEM (n=9-10) with letters indicating significant differences between treatments. Significance between lines within treatments and within treatments between lines determined by one- or two-way ANOVA, Tukey-Kramer HSD, ($P \leq 0.05$). Significant differences were observed between treatments with decreasing [K^+] in leaves with increasing NaCl treatments. Root [K^+] remains consistent with increasing NaCl treatment in most lines. No significant differences were observed between lines parental or crossed line within treatments. Crossed line within treatments.

5.4. Discussion

The aim of this chapter was to develop dual enhancer trap lines which expressed reporter genes in different cell types of Arabidopsis root. To facilitate this it was necessary to confirm the root cell-type specific location of CFP protein fluorescence in *HAP1-VP16* enhancer lines, HAP1D and HAP1C, and that the plants performed similar to wild-type under saline growth conditions. Confocal microscopy demonstrated that HAP1C enhancer-trap line fluorescence is primary in the root cortex and is found throughout the entire root system, including lateral roots (Figure 5.4). Similarly, the HAP1D enhancer-trap line fluorescence is root specific, expressed along the length of the root, and is confined to the root epidermal cells (Figure 5.5). The nuclear localisation of H2B::CFP did make visualisation difficult in larger cells, where the total cell volume to nucleus volume ratio is much higher, especially in epidermal and cortical cells of the mature root zone. The root-epidermal (HAP1D) or cortical (HAP1C) fluorescence patterns between these two lines can easily be observed in the root tip, where cell density is at its highest and so visualisation of the nucleus localised H2B::CFP is most distinct. Additional work may be required to further confirm the expression pattern in these lines, potentially through the use of a reporter gene more suitable for fixing and dissection, such as *β-glucuronidase* (GUS). The development of UAS_{HAP1} transactivation constructs to enable the expression of such reporter genes and other GOIs using the *HAP1-VP16* enhancer trap system is described in the following chapter.

The *GAL-VP16* enhancer-trap line J2371*C was confirmed to have with root pericycle specific expression (section 5.3.1.1) as previously observed by (Møller *et al.*, 2009), and potentially additionally leaf vascular expression. Importantly, Both *GAL4-VP16* and *HAP1-VP16* enhancer-trap lines selected for also showed no changes in fluorescence patterns under increased salinity (section 5.3.1.4) indicating that expression of the enhancer-trap remains relatively constant under increasing salinity.

Following this initial characterisation, several dual *GAL4-VP16* and *HAP1-VP16* enhancer-trap lines were developed (section 5.3.2). The fluorescence patterns of the two reporters, mGFP5-ER and H2B::mCFP, as determined by confocal microscopy in the dual-enhancer trap lines appears stable and similar to that of the parental lines, without any indication of cross activation between the two enhancer-trap constructs. Salinity screening of parental and dual enhancer-trap lines in mini-hydroponics (section 5.3.2) shows no significant difference in Na^+, K^+ accumulation or biomass production between

lines, indicating that there is no significant impact from the expression of the *GAL4-VP16* or *HAP1-VP16* enhancer-traps individually or in combination.

The relatively constant fluorescence in the specified tissues indicates that the enhancer-trap lines selected are not salt responsive. A decrease in fluorescence may have indicated repression of the enhancer-trap under increased salinity which would have impacted their use in later salinity experiments. Further work could be done to confirm the relative and/or absolute expression levels of each enhancer-trap by such techniques such as RT-PCR or Q-PCR. The expression patterns in specific tissues could be similarly confirmed by techniques such as RT-PCR or *in situ* PCR (Byrt *et al.*, 2014; Haase *et al.*, 1990).

The high expression in the root tip of the *HAP1-VP16* parental lines and dual enhancer-trap lines may be of concern, especially when these lines will be later used to drive the cell-type specific expression of Na^+ transporters. Expression of genes involved in Na^+ sequestration, such as *AtNHX1* or *AtAVP1* may lead to more rapid accumulation of Na^+ to toxic levels in the root tip, which may limit the overall root growth in saline conditions. However, as substantial Na^+ uptake may occur at the root tip via the endodermal cells which have to develop a Casparian band to exclude Na^+ expression of Na^+ transporters capable of effluxing Na^+ out of these cells directly, such as *AtSOS1,* may prove very beneficial. Indeed, *AtSOS1* is reported localised to the root tip plasma membrane natively (Shi *et al.*, 2002).

The material generated in this chapter will be used to allow the expression of multiple salinity tolerance genes in specific and distinct cell types, specifically the root-pericycle and either the root-epidermis or root-cortex, via the use of $GAL4_{UAS}$ and $HAP1_{UAS}$ transactivation constructs developed in the following chapter.

Chapter 6

Vector Construction for cell-type specific over-expression of GOIs in dual enhancer-trap Arabidopsis lines

Chapter 6 - Vector construction for cell-type specific expression of multiple *GOIs* in dual enhancer-trap Arabidopsis lines

6.1. Introduction

In the previous chapter, a number of lines with cell-type specific expression of two enhancer-traps, *GAL4-VP16* and *HAP1-VP16*, in the root-stele and root-cortex or root-stele and root-epidermis were developed and characterised for salinity tolerance and cell-type specific expression. In order to drive the expression of transgenes via the *GAL4-VP16* or *HAP1-VP16* transcriptional activators in these cell-types, trans-activation constructs are required.

The *GAL4-VP16* trans-activation construct *pG/UAS$_{GAL4}$* has previously been developed and used to express several salinity tolerance genes, such as *AtHKT1;1* (Møller, 2008) or *AtAVP1* (El-Hussieny, 2006) and has been shown to be able to alter Na^+ transport in Arabidopsis *GAL4-VP16* enhancer-trap lines (Møller *et al.*, 2009). To our knowledge, a *HAP1-VP16* trans-activation construct for the expression of transgenes has not previously been developed or trialled in plants, although a previous attempt been has made by colleagues at the University of Adelaide (Yew, 2011).

6.1.1. Aim of this study

This aim of work described in this chapter was to develop *HAP1-VP16* trans-activation DNA constructs that would allow the cell-type specific expression of selected transgenes, through the use of the *HAP1-VP16* enhancer-traps previously characterised or when transformed into the dual Arabidopsis enhancer-trap lines developed and characterised in Chapter 5. Using these constructs, we aimed to drive the over expression of selected transgenes (Table 6.1) in specific cell-types and alter Na^+. Progress towards these aims are presented, and future prospects for use of this system are discussed.

Table 6.1: Selected transgenes for root cell-type specific expression in Arabidopsis dual *GAL4-VP16* and *HAP1-VP16* enhancer-trap lines.
Information included; Gene name; locus and species of origin

Gene Name	Gene Locus	Original species
AtAVP1	At1g78920[1]	*Arabidopsis thaliana*
AtHKT1;1	At4g10310[2]	*Arabidopsis thaliana*
AtSOS1	At2g01980[3]	*Arabidopsis thaliana*
AtNHX1	At5g27150[4]	*Arabidopsis thaliana*
PpENA1	PHYPADRAFT_105562[5]	*Physcomitrella patens*

[1] http://www.ncbi.nlm.nih.gov/gene/844231
[2] http://www.ncbi.nlm.nih.gov/gene/826623
[3] http://www.ncbi.nlm.nih.gov/gene/814729
[4] http://www.ncbi.nlm.nih.gov/gene/832773
[5] http://www.ncbi.nlm.nih.gov/gene/5923286

6.2. Methods and Materials

6.2.1. Preparation of binary vectors for cell-type specific expression of genes of interest

6.2.1.1. Vector construction starting material

The vectors in Table 6.2 were used as starting material for the construction of Gateway®-enabled destination vectors described in this chapter. Additional vector maps are presented in Appendix II: Vectors Maps.

Table 6.2: Summary of vectors used for *UAS$_{HAP1}$*:Gateway® vector construction. Information includes: Vector source; Antibiotics for bacterial and plant transformation selection; intended purpose; and whether the vector is compatible with the Gateway®-cloning system. All Gateway®-enabled destination vectors, designed for plant transformation, are propagated in *E. coli* DB3.1 cells. All other vectors are propagated in *E. coli* Top-10® or DH5α cells. Bacterial and plant selectable markers: kanamycin (Kan.), chloramphenicol (Chlor.), hygromycin B (Hyg.) and glufosinate ammonoium (BASTA).

Vector	Source	Selectable marker		Purpose	Gateway® enabled
		Bacterial	*Plant*		
pMDC43	Uni. Zurich	Kan. & Chlor.	Hyg.	Hyg selectable Gateway® Vector	Yes
pMDC123	Uni. Zurich	Kan. & Chlor.	BASTA	BASTA selectable Gateway® vector	Yes
pTOOL36	Uni. Zurich	Kan. & Chlor.	Hyg.	Source of *nos* terminator	Yes
pET-HAP1	J. Hassloff Uni. Cambridge	Kan.	Kan.	Source of UAS$_{HAP1}$, *HAP1-VP16* & *H2B::CFP*	No
pGOF-UAS$_{GAL4}$: AtHKT1;1	I. Moller Uni. Cambridge	Kan.	BASTA	Source of *UAS$_{GAL4}$: AtHKT1;1*	No

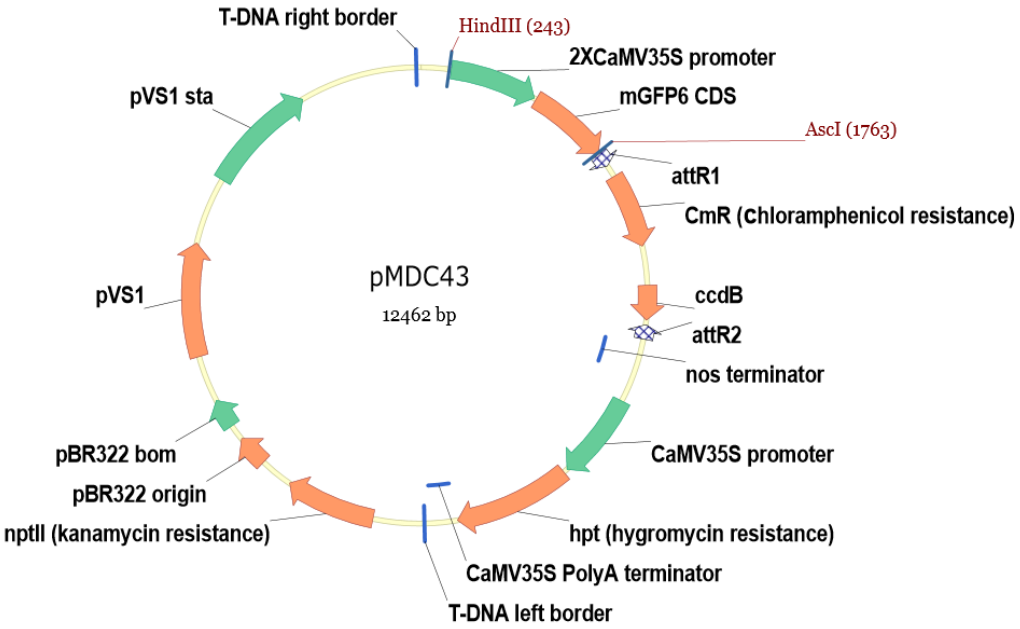

Figure 6.1: Schematic diagram of the destination vector *pMDC43*
The *pMDC43* vector was primarily developed (Dettmer & Friml, 2011) to enable the generation and expression in planta of N-terminus mGFP6 tagged genes of interest, via the Gateway® LR recombination site. From the T-DNA right border (clockwise) to the T-DNA left border: the T-DNA cassette contains [restriction sites HindIII (269 bp) and AscI (1763 bp) flanking 2 repeats of the Cauliflower Mosaic Virus 35S (*2×CaMV35S*) promoter upstream of a unterminated *mGFP6* CDS, a Gateway® recombination cassette [comprised of Gateway® recombination sites (*attR1* and *attR2*) flanking: chloramphenicol resistance gene (*CmR*) for bacterial selection, and the *ccdB* plasmid maintenance gene (requiring *ccdB* resistant E. coli strains such as DB3.1 or Invitrogen® OneShot® Survival 2)], bacterial nopaline synthase (*nos*) terminator, a Cauliflower Mosaic Virus 35S (*CaMV35S*) promoter driving the *Hygromycin phosphotransferase* (*hpt*) gene (Hygromycin B resistance for in planta selection) followed by a *CaMV35S* polyA terminator sequence; T-DNA left border sequence]. The remaining vector consists of: the *neomycin phosphotransferase* (*nptII*) gene (kanamycin resistance for bacterial selection); *pBR322 replication origin* (*pBR322 ori*) and *basis of mobilisation* (*pBR322 bom*) sequences for vector propagation in *E. coli*; and *pVS1 replication* (*pVS1 rep*) and *stability* (*pVS1 sta*) sites for vector propagation in *A. tumefaciens* . Primer binding sites used for sequencing the modified promoter sequence (Table 6.4: sqUpRB_1, sqDownRB_1, sqUpattR1_1 and sqCMr_Mid F1) and plant genotyping (Table 6.4: HYG1-F and HYG1-R) have also been included.

6.2.1.2. Plasmids containing cDNA of selected transporters

Plasmids containing cDNAs of transporters selected for use in this study were kindly obtained from Dr. Darren Plett, Dr. Joanna Sundstrom and Dr. Andrew Jacobs (University of Adelaide, ACPFG). Full details of cDNA plasmids are provided in Table 6.3.

Table 6.3: Summary of entry vectors containing GOIs used for the construction of binary expression vectors.
Information includes: vector source; cDNA species of origin; bacterial selectable marker. All entry vectors are Gateway® enabled and propagated in *E. coli* DH5α or Top-10® cell lines.

Vector	Source	cDNA origin	Bacterial selection
pCR8/GW-TOPO	Invitrogen®	n/a	Spec.
pENTR-D-TOPO	Invitrogen®	n/a	Kan.
pCR8-GW-TOPO TA+AtAVP1	D. Plett (ACPFG)	*A. thaliana*	Spec.
pCR8-GW-TOPO TA+AtHKT1;1	J. Sundstrom (ACPFG)	*A. thaliana*	Spec.
pCR8-GW-TOPO TA+AtNHX1	D. Plett (ACPFG)	*A. thaliana*	Spec.
pCR8-GW-TOPO TA+AtSOS1	D. Plett (ACPFG)	*A. thaliana*	Spec.
pENTR-D-TOPO::PpENA1	A. Jacobs (ACPFG)	*P. patens*	Kan
pCR8-GW-TOPO TA+uidA	A. Jacobs (ACPFG)	n/a	Spec.
pCR8-GW-TOPO TA+mGFP6-ER	A. Jacobs (ACPFG)	n/a	Spec.

6.2.2. *HAP1-VP16* enhancer trap, *pET-HAP1* and sequence information

Initial sequence data of the *HAP1-VP16* T-DNA construct, *pET-HAP1* and the construct itself was kindly provided by S. Henderson and M. Gilliham (University of Adelaide, Waite Campus) and was originally developed by Dr. J. Hassloff (University of Cambridge). Further sequence analysis of the *pET-HAP1* construct was conducted to identify all the components of the T-DNA region through NCBI blast and comparisons made using VectorNTI (2.2.1).

6.2.3. Cloning and vector construction

Development of Gateway®-enabled constructs are discussed below. PCR amplification of fragments for cloning and vector construction were conducted in 25 µL reactions using a proof-reading DNA polymerase described in section 2.2.2 (cloning PCR) to reduce replication errors. Amplified fragments were cloned into *pCR8/GW-TOPO* (section 2.2.7) and subsequently sequenced as per section 2.2.13 with primers flanking the inserted DNA (primers: Table 6.4: GW1 and GW2). Plasmid DNA was linearised by restriction enzyme (RE) digest as per section 2.2.3. A-Tailing of blunt-ended RE products where necessary was done as per section 2.2.2 (A-Tailing PCR). Ligation of plasmid

fragments was conducted with T4 DNA ligase (section 2.2.6). Sequencing across modified plasmids was done as per section 2.2.13 with primers flanking the inserted DNA and Gateway® recombination site (primers: Table 6.4: sqUpRB_1, sqUpattR1_1, SqDownRB_1, sqCMr_Mid_F1)

6.2.4. Preparation of binary vectors for cell-type specific expression of genes of interest and transformation into Arabidopsis

Selected GOIs cDNAs in various Gateway® entry vectors (Table 6.3) were recombined into Gateway®-enabled binary constructs via Gateway® recombination as per section 2.2.8 and subsequently transformed into *Agrobacterium* for use in Arabidopsis transformation. The vectors developed are outlined in Table 6.5.

Parental *GAL4-VP16* and *HAP1-VP16* enhancer-trap lines, J2371*C, HAP1C, HAP1D and dual enhancer trap lines developed in Chapter 5, were transformed with these *Agrobacterium* cultures via the floral dip protocol per section 2.3.6.2, and selected on appropriate selection media s per section 2.3.7.

Genomic DNA (gDNA) was extracted from leaf tissue of resistant plants with the Edwards extraction protocol (section 2.2.20) and genotyping PCR carried out as per section 2.2.2, with primers specific to transformed constructs (Primers: Table 6.4 - Hyg1 and Hyg2 or Basta_F and Basta_R), *GAL4-VP16* (Primers: Table 5.1 - GFPiF and GFPiR) or *HAP1-VP16* (Primers: Table 5.1: CFP51 and CFP3RC1)

Table 6.4: Primers for vector construction, sequencing and genotyping Arabidopsis *GAL4-VP16* and *HAP1-VP16* lines transformed lines. Information included; primer length (b), sequence, expected product length (bp), PCR conditions and intended purpose. PCRs conducted as per section 2.2.2 with specified PCR conditions, 35 cycles. BigDye® sequencing reactions conducted as per section 2.2.13. Additional genotyping primers in Table 5.1.

Primer	Length (bp)	Sequence (5′ - 3′)	Amplicon size (bp)	PCR conditions	Purpose
sqUpRB_1	20	AGAAAACGCCAGGAAAAGGG	N/A	BigDye® sequencing PCR	Sequencing of Gateway® constructs
sqUpattR1_1	22	CGCCGGATCCTAACTCAAAATC			
SqDownRB_1	20	AGGCGGGAAACGACAATCTG			
sqCMr_Mid_F1	20	GATGAGCATTCATCAGGCGG			
GW1	25	GTTGCAACAAATTGATGAGCAATGC			Sequencing of *pCR8/GW-TOPO* inserts
GW2	25	GTTGCAACAAATTGATGAGCAATTA			
BamHI-UAS(Fwd)	30	AGTCGGATCCCAAGCTTAGCACGGACTTAT	137	Anneal:60°C Extend:25 s	Amplification of 5×UAS_{HAP1}
AscI-HAP1::UAS (Rev)	32	AGTCGGCGCGCCCTTCTAGACCGACCGATAAG			
BamHI-UAS(Fwd)	30	AGTCGGATCCCAAGCTTAGCACGGACTTAT	226	Anneal:60°C Extend:60s	Amplification of 5×UAS_{HAP1}:minCaMV35s
Min35s_AscI_R	28	GGCGCGCCGTCCTCTCCAAATGAAATGA			
PacI-HAP1VP16_F	29	TAATTAATGGATCTTCGCAAGACCCTTC	915	Anneal:60°C Extend:60s	Amplification of *minCaMV35S*: HAP1-VP16:nosT
HAP1VP16-KpnI_R	26	GGTACCCAGATTGTCGTTTCCCGCCT			
KpnI-UASCFP_F	26	GGTACCCGATTCATTAATGCAGCTGG	1915	Anneal:60°C Extend:60s	Amplification of *5×UAS_{HAP1}:* minCaMV35s:H2B::CFP:nos T
UASCFP_NosT_R	24	CAGTCACGACGTTGTAAAACGACG			
Hyg1	20	GTCGATCGACAGATCCGGTC	815	Anneal:60°C Extend:60s	Genotyping of *hpt* containing constructs: *pGOR1, pGOR2*
Hyg2	20	GGGAGTTTAGCGAGAGCCTG			
Basta_F	20	GACTTCAGCAGGTGGGTGTA	377	Anneal: 62°C Extend:30s	Genotyping for presence of *bar* containing constructs *pGOF-$UAS_{GAL4,}$ pGOR3* & *pGOR4*
Basta_R	17	AAATCTCGGTGACGGGC			

6.3. Results and Discussion

6.3.1. Development of Gateway® enabled destination vectors for expression of transgenes

A number Gateway® enabled binary vectors were constructed to enable cell-type specific expression of genes of interest using the *HAP1-VP16* enhancer-trap system in Arabidopsis to examine the role of these GOIs when they are expressed in a cell-type specific manner with an aim to alter Na^+ transport in the plants previously developed in Chapter 4 (Table 6.5).

The binary vector, *pMDC43* (Figure 6.1), was selected to form the backbone of these vectors for a number of reasons;

Primarily, it was selected for the presence of the *Hygromycin phosphotransferase* (*hpt*) gene which confers in planta resistance to the antibiotic Hygromycin B, which was to be used as the plant selectable marker. This choice was critical as both the *GAL4-VP16* and *HAP1-VP16* enhancer-trap lines are already resistant to kanamycin, conferred by the original enhancer-trap constructs, and BASTA resistance was used for the selection of the *pG/UAS$_{GAL4}$:GOI* trans-activation constructs used to drive *AtHKT1;1* or *AtAVP1* in the *GAL4-VP16* enhancer-trap lines.

pMDC43 also includes a LR Gateway® cloning site to allow the easy integration of different cDNA sequences by LR recombination and compatible cloning sites which allowed the replacement of the original CaMV35S promoter and *mGFP6* CDS upstream of the LR Gateway® cloning site with the *UAS$_{HAP1}$* sequences

The pMDC-series vectors also include a number of other desirable features outside of the T-DNA region including; *neomycin phosphotransferase* (*nptII*) confering kanamycin resistance for bacterial selection; the *pBR322* replication origin (*pBR322 ori*) and basis of mobilisation (*pBR322 bom*) sites for vector propagation in *E. coli*; and *pVS1* origin of replication (*pVS1 rep*) and stability (*pVS1 sta*) sites for vector propagation in *Agrobacterium*. The presence of the *pVS1* sites allows effective transformation with *Agrobacterium* without a helper plasmid required for transformation in earlier plant transformation constructs such as the *pGreen* vector series (Hellens *et al.*, 2000).

6.3.1.1. *pGOR1/UAS$_{HAP1}$*:Gateway® for cell-type specific expression of GOIs in Arabidopsis HAP1-VP16 enhancer-trap lines – Hygromycin *in planta* selection

The repeats of the *HAP1* upstream activation sequence (*5×UAS$_{HAP1}$*) from the *pET-HAP1* plasmid (Figure 5.1) were amplified by PCR (primers: Table 6.4: BamHI-UAS(Fwd) and AscI-HAP1::UAS(Rev)) producing a 137 bp fragment which was subsequently cloned into the pCR8/GW-TOPO vector. A single clone was sequenced to confirm the cloned sequence and was digested with restriction enzymes HindIII and AscI. The 115 bp fragment containing the *5×UAS$_{HAP1}$* with over-hangs was isolated by gel electrophoresis. The *pMDC43* vector (Figure 6.1) was digested with HindIII and AscI to remove the *2×CaMV35S* promoter and *mGFP6* CDS upstream of the Gateway® cloning site and gel electrophoresis was conducted to separate vector backbone (10942 bp) with compatible ends. The two compatible fragments were ligated, as per section 2.2.6, to generate *pGOR1/UAS$_{HAP1}$:Gateway®* (Figure 6.2).

The *pGOR1/UAS$_{HAP1}$:Gateway®* construct lacks the minimal *CaMV35S* promoter sequence originally found in the *pET-HAP1* construct, in order compare levels of expression with or without this element. Potentially, different levels of expression could be possible with modification to this promoter sequence which may be desirable in some cases to fine tune expression of selected transgenes.

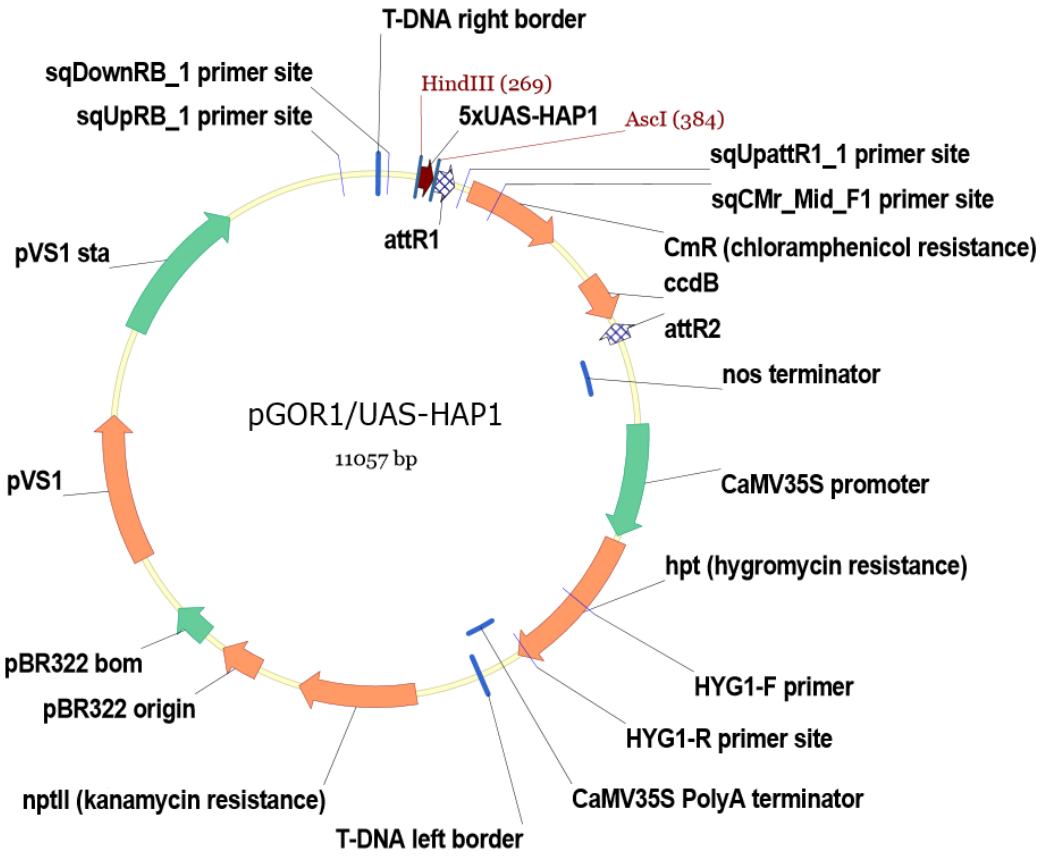

Figure 6.2: Schematic diagram of the destination vector *pGOR1/UAS$_{HAP1}$*:Gateway®.
From the T-DNA right border (clockwise) to the T-DNA left border: the T-DNA cassette contains restriction sites *HindIII* (269 bp) and *AscI* (384 bp) flanking, 5 repeats of the *HAP1* upstream activation sequence *UAS$_{HAP1}$* (5×UAS-HAP1), a Gateway® recombination cassette (see Figure 6.1 for details), a bacterial nopaline synthase (*nos*) terminator sequence, a Cauliflower Mosaic Virus 35S (*CaMV35S*) promoter driving the *Hygromycin phosphotransferase* (*hpt*) gene (Hygromycin B resistance for in planta selection) followed by a CaMV35S polyA terminator sequence; T-DNA left border sequence. For details of other vector components, see parent vector *pMDC43* (Figure 6.1).

6.3.1.2. *pGOR2/UAS$_{HAP1}$-min35s*:Gateway® for enhanced cell-type specific expression of GOIs in Arabidopsis *HAP1-VP16* enhancer trap lines – Hygromycin selection

For increased expression of transgenes *in planta*, a second UAS$_{HAP1}$ Gateway® construct was developed to the minimal *CaMV35S* promoter element from the *pET-HAP1* construct. The five repeats of the HAP1 upstream activation sequence (*5×HAP1*$_{UAS}$) plus the 92 bp minimal *CaMV35S* promoter from the *pET-HAP1* plasmid was amplified by PCR (primers: BamHI-UAS(Fwd) and AscI-min35S-(Rev)), producing a 226 bp fragment which was subsequently cloned into pCR8/GW-TOPO vector and sequenced to verify the cloned sequence. The subsequent vector was digested with restriction enzymes HindIII and AscI and the 208 bp fragment containing the *5×UAS$_{HAP1}$-minCaMv35S* with over-hangs was isolated by gel electrophoresis. The *pMDC43* vector (Figure 6.1) was likewise digested with HindIII and AscI to remove the *2xCaMV35s* promoter and *mGFP6* CDS upstream of the Gateway® cloning site and gel electrophoresis was conducted to separate vector backbone (10942 bp) now with compatible HindIII and AscI overhangs. The two compatible fragments were ligated to generate *pGOR2/UAS$_{HAP1}$-min35S:Gateway*® (Figure 6.3).

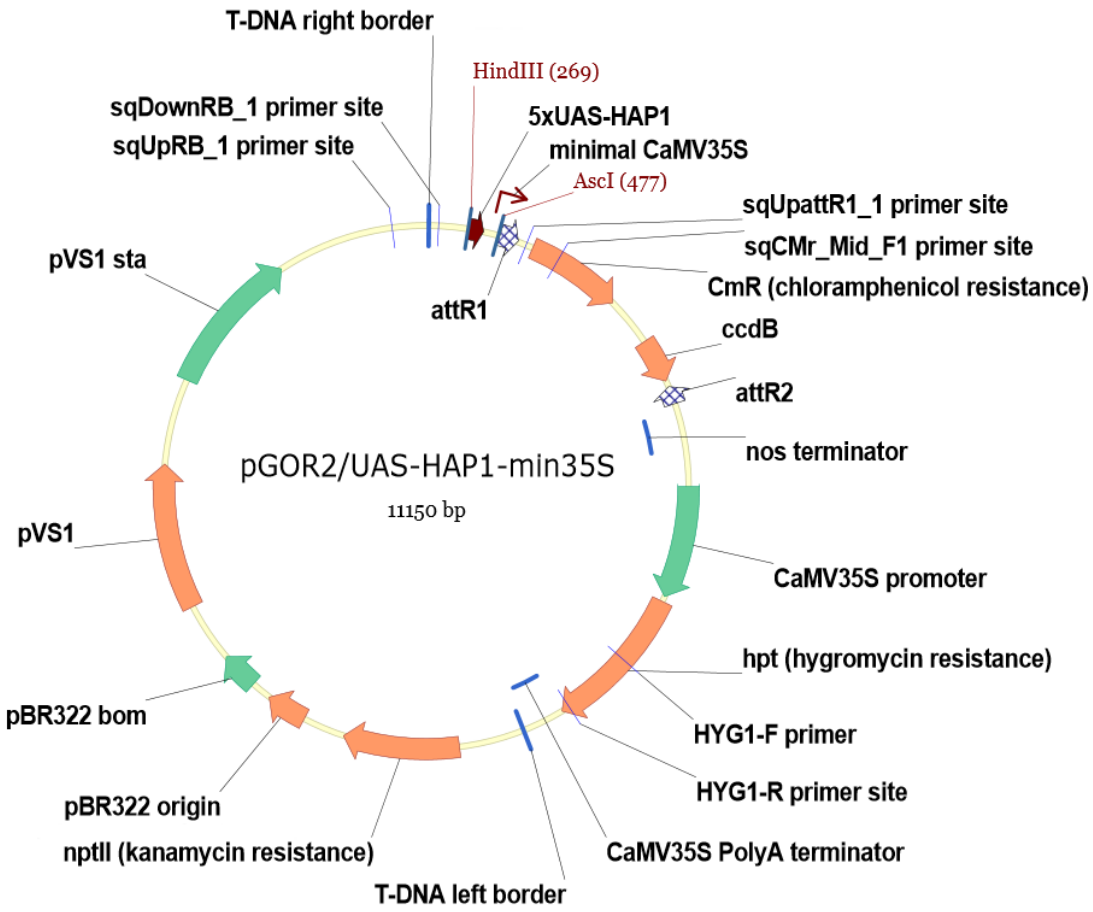

Figure 6.3: Schematic diagram of the destination vector *pGOR2/UAS$_{HAP1}$-min35s:Gateway*®.
From the T-DNA right border (clockwise) to the T-DNA left border: the T-DNA cassette contains restriction sites *HindIII*(269 bp) and *AscI*(384 bp) flanking 5 tandem repeats of the *HAP1* upstream activation sequence (5×UAS-HAP1) followed by a 92 bp minimal *CaMV35S* promoter element, a Gateway® recombination cassette (see Figure 6.1 for details), a bacterial *nopaline synthase* (*nos*) terminator sequence, a *CaMV35S* promoter driving the *Hygromycin phosphotransferase* (*hpt*) gene (Hygromycin B for *in planta* selection) followed by a CaMV35S polyA terminator sequence; T-DNA left border sequence. For details of other vector components, see parent vector *pMDC43* (Figure 6.1)

6.3.1.3. *pGOR3/UAS$_{HAP1}$-min35s:Gateway®* for cell-type specific expression of GOIs in Arabidopsis HAP1-VP16 enhancer-trap lines – BASTA selection

Due to difficulties with in planta selection of transformants under Hygromycin B using the *pGOR1/UAS$_{HAP1}$:Gateway®* and *pGOR2/UAS$_{HAP1}$-min35S:Gateway®* vectors another Gateway® enabled vector was developed with the phosphinothricin acetyltransferase (*bar*) gene conferring glufosinate ammonium resistance, allowing in planta selection by BASTA foliar spraying (Weigel & Glazebrook, 2006).

No suitable pMDC-series vectors with *bar* were available and needed to be developed. pMDC123 (Appendix Figure 1), while containing *bar*, lacks a terminator sequence downstream of the Gateway® recombination site. To correct this, *pTOOL36* (Appendix Figure 2) was digested with SacI and BsaXI to produce a 461 bp fragment containing the nopaline synthase (*nos*) terminator and isolated by gel electrophoresis. *pMDC123* was subsequently linearised by restriction enzyme digest with SacI and BsaXI creating compatible ends downstream of the Gateway® recombination cassette. The fragment contain *nopaline synthase* (*nos*) terminator was ligated into the digested *pMDC123* backbone, creating *pMDC123+nosT* (Appendix Figure 3).

pMDC123+nosT was subsequently linearised by restriction enzyme digest with HindIII and AscI and producing compatible ends. The five tandem repeats of HAP1 upstream activation sequence (*5×UAS$_{HAP1}$*) plus the 92 bp minimal *CaMV35S* promoter was isolated from pCR8/GW-TOPO TA+(BamHI)-HAP1-UAS-min35s-(AscI) vector by restriction enzyme digest as for *pGOR2/UASHAP1-min35s:*Gateway® (section 6.3.1.2). The two compatible fragments were ligated as per section 2.2.6 to generate *pGOR3/UAS$_{HAP1}$-min35S:Gateway®* (Figure 6.4).

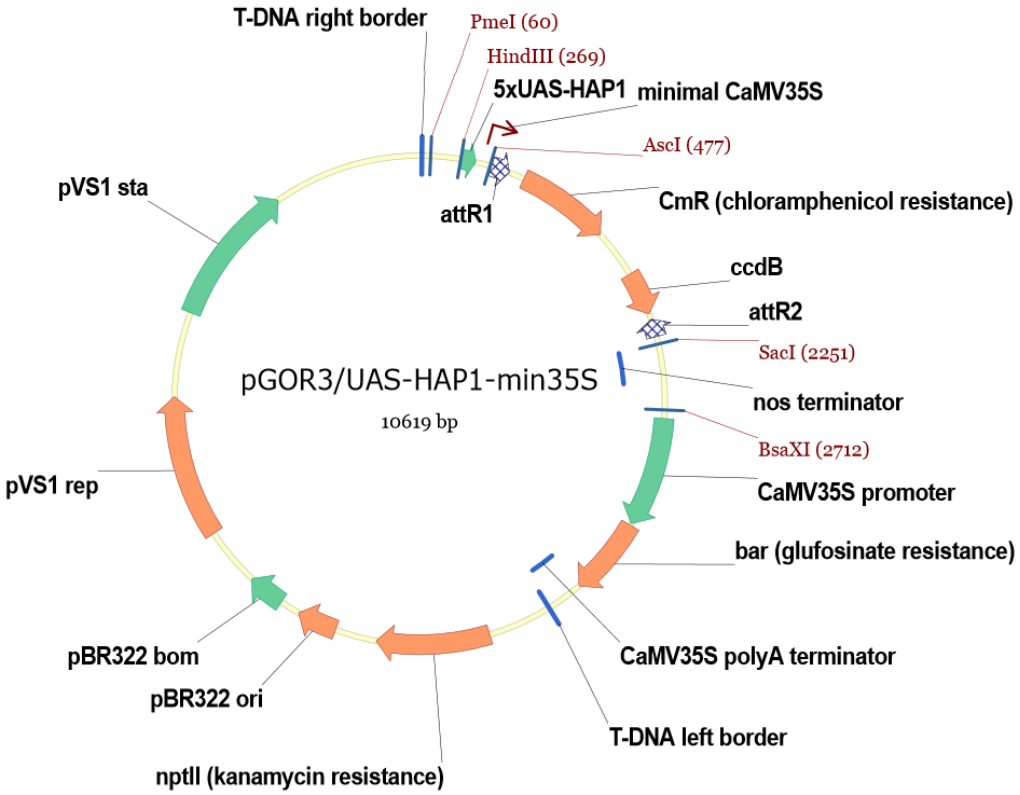

Figure 6.4: Schematic diagram of the destination vector *pGOR3/UAS$_{HAP1}$-min35S:Gateway*®.
From the T-DNA right border (clockwise) to the T-DNA left border: the T-DNA cassette contains [restriction sites *HindIII*(269 bp) and *AscI*(384 bp) flanking 5 repeats of the HAP1 upstream activation sequence *UAS$_{HAP1}$* (5xUAS-HAP1) followed by a 92 bp minimal CaMV35S promoter element, a Gateway® recombination cassette (see Figure 6.1 for details), a bacterial nopaline synthase (*nos*) terminator sequence, a *CaMV35S* promoter driving the phosphinothricin acetyltransferase (*bar*) gene (Glufosinate resistance for Basta in planta selection - originally from *pMDC123+nosT*) followed by a CaMV35S polyA terminator sequence]. For details of other vector components, see parent vector *pMDC123+nosT*

6.3.1.4. *pGOR4/Dual-UASG$_{AL4}$/HAP1-AtHKT1;1::Gateway*® for cell-type specific expression of two transgenes simultaneously in Arabidopsis GAL4-VP16 and HAP1-VP16 enhancer-trap lines

To reduce the overall number of transformation events in the dual HAP1-VP16 and GAL4-VP16 enhancer-trap lines developed in Chapter 5 (Table 5.2) an additional construct was produced with AtHKT1;1 cDNA downstream of *UAS$_{GAL4}$:minimal-CaMV35S* promoter (as in *pG/UAS$_{GAL4}$-AtHKT1;1*, Appendix Figure 4) and a Gateway® site downstream stream of the UAS$_{HAP1}$-minCaMV35S promoter (as in *pGOR3/UAS$_{HAP1}$-min35S::Gateway*®, Figure 6.4). This construct would potentially allow the expression of *AtHTK1;1* and a secondary *GOI* in different cells-types in lines with both *GAL4-VP16* and *HAP1-VP16* enhancer-traps.

To generate this construct, *pGOR3/UAS$_{HAP1}$-min35S::Gateway*® was linerised by digestion with restriction enzyme PmeI producing a blunt ended product. The *pG/UAS$_{GAL}$-AtHKT1;1* was digested with SacI and KpnI to isolate a 2057 bp fragment with 3′ overhangs which were filled in by use of T4 DNA polymerase (section 2.2.2) to produce a compatible blunt-ended fragment. The two fragments were ligated together to produce *pGOR4/DUAL-UAS$_{GAL4}$:AtHKT1;1-UAS$_{HAP1}$:Gateway*® (Figure 6.5).

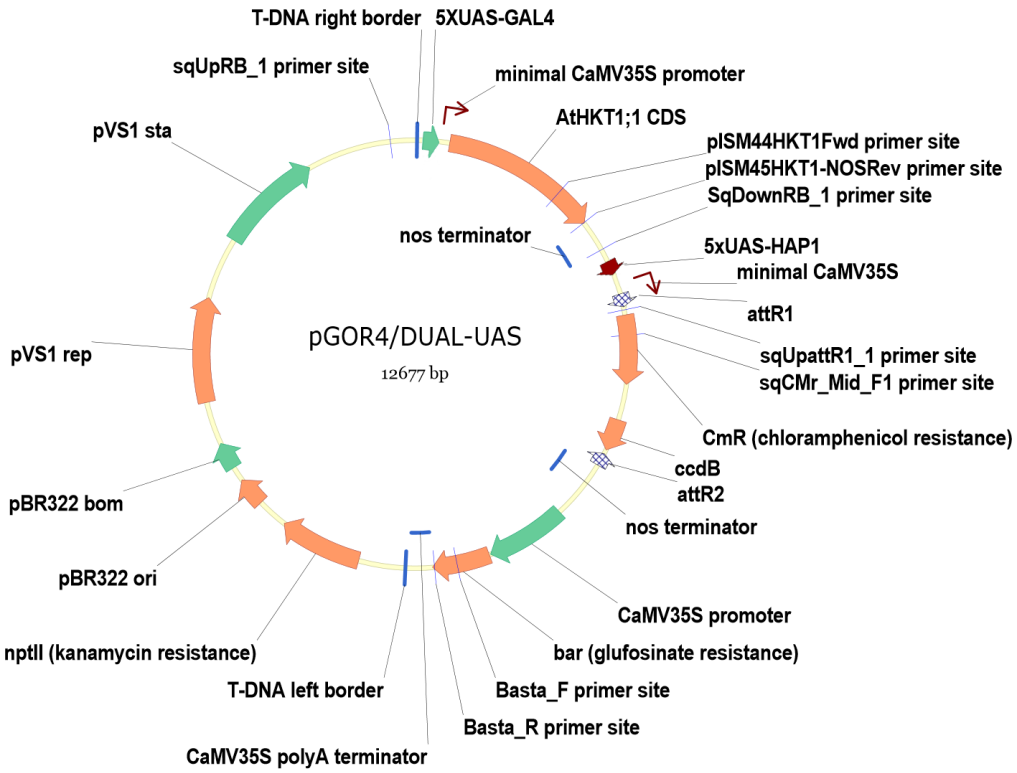

Figure 6.5: Schematic diagram of the destination vector *pGOR4/DUAL-UAS$_{GAL4}$:AtHKT1;1:UAS$_{HAP1}$-min35s:Gateway®*.
From the T-DNA right border (clockwise) to the T-DNA left border: the T-DNA cassette contains [The *UAS$_{GAL4}$:AtHKT1;1* region from *pG/UAS$_{GAL4}$-AtHKT1;1*(Appendix Figure 4) [5 repeats of the GAL4 upstream activation sequence (5×UAS-GAL4); a minimal Cauliflower Mosaic Virus 35S (*CaMV35S*) promoter; *AtHKT1;1* CDS from Arabidopsis ecotype Col-0 followed by the nopaline synthase (*nos*) terminator a bacterial nopaline synthase (nos) promoter]; 5 repeats of the HAP1 upstream activation sequence *UAS$_{HAP1}$* (5×UAS-HAP1) followed by a 92 bp minimal CaMV35S promoter element, a Gateway® recombination cassette (see Figure 6.1 for details), a bacterial nopaline synthase (*nos*) terminator sequence, a CaMV35S promoter driving the phosphinothricin acetyltransferase (*bar*) gene (BASTA in planta selection) followed by a CaMV35S polyA terminator sequence] For details of other vector components, see parent vector *pGOR3/UAS$_{HAP1}$-min35S:Gateway®* (Figure 6.4). Binding sites of sequencing primers (sqUpattR1_1, sqCMr_Mid_F1) and genotyping primers (pISM44HKTFwd, pISM45HKT-NOSRev, Basta_F, Basta_R) (Table 6.4) are also included.

6.3.1.5. *pPromoterEnhancer* for characterisation of native promoters and expression of GOIs with use of *the pGOR/UAS$_{HAP1}$-series* constructs.

The *GAL4-VP16* Arabidopsis enhancer-trap lines have been used extensively expressing transgenes in selected cell-types (Laplaze *et al.*, 2005; Møller *et al.*, 2009; Sabatini *et al.*, 1999) and for analysis of cell-function by cell-type toxin-mediated cell ablation (Weijers *et al.*, 2003). While convenient in some cases, the use of these lines does pose potential issues. Effective characterisation of enhancer trap lines can be time consuming, as seen in Chapter 4, as the integration of the enhancer-trap itself may interrupt expression of genes in the cell-types examined, potentially leading to pleiotropic affects in these cell-types or affecting growth overall. Furthermore, expression of *GOIs* via the trans-activation cassettes are limited to the expression pattern of the captured enhancer element, which is cell-type specific but is lacking temporal or other regulatory elements.

One potential work around, is the use of *GAL4-VP16* transcriptional activator under the control of cloned native promoters. This technique has successfully been used in Arabidopsis with cell-type specific promoters, driving the expression of the *GAL4-VP16* transcriptional activator, in turn driving the expression of *GOIs* in *GAL4$_{UAS}$* transactivation cassettes (Gallois *et al.*, 2004; Sabatini *et al.*, 2003). To date, the development of a similar system with the use of *HAP1-VP16* transcriptional activator has not been achieved and so was developed and designed to be used in conjunction with the *pGOR-UAS$_{HAP1}$* trans-activation constructs.

The -46 minimal *CaMV35S* promoter and downstream *HAP1-VP16* transcriptional activator and *nos* terminator was PCR amplified from the *pET-HAP1* construct (Table 6.4: Primers - PacI-HAP1VP16_F and HAP1VP16-KpnI_R), which also added PacI and KpnI restriction enzyme sites to respective ends, and was TA cloned into pCR8 forming pCR8/GW-TOPO TA+(PacI)-minCaMV35S-HAP1-VP16-nosT-(KpnI).

The *5×UASHAP1-minimalCaMV35S* promoter fused upstream of *H2B::CFP* and *nos* terminator was PCR amplified from the *pET-HAP1* adding a adding a 5′ KpnI site (Table 6.4: primers - KpnI-UASCFP_F, and UASCFP_NosT_R) and TA cloned into pCR8 forming pCR8/GW-TOPO TA+(KpnI)-HAP1UAS-min35s- H2B:CFP-(SacI)-nosT.

pMDC123+nosT was linerised by digest with restriction enzymes PacI and SacI which cut downstream of the Gateway® recombination cassette and upstream of the in planta

selectable marker (*bar*). The two above pCR8 clones were digested with either; PacI and KpnI, or KpnI and SacI forming compatible ends.

The three fragments were then ligated together to form *pPromoterEnhancer* (Figure 6.6), with the Gateway®-recombination cassette upstream of the *HAP1-VP16* transcriptional activator CDS, to allow introduction of cloned promoters by LR recombination, as well as the UAS_{HAP1} and reporter gene *H2B::CFP* to verify expression of the construct by confocal microscopy. The presence of the BASTA selectable marker makes it compatible with the Hygromycin selectable transactivation cassettes *pGOR1/*UAS_{HAP1} and *pGOR2/*UAS_{HAP1}*-min35s*

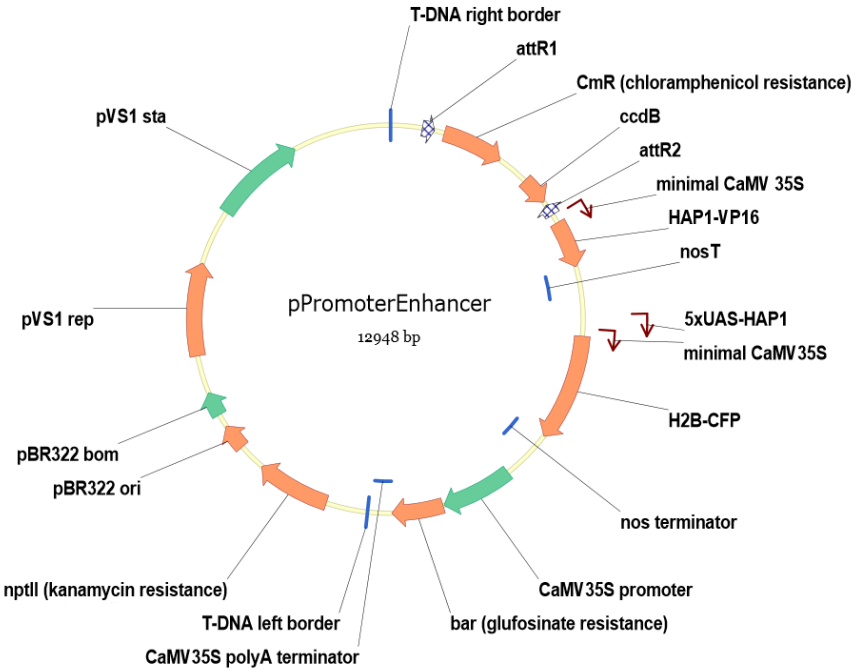

Figure 6.6: Schematic diagram of the destination vector pPromoterEnhancer.
From the T-DNA right border (clockwise) to the T-DNA left border: the T-DNA cassette contains [The UASGAL4::AtHKT1;5 region from pG/UAS-AtHKT1;1(FIGURE!!) [5 repeats of the GAL4 upstream activation sequence (5XUAS-GAL4); a minimal Cauliflower Mosaic Virus 35S (CaMV35S) promoter; AtHKT1;5 CDS from A. thaliana ecotype Col-0 followed by the nopaline synthase (nos) terminator a bacterial nopaline synthase (nos) promoter]; 5 repeats of the HAP1 upstream activation sequence UAS_{HAP1} (5xUAS-HAP1) followed by a 92 bp minimal CaMV35S promoter element, a Gateway® recombination cassette (see Figure 6.1 for details), a bacterial nopaline synthase (nos) terminator sequence, a CaMV35S promoter driving the phosphinothricin acetyltransferase (bar) gene (BASTA in planta selection) followed by a CaMV35S polyA terminator sequence] For details of other vector components, see parent vector *pGOR3/UAS_{HAP1}-min35S:Gateway®* (Figure 6.4).

6.3.2. Development of GOI expression vectors for transformation into *Arabidopsis*

LR recombination was carried out between *pGOR1-UAS$_{HAP1}$::Gateway*® and pGOR2-*UAS$_{HAP1}$-min35s::Gateway*® constructs and selected GOIs entry vectors (Table 6.3) to produce destination vectors (Table 6.5, vectors 7 – 14, 16 – 23). They were subsequently transformed into *Agrobacterium* and Colony PCR was conducted on all cultures prior to use in plant transformation.

Table 6.5: Overview of the vectors constructed, destination and expression vectors generated, transformation into *A. tumefaciens* and Arabidopsis
Information included; Vectors developed, and current progress of transformation

	Vector		*Vector constructed*	*In A. tumefaciens*	*In Arabidopsis*
1	*pCR8/GW-TOPO TA+(BamHI)-UAS$_{HAP1}$-(AscI)*		✓	N/A	N/A
2	*pCR8/GW-TOPO-TA+(BamHI)-UAS$_{HAP1}$-min35s-(AscI)*		✓	N/A	N/A
3	*pCR8/GW-TOPO TA+(PacI)-minCaMV35s-HAP1-VP16-nosT-(KpnI)*		✓	N/A	N/A
4	*pCR8/GW-TOPO TA+(KpnI)-UAS$_{HAP1}$-min35s-H2B::CFP-(SacI)-nosT*		✓	N/A	N/A
5	*pMDC123+nosT*		✓	N/A	N/A
6	*pGOR1/UAS$_{HAP1}$:Gateway®*		✓	N/A	N/A
7	*pGOR1/UAS$_{HAP1}$:*	*AtAVP1*	✓	✓	×
8		*AtHKT1;1*	✓	✓	×
9		*AtNHX1*	✓	✓	×
10		*AtSOS1*	✓	✓	×
11		*PpENA1*	✓	✓	×
12		*mGFP6-ER*	✓	✓	×
13		*uidA*	✓	✓	×
14	*pGOR2/UAS$_{HAP1}$-min35s:Gateway®*		✓	N/A	N/A
15	*pGOR2/UAS$_{HAP1}$-min35s:*	*AtAVP1*	✓	✓	×
16		*AtHKT1;1*	✓	✓	×
17		*AtNHX1*	✓	✓	×
18		*AtSOS1*	✓	✓	×
19		*PpENA1*	✓	✓	×
20		*mGFP6-ER*	✓	✓	×
21		*uidA*	✓	✓	×
22	*pGOR3/UAS$_{HAP1}$-min35s:Gateway® (BASTA selectable)*		✓	N/A	N/A
23	*pGOR4/Dual-UAS:Gateway®*		✓	N/A	N/A
24	*pPromoterEnhancer:Gateway®*		✓	N/A	N/A
25	*pPromoterEnhancer:*	*promCER2*	✓	×	×
26	*pPromoterEnhancer:*	*CaMV35S*	✓	×	×

✓: Stage completed ×: Stage incomplete N/A: Not applicable

6.3.3. Transformation of *pGOR-series* expression vectors into Arabidopsis enhancer trap lines proved unsuccessful

In total, 6 rounds of transformation of T_7F_4 Arabidopsis dual *GAL4-VP16* and *HAP1-VP16* enhancer-trap lines and T_7 parental enhancer trap lines were carried out with *Agrobacterium* containing *pGOR1/UAS$_{HAP1}$* (Table 6.5, vectors 7 - 14) or *pGOR2/UAS$_{HAP1}$-min35s* (Table 6.5, vectors 16 - 23) series vectors containing various GOI cDNAs. Unfortunately, despite numerous attempts to obtain transformants, difficulties with Hygromycin B selection, thrips infestations and malfunctions in growth room conditions prevented sufficient numbers of transformants being recovered from selection for further analysis during the timeframe of this project. Development of the *pGOR3* and *pGOR4* series vectors with BASTA selection was conducted late in this project due to the difficulties with Hygromycin B selection and so have not been thoroughly tested.

To optimise transformation, floral dip with and without vacuum infiltration, floral spraying and application of *Agrobacterium* solution directly to florets by pipette and by paint-brush was attempted with increasing numbers of plants (≈ 4 - 12 plants per construct) and at several flowering stages to improve efficiency.

Selection was trialled on 0.5 × MS selection plates (section 2.3.7) containing various concentration of Hygromycin B (15, 20, 40, 50 µg/mL) were conducted in order to obtain transformants for analysis. Under high (40 – 50 µg/mL) Hygromycin B concentration, plants either failed to germinate or rapidly vitrified. Lower (15, 20 µg/mL) concentrations failed to distinguish transformed and untransformed individuals.

Supplementation of selection media with 0.5% v/v sucrose assisted with C24 germination, but lead to excessive fungal and *Agrobacterium* growth, even with the addition of 200 µg/mL cefotaxmine added to control *Agrobacterium* growth. Several different gelling medias were trialled, described in section 2.3.3, to improve selection, but quarantine restrictions on use of certain gelling agents for plant growth forced the use of Gelrite® gellum gum. Difficulties with the use of this gelling agent for selection with Hygromycin B, were also encountered by colleagues using it for rice embryo transformation (Aris Hairmansis, Melissa Pickering ACPFG – personal communication).

Genomic DNA was extracted from a number of plants surviving lower Hygromycin B concentrations but genotyping by PCR for the presence of *hpt* failed to detect to the presence of pGOR1 or pGOR2 series constructs in recovered plants (not shown).

A very small number of plants (6) were recovered in early trial transformation with F_1 plant material, however these plants were subsequently lost due to an over-heating event in the growth chamber before seed set. This early success is why we persisted with transformation of developed constructs and Hygromycin B selection, despite the above difficulties. Several different Hygromycin B selection techniques were also examined, such as examination of hypocotyl length in dark grown plants which can help identify transformants (Harrison *et al.*, 2006), selection on sand (Davis *et al.*, 2009) and in liquid culture (Nichols *et al.*, 1997), both techniques also failed to identify transformants in this case.

Hygromycin B selection of T_1 plants of the parental *HAP1-VP16* enhancer-trap lines (HAP1C and HAP1D) and wild-type *C24* plants transformed with reporter genes *uidA* and *mGFP6-ER* trans-activation constructs also proved unsuccessful.

6.3.4. Possible reasons for the difficulties in Arabidopsis transformation and selection

While poor Arabidopsis plant growth conditions have been significant issue during this project (also seen in Chapter 4), several other possible reasons for the poor transformation and selection efficiency of the developed *HAP1-VP16* enhancer-trap lines with the pGOR-UAS$_{HAP1}$ series trans-activation constructs exist.

The major factor would be the recalcitrance of the Arabidopsis ecotype C24, the background for both the *GAL4-VP16* and *HAP1-VP16* enhancer-trap lines used in the project, to floral dip transformation. Although the C24 ecotype has been used extensively for *Agrobacterium* root transformation (Valvekens *et al.*, 1988), the efficiency by the floral dip-transformation method (Clough & Bent, 1998) is limited (maximum 0.33% reported by Ghedira *et al.* (2013)) compared to the other Arabidopsis ecotype used in this research project, Col-0, which has a much higher reported transformation efficiency by floral-dip transformation (up to 1.57% reported by Ghedira *et al.* (2013)).

The floral dip protocol has been used for transformation of both C24 and *GAL4-VP16* enhancer-trap lines previously within this lab (El-Hussieny, 2006; Møller, 2008), however, in these cases BASTA foliar selection of soil grown plants was used which

allowed the screening of much larger quantities of T_1 seeds without the added difficulties of selection of MS plates.

The reduced transformation efficiency of C24 was further experienced first-hand, as Col-0 plants were also transformed simultaneously as part of side project (Appendix VII: Investigation of polar localisation of Na+ transporters; *AtHKT1;*1) which were successfully selected under Hygromycin B and recovered for analysis.

Significant issues were encountered with contamination of selection plates, despite seed sterilisation and use sterile conditions while plating. It is likely that the supplementation of selection media with sucrose required for germination and the high humidity due to the use of Gelrite® gellum gum gelling agent. Excessive 'sweating' of the Gelrite® media lead to wetting of micropore™ tape used to seal plates which may have facilitated entry of microorganisms into the plates. However, if paraffin wax or cling-wrap was used to seal the plates, seedlings become quickly vitrified due to the excessive humidity. Plants may have been recovered from selection if other gelling agents had been available for use. Additionally, the PC2 requirement for growth of transgenic plant material meant that selection had to be conducted in growth chambers with soil grown plants. Despite bleaching and segregation of plants and plates, the presence of thrips and fungus gnats may have also contribute to contamination.

Another cause may be due to the already high transgene load in these lines. The dual enhancer-trap lines contain at least two T-DNA insertions, each using the *CaMV35S* promoter driving the *NptI* selectable marker. It has long been established that multiple transgene insertions can result in transcriptional gene (TG) silencing (Schubert *et al.*, 2004). More recently, some studies have suggested transcriptional gene silencing of *CaMV35S* promoter driven transgenes can occur through the production of *CaMV35S* promoter specific siRNAs in some T-DNA insertion lines containing the *CaMV35S* promoter (Daxinger *et al.*, 2008; Mlotshwa *et al.*, 2010). The multiple copies of *CaMV35S* promoter from both the *GAL4-VP16* and *HAP1-VP16* enhancer-traps, and from the *pGOF-UAS$_{GAL}$:AtHKT1;1* trans-activation construct could contribute to the silencing of the *CaMV35S* driven *hpt* selectable in marker the *pGOR* series constructs, preventing effective selection. Although, is not likely as T_1 plants of wild-type C24 plants transformed with reporter constructs, *pGOR1/UAS$_{HAP1}$*:(*mGFP6-ER* or *uidA*) and *pGOR2/UAS$_{HAP1}$-min35s*:(*mGFP6-ER* or *uidA*), constructs were also not recoverable.

6.4. Conclusions and Future Directions

During this project, a number of vectors were developed that would allow the expression transgenes in specific cell-types in conjunction with the *HAP1-VP16* and/or *GAL4-VP16* enhancer trap systems in Arabidopsis. *In planta* analysis of the effect of selected GOIs expression was unfortunately no able to be completed during the course of this study due to issues with selection and recovery of a suitable number of plants for analysis. Numerous attempts were made to transform and select for *HAP1-VP16*, *GAL4-VP16* and dual-enhancer trap lines containing the *pGOR-UAS*$_{\text{HAP1}}$ series of trans-activation vectors, however various reasons prevented obtaining enough transformants for analysis in the timeframe of this work and have been discussed above. The very low rate of success in selection under Hygromycin B is likely due to a combination of the relatively low transformation efficiency of the Arabidopsis C24 ecotype via floral dip, combined with issues with the use Hygromycin B selection and possible transgene silencing due to the heavy transgene load in these lines.

Further work and optimisation of transformation and Hygromycin B selection of enhancer-trap lines with the *pGOR1* and *pGOR2 GOI* constructs would achievable given improved growth facilities and further optimisation of the Hygromycin B selection in the enhancer-trap lines.

The BASTA selectable *UAS*$_{HAP1}$ trans-activation vectors (*pGOR3* and *pGOR4*) were generated too late into this project in an attempt transformation and select transgenic plant material for analysis before the end of this project. However, due to limited time plant transformation vectors containing selected *GOIs* were not generated and no proper attempt was made to transform and select plants with these vectors. It is likely, however, the ability to select a larger number of plants ease of selection by BASTA foliar spraying a suitable number of transformants will be obtainable. The size of the T-DNA insert of the *pGOR4* dual *UAS*$_{GAL4}$ and *UAS*$_{HAP1}$ trans-activation construct may also be of concern as it has been observed that Arabidopsis transformation efficiency decreases with insert size (Hellens *et al.*, 2000 and references therein). Additionally, it is possible that *Agrobacterium*-mediated Arabidopsis root transformation (Valvekens *et al.*, 1988) may be more successful than floral dip transformation for the ecotype used C24. Although, some preliminary investigation was made into using this technique, no serious attempt was made due to time constraints.

Chapter 7

General Discussion and Future Directions

Chapter 7 - General Discussion and Future Directions

7.1. Review of the aims and hypotheses

Excessive soil salinity has a major impact on plant growth and agronomic yield, both in Australia and worldwide. While the impact of soil salinity is multifaceted like many other abiotic stresses, with both ionic and non-ionic components, the focus of this thesis has been on the ionic stress component. Ionic stress is the negative effect of the often slow accumulation toxic ions, primarily Na^+, in above-ground tissues to levels which interfere with cellular processes leading to premature leaf senescence and reduced growth. One mechanism to allow plants to grow on salt affected soils by reducing, or at least slowing, the accumulation of Na^+ in above ground tissues. This reduction could be achieved by three mechanisms within roots;

1) Sequestering Na^+ within the root
2) Preventing Na^+ in the root from being loaded into the transpiration stream
3) Or reducing the overall uptake of Na^+ from the soil.

In this project, the overall aim was to investigate ways to minimise the accumulation of Na^+ in the shoot by manipulating Na^+ transport within the root. This was to be done by root cell-type specific expression of selected genes hypothesised to play a role in the above three processes (see also Chapter 1). This approach has been trialled in a number of previous studies with some success (Hairmansis, 2014; Møller *et al.*, 2009; Plett *et al.*, 2010a; Plett *et al.*, 2010b)

Initial work in this thesis focused on re-assessing previously developed Arabidopsis or barley lines with root cell-type specific over-expression of native genes involved with these processes with previous preliminary results suggesting a reduced shoot Na^+ phenotype.

Targeting Na^+ sequestration, the over-expression of *vacuolar H^+-pyrophosphatases* (*H^+-PPases*) was initially thought to play a role in Na^+ sequestration by assisting with energising of the tonoplast membrane, promoting Na^+ translocation into the vacuole by H^+/Na^+ antiporters (*NHXs*). Over-expression of *H^+-PPases* in the root cortical cells was hypothesised to allow greater Na^+ sequestration in these root cell-types, thereby reducing Na^+ transport to the shoot. This hypothesis was examined in a series of hydroponics experiments in barley lines with potential root cortical over-expression of barley *H^+-*

PPase, HvHVP1 (Chapter 3) and in Arabidopsis lines with root epidermal and/or root cortical over-expression of the Arabidopsis *H^+-PPase, AtAVP1* (Chapter 4).

To reduce Na^+ from reaching the transpiration stream and thereby the shoot, over-expression of class I *HKT* Na^+ transporters has proved successful in a number of previous studies (Byrt *et al.*, 2014; Møller *et al.*, 2009; Plett *et al.*, 2010a; Plett *et al.*, 2010b). While compelling evidence for the importance of xylem retrieval of Na^+ and reducing shoot Na^+ content exists in Arabidopsis and wheat, the importance of shoot Na^+ exclusion in barley is relatively unknown. To examine the potential for xylem Na^+ retrieval and its impact on salinity tolerance in barley, lines with potential root vascular over-expression of *HvHKT1;5* (Chapter 3) were examined in a series of hydroponics experiments. Additional work was conducted to verify the putative cell-type specific promoters used to drive root tissue-type specific expression of these genes (*HvHKT1;5* and *HvHVP1*) and to migrate promising lines closer to field trials.

Following this initial work, the major aim of the project was the development of a system for the expression of multiple transgenes in specific and distinct root cell-types. When used with known salinity tolerance genes, it would allow such genes to work in a coordinated manner and potentially improve plant salinity tolerance greater than if simply expressed individually. Such a system would assist in characterisation of multiple GOIs when expressed in specific cell-types. This was done by the development of dual enhancer-trap (*GAL4-VP16* and *HAP1-VP16*) Arabidopsis lines (Chapter 5) which would enable the cell-type specific expression of GOIs via the use of trans-activation constructs (developed in Chapter 6). Co-expression of multiple transgenes in specific cell-types could ultimately enable the enhancement of the multiple Na^+ tolerance mechanisms previously mentioned.

Mirroring this work in Arabidopsis, we also attempted the root cell-type specific co-expression of salinity tolerance genes, *HvHKT1;5* and *HvHVP1*, potentially targeting both the xylem Na^+ retrieval and root Na^+ sequestration mechanisms in combination. This was examined by hybridisation of the lines with putative cell-type specific over-expression of these genes (previously characterised in Chapter 3) and screening developed material in a series of supported hydroponics experiments to see if there was an improvement in overall plant salinity tolerance and/or reduction in shoot Na^+ accumulation.

7.2. Summary of the findings of this study

7.2.1. *H*$^+$*-PPases* in the outer root have little role in salinity tolerance

7.2.1.1. There was no observable effect on Na^+ profile and plant biomass by *H*$^+$*-PPase* over-expression in the outer root in Arabidopsis or barley.

Early experimental barley work (Chapter 3) examined the role of root-cortex specific expression of the vacuolar *H*$^+$*-PPase HvHVP1*. Previous preliminary mini-hydroponics experiments showed an altered Na^+ phenotype in lines expressing *HvHVP1* under the control of the putative root-cortex specific promoter *proC34* (Krishnan, 2013). In the mini-hydroponics experiments conducted during this study, there was no significant difference in Na^+ accumulation or plant biomass compared to null segregants. Although, there is now some evidence for the unsuitability of the *proC34* promoter used to drive *HvHVP1* in these lines.

Following on from this work, the role of root-cortex and -epidermal specific expression of the vacuolar *H*$^+$*-PPase, AtAVP1,* in the Arabidopsis ecotype C24 was examined via the use of the *GAL4-VP16* enhancer-trap and trans-activation system. Similarly, these experiments failed to confirm any significant alteration in Na^+ accumulation or transport through-out the plant as seen in the previous study conducted in soil by El-Hussieny (2006). Nor was there a significant improvement of plant biomass or salinity tolerance as seen in previous studies where *AtAVP1* has been constitutively over-expressed (Bao *et al.*, 2009; Gaxiola *et al.*, 2001; Park *et al.*, 2005; Pasapula *et al.*, 2011; Schilling, 2014; Schilling *et al.*, 2014)

7.2.1.2. An alternate role for vacuolar *H*$^+$*-PPases* and their role in salt tolerance

In this study, we were unable to demonstrate that over-expression of vacuolar *H*$^+$*-PPases* in the root-cortex/epidermal tissues in Arabidopsis or barley altered Na^+ transport or improved salinity tolerance. The potential for an altered Na^+ profile or improved salt tolerance in the material screened may exist, possibly masked by the hydroponics experimental setup, the length and/or severity of the Na^+ stress treatment or technical issues regarding the suitability of the cell-type specific promoters used. However, considering the number of lines screened and similar results in two different plant system, it is also possible that vacuolar *H*$^+$*-PPases* contribute little to plant salinity tolerance when over-expressed in part of the outer root.

New hypotheses as to the function of vacuolar *H^+-PPases*, in plants may explain the lack of an improved salinity tolerance phenotype in the examined lines. Recent experimental work suggests that, at least in Arabidopsis, the vacuolar H^+-*PPase AtAVP1* acts in the sieve element-companion cells of plant vasculature and plays a role in PPi homeostasis important for phloem loading (Pizzio *et al.*, 2015). While constitutive over-expression of *AtAVP1* in a variety of species has been shown to improve plant growth and abiotic stress tolerance (Bao *et al.*, 2009; Gaxiola *et al.*, 2001; Park *et al.*, 2005; Pasapula *et al.*, 2011; Schilling, 2014; Schilling *et al.*, 2014) it is possible that these improvements are the result of the phloem expressed *H^+-PPase*, while mis-expressed *H^+-PPase* in other tissues plays little role. It is conceivable that the over-expression of the barley homologue, *HvHVP1*, in the root cortex as examined in the study may produce a similar result.

7.2.2. Reducing Shoot Na^+ in barley by xylem retrieval by *HvHTK1;5* may play little role in the salt tolerance of barley

Hydroponics experiments examining barley lines with putative root stele-specific over-expression of the barley Na^+ transporter *HvHKT1;5* (Chapter 3) were unable to reproduce the preliminary mini-hydroponics experiments which showing an reduced leaf [Na^+] phenotype under salt stress conditions. The lack of a detectable phenotype in the root vasculature cell-type specific *HvHKT1;5* OX barley lines may simply be due to the choice of the *proS147* promoter. Previous work in Arabidopsis and wheat support the role of HKTs in xylem Na^+ retrieval (Byrt *et al.*, 2014; Møller *et al.*, 2009; Plett *et al.*; Plett *et al.*, 2010b) and identification and use of new barley root cell-type specific promoter sequences to drive *HvHKT1;5* in the root vasculature may be able to alter the Na^+ accumulation profile and improve salt tolerance.

However, the importance of shoot Na^+ exclusion in barley for salt tolerance may be limited as barley maintains higher shoot [Na^+] than less tolerant species such as wheat (Colmer *et al.*; Munns & James, 2003). Interestingly, over-expression of the *HvHKT2;1* in barley also leads to increased Na^+ accumulation in the shoot and increased relative growth compared to wild-type plants (Mian *et al.*, 2011). It may be that excluding Na^+ from the shoot in barley has little effect on overall salinity tolerance.

7.2.3. Thorough characterisation of putative cell-type specific promoters is vital prior to their use to drive GOIs

The previous sections highlight the need for thorough characterisation of cell-type specific promoters in the species into which they are ultimately are to be used. Although both *HvHVP1* and *HvHKT1;5* genes are expressed (as determined by RT-PCR) by the putative cell-type specific promoters, *proC34* and *proS147* respectively, in the barley material examined in this study conclusions about the over-expression of these genes are poor due to doubt surrounding the expression patterns and levels of expression. Further work to verify the expression levels and the tissue specificity by Q-PCR (Exner, 2010) and/or *in situ* RT-PCR (Przybecki *et al.*, 2006) would help greatly to support the conclusions outlined.

Future research should focus on the thorough identification and characterisation of cell-type specific promoters prior to their use to drive the expression of GOIs. Although it is understandable that this is not always practicable in shorter research projects.

7.2.4. Pyramiding of transgenes by hybridisation is feasible, if challenging – advice for future studies.

During this project we successfully developed both Arabidopsis and barley transgenic lines expressing multiple transgenes by hybridisation of lines with separate transformation events. However, this approach raises some special challenges when working with transgenic plant material; Producing sufficient crosses from a sufficient number of independent transgenic lines for proper analysis is difficult, and inheritance of transgenes may be complicated particularly where the exact number of T-DNA inserts is uncertain or with non-homozygous material as used in this study. While these issues are in themselves not technically challenging, but rather logistically challenging, the relatively slow reproduction of crop species (maximum of three generations a year for barley) compared to model species such as Arabidopsis makes this technique risky for short term research projects.

It is also recommended there is thorough characterisation of the lines to verify potential phenotypes prior to hybridisation and not to conduct hybridisation of unproven lines in hopes of strengthening a potentially weak phenotype as done in the barley component of this project. An exception can be made where different transgenes are known to interact and are required for proper function. However, in these cases it would be wise to use multi-gene T-DNA cassettes, such as that developed in section 6.3.1.4, which would

provide the added benefit of greatly simplify tracking the inheritance of the transgenes over the generations. Future researchers willing to use this technique in crop species should proceed with caution.

7.2.5. The use of Arabidopsis enhancer-trap lines for cell-type specific over expression of multiple GOIs provides exciting avenues for research.

The primary aim this thesis was to develop a system that would allow the over expression of multiple genes, in different but specific-cell types. During this study, several F_4 Arabidopsis lines with stable and constitutive cell-type specific expression of reporter genes *mGFP5-ER* in the root-stele and *CFP::H2B* in the root epidermis and/or root cortex were successfully developed through the use of a number of *GAL4-VP16* and *HAP1-VP16* enhancer-trap lines (Chapter 5). When screened on plates and in mini-hydroponics, reporter gene expression was stable and plants had similar biomass, Na^+ and K^+ content to the original parental lines. A number of trans-activation constructs were successfully developed Chapter 6, however difficulties experienced throughout this thesis in obtaining sufficient transgenic material for examination severely limited the experimental output of this work. A number of potentials reasons exist that prevented obtaining sufficient transformants for analysis. These include;

1) multiple transgenic events present in the transformed dual enhancer-trap lines may negatively affect plant growth and selection,
2) the relatively low efficiency of transformation by floral dip in the Arabidopsis C24 ecotype compared to other ecotypes routinely used,
3) the use Hygromycin B as the selectable marker in the C24 ecotype.

Greater progress could have been made with more material and further optimisation of the Arabidopsis transformation and selection techniques. Despite these issues, significant progress was made to allow the use of this system for future research purposes. Additional constructs with BASTA selection were developed, however further work will be required to transform and test these constructs in Arabidopsis as this was not possible during the course of this PhD project.

7.3. Future work and research directions

There remains further work that could be done to verify the presence or absence of an altered shoot [Na^+] phenotype in material developed and examined in this study. Additional hydroponics experiments and/or soil experiments could be conducted with the Arabidopsis OX material and the barley OX lines developed in this study. Options for both have been discussed in relevant chapters. However, further experiments with these lines without a strong observable phenotype is not advisable.

The current cell-type specific *H^+-PPase* OX plant material, both in Arabidopsis and barley, used in this study is probably best abandoned. The lack of a observable phenotype with this material and with recent hypothesises regarding the native role of *H^+-PPase* coming forward, further examination of these lines may have little pay-off. However, an interesting study would be to examine constitutive, or root stele specific overexpression, of *HvHVP1* in barley to see if plant biomass and abiotic stress tolerance is improved as has been seen when *AtAVP1* is similarly over-expressed in barley (Schilling, 2014; Schilling *et al.*, 2014).

Similarly, the lack of an detectable phenotype in the hydroponics experiments presented in this study for both the *HvHKT1;5* OX the dual *HvHVP1*/*HvHKT1;5* OX lines makes further experiments risky. However, the native role of *HvHKT1;5* and the significance of shoot Na^+ exclusion in barley deserves further study, perhaps through siRNA knock-down or constitutive over-expression studies of *HvHKT1;5*.

Beyond the future work already suggested and tidying up technical issues raised by this project, several avenues of further research in relation to Na^+ tolerance are discussed below.

7.3.1. Further studies using resources developed during this project.

Significant material was generated during the course of this project which may provide future research opportunities. The Arabidopsis dual enhancer-trap lines developed and characterised during the course of this study will provide a useful research tool for further studies into root ion-transport mechanisms. The lines themselves could be of use to examine genes/proteins co-operating in different root cell-types simultaneously through the use of fluorescent activated cell sorting (FACS) (Bargmann & Birnbaum, 2010). Protoplasts extracted from stressed/un-stressed roots could be separated based on the mGFP5-ER and/or H2B::CFP reporter fluorescence and gene expression and/or protein abundance examined by various techniques. This approach has been previously trialled and potential gene candidates involved in salinity tolerance identified (Evrard, 2012).

Similarly, the Gateway®-enabled *UAS$_{HAP1}$* trans-activation vectors developed in Chapter 6 could be used in other *HAP1-VP16* enhancer-trap lines for cell-type specific expression of other GOIs or for cell-type specific silencing of endogenous genes by RNAi (Burgos-Rivera & Dawe, 2012; Filichkin *et al.*, 2007)

7.3.2. New methods for cell-type specific over-expression of salinity tolerance genes

We have seen in this study the difficulties with obtaining and using cell-type specific promoters in complex plant species such barley, despite a significant amount of promoter and expression data being available in other monocots such as rice and maize. However, as greater genetic and expression information resources become available, such as the release of the barley genome recently published (International Barley Genome Sequencing Consortium, 2012), the identification and cloning of native barley promoters is becoming simpler.

The development of "synthetic" promoters composed of elements of known function would be ideal, removing much of the ambiguity surrounding "native" promoter use. However, significant work to characterise promoters is required, both *in silico* and *in planta* with commercially relevant species, to identify functional promoter elements before this approach can be used. Several major technological hurdles exist, such as high-throughput promoter analysis *in planta*, before this approach is feasible.

Moving away from cell-type specific over-expression of transgenes, the developing CRISPR-Cas9 genome editing techniques for plants (Feng *et al.*, 2013; Ran *et al.*, 2013), provides the exciting possibility to do *in planta* site directed mutagenesis. This technique may allow modifications to either native promoter elements to enhance expression or modifications to coding of native genes to alter their function and improve plant abiotic stress tolerance. Although not currently achievable, there is the possibility that this technology could be used for site-specific integration of larger DNA fragments such as promoter elements and potentially entire transgenes in the future.

The use of these techniques will possibly reduce some of the risk of using promoters taken from different species as attempted in this study, and provide novel ways to control the expression of transgenes not possible when using "native" promoters.

7.3.3. New avenues of research for examining ion transport through plants

During the course of this project, several additional research avenues were investigated which have not been discussed in the experimental chapters of this thesis. One side avenue was the possibility of directional Na^+ transport in Arabidopsis by *AtHKT1;1* and *AtSOS1* introduced briefly in Chapter 1. Directional transport across individual cells of compounds such as nutrients and hormones through both individual cells and tissues requires the localisation of transporters onto specific and often opposing membranes of a cell. Such localisation of transporters has been previously observed and extensively studied in Drosophila (Tepass *et al.*, 2001), and in plants, particularly auxin transporters involved in apical to basal (shoot to root) auxin transport (Gao *et al.*, 2008). In recent years, increasing numbers of plant proteins involved in directional nutrient transport are being characterised. Several key examples include; silicon transport in rice via the silicic acid channel Lsi1 (*OsNIP2;1*) (Ma *et al.*, 2006) and exporter Lsi2 (Ma *et al.*, 2007); and boron transport in Arabidopsis via Borate acid channel *NIP5;1* and exporter *BOR1* (Takano *et al.*, 2010). Evidence for such directional sorting of AtSOS1 and AtHKT1;1 would support their roles Na^+ efflux from the root and of xylem N^+ retrieval respectively.

Preliminary bioinformatics work into this area identified the presence of potential tyrosine sorting motifs in both AtSOS1 and AtHKT1;1 (Appendix figure 25 and 26), similar to those responsible for the membrane sorting of *NIP5;1* (Takano *et al.*, 2010). Constructs with N′- and C′-terminally *mGFP6* tagged versions of *AtHKT1*;1 and *AtSOS1* were developed (Appendix figure 7 to Appendix figure 10) and transformed into Arabidopsis ecotype Columbia. Unfortunately, in-depth screening of this material was not possible during the time-frame of this project. However, further work into this area would be of great interest as it may open up new ways to control Na^+ transport by controlling the localisation and thereby, in part, the function of the transporters.

7.4. Final remarks

Ultimately, work such as this aims to improve plant yield overall and/or improve yield stability under high soil salinity conditions. As global food production is threatened by increasing soil salinity, innovative ways to improve plant salinity tolerance are required. A targeted molecular approach to manipulating Na^+ transport *in planta* through the use of biotechnology, such as in this study, provides but one way to improve plant Na^+ stress tolerance.

During the course of this project, significant amounts of plant material were generated and screened to assess the potential for altering root to shoot transport Na^+ through the root cell-type specific expression of Na^+ transporters (*HKTs*), and genes potentially related to Na^+ sequestration (H^+-*PPases*). Techniques to enable pyramiding these genes in Arabidopsis were developed and cell-type co-expression of these genes in barley was trialled. Although no significant improvement in plant salinity tolerance was detected in the hydroponics experiments conducted with this material, the lessons and techniques developed in this project, particularly in trialling cell-type specific expression of multiple transgenes, may be applied to other gene combinations or even other abiotic stresses. The fact that experiments conducted during this project were not able to replicate earlier preliminary work results demonstrates the inherent risk involved in research, especially in carrying on others work and narrowly focusing on a single desired phenotype.

Advances in genomics, transcriptomics and bioinformatics has already made the identification of promoters and genes simpler allowing such research to be conducted more rapidly and in greater detail than allowed in the current study. Additionally, these techniques also open up potentially exciting future research avenues discussed previously.

However, future researchers should keep in mind the ultimate reason for research into plant abiotic stress tolerance and the need to migrate current knowledge from model species to commercially relevant species in ensuring global food security.

Appendices

Appendix I: Primers

Appendix Table 1: Summary of primers used for vector construction, genotyping and sequencing throughout experimental chapters
Information included; Primer ID, length and sequence

Primer	Length (bp)	Sequence (5′ - 3′)
AscI-HAP1::UAS (Rev)	32	AGTCGGCGCGCCCTTCTAGACCGACCGATAAG
BamHI-UAS(Fwd)	30	AGTCGGATCCCAAGCTTAGCACGGACTTAT
Basta_F	20	TACACCCACCTGCTGAAGTC
Basta_R	17	AAATCTCGGTGACGGGC
CFP3RC1	22	TCCTGCTGGTAGTGGTCGGCGA
CFP51	22	TCGAGCTGGACGGCGACGTAAA
GFP3RC1	28	TTACGTTTCTCGTTCAGCTTTTTTGTAC
GFP3RC2	20	TTAGTGGTGGTGGTGGTGGT
GFP51	29	ATGAGTAAAGGAGAAGAACTTTTCACTGG
GFPHKT1	54	TTGTACAAAAAAGCTGAACGAGAAACGATGGACAGAGTGGTG GCAAAAATAGCA
GFPHKTRC1	51	GCTATTTTTGCCACCACTCTGTCCATCGTTTCTCGTTCAGCT TTTTTGTAC
GFPiF	20	TCAAGGAGGACGGAAACATC
GFPiR	20	AAAGGGCAGATTGTGTGGAC
GFPSOS1	48	GTACAAAAAAGCTGAACGAGAAACGGGGATGACGACTGTAAT CGACGC
GFPSOSRC1	48	GCGTCGATTACAGTCGTCATCCCCGTTTCTCGTTCAGCTTTT TTGTAC
gtMK15_F	20	GCACTTGAGGACGACGTTGT
gtMK15_R	23	TGAACGACTGATCGAGAGCA
gtMK25_F	20	GTGGGCATGTTGGTCTTCAT
gtMK25_R	25	GGAGTAGTAGTGGAATGCAGTGA
GUSiF	20	GGCACAGCACATCAAAGAGA
GUSiR	20	CTGATAGCGCGTGACAAAAA
GW1	25	GTTGCAACAAATTGATGAGCAATGC
GW2	25	GTTGCAACAAATTGATGAGCAATTA
HAP1VP16-KpnI_R	26	GGTACCCAGATTGTCGTTTCCCGCCT
HKT_SqP1	20	CTGCGCCTTTGAATGGACCT
HKT_SqP2	24	TTGAGACTGTTACTGATTATCGCG
HKT3RC1	26	TTAGGAAGACGAGGGGTAAAGAATCC
HKT3RC2_NoStop	25	CCCGAAGACGAGGGGTAAAGAATCC
HKT51	26	ATGGACAGAGTGGTGGCAAAAATAGC
HKTGFP1	58	GCATGGATTCTTTACCCCTCGTCTTCCGGGATGAGTAAAGGA GAAGAACTTTTCACTG
HKTGFPRC1	59	CCAGTGAAAAGTTCTTCTCCTTTACTCATCCCGGAAGACGAG GGGTAAAGAATCCATGC
HvGAP-F	21	GTGAGGCTGGTGCTGATTACG
HvGAP-R	22	TGGTGCAGCTAGCATTTGAGAC
HvHKT15_SF2	16	CGGCTACGACCACCTC

HvHVP1_SF3		ACGACCGTTGATGTCCTGA
Hyg1	20	GTCGATCGACAGATCCGGTC
HYG1-F	22	TCACTGGCAAACTGTGATGGAC
HYG1-R	22	GGTTTCCACTATCGGCGAGTAC
Hyg2	20	GGGAGTTTAGCGAGAGCCTG
KpnI-UASCFP_F	26	GGTACCCGATTCATTAATGCAGCTGG
Min35s_AscI_R	28	GGCGCGCCGTCCTCTCCAAATGAAATGA
NOS_R	25	CATCGCAAGACCGGCAACAGGATTC
PacI-HAP1VP16_F	29	TAATTAATGGATCTTCGCAAGACCCTTC
pISM42AtAct2Fwd	20	GCCCAGAAGTCTTGTTCCAG
pISM48AVPFwd	21	GATGCTTCCATCAAGGAAATG
pISM49AVP-NOSRev	24	CCCCTCGAGTTAGAAGTACTTGAA
SOS_SqP1	23	CTTGCTGTCCCTGGAGTTCTTAT
SOS_SqP1	22	TTTGCAAGGACAGCCTTTAAAG
SOS_SqP2	21	GCCCCCAAGAAACGAATATTG
SOS_SqP3	25	GCAATTGTATGATTTTCTAGGGGAG
SOS_SqP4	24	GCATCCAACTTTTTCTCACGGTAG
SOS_SqP5	23	GACGAGAGCAAGAGCAATCATCT
SOS3RC1	22	TCATAGATCGTTCCTGAAAACG
SOS3RC2-No_Stop	22	GGGTAGATCGTTCCTGAAAACG
SOS51	20	ATGACGACTGTAATCGACGC
SOSGFP1	51	CGTTTTCAGGAACGATCTACCCATGAGTAAAGGAGAAGAACTTTTCACTGG
SOSGFPRC1	51	CCAGTGAAAAGTTCTTCTCCTTTACTCATGGGTAGATCGTTCCTGAAAACG
sqCMr_Mid_F1	20	GATGAGCATTCATCAGGCGG
SqDownRB_1	20	AGGCGGGAAACGACAATCTG
sqUpattR1_1	22	CGCCGGATCCTAACTCAAAATC
sqUpRB_1	20	AGAAAACGCCAGGAAAAGGG
SUC2_F	22	TATGCATGCAAAATAGCACACC
SUC2_R	25	GTTGACAAACCAAGAAAGTAAGAAA
UASCFP_NosT_R	24	CAGTCACGACGTTGTAAAACGACG
VRT2_F	24	CCGAATGTACTGCCGTCATCACAG
VRT2_R	27	TGGCAGAGGAAAATATGCGCTTGA

Appendix II: Vectors Maps

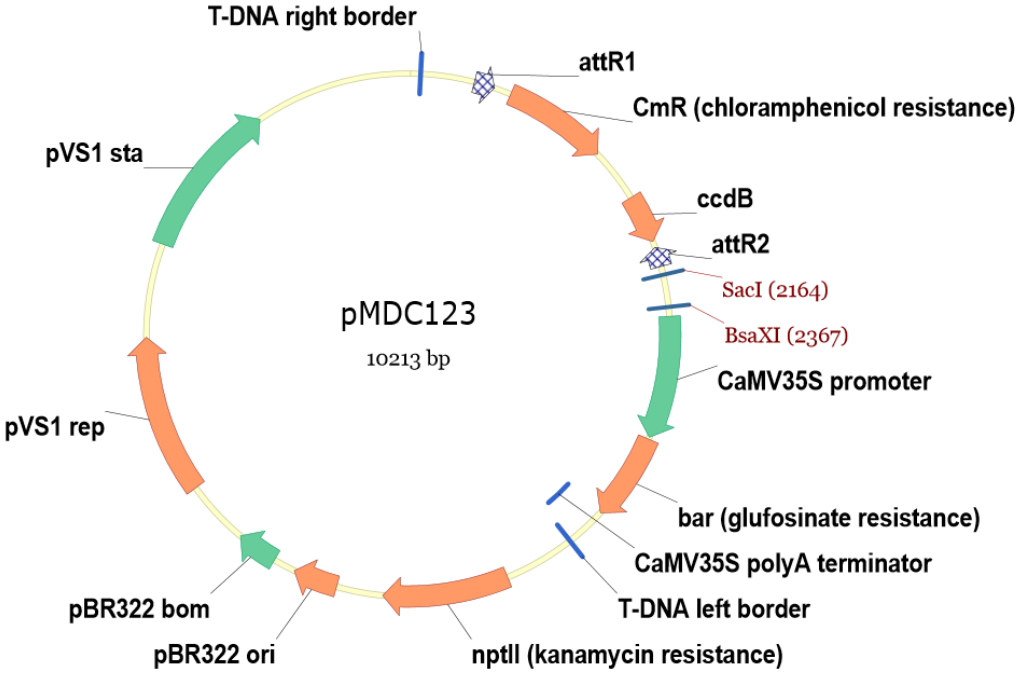

Appendix Figure 1: Schematic diagram of the destination vector *pMDC123*.
From the T-DNA right border (clockwise) to the T-DNA left border: the T-DNA cassette contains [Gateway® recombination cassette [comprised of Gateway® recombination sites (*attR1* and *attR2*) flanking: chloramphenicol resistance gene (*CmR*) for bacterial selection, and the *ccdB* plasmid maintenance gene (requiring *ccdB* resistance *E. coli* strains such as DB3.1 or Invitrogen® OneShot® Survival 2)], restriction sites for the addition of a terminator in pMDC123+nosT, *SacI*(2164) and *BasXI*(2367), a Cauliflower Mosaic Virus 35S (*CaMV35S*) promoter driving a *phosphinothricin acetyltransferase* (*bar*) gene (Glufosinate resistance for BASTA *in planta* selection) followed by a *CaMV35S* polyA terminator sequence; T-DNA left border sequence]. The remaining vector consists of: the *neomycin phosphotransferase* (*nptII*) gene (kanamycin resistance for bacterial selection); *pBR322* replication origin (*pBR322 ori*) and basis of mobilisation (*pBR322 bom*) sequences for vector propagation in *E. coli*; and *pVS1* replication (*pVS1 rep*) and stability (*pVS1 sta*) sites for vector propagation in *Agrobacterium*.

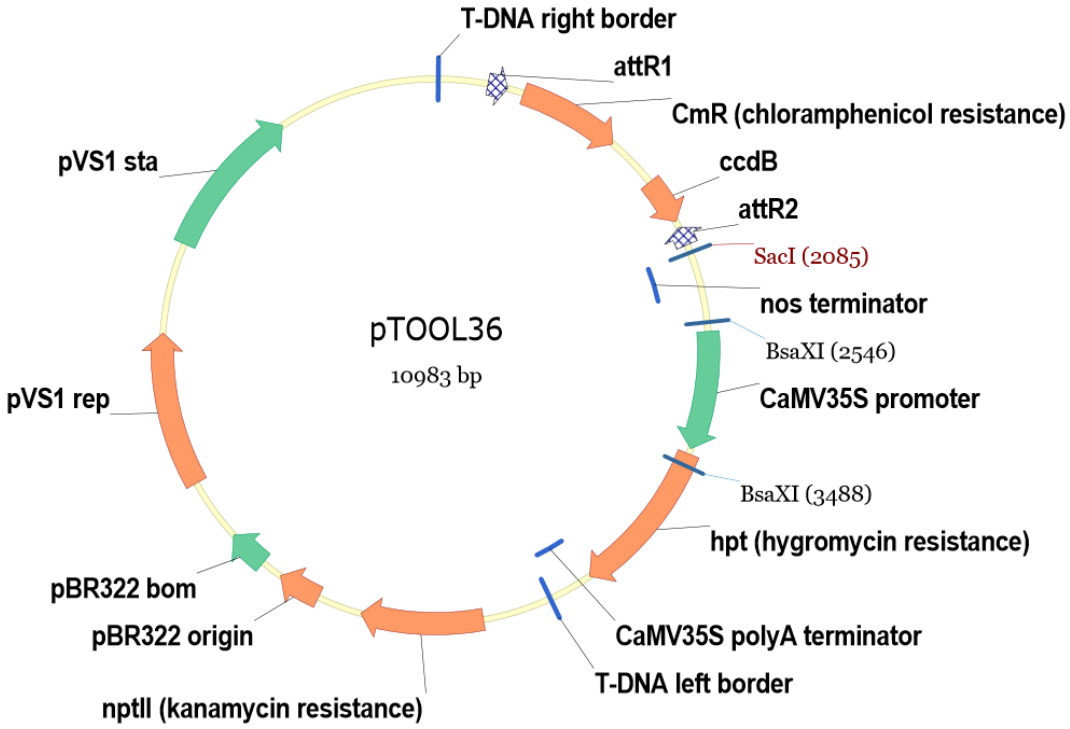

Appendix Figure 2: Schematic diagram of the destination vector *pTOOL36*.
From the T-DNA right border (clockwise) to the T-DNA left border: the T-DNA cassette contains [Gateway® recombination cassette [comprised of Gateway® recombination sites (*attR1* and *attR2*) flanking: chloramphenicol resistance gene (*CmR*) for bacterial selection, and the *ccdB* plasmid maintenance gene (requiring *ccdB* resistance *E. coli* strains such as DB3.1 or Invitrogen® OneShot® Survival 2)], restriction sites SacI (at 2085 bp) and BasXI (at 2367 and 3488 bps) flanking the bacterial nopaline synthase (*nos*) terminator (to be removed and inserted into *pMDC123+nosT*), a Cauliflower Mosaic Virus 35S (*CaMV35S*) promoter driving the *hygromycin phosphotransferase* (*hpt*) gene (Hygromycin B resistance for *in planta* selection) followed by a *CaMV35S* polyA terminator sequence; T-DNA left border sequence]. The remaining vector consists of: the *neomycin phosphotransferase* (*nptII*) gene (kanamycin resistance for bacterial selection); *pBR322* replication origin (*pBR322 ori*) and basis of mobilisation (*pBR322 bom*) sites for vector propagation in *E. coli*; and *pVS1* replication (*pVS1 rep*) and stability (*pVS1 sta*) sites for vector propagation in *Agrobacterium*.

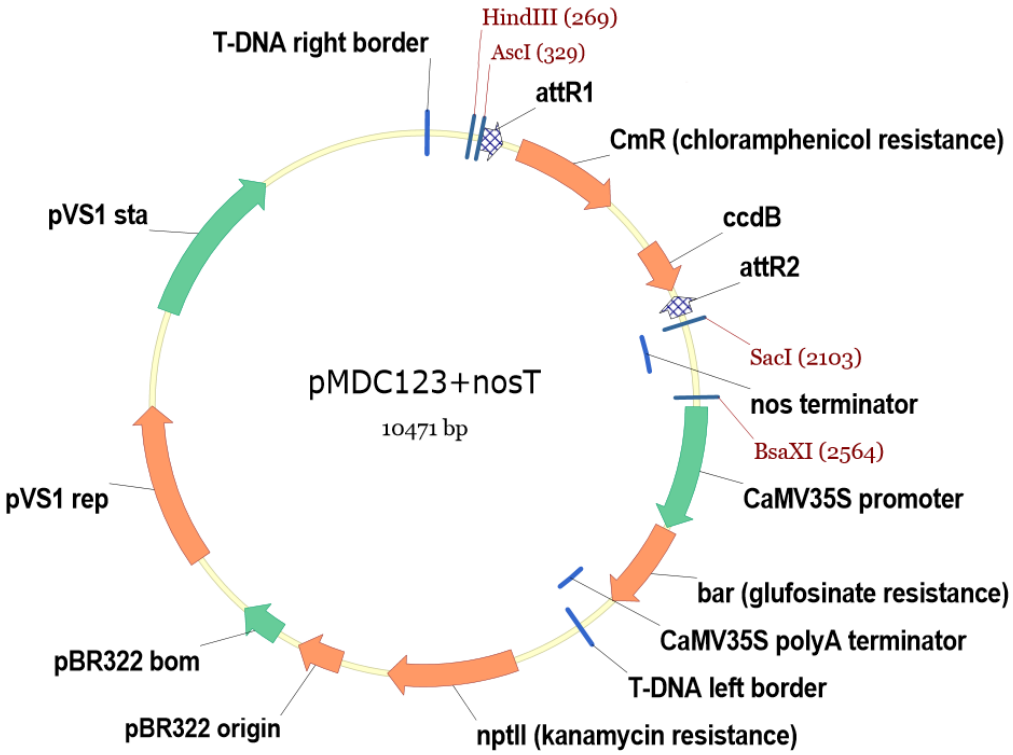

Appendix Figure 3: Schematic diagram of the destination vector *pMDC123+nosT*. From the T-DNA right border (clockwise) to the T-DNA left border: the T-DNA cassette contains [restriction sites HindIII(at 269 bp) and AscI(at 329 bp) for later cloning of promoter sequences, Gateway® recombination cassette [comprised of Gateway® recombination sites (*attR1* and *attR2*) flanking: chloramphenicol resistance gene (*CmR*) for bacterial selection, and the *ccdB* plasmid maintenance gene (requiring *ccdB* resistance *E. coli* strains such as DB3.1 or Invitrogen® OneShot® Survival 2)], restriction sites used for the addition of the bacterial nopaline synthase (*nos*) terminator from *pTOOL36*, SacI (at 2103 bp) and BasXI (at 2564bps), a Cauliflower Mosaic Virus 35S (*CaMV35S*) promoter driving a *phosphinothricin acetyltransferase* (*bar*) gene (Glufosinate resistance for BASTA *in planta* selection) followed by a *CaMV35S* polyA terminator sequence; T-DNA left border sequence]. The remaining vector consists of: the *neomycin phosphotransferase* (*nptII*) gene (kanamycin resistance for bacterial selection); *pBR322* replication origin (*pBR322 ori*) and basis of mobilisation (*pBR322 bom*) sites for vector propagation in *E. coli*; and *pVS1* replication (*pVS1 rep*) and stability (*pVS1 sta*) sites for vector propagation in *Agrobacterium*.

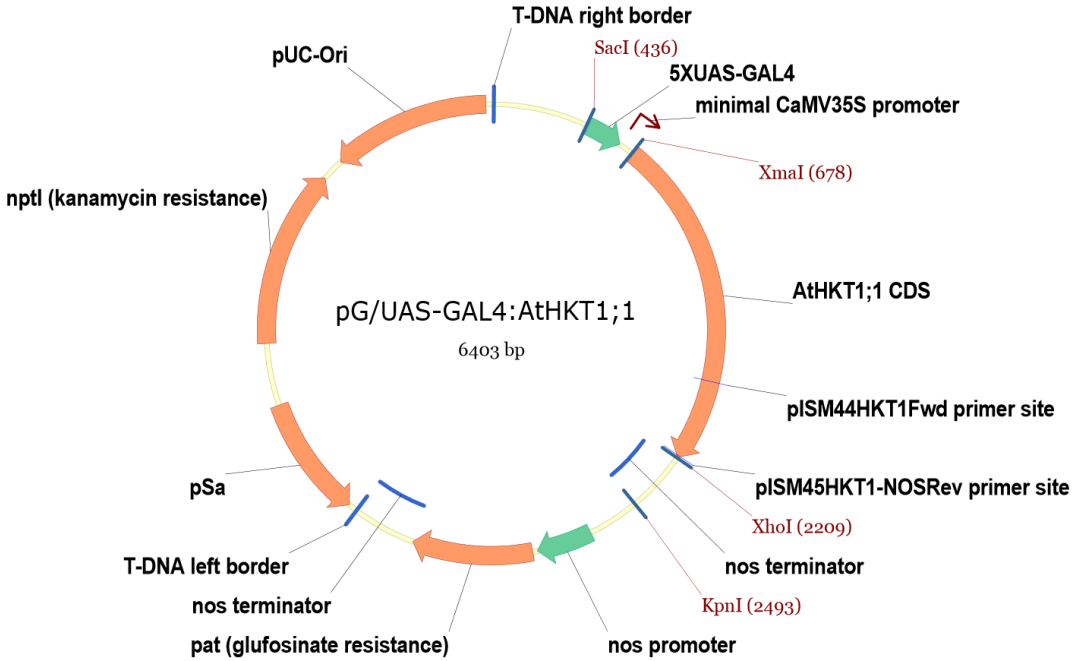

Appendix Figure 4: Schematic diagram of the expression vector *pGOF-UAS$_{GAL4}$:AtHKT1;1* used to drive the expression of *AtHKT1;1* in Arabidopsis *GAL4-VP16* enhancer trap-line J2731*C.

From the T-DNA right border (clockwise) to the T-DNA left border: the T-DNA cassette contains [5 repeats of the *GAL4* upstream activation sequence (5×UAS-GAL4); a minimal Cauliflower Mosaic Virus 35S (*CaMV35S*) promoter; *AtHKT1;1* CDS from Arabidopsis ecotype Col-0 (inserted via restriction enzyme sites, XmaI and XhoI); bacterial *nopaline synthase* (*nos*) terminator; bacterial *nopaline synthase* (*nos*) promoter; *phosphinothricin acetyltransferase* (*pat*) gene (Glufosinate resistance for BASTA *in planta* selection); nos terminator, T-DNA left border sequence]. The remaining vector consists of the *pSa* replication origin (*pSa* - Requiring the Agrobacterium strain for transformation to be co-transformed with the *pSoup* helper plasmid for successful replication in *Agrobacterium*), *neomycin phosphotransferase* (*nptI*) gene (Kanamycin resistance for bacterial selection) and the *pUC* replication origin (*pUC-Ori*) for *E. coli* replication. The primer binding sites for detecting the expression of AtHKT1;1 by semi-Q PCR (pISM44HKT1Fwd & pISM45HKT1-NOSRev) are also displayed. Adapted from (Møller, 2008)

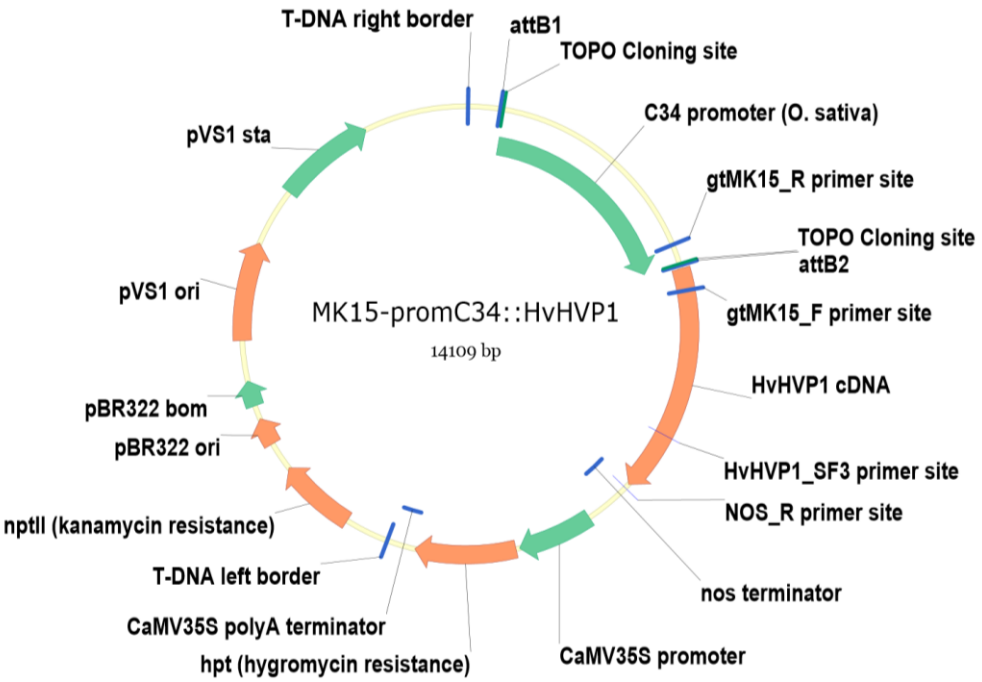

Appendix figure 5: Schematic diagram of the expression vector *pMK15-promC34::HvHVP1* for root cortex-specific expression of *HvHVP1* in barley
From the T-DNA right border (clockwise) to the T-DNA left border: the T-DNA cassette contains [*attB1* and *attB2* recombination sites flanking the putative cortical *proC34* promoter from *O. sativa*, followed by the HvHVP1 cDNA and bacterial *nopaline synthase* (*nos*) terminator; a bacterial *nopaline synthase* (*nos*) promoter;; nos terminator, T-DNA left border sequence]. The remaining vector is identical to the parent vector *pTOOL36* (Appendix Figure 2). The primer binding sites for genotyping (Table 3.4: gtMK15_R & gtMK15_F) and detecting the expression of *HvHVP1::nosT* by RT-PCR (Table 3.4: HvHVP1_SF3 & NOS_R) are also displayed. (Adapted from Krishnan, 2013)

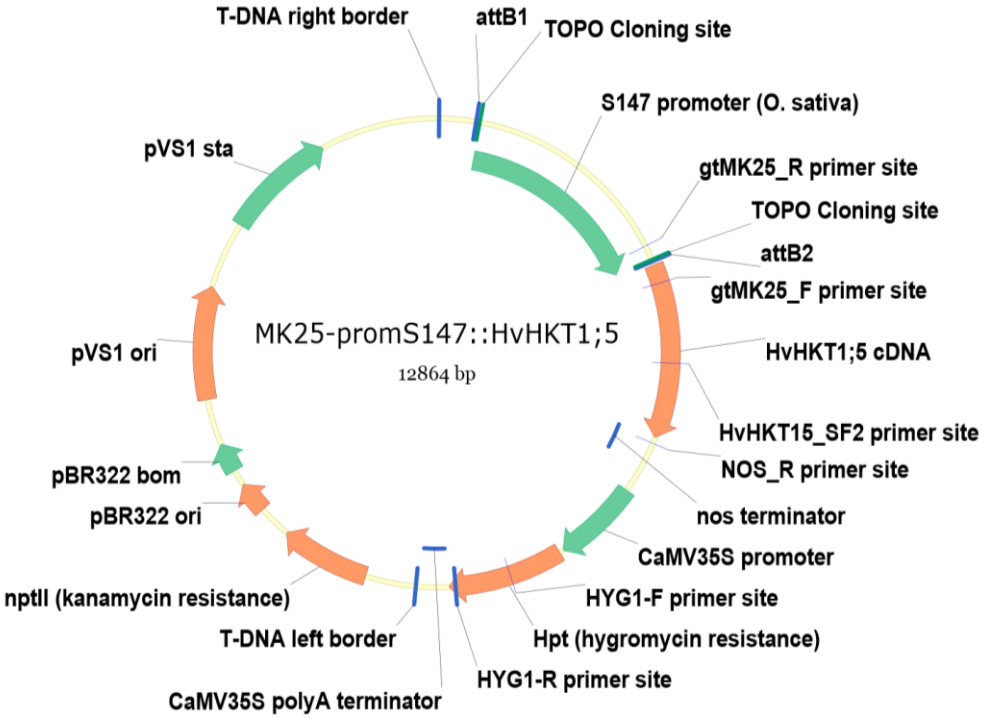

Appendix figure 6: Schematic diagram of the expression vector *pMK25-proS147::HvHKT1;5* for root stele-specific expression of *HvHKT1;5* in barley
From the T-DNA right border (clockwise) to the T-DNA left border: the T-DNA cassette contains [*attB1* and *attB2* recombination sites flanking the putative stelar promoter *proS147* from *O. sativa*, followed by the *HvHKT1;5* cDNA and bacterial *nopaline synthase* (*nos*) terminator; a bacterial *nopaline synthase* (*nos*) promoter;; nos terminator, T-DNA left border sequence]. The remaining vector is identical to the parent vector *pTOOL36* (Appendix Figure 2). The primer binding sites for genotyping (Table 3.4: gtMK25_R & gtMK25_F) and detecting the expression of *HvHVP1::nosT* by RT-PCR (Table 3.4: HvHKT1;5_SF2 & NOS_R) are also displayed. (Adapted from Krishnan, 2013)

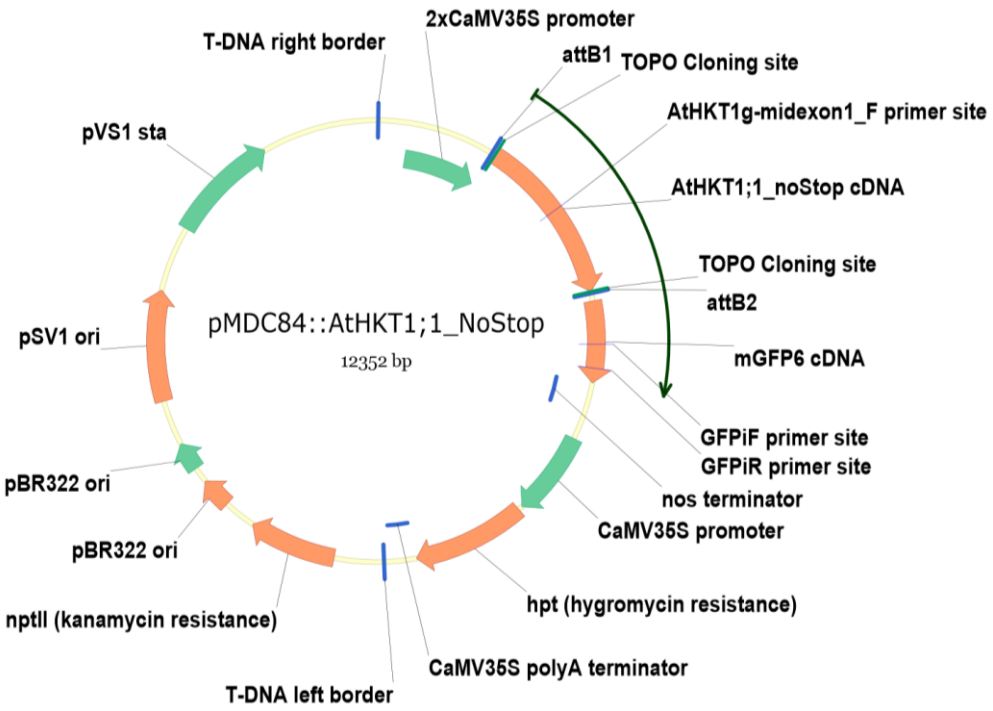

Appendix figure 7: Schematic diagram of *pMDC84::AtHTK1;1* for constitutive over-expression of C-terminally mGFP6 tagged AtHKT1;1 *in planta*

From the T-DNA right border (clockwise) to the T-DNA left border: the T-DNA cassette contains [2 repeats of the Cauliflower Mosaic Virus 35S (*2×CaMV35S*) promoter, unterminated *AtHKT1;1* cDNA added by Gateway® LR recombination upstream and in-frame with *mGFP6* CDS, bacterial nopaline synthase (*nos*) terminator, a *CaMV35S* promoter driving the *Hygromycin phosphotransferase* (*hpt*) gene (Hygromycin B resistance for *in planta* selection) followed by a *CaMV35S* polyA terminator sequence; T-DNA left border sequence]. For details of other vector components, see related parent vector *pMDC43* (Figure 6.1). Primer binding sites for sequencing (AtHKT1g-midexon1_F) and for plant genotyping (Table 6.4: HYG1-F and HYG1-R, GFPiF and GFPiR) have also been included.

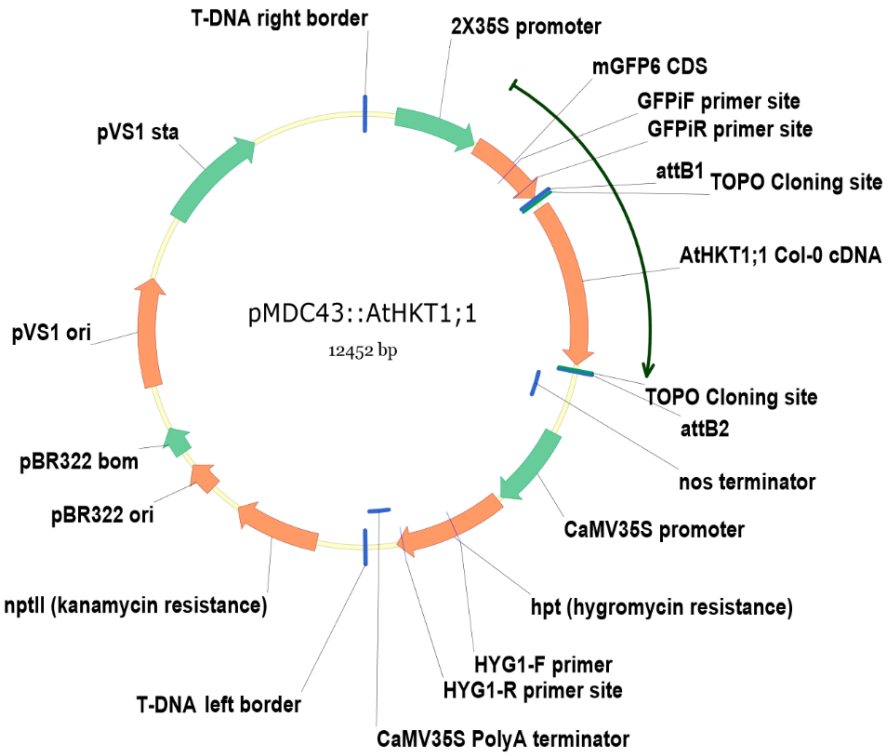

Appendix figure 8: Schematic diagram of *pMDC83::AtSOS1* for constitutive over-expression of N-terminally mGFP6 tagged AtHTK1;1 *in planta*
From the T-DNA right border (clockwise) to the T-DNA left border: the T-DNA cassette contains [2 repeats of the Cauliflower Mosaic Virus 35S (*2×CaMV35S*) promoter, unterminated *mGFP6* CDS upstream of *AtHKT1;1* cDNA added by Gateway® LR recombination, bacterial nopaline synthase (*nos*) terminator, a *CaMV35S* promoter driving the *Hygromycin phosphotransferase* (*hpt*) gene (Hygromycin B resistance for *in planta* selection) followed by a *CaMV35S* polyA terminator sequence; T-DNA left border sequence]. For details of other vector components, see related parent vector *pMDC43* (Figure 6.1). Primer binding sites used for plant genotyping (Table 6.4: HYG1-F and HYG1-R, GFPiF and GFPiR) have also been included.

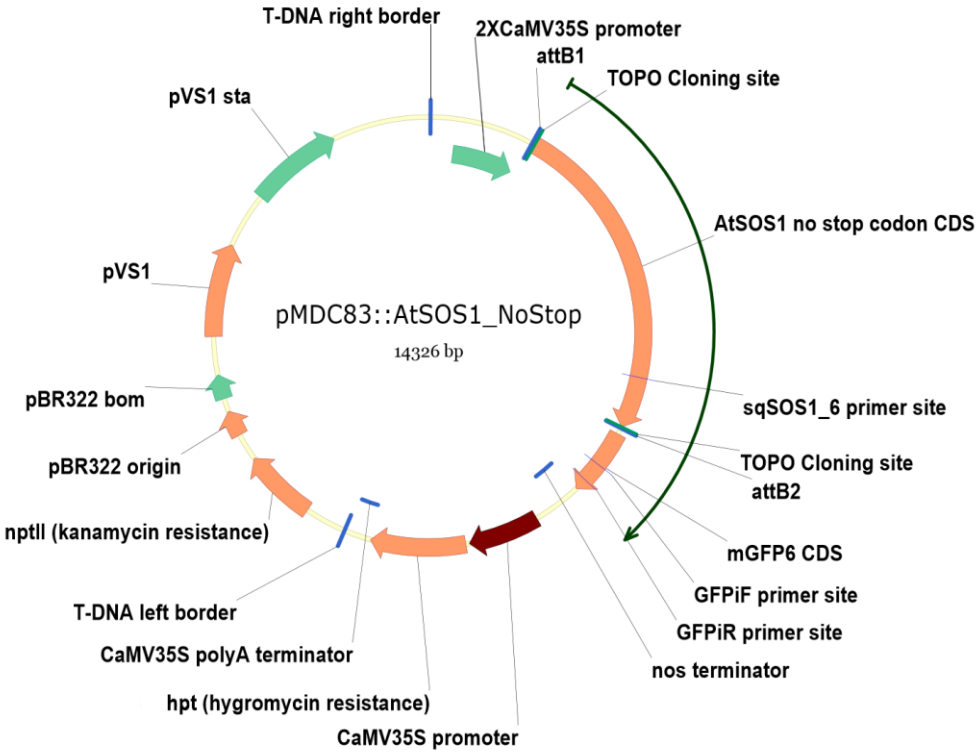

Appendix figure 9: Schematic diagram of *pMDC83::AtSOS1* for constitutive over-expression of C-terminally mGFP6 tagged AtSOS1 *in planta*
From the T-DNA right border (clockwise) to the T-DNA left border: the T-DNA cassette contains [2 repeats of the Cauliflower Mosaic Virus 35S (*2×CaMV35S*) promoter, an unterminated *AtSOS1* cDNA added by Gateway® LR recombination upstream and in-frame of *mGFP6* CDS, bacterial nopaline synthase (*nos*) terminator, a *CaMV35S* promoter driving the *Hygromycin phosphotransferase* (*hpt*) gene (Hygromycin B resistance for *in planta* selection) followed by a *CaMV35S* polyA terminator sequence; T-DNA left border sequence]. For details of other vector components, see related parent vector *pMDC43* (Figure 6.1). Primer binding sites used for plant genotyping (Table 6.4: HYG1-F and HYG1-R, GFPiF and GFPiR) have also been included.

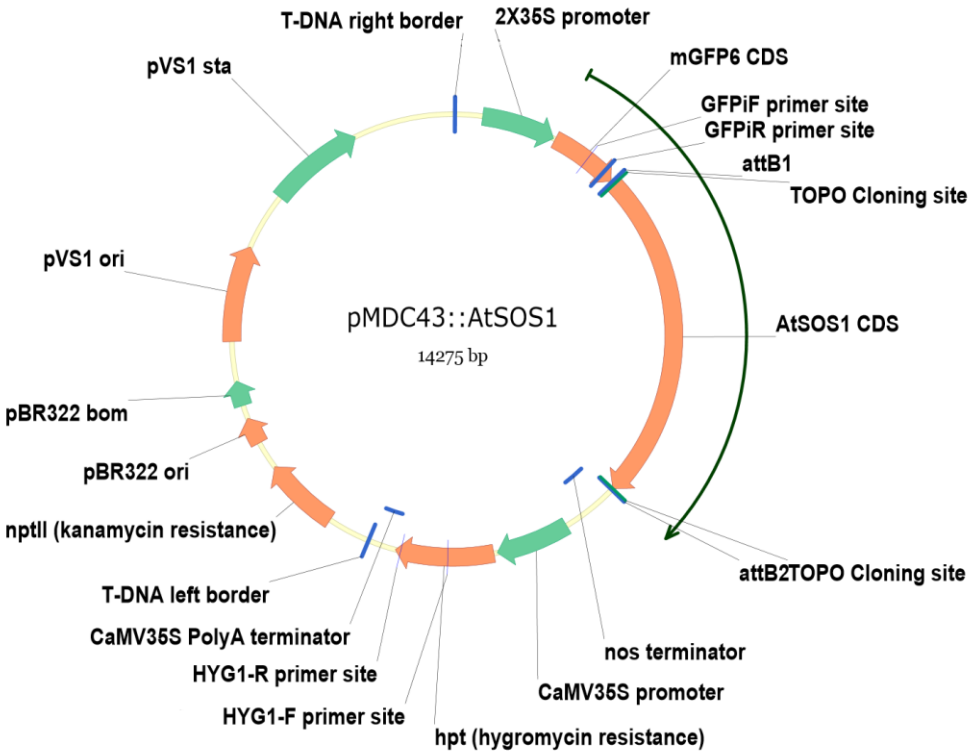

Appendix figure 10: Schematic diagram of *pMDC43::AtSOS1* for constitutive over-expression of N-terminally mGFP6 tagged AtSOS1 *in planta*

From the T-DNA right border (clockwise) to the T-DNA left border: the T-DNA cassette contains [2 repeats of the Cauliflower Mosaic Virus 35S (*2×CaMV35S*) promoter, unterminated *mGFP6* CDS upstream and in-frame with *AtSOS1* cDNA added by Gateway® LR recombination, bacterial nopaline synthase (*nos*) terminator, a *CaMV35S* promoter driving the *Hygromycin phosphotransferase* (*hpt*) gene (Hygromycin B resistance for *in planta* selection) followed by a *CaMV35S* polyA terminator sequence; T-DNA left border sequence]. For details of other vector components, see parent vector *pMDC43* (Figure 6.1). Primer binding sites used for plant genotyping (Table 6.4: HYG1-F and HYG1-R, GFPiF and GFPiR) have also been included.

Appendix III: Supplementary hydroponics data

Supplementary Arabidopsis hydroponics data

Arabidopsis hydroponics experiment #1 - tabulated data

Appendix Table 2: Mini-hydroponics experiment #1 – J1551 + *pGOF-UAS$_{GAL4}$::AtAVP1*

To assessing the effect of salinity tolerance of root cell-type specific expression of *AtAVP1* via the *pGOF-UAS$_{GAL4}$::AtAVP1* transactivation construct in the *GAL4-VP16* enhancer-trap line J1551, T_4 lines, a null segregants line, Wild-type C24, and the parental line, J1551, were screened in supported hydroponics (2.3.8) and exposed to 0, 50 or 100 mM additional NaCl (plus additional $CaCl_2$ to maintain Ca^{2+} activity). Plants were harvested after 7 days growth. Root and shoot fresh and dry weight were measured. Root and youngest fully-expanded leaf Na^+, K^+ and as per section 2.4.4.1. Data tabulated is mean measurements ± S.E.M. Significant differences ($P \leq 0.05$) from the null line determined by one-way ANOVA, Tukey-Cramer HSD test and are highlighted in yellow.

		Shoot FW (g)		Root FW (g)		Root:Shoot Ratio FW	
0 mM NaCl	*J1551 UAS::AtAVP1-2*	0.68±0.12(n=6)	+10.79%	0.1±0.02(n=6)	+29.42%	0.14±0.01(n=6)	+11.28%
	J1551 UAS::AtAVP1-5	0.4±0.06(n=5)	-35.04%	0.05±0.01(n=5)	-36.55%	0.12±0.01(n=5)	-5.32%
	J1551 UAS::AtAVP1-6	0.6±0.05(n=5)	-2.79%	0.07±0.01(n=5)	-13.51%	0.11±0.003(n=5)	-10.73%
	J1551 UAS::AtAVP1-10	0.33±0.05(n=5)	**-46.84%**	0.04±0.01(n=5)	-42.08%	0.14±0.03(n=5)	+10.47%
	J1551 null	0.62±0.08(n=7)	0%	0.08±0.01(n=7)	0%	0.13±0.01(n=7)	0%
	J1551 Untransformed	0.76±0.15(n=10)	+22.7%	0.11±0.02(n=10)	+43.59%	0.15±0.01(n=10)	+16.55%
	C24	1.36±0.09(n=6)	**+120.38%**	0.16±0.01(n=6)	**+107.6%**	0.12±0.01(n=6)	-5.7%
		Shoot FW (g)		**Root FW (g)**		**Root:Shoot Ratio FW**	
50 mM NaCl	*J1551 UAS::AtAVP1-2*	0.7±0.11(n=6)	+12.99%	0.13±0.02(n=6)	+18.08%	0.18±0.02(n=6)	+6.93%
	J1551 UAS::AtAVP1-5	0.74±0.13(n=4)	+19.89%	0.15±0.04(n=4)	+44.25%	0.2±0.02(n=4)	+18.03%
	J1551 UAS::AtAVP1-6	0.88±0.13(n=5)	+42.39%	0.14±0.02(n=5)	+31.89%	0.16±0.01(n=5)	-6.01%
	J1551 UAS::AtAVP1-10	0.89±0.24(n=4)	+43.24%	0.15±0.04(n=4)	+44.69%	0.18±0.01(n=4)	+4.47%
	J1551 null	0.62±0.09(n=3)	0%	0.11±0.02(n=3)	0%	0.17±0.01(n=3)	0%
	J1551 Untransformed	0.81±0.11(n=9)	+31.09%	0.15±0.02(n=9)	+38.51%	0.18±0.01(n=9)	+3.86%
	C24	0.8±0.24(n=3)	+30.01%	0.12±0.04(n=3)	+14.25%	0.15±0.01(n=3)	-13.62%
		Shoot FW (g)		**Root FW (g)**		**Root:Shoot Ratio FW**	
100 mM NaCl	*J1551 UAS::AtAVP1-2*	0.6±0.6(n=6)	+25.04%	0.12±0.12(n=6)	+8.58%	0.2±0.2(n=6)	-18.31%
	J1551 UAS::AtAVP1-5	0.42±0.42(n=5)	-11.88%	0.09±0.09(n=5)	-17.8%	0.22±0.22(n=5)	-10.34%
	J1551 UAS::AtAVP1-6	0.61±0.61(n=5)	+27.57%	0.14±0.14(n=5)	+26.04%	0.23±0.23(n=5)	-8.05%
	J1551 UAS::AtAVP1-10	0.68±0.68(n=6)	+41.75%	0.15±0.15(n=6)	+31.3%	0.22±0.22(n=6)	-10.37%
	J1551 null	0.48±0.48(n=7)	0%	0.11±0.11(n=7)	0%	0.25±0.25(n=7)	0%
	J1551 Untransformed	0.61±0.61(n=6)	+26.08%	0.13±0.13(n=6)	+18.29%	0.23±0.23(n=6)	-6.6%
	C24	0.73±0.73(n=6)	**+51.25%**	0.16±0.16(n=6)	**+40.96%**	0.22±0.22(n=6)	-10.52%
		Root [Na^+] (µmoles.g^{-1} DW)		**Root [K^+] (µmoles.g^{-1} DW)**		**Root [Na^+]:[K^+] (DW)**	
0 mM NaCl	*J1551 UAS::AtAVP1-2*	24.26±5.26(n=5)	+14.37%	1078.41±187.79(n=5)	-5.98%	0.02±0.005(n=5)	+21.62%
	J1551 UAS::AtAVP1-5	17.06±2.21(n=5)	-19.54%	1270.51±194.49(n=5)	+10.77%	0.02±0.01(n=5)	-12.06%
	J1551 UAS::AtAVP1-6	20.72±5.2(n=5)	-2.32%	1169.66±97.8(n=5)	+1.97%	0.02±0.003(n=5)	-12.34%
	J1551 UAS::AtAVP1-10	19.42±3.04(n=5)	-8.42%	1473.03±173.15(n=5)	+28.42%	0.01±0.003(n=5)	-28.96%
	J1551 null	21.21±2.83(n=7)	0%	1147.01±92.35(n=7)	0%	0.02±0.004(n=7)	0%
	J1551 Untransformed	19.68±2.55(n=9)	-7.21%	1366.36±120.62(n=9)	+19.12%	0.02±0.003(n=9)	-20.44%
	C24	29.05±4.99(n=6)	+36.98%	1696.39±49.8(n=6)	**+47.9%**	0.02±0.003(n=6)	-12.89%
		Root [Na^+] (µmoles.g^{-1} DW)		**Root [K^+] (µmoles.g^{-1} DW)**		**Root [Na^+]:[K^+] (DW)**	
50 mM NaCl	*J1551 UAS::AtAVP1-2*	212.09±25.74(n=6)	+8.33%	1438.96±44.55(n=6)	+6.17%	0.15±0.01(n=6)	+1.37%
	J1551 UAS::AtAVP1-5	205.51±32.37(n=4)	+4.97%	1360.69±73.07(n=4)	+0.39%	0.15±0.02(n=4)	+4.03%
	J1551 UAS::AtAVP1-6	203.75±41.32(n=5)	+4.07%	1344.34±54.24(n=5)	-0.81%	0.15±0.03(n=5)	+3.59%
	J1551 UAS::AtAVP1-10	172.62±9.41(n=4)	-11.83%	1595.75±169.3(n=4)	+17.74%	0.11±0.01(n=4)	-22.47%
	J1551 null	195.78±10.55(n=3)	0%	1355.34±68.53(n=3)	0%	0.14±0.005(n=3)	0%
	J1551 Untransformed	213.65±20.42(n=9)	+9.13%	1293.24±134.89(n=9)	-4.58%	0.19±0.05(n=9)	+32.75%
	C24	196.87±50.25(n=3)	+0.56%	1030.54±116.43(n=3)	**-23.96%**	0.2±0.07(n=3)	+38.43%
		Root [Na^+] (µmoles.g^{-1} DW)		**Root [K^+] (µmoles.g^{-1} DW)**		**Root [Na^+]:[K^+] (DW)**	
100 mM NaCl	*J1551 UAS::AtAVP1-2*	418.09±418.09(n=6)	+3.79%	1627.37±1627.37(n=6)	-6.44%	0.26±0.26(n=6)	+13.51%
	J1551 UAS::AtAVP1-5	533.59±533.59(n=5)	+32.46%	1765.76±1765.76(n=5)	+1.51%	0.3±0.3(n=5)	+28.89%
	J1551 UAS::AtAVP1-6	336.39±336.39(n=5)	-16.49%	1548.24±1548.24(n=5)	-10.99%	0.22±0.22(n=5)	-5.86%
	J1551 UAS::AtAVP1-10	419.84±419.84(n=6)	+4.22%	1571.58±1571.58(n=6)	-9.65%	0.27±0.27(n=6)	+17.58%
	J1551 null	402.83±402.83(n=7)	0%	1739.47±1739.47(n=7)	0%	0.23±0.23(n=7)	0%
	J1551 Untransformed	442.9±442.9(n=6)	+9.95%	1700.04±1700.04(n=6)	-2.27%	0.26±0.26(n=6)	+12.25%
	C24	358.18±358.18(n=6)	-11.08%	1537.2±1537.2(n=6)	-11.63%	0.25±0.25(n=6)	+8.37%

Continued onto next page

		Leaf [Na^+] (µmoles.g^{-1} DW)		Leaf [K^+] (µmoles.g^{-1} DW)		Leaf [Na^+]:[K^+] DW	
0 mM NaCl	*J1551 UAS::AtAVP1-2*	109.14±11.21(n=6)	+2.98%	1478.11±30.96(n=6)	-2.8%	0.07±0.01(n=6)	+6.9%
	J1551 UAS::AtAVP1-5	104.28±12.68(n=4)	-1.6%	1497.36±103.49(n=4)	-1.53%	0.07±0.01(n=4)	+0.87%
	J1551 UAS::AtAVP1-6	124.93±26.2(n=4)	+17.89%	1641.38±105.94(n=4)	+7.94%	0.07±0.01(n=4)	+6.48%
	J1551 UAS::AtAVP1-10	106.06±8.57(n=5)	+0.08%	1650.89±40.43(n=5)	+8.57%	0.06±0.005(n=5)	-7.82%
	J1551 null	105.98±6.94(n=7)	0%	1520.62±45.77(n=7)	0%	0.07±0.004(n=7)	0%
	J1551 Untransformed	104.84±7.55(n=10)	-1.08%	1468.37±44.69(n=10)	-3.44%	0.07±0.01(n=10)	+3.95%
	C24	96.22±10.82(n=5)	-9.21%	1377.23±34.62(n=5)	**-9.43%**	0.07±0.01(n=5)	+1.59%
		Leaf [Na^+] (µmoles.g^{-1} DW)		**Leaf [K^+] (µmoles.g^{-1} DW)**		**Leaf [Na^+]:[K^+] DW**	
50 mM NaCl	*J1551 UAS::AtAVP1-2*	1164.37±95.03(n=5)	+11.11%	681.4±61.83(n=5)	-0.78%	1.77±0.25(n=5)	+15.25%
	J1551 UAS::AtAVP1-5	1176.37±75.98(n=4)	+12.26%	712.3±51.78(n=4)	+3.72%	1.69±0.2(n=4)	+9.62%
	J1551 UAS::AtAVP1-6	1109.64±109.5(n=5)	+5.89%	742.47±54.22(n=5)	+8.11%	1.55±0.24(n=5)	+0.78%
	J1551 UAS::AtAVP1-10	1189.12±71.63(n=4)	+13.48%	733.81±14.08(n=4)	+6.85%	1.62±0.11(n=4)	+5.52%
	J1551 null	1047.9±100.74(n=3)	0%	686.77±74.28(n=3)	0%	1.54±0.12(n=3)	0%
	J1551 Untransformed	1093.42±57.09(n=9)	+4.34%	766.94±32.35(n=9)	+11.67%	1.45±0.1(n=9)	-5.87%
	C24	1240.16±59.95(n=3)	+18.35%	770.91±50.08(n=3)	+12.25%	1.63±0.18(n=3)	+6.05%
		Leaf [Na^+] (µmoles.g^{-1} DW)		**Leaf [K^+] (µmoles.g^{-1} DW)**		**Leaf [Na^+]:[K^+] DW**	
100 mM NaCl	*J1551 UAS::AtAVP1-2*	1668.41±1668.41(n=6)	+11.26%	678.39±678.39(n=6)	+10.83%	2.6±2.6(n=6)	-0.25%
	J1551 UAS::AtAVP1-5	1605.32±1605.32(n=4)	+7.05%	574.94±574.94(n=4)	-6.08%	2.78±2.78(n=4)	+7.03%
	J1551 UAS::AtAVP1-6	1658.94±1658.94(n=5)	+10.63%	590.11±590.11(n=5)	-3.6%	2.87±2.87(n=5)	+10.42%
	J1551 UAS::AtAVP1-10	1577.35±1577.35(n=6)	+5.19%	630.48±630.48(n=6)	+3%	2.53±2.53(n=6)	-2.88%
	J1551 null	1499.58±1499.58(n=6)	0%	612.13±612.13(n=6)	0%	2.6±2.6(n=6)	0%
	J1551 Untransformed	1647.16±1647.16(n=6)	+9.84%	829.28±829.28(n=6)	+35.47%	2.16±2.16(n=6)	-16.93%
	C24	1818.19±1818.19(n=6)	+21.25%	664.57±664.57(n=6)	+8.57%	2.95±2.95(n=6)	+13.25%
		Shoot DW (g)		**Root DW (g)**			
0 mM NaCl	*J1551 UAS::AtAVP1-2*	0.04±0.01(n=6)	+5.71%	0.01±0.001(n=6)	+8.54%		
	J1551 UAS::AtAVP1-5	0.02±0.005(n=5)	-34.39%	0±0.001(n=5)	-32.23%		
	J1551 UAS::AtAVP1-6	0.04±0.004(n=5)	-6.24%	0.01±0(n=5)	+13.8%		
	J1551 UAS::AtAVP1-10	0.02±0.002(n=5)	**-48.55%**	0±0(n=5)	**-63.32%**		
	J1551 null	0.04±0.01(n=7)	0%	0±0.001(n=7)	0%		
	J1551 Untransformed	0.05±0.01(n=10)	+19%	0.01±0.001(n=10)	+24.3%		
	C24	0.08±0.01(n=6)	**+99.07%**	0.01±0.001(n=6)	**+97.7%**		
		Shoot DW (g)		**Root DW (g)**			
50 mM NaCl	*J1551 UAS::AtAVP1-2*	0.05±0.01(n=6)	+21.86%	0.01±0.002(n=6)	+20.2%		
	J1551 UAS::AtAVP1-5	0.05±0.01(n=4)	+31.89%	0.01±0.001(n=4)	+37.2%		
	J1551 UAS::AtAVP1-6	0.06±0.01(n=5)	**+63.99%**	0.01±0.001(n=5)	+30.81%		
	J1551 UAS::AtAVP1-10	0.06±0.02(n=4)	+52.19%	0.01±0.002(n=4)	+43.27%		
	J1551 null	0.04±0.005(n=3)	0%	0.01±0.001(n=3)	0%		
	J1551 Untransformed	0.06±0.01(n=9)	+57.43%	0.01±0.001(n=9)	+22.13%		
	C24	0.05±0.02(n=3)	+34.15%	0.01±0.002(n=3)	+4.33%		
		Shoot DW (g)		**Root DW (g)**			
100 mM NaCl	*J1551 UAS::AtAVP1-2*	0.05±0.05(n=6)	+28.78%	0.01±0.01(n=6)	+21.62%		
	J1551 UAS::AtAVP1-5	0.03±0.03(n=5)	-10.11%	0.01±0.01(n=5)	-15.38%		
	J1551 UAS::AtAVP1-6	0.05±0.05(n=5)	+28.66%	0.01±0.01(n=5)	+8.59%		
	J1551 UAS::AtAVP1-10	0.05±0.05(n=6)	+43.29%	0.01±0.01(n=6)	+37.84%		
	J1551 null	0.04±0.04(n=7)	0%	0.01±0.01(n=7)	0%		
	J1551 Untransformed	0.05±0.05(n=6)	+35.4%	0.01±0.01(n=6)	+34.61%		
	C24	0.06±0.06(n=6)	**+54.25%**	0.01±0.01(n=6)	+35.3%		

End of table

Appendix Table 3: Mini-hydroponics experiment #1 – J1422 + *pGOF-UAS$_{GAL4}$::AtAVP1*

To assessing the effect of salinity tolerance of root cell-type specific expression of *AtAVP1* via the *pGOF-UAS$_{GAL4}$::AtAVP1* transactivation construct in the *GAL4-VP16* enhancer-trap line J1422, T_4 lines, a null segregants line, wild-type C24, and the parental line, J1422, were screened in supported hydroponics (2.3.8) and exposed to 0, 50 or 100 mM additional NaCl (plus additional $CaCl_2$ to maintain Ca^{2+} activity). Plants were harvested after 7 days growth. Root and shoot fresh and dry weight were measured. Root and youngest fully-expanded leaf Na^+, K^+ and as per section 2.4.4.1. Data tabulated is mean measurements ± S.E.M. Significant differences ($P \leq 0.05$) from the null line determined by one-way ANOVA, Tukey-Cramer HSD test and are highlighted in yellow.

		Shoot FW (g)		Root FW (g)		Root:Shoot Ratio FW	
0 mM NaCl	*J1422 UAS::AtAVP1-6*	1.34±0.22(n=8)	-21.8%	0.18±0.03(n=8)	-16.12%	0.14±0.01(n=8)	+5.74%
	J1422 UAS::AtAVP1-18	1.24±0.17(n=6)	-27.85%	0.17±0.02(n=6)	-23.06%	0.14±0.01(n=6)	+6.02%
	J1422 UAS::AtAVP1-5	1.56±0.24(n=6)	-9.02%	0.2±0.03(n=6)	-8.6%	0.14±0.02(n=6)	+5.18%
	J1422 UAS::AtAVP1-16	1.42±0.2(n=7)	-16.95%	0.19±0.03(n=7)	-10.44%	0.13±0.01(n=7)	+4.01%
	J1422 null	1.72±0.32(n=7)	0%	0.21±0.03(n=7)	0%	0.13±0.01(n=7)	0%
	J1422 Untransformed	1.17±0.15(n=6)	-31.68%	0.17±0.03(n=6)	-20.7%	0.14±0.01(n=6)	+10.26%
	C24	1.85±0.29(n=6)	+7.91%	0.21±0.03(n=6)	-4.34%	0.11±0.01(n=6)	-12.03%
		Shoot FW (g)		Root FW (g)		Root:Shoot Ratio FW	
50 mM NaCl	*J1422 UAS::AtAVP1-6*	1.92±0.27(n=6)	+13.62%	0.34±0.06(n=6)	+10.44%	0.17±0.01(n=6)	-5.47%
	J1422 UAS::AtAVP1-18	1.44±0.14(n=7)	-14.78%	0.24±0.03(n=7)	-22.23%	0.16±0.01(n=7)	-8.52%
	J1422 UAS::AtAVP1-5	1.66±0.23(n=7)	-1.7%	0.28±0.05(n=7)	-7.9%	0.16±0.01(n=7)	-8.25%
	J1422 UAS::AtAVP1-16	1.68±0.26(n=7)	-0.89%	0.3±0.05(n=7)	-2.25%	0.18±0.01(n=7)	+0.31%
	J1422 null	1.69±0.22(n=7)	0%	0.3±0.04(n=7)	0%	0.18±0.01(n=7)	0%
	J1422 Untransformed	1.93±0.15(n=6)	+14.06%	0.35±0.04(n=6)	+14.25%	0.18±0.01(n=6)	+1.08%
	C24	1.74±0.3(n=7)	+2.77%	0.3±0.05(n=7)	-1.72%	0.17±0.01(n=7)	-4.16%
		Shoot FW (g)		**Root FW (g)**		**Root:Shoot Ratio FW**	
100 mM NaCl	*J1422 UAS::AtAVP1-6*	1.27±1.27(n=6)	-2.5%	0.28±0.28(n=6)	-3.58%	0.21±0.21(n=6)	-2.44%
	J1422 UAS::AtAVP1-18	1.19±1.19(n=7)	-8.72%	0.26±0.26(n=7)	-11.19%	0.22±0.22(n=7)	+1.48%
	J1422 UAS::AtAVP1-5	1.46±1.46(n=6)	+12.19%	0.32±0.32(n=6)	+11.04%	0.22±0.22(n=6)	+2.4%
	J1422 UAS::AtAVP1-16	1.02±1.02(n=7)	-21.62%	0.24±0.24(n=7)	-17.99%	0.23±0.23(n=7)	+7.55%
	J1422 null	1.3±1.3(n=7)	0%	0.29±0.29(n=7)	0%	0.22±0.22(n=7)	0%
	J1422 Untransformed	1.36±1.36(n=6)	+4.72%	0.3±0.3(n=6)	+3.82%	0.21±0.21(n=6)	-1.99%
	C24	1.44±1.44(n=5)	+10.61%	0.33±0.33(n=5)	+14.75%	0.23±0.23(n=5)	+4.24%
		Root [Na^+] (µmoles.g^{-1} DW)		**Root [K^+] (µmoles.g^{-1} DW)**		**Root [Na^+]:[K^+] (DW)**	
0 mM NaCl	*J1422 UAS::AtAVP1-6*	26.47±4.26(n=8)	**+80.97%**	1230.3±177.2(n=8)	+21.59%	0.02±0.01(n=8)	+67.88%
	J1422 UAS::AtAVP1-18	20.79±3.41(n=6)	+42.18%	1372.1±103.14(n=6)	+35.6%	0.02±0.002(n=6)	+5.88%
	J1422 UAS::AtAVP1-5	20.8±3.85(n=6)	+42.19%	1373.23±109.97(n=6)	+35.71%	0.02±0.003(n=6)	+4.14%
	J1422 UAS::AtAVP1-16	27.28±4.01(n=7)	**+86.55%**	1389.38±54.7(n=7)	**+37.31%**	0.02±0.003(n=7)	+37.99%
	J1422 null	14.63±2.44(n=7)	0%	1011.87±144.91(n=7)	0%	0.01±0.001(n=7)	0%
	J1422 Untransformed	25.92±3.78(n=6)	**+77.24%**	1322.62±56.88(n=6)	+30.71%	0.02±0.002(n=6)	+32.97%
	C24	35.5±7.25(n=6)	**+142.74%**	1362.97±69.67(n=6)	+34.7%	0.03±0.01(n=6)	+82.06%
		Root [Na^+] (µmoles.g^{-1} DW)		**Root [K^+] (µmoles.g^{-1} DW)**		**Root [Na^+]:[K^+] (DW)**	
50 mM NaCl	*J1422 UAS::AtAVP1-6*	186.69±20.32(n=4)	-11.65%	1221.21±116.46(n=4)	-20.02%	0.15±0.005(n=4)	+5.74%
	J1422 UAS::AtAVP1-18	201.21±9.3(n=7)	-4.78%	1386.33±168.57(n=7)	-9.2%	0.18±0.05(n=7)	+27.3%
	J1422 UAS::AtAVP1-5	195.96±9.84(n=6)	-7.26%	1651.75±43.1(n=6)	+8.18%	0.12±0.005(n=6)	-17.73%
	J1422 UAS::AtAVP1-16	194.21±25.75(n=7)	-8.09%	1424.68±149.41(n=7)	-6.69%	0.14±0.01(n=7)	-4.69%
	J1422 null	211.3±29.38(n=7)	0%	1526.81±95.03(n=7)	0%	0.14±0.02(n=7)	0%
	J1422 Untransformed	270.08±60.13(n=6)	+27.82%	1567.25±65.67(n=6)	+2.65%	0.17±0.03(n=6)	+17.24%
	C24	238.46±32.85(n=7)	+12.85%	1556.95±76.81(n=7)	+1.97%	0.16±0.03(n=7)	+8.93%
		Root [Na^+] (µmoles.g^{-1} DW)		**Root [K^+] (µmoles.g^{-1} DW)**		**Root [Na^+]:[K^+] (DW)**	
100 mM NaCl	*J1422 UAS::AtAVP1-6*	422.55±422.55(n=6)	-5.25%	1235.76±1235.76(n=6)	-6.59%	0.35±0.35(n=6)	-9.49%
	J1422 UAS::AtAVP1-18	368.05±368.05(n=6)	-17.47%	1222.74±1222.74(n=5)	-7.58%	0.31±0.31(n=5)	-19.76%
	J1422 UAS::AtAVP1-5	449.19±449.19(n=6)	+0.73%	1250.64±1250.64(n=6)	-5.47%	0.38±0.38(n=6)	-1.84%
	J1422 UAS::AtAVP1-16	521.05±521.05(n=7)	+16.84%	1455.26±1455.26(n=7)	+10%	0.39±0.39(n=7)	+1.26%
	J1422 null	445.95±445.95(n=7)	0%	1322.95±1322.95(n=7)	0%	0.39±0.39(n=7)	0%
	J1422 Untransformed	401.78±401.78(n=6)	-9.9%	1243.19±1243.19(n=6)	-6.03%	0.36±0.36(n=6)	-7.33%
	C24	473.88±473.88(n=5)	+6.26%	1484.12±1484.12(n=5)	+12.18%	0.37±0.37(n=5)	-3.29%

Table continued onto next page

		Leaf [Na^+] (µmoles.g^{-1} DW)		Leaf [K^+] (µmoles.g^{-1} DW)		Leaf [Na^+]:[K^+] DW	
0 mM NaCl	*J1422 UAS::AtAVP1-6*	105.82±6.17(n=8)	**+46.77%**	1454.88±68.06(n=8)	+12.23%	0.07±0.005(n=8)	**+32.21%**
	J1422 UAS::AtAVP1-18	84.05±8.74(n=6)	+16.58%	1519.79±52.14(n=6)	+17.23%	0.05±0.005(n=6)	-1.21%
	J1422 UAS::AtAVP1-5	109.05±17.36(n=6)	+51.26%	1579.8±84.87(n=6)	+21.86%	0.07±0.01(n=6)	+26.91%
	J1422 UAS::AtAVP1-16	96.46±9.48(n=7)	+33.8%	1312.76±60.3(n=7)	+1.26%	0.07±0.01(n=7)	+31.99%
	J1422 null	72.1±10.06(n=7)	0%	1296.39±142.7(n=7)	0%	0.06±0.01(n=7)	0%
	J1422 Untransformed	99.35±13.95(n=6)	+37.81%	1448.28±76.19(n=6)	+11.72%	0.07±0.01(n=6)	+25.17%
	C24	114.09±12.36(n=6)	**+58.24%**	1430.24±54.34(n=6)	+10.33%	0.08±0.01(n=6)	**+45.24%**
		Leaf [Na^+] (µmoles.g^{-1} DW)		Leaf [K^+] (µmoles.g^{-1} DW)		Leaf [Na^+]:[K^+] DW	
50 mM NaCl	*J1422 UAS::AtAVP1-6*	1354.43±121.03(n=6)	-6.24%	822.46±83.58(n=6)	+5.59%	1.78±0.27(n=6)	-5.28%
	J1422 UAS::AtAVP1-18	1622.95±250.63(n=5)	+12.35%	879.09±90.19(n=5)	+12.86%	1.83±0.13(n=5)	-2.67%
	J1422 UAS::AtAVP1-5	1621.4±182.24(n=6)	+12.24%	690.09±85.27(n=6)	-11.41%	2.66±0.56(n=6)	+41.61%
	J1422 UAS::AtAVP1-16	1695.15±132.7(n=6)	+17.35%	670.8±38.64(n=6)	-13.88%	2.58±0.25(n=6)	+37.12%
	J1422 null	1444.54±65.78(n=4)	0%	778.95±45.54(n=4)	0%	1.88±0.16(n=4)	0%
	J1422 Untransformed	1201.28±190.69(n=5)	-16.84%	819.12±50.04(n=5)	+5.16%	1.52±0.28(n=5)	-19.21%
	C24	1268.9±286.78(n=5)	-12.16%	566.1±129.24(n=5)	-27.33%	2.3±0.24(n=5)	+22.26%
		Leaf [Na^+] (µmoles.g^{-1} DW)		**Leaf [K^+] (µmoles.g^{-1} DW)**		**Leaf [Na^+]:[K^+] DW**	
100 mM NaCl	*J1422 UAS::AtAVP1-6*	2123.53±2123.53(n=6)	+7.62%	568.2±568.2(n=6)	+0.03%	3.87±3.87(n=6)	+8.53%
	J1422 UAS::AtAVP1-18	2002.65±2002.65(n=7)	+1.5%	600.06±600.06(n=7)	+5.64%	3.47±3.47(n=7)	-2.66%
	J1422 UAS::AtAVP1-5	2244.55±2244.55(n=6)	+13.76%	486.95±486.95(n=6)	-14.27%	4.68±4.68(n=6)	**+31.49%**
	J1422 UAS::AtAVP1-16	1887.72±1887.72(n=7)	-4.33%	565.95±565.95(n=7)	-0.36%	3.64±3.64(n=7)	+2.28%
	J1422 null	1973.08±1973.08(n=7)	0%	568.02±568.02(n=7)	0%	3.56±3.56(n=7)	0%
	J1422 Untransformed	1939.91±1939.91(n=6)	-1.68%	658.27±658.27(n=6)	+15.89%	3.53±3.53(n=6)	-0.82%
	C24	2005.55±2005.55(n=5)	+1.65%	660.35±660.35(n=5)	+16.25%	3.86±3.86(n=5)	+8.43%
		Shoot DW (g)		**Root DW (g)**			
0 mM NaCl	*J1422 UAS::AtAVP1-6*	0.09±0.02(n=8)	-20.51%	0.01±0.002(n=8)	-18.51%		
	J1422 UAS::AtAVP1-18	0.08±0.01(n=6)	-34.17%	0.01±0.002(n=6)	-26.68%		
	J1422 UAS::AtAVP1-5	0.1±0.02(n=6)	-12.96%	0.01±0.002(n=6)	-2.7%		
	J1422 UAS::AtAVP1-16	0.09±0.01(n=7)	-21.9%	0.01±0.002(n=7)	-11.93%		
	J1422 null	0.12±0.02(n=7)	0%	0.01±0.003(n=7)	0%		
	J1422 Untransformed	0.07±0.01(n=6)	-36.65%	0.01±0.002(n=6)	-23.42%		
	C24	0.11±0.02(n=6)	-3.42%	0.01±0.001(n=6)	-10.84%		
		Shoot DW (g)		**Root DW (g)**			
50 mM NaCl	*J1422 UAS::AtAVP1-6*	0.13±0.02(n=6)	+2.99%	0.02±0.003(n=6)	-4%		
	J1422 UAS::AtAVP1-18	0.11±0.01(n=7)	-15.61%	0.02±0.002(n=7)	-23.41%		
	J1422 UAS::AtAVP1-5	0.14±0.03(n=7)	+4.34%	0.02±0.003(n=7)	-10.65%		
	J1422 UAS::AtAVP1-16	0.12±0.02(n=7)	-10.22%	0.02±0.003(n=7)	-7.21%		
	J1422 null	0.13±0.02(n=7)	0%	0.02±0.004(n=7)	0%		
	J1422 Untransformed	0.13±0.01(n=6)	+1.93%	0.02±0.003(n=6)	-7.75%		
	C24	0.12±0.02(n=7)	-9.78%	0.02±0.003(n=7)	-12.51%		
		Shoot DW (g)		**Root DW (g)**			
100 mM NaCl	*J1422 UAS::AtAVP1-6*	0.1±0.1(n=6)	+5.04%	0.02±0.02(n=6)	-2.12%		
	J1422 UAS::AtAVP1-18	0.09±0.09(n=7)	-11.85%	0.02±0.02(n=7)	-17.78%		
	J1422 UAS::AtAVP1-5	0.11±0.11(n=6)	+13.24%	0.02±0.02(n=6)	+10.94%		
	J1422 UAS::AtAVP1-16	0.08±0.08(n=7)	-16.11%	0.01±0.01(n=7)	-27.5%		
	J1422 null	0.1±0.1(n=7)	0%	0.02±0.02(n=7)	0%		
	J1422 Untransformed	0.11±0.11(n=6)	+7.65%	0.02±0.02(n=6)	-1.65%		
	C24	0.11±0.11(n=5)	+8.71%	0.02±0.02(n=5)	+9.92%		

End of table

Arabidopsis hydroponics experiment #2 - tabulated data

Appendix Table 4: Mini-hydroponics experiment #2 – J1551 + *pGOF-UAS$_{GAL4}$::AtAVP1*

To assessing the effect of salinity tolerance of root cell-type specific expression of *AtAVP1* via the *pGOF-UAS$_{GAL4}$::AtAVP1* transactivation construct in the *GAL4-VP16* enhancer-trap line J1551, T_4 lines, a null segregants line, and the parental line, J1551, were screened in supported hydroponics (2.3.8) and exposed to 0, 50 or 100 mM additional NaCl (plus additional $CaCl_2$ to maintain Ca^{2+} activity). Plants were harvested after 7 days growth. Root and shoot fresh and dry weight were measured. Root and youngest fully-expanded leaf Na^+, K^+ and as per section 2.4.4.1. Data tabulated is mean measurements ± S.E.M. Significant differences ($P \leq 0.05$) from the null line determined by one-way ANOVA, Tukey-Cramer HSD test and are highlighted in yellow.

		Shoot FW (g)		Root FW (g)		Root:Shoot Ratio FW	
0 mM NaCl	*J1551 UAS::AtAVP1-2*	1.46±0.26(n=4)	**-36.32%**	0.26±0.04(n=4)	-27.28%	0.18±0.03(n=4)	+18.88%
	J1551 UAS::AtAVP1-5	2±0.18(n=7)	-12.56%	0.3±0.04(n=7)	-15.57%	0.14±0.01(n=7)	-5.7%
	J1551 UAS::AtAVP1-6	1.59±0.23(n=7)	**-30.55%**	0.26±0.08(n=7)	-24.49%	0.15±0.02(n=7)	+0.25%
	J1551 UAS::AtAVP1-10	1.67±0.2(n=9)	**-27.2%**	0.26±0.04(n=9)	-24.7%	0.16±0.01(n=9)	+2.07%
	J1551 null	2.29±0.1(n=10)	0%	0.35±0.03(n=10)	0%	0.15±0.01(n=10)	0%
	J1551 Untransformed	2.31±0.31(n=6)	+0.84%	0.34±0.07(n=6)	-2.89%	0.14±0.01(n=6)	-6.52%
		Shoot FW (g)		**Root FW (g)**		**Root:Shoot Ratio FW**	
50 mM NaCl	*J1551 UAS::AtAVP1-2*	1.7±0.28(n=4)	-15.81%	0.3±0.08(n=4)	-22.75%	0.19±0.05(n=4)	-1.14%
	J1551 UAS::AtAVP1-5	1.93±0.24(n=5)	-4.57%	0.36±0.08(n=5)	-9.63%	0.18±0.02(n=5)	-8.61%
	J1551 UAS::AtAVP1-6	2.08±0.28(n=6)	+2.95%	0.35±0.09(n=6)	-10.22%	0.17±0.03(n=6)	-14.03%
	J1551 UAS::AtAVP1-10	1.7±0.3(n=7)	-15.72%	0.36±0.07(n=7)	-9.8%	0.2±0.01(n=7)	+5.49%
	J1551 null	2.02±0.13(n=10)	0%	0.39±0.04(n=10)	0%	0.19±0.01(n=10)	0%
	J1551 Untransformed	1.32±0.09(n=6)	**-34.53%**	0.28±0.05(n=6)	-28.26%	0.22±0.04(n=6)	+12.26%
		Shoot FW (g)		**Root FW (g)**		**Root:Shoot Ratio FW**	
100 mM NaCl	*J1551 UAS::AtAVP1-2*	1.72±1.72(n=5)	-6.7%	0.53±0.53(n=5)	-6.22%	0.32±0.32(n=5)	+4.56%
	J1551 UAS::AtAVP1-5	1.49±1.49(n=6)	-18.94%	0.5±0.5(n=6)	-10.39%	0.36±0.36(n=6)	+20.09%
	J1551 UAS::AtAVP1-6	1.57±1.57(n=5)	-14.71%	0.46±0.46(n=5)	-18.52%	0.3±0.3(n=5)	-2.45%
	J1551 UAS::AtAVP1-10	1.65±1.65(n=7)	-10.11%	0.52±0.52(n=7)	-7.16%	0.32±0.32(n=7)	+5.64%
	J1551 null	1.84±1.84(n=10)	0%	0.56±0.56(n=10)	0%	0.3±0.3(n=10)	0%
	J1551 Untransformed	1.71±1.71(n=3)	-7.07%	0.44±0.44(n=3)	-21.91%	0.26±0.26(n=3)	-15.21%
		Root [Na^+] (µmoles.g^{-1} DW)		**Root [K^+] (µmoles.g^{-1} DW)**		**Root [Na^+]:[K^+] (DW)**	
0 mM NaCl	*J1551 UAS::AtAVP1-2*	20.31±0.79(n=4)	-25.19%	2082.2±67.09(n=4)	+17.93%	0.01±0(n=4)	-37.47%
	J1551 UAS::AtAVP1-5	38.69±10.67(n=7)	+42.56%	2034.64±33.45(n=7)	+15.24%	0.02±0.01(n=7)	+23.73%
	J1551 UAS::AtAVP1-6	24.5±2.45(n=6)	-9.74%	2185.25±106.91(n=6)	**+23.77%**	0.01±0.001(n=6)	-27.02%
	J1551 UAS::AtAVP1-10	24.98±1.86(n=8)	-7.98%	1988.2±94.49(n=8)	+12.61%	0.01±0.001(n=8)	-18.48%
	J1551 null	27.14±3.23(n=10)	0%	1765.58±111.01(n=10)	0%	0.02±0.002(n=10)	0%
	J1551 Untransformed	19.92±2.43(n=6)	-26.61%	1854.1±144.1(n=6)	+5.01%	0.01±0.001(n=6)	-31.67%
		Root [Na^+] (µmoles.g^{-1} DW)		**Root [K^+] (µmoles.g^{-1} DW)**		**Root [Na^+]:[K^+] (DW)**	
50 mM NaCl	*J1551 UAS::AtAVP1-2*	448.15±61.21(n=4)	-12.36%	1965.4±171.19(n=4)	+0.03%	0.23±0.02(n=4)	-13.37%
	J1551 UAS::AtAVP1-5	478.08±56.87(n=5)	-6.51%	2008.15±111.11(n=5)	+2.2%	0.24±0.02(n=5)	-9.95%
	J1551 UAS::AtAVP1-6	454.06±67.67(n=6)	-11.21%	1997.44±69.15(n=6)	+1.66%	0.23±0.04(n=6)	-12.85%
	J1551 UAS::AtAVP1-10	452.2±42.12(n=7)	-11.57%	2031.84±94.21(n=7)	+3.41%	0.22±0.02(n=7)	-14.48%
	J1551 null	511.38±33.27(n=10)	0%	1964.85±117.67(n=10)	0%	0.26±0.01(n=10)	0%
	J1551 Untransformed	494.62±39.96(n=6)	-3.28%	2151.95±107.21(n=6)	+9.52%	0.23±0.02(n=6)	-11.19%
		Root [Na^+] (µmoles.g^{-1} DW)		**Root [K^+] (µmoles.g^{-1} DW)**		**Root [Na^+]:[K^+] (DW)**	
100 mM NaCl	*J1551 UAS::AtAVP1-2*	627.97±627.97(n=5)	-8.4%	2098.8±2098.8(n=5)	-7.07%	0.3±0.3(n=5)	-2.36%
	J1551 UAS::AtAVP1-5	761.9±761.9(n=6)	+11.14%	2171.95±2171.95(n=6)	-3.83%	0.35±0.35(n=6)	+15.25%
	J1551 UAS::AtAVP1-6	604.08±604.08(n=5)	-11.88%	2206.27±2206.27(n=5)	-2.31%	0.27±0.27(n=5)	-10.58%
	J1551 UAS::AtAVP1-10	740.82±740.82(n=5)	+8.07%	2133.65±2133.65(n=5)	-5.53%	0.35±0.35(n=5)	+16.01%
	J1551 null	685.52±685.52(n=10)	0%	2258.5±2258.5(n=10)	0%	0.3±0.3(n=10)	0%
	J1551 Untransformed	636.44±636.44(n=3)	-7.16%	1990.24±1990.24(n=3)	**-11.88%**	0.32±0.32(n=3)	+5.17%

Table continued onto next page

		Leaf [Na⁺] (µmoles.g⁻¹ DW)		Leaf [K⁺] (µmoles.g⁻¹ DW)		Leaf [Na⁺]:[K⁺] DW	
0 mM NaCl	*J1551 UAS::AtAVP1-2*	162.91±11.65(n=4)	**+32.76%**	1763.39±98.98(n=4)	+12.68%	0.09±0.003(n=4)	+16.47%
	J1551 UAS::AtAVP1-5	123.92±13.43(n=7)	+0.99%	1555.25±60.9(n=7)	-0.62%	0.08±0.01(n=7)	+1.78%
	J1551 UAS::AtAVP1-6	127.05±18.48(n=7)	+3.54%	1582±60.04(n=7)	+1.09%	0.08±0.01(n=7)	+2.04%
	J1551 UAS::AtAVP1-10	145.93±14.48(n=9)	+18.93%	1538.25±40.43(n=9)	-1.7%	0.1±0.01(n=9)	+21.28%
	J1551 null	122.71±6.71(n=10)	0%	1564.89±49.48(n=10)	0%	0.08±0.01(n=10)	0%
	J1551 Untransformed	141.44±10.94(n=6)	+15.27%	1602.74±44.24(n=6)	+2.42%	0.09±0.01(n=6)	+12.08%
		Leaf [Na⁺] (µmoles.g⁻¹ DW)		**Leaf [K⁺] (µmoles.g⁻¹ DW)**		**Leaf [Na⁺]:[K⁺] DW**	
50 mM NaCl	*J1551 UAS::AtAVP1-2*	1303.2±174.09(n=4)	+4.13%	711.39±210.16(n=4)	+31.19%	2.09±0.3(n=4)	-18.7%
	J1551 UAS::AtAVP1-5	1168.15±135.07(n=5)	-6.66%	584.22±44.02(n=5)	+7.74%	2.04±0.29(n=5)	-20.48%
	J1551 UAS::AtAVP1-6	1056.05±87.25(n=5)	-15.61%	520.29±84.67(n=5)	-4.05%	2.38±0.56(n=5)	-7.56%
	J1551 UAS::AtAVP1-10	1119.68±125.41(n=7)	-10.53%	573.08±45.85(n=7)	+5.68%	2.09±0.34(n=7)	-18.79%
	J1551 null	1251.46±196.45(n=10)	0%	542.26±55.74(n=10)	0%	2.57±0.51(n=10)	0%
	J1551 Untransformed	1079.69±23.71(n=6)	-13.73%	635.53±82.71(n=6)	+17.2%	1.89±0.3(n=6)	-26.52%
		Leaf [Na⁺] (µmoles.g⁻¹ DW)		**Leaf [K⁺] (µmoles.g⁻¹ DW)**		**Leaf [Na⁺]:[K⁺] DW**	
100 mM NaCl	*J1551 UAS::AtAVP1-2*	2997.95±2997.95(n=5)	**+36.2%**	433.95±433.95(n=5)	+7.36%	6.92±6.92(n=5)	+22.28%
	J1551 UAS::AtAVP1-5	2574.81±2574.81(n=6)	+16.98%	508.5±508.5(n=6)	+25.8%	5.79±5.79(n=6)	+2.33%
	J1551 UAS::AtAVP1-6	2810.94±2810.94(n=5)	**+27.71%**	487.69±487.69(n=5)	+20.66%	6.1±6.1(n=5)	+7.78%
	J1551 UAS::AtAVP1-10	2245.56±2245.56(n=7)	+2.02%	474.66±474.66(n=7)	+17.43%	5.28±5.28(n=7)	-6.8%
	J1551 null	2201.1±2201.1(n=10)	0%	404.2±404.2(n=10)	0%	5.66±5.66(n=10)	0%
	J1551 Untransformed	2400.17±2400.17(n=3)	+9.04%	508.36±508.36(n=3)	+25.77%	4.8±4.8(n=3)	-15.27%
		Shoot DW (g)		**Root DW (g)**			
0 mM NaCl	*J1551 UAS::AtAVP1-2*	0.1±0.01(n=4)	**-40.67%**	0.01±0.001(n=4)	-32.64%		
	J1551 UAS::AtAVP1-5	0.14±0.01(n=7)	-13.14%	0.02±0.002(n=7)	-19.1%		
	J1551 UAS::AtAVP1-6	0.11±0.01(n=7)	**-30.68%**	0.01±0.005(n=7)	-20.11%		
	J1551 UAS::AtAVP1-10	0.13±0.02(n=9)	-21.95%	0.01±0.002(n=9)	**-32.61%**		
	J1551 null	0.16±0.01(n=10)	0%	0.02±0.002(n=10)	0%		
	J1551 Untransformed	0.16±0.02(n=6)	-2.74%	0.02±0.003(n=6)	-9.66%		
		Shoot DW (g)		**Root DW (g)**			
50 mM NaCl	*J1551 UAS::AtAVP1-2*	0.13±0.02(n=4)	-12.49%	0.01±0.004(n=4)	-21.23%		
	J1551 UAS::AtAVP1-5	0.14±0.02(n=5)	-1.8%	0.02±0.004(n=5)	-1.63%		
	J1551 UAS::AtAVP1-6	0.15±0.02(n=6)	+4.92%	0.02±0.004(n=6)	+2.58%		
	J1551 UAS::AtAVP1-10	0.12±0.02(n=7)	-14.28%	0.01±0.003(n=7)	-15.72%		
	J1551 null	0.14±0.01(n=10)	0%	0.02±0.002(n=10)	0%		
	J1551 Untransformed	0.09±0.01(n=6)	**-36.11%**	0.01±0.002(n=6)	**-30.15%**		
		Shoot DW (g)		**Root DW (g)**			
100 mM NaCl	*J1551 UAS::AtAVP1-2*	0.13±0.13(n=5)	-11.91%	0.02±0.02(n=5)	-3.92%		
	J1551 UAS::AtAVP1-5	0.13±0.13(n=6)	-14.05%	0.02±0.02(n=6)	-11.51%		
	J1551 UAS::AtAVP1-6	0.12±0.12(n=5)	-16.6%	0.02±0.02(n=5)	-15.14%		
	J1551 UAS::AtAVP1-10	0.13±0.13(n=7)	-8.14%	0.02±0.02(n=7)	-4.75%		
	J1551 null	0.15±0.15(n=10)	0%	0.02±0.02(n=10)	0%		
	J1551 Untransformed	0.14±0.14(n=3)	-6.94%	0.02±0.02(n=3)	-15.04%		

End of table

Appendix Table 5: Mini-hydroponics experiment #2 – J1422 + *pGOF-UAS$_{GAL4}$::AtAVP1*

To assessing the effect of salinity tolerance of root cell-type specific expression of *AtAVP1* via the *pGOF-UAS$_{GAL4}$::AtAVP1* transactivation construct in the *GAL4-VP16* enhancer-trap line J1422, T_4 lines, a null segregants line, and the parental line, J1422, were screened in supported hydroponics (2.3.8) and exposed to 0, 50 or 100 mM additional NaCl (plus additional $CaCl_2$ to maintain Ca^{2+} activity). Plants were harvested after 7 days growth. Root and shoot fresh and dry weight were measured. Root and youngest fully-expanded leaf Na^+, K^+ and as per section 2.4.4.1. Data tabulated is mean measurements ± S.E.M. Significant differences ($P \leq 0.05$) from the null line determined by one-way ANOVA, Tukey-Cramer HSD test and are highlighted in yellow.

		Shoot FW (g)		Root FW (g)		Root:Shoot Ratio FW	
0 mM NaCl	*J1422 UAS::AtAVP1-6*	2.17±0.24(n=8)	-16.74%	0.26±0.02(n=8)	-22.69%	0.12±0.01(n=8)	-2.64%
	J1422 UAS::AtAVP1-18	2.98±0.44(n=7)	+14.55%	0.4±0.06(n=7)	+17.58%	0.13±0.01(n=7)	+5.49%
	J1422 UAS::AtAVP1-5	3.54±0.66(n=6)	+36%	0.43±0.09(n=6)	+28.1%	0.12±0.01(n=6)	-4.96%
	J1422 UAS::AtAVP1-16	2.75±0.43(n=10)	+5.78%	0.36±0.06(n=10)	+7.02%	0.13±0.01(n=10)	+5%
	J1422 null	2.6±0.34(n=10)	0%	0.34±0.05(n=10)	0%	0.13±0.01(n=10)	0%
	J1422 Untransformed	2.52±0.5(n=3)	-3.27%	0.31±0.06(n=3)	-8.41%	0.12±0.002(n=3)	-2.3%
		Shoot FW (g)		**Root FW (g)**		**Root:Shoot Ratio FW**	
50 mM NaCl	*J1422 UAS::AtAVP1-6*	3.12±0.3(n=10)	+20.28%	0.49±0.05(n=10)	+23.61%	0.16±0.01(n=10)	+7.91%
	J1422 UAS::AtAVP1-18	2.7±0.39(n=8)	+4.13%	0.42±0.05(n=8)	+6.04%	0.16±0.01(n=8)	+8.12%
	J1422 UAS::AtAVP1-5	2.43±0.36(n=7)	-6.24%	0.39±0.06(n=7)	-1.07%	0.16±0.01(n=7)	+12.84%
	J1422 UAS::AtAVP1-16	2.5±0.32(n=11)	-3.61%	0.37±0.05(n=11)	-5.92%	0.15±0.01(n=11)	+1.73%
	J1422 null	2.6±0.36(n=8)	0%	0.39±0.07(n=8)	0%	0.15±0.01(n=8)	0%
	J1422 Untransformed	2.65±0.55(n=3)	+2.16%	0.49±0.13(n=3)	+24.29%	0.18±0.03(n=3)	+26.6%
		Shoot FW (g)		**Root FW (g)**		**Root:Shoot Ratio FW**	
100 mM NaCl	*J1422 UAS::AtAVP1-6*	2.54±2.54(n=6)	+3.4%	0.57±0.57(n=6)	-0.23%	0.22±0.22(n=6)	-4.57%
	J1422 UAS::AtAVP1-18	2.07±2.07(n=8)	-15.64%	0.51±0.51(n=8)	-10.82%	0.24±0.24(n=8)	+4.7%
	J1422 UAS::AtAVP1-5	1.88±1.88(n=7)	-23.25%	0.42±0.42(n=7)	-27.4%	0.22±0.22(n=7)	-6.65%
	J1422 UAS::AtAVP1-16	2.34±2.34(n=6)	-4.67%	0.49±0.49(n=6)	-14.36%	0.21±0.21(n=6)	-9.72%
	J1422 null	2.46±2.46(n=9)	0%	0.57±0.57(n=9)	0%	0.23±0.23(n=9)	0%
	J1422 Untransformed	2.79±2.79(n=3)	+13.75%	0.65±0.65(n=3)	+13.38%	0.24±0.24(n=3)	+1.86%
		Root [Na^+] (µmoles.g^{-1} DW)		**Root [K^+] (µmoles.g^{-1} DW)**		**Root [Na^+]:[K^+] (DW)**	
0 mM NaCl	*J1422 UAS::AtAVP1-6*	31.69±1.75(n=8)	-14.97%	2026.86±170.67(n=8)	+1.47%	0.02±0.001(n=8)	-14.18%
	J1422 UAS::AtAVP1-18	28.38±4.05(n=7)	-23.84%	1792.05±42.06(n=7)	**-10.29%**	0.02±0.002(n=7)	-14.77%
	J1422 UAS::AtAVP1-5	36.4±3.97(n=6)	-2.31%	1870.97±59.5(n=6)	-6.33%	0.02±0.002(n=6)	+3.54%
	J1422 UAS::AtAVP1-16	29.13±2.07(n=10)	-21.83%	1980.57±62.9(n=10)	-0.85%	0.01±0.001(n=10)	-20.14%
	J1422 null	37.27±6.69(n=10)	0%	1997.51±55.74(n=10)	0%	0.02±0.003(n=10)	0%
	J1422 Untransformed	29.69±3.03(n=3)	-20.33%	1897.26±31.86(n=3)	-5.02%	0.02±0.002(n=3)	-16.14%
		Root [Na^+] (µmoles.g^{-1} DW)		**Root [K^+] (µmoles.g^{-1} DW)**		**Root [Na^+]:[K^+] (DW)**	
50 mM NaCl	*J1422 UAS::AtAVP1-6*	535.38±41.08(n=10)	**+47.21%**	2118.38±253.24(n=10)	+3.51%	0.27±0.02(n=10)	**+51.33%**
	J1422 UAS::AtAVP1-18	369.13±40.43(n=8)	+1.5%	1867.86±137.97(n=8)	-8.73%	0.21±0.04(n=8)	+19.68%
	J1422 UAS::AtAVP1-5	392.03±20.33(n=7)	+7.8%	1864.04±113.68(n=7)	-8.92%	0.21±0.01(n=7)	**+19.22%**
	J1422 UAS::AtAVP1-16	508.28±45.69(n=11)	**+39.76%**	1906.77±48.95(n=11)	-6.83%	0.27±0.03(n=11)	**+52.59%**
	J1422 null	363.67±27.41(n=8)	0%	2046.51±121.04(n=8)	0%	0.18±0.01(n=8)	0%
	J1422 Untransformed	327.18±80.17(n=3)	-10.03%	1817.07±147.54(n=3)	-11.21%	0.18±0.05(n=3)	+4.07%
		Root [Na^+] (µmoles.g^{-1} DW)		**Root [K^+] (µmoles.g^{-1} DW)**		**Root [Na^+]:[K^+] (DW)**	
100 mM NaCl	*J1422 UAS::AtAVP1-6*	767.22±767.22(n=4)	-14.31%	2084.43±2084.43(n=4)	+2.96%	0.37±0.37(n=4)	-20.39%
	J1422 UAS::AtAVP1-18	840.59±840.59(n=7)	-6.12%	1545.32±1545.32(n=7)	-23.67%	0.55±0.55(n=7)	+19.04%
	J1422 UAS::AtAVP1-5	733.2±733.2(n=7)	-18.11%	1876.83±1876.83(n=7)	-7.29%	0.39±0.39(n=7)	-14.51%
	J1422 UAS::AtAVP1-16	670.21±670.21(n=6)	-25.15%	1917.4±1917.4(n=6)	-5.29%	0.36±0.36(n=6)	-22.52%
	J1422 null	895.39±895.39(n=9)	0%	2024.52±2024.52(n=9)	0%	0.46±0.46(n=9)	0%
	J1422 Untransformed	598.83±598.83(n=3)	-33.12%	2462.68±2462.68(n=3)	+21.64%	0.23±0.23(n=3)	-49.59%

Table continued onto next page

		Leaf [Na^+] (µmoles.g^{-1} DW)		Leaf [K^+] (µmoles.g^{-1} DW)		Leaf [Na^+]:[K^+] DW	
0 mM NaCl	*J1422 UAS::AtAVP1-6*	74.55±6.9(n=8)	-4.52%	1518.91±145.33(n=8)	-5.3%	0.05±0.01(n=8)	+3.61%
	J1422 UAS::AtAVP1-18	86.35±6.06(n=7)	+10.59%	1495.57±186.06(n=7)	-6.76%	0.07±0.02(n=7)	+32.42%
	J1422 UAS::AtAVP1-5	86.93±4.5(n=6)	+11.33%	1452.59±132.69(n=6)	-9.44%	0.06±0.01(n=6)	+19.59%
	J1422 UAS::AtAVP1-16	97.29±6.93(n=10)	**+24.6%**	1268±132.77(n=10)	-20.95%	0.09±0.01(n=10)	**+66.48%**
	J1422 null	78.08±4.91(n=10)	0%	1603.99±100.74(n=10)	0%	0.05±0.01(n=10)	0%
	J1422 Untransformed	72±10.19(n=3)	-7.79%	1617.86±247.24(n=3)	+0.86%	0.05±0.01(n=3)	-8.01%
		Leaf [Na^+] (µmoles.g^{-1} DW)		**Leaf [K^+] (µmoles.g^{-1} DW)**		**Leaf [Na^+]:[K^+] DW**	
50 mM NaCl	*J1422 UAS::AtAVP1-6*	1684.54±86.86(n=10)	+3.33%	915.13±82.8(n=10)	+26.19%	2.04±0.28(n=10)	-18.99%
	J1422 UAS::AtAVP1-18	1753.22±99.33(n=8)	+7.54%	739.77±79.69(n=8)	+2.01%	2.67±0.42(n=8)	+6.2%
	J1422 UAS::AtAVP1-5	1527.79±168.47(n=7)	-6.29%	984.81±60.03(n=7)	**+35.8%**	1.61±0.22(n=7)	-36.11%
	J1422 UAS::AtAVP1-16	1544.39±121.19(n=11)	-5.27%	828.22±82.21(n=11)	+14.2%	2.23±0.46(n=11)	-11.19%
	J1422 null	1630.27±165.84(n=8)	0%	725.21±69.75(n=8)	0%	2.51±0.41(n=8)	0%
	J1422 Untransformed	1600.39±171(n=3)	-1.83%	750.83±105.29(n=3)	+3.53%	2.2±0.35(n=3)	-12.36%
		Leaf [Na^+] (µmoles.g^{-1} DW)		**Leaf [K^+] (µmoles.g^{-1} DW)**		**Leaf [Na^+]:[K^+] DW**	
100 mM NaCl	*J1422 UAS::AtAVP1-6*	3360.93±3360.93(n=6)	+9.11%	538.74±538.74(n=6)	+0.78%	6.28±6.28(n=6)	+0.61%
	J1422 UAS::AtAVP1-18	3081.79±3081.79(n=8)	+0.05%	568.69±568.69(n=8)	+6.38%	5.49±5.49(n=8)	-12.03%
	J1422 UAS::AtAVP1-5	3372.1±3372.1(n=7)	+9.48%	539.29±539.29(n=7)	+0.88%	6.73±6.73(n=7)	+7.83%
	J1422 UAS::AtAVP1-16	3339.17±3339.17(n=6)	+8.41%	461.72±461.72(n=6)	-13.63%	7.82±7.82(n=6)	+25.25%
	J1422 null	3080.18±3080.18(n=8)	0%	534.58±534.58(n=8)	0%	6.24±6.24(n=8)	0%
	J1422 Untransformed	3966.53±3966.53(n=3)	+28.78%	514.53±514.53(n=3)	-3.75%	7.67±7.67(n=3)	+22.83%
		Shoot DW (g)		**Root DW (g)**			
0 mM NaCl	*J1422 UAS::AtAVP1-6*	0.17±0.02(n=8)	+8.83%	0.02±0.001(n=8)	-19.33%		
	J1422 UAS::AtAVP1-18	0.22±0.03(n=7)	+36.21%	0.02±0.003(n=7)	+17.4%		
	J1422 UAS::AtAVP1-5	0.25±0.05(n=6)	+56.61%	0.02±0.01(n=6)	+23.66%		
	J1422 UAS::AtAVP1-16	0.16±0.04(n=10)	+3.07%	0.02±0.003(n=10)	+6.23%		
	J1422 null	0.16±0.04(n=10)	0%	0.02±0.003(n=10)	0%		
	J1422 Untransformed	0.17±0.04(n=3)	+8.48%	0.02±0.003(n=3)	-9.3%		
		Shoot DW (g)		**Root DW (g)**			
50 mM NaCl	*J1422 UAS::AtAVP1-6*	0.21±0.02(n=10)	+14.88%	0.02±0.002(n=10)	+15.71%		
	J1422 UAS::AtAVP1-18	0.2±0.04(n=8)	+10.05%	0.02±0.003(n=8)	+0.94%		
	J1422 UAS::AtAVP1-5	0.16±0.02(n=7)	-11.51%	0.02±0.003(n=7)	+3.4%		
	J1422 UAS::AtAVP1-16	0.19±0.02(n=11)	+1.43%	0.02±0.002(n=11)	-7.1%		
	J1422 null	0.18±0.03(n=8)	0%	0.02±0.003(n=8)	0%		
	J1422 Untransformed	0.18±0.04(n=3)	-1.9%	0.02±0.003(n=3)	+9.33%		
		Shoot DW (g)		**Root DW (g)**			
100 mM NaCl	*J1422 UAS::AtAVP1-6*	0.26±0.26(n=6)	+6.55%	0.03±0.03(n=6)	-1.61%		
	J1422 UAS::AtAVP1-18	0.21±0.21(n=8)	-13.99%	0.03±0.03(n=8)	-8.02%		
	J1422 UAS::AtAVP1-5	0.19±0.19(n=7)	-19.01%	0.02±0.02(n=7)	-21.06%		
	J1422 UAS::AtAVP1-16	0.21±0.21(n=6)	-13.21%	0.03±0.03(n=6)	-11.98%		
	J1422 null	0.24±0.24(n=9)	0%	0.03±0.03(n=9)	0%		
	J1422 Untransformed	0.26±0.26(n=3)	+6.16%	0.03±0.03(n=3)	+3.44%		

End of table

Supplementary Barley Hydroponics data

Barley supported hydroponics experiment #1 tabulated data

Appendix Table 6: Supported hydroponics experiment #1
To assessing salinity tolerance of lines with expression of *HvHVP1* or *HvHKT1;5* under the control of putative cell-type specific promoter *proC34* or *proS147* respectively, selected T_3 lines and segregants were screened in supported hydroponics and exposed to either 0 or 200 mM additional NaCl on emergence of the 3rd leaf. Plants were harvested after 21 days growth. Root and shoot fresh and dry weight were measured. Root and 4th leave Na^+, K^+ and Cl^- content were measured as per section 2.4.4.1. Data tabulated is mean measurements ± S.E.M. Significant differences ($P \leq 0.05$) from the grouped null segregants determined by one-way ANOVA, Tukey-Cramer HSD test and are highlighted in yellow.

		Shoot FW (g)		Root FW (g)		Root:Shoot FW	
0 mM NaCl	*proC34:HvHVP1* -310.3 A	7.72±0.68(n=9)	+3.5%	1.7±0.18(n=9)	+7.4%	0.22±0.01(n=9)	+3.1%
	proC34:HvHVP1 -310.3 B	5.41±0.25(n=8)	**-27.4%**	1.13±0.08(n=8)	**-28.2%**	0.21±0.01(n=8)	-1.3%
	proC34:HvHVP1 -310.8 A	6.93±0.29(n=8)	-7%	1.5±0.08(n=8)	-5.2%	0.22±0.01(n=8)	+1.8%
	proC34:HvHVP1 -310.8 B	7.98±0.39(n=7)	+7.1%	1.78±0.13(n=7)	+12.5%	0.22±0.01(n=7)	+4.4%
	proS147:HvHKT1;5 -316.10 A	8.33±0.33(n=7)	+11.8%	1.8±0.09(n=7)	+14%	0.22±0.004(n=7)	+1.8%
	proS147:HvHKT1;5 -316.10 B	7.18±1(n=8)	-3.7%	1.54±0.16(n=8)	-2.6%	0.22±0.01(n=8)	+4.8%
	proS147:HvHKT1;5 -316.20 A	7.4±0.4(n=9)	-0.7%	1.69±0.12(n=9)	+6.9%	0.23±0.01(n=9)	+7.1%
	proS147:HvHKT1;5 -316.20 B	7.71±0.45(n=8)	+3.5%	1.62±0.12(n=8)	+2.6%	0.21±0.01(n=8)	-1.4%
	Null segregants	7.45±0.51(n=10)	N/A	1.58±0.12(n=10)	N/A	0.21±0.01(n=10)	N/A
		Shoot FW (g)		**Root FW (g)**		**Root:Shoot FW**	
200 mM NaCl	*proC34:HvHVP1* -310.3 A	3.36±0.24(n=9)	-17.6%	1.11±0.07(n=9)	-17.6%	0.33±0.01(n=9)	+0.1%
	proC34:HvHVP1 -310.3 B	2.76±0.25(n=8)	**-32.2%**	0.91±0.06(n=8)	**-32.2%**	0.34±0.02(n=8)	+1.4%
	proC34:HvHVP1 -310.8 A	3.53±0.2(n=8)	-13.4%	1.12±0.06(n=8)	**-17.2%**	0.32±0.01(n=8)	-4.5%
	proC34:HvHVP1 -310.8 B	3.76±0.25(n=9)	-7.6%	1.14±0.06(n=9)	-15%	0.31±0.01(n=9)	-7.4%
	proS147:HvHKT1;5 -316.10 A	4.03±0.2(n=8)	-1.1%	1.33±0.09(n=8)	-1.2%	0.33±0.01(n=8)	-0.9%
	proS147:HvHKT1;5 -316.10 B	3.8±0.28(n=8)	-6.8%	1.26±0.12(n=8)	-6.3%	0.33±0.02(n=8)	-0.3%
	proS147:HvHKT1;5 -316.20 A	3.96±0.17(n=9)	-2.7%	1.28±0.05(n=9)	-5.2%	0.33±0.02(n=9)	-1.7%
	proS147:HvHKT1;5 -316.20 B	3.51±0.32(n=9)	-13.9%	1.17±0.11(n=9)	-13.1%	0.33±0.01(n=9)	-0.1%
	Null segregants	4.07±0.29(n=8)	N/A	1.35±0.09(n=8)	N/A	0.33±0.01(n=8)	N/A
		Shoot DW (g)		**Root DW (g)**		**Root:Shoot DW**	
0 mM NaCl	*proC34:HvHVP1* -310.3 A	0.63±0.06(n=9)	+3%	0.1±0.01(n=9)	-1%	0.16±0.01(n=9)	-4.7%
	proC34:HvHVP1 -310.3 B	0.45±0.04(n=8)	**-25.7%**	0.08±0.01(n=8)	**-24.6%**	0.17±0.01(n=8)	+2.7%
	proC34:HvHVP1 -310.8 A	0.56±0.02(n=8)	-7.3%	0.09±0.01(n=8)	-11.5%	0.16±0.01(n=8)	-4.6%
	proC34:HvHVP1 -310.8 B	0.6±0.08(n=7)	-1.2%	0.11±0.01(n=7)	+6.9%	0.2±0.03(n=7)	+20.1%
	proS147:HvHKT1;5 -316.10 A	0.69±0.04(n=7)	+13%	0.1±0.01(n=7)	-4.2%	0.14±0.02(n=7)	-13.6%
	proS147:HvHKT1;5 -316.10 B	0.58±0.09(n=8)	-4.2%	0.1±0.01(n=8)	-3.3%	0.17±0.01(n=8)	+4.9%
	proS147:HvHKT1;5 -316.20 A	0.61±0.04(n=9)	-0.3%	0.1±0.01(n=9)	+4.3%	0.17±0.01(n=9)	+5.1%
	proS147:HvHKT1;5 -316.20 B	0.62±0.05(n=8)	+2.3%	0.1±0.01(n=8)	-1.3%	0.16±0.01(n=8)	-1.4%
	Null segregants	0.61±0.05(n=10)	N/A	0.1±0.01(n=10)	N/A	0.16±0.01(n=10)	N/A
		Shoot DW (g)		**Root DW (g)**		**Root:Shoot DW**	
200 mM NaCl	*proC34:HvHVP1* -310.3 A	0.36±0.03(n=9)	-15%	0.08±0.01(n=9)	-20.9%	0.23±0.01(n=9)	-5.5%
	proC34:HvHVP1 -310.3 B	0.29±0.03(n=8)	**-31.2%**	0.07±0(n=8)	**-35.9%**	0.23±0.01(n=8)	-4%
	proC34:HvHVP1 -310.8 A	0.37±0.02(n=8)	-13.4%	0.08±0(n=8)	-21.3%	0.22±0.01(n=8)	-7.8%
	proC34:HvHVP1 -310.8 B	0.39±0.03(n=9)	-8.3%	0.09±0(n=9)	-15.2%	0.23±0.01(n=9)	-5.4%
	proS147:HvHKT1;5 -316.10 A	0.43±0.03(n=8)	+2.7%	0.09±0.01(n=8)	-8.2%	0.22±0.01(n=8)	-9.9%
	proS147:HvHKT1;5 -316.10 B	0.4±0.03(n=8)	-6.2%	0.09±0.01(n=8)	-13%	0.22±0.01(n=8)	-7%
	proS147:HvHKT1;5 -316.20 A	0.41±0.02(n=9)	-2.9%	0.1±0(n=9)	+0.6%	0.25±0.02(n=9)	+6.2%
	proS147:HvHKT1;5 -316.20 B	0.36±0.03(n=9)	-14.3%	0.08±0.01(n=9)	-17.7%	0.23±0.01(n=9)	-4%
	Null segregants	0.42±0.03(n=8)	N/A	0.1±0.01(n=8)	N/A	0.24±0.01(n=8)	N/A

Table continued onto next page

		Leaf [Na^+] (µmoles.g^{-1} DW)		Leaf [K^+] (µmoles.g^{-1} DW)		Leaf [Na^+]:[K^+] DW	
0 mM NaCl	*proC34:HvHVP1* -310.3 A	171.84±7.63(n=9)	-4.1%	1862.65±54.53(n=9)	-3.3%	0.09±0(n=9)	-1.4%
	proC34:HvHVP1 -310.3 B	172.29±7.8(n=8)	-3.8%	1817.51±39.85(n=8)	-5.7%	0.1±0(n=8)	+1.2%
	proC34:HvHVP1 -310.8 A	192.95±7.68(n=8)	+7.7%	1857.1±26.67(n=8)	-3.6%	0.1±0(n=8)	+10.7%
	proC34:HvHVP1 -310.8 B	182.75±5.65(n=7)	+2%	1957.44±84.79(n=7)	+1.6%	0.09±0(n=7)	-0%
	proS147:HvHKT1;5 -316.10 A	195.67±9.27(n=7)	+9.2%	1792.83±40.51(n=7)	-7%	0.11±0(n=7)	+16.2%
	proS147:HvHKT1;5 -316.10 B	188.71±11.03(n=8)	+5.4%	1848.35±46.97(n=8)	-4.1%	0.1±0(n=8)	+8.6%
	proS147:HvHKT1;5 -316.20 A	173.84±6.77(n=9)	-2.9%	1825.09±33.07(n=9)	-5.3%	0.1±0(n=9)	+1.5%
	proS147:HvHKT1;5 -316.20 B	163.87±6.27(n=8)	-8.5%	1884.37±53.98(n=8)	-2.2%	0.09±0(n=8)	-7.3%
	Null segregants	179.11±9.73(n=10)	N/A	1927.1±57.39(n=10)	N/A	0.09±0.01(n=10)	N/A
		Leaf [Na^+] (µmoles.g^{-1} DW)		**Leaf [K^+] (µmoles.g^{-1} DW)**		**Leaf [Na^+]:[K^+] DW**	
200 mM NaCl	*proC34:HvHVP1* -310.3 A	2769.57±156.01(n=8)	+5.3%	296.7±28.98(n=8)	+7%	10.04±1.23(n=8)	+1.8%
	proC34:HvHVP1 -310.3 B	2449.09±39.4(n=8)	**-6.9%**	248.52±11.52(n=8)	-10.4%	10.01±0.52(n=8)	+1.4%
	proC34:HvHVP1 -310.8 A	2658.21±64.01(n=8)	+1.1%	299.44±31.71(n=8)	+8%	9.42±0.78(n=8)	-4.5%
	proC34:HvHVP1 -310.8 B	2521.27±29.65(n=9)	-4.1%	284.74±15.78(n=9)	+2.7%	9.08±0.52(n=9)	-7.9%
	proS147:HvHKT1;5 -316.10 A	2668.66±41.67(n=8)	+1.5%	344.29±39.84(n=8)	+24.2%	8.56±1.03(n=8)	-13.2%
	proS147:HvHKT1;5 -316.10 B	2488.84±111.9(n=8)	-5.4%	397.83±69.17(n=8)	+43.5%	7.94±1.45(n=8)	-19.5%
	proS147:HvHKT1;5 -316.20 A	2538.34±39.33(n=9)	-3.5%	328.63±33.15(n=9)	+18.6%	8.34±0.78(n=9)	-15.4%
	proS147:HvHKT1;5 -316.20 B	2477.9±47.19(n=9)	-5.8%	322.24±32.77(n=9)	+16.2%	8.4±0.91(n=9)	-14.8%
	Null segregants	2629.98±57.12(n=8)	N/A	277.21±26.24(n=8)	N/A	9.86±0.6(n=8)	N/A
		Root [Na^+] (µmoles.g^{-1} DW)		**Root [K^+] (µmoles.g^{-1} DW)**		**Root [Na^+]:[K^+] DW**	
0 mM NaCl	*proC34:HvHVP1* -310.3 A	129.85±7.1(n=9)	+0.4%	1739.61±72.42(n=9)	-4.1%	0.07±0.003(n=9)	+4.6%
	proC34:HvHVP1 -310.3 B	132.78±7.24(n=8)	+2.7%	1850.57±39.39(n=8)	+2%	0.07±0.004(n=8)	+0.3%
	proC34:HvHVP1 -310.8 A	134.4±2.71(n=8)	+3.9%	1879.49±52.41(n=8)	+3.6%	0.07±0.003(n=8)	+0.6%
	proC34:HvHVP1 -310.8 B	131.33±3.11(n=7)	+1.6%	1811.11±58.12(n=7)	-0.1%	0.07±0.002(n=7)	+1.7%
	proS147:HvHKT1;5 -316.10 A	137.64±4.82(n=6)	+6.5%	1861.16±40.82(n=6)	+2.6%	0.07±0.003(n=6)	+3.5%
	proS147:HvHKT1;5 -316.10 B	128.77±8.62(n=8)	-0.4%	1777.66±67.37(n=8)	-2%	0.07±0.004(n=8)	+1.5%
	proS147:HvHKT1;5 -316.20 A	127.53±3.2(n=9)	-1.4%	1760.4±29.25(n=9)	-2.9%	0.07±0.002(n=9)	+1.5%
	proS147:HvHKT1;5 -316.20 B	137.16±2.87(n=7)	+6.1%	1838.43±41.96(n=7)	+1.4%	0.07±0.002(n=7)	+4.6%
	Null segregants	129.29±4.98(n=10)	N/A	1813.41±61.61(n=10)	N/A	0.07±0.002(n=10)	N/A
		Root [Na^+] (µmoles.g^{-1} DW)		**Root [K^+] (µmoles.g^{-1} DW)**		**Root [Na^+]:[K^+] DW**	
200 mM NaCl	*proC34:HvHVP1* -310.3 A	1931.27±58.46(n=9)	+7.9%	513.43±16.98(n=9)	+11.2%	3.8±0.19(n=9)	-2.6%
	proC34:HvHVP1 -310.3 B	1927.66±69.35(n=8)	+7.7%	435.5±22.13(n=8)	-5.7%	4.5±0.26(n=8)	+15.2%
	proC34:HvHVP1 -310.8 A	1957.97±41.02(n=8)	+9.3%	489.24±23.92(n=8)	+6%	4.09±0.27(n=8)	+4.8%
	proC34:HvHVP1 -310.8 B	1786.01±30.83(n=9)	-0.3%	480.14±19.86(n=9)	+4%	3.76±0.13(n=9)	-3.6%
	proS147:HvHKT1;5 -316.10 A	1940.52±68.53(n=8)	+8.4%	429.6±17.09(n=8)	-7%	4.55±0.2(n=8)	**+16.7%**
	proS147:HvHKT1;5 -316.10 B	1995.83±69.23(n=8)	+11.5%	478.01±15.55(n=8)	+3.5%	4.19±0.16(n=8)	+7.5%
	proS147:HvHKT1;5 -316.20 A	1731.08±74.94(n=9)	-3.3%	438.69±21.9(n=9)	-5%	3.98±0.14(n=9)	+2%
	proS147:HvHKT1;5 -316.20 B	1883.05±31.99(n=9)	+5.2%	499.5±24.67(n=9)	+8.2%	3.84±0.2(n=9)	-1.5%
	Null segregants	1790.63±98.89(n=8)	N/A	461.69±23.91(n=8)	N/A	3.9±0.19(n=8)	N/A
		Leaf [Cl^-] (µM.g^{-1} DW)		**Root [Cl^-] (µnoles.g^{-1} DW)**		**Number of Tillers**	
0 mM NaCl	*proC34:HvHVP1* -310.3 A	881.87±124.83(n=9)	+8.3%	78.85±3.74(n=8)	+5.8%	2.67±0.24(n=9)	-0%
	proC34:HvHVP1 -310.3 B	663.33±79.03(n=8)	**-18.5%**	106.25±7(n=8)	**+42.6%**	2.57±0.2(n=7)	-3.6%
	proC34:HvHVP1 -310.8 A	865.48±60.37(n=8)	+6.3%	83.26±4.89(n=8)	+11.7%	2.63±0.18(n=8)	-1.6%
	proC34:HvHVP1 -310.8 B	883.94±48.14(n=7)	+8.6%	76.54±4.84(n=7)	+2.7%	2.67±0.21(n=6)	-0%
	proS147:HvHKT1;5 -316.10 A	814.69±22.04(n=7)	+0.1%	105.75±25.35(n=7)	+41.9%	3±0.26(n=6)	+12.5%
	proS147:HvHKT1;5 -316.10 B	790.55±38.27(n=8)	-2.9%	70.7±9.76(n=6)	-5.1%	2.5±0.38(n=8)	-6.3%
	proS147:HvHKT1;5 -316.20 A	842.96±119.89(n=9)	+3.6%	84.32±4.53(n=8)	+13.2%	3±0.22(n=7)	+12.5%
	proS147:HvHKT1;5 -316.20 B	798.67±42.39(n=8)	-1.9%	73.69±3(n=7)	-1.1%	3±0(n=6)	+12.5%
	Null segregants	814.03±15.49(n=10)	N/A	74.51±2.92(n=10)	N/A	2.67±0.24(n=9)	N/A
		Leaf [Cl^-] (µM.g^{-1} DW)		**Root [Cl^-] (µnoles.g^{-1} DW)**		**Number of Tillers**	
200 mM NaCl	*proC34:HvHVP1* -310.3 A	1341.25±151.87(n=9)	+0.7%	436.34±23.33(n=9)	**+26%**	1.89±0.31(n=9)	-31.3%
	proC34:HvHVP1 -310.3 B	1163.09±58.68(n=8)	-12.7%	392.21±22.12(n=8)	+13.3%	1.63±0.26(n=8)	**-40.9%**
	proC34:HvHVP1 -310.8 A	1362.26±38.13(n=8)	+2.3%	363.27±24.45(n=8)	+4.9%	1.71±0.36(n=7)	**-37.7%**
	proC34:HvHVP1 -310.8 B	1251.42±30.57(n=9)	-6.1%	379.31±42.2(n=9)	+9.5%	2.78±0.15(n=9)	+1%
	proS147:HvHKT1;5 -316.10 A	1508.98±87.11(n=8)	+13.3%	383.8±29.18(n=8)	+10.8%	2.38±0.32(n=8)	-13.6%
	proS147:HvHKT1;5 -316.10 B	1254.29±82.9(n=8)	-5.9%	394.74±46.6(n=8)	+14%	2.86±0.34(n=7)	+3.9%
	proS147:HvHKT1;5 -316.20 A	1317.89±33.16(n=9)	-1.1%	316.33±26.27(n=9)	-8.6%	2.25±0.31(n=8)	-18.2%
	proS147:HvHKT1;5 -316.20 B	1233.33±29.44(n=9)	-7.4%	355.02±18.76(n=9)	+2.5%	1.89±0.35(n=9)	-31.3%
	Null segregants	1332.26±67.3(n=8)	N/A	346.28±15.86(n=7)	N/A	2.75±0.31(n=8)	N/A

End of table

Barley mini-hydroponics experiment #2 tabulated data

Appendix Table 7: Mini-hydroponics experiment #2

To assessing salinity tolerance of lines with co-ordinated expression of *proC34:HvHVP1* and *proS147:HvHKT1;5*, selected T_5F_3 line, segregants and parental lines were screened in mini-hydroponics and exposed to either 0 or 150 mM additional NaCl on emergence of the 3rd leaf. Plants were harvested after 14 days growth. Root and shoot fresh and dry weight were measured. Root and 4th leave Na^+, K^+ and Cl^- content were measured as per section 2.4.4.1.

Data tabulated is mean measurements ± S.E.M. significant differences ($P \leq 0.05$) from the T_5F_3 null line determined by one-way ANOVA, Tukey-Cramer HSD test and are highlighted in yellow.

		Shoot fresh weight (g)		Root fresh weight (g)		Root:Shoot ratio FW	
0 mM NaCl	*T_5 316.10 S::HvHKT1;5*	2.7±0.08(n=6)	**-19.93%**	1.52±0.12(n=6)	-3.24%	0.57±0.05(n=6)	+20.59%
	T_5F_3 HvHKT1;5/null	3.39±0.11(n=12)	+0.53%	1.51±0.11(n=12)	-4.14%	0.44±0.02(n=12)	-5.84%
	T_5F_3 A - HvHKT1;5/HvHVP1	3.12±0.11(n=6)	-7.41%	1.64±0.11(n=6)	+4.28%	0.52±0.02(n=6)	+11.21%
	T_5F_3 B - HvHKT1;5/HvHVP1	3.13±0.22(n=6)	-6.96%	1.31±0.15(n=6)	-16.58%	0.42±0.04(n=6)	-10.78%
	T_5F_3 null/null	3.37±0.14(n=14)	N/A	1.57±0.13(n=14)	N/A	0.47±0.04(n=14)	N/A
	T_5F_3 C - HvHVP1/HvHKT1;5	3.35±0.27(n=4)	-0.53%	1.59±0.18(n=4)	+0.68%	0.47±0.04(n=4)	+0.23%
	T_5F_3 D - HvHVP1/HvHKT1;5	3.18±0.19(n=7)	-5.71%	1.83±0.44(n=7)	+15.97%	0.55±0.1(n=7)	+16.82%
	T_5F_3 HvHVP1/null	3.09±0.11(n=18)	-8.17%	1.57±0.12(n=18)	-0.34%	0.5±0.03(n=18)	+6.18%
	T_5 310.8 C::HvHVP1	2.93±0.11(n=5)	-13.12%	1.55±0.1(n=5)	-1.8%	0.53±0.03(n=5)	+11.97%
	WT - GP	3.21±0.18(n=6)	-4.74%	1.56±0.22(n=6)	-0.7%	0.49±0.06(n=6)	+3.18%
		Shoot fresh weight (g)		**Root fresh weight (g)**		**Root:Shoot ratio FW**	
150 mM NaCl	*T_5 316.10 S::HvHKT1;5*	1.44±0.08(n=7)	-10.53%	0.73±0.05(n=7)	-5.77%	0.51±0.02(n=7)	+5.19%
	T_5F_3 HvHKT1;5/null	1.63±0.09(n=10)	+1.35%	0.8±0.05(n=10)	+2.42%	0.49±0.01(n=10)	+0.69%
	T_5F_3 A - HvHKT1;5/HvHVP1	1.55±0.16(n=6)	-3.81%	0.75±0.08(n=6)	-3.17%	0.49±0.02(n=6)	+2.21%
	T_5F_3 B - HvHKT1;5/HvHVP1	1.53±0.25(n=5)	-4.75%	0.71±0.13(n=5)	-8.28%	0.46±0.02(n=5)	-3.98%
	T_5F_3 null/null	1.61±0.07(n=16)	N/A	0.78±0.04(n=16)	N/A	0.48±0.01(n=16)	N/A
	T_5F_3 C - HvHVP1/HvHKT1;5	1.61±0.05(n=5)	+0.23%	0.74±0.06(n=5)	-4.41%	0.46±0.03(n=5)	-4.9%
	T_5F_3 D - HvHVP1/HvHKT1;5	1.68±0.12(n=6)	+4.7%	0.83±0.05(n=6)	+6.71%	0.5±0.03(n=6)	+3.3%
	T_5F_3 HvHVP1/null	1.69±0.07(n=20)	+5.31%	0.83±0.04(n=20)	+6.92%	0.49±0.01(n=20)	+1.44%
	T_5 310.8 C::HvHVP1	1.35±0.14(n=6)	-16.26%	0.7±0.06(n=6)	-10.47%	0.52±0.02(n=6)	**+8.67%**
	WT - GP	1.57±0.06(n=5)	-2.38%	0.73±0.05(n=5)	-5.7%	0.47±0.04(n=5)	-2.34%
		4th Leaf [Na^+] (µmoles.g^{-1} DW)		**4th Leaf [K^+] (µmoles.g^{-1} DW)**		**4th Leaf [Na^+]:[K^+] DW**	
0 mM NaCl	*T_5 316.10 S::HvHKT1;5*	39.21±2.44(n=6)	-5.86%	1.52±0.12(n=6)	+2.03%	0.57±0.05(n=6)	-7.59%
	T_5F_3 HvHKT1;5/null	41.14±1.85(n=12)	-1.23%	1.51±0.11(n=12)	+0.42%	0.44±0.02(n=12)	-1.12%
	T_5F_3 A - HvHKT1;5/HvHVP1	40.93±2.83(n=6)	-1.72%	1.64±0.11(n=6)	+2.98%	0.52±0.02(n=6)	-4.33%
	T_5F_3 B - HvHKT1;5/HvHVP1	41.14±1.83(n=6)	-1.21%	1.31±0.15(n=6)	+2.43%	0.42±0.04(n=6)	-3.2%
	T_5F_3 null/null	41.65±2.24(n=14)	N/A	1.57±0.13(n=14)	N/A	0.47±0.04(n=14)	N/A
	T_5F_3 C - HvHVP1/HvHKT1;5	39.13±2.59(n=4)	-6.04%	1.59±0.18(n=4)	+3.1%	0.47±0.04(n=4)	-8.67%
	T_5F_3 D - HvHVP1/HvHKT1;5	44.01±3.33(n=6)	+5.68%	1.83±0.44(n=7)	+8.35%	0.55±0.1(n=7)	-2.54%
	T_5F_3 HvHVP1/null	41.8±1.43(n=18)	+0.36%	1.57±0.12(n=18)	+3.33%	0.5±0.03(n=18)	-3.96%
	T_5 310.8 C::HvHVP1	34.89±3.67(n=5)	-16.23%	1.55±0.1(n=5)	-2.71%	0.53±0.03(n=5)	-14.27%
	WT - GP	38.31±2.24(n=6)	-8.02%	1.56±0.22(n=6)	+0.6%	0.49±0.06(n=6)	-8.13%
		4th Leaf [Na^+] (µmoles.g^{-1} DW)		**4th Leaf [K^+] (µmoles.g^{-1} DW)**		**4th Leaf [Na^+]:[K^+] DW**	
150 mM NaCl	*T_5 316.10 S::HvHKT1;5*	1649.4±48.38(n=7)	-7.8%	858.11±68.07(n=7)	-4.81%	2.01±0.19(n=7)	-0.6%
	T_5F_3 HvHKT1;5/null	1748.34±38.18(n=10)	-2.27%	878.84±32.19(n=10)	-2.52%	2.02±0.1(n=10)	+0.05%
	T_5F_3 A - HvHKT1;5/HvHVP1	1920.99±61.38(n=6)	+7.38%	923.08±45.19(n=6)	+2.39%	2.09±0.07(n=6)	+3.67%
	T_5F_3 B - HvHKT1;5/HvHVP1	1839.27±25.04(n=5)	+2.81%	875.61±53.61(n=5)	-2.87%	2.14±0.16(n=5)	+5.91%
	T_5F_3 null/null	1789.01±50.94(n=16)	N/A	901.52±29.52(n=16)	N/A	2.02±0.09(n=16)	N/A
	T_5F_3 C - HvHVP1/HvHKT1;5	1753.6±82.03(n=5)	-1.98%	908.09±38.28(n=5)	+0.73%	1.94±0.1(n=5)	-3.9%
	T_5F_3 D - HvHVP1/HvHKT1;5	1726.82±84.85(n=6)	-3.48%	875.17±31.82(n=6)	-2.92%	1.99±0.15(n=6)	-1.23%
	T_5F_3 HvHVP1/null	1741.97±51.86(n=19)	-2.63%	889.78±22.95(n=19)	-1.3%	1.99±0.09(n=19)	-1.57%
	T_5 310.8 C::HvHVP1	1540.41±97.06(n=6)	-13.9%	999.45±54.28(n=6)	+10.86%	1.58±0.17(n=6)	-21.63%
	WT - GP	1740.7±209.83(n=4)	-2.7%	938.67±52.48(n=4)	4.12%	1.86±0.21(n=4)	-7.72%

Table continued onto next page

		Root [Na^+] (µmoles.g^{-1} DW)		Root [K^+] (µmoles.g^{-1} DW)		Root [Na^+]:[K^+] DW	
0 mM NaCl	*T_5 316.10 S::HvHKT1;5*	60.08±2.75(n=6)	+0.32%	1.52±0.12(n=6)	+3.41%	0.57±0.05(n=6)	-3.3%
	T_5F_3 HvHKT1;5/null	61.43±1.54(n=12)	+2.58%	1.51±0.11(n=12)	-0.72%	0.44±0.02(n=12)	+3.45%
	T_5F_3 A - HvHKT1;5/HvHVP1	60.73±4.52(n=6)	+1.4%	1.64±0.11(n=6)	-1.11%	0.52±0.02(n=6)	+3.47%
	T_5F_3 B - HvHKT1;5/HvHVP1	62.53±4.19(n=6)	+4.41%	1.31±0.15(n=6)	+3.76%	0.42±0.04(n=6)	+0.49%
	T_5F_3 null/null	59.89±1.52(n=14)	N/A	1.57±0.13(n=14)	N/A	0.47±0.04(n=14)	N/A
	T_5F_3 C - HvHVP1/HvHKT1;5	57.93±4.46(n=4)	-3.27%	1.59±0.18(n=4)	-5.5%	0.47±0.04(n=4)	+2.13%
	T_5F_3 D - HvHVP1/HvHKT1;5	63.85±4.18(n=7)	+6.62%	1.83±0.44(n=7)	-4.57%	0.55±0.1(n=7)	**+11.59%**
	T_5F_3 HvHVP1/null	62.86±1.49(n=18)	+4.96%	1.57±0.12(n=18)	-0.08%	0.5±0.03(n=18)	+6.15%
	T_5 310.8 C::HvHVP1	61.05±3.55(n=5)	+1.94%	1.55±0.1(n=5)	+3.61%	0.53±0.03(n=5)	-1.92%
	WT - GP	57.54±1.19(n=6)	-3.92%	1.56±0.22(n=6)	-2.54%	0.49±0.06(n=6)	-1.25%
		Root [Na^+] (µmoles.g^{-1} DW)		**Root [K^+] (µmoles.g^{-1} DW)**		**Root [Na^+]:[K^+] DW**	
150 mM NaCl	*T_5 316.10 S::HvHKT1;5*	2704.57±58.13(n=7)	+1.67%	570.1±27.75(n=7)	-6.09%	4.79±0.18(n=7)	+5.89%
	T_5F_3 HvHKT1;5/null	2674.48±54.9(n=10)	+0.54%	586.43±19.91(n=10)	-3.4%	4.62±0.22(n=10)	+2.1%
	T_5F_3 A - HvHKT1;5/HvHVP1	2746.66±113.09(n=6)	+3.25%	526.96±20.93(n=6)	-13.19%	5.24±0.27(n=6)	+15.88%
	T_5F_3 B - HvHKT1;5/HvHVP1	2745.64±66.48(n=5)	+3.21%	596.09±34.69(n=5)	-1.8%	4.67±0.28(n=5)	+3.16%
	T_5F_3 null/null	2660.21±60.29(n=16)	N/A	607.05±32.6(n=16)	N/A	4.52±0.22(n=16)	N/A
	T_5F_3 C - HvHVP1/HvHKT1;5	2738.53±165.87(n=5)	+2.94%	523.05±31.84(n=5)	-13.84%	5.34±0.55(n=5)	+18.06%
	T_5F_3 D - HvHVP1/HvHKT1;5	2531.92±117.01(n=6)	-4.82%	560.9±20.14(n=6)	-7.6%	4.52±0.17(n=6)	-0.09%
	T_5F_3 HvHVP1/null	2624.9±57.08(n=20)	-1.33%	559.79±17.51(n=20)	-7.78%	4.74±0.12(n=20)	+4.8%
	T_5 310.8 C::HvHVP1	2601.97±80.39(n=6)	-2.19%	623.97±14.29(n=6)	+2.79%	4.17±0.11(n=6)	-7.76%
	WT - GP	2401.74±106.39(n=5)	-9.72%	525.53±30.25(n=5)	-13.43%	4.62±0.3(n=5)	2.05%
		4th Leaf [Cl^-] (µmoles.g^{-1} DW)		**Root [Cl^-] (µmoles.g^{-1} DW)**			
0 mM NaCl	*T_5 316.10 S::HvHKT1;5*	503.57±37.57(n=6)	-8.15%	1.52±0.12(n=6)	+34.03%		
	T_5F_3 HvHKT1;5/null	532.51±32.56(n=12)	-2.87%	1.51±0.11(n=12)	-3.22%		
	T_5F_3 A - HvHKT1;5/HvHVP1	546.9±32.79(n=6)	-0.24%	1.64±0.11(n=6)	+1.16%		
	T_5F_3 B - HvHKT1;5/HvHVP1	531.66±31.47(n=6)	-3.02%	1.31±0.15(n=6)	-3%		
	T_5F_3 null/null	548.24±23.6(n=14)	N/A	1.57±0.13(n=14)	N/A		
	T_5F_3 C - HvHVP1/HvHKT1;5	583.02±44.23(n=4)	+6.34%	1.59±0.18(n=4)	-2.23%		
	T_5F_3 D - HvHVP1/HvHKT1;5	622.11±60.08(n=6)	+13.47%	1.83±0.44(n=7)	-6.13%		
	T_5F_3 HvHVP1/null	546.09±18.58(n=18)	-0.39%	1.57±0.12(n=18)	-0.73%		
	T_5 310.8 C::HvHVP1	471.49±51.38(n=5)	-14%	1.55±0.1(n=5)	-13.94%		
	WT - GP	512.46±35.26(n=6)	-6.53%	1.56±0.22(n=6)	-1.08%		
		Shoot fresh weight (g)		**Root fresh weight (g)**			
150 mM NaCl	*T_5 316.10 S::HvHKT1;5*	1.44±0.08(n=7)	-10.53%	0.73±0.05(n=7)	-5.77%		
	T_5F_3 HvHKT1;5/null	1.63±0.09(n=10)	+1.35%	0.8±0.05(n=10)	+2.42%		
	T_5F_3 A - HvHKT1;5/HvHVP1	1.55±0.16(n=6)	-3.81%	0.75±0.08(n=6)	-3.17%		
	T_5F_3 B - HvHKT1;5/HvHVP1	1.53±0.25(n=5)	-4.75%	0.71±0.13(n=5)	-8.28%		
	T_5F_3 null/null	1.61±0.07(n=16)	N/A	0.78±0.04(n=16)	N/A		
	T_5F_3 C - HvHVP1/HvHKT1;5	1.61±0.05(n=5)	+0.23%	0.74±0.06(n=5)	-4.41%		
	T_5F_3 D - HvHVP1/HvHKT1;5	1.68±0.12(n=6)	+4.7%	0.83±0.05(n=6)	+6.71%		
	T_5F_3 HvHVP1/null	1.69±0.07(n=20)	+5.31%	0.83±0.04(n=20)	+6.92%		
	T_5 310.8 C::HvHVP1	1.35±0.14(n=6)	-16.26%	0.7±0.06(n=6)	-10.47%		
	WT - GP	1.57±0.06(n=5)	-2.38%	0.73±0.05(n=5)	-5.7%		

End of table

Barley supported hydroponics experiment #2 tabulated data

Appendix Table 8: Supported hydroponics experiment #2

To assessing salinity tolerance of lines with co-ordinated expression of *proC34:HvHVP1* and *proS147:HvHKT1;5*, selected T_6F_4 line, segregants and parental lines were screened in supported hydroponics and exposed to either 0 or 200 mM additional NaCl (plus additional $CaCl_2$ to maintain Ca^{2+} activity) on emergence of the 3rd leaf. Plants were harvested after 21 days growth. Root and shoot fresh and dry weight were measured. Root and 4th leave Na^+, K^+ and Cl^- content were measured as per section 2.4.4.1. Data tabulated is mean measurements ± S.E.M. significant differences ($P \leq 0.05$) from the T_6F_4 null line determined by one-way ANOVA, Tukey-Cramer HSD test and are highlighted in yellow.

		Total shoot FW (g)		Total Root FW (g)		Root:Shoot ratio FW	
0 mM NaCl	*T_6 316.10 S::HvHKT1;5*	13.17±1.07(n=5)	+12.42%	3.22±0.31(n=5)	+8.4%	0.24±0.01(n=5)	-4.1%
	T_6F_4 HvHKT1;5/null	11.04±1.14(n=6)	-5.74%	3.23±0.38(n=6)	+8.95%	0.29±0.02(n=6)	+15.07%
	T_6F_4 A - HvHKT1;5/HvHVP1	16.63±1.86(n=6)	**+41.97%**	3.98±0.34(n=6)	**+34.26%**	0.25±0.02(n=6)	-3.04%
	T_6F_4 B - HvHKT1;5/HvHVP1	12.84±0.3(n=12)	+9.66%	3.4±0.15(n=12)	+14.55%	0.26±0.01(n=12)	+3.82%
	T_6F_4 null/null	11.71±0.5(n=10)	N/A	2.97±0.14(n=10)	N/A	0.25±0.01(n=10)	N/A
	T_6F_4 C - HvHVP1/HvHKT1;5	15.78±1.06(n=12)	**+34.78%**	4.25±0.3(n=12)	**+43.11%**	0.27±0.01(n=12)	+6.27%
	T_6F_4 D - HvHVP1/HvHKT1;5	12.12±1.15(n=5)	+3.49%	3.45±0.27(n=5)	+16.35%	0.29±0.02(n=5)	+14.03%
	T_6 HvHVP1/null	11±0.87(n=6)	-6.11%	3.15±0.26(n=6)	+6.24%	0.29±0.01(n=6)	+12.68%
	T_6 310.8 C::HvHVP1	13.7±0.83(n=5)	**+17.01%**	3.95±0.33(n=5)	**+33.11%**	0.29±0.01(n=5)	+12.61%
	T_6 null	11.49±0.95(n=10)	-1.9%	3.27±0.31(n=10)	+10.16%	0.28±0.01(n=10)	+11.72%
		Total plant DW (g)		**Total Root FW (g)**		**Root:Shoot ratio FW**	
200 mM NaCl	*T_6 316.10 S::HvHKT1;5*	0.67±0.06(n=6)	+5.47%	2.32±0.23(n=6)	+18.31%	0.49±0.03(n=6)	+8.36%
	T_6F_4 HvHKT1;5/null	0.57±0.02(n=6)	-9.82%	1.9±0.11(n=6)	-3.32%	0.46±0.02(n=6)	+2.36%
	T_6F_4 A - HvHKT1;5/HvHVP1	0.81±0.07(n=5)	**+28.7%**	2.62±0.22(n=5)	**+33.53%**	0.46±0.04(n=5)	+3.32%
	T_6F_4 B - HvHKT1;5/HvHVP1	0.66±0.04(n=11)	+3.92%	2.15±0.12(n=11)	**+9.62%**	0.47±0.03(n=11)	+4.44%
	T_6F_4 null/null	0.63±0.05(n=11)	N/A	1.96±0.12(n=11)	N/A	0.45±0.03(n=11)	N/A
	T_6F_4 C - HvHVP1/HvHKT1;5	0.79±0.05(n=12)	**+24.6%**	2.5±0.13(n=12)	**+27.22%**	0.44±0.02(n=12)	-2.44%
	T_6F_4 D - HvHVP1/HvHKT1;5	0.71±0.06(n=7)	+12.16%	2.38±0.23(n=7)	**+21.49%**	0.44±0.03(n=7)	-1.6%
	T_6 HvHVP1/null	0.63±0.04(n=6)	-0.11%	2.11±0.24(n=6)	+7.63%	0.46±0.02(n=6)	+1.91%
	T_6 310.8 C::HvHVP1	0.86±0.08(n=6)	+36.92%	2.63±0.18(n=6)	**+33.87%**	0.43±0.02(n=6)	-4.9%
	T_6 null	0.68±0.04(n=11)	8.02%	2.17±0.13(n=11)	10.75%	0.44±0.02(n=11)	-2.03%
		Total shoot DW (g)		**Total Root DW (g)**		**Root:Shoot ratio DW**	
0 mM NaCl	*T_6 316.10 S::HvHKT1;5*	0.89±0.08(n=5)	+9.27%	0.15±0.01(n=5)	+10.23%	0.17±0.01(n=5)	-0.47%
	T_6F_4 HvHKT1;5/null	0.74±0.09(n=6)	-8.73%	0.15±0.03(n=6)	+8.98%	0.2±0.02(n=6)	+14.34%
	T_6F_4 A - HvHKT1;5/HvHVP1	1.09±0.08(n=6)	+34.51%	0.19±0.03(n=6)	+42.7%	0.17±0.01(n=6)	+1.62%
	T_6F_4 B - HvHKT1;5/HvHVP1	0.89±0.03(n=12)	+8.76%	0.17±0.01(n=12)	+28.21%	0.2±0.01(n=12)	+16.32%
	T_6F_4 null/null	0.81±0.05(n=10)	N/A	0.14±0.01(n=10)	N/A	0.17±0.01(n=10)	N/A
	T_6F_4 C - HvHVP1/HvHKT1;5	1.04±0.07(n=12)	+28.38%	0.19±0.02(n=12)	+42.65%	0.18±0.01(n=12)	+7.41%
	T_6F_4 D - HvHVP1/HvHKT1;5	0.79±0.1(n=5)	-2.5%	0.17±0.01(n=5)	+23.93%	0.22±0.02(n=5)	+27.95%
	T_6 HvHVP1/null	0.72±0.06(n=6)	-11.03%	0.16±0.02(n=6)	+15.81%	0.21±0.02(n=6)	+25.28%
	T_6 310.8 C::HvHVP1	0.89±0.08(n=5)	+9.36%	0.19±0.02(n=5)	+36.85%	0.21±0.01(n=5)	+23.24%
	T_6 null	0.78±0.08(n=10)	-4.21%	0.15±0.02(n=10)	+13.46%	0.2±0.01(n=10)	+18.43%
		Total shoot DW (g)		**Total Root DW (g)**		**Root:Shoot ratio DW**	
200 mM NaCl	*T_6 316.10 S::HvHKT1;5*	0.53±0.05(n=6)	+1.05%	0.13±0.02(n=6)	+27.5%	0.25±0.02(n=6)	+22.39%
	T_6F_4 HvHKT1;5/null	0.46±0.02(n=6)	-12.9%	0.11±0.01(n=6)	+5.56%	0.24±0.01(n=6)	+18.22%
	T_6F_4 A - HvHKT1;5/HvHVP1	0.67±0.06(n=5)	+27.26%	0.14±0.01(n=5)	+35.9%	0.22±0.01(n=5)	+5.01%
	T_6F_4 B - HvHKT1;5/HvHVP1	0.53±0.04(n=11)	+0.93%	0.13±0.01(n=11)	+18.82%	0.24±0.01(n=11)	+17.33%
	T_6F_4 null/null	0.53±0.04(n=11)	N/A	0.11±0.01(n=11)	N/A	0.21±0.01(n=11)	N/A
	T_6F_4 C - HvHVP1/HvHKT1;5	0.66±0.04(n=12)	+24.5%	0.13±0.01(n=12)	+25.12%	0.2±0.01(n=12)	-0.64%
	T_6F_4 D - HvHVP1/HvHKT1;5	0.58±0.05(n=7)	+9.92%	0.13±0.01(n=7)	+23.32%	0.23±0.01(n=7)	+9.71%
	T_6 HvHVP1/null	0.52±0.03(n=6)	-2.03%	0.12±0.01(n=6)	+9.41%	0.23±0.01(n=6)	+9.53%
	T_6 310.8 C::HvHVP1	0.71±0.06(n=6)	+35.62%	0.15±0.02(n=6)	+43.4%	0.21±0.01(n=6)	+3.06%
	T_6 null	0.56±0.03(n=11)	6.28%	0.12±0.01(n=11)	16.69%	0.22±0.01(n=11)	7.54%

Table continues onto next page

		4th Leaf [Na+] (µmoles.g-1 DW)		4th Leaf [K+] (µmoles.g-1 DW)		4th Leaf [Na+]:[K+] DW	
0 mM NaCl	T_6 316.10 S::HvHKT1;5	152.12±7.02(n=4)	**-11%**	1571.59±58.34(n=4)	**-14.15%**	0.1±0(n=4)	+3.49%
	T_6F_4 HvHKT1;5/null	158.21±4.55(n=6)	-7.44%	1652.97±41.97(n=6)	**-9.71%**	0.1±0(n=6)	+2.42%
	T_6F_4 A - HvHKT1;5/HvHVP1	168.62±4.45(n=4)	-1.35%	1814.62±101.75(n=4)	-0.88%	0.09±0.01(n=4)	+0.26%
	T_6F_4 B - HvHKT1;5/HvHVP1	158.61±7.58(n=12)	-7.2%	1761.04±52.66(n=12)	-3.8%	0.09±0(n=12)	-2.93%
	T_6F_4 null/null	170.93±4.7(n=9)	N/A	1830.68±48.72(n=9)	N/A	0.09±0(n=9)	N/A
	T_6F_4 C - HvHVP1/HvHKT1;5	150.04±7.59(n=11)	**-12.22%**	1761.76±81.69(n=11)	-3.76%	0.09±0(n=11)	-8.11%
	T_6F_4 D - HvHVP1/HvHKT1;5	148.29±10.26(n=5)	**-13.25%**	1854.96±67.27(n=5)	+1.33%	0.08±0(n=5)	-14.68%
	T_6 HvHVP1/null	143.6±10.55(n=6)	**-15.99%**	1862.73±147.23(n=6)	+1.75%	0.08±0.01(n=6)	-15.22%
	T_6 310.8 C::HvHVP1	158.17±8.36(n=5)	-7.46%	1839.02±44.86(n=5)	+0.46%	0.09±0.01(n=5)	-7.61%
	T_6 null	158.79±9.35(n=10)	-7.1%	1728.3±64.22(n=10)	-5.59%	0.09±0(n=10)	-2.03%
		4th Leaf [Na+] (µmoles.g-1 DW)		4th Leaf [K+] (µmoles.g-1 DW)		4th Leaf [Na+]:[K+] DW	
200 mM NaCl	T_6 316.10 S::HvHKT1;5	1843.35±67.77(n=6)	-4.91%	416.79±39.32(n=6)	+24.62%	4.67±0.56(n=6)	-23.44%
	T_6F_4 HvHKT1;5/null	2106.37±123.8(n=6)	+8.66%	344.48±35.15(n=6)	+3%	6.66±1.12(n=6)	+9.2%
	T_6F_4 A - HvHKT1;5/HvHVP1	1820.9±160.26(n=5)	-6.06%	411.32±72.31(n=5)	+22.98%	4.99±1.01(n=5)	-18.18%
	T_6F_4 B - HvHKT1;5/HvHVP1	2017.09±186.84(n=11)	+4.06%	422.72±28.43(n=11)	+26.39%	5.24±0.81(n=11)	-14%
	T_6F_4 null/null	1938.46±88.11(n=11)	N/A	334.46±18.08(n=11)	N/A	6.09±0.61(n=11)	N/A
	T_6F_4 C - HvHVP1/HvHKT1;5	1776.35±62.1(n=12)	-8.36%	421.55±31.01(n=12)	+26.04%	4.43±0.32(n=12)	-27.31%
	T_6F_4 D - HvHVP1/HvHKT1;5	2192.12±280.18(n=6)	+13.09%	386±48.76(n=6)	+15.41%	6.6±1.55(n=6)	+8.33%
	T_6 HvHVP1/null	1983.81±184.4(n=6)	+2.34%	437.92±31.21(n=6)	+30.94%	4.67±0.57(n=6)	-23.35%
	T_6 310.8 C::HvHVP1	1867.11±141.11(n=6)	-3.68%	384.19±31.49(n=6)	+14.87%	5.16±0.81(n=6)	-15.33%
	T_6 null	1639.87±116.47(n=10)	-15.4%	422.05±45.49(n=10)	26.19%	4.38±0.65(n=10)	-28.14%
		Root [Na+] (µmoles.g-1 DW)		Root [K+] (µmoles.g-1 DW)		Root [Na+]:[K+] DW	
0 mM NaCl	T_6 316.10 S::HvHKT1;5	120.33±5.89(n=5)	-4.01%	1495.96±68.09(n=5)	**-6.96%**	0.08±0(n=5)	+3.27%
	T_6F_4 HvHKT1;5/null	126.11±4.13(n=6)	+0.6%	1574.77±75.52(n=6)	-2.06%	0.08±0.01(n=6)	+3.87%
	T_6F_4 A - HvHKT1;5/HvHVP1	110.93±3.72(n=6)	-11.5%	1562.64±98.85(n=6)	-2.81%	0.07±0(n=6)	-7.93%
	T_6F_4 B - HvHKT1;5/HvHVP1	113.02±5.38(n=9)	-9.84%	1554.17±100.25(n=9)	-3.34%	0.07±0(n=9)	-5.71%
	T_6F_4 null/null	125.36±7.12(n=9)	N/A	1607.87±29.54(n=9)	N/A	0.08±0(n=9)	N/A
	T_6F_4 C - HvHVP1/HvHKT1;5	128.14±7.66(n=11)	+2.22%	1584.33±62.89(n=11)	-1.46%	0.08±0(n=11)	+3.53%
	T_6F_4 D - HvHVP1/HvHKT1;5	120.3±2.17(n=4)	-4.03%	1646.62±89.23(n=4)	+2.41%	0.07±0(n=4)	-5.54%
	T_6 HvHVP1/null	117.71±3.75(n=5)	-6.1%	1625.37±84.97(n=5)	+1.09%	0.07±0.01(n=5)	-6.21%
	T_6 310.8 C::HvHVP1	107.77±9.19(n=5)	-14.03%	1420.53±91.47(n=5)	-11.65%	0.08±0(n=5)	-2.91%
	T_6 null	116.18±3.37(n=9)	-7.32%	1543.54±57.55(n=9)	-4%	0.08±0(n=9)	-3.17%
		Root [Na+] (µmoles.g-1 DW)		Root [K+] (µmoles.g-1 DW)		Root [Na+]:[K+] DW	
200 mM NaCl	T_6 316.10 S::HvHKT1;5	1817.14±61.03(n=6)	+2.59%	362.74±58.53(n=6)	-9.02%	5.44±0.6(n=6)	+14.95%
	T_6F_4 HvHKT1;5/null	1788.66±49.09(n=6)	+0.98%	363.33±43.89(n=6)	-8.88%	5.23±0.53(n=6)	+10.46%
	T_6F_4 A - HvHKT1;5/HvHVP1	1815.58±83.75(n=5)	+2.5%	376.98±41.83(n=5)	-5.45%	5.21±0.96(n=5)	+10.08%
	T_6F_4 B - HvHKT1;5/HvHVP1	1746.42±69.33(n=11)	-1.4%	397.58±31.13(n=11)	-0.29%	4.62±0.35(n=11)	-2.4%
	T_6F_4 null/null	1771.28±51.41(n=11)	N/A	398.73±34.5(n=11)	N/A	4.74±0.36(n=11)	N/A
	T_6F_4 C - HvHVP1/HvHKT1;5	1795.56±43.29(n=12)	+1.37%	379.07±25.13(n=12)	-4.93%	4.97±0.34(n=12)	+4.92%
	T_6F_4 D - HvHVP1/HvHKT1;5	1736.73±119.45(n=7)	-1.95%	393.32±49.14(n=7)	-1.36%	5.05±0.88(n=7)	+6.54%
	T_6 HvHVP1/null	1828.08±107.53(n=5)	+3.21%	358.65±48.95(n=5)	-10.05%	5.36±0.51(n=5)	+13.06%
	T_6 310.8 C::HvHVP1	1905.26±53.73(n=5)	+7.56%	463.51±31.3(n=5)	+16.25%	4.19±0.31(n=5)	-11.61%
	T_6 null	1704.68±90(n=11)	-3.76%	346.4±25.26(n=11)	-13.12%	5.16±0.45(n=11)	9.03%
		4th Leaf [Cl-] (µmoles.g-1 DW)		Root [Cl-] (µmoles.g-1 DW)		Number of Tillers	
0 mM NaCl	T_6 316.10 S::HvHKT1;5	685.36±39.75(n=5)	-10.1%	178.35±19.67(n=5)	+1.74%	5.2±0.37(n=5)	**+30%**
	T_6F_4 HvHKT1;5/null	778.3±29.37(n=6)	+2.09%	174.6±15.17(n=5)	-0.4%	3.83±0.4(n=6)	-4.17%
	T_6F_4 A - HvHKT1;5/HvHVP1	822.39±35(n=6)	+7.87%	142.57±9.08(n=6)	-18.67%	5.17±0.48(n=6)	**+29.17%**
	T_6F_4 B - HvHKT1;5/HvHVP1	750.22±24.21(n=12)	-1.59%	143.25±8.04(n=12)	**-18.28%**	4.5±0.19(n=12)	+12.5%
	T_6F_4 null/null	762.37±24.79(n=10)	N/A	175.29±13.04(n=10)	N/A	4±0.26(n=10)	N/A
	T_6F_4 C - HvHVP1/HvHKT1;5	708.27±26.86(n=12)	-7.1%	158.47±6.17(n=12)	-9.6%	5.17±0.42(n=12)	**+29.17%**
	T_6F_4 D - HvHVP1/HvHKT1;5	701±40.09(n=5)	-8.05%	155.13±14.63(n=5)	-11.5%	4.4±0.51(n=5)	+10%
	T_6 HvHVP1/null	790.51±56.49(n=6)	+3.69%	157.56±7.8(n=6)	-10.12%	4±0.37(n=6)	0%
	T_6 310.8 C::HvHVP1	691.32±39.44(n=5)	-9.32%	152.89±7.58(n=5)	-12.78%	5±0.63(n=5)	+25%
	T_6 null	683.14±47.84(n=9)	-10.39%	173.15±15.77(n=10)	-1.22%	4.1±0.35(n=10)	+2.5%
		4th Leaf [Cl-] (µmoles.g-1 DW)		Root [Cl-] (µmoles.g-1 DW)		Number of Tillers	
200 mM NaCl	T_6 316.10 S::HvHKT1;5	1612.63±177.24(n=6)	+13.56%	541.61±53.62(n=6)	-7.62%	4±0.26(n=6)	+15.79%
	T_6F_4 HvHKT1;5/null	1727.02±122.14(n=6)	+21.62%	599.28±32.64(n=6)	+2.22%	3.17±0.17(n=6)	-8.33%
	T_6F_4 A - HvHKT1;5/HvHVP1	1487.91±209.6(n=5)	+4.78%	567.2±24.31(n=5)	-3.25%	4.2±0.37(n=5)	+21.58%
	T_6F_4 B - HvHKT1;5/HvHVP1	1628.6±199.18(n=11)	+14.68%	581.63±28.6(n=11)	-0.79%	4±0.19(n=11)	+15.79%
	T_6F_4 null/null	1420.07±80.11(n=11)	N/A	586.27±53.15(n=11)	N/A	3.45±0.21(n=11)	N/A
	T_6F_4 C - HvHVP1/HvHKT1;5	1337.94±69.08(n=12)	-5.78%	571.73±18.46(n=12)	-2.48%	4.25±0.3(n=12)	+23.03%
	T_6F_4 D - HvHVP1/HvHKT1;5	1873.16±265.43(n=6)	+31.91%	522.52±24.38(n=7)	-10.87%	4.57±0.75(n=7)	+32.33%
	T_6 HvHVP1/null	1586.87±214.71(n=6)	+11.75%	611.54±26.86(n=6)	+4.31%	3±0.37(n=6)	-13.16%
	T_6 310.8 C::HvHVP1	1516.17±229.19(n=5)	+6.77%	546.39±85.29(n=6)	-6.8%	5±0.45(n=6)	+44.74%
	T_6 null	1284.35±97.71(n=11)	-9.56%	607.19±72.44(n=11)	3.57%	3.82±0.23(n=11)	10.53%

End of table

Appendix IV: Media, Solutions and Equipment

Appendix IV: Sequencing Reaction clean-up

0.2 mM MgSO4 in 70 % Ethanol for MgSO4 post-sequencing clean-up

Component	Final Concentration	Weight/ Volume
1 M $MgSO_4$	0.2 mM	20 µL
100 % Ethanol	70 % v/v	7 mL
Milli-Q H_2O	-	3 ml
Notes: Stable at room temperature for approximately 1 week. Make up fresh if white precipitate forms.		

1M $MgSO_4$

Component	Final Concentration	Weight/ Volume
$MgSO_4$	1 M	120.37 g
Milli-Q H_2O	-	1 L
Notes: Stable at room temperature. Shake before use as precipitate may form.		

Appendix IV: Plant DNA Extraction solutions

Freeze Dry Extraction Buffer

Component	Final Concentration	Weight/Volume
Tris-HCL pH 7.5	0.1 M	
0.5 M EDTA pH 8.0	0.05 M	
Sodium dodecyl sulphate (SDS)	1.25 % v/v	
Milli-Q H_2O	-	To 1 L
Notes: Require 600 µL per sample.		

Appendix IV: Alkaline Lysis extraction of Plasmid DNA from *E. Coli*

Alkaline extraction Solution I

Component	Final Concentration	Weight/volume
Glucose	50 mM	4.95 g
Tris-HCL	2.3 % w/v	1.15 g
0.5 M EDTA	25 mM	3.33 mL
Milli-Q H_2O		Final volume of 500 mL
Notes: Require 100 µL per sample		

Alkaline extraction Solution II

Component	Final Concentration	Weight/volume
Sodium Hydroxide (NaOH)	0.2 M	4 g
20 % SDS Stock	1 % v/v	25 mL
Milli-Q H_2O	-	Final volume of 500 mL
Notes: Require 200 µL per sample		

Alkaline extraction Solution III

Component	Final Concentration	Weight/volume
Potassium acetate CH_3CO_2K	3 M	147 g
Milli-Q H_2O		Final volume of 500 mL
Notes: Adjust to pH 4.8 with 100% acetic acid (57.5 mL) Require 150 µL per sample		

Appendix IV: Arabidopsis Basal Nutrient Solution

Arabidopsis basal nutrient solution (B.N.S) adapted from Conn *et al.* (2013). Prepare stock solutions (1 through 10) separately as below in Appendix Table 9 and keep at 4°C protected from light for long term storage. NaFe(III)EDTA will form a precipitate if added to other micronutrients at stock concentrations and so is kept separate. Add specified volume of stock solutions to hydroponics tanks filled with 10 L of RO H2O to form B.N.S. Adjust final pH in tank to 5.6 with 1 M KOH (≈100 µL)

Appendix Table 9: Composition of Arabidopsis Basal Nutrient solutions for mini hydroponic growth.

Information included; Components of Macro- and micro-nutrient stock solutions (1 through 10), Molecular weight (MW), grams for each components to be added to Milli-Q H_2O to form stock solution; concentration of stock solution; Volume of each stock to be added to 10 L of RO H_2O to form nutrient solution (N.S.) and final B.N.S. concentration.

stock solutions (components)	MW ($g.mol^{-1}$)	g/L of Milli-Q H_2O for Stock	Stock Conc.	Volume/10L of N.S.	Final Conc.
Macronutrients					
1) NH_4NO_3	80	80 g	1 M	20 mL	2 mM
2) KNO_3	101.1	101.1 g	1 M	30 mL	3 mM
3) $CaCl_2$	101.98	101.98 g	1 M	1 mL	0.1 mM
4) KCl	74.55	74.55 g	1 M	20 mL	2 mM
5) $Ca(NO_3)_2•4H_2O$	236.1	94.44 g	0.4 M	50 mL	2 mM
6) $MgSO_4•7H_2O$	246.5	98.60 g	0.4 M	50 mL	2 mM
7) KH_2PO_4	136.1	13.61 g	0.1 M	60 mL	0.6 mM
8) NaCl	58.44	58.44 g	1 M	15 mL	1.5 mM
Micronutrients					
9) NaFe(III)EDTA	367.1	18.36 g	50 mM	10 mL	50mM
10) H_3BO_3	61.8	3.09 g	50 mM	10 mL	50 µM
$MnCl_2•4H_2O$	197.9	0.99 g	5 mM		5 µM
$ZnSO_4•7H_2O$	287.5	2.875 g	10 mM		10 µM
$CuSO_4•5H_2O$	249.7	0.125 g	0.5 mM		0.5 µM
$Na_2MoO_3.2H_2O$	242.0	0.0245	0.1 mM		0.1 µM

Appendix Table 10: Nutrient concentration and activity in mini-hydroponics with increasing additional NaCl (0 mM, 50 mM or 100 mM)

Macro- and micro-nutrient concentration and activity, under increasing NaCl concentrations (0 mM, 50 mM and 150 mM), with additional $CaCl_2$ (0 mM, 0.7mM, 1.4 mM) added to maintain Ca^{+2} activity. Calculated using Visual MinTEQ V 3.1 (Gustafsson, 2012), pH 5.6 and temperature of 22°C.

Macronutrients		*Concentration (mM)*			*Activity (mM)*		
Element	State	0 mM	50 mM	100 mM	0 mM	50 mM	100 mM
K	K^{+1}	5.6	5.6	5.6	4.7932	4.3672	4.1598
Ca	Ca^{+2}	2.1	2.8	3.5	1.0381	1.0156	1.0793
Mg	Mg^{+2}	2	2	2	1.0256	0.72241	0.60047
NH_4	$NH4^{+1}$	2	2	2	1.717	1.5892	1.533
Cl	Cl^{-1}	3.71	55.11	106.51	3.1863	43.084	79.265
NO_3	NO_3^{-1}	9	9	9	7.7512	7.0982	6.7921
SO_4	SO_4^{-2}	2.0105	2.0105	2.0105	0.89118	0.64299	0.53378
PO_4	$PO4^{3-}$	0.6	0.6	0.6	1.8487	1.6084	1.4741
Na	Na^{+1}	1.5502	51.55	101.55	1.3317	40.307	75.589
Micronutrients		*Concentration (mM)*			*Activity*		
Element	State	0 mM	50 mM	100 mM	0 mM	50 mM	100 mM
Fe	Fe^{2+}	0.05	0.05	0.05	21.92µM	17.24µM	15.24µM
Mn	Mn^{2+}	0.005	0.005	0.005	2.53µM	1.89µM	1.62µM
Zn	Zn^{2+}	0.01	0.01	0.01	4.95µM	3.60µM	3.04µM
Cu	Cu^{2+}	0.0005	0.0005	0.0005	230.62nM	174.84nM	150.98nM
Mo	MoO_4^{2-}	0.0001	0.0001	0.0001	30.68nM	27.82nM	25.82nM

Appendix IV: Barley hydroponics growth solutions

Appendix Table 11: Composition of barley nutrient solution for mini- and supported- hydroponics growth.

Information included; Components of Macro- and micro-nutrient stock solutions (1 through 10), Molecular weight (MW), grams for each components to be added to Milli-Q H_2O to form stock solution; concentration of stock solution; Volume of each stock to be added for each L of RO H_2O in hydroponics tanks (10 L for mini, 80 L for supported) to form nutrient solution (N.S.) and final concentration.

stock solutions (components)	MW ($g.mol^{-1}$)	g/L of Milli-Q H_2O for Stock	Stock Conc.	Volume/L of N.S.	Final Conc.
Macronutrients					
1) NH_4NO_3	80	80 g	1 M	5 mL	5.0 mM
KNO_3	101.1	101.1 g	1 M		5.0 mM
2) $Ca(NO_3)_2•4H_2O$	236.1	69.44 g	0.4 M	5 mL	2.0 mM
3) $MgSO_4•7H_2O$	246.5	72.5 g	0.4 M	5 mL	2.0 mM
KH_2PO_4	136.1	2.72 g	0.1 M		0.1 mM
4) $Na_2Si_3O_7$	122.0	89.6 mL	1 M	5 mL	0.5 mM
Micronutrients					
5) NaFe(III)EDTA	367.1	18.36 g	50 mM	1 mL	50mM
6) $MnCl_2•4H_2O$	197.9	0.99 g	5 mM	1 mL	5 µM
$ZnSO_4•7H_2O$	287.5	2.875 g	10 mM		10 µM
$CuSO_4•5H_2O$	249.7	0.125 g	0.5 mM		0.5 µM
$Na_2MoO_3.2H_2O$	242.0	0.0245	0.1 mM		0.1 µM

Notes:
All macronutrient stocks made up in 1L of Milli-Q H_2O.
$Na_2Si_3O_7$ sourced as sodium silicate in NaOH solution in (Sigma-Aldrich Co. Llc., Castle Hill, NSW, Australia. Cat. No. 338443-1L)
Store at 4°C and protected from light for long term storage.
Do not autoclave.
Adjustment of pH not required until used in growth solution.

For use in mini-hydroponics (10 L) system:
Fill tanks with 9780 mL of reverse osmosis H_2O
Add 50 mL of each macronutrient solution and 10 mL of each micronutrient solution to tanks.
Mix and adjust pH with 1M HCL to 6.5. Generally requires 3.2 mL.
For use in supported hydroponics (80 L) system:
Fill tanks with 78240 mL of reverse osmosis H_2O.
Add required volume of stock (400 mL of macronutrient stocks) of solution directly to tanks filled with reverse osmosis H_2O. Mix and adjust pH with 1 M HCL to 6.5.

Micronutrients solution (6) originally contained additional 50 µM H_3BO_3, however boron toxicity was observed in early hydroponics experiments due to excess boron in RO H_2O supply and so was left out from barley hydroponic solutions used in this thesis.
Adapted from (Genc *et al.*, 2007; Shavrukov *et al.*, 2012)

Appendix Table 12: Barley nutrient concentration and activity in mini and supported hydroponics with increasing additional NaCl (0 mM, 150 mM or 200 mM)

Macro- and micro-nutrient concentration and activity, under increasing NaCl concentrations (0 mM, 150 mM and 200 mM), with additional $CaCl_2$ (0 mM, 2.1 mM, 2.8 mM) added to maintain Ca^{2+} activity. Calculated using Visual MinTEQ V 3.1 (Gustafsson, 2012), pH 6.5 and temperature of 24°C.

Macronutrients		*Concentration (mM)*			*Activity (mM)*		
Element	State	0 mM	50 mM	100 mM	0 mM	150 mM	200 mM
K	K^+	5	5	5	4.304	3.593	3.508
Ca	Ca^{+2}	2	4.1	4.8	0.956	1.112	1.210
Mg	Mg^{+2}	2	2	2	0.985	0.519	0.475
NH_4	NH_4^+	0.2	0.2	0.2	0.173	0.150	0.148
Cl	Cl^-	0.01	154.21	205.61	0.009	111.180	144.680
NO_3	NO_3^-	9.2	9.2	9.2	7.991	6.750	6.616
SO_4	SO_4^{-2}	2.0105	2.0105	2.0105	0.931	0.472	0.427
Na	Na^+	0.5502	150.5502	200.5502	0.475	108.360	140.910
Micronutrients		*Concentration (mM)*			*Activity*		
Element	State	0 mM	150 mM	200 mM	0 mM	150 mM	200 mM
Fe	Fe^{+2}	0.05	0.05	0.05	14.301 µM	11.499 µM	11.201 µM
Mn	Mn^{+2}	0.005	0.005	0.005	2.001 µM	1.338 µM	1.2699 µM
Zn	Zn^{+2}	0.01	0.01	0.01	4.137 µM	2.512 µM	2.3298 µM
Cu	Cu^{+2}	0.0005	0.0005	0.0005	98.16 nM	90.115 nM	88.507 nM
PO4	PO_4^{-3}	2	2	2	0.303 nM	0.195 nM	0.17926 nM

Appendix IV: Antibiotics and selective agents

100 mg/mL Ampicillin Stock in Milli-Q H_2O

Component	Final Concentration	Weight/Volume
Ampicillin (Sigma-Aldrich Co. Llc., Castle Hill, NSW, Australia. Cat. No. A1593)	100 mg/mL	100 mg
Milli-Q H_2O		1 mL
Notes: Store at -20 °C Use 100 µL per 100 mL of media for final concentration of 100 µg/mL		

100 mg/mL Kanamycin A Stock in Milli-Q H_2O

Component	Final Concentration	Weight/Volume
Kanamycin sulfate from *Streptomyces kanamyceticus* (Sigma-Aldrich, Cat. No. K4378)	100 mg/mL	100 mg
Milli-Q H_2O	-	1 mL
Notes: Store at -20 °C Use 100 µL per 100 mL of media for final concentration of 100 µg/mL		

25 mg/mL Chloramphenicol Stock in 100 % Ethanol

Component	Final concentration	Weight/Volume
Chloramphenicol (Sigma-Aldrich, Cat. No. C0378)	25 mg/mL	250 mg
100 % Ethanol	-	10 mL
Notes: Store at -20 °C Use 100 µL per 100 mL of media for final concentration of 100 µg/mL		

50 mg/mL Hygromycin B Stock in 100 % Ethanol

Component	Final concentration	Weight/Volume
Hygromycin B from *Streptomyces hygroscopicus* (Sigma-Aldrich, Cat. No.H9773)	50 mg/mL	500 mg
100 % Ethanol	-	10 mL
Notes: Store at -20 °C Use 100 µL per 100 mL of media for final concentration of 50 µg/mL		

50 mg/mL Carbenicillin Stock in Milli-Q H_2O

Component	Final Concentration	Weight/Volume
Carbenicillin Disodium Salt (Sigma-Aldrich, Cat. No.C3416)	50 mg/mL	50 mg
Milli-Q H_2O	-	1 mL
Notes: Store at -20 °C Use 100 µL per 100 mL of media for final concentration of 50 µg/mL		

50 mg/mL Rifampicin Stock in Dimethyl sulfoxide (DMSO)

Component	Final Concentration	Weight/Volume
Rifampicin (Sigma-Aldrich, Cat. No. R7382)	50 mg/mL	50 mg
Dimethyl sulfoxide (DMSO) (Sigma-Aldrich, Cat. No. D4540)	-	1 mL
Notes: Store at -20 °C Protect from light Use 100 µL per 100 mL of media for final concentration of 50 µg/mL		

200 mg/mL Cefotaxime Stock in Milli-Q H_2O

Component	Final Concentration	Weight/Volume
Cefotaxime sodium salt (Sigma-Aldrich, Cat. No.C7039)	200 mg/mL	200 mg
Milli-Q H_2O	-	1 mL
Notes: Store at -20 °C Protect from light Use 100 µL per 100 mL of media for final concentration of 200 µg/mL		

Appendix IV: Loading Dyes

10× Sucrose DNA Loading Dye

Component	Final Concentration	Weight/Volume
Bromophenol Blue	0.4 % w/v	0.083 g
Xylene Cyanol	0.4 % w/v	0.083 g
Sucrose	65 % w/v	13 g
autoclaved Milli-Q H_2O	-	20 mL

Notes:
Dissolve sucrose into warm H2O. Allow to cool then add dyes.
Aliquot into 1 mL volumes. Store at -20 °C.
Use 1 µL per 10 µL of sample.
Approximate running size on Agarose gels:

	1 % gel	2 % gel
Xylene cyanol	≈5000 bp	≈500 bp
Bromophenol blue	≈500 bp	≈50 bp

6 × Orange G Loading Dye

Component	Final Concentration	Component
Orange G	0.4% w/v	0.083 g
Sucrose	40 % w/v	8 g
autoclaved Milli-Q H_2O	-	Final volume of 20 mL

Notes:
Dissolve sucrose into warm H_2O. Allow to cool then add dye.
Aliquot into 1 mL volumes. Store at -20 °C.
Use 1 µL per 5 µL of sample.
Approximate running size on Agarose gels:

	1 % gel	2 % gel
Orange G	≈100 bp	≈50 bp

Appendix IV: Bromocresol purple pH indicator gel

Bromocresol purple pH indicator gel

Component	Final Concentration	Weight/Volume
Bromocresol purple dye	0.06 $g.L^{-1}$	0.06 g
Agarose	0.75 % w/v	7.5 g
Milli-Q H_2O	-	Final volume of 1 L

Notes:
pH to 6.5 with 0.5 M NaOH while stirring – solution will appear purple
Microwave until agarose dissolves and keep stirring to prevent settling until solution is cooled to 30 °C.

Appendix IV: 50 × Tris base, acetic acid and EDTA (TAE) Buffer Stock

50× TAE Buffer Stock

Component	Final Concentration	Weight/Volume
TRIS-hydrochloride (Tris-HCl)	2 M	968 g
0.5 M EDTA Stock Solution	50 mM	400 mL
Glacial Acetic Acid	5.7 % v/v	228 mL
Milli-Q H_2O	-	Final volume of 4 L
Notes: Adjustment of final pH not required. pH 8.0 Use 400 mL 50 × TAE in 20 L of RO H_2O to make 1 × TAE for gel electrophoresis		

Appendix IV: 0.5 M Ethylenediamine tetra acetic acid (EDTA) Stock Solution

0.5 M Ethylenediamine tetra acetic acid (EDTA) Stock Solution

Component	Final Concentration	Weight/Volume
$Na_2EDTA.2H_2O$	0.5 M	186.1 g
Milli-Q H_2O		Final volume of 1 L
Notes: Buffer with NaOH pellets (approx.. 15 g) to pH 8.0 Na_2EDTA will not enter solution until pH is adjusted.		

Appendix IV: Media

Appendix IV: Luria Broth (LB medium)

Component	Final Concentration	Weight/Volume
Bacto Tryptone Bacto-tryptone (DB Co. Australia, North Ryde, NSW, Australia. Cat. No: 211705)	1 % w/v	10 g
Yeast extract (DB Co. Australia, North Ryde, NSW, Australia. Cat. No: 212750)	0.5 % w/v	5 g
Sodium Chloride (NaCl)	1 % w/v	10 g
Milli-Q H_2O	-	Final volume of 1 L
Notes: Adjust to pH 7.5 with 1M NaOH. Autoclave before use.		

Appendix IV: Luria Broth Agar (LBA)

Component	Final Concentration	Weight/Volume
Difco™ granulated Agar (DB Co. Australia, North Ryde, NSW, Australia. Cat. No: 214530)	1.5 % w/v	1.5g
LB media	-	100 mL
Notes: Autoclave before use. To make LBA plates, microwave and allow to cool to 60°C before adding antibiotics if required.		

Appendix IV: Super Optimal Broth (SOB medium)

Component	Final Concentration	Weight/Volume
Bacto-tryptone (DB Co. Australia, North Ryde, NSW, Australia. Cat. No: 211705)	2 % w/v	20 g
Yeast extract (DB Co. Australia, North Ryde, NSW, Australia. Cat. No: 212750)	0.5 % w/v	5 g
Sodium Chloride (NaCl)	0.06 % w/v	0.6 g
Potassium Chloride (KCl)	0.019 % w/v	0.19 g
Milli-Q H_2O	-	Final volume of 1 L
Notes: Adjust to pH 7.5 with 1 M NaOH Autoclave before use. Stable at room temperature.		

Appendix IV: GUS Staining Buffer

β-glucuronidase (GUS) stain

Component	Weight/Volume
1 M Na Phosphate Buffer pH 7.0	1000 µL
0.5 M EDTA Stock	400 µL
10 % Triton X-100 Stock	200 µL
0.1 M Potassium Ferrocyanide	400 µL
0.1 M Potassium Ferricyanide	400 µL
40 mg/mL X-Gluc	250 µL
25 mg/mL Chloramphenicol	200 µL
Milli-Q H_2O	17.15 mL
Total:	20 mL

Notes:
Prepare on ice and protect from light.
GUS stain can be stored short-term (1-2 weeks) at -20 °C before use.
Adapted from (Jefferson *et al.*, 1987)

10 % Triton X-100 Stock

Component	Final Concentration	Weight/Volume
Triton X-100	10 % v/v	10 mL
Milli-Q H_2O	-	90 mL

Notes:
Triton X-100 sourced from:
Heat to 65 °C to dissolve Triton X-100 then autoclave.

0.1 M Potassium ferrocyanide ($K_4[Fe(CN)_6]$) Stock

Component	MW	Weight/Volume
Potassium ferrocyanide ($K_4[Fe(CN)_6].3H_2O$)	422.388 $g.mol^{-1}$	4.2241 g
Milli-Q H_2O	-	100 mL

Notes:
Store at 4 °C and protect from light

0.1 M Potassium ferricyanide ($K_3[Fe(CN)_6]$) Stock

Component	MW	Weight/Volume
Potassium ferricyanide ($K_4[Fe(CN)_6]$)	329.24 $g.mol^{-1}$	3.2926 g
Milli-Q H_2O	-	100 mL

Notes:
Store at 4 °C and protect from light

40 mg/ml X-Gluc Stock in DMF

Component	Final Concentration	Weight/Volume
5-Bromo-4-chloro-3-indolyl-β-D-glucuronide (X-Gluc)	40 mg/mL	0.04 g
Dimethylformamide (DMF)	-	1 mL
Notes: Store at -20 °C and X-Gluc ourced from: Gold Biotechnology® Inc., St. Louis, MO, USA via Everest Resources Pty. Ltd., Boondall, QLD, Australia, Cat. No. N1030011-3/1		

1 M Na Phosphate Buffer pH 7.0

Component	MW	Final Concentration	Weight / Volume
Disodium phosphate dihydrate (Na_2HPO_4)	141.96 g.mol-1	1 M	35.49 g
Sodium dihydrogen phosphate monohydrate ($NaH_2PO_4.H_2O$)	137.99 g.mol-1	1 M	34.50 g
Milli-Q H_2O	-	-	250 mL
Notes: Adjust pH to 7.0 with 1 M NaOH Autoclave before use			

Appendix IV: Chloride analysis solutions

Combined Acid Buffer

Component	Final Concentration	Weight/Volume
Glacial acetic acid	10.9 % v/v	109 mL
69.5 % Nitric Acid	0.6255 % v/v	9 mL
Milli-Q H_2O	-	Final volume of 1 L
Notes: Stable at room temperature.		

Gelatine Solution

Component	Final Concentration	Weight/Volume
Gelatine	0.12 % w/v	1.2 g
Milli-Q H_2O	-	1 L
Notes: Using a heating magnetic stirrer, apply gentle heat and stir until dissolved. Store at 4 °C. Allow to warm to room temperature before use.		

Appendix IV: Milli-Q Ultra-Pure H_2O

Ultra-pure H_2O (18.2 MΩ·cm at 25 °C) was sourced from a Milli-Q Plus Laboratory Water purification system (EMD Millipore® Corp. Billerica, MA, USA) using a RephiQuatro U Pack 1 filter (RephiLe Biosciences, Ltd. Boston, MA, USA, Cat. No. RR100Q101). Unless specified otherwise, Milli-Q H_2O was autoclaved prior to use.

Appendix IV: Electromagnet for extraction of ball-bearings

To assist with the removal of stainless steel ball-bearings used for grinding of plant tissues for RNA and gDNA extractions an electromagnetic wand was developed. Previously, a small rare-earth magnet was used to draw the ball-bearings from the tube, however it was difficult to remove ball-bearings from the magnet once completed and use posed a risk of contaminating samples and safety hazard by splashing of extraction buffers. The electromagnet outlined below in Appendix Figure 11, allows the extraction of ball-bearings when activated by the push switch, which then fall away when the switch is released. This allows rapid and safe processing of large number of samples with reduced cross contamination. Although not shown below, a rubber glove over the magnet (L1) protects the magnet from extraction buffer solutions and assists in reducing cross contamination of samples.

Appendix Figure 11: Schematic diagram of electromagnet wand developed.
Overview (a) and (b) circuit diagram of the electromagnetic wand and (c) tabulated parts list.

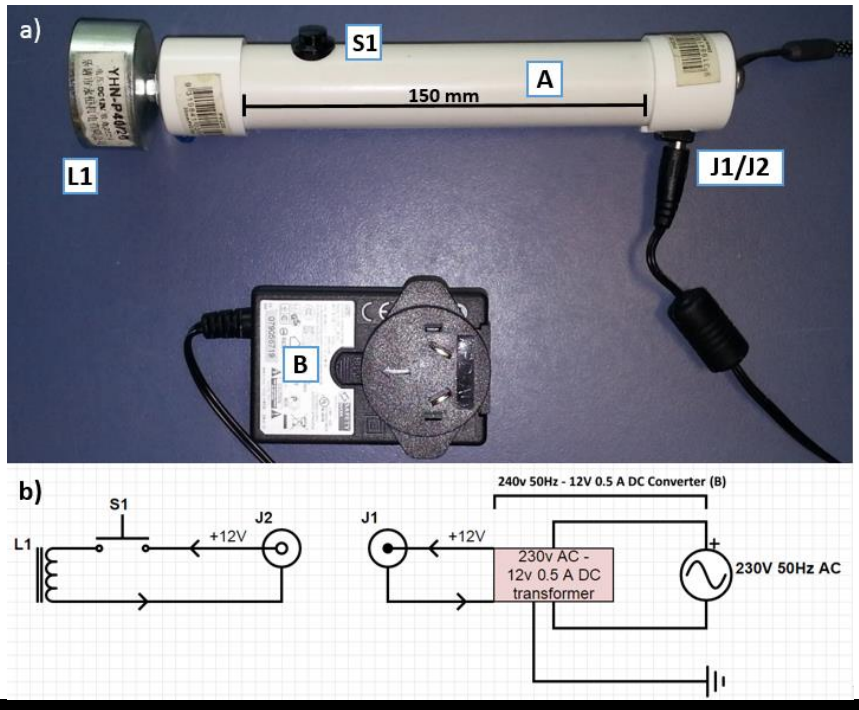

c)	Parts list
L1	Electromagnet coil (25kg lift, max input:12V 0.67A 8W) Part No: YHN-P40/20 Attached to tubing via 5 mm bolt.
S1	SPST push switch (N/O) (Jaycar Electronics Pty. Ltd., Adelaide, Australia, Cat. No: SP0700)
A	150 mm length 25 mm PCV tubing – capped
J1-2	low voltage DC 2.5mm plug/socket (Jaycar Electronics Pty. Ltd., Adelaide, Australia, Cat. No:PS0520)
B	240AC 50Hz – 12V 1.5A DC converter with 2.5mm male plug

Appendix V: Promoter Sequences

>minimal Cauliflower Mosaic Virus 35S (*CaMV35s*) promoter sequence (92bp)

```
   1  TACTCCACGT CCATAAGGGA CACATCACAA TCCCACTATC CTTCGCAAGA CCCTTCCTCT
  61  ATATAAGGAA GTTCATTTCA TTTGGAGAGG AC
```

>1×*HAP1* Upstream activation sequence (UAS_{HAP1}) motif (18bp)

```
   1  CACGGACTTA TCGGTCGG
```

>5 repeats of $HAP1_{UAS}$ fused to minimal *CAMV35s* promoter (5×$HAP1_{UAS}$*:minimal_CaMV35s*) (193bp)

```
   1  TAGCACGGAC TTATCGGTCG GAGCACGGAC TTATCGGTCG GAGCACGGAC TTATCGGTCG
  61  GAGCACGGAC TTATCGGTCG GAGCACGGAC TTATCGGTCG GTACTCCACG TCCATAAGGG
 121  ACACATCACA ATCCCACTAT CCTTCGCAAG ACCCTTCCTC TATATAAGGA AGTTCATTTC
 181  ATTTGGAGAG GAC
```

>1×*GAL4* Upstream activation sequence (UAS_{GAL4}) motif (17 bp)

```
   1  CGGAGTACTG TCCTCCG
```

>5 repeats of $GAL4_{UAS}$ fused to minimal *CAMV35s* promoter (5×$GAL4_{UAS}$*:minimal_CaMV35s*) (206bp)

```
   1  GGTCGGAGTA CTGTCCTCCG AGCGGAGTAC TGTCCTCCGA GCGGAGTACT GTCCTCCGAG
  61  CGGAGTACTG TCCTCCGAGC GGAGTACTGT CCTCCGAGCG GAGACTCTAG AAGCTACTCC
 121  ACGTCCATAA GGGACACATC ACAATCCCAC TATCCTTCGC AAGACCCTTC CTCTATATAA
 181  GGAAGTTCAT TTCATTTGGA GAGGAC
```

Alignment of *HAP1* (UAS_{HAP1}) and GAL4 (UAS_{GAL4}) Upstream activation motifs (* indicates conserved nucleotides)

```
UASHAP1   CACGGACT- - TATCGGTCGG - 18 bp
UASGAL4   - - CGGAGTACTGTCC- TCCG - 17 bp
            * * * *   *    *  * *    * *  *
```

>*proC34*–putative root cortex-specific promoter (Rice cv. Nipponbare) sequence (2486bp)

```
   1  GCCAACTGAA ACGCCACGTC ATGCTGAACG TTAATGGGGA GGAAGGTGCT TTTACCCATG
  61  TCAATTCCTT CTTTTTACCA TGCATCCCCC GTTCGTTTTC CCATGATTTT AGATACTTTT
 121  TTTTTGTCCC CGATCGAATC ACAGATCATT TTTCATTACT GCAGTTGCAA GGATGTGGCA
 181  AAAAATATCA TCTAGACCAG TTGGTTGATT TGTCACCTAC ATTTATTCAG ATCTAATAAG
 241  AATATAAGTC AACAAGTTGG TTTTTAAATT CGATGTGTAT ATATCTTTAA GCCGACGATA
 301  TGTATTTCAG TAATGACCTT TACCCGGTGA AGCTTTTTTT TCTTAATTGG TATATACAGG
 361  ATAATAGTAT GTTTTAAACT CTCTATCAAG AAAGAGCAGC TAAGCTGGAT GGGCTCTCCA
 421  ATTTATGTTA ATTTAATAAT TCCCTCGATA ACAAGATAAA TGATCTCCAG TCATTTCTTG
 481  ACCATTGTTC TACTTTACCT ATGACTTTAT AAAATCCTGT AGCAACGTGC TGAGTATCAC
 541  CCAATAAACA TAAGAAAACA CACCATGCAT GTTCTAGTGA GCATCTTGAT GCTGGTAGGA
 601  TAACTAGCGA GCTAAATAAA GCTAAGGGTC GGATGCGACA TGGGTGCTAG CGAATAGAGC
 661  TTTTCTGCCT TGTTAGGGTG CGTTTGGAAT CAGCTGTTGC ATGTCCGAGC AGTATATGAG
 721  CGCGTGATTA ATTAAGTATT TTCTTTTTTT TCAAAAATAG ATAATATAAT TTTTTAAGCA
 781  ACTTTCGTAT ATAAACTTTT TTTAAAAAAC ACGCCGTTTA GTAGTTTAAA AAACGTGCGC
 841  GCGAAATACA ACGGAGAGGG ATTGGAAACA CAGGATTCCA AACACAGCCT GAATCGTCAT
 901  TGATACAAGG AAAGATGGGA GGAGGAACAA GAGGGAGAGG AGCAATAGTT TGGGGGATGA
 961  TCCCCTCCAT TAATTTCTCA TTCTGGATCT GTGCTACTTC CTCCGTTTCA TAATATAAGT
1021  CATTCTAGCA TTTATCTATC TAGATTCATT AATATCAATA TGAATGTGGA AAATACCAGA
1081  ATGACTTACA TTGTGAAACG GGGGAGAGTA GCTAGGAATG GATAAATAAA TAATGTTATC
1141  CCAAACAGAA AAAGTTACGT ACGGCCGGGT ATGTGCTTCA CGTGAAATGG GAAATATATA
1201  CAATCAATGA CGACTAATTT GGCAGCAAAC ATGCATGCAT GGGCCAGTTA ATTAATTATG
1261  CTAAATGGAT AGTTTGATTC GATGAGCAGC CGGACGACTG AGGCTTTCTT TTGTTGGGAA
1321  AAAAATTAGG TTTGATTGTC ACATCAGATA TACGGATATA CATTTGAAGT ATTAAACGTA
1381  GTTTAAAAAC AAAATAAATT ATAGATTCTA CTAAAAAACT GCGAGATAAA TTTATTAAGC
1441  CTAATTAATT CGTTATTAGC AAATGCTTAC TGTAGCACCA CATTGTCAAA TCATGGTGCA
1501  ATTTGGTTTA AAAATTTTGT CTCGTAATTT ACACGTAATA TGTGTAATTG GTTTTTTCCT
1561  ACATTAAATA CTTCATGCGT ATGTCTAAAC ATTTGATGTG ACAGTGTGAA ATTTTTTTTT
1621  TAAATAGGGC CTGAGAGCAA AACACATGCT GCATGAATAG TAGTCGCTCG CTCGTGTATC
1681  ATACTTAAAG AAAGTTTAAC TAGGAAAAAA AAACCTACTT CATATATAAA ATCACAAGAC
1741  CTTTTATCCA AAAATTGAAA CTTTCAACTA AAAGTTCAAA AAAATTATAC TCTTGGCTCA
1801  AACTTTCAAT ATAAAAACCC AAAACTTCTA ATCCAAAAAC TGAAACTTCC CAAAAAAATC
1861  AAAAACTTTG TGCTCATGGC TCTCAATCTT TCGATACGAA GTTACAGAAT CATGGTAGGG
1921  TAGCTAGCTA AATAAAGGGA CGGATGCGAT ATGGGTGCTA GCGAATAGAG CCTTTCTACC
1981  TTGCTGAATC GTCATTGATA ATTAGGGGAG GAGGAACAAG AGGGAAAGGA GCAATAGTTT
2041  GGGGATGATC CCCTCCATTG AATAATTTCT CATTCTGGAT CCGTGCTAGG GATGGATCAA
2101  TAATGTTATC CCAAACAGAA ACAGCTAGTG TTAGGTACGG GTATGTGCTT CACGTGAAAT
2161  GGGAAATATA TACAATCAAC GATGACTAAT TTGGTAGTAA GCATACATGC ATGGGCCAAT
2221  TAATTAATTA TGCTAAATGG ATATAGTTTG ATTCGATCAG CAGCTGAACG ACTGATCGAG
2281  AGCAAAACAC ATGCATAATG CATAATGCAT TAATTTATAT ATATGAATAG TAGTCGCTCG
2341  CTCGTGTATC ACGCATAAAT TATATATCAA TGATCGATCA CATGCAACAC CGGCAAATTA
2401  AATTGACCCA TCATCGATCC ATCTAGCTAG CTATGCCTAT ATATATACGC CATATGCATG
2461  ATAAATAC
```

>*proS147*–putative root stele specific promoter (Rice cv. Nipponbare) sequence (2000 bp)

```
   1  CTGATGATCG ACCACTATTA GACATCGGGT TATTAGAGGC GATCCAAAAA CCCCACTAGA
  61  GATGGTTTTG TGAATTGTCT ATGCACGTGC GTCATTGCAA TCTGCCTTAG ACATATTTCA
 121  ACAAATAAGT CAGAAAAACC TACCCACATA ATCTACTTAC CAGAGATAGT AAAAAAACCG
 181  CCTTAGACAT ATGTCTTGTC AATACAATTA TGAACGAGGT ACAATATTAT ATTATATATA
 241  TTTACAGACA ATTATGTCCT ATGAGGATTT CTTATTTAAT ATTTATGGTT TTATGGATCT
 301  ATCTTATGAC TATATCTCTA GAATTAATTA GTACTCCACC TCAAACATCA TGTCCTAGCT
 361  AGGCCCGTTC GGTTTATATT ATTGAGTGGA TAAAATTGAC ATATATTATT TACTTAATTA
 421  TAGAGATAGA ATAAATATTT TAAAATATAA ACTTAAAAAA TATCATCCTA AGATATAAGC
 481  ATTAGTGGCT ATGATTTTAG ACATACATTT ATCCAGATTG ATAGCTAAAA ATAGTTATAT
 541  TTTAGGATAA AGGCAGTACC TTAAAACAAG TGGTCTAAAC AATCCAATAC AAGGATGCAT
 601  TTTTGAAGCG TTGAGCGAAT AATCCATTTG CATAATCCAG CGAATATGTT GTTGTATGTA
 661  TCGGACATTG ACAATATTAT CTGTAGAATA TAGCTTTAAT CTCCAATTTT TATTTAAAAA
 721  ATATGTTATA TTTGAAAAGA TAATGAAATT TGTGATCGTG TTTGGATTCA ACCCGAGTTC
 781  AAATCCTGGT TACAAATAGA AACATTTACG CTTAGAATCG ACCTATAGAG ACAGGGTCCT
 841  CGTGTATTAG ACACAGGTTG CCTGTTTGGT AGAGCTCTAA CTCCTAAATT TAGCTCCAGG
 901  AGTTGGGTCT AGAATGGAGT TGTGGAGCTG CCTAAACCCA GCTCCACCTC TCTAGTTCAT
 961  TCTATGAGAG AGCTCCACCT AACTCTGCTT CTATTTTAGG TGGAGCTGGA GTTGAAGCTG
1021  TGCCAAATAG GCCCTTAATT AAGGCACGAT TCATAGGGGA TAGCTCCTGT CATCCTGTGC
1081  AGGGGACCTG CTTCTATGGC CTTTCTTGAA TCCAAATTTA GGTATTTCTT ATTTGAAATA
1141  CCTTGGGTAG GTATTTAATT TCCCTTAAAG CCGAGGGTTT CTTTAAAAAA AGAAATGAAA
1201  TTTCGATATT TTGATAGTAT TGTTTTTCAA TAGAATTTTT TTTTCATGTT TTCAATCTAC
1261  TCACTCCTAT TCAGAGAAGT ACTGACAGCA ATGTTTAACC CCACCTAACC CAAAATCACT
1321  AATTTTTTGT ACTCAATGGA GTATCTTGCT AGATTTTCCA ATTAAGCACA TAATCGTACA
1381  TGCATGCATG TACATTCCAC AAAGGATGTA TACATGCATA CTCCAGGAGT ATTAGTGATG
1441  TCATCCGCAG GGATATGGAA CTGTCACTTC TTCAGAGACT TCAGTGAAAA GTAACACTTG
1501  TTTAAGAACA GAGATATCCT ATATCCAACG TCGCCGCAGG TAGTGGAGTT TACAGAAATC
1561  TTTTAACTTG CTAGTGGACG CACGACGCAT GTTGGGGCGA AACTGCGTAT GAAAATTTTC
1621  GTTATCTTCC CCAAATTTTC CACCCATATC GTGCAGGTAT TCCACAGACC AAGGATACAT
1681  ATATTATGCA TATTTATGCA CGTGATTACA CTGCATAAAC AAACAGTTAG TGGGACTGTA
1741  ACAAGACAAT CAAGCAAAAA TAGGTTGTGT CTTACGTAAG AGTAATAATT AACACAGACA
1801  CAGCTAGCTC GTATTGTGGT TTAATTGTGG ATTCCTACTC AAACTACACA CAATGAACAG
1861  ATTAATTTGG AGTAGTAGTG GAATGCAGTG AATATAATCA TGTACTACAG CAGTATATTA
1921  TGCAAGTAGT CCACTTCTTC AGGGTTCAGG GGTTGCCTTT TACGCCTGTA TAAATTGGTA
1981  CTCTTGCGTA GTTTACAAGC
```

Appendix VI: Supplementary micrographs

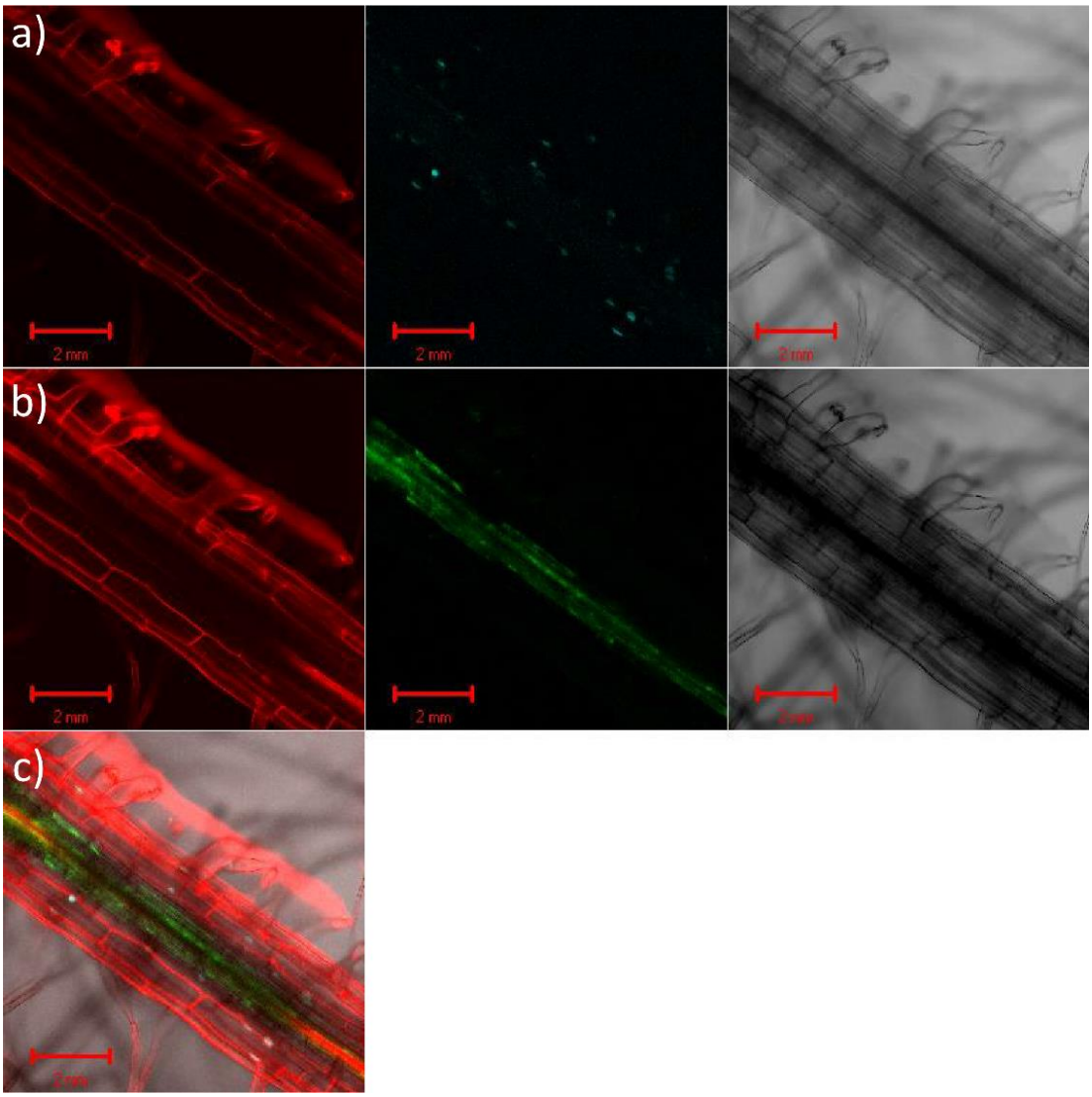

Appendix figure 12: Supplementary confocal micrographs of roots dual enhancer-trap line HAP1C-J2371*c shows the presence of mGFP5-ER and H2B::CFP fluorescence in separate and distinct root-cell types.
Representative multilayer confocal image of a 3 week old seedlings of dual *HAP1-VP16* and *GAL4-VP16* enhancer-trap line HAP1C-J2371*C A, grown on vertical MS plates (as per section 2.3.3) and imaged by confocal microscopy (as per section 2.6). CFP layer (a), GFP layer (b) and merged GFP/CFP layers (c). Cells walls stained with propidium iodine appear red, ER localised mGFP-ER fluorescence appears green, nuclear localised H2B::CFP fluorescence appears blue, bright field image in grey. CFP fluorescence can be seen in the cortical/epidermal cell types, GFP fluorescence in the root stele.

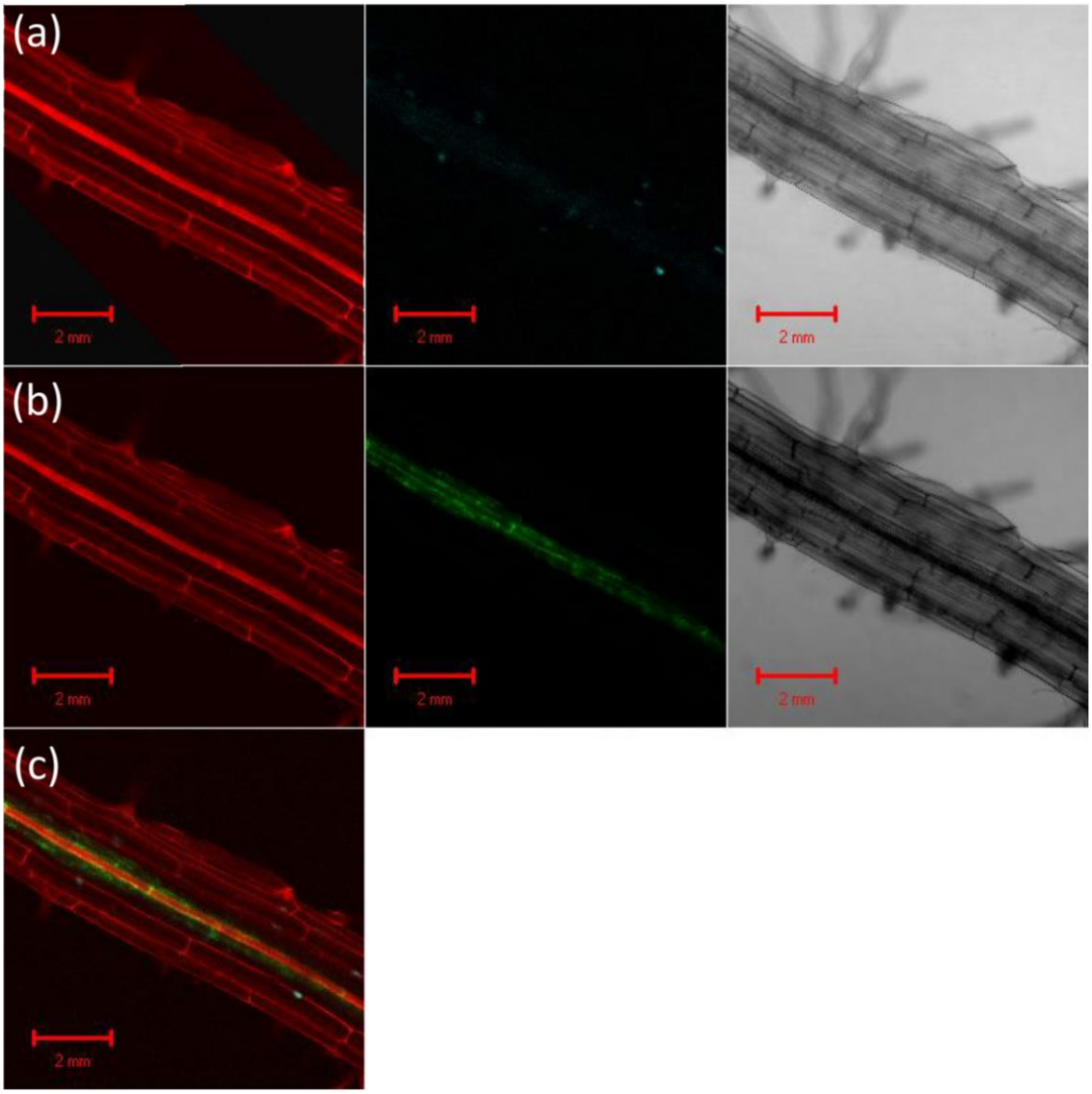

Appendix figure 13: Supplementary confocal micrographs of roots dual enhancer-trap line HAP1D-J2371*c shows the presence of mGFP5-ER and H2B::CFP fluorescence in separate and distinct root-cell types.
Representative multilayer confocal image of a 3 week old seedlings of dual *HAP1-VP16* and *GAL4-VP16* enhancer-trap line HAP1D-J2371*C A, grown on vertical MS plates (as per section 2.3.3) and imaged by confocal microscopy (as per section 2.6). CFP layer (a), GFP layer (b) and merged GFP/CFP layers (c). Cells walls stained with propidium iodine appear red, ER localised mGFP-ER fluorescence appears green, nuclear localised H2B::CFP fluorescence appears blue, bright field image in grey. CFP fluorescence can be seen in the cortical/epidermal cell types, GFP fluorescence in the root stele.

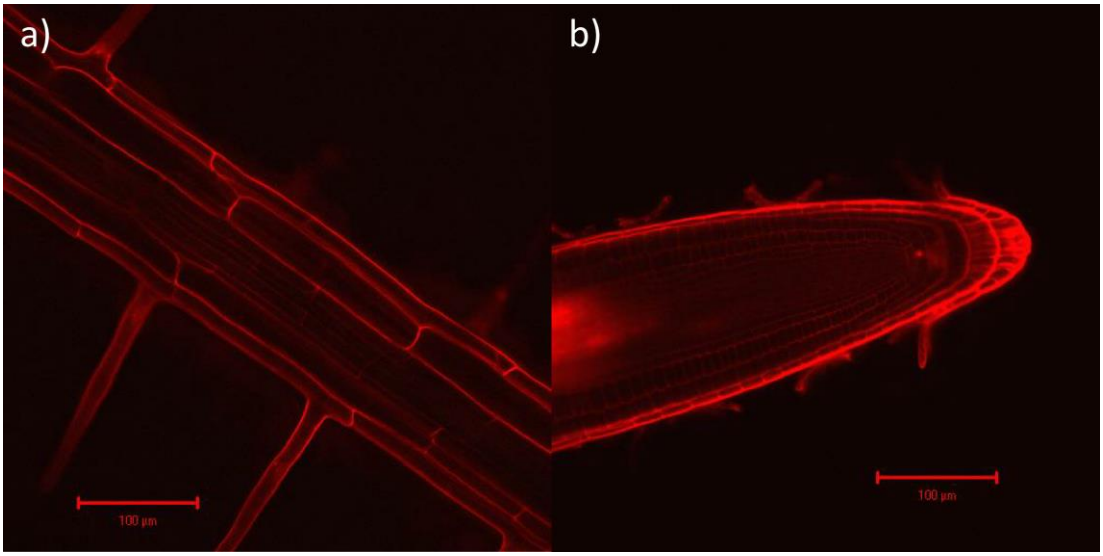

Appendix figure 14: Confocal micrographs of roots of wild-type Arabidopsis C24 for mGFP5-ER and H2B::CFP fluorescence.
Representative confocal images of 3 week old seedlings of wild-type Arabidopsis C24, grown on vertical MS plates (as per section 2.3.3) and imaged for mGFP-ER and H2B::CFP fluorescence by confocal microscopy (as per section 2.6). Mature root (a) and root tip (b).
Approximately 10 seedlings screened per line. GFP or CFP fluorescence was not detected in any tissues.

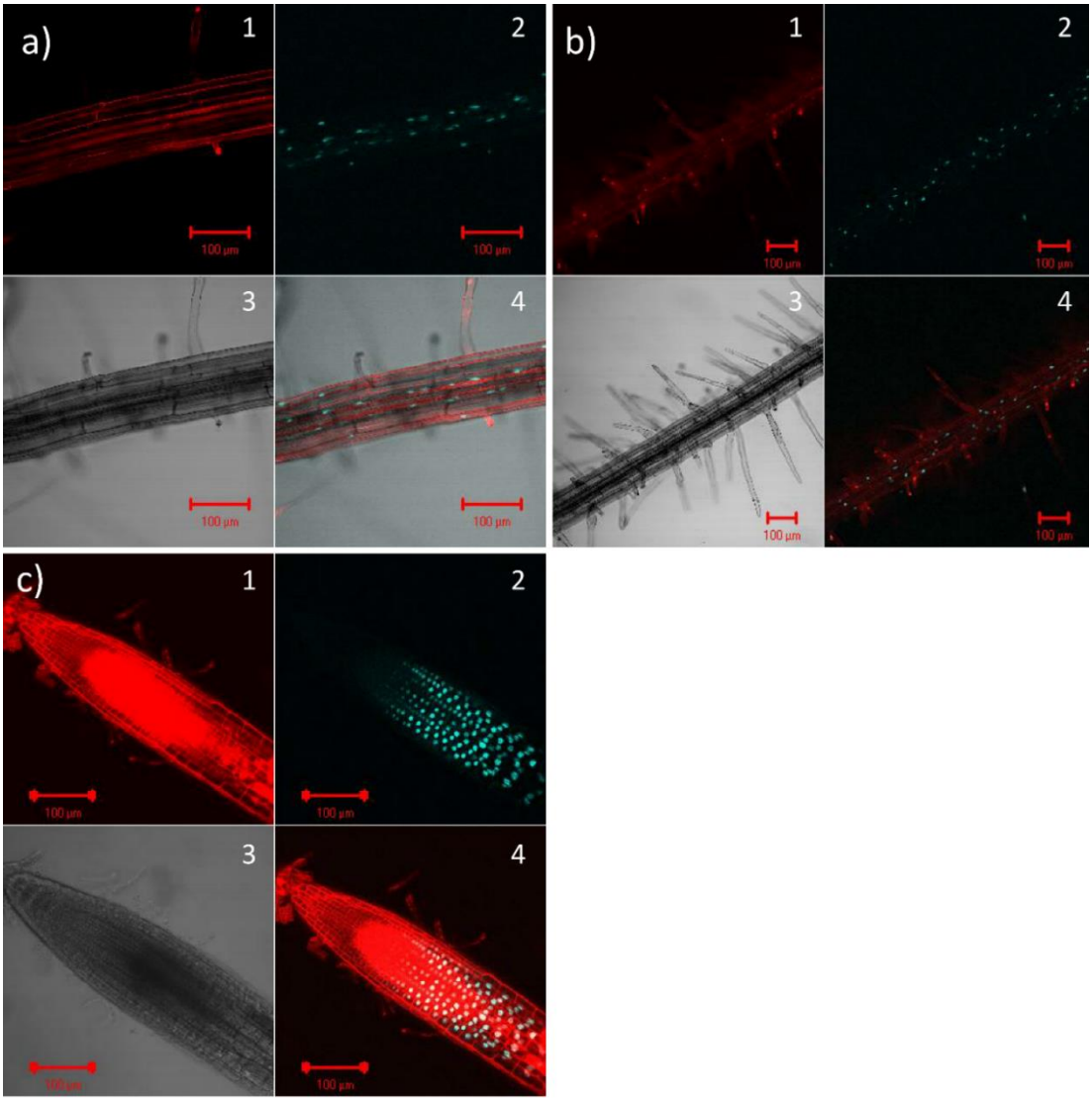

Appendix figure 15: Unmerged confocal micrographs of roots of *HAP1-VP16* enhancer-trap line HAP1C shows the presence of H2B::CFP fluorescence in the root cortex

Representative unmerged confocal images of 3 week old seedlings of *HAP1-VP16* enhancer-trap line, HAP1C grown on vertical MS plates (as per section 2.3.3) and imaged by confocal microscopy (as per section 2.6). Propidium iodine stained cell walls (1), nuclear localised H2B::CFP fluorescence (2), bright field image (3) and merged PI and CPF images (4). Images taken under a range of focal distances (scale bars shown), examining inner mature root (a), outer mature root (b) and root tip (c). Approximately 10 seedlings screened per line. CFP fluorescence (via H2B::CFP) was detected primarily in root-cortex.

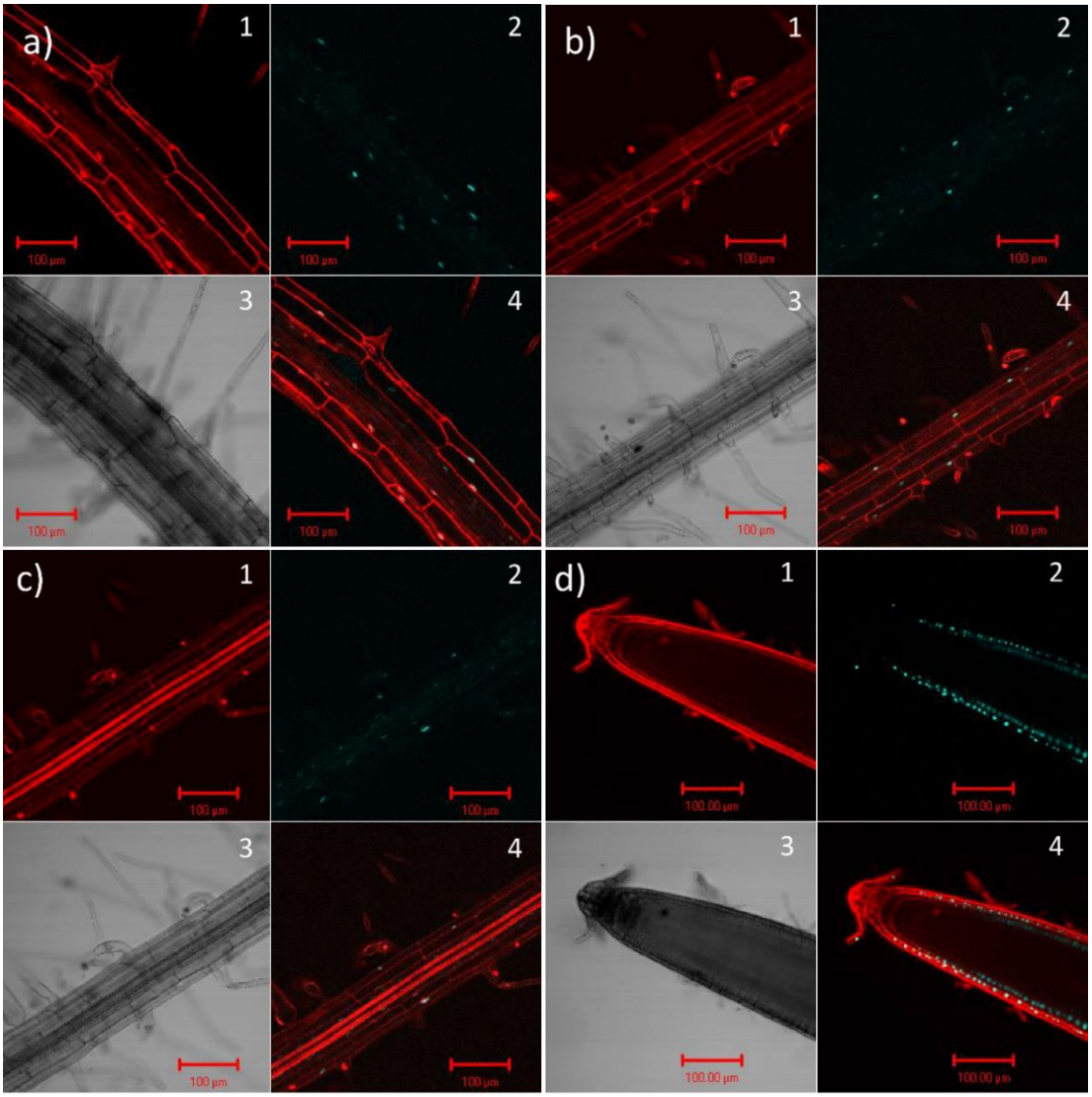

Appendix figure 16: Unmerged confocal micrographs of roots of *HAP1-VP16* enhancer-trap line HAP1D shows the presence of H2B::CFP fluorescence in the root epidermis

Representative unmerged confocal images of 3 week old seedlings of *HAP1-VP16* enhancer-trap line, HAP1D grown on vertical MS plates (as per section 2.3.3) and imaged by confocal microscopy (as per section 2.6). Propidium iodine stained cell walls (1), nuclear localised H2B::CFP fluorescence (2), bright field image (3) and merged PI and CPF images (4). Images taken under a range of focal distances (scale bars shown), examining root maturation zone (a) and outer mature root (b), inner mature root (c) and root tip (d). Approximately 10 seedlings screened per line. CFP fluorescence (via H2B::CFP) was detected primarily in root-epidermis.

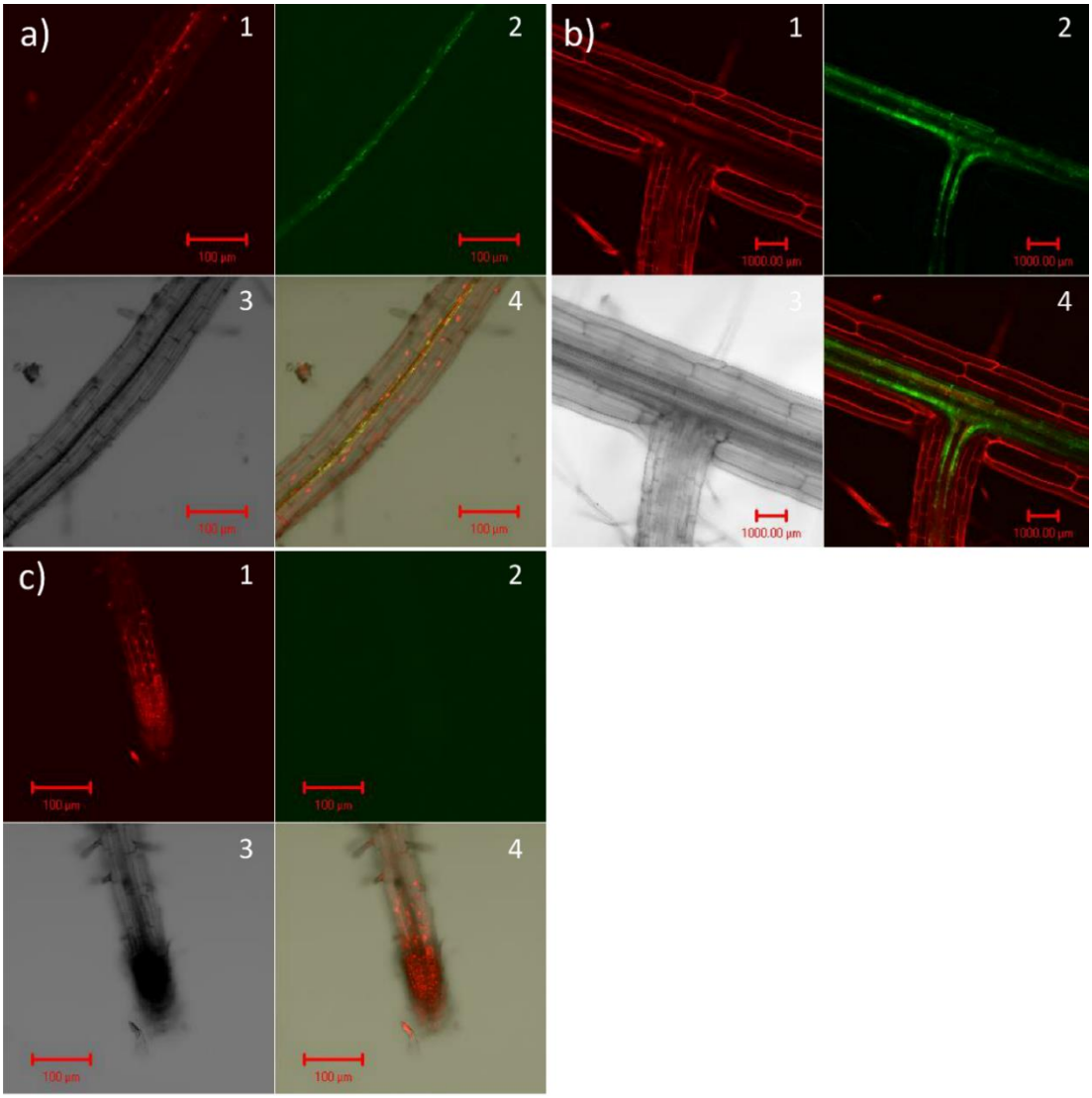

Appendix figure 17: Unmerged confocal micrographs of roots of *GAL4-VP16* enhancer-trap line J2371*C shows the presence of mGFP-ER fluorescence in the root pericycle

Representative unmerged confocal images of 3 week old seedlings of *GAL4-VP16* enhancer-trap line, J2371*C grown on vertical MS plates (as per section 2.3.3) and imaged by confocal microscopy (as per section 2.6). Propidium iodine stained cell walls (1), nuclear localised mGFP-ER fluorescence (2), bright field image (3) and merged PI and GFP images (4). Images taken under a range of focal distances (scale bars shown), examining mature root (a), outer lateral root (b) and root tip (c). Approximately 10 seedlings screened per line. GFP fluorescence (via mGFP-ER) was detected primarily in root-stele.

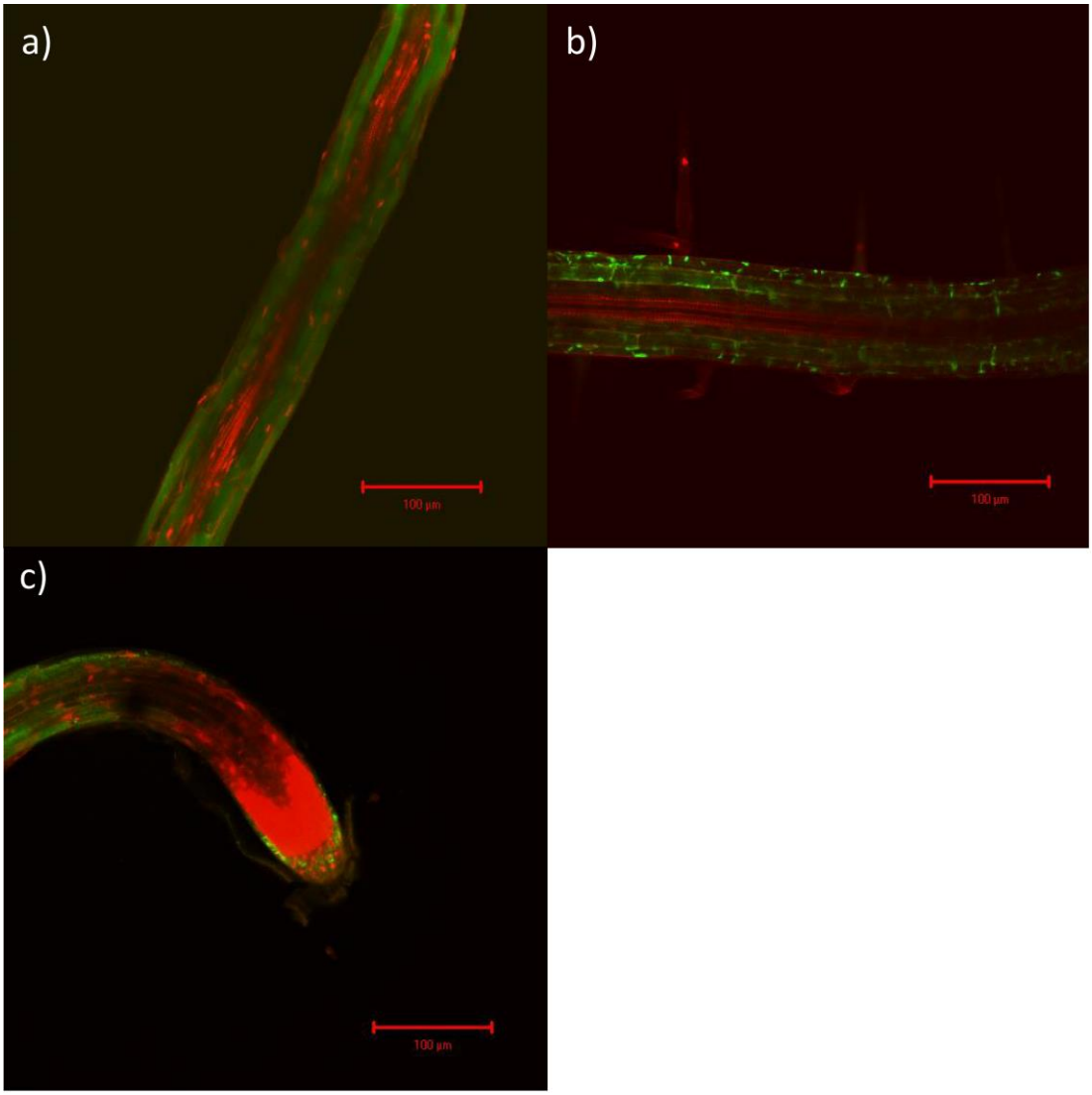

Appendix figure 18: Confocal micrographs of roots of *GAL4-VP16* enhancer-trap line J1422 shows the presence of mGFP-ER fluorescence in the root vasculature
Representative confocal images of 3 week old seedlings of *GAL4-VP16* enhancer-trap line, grown on vertical MS plates (as per section 2.3.3) and imaged by confocal microscopy (as per section 2.6). Cells walls stained with propidium iodine appear red, Endoplasmic reticulum localised mGFP-ER fluorescence appears green. Images taken under a range of focal distances (scale bars shown), examining root maturation zone (a), mature root (b) and root tip (c). Approximately 10 seedlings screened per line. GFP fluorescence (via mGFP5-ER) was detected primarily in root cortical and epidermal cells.

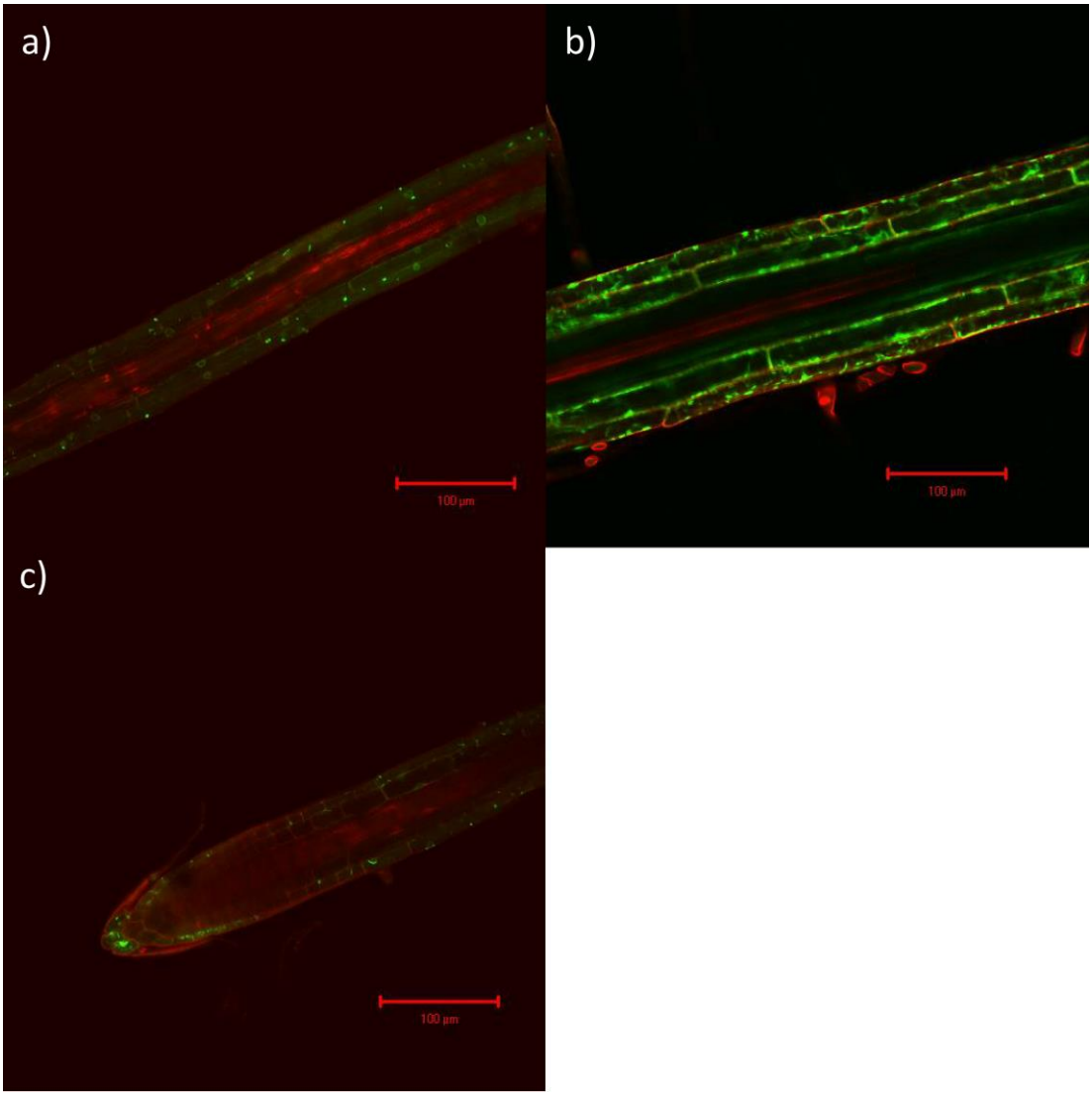

Appendix figure 19: Confocal micrographs of roots of *GAL4-VP16* enhancer-trap line J1551 shows the presence of mGFP-ER fluorescence in the root vasculature
Representative confocal images of 3 week old seedlings of *GAL4-VP16* enhancer-trap line, grown on vertical MS plates (as per section 2.3.3) and imaged by confocal microscopy (as per section 2.6). Cells walls stained with propidium iodine appear red, Endoplasmic reticulum localised mGFP-ER fluorescence appears green. Images taken under a range of focal distances (scale bars shown), examining root maturation zone (a), mature root (b) and root tip (c). Approximately 10 seedlings screened per line. GFP fluorescence (via mGFP5-ER) was detected primarily in root cortical and epidermal cells.

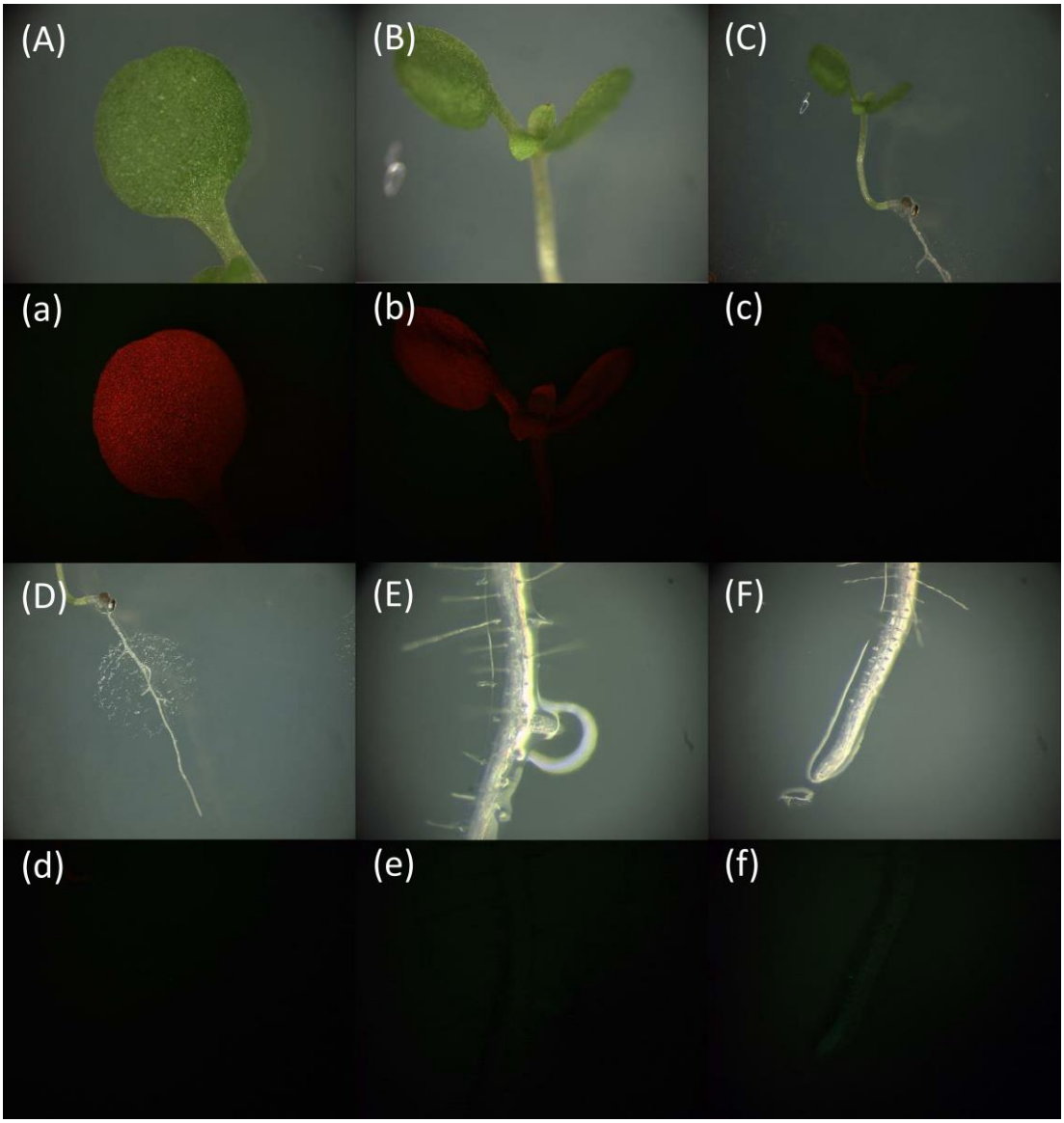

Appendix figure 20: Epifluorescence stereo micrographs of root and shoots of wild-type Arabidopsis C24 for mGFP5-ER fluorescence

Representative images of 3 week old seedlings of wild-type Arabidopsis C24, grown on vertical MS plates (as per section 2.3.3) and imaged for mGFP-ER florescence by epifluorescence stereo microscopy (as per section 2.6). Images taken under bright field (A-F) and GFP2 (a-f) filters under a range of focal distances, examining shoots (A-C) and roots (D-F). Approximately 10 seedlings screened per line. GFP fluorescence was not detected in any tissues.

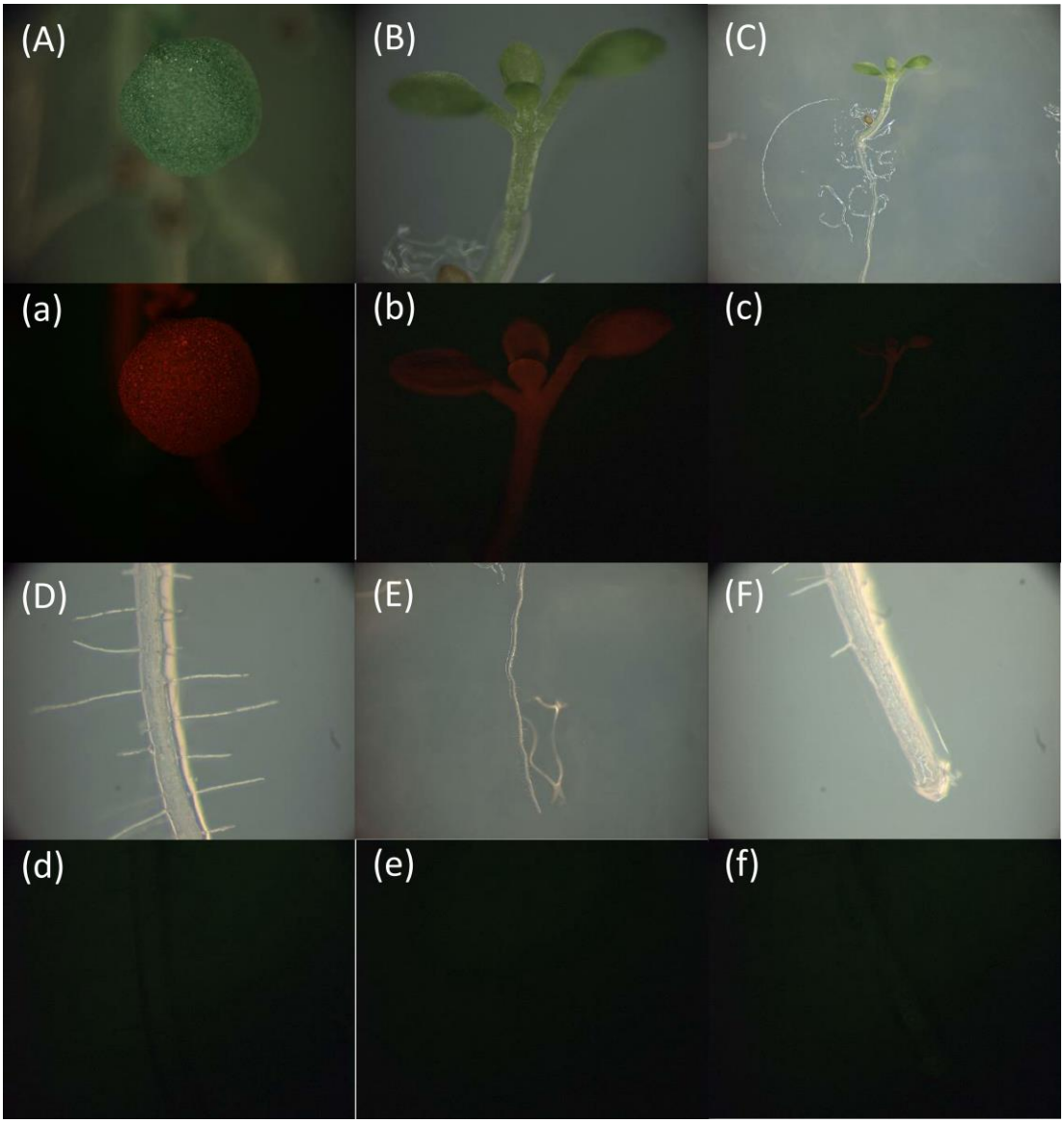

Appendix figure 21: HAP1C Epifluorescence stereo micrographs of root and shoots of *HAP1-VP16* enhancer-trap line HAP1C for mGFP5-ER fluorescence

Representative images of 3 week old seedlings of *HAP1-VP16* enhancer-trap line HAP1C, grown on vertical MS plates (as per section 2.3.3) and imaged for mGFP-ER florescence by epifluorescence stereo microscopy (as per section 2.6). Images taken under bright field (A-F) and GFP2 (a-f) filters under a range of focal distances, examining shoots (A-C) and roots (D-F). Approximately 10 seedlings screened per line. GFP fluorescence was not detected in any tissues.

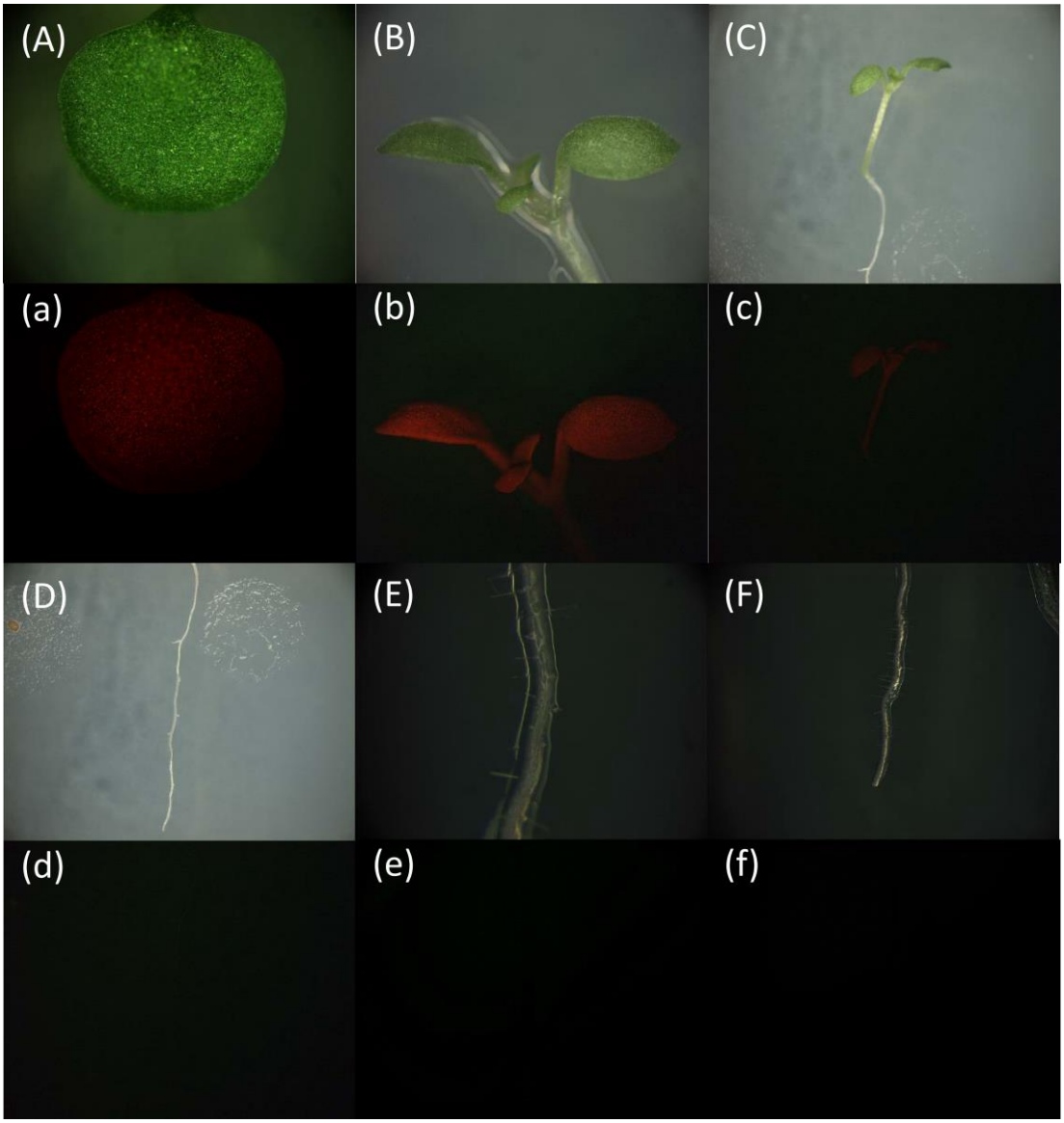

Appendix figure 22: HAP1D Epifluorescence stereo micrographs of root and shoots of *HAP1-VP16* enhancer-trap line HAP1D for mGFP5-ER fluorescence

Representative images of 3 week old seedlings of *HAP1-VP16* enhancer-trap line HAP1D, grown on vertical MS plates (as per section 2.3.3) and imaged for mGFP-ER florescence by epifluorescence stereo microscopy (as per section 2.6). Images taken under bright field (A-F) and GFP2 (a-f) filters under a range of focal distances, examining shoots (A-C) and roots (D-F). Approximately 10 seedlings screened per line. GFP fluorescence was not detected in any tissues.

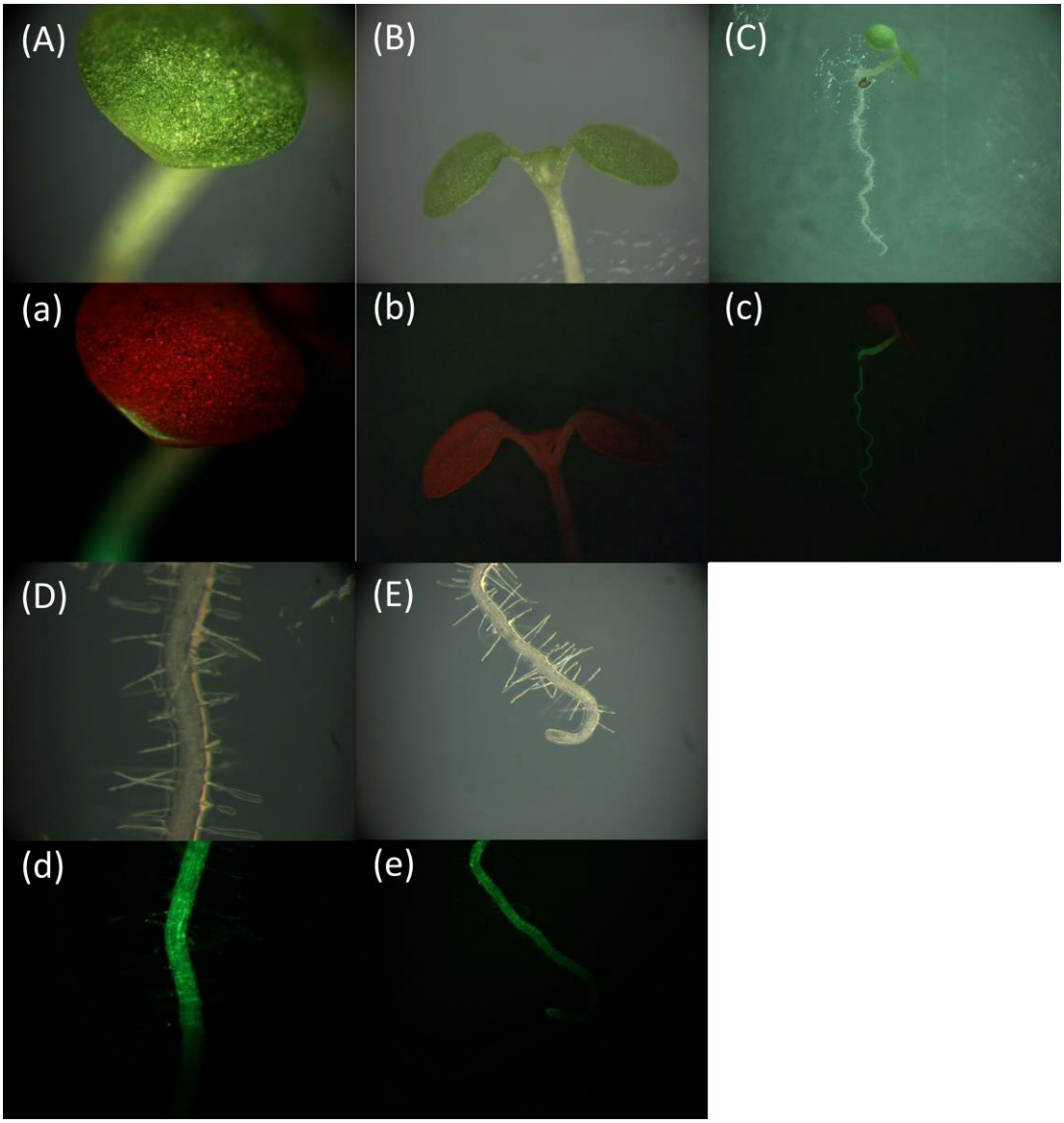

Appendix figure 23: Epifluorescence stereo micrographs of root and shoots of *GAL4-VP16* enhancer-trap line J1422 for mGFP5-ER fluorescence
Representative images of 3 week old seedlings of *GAL4-VP16* enhancer-trap line, J1422, grown on vertical MS plates (as per section 2.3.3) and imaged for mGFP-ER florescence by epifluorescence stereo microscopy (as per section 2.6). Images taken under bright field (A-E) and GFP2 (a-e) filters under a range of focal distances, examining shoots (A-C) and roots (D-E). Approximately 10 seedlings screened per line. GFP fluorescence was not detected in any tissues.

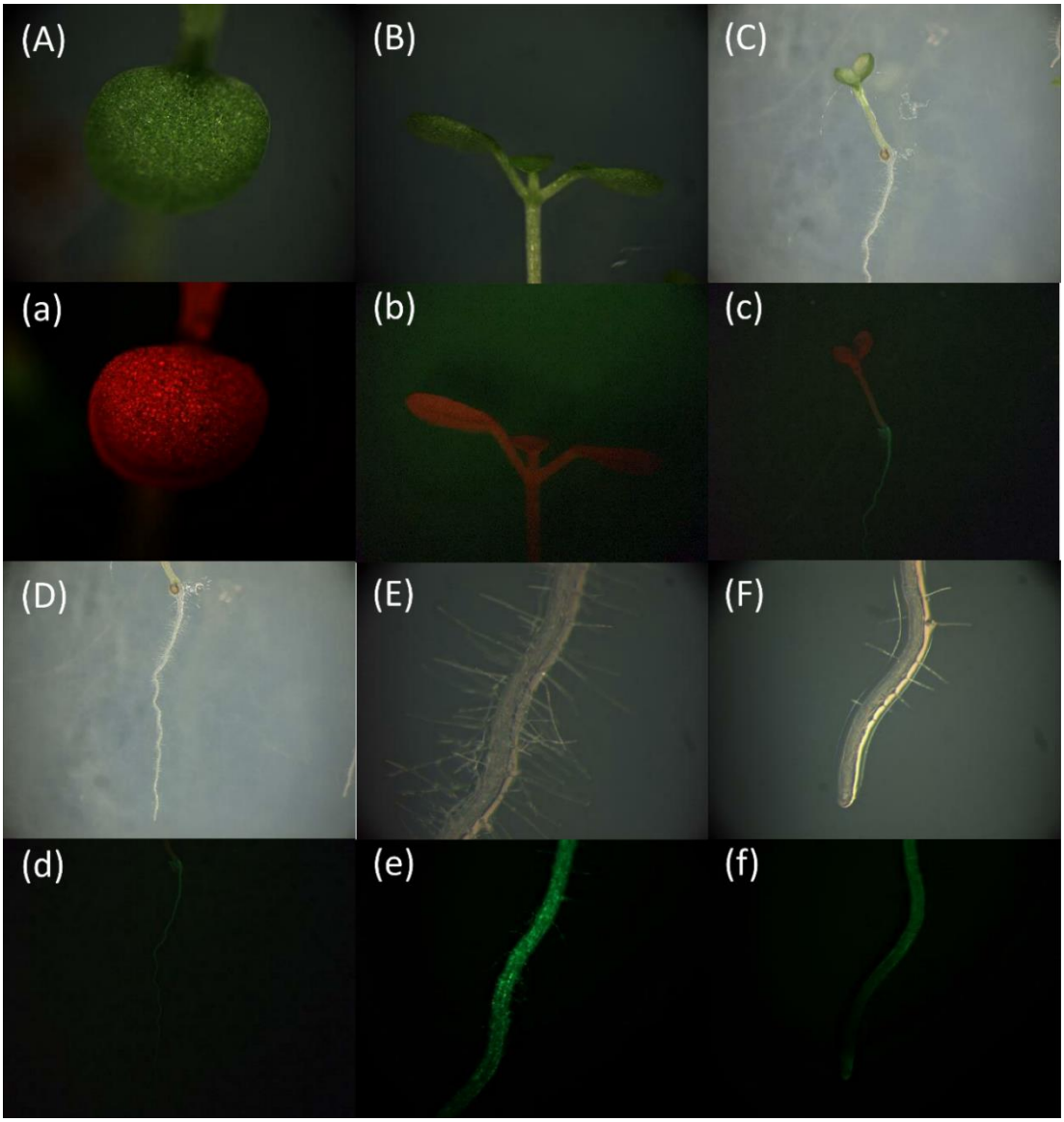

Appendix figure 24: Epifluorescence stereo micrographs of root and shoots of *GAL4-VP16* enhancer-trap line J1551 for mGFP5-ER fluorescence
Representative images of 3 week old seedlings of *GAL4-VP16* enhancer-trap line, J1551, grown on vertical MS plates (as per section 2.3.3) and imaged for mGFP-ER florescence by epifluorescence stereo microscopy (as per section 2.6). Images taken under bright field (A-F) and GFP2 (a-f) filters under a range of focal distances, examining shoots (A-C) and roots (D-F). Approximately 10 seedlings screened per line. GFP fluorescence was not detected in any tissues.

Appendix VII: Investigation of polar localisation of Na^+ transporters; *AtHKT1;1* and *AtSO1*

Preliminary investigation was undertaken into the potential for sub-cellular localisation of Arabidopsis Na^+ transporters, *AtHKT1;1* and *AtSOS1* when expressed in roots. To do this, bio-informatics analysis was carried out to identify potential tyrosine-sorting motifs present in the protein sequences. Transmembrane domains of both *AtHKT1;1* and *AtSOS1* were predicted by http://topcons.net/ (Bernsel *et al.*, 2009). Several potential intracellular Tyrosine sorting motifs (YxxΦ, where 'Y' is Tyrosine, 'x' is any amino acid, and 'Φ' is any large hydrophobic residue) were identified in both AtHKT1;1 (Appendix figure 25) and AtSOS1 (Appendix figure 26) protein sequences. Constructs containing the open reading frame (ORF) of *AtHKT1;1* and *AtSOS1*, N- or C-terminally tagged with plant optimised monomeric green fluorescent protein (*mGFP6*) and driven by the constitutive *2×CaMV35S* promoter were generated (Appendix figure 7, Appendix figure 8, Appendix figure 9 and Appendix figure 10). Overall orientation of transmembrane domains was predicated to be maintained with the addition of the GFP-tag sequences (Appendix figure 27 and Appendix figure 28).

These constructs were then to be transformed into Arabidopsis Col-0 to attempt to visualise potential sub-cellular sorting of these transporters however, additional screening of these lines was not possible during this project.

AtHKT1;1	
Motif	Orientation
Y28FLF	transmembrane
Y158SVV	transmembrane
Y164HLV	transmembrane
Y179VNF	non-cytoplasmic
Y265GYI	cytoplasmic
Y277SHL	cytoplasmic
Y320YEKL	non-cytoplasmic
Y363TLF	transmembrane
Y438GNV	non-cytoplasmic
Y485GRF	transmembrane

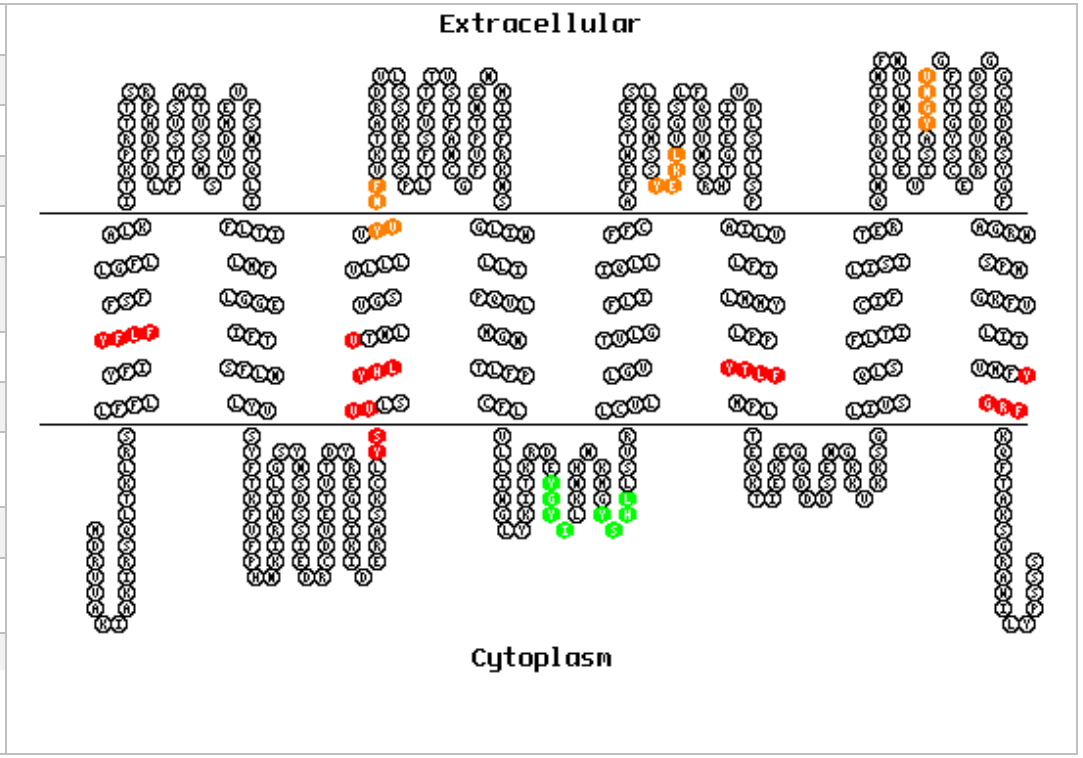

Appendix figure 25: Presence of potential tyrosine sorting motifs in AtHKT1;1 protein sequence

List of potential tyrosine sorting motifs (YxxΦ, where 'Y' is Tyrosine, 'x' is any amino acid, and 'Φ' is any large hydrophobic residue) in AtHKT1;1 protein sequence and motif orientation. Extracellular motifs (orange), transmembrane motifs (red), cytoplasmic motifs (green). Transmembrane domains and orientation predicted with TOPCONS (Bernsel *et al.*, 2009). Figures prepared using TOPO2 (Johns, 1996)

AtSOS1	
Motif	Orientation
Y11RFL	non-cytoplasmic
Y295AAF	transmembrane
Y358VYI	transmembrane
Y360IQL	transmembrane
Y373PLL	transmembrane
Y469EML	cytoplasmic
Y543WEM	cytoplasmic
Y590YNF	cytoplasmic
Y591NFL	cytoplasmic
Y606FAV	cytoplasmic
Y634DFL	cytoplasmic
Y682SVL	cytoplasmic
Y812EVL	cytoplasmic
Y1069KKL	cytoplasmic

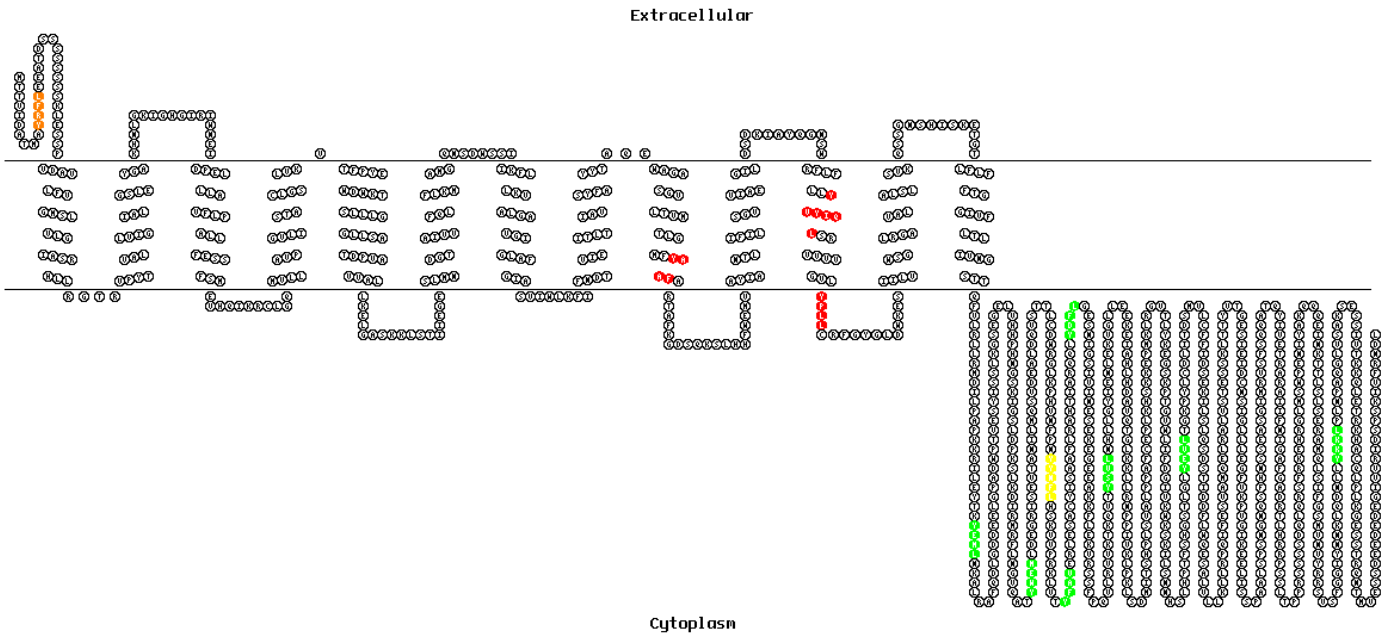

Appendix figure 26: Presence of potential tyrosine sorting motifs in AtSOS1 protein sequence

List of potential tyrosine sorting motifs (YxxΦ, where 'Y' is Tyrosine, 'x' is any amino acid, and 'Φ' is any large hydrophobic residue) in AtSOS1 protein sequence and motif orientation. Extracellular motifs (orange) , transmembrane motifs (red), cytoplasmic motifs (green), overlapping motifs (yellow). Transmembrane domains and orientation predicted with TOPCONS (Bernsel *et al.*, 2009). Figures prepared using TOPO2 (Johns, 1996)

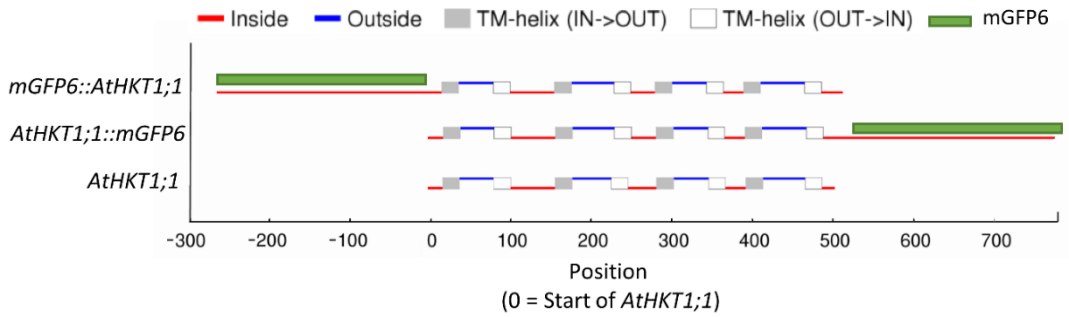

Appendix figure 27: Consensus topology of predicted transmembrane spanning domains and relative position of *mGFP6* tags of N-and C- terminally tagged *AtHKT1;1*.
The number of transmembrane domains and overall topology is predicted to be similar to that of the unmodified *AtHKT1;1* following the addition of either N′- or C′-terminal *mGFP6* tags. Position on the x-axis refers to the peptide number, relative to the starting peptide of the un-modified *AtHKT1;1*. Red lines represent cytoplasmic-side peptides; blue lines represent non-cytoplasmic-side peptides; grey and white boxes represent transmembrane spanning helices from intracellular to extracellular and from extracellular to intracellular respectively; green lines represent the *mGFP6* tag domain. Consensus based on the predictions of via TOPCONS (Bernsel *et al.*, 2009).

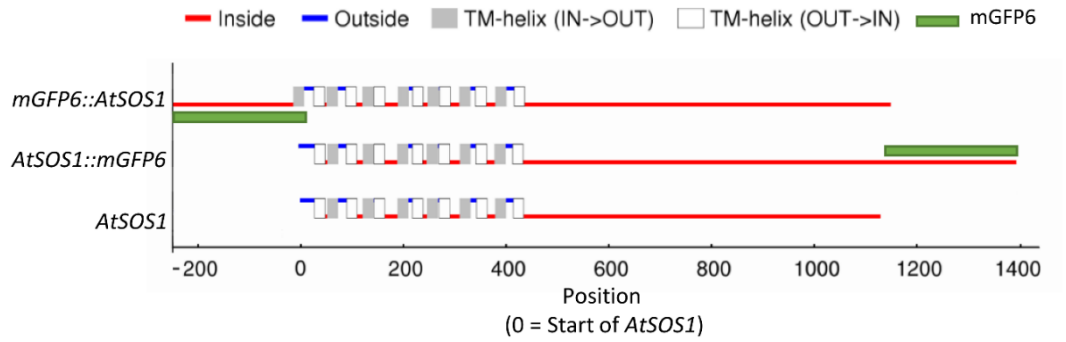

Appendix figure 28: Consensus topology of predicted transmembrane spanning domains and relative position of *mGFP6* tags of N-and C-terminally tagged *AtSOS1*.
The number of transmembrane domains and overall topology is predicted to be similar to that of the unmodified *AtSOS1* following the addition of either N- or C-terminal *mGFP6* tags. The inclusion of the N-terminal *mGFP6* tag potentially results in an extra transmembrane domain. Position on the x-axis refers to the peptide number, relative to the starting peptide of the unmodified *AtSOS1*. Red lines represent cytoplasmic-side peptides; blue lines represent non-cytoplasmic-side peptides; grey and white boxes represent transmembrane spanning helices from intracellular to extracellular and from extracellular to intracellular respectively; green lines represent the mGFP6 tag domain. Consensus based on the predictions of via TOPCONS (Bernsel *et al.*, 2009).

References

ABARES. (2015). *Agricultural commodities - March Quarter 2015*. Australian Government.

Abe, S., Nagasaka, K., Hirayama, Y., Kozuka-Hata, H., Oyama, M., Aoyagi, Y., . . . Hirota, T. (2011). The initial phase of chromosome condensation requires Cdk1-mediated phosphorylation of the CAP-D3 subunit of condensin II. *Genes Dev, 25*(8), 863-874.

Apse, M. P., Aharon, G. S., Snedden, W. A., & Blumwald, E. (1999). Salt tolerance conferred by overexpression of a vacuolar Na^+/H^+ antiport in Arabidopsis. *Science, 285*(5431), 1256-1258.

Apse, M. P., & Blumwald, E. (2007). Na^+ transport in plants. *FEBS Lett, 581*(12), 2247-2254.

AQIS. (2012, 13 Nov 2014). In vivo use of imported biological products in non-laboratory animals. 2013, from http://www.agriculture.gov.au/biosecurity/import/biological/checklist/in-vivo

Aslam, Z., Jeschke, W. D., Barrettlennard, E. G., Setter, T. L., Watkin, E., & Greenway, H. (1986). Effects of external NaCl on the growth of *Atriplex amnicola* and the ion relations and carbohydate status of the leaves. *Plant Cell and Environment, 9*(7), 571-580.

Banuelos, M. A., Haro, R., Fraile-Escanciano, A., & Rodriguez-Navarro, A. (2008). Effects of polylinker uATGs on the function of grass HKT1 transporters expressed in yeast cells. *Plant Cell Physiol, 49*(7), 1128-1132.

Bao, A. K., Wang, S. M., Wu, G. Q., Xi, J. J., Zhang, J. L., & Wang, C. M. (2009). Overexpression of the Arabidopsis H^+-PPase enhanced resistance to salt and drought stress in transgenic alfalfa (*Medicago sativa L.*). *Plant Science, 176*(2), 232-240.

Bargmann, B. O., & Birnbaum, K. D. (2010). Fluorescence activated cell sorting of plant protoplasts. *J Vis Exp*(36).

Barragán, V., Leidi, E. O., Andrés, Z., Rubio, L., De Luca, A., Fernández, J. A., . . . Pardo, J. M. (2012). Ion Exchangers NHX1 and NHX2 Mediate Active Potassium Uptake into Vacuoles to Regulate Cell Turgor and Stomatal Function in Arabidopsis. *The Plant Cell, 24*(3), 1127-1142.

Benito, B., Garciadeblas, B., & Rodriguez-Navarro, A. (2002). Potassium- or sodium-efflux ATPase, a key enzyme in the evolution of fungi. *Microbiology, 148*(Pt 4), 933-941.

Benito, B., & Rodriguez-Navarro, A. (2003). Molecular cloning and characterization of a sodium-pump ATPase of the moss Physcomitrella patens. *Plant J, 36*(3), 382-389.

Bernsel, A., Viklund, H., Hennerdal, A., & Elofsson, A. (2009). TOPCONS: consensus prediction of membrane protein topology. *Nucleic Acids Res, 37*(Web Server issue), W465-468.

Berthomieu, P., Conejero, G., Nublat, A., Brackenbury, W. J., Lambert, C., Savio, C., . . . Casse, F. (2003). Functional analysis of AtHKT1 in Arabidopsis shows that Na^+ recirculation by the phloem is crucial for salt tolerance. *EMBO Journal, 22*(9), 2004-2014.

Blaha, G., Stelzl, U., Spahn, C. M. T., Agrawal, R. K., Frank, J., & Nierhaus, K. H. (2000). Preparation of functional ribosomal complexes and effect of buffer conditions on tRNA positions observed by cryoelectron microscopy *Rna-Ligand Interactions Pt A* (Vol. 317, pp. 292-309).

Blumwald, E., Aharon, G. S., & Apse, M. P. (2000). Sodium transport in plant cells. *Biochim Biophys Acta, 1465*(1-2), 140-151.

Brand, A. H., & Perrimon, N. (1993). Targeted gene expression as a means of altering cell fates and generating dominant phenotypes. *Development, 118*(2), 401-415.

Brenner, S., Johnson, M., Bridgham, J., Golda, G., Lloyd, D. H., Johnson, D., . . . Corcoran, K. (2000). Gene expression analysis by massively parallel signature sequencing (MPSS) on microbead arrays. *Nature Biotechnology, 18*(6), 630-634.

Brini, F., Hanin, M., Mezghani, I., Berkowitz, G. A., & Masmoudi, K. (2007). Overexpression of wheat Na^+/H^+ antiporter *TNHX1* and H^+-pyrophosphatase *TVP1* improve salt- and drought-stress tolerance in *Arabidopsis thaliana* plants. *Journal of Experimental Botany, 58*(2), 301-308.

Burgos-Rivera, B., & Dawe, R. K. (2012). An Arabidopsis Tissue-Specific RNAi Method for Studying Genes Essential to Mitosis. *PLoS One, 7*(12), e51388.

Byrt, C. S., Xu, B., Krishnan, M., Lightfoot, D. J., Athman, A., Jacobs, A. K., . . . Gilliham, M. (2014). The Na(+) transporter, TaHKT1;5-D, limits shoot Na(+) accumulation in bread wheat. *Plant J, 80*(3), 516-526.

Carden, D. E., Walker, D. J., Flowers, T. J., & Miller, A. J. (2003). Single-cell measurements of the contributions of cytosolic Na(+) and K(+) to salt tolerance. *Plant Physiol, 131*(2), 676-683.

Clark, R. M., Wagler, T. N., Quijada, P., & Doebley, J. (2006). A distant upstream enhancer at the maize domestication gene tb1 has pleiotropic effects on plant and inflorescent architecture. *Nat Genet, 38*(5), 594-597.

Clough, S. J., & Bent, A. F. (1998). Floral dip: a simplified method for Agrobacterium-mediated transformation of *Arabidopsis thaliana*. *Plant Journal, 16*(6), 735-743.

Colmer, T. D., Munns, R., & Flowers, T. J. (2005). Improving salt tolerance of wheat and barley: future prospects. *Australian Journal of Experimental Agriculture, 45*(11), 1425-1443.

Conn, S. J., Hocking, B., Dayod, M., Xu, B., Athman, A., Henderson, S., . . . Gilliham, M. (2013). Protocol: optimising hydroponic growth systems for nutritional and physiological analysis of Arabidopsis thaliana and other plants. *Plant Methods, 9*(1), 4.

Curtis, M. D., & Grossniklaus, U. (2003). A gateway cloning vector set for high-throughput functional analysis of genes in planta. *Plant Physiol, 133*(2), 462-469.

Davenport, R. J., Munoz-Mayor, A., Jha, D., Essah, P. A., Rus, A., & Tester, M. (2007). The Na^+ transporter *AtHKT1;1* controls retrieval of Na^+ from the xylem in Arabidopsis. *Plant Cell and Environment, 30*(4), 497-507.

Davenport, R. J., & Tester, M. (2000). A weakly voltage-dependent, nonselective cation channel mediates toxic sodium influx in wheat. *Plant Physiology, 122*(3), 823-834.

Davis, A. M., Hall, A., Millar, A. J., Darrah, C., & Davis, S. J. (2009). Protocol: Streamlined sub-protocols for floral-dip transformation and selection of transformants in Arabidopsis thaliana. *Plant Methods, 5*, 3.

Daxinger, L., Hunter, B., Sheikh, M., Jauvion, V., Gasciolli, V., Vaucheret, H., . . . Furner, I. (2008). Unexpected silencing effects from T-DNA tags in Arabidopsis. *Trends in Plant Science, 13*(1), 4-6.

De Boer, A. H. (1999). Potassium translocation into the root xylem. *Plant Biology, 1*(1), 36-45.

De Laat, W., & Grosveld, F. (2003). Spatial organization of gene expression: the active chromatin hub. *Chromosome Research, 11*(5), 447-459.

Demidchik, V., & Tester, M. (2002). Sodium fluxes through nonselective cation channels in the plasma membrane of protoplasts from Arabidopsis roots. *Plant Physiology, 128*(2), 379-387.

Dettmer, J., & Friml, J. (2011). Cell polarity in plants: When two do the same, it is not the same. *Current Opinion in Cell Biology, 23*(6), 686-696.

Dolan, L., Janmaat, K., Willemsen, V., Linstead, P., Poethig, S., Roberts, K., & Scheres, B. (1993). Cellular organisation of the Arabidopsis thaliana root. *Development, 119*(1), 71-84.

Dubcovsky, J., Maria, G. S., Epstein, E., Luo, M. C., & Dvorak, J. (1996). Mapping of the K(+)/Na (+) discrimination locus Kna1 in wheat. *Theor Appl Genet, 92*(3-4), 448-454.

Edwards, K., Johnstone, C., & Thompson, C. (1991). A simple and rapid method for the preparation of plant genomic DNA for PCR analysis. *Nucleic Acids Res., 19*(6), 1349-1349.

El-Hussieny, G. S. (2006). *Control of shoot elemental accumulation by cell type-specific alteration of gene function in roots.* (Doctor of Philosophy), University of Cambridge, Cambridge.

Engineer, C. B., Fitzsimmons, K. C., Schmuke, J. J., Dotson, S. B., & Kranz, R. G. (2005). Development and evaluation of a Gal4-mediated LUC/GFP/GUS enhancer trap system in Arabidopsis. *BMC Plant Biol, 5*, 9.

Enstone, D. E., Peterson, C. A., & Ma, F. S. (2002). Root endodermis and exodermis: Structure, function, and responses to the environment. *Journal of Plant Growth Regulation, 21*(4), 335-351.

Evrard, A. (2012). *Cell type-specific transcriptional responses of plants to salinity* (Doctor of Philosophy Conventional), University of Adelaide, Adelaide.

Exner, V. (2010). Quantitative real time PCR in plant developmental biology. *Methods Mol Biol, 655*, 275-291.

FAO. (2000). Problem Soils Database - Saline soils. Retrieved 21st March, 2011, from http://www.fao.org/ag/AGL/agll/prosoil/saline.htm

Feng, Z., Zhang, B., Ding, W., Liu, X., Yang, D.-L., Wei, P., . . . Zhu, J.-K. (2013). Efficient genome editing in plants using a CRISPR/Cas system. *Cell Res, 23*(10), 1229-1232.

Ferjani, A., Segami, S., Horiguchi, G., Muto, Y., Maeshima, M., & Tsukaya, H. (2011). Keep an Eye on PPi: The Vacuolar-Type H(+)-Pyrophosphatase Regulates Postgerminative Development in Arabidopsis. *The Plant Cell, 23*(8), 2895-2908.

Filichkin, S. A., DiFazio, S. P., Brunner, A. M., Davis, J. M., Yang, Z. K., Kalluri, U. C., . . . Strauss, S. H. (2007). Efficiency of gene silencing in Arabidopsis: direct inverted repeats vs. transitive RNAi vectors. *Plant Biotechnol J, 5*(5), 615-626.

Finnie, C., Steenholdt, T., Roda Noguera, O., Knudsen, S., Larsen, J., Brinch-Pedersen, H., . . . Svensson, B. (2004). Environmental and transgene expression effects on the barley seed proteome. *Phytochemistry, 65*(11), 1619-1627.

Flowers, T. J. (2004). Improving crop salt tolerance. *Journal of Experimental Botany, 55*(396), 307-319.

Flowers, T. J., Munns, R., & Colmer, T. D. (2015). Sodium chloride toxicity and the cellular basis of salt tolerance in halophytes. *Annals of Botany, 115*(3), 419-431.

Fukuda, A., Chiba, K., Maeda, M., Nakamura, A., Maeshima, M., & Tanaka, Y. (2004a). Effect of salt and osmotic stresses on the expression of genes for the vacuolar H^+-pyrophosphatase, H^+-ATPase subunit A, and Na^+/H^+ antiporter from barley. *Journal of Experimental Botany, 55*(397), 585-594.

Fukuda, A., Nakamura, A., Tagiri, A., Tanaka, H., Miyao, A., Hirochika, H., & Tanaka, Y. (2004b). Function, intracellular localization and the importance in salt tolerance of a vacuolar Na(+)/H(+) antiporter from rice. *Plant Cell Physiol, 45*(2), 146-159.

Gallois, J.-L., Nora, F. R., Mizukami, Y., & Sablowski, R. (2004). WUSCHEL induces shoot stem cell activity and developmental plasticity in the root meristem. *Genes & Development, 18*(4), 375-380.

Gao, X., Nagawa, S., Wang, G., & Yang, Z. (2008). Cell polarity signaling: focus on polar auxin transport. *Mol Plant, 1*(6), 899-909.

Gardner, M. J., Baker, A. J., Assie, J. M., Poethig, R. S., Haseloff, J. P., & Webb, A. A. (2009). *GAL4 GFP* enhancer trap lines for analysis of stomatal guard cell development and gene expression. *Journal of Experimental Botany, 60*(1), 213-226.

Gaxiola, R. A., Fink, G. R., & Hirschi, K. D. (2002). Genetic manipulation of vacuolar proton pumps and transporters. *Plant Physiol, 129*(3), 967-973.

Gaxiola, R. A., Li, J., Undurraga, S., Dang, L. M., Allen, G. J., Alper, S. L., & Fink, G. R. (2001). Drought- and salt-tolerant plants result from overexpression of the *AVP1* H^+-pump. *Proc Natl Acad Sci U S A, 98*(20), 11444-11449.

Gaxiola, R. A., Rao, R., Sherman, A., Grisafi, P., Alper, S. L., & Fink, G. R. (1999). The *Arabidopsis thaliana* proton transporters, *AtNhx1* and *Avp1*, can function in cation detoxification in yeast. *Proc Natl Acad Sci U S A, 96*(4), 1480-1485.

Gaxiola, R. A., Sanchez, C. A., Paez-Valencia, J., Ayre, B. G., & Elser, J. J. (2012). Genetic manipulation of a "vacuolar" H(+)-PPase: from salt tolerance to yield enhancement under phosphorus-deficient soils. *Plant Physiol, 159*(1), 3-11.

Genc, Y., McDonald, G. K., & Tester, M. (2007). Reassessment of tissue Na^+ concentration as a criterion for salinity tolerance in bread wheat. *Plant Cell Environ, 30*(11), 1486-1498.

Ghassemi, F., Jakeman, A. J., & Nix, H. A. (1995). *Salinisation of land and water resources : human causes, extent, management, and case studies*. Sydney, New South Wales: NSW University Press.

Ghedira, R., De Buck, S., Nolf, J., & Depicker, A. (2013). The Efficiency of Arabidopsis thaliana Floral Dip Transformation Is Determined Not Only by the Agrobacterium Strain Used but Also by the Physiology and the Ecotype of the Dipped Plant. *Molecular Plant-Microbe Interactions, 26*(7), 823-832.

Gonzalez, N., De Bodt, S., Sulpice, R., Jikumaru, Y., Chae, E., Dhondt, S., . . . Inze, D. (2010). Increased leaf size: different means to an end. *Plant Physiol, 153*(3), 1261-1279.

Greenway, H., & Munns, R. (1980). Mechanisms of salt tolerance in non-halophytes. *Annual Review of Plant Physiology and Plant Molecular Biology, 31*, 149-190.

Greenway, H., & Munns, R. (1983). Interactions between growth, uptake of Cl− and Na+, and water relations of plants in saline environments. II. Highly vacuolated cells. *Plant, Cell & Environment, 6*(7), 575-589.

Gustafsson, J. P. (2012). Visual MINTEQ ver. 3.0. 2012. 2012

Haase, A. T., Retzel, E. F., & Staskus, K. A. (1990). Amplification and detection of lentiviral DNA inside cells. *Proceedings of the National Academy of Sciences, 87*(13), 4971-4975.

Hairmansis, A. (2014). *Modifying sodium transport to improve salinity tolerance of commercial rice cultivars (Oryza sativa L.).* (Doctor of Philosophy Conventional), The University of Adelaide, Adelaide, South Australia.

Haro, R., Banuelos, M. A., Senn, M. E., Barrero-Gil, J., & Rodriguez-Navarro, A. (2005). HKT1 mediates sodium uniport in roots. Pitfalls in the expression of HKT1 in yeast. *Plant Physiol, 139*(3), 1495-1506.

Harrison, S. J., Mott, E. K., Parsley, K., Aspinall, S., Gray, J. C., & Cottage, A. (2006). A rapid and robust method of identifying transformed Arabidopsis thaliana seedlings following floral dip transformation. *Plant Methods, 2*(1), 19.

Haseloff, J. (1999). GFP variants for multispectral imaging of living cells *Methods in Cell Biology, Vol 58* (Vol. 58, pp. 139).

Haseloff, J., Bauch, M., Boisnard-Lorig, C., Hodge, S., Laplaze, L., Runions, J., & Kurup, S. (2003). Gene expression construct of HAP1 adapted for plant cells: Google Patents.

Haseloff, J., Bauch, M., Boisnard-Lorig, C., Hodge, S., Laplaze, L., Runions, J., & Kurup, S. (2005). Patent, United States of America Patent No.

He, C., Yan, J., Shen, G., Fu, L., Holaday, A. S., Auld, D., . . . Zhang, H. (2005). Expression of an Arabidopsis vacuolar sodium/proton antiporter gene in cotton improves photosynthetic performance under salt conditions and increases fiber yield in the field. *Plant Cell Physiol, 46*(11), 1848-1854.

Heckman, J. R., & Strick, J. E. (1996). Teaching Plant-Soil Relationships with Color Images of Rhizosphere pH. *J. Nat. Resour. Life Sci. Educ., 25*(1), 13-17.

Hellens, R. P., Edwards, E. A., Leyland, N. R., Bean, S., & Mullineaux, P. M. (2000). pGreen: a versatile and flexible binary Ti vector for Agrobacterium-mediated plant transformation. *Plant Mol Biol, 42*(6), 819-832.

Höfgen, R., & Willmitzer, L. (1988). Storage of competent cells for Agrobacterium transformation. *Nucleic Acids Research, 16*(20), 9877.

Holme, I. B., Wendt, T., & Holm, P. B. (2013). Intragenesis and cisgenesis as alternatives to transgenic crop development. *Plant Biotechnol J, 11*(4), 395-407.

Holwerda, B. C., Galvin, N. J., Baranski, T. J., & Rogers, J. C. (1990). In Vitro Processing of Aleurain, a Barley Vacuolar Thiol Protease. *The Plant Cell Online, 2*(11), 1091-1106.

Hon, T., Hach, A., Tamalis, D., Zhu, Y. H., & Zhang, L. (1999). The yeast heme-responsive transcriptional activator Hap1 is a preexisting dimer in the absence of heme. *Journal of Biological Chemistry, 274*(32), 22770-22774.

Horie, T., Hauser, F., & Schroeder, J. I. (2009). HKT transporter-mediated salinity resistance mechanisms in Arabidopsis and monocot crop plants. *Trends Plant Sci, 14*(12), 660-668.

International Barley Genome Sequencing Consortium. (2012). A physical, genetic and functional sequence assembly of the barley genome. *Nature, 491*(7426), 711-716.

Jacobs, A., Ford, K., Kretschmer, J., & Tester, M. (2011). Rice plants expressing the moss sodium pumping ATPase *PpENA1* maintain greater biomass production under salt stress. *Plant Biotechnol J, 9*(8), 838-847.

Jacobs, A., Lunde, C., Bacic, A., Tester, M., & Roessner, U. (2007). The impact of constitutive heterologous expression of a moss Na^+ transporter on the metabolomes of rice and barley. *Metabolomics, 3*(3), 307-317.

Jain, M., Nijhawan, A., Arora, R., Agarwal, P., Ray, S., Sharma, P., . . . Khurana, J. P. (2007). F-box proteins in rice. Genome-wide analysis, classification, temporal and spatial gene expression during panicle and seed development, and regulation by light and abiotic stress. *Plant Physiol, 143*(4), 1467-1483.

Jefferson, R. A., Kavanagh, T. A., & Bevan, M. W. (1987). GUS fusions: beta-glucuronidase as a sensitive and versatile gene fusion marker in higher plants. *The EMBO Journal, 6*(13), 3901-3907.

Jha, D., Shirley, N., Tester, M., & Roy, S. J. (2010). Variation in salinity tolerance and shoot sodium accumulation in Arabidopsis ecotypes linked to differences in the natural expression levels of transporters involved in sodium transport. *Plant Cell Environ, 33*(5), 793-804.

Johns, S. J. (1996). TOPO2, Transmembrane protein display software. Retrieved 1-2-2015, 2015, from http://www.sacs.ucsf.edu/TOPO2/

Johnson, A. A., Hibberd, J. M., Gay, C., Essah, P. A., Haseloff, J., Tester, M., & Guiderdoni, E. (2005). Spatial control of transgene expression in rice (Oryza sativa L.) using the GAL4 enhancer trapping system. *Plant J, 41*(5), 779-789.

Karakas, B., Ozias-Akins, P., Stushnoff, C., Suefferheld, M., & Rieger, M. (1997). Salinity and drought tolerance of mannitol-accumulating transgenic tobacco. *Plant, Cell & Environment, 20*(5), 609-616.

Katerji, N., van Hoorn, J. W., Hamdy, A., & Mastrorilli, M. (2003). Salinity effect on crop development and yield, analysis of salt tolerance according to several classification methods. *Agricultural Water Management, 62*(1), 37-66.

Kiegle, E., Moore, C. A., Haseloff, J., Tester, M. A., & Knight, M. R. (2000). Cell-type-specific calcium responses to drought, salt and cold in the Arabidopsis root. *Plant J, 23*(2), 267-278.

Kim, Y. S., Kim, I. S., Choe, Y. H., Bae, M. J., Shin, S. Y., Park, S. K., . . . Yoon, H. S. (2014). Overexpression of the Arabidopsis vacuolar H+-pyrophosphatase AVP1 gene in rice plants improves grain yield under paddy field conditions. *The Journal of Agricultural Science, 152*(06), 941-953.

Klimyuk, V. I., Nussaume, L., Harrison, K., & Jones, J. D. (1995). Novel GUS expression patterns following transposition of an enhancer trap Ds element in Arabidopsis. *Mol Gen Genet, 249*(4), 357-365.

Kovalchuk, N., Li, M., Wittek, F., Reid, N., Singh, R., Shirley, N., . . . Lopato, S. (2010). Defensin promoters as potential tools for engineering disease resistance in cereal grains. *Plant Biotechnol J, 8*(1), 47-64.

Krishnan, M. (2013). *Cell type-specific manipulation of salt tolerance genes in wheat and barley* (Doctor of Philosophy Conventional), University of Adelaide, Adelaide.

Lan, C., Lee, H. C., Tang, S., & Zhang, L. (2004). A novel mode of chaperone action: heme activation of Hap1 by enhanced association of Hsp90 with the repressed Hsp70-Hap1 complex. *J Biol Chem, 279*(26), 27607-27612.

Laplaze, L., Parizot, B., Baker, A., Ricaud, L., Martiniere, A., Auguy, F., . . . Haseloff, J. (2005). GAL4-GFP enhancer trap lines for genetic manipulation of lateral root development in Arabidopsis thaliana. *Journal of Experimental Botany, 56*(419), 2433-2442.

Li, J., Yang, H., Peer, W. A., Richter, G., Blakeslee, J., Bandyopadhyay, A., . . . Gaxiola, R. (2005). Arabidopsis H+-PPase AVP1 regulates auxin-mediated organ development. *Science, 310*(5745), 121-125.

Li, Z., Baldwin, C. M., Hu, Q., Liu, H., & Luo, H. (2010). Heterologous expression of *Arabidopsis* H^+-pyrophosphatase enhances salt tolerance in transgenic creeping bentgrass (*Agrostis stolonifera L.*). *Plant Cell Environ, 33*(2), 272-289.

Lunde, C., Drew, D. P., Jacobs, A. K., & Tester, M. (2007). Exclusion of Na^+ via sodium ATPase (*PpENA1*) ensures normal growth of *Physcomitrella patens* under moderate salt stress. *Plant Physiol, 144*(4), 1786-1796.

Ma, J. F., Tamai, K., Yamaji, N., Mitani, N., Konishi, S., Katsuhara, M., . . . Yano, M. (2006). A silicon transporter in rice. *Nature, 440*(7084), 688-691.

Ma, J. F., Yamaji, N., Mitani, N., Tamai, K., Konishi, S., Fujiwara, T., . . . Yano, M. (2007). An efflux transporter of silicon in rice. *Nature, 448*(7150), 209-212.

Maathuis, F. J. M., & Amtmann, A. (1999). K^+Nutrition and Na^+Toxicity: The Basis of Cellular K^+/Na^+Ratios. *Annals of Botany, 84*(2), 123-133.

Mantis, J., & Tague, B. (2000). Comparing the utility of β-glucuronidase and green fluorescent protein for detection of weak promoter activity inArabidopsis thaliana. *Plant Molecular Biology Reporter, 18*(4), 319-330.

Maser, P., Eckelman, B., Vaidyanathan, R., Horie, T., Fairbairn, D. J., Kubo, M., . . . Schroeder, J. I. (2002). Altered shoot/root Na^+ distribution and bifurcating salt sensitivity in Arabidopsis by genetic disruption of the Na^+ transporter *AtHKT1*. *FEBS Lett, 531*(2), 157-161.

Mian, A., Oomen, R. J., Isayenkov, S., Sentenac, H., Maathuis, F. J., & Very, A. A. (2011). Over-expression of an Na+-and K+-permeable HKT transporter in barley improves salt tolerance. *Plant J, 68*(3), 468-479.

Mlotshwa, S., Pruss, G. J., Gao, Z., Mgutshini, N. L., Li, J., Chen, X., . . . Vance, V. (2010). Transcriptional silencing induced by Arabidopsis T-DNA mutants is associated with 35S promoter siRNAs and requires genes involved in siRNA-mediated chromatin silencing. *The Plant Journal, 64*(4), 699-704.

Møller, I. S. (2008). *Na^+ exclusion and salinity tolerance in Arabidopsis thaliana.* (Doctor of Philosophy Conventional), PhD Thesis, University of Cambridge, Cambridge.

Møller, I. S., Gilliham, M., Jha, D., Mayo, G. M., Roy, S. J., Coates, J. C., . . . Tester, M. (2009). Shoot Na+ exclusion and increased salinity tolerance engineered by cell type-specific alteration of Na+ transport in Arabidopsis. *Plant Cell, 21*(7), 2163-2178.

Møller, I. S., & Tester, M. (2007). Salinity tolerance of Arabidopsis: a good model for cereals? *Trends Plant Sci, 12*(12), 534-540.

Monaco, M. K., Stein, J., Naithani, S., Wei, S., Dharmawardhana, P., Kumari, S., . . . Ware, D. (2014). Gramene 2013: comparative plant genomics resources. *Nucleic Acids Res, 42*(Database issue), D1193-1199.

Munns, R. (2002). Comparative physiology of salt and water stress. *Plant Cell Environ, 25*(2), 239-250.

Munns, R., & Gilliham, M. (2015). Salinity tolerance of crops – what is the cost? *New Phytologist*, n/a-n/a.

Munns, R., Guo, J. M., Passioura, J. B., & Cramer, G. R. (2000). Leaf water status controls day-time but not daily rates of leaf expansion in salt-treated barley. *Australian Journal of Plant Physiology, 27*(10), 949-957.

Munns, R., & James, R. A. (2003). Screening methods for salinity tolerance: a case study with tetraploid wheat. *Plant and Soil, 253*(1), 201-218.

Munns, R., James, R. A., Xu, B., Athman, A., Conn, S. J., Jordans, C., . . . Gilliham, M. (2012). Wheat grain yield on saline soils is improved by an ancestral Na + transporter gene. *Nature Biotechnology, 30*(4), 360-364.

Munns, R., & Tester, M. (2008). Mechanisms of salinity tolerance. *Annu Rev Plant Biol, 59*, 651-681.

Nauer, E. M., Roistach.Cn, & Labanaus.Ck. (1967). EFFECTS OF MIX COMPOSITION FERTILIZATION AND PH ON CITRUS GROWN IN U C-TYPE POTTING MIXTURES UNDER GREENHOUSE CONDITIONS. *Hilgardia, 38*(15), 557-&.

Nichols, K. W., Heck, G. R., & Fernandez, D. E. (1997). Simplified selection of transgenic Arabidopsis thaliana seed in liquid culture. *Biotechniques, 22*(1), 62-63.

Ouyang, S., Zhu, W., Hamilton, J., Lin, H., Campbell, M., Childs, K., . . . Buell, C. R. (2007). The TIGR Rice Genome Annotation Resource: improvements and new features. *Nucleic Acids Res, 35*(Database issue), D883-887.

Paez-Valencia, J., Patron-Soberano, A., Rodriguez-Leviz, A., Sanchez-Lares, J., Sanchez-Gomez, C., Valencia-Mayoral, P., . . . Gaxiola, R. (2011). Plasma membrane localization of the type I H(+)-PPase AVP1 in sieve element-companion cell complexes from Arabidopsis thaliana. *Plant Sci, 181*(1), 23-30.

Paez-Valencia, J., Sanchez-Lares, J., Marsh, E., Dorneles, L. T., Santos, M. P., Sanchez, D., . . . Gaxiola, R. A. (2013). Enhanced proton translocating pyrophosphatase activity improves nitrogen use efficiency in Romaine lettuce. *Plant Physiol, 161*(3), 1557-1569.

Park, S., Li, J., Pittman, J. K., Berkowitz, G. A., Yang, H., Undurraga, S., . . . Gaxiola, R. A. (2005). Up-regulation of a H^+-pyrophosphatase (H^+-PPase) as a strategy to engineer drought-resistant crop plants. *Proc Natl Acad Sci U S A, 102*(52), 18830-18835.

Pasapula, V., Shen, G., Kuppu, S., Paez-Valencia, J., Mendoza, M., Hou, P., . . . Payton, P. (2011). Expression of an Arabidopsis vacuolar H^+-pyrophosphatase gene (*AVP1*) in cotton improves drought- and salt tolerance and increases fibre yield in the field conditions. *Plant Biotechnol J, 9*(1), 88-99.

Patel, R. V., Nahal, H. K., Breit, R., & Provart, N. J. (2012). BAR expressolog identification: expression profile similarity ranking of homologous genes in plant species. *Plant J, 71*(6), 1038-1050.

Peng, Y. H., Zhu, Y. F., Mao, Y. Q., Wang, S. M., Su, W. A., & Tang, Z. C. (2004). Alkali grass resists salt stress through high [K^+] and an endodermis barrier to Na^+. *Journal of Experimental Botany, 55*(398), 939-949.

Pizzio, G. A., Paez-Valencia, J., Khadilkar, A. S., Regmi, K. C., Patron-Soberano, A., Zhang, S., . . . Gaxiola, R. A. (2015). Arabidopsis proton-pumping pyrophosphatase AVP1 expresses strongly in phloem where it is required for PPi metabolism and photosynthate partitioning. *Plant Physiology*.

Platten, J. D., Cotsaftis, O., Berthomieu, P., Bohnert, H., Davenport, R. J., Fairbairn, D. J., . . . Tester, M. (2006). Nomenclature for HKT transporters, key determinants of plant salinity tolerance. *Trends in Plant Science, 11*(8), 372-374.

Plett, D. C., Johnson, A., Jacobs, A., & Tester, M. (2010a). Cell type-specific expression of sodium transporters improves salinity tolerance of rice. *GM Crops, 1*(5), 273-275.

Plett, D. C., & Møller, I. S. (2010). Na^+ transport in glycophytic plants: what we know and would like to know. *Plant Cell and Environment, 33*(4), 612-626.

Plett, D. C., Safwat, G., Gilliham, M., Møller, I. S., Roy, S., Shirley, N., . . . Tester, M. (2010b). Improved salinity tolerance of rice through cell type-specific expression of *AtHKT1;1*. *PLoS One, 5*(9), e12571.

Porto, M. S., Pinheiro, M. P., Batista, V. G., dos Santos, R. C., Filho Pde, A., & de Lima, L. M. (2014). Plant promoters: an approach of structure and function. *Molecular Biotechnology, 56*(1), 38-49.

Przybecki, Z., Siedlecka, E., Filipecki, M., & Urbanczyk-Wochniak, E. (2006). In situ reverse transcription PCR on plant tissues. *Methods Mol Biol, 334*, 181-198.

Quarrie, S. A., & Mahmood, A. (1993). Improving salt tolerance in hexaploid wheat. *Institue of Plant Research and John Innes Centre Annual Report 1992*, 4.

Ran, F. A., Hsu, P. D., Wright, J., Agarwala, V., Scott, D. A., & Zhang, F. (2013). Genome engineering using the CRISPR-Cas9 system. *Nature protocols, 8*(11), 2281-2308.

Ren, Z. H., Gao, J. P., Li, L. G., Cai, X. L., Huang, W., Chao, D. Y., . . . Lin, H. X. (2005). A rice quantitative trait locus for salt tolerance encodes a sodium transporter. *Nat Genet, 37*(10), 1141-1146.

Rengasamy, P. (2002). Transient salinity and subsoil constraints to dryland farming in Australian sodic soils: an overview. *Australian Journal of Experimental Agriculture, 42*(3), 351-361.

Rengasamy, P. (2006). World salinization with emphasis on Australia. *Journal of Experimental Botany, 57*(5), 1017-1023.

Roy, S. J., Negrao, S., & Tester, M. (2014). Salt resistant crop plants. *Curr Opin Biotechnol, 26*(0), 115-124.

Rozen, S., & Skaletsky, H. (1999). Primer3 on the WWW for general users and for biologist programmers *Bioinformatics methods and protocols* (pp. 365-386): Springer.

Rus, A., Yokoi, S., Sharkhuu, A., Reddy, M., Lee, B. H., Matsumoto, T. K., . . . Hasegawa, P. M. (2001). *AtHKT1* is a salt tolerance determinant that controls Na^+ entry into plant roots. *Proc Natl Acad Sci U S A, 98*(24), 14150-14155.

Sabatini, S., Beis, D., Wolkenfelt, H., Murfett, J., Guilfoyle, T., Malamy, J., . . . Scheres, B. (1999). An auxin-dependent distal organizer of pattern and polarity in the Arabidopsis root. *Cell, 99*(5), 463-472.

Sabatini, S., Heidstra, R., Wildwater, M., & Scheres, B. (2003). SCARECROW is involved in positioning the stem cell niche in the Arabidopsis root meristem. *Genes & Development, 17*(3), 354-358.

Sarafian, V., Kim, Y., Poole, R. J., & Rea, P. A. (1992). Molecular cloning and sequence of cDNA encoding the pyrophosphate-energized vacuolar membrane proton pump of Arabidopsis thaliana. *Proc Natl Acad Sci U S A, 89*(5), 1775-1779.

Sato, Y., Takehisa, H., Kamatsuki, K., Minami, H., Namiki, N., Ikawa, H., . . . Nagamura, Y. (2013). RiceXPro Version 3.0: expanding the informatics resource for rice transcriptome. *Nucleic Acids Research, 41*(D1), D1206-D1213.

Sauer, M., & Friml, J. (2010). Immunolocalization of proteins in plants. *Methods Mol Biol, 655*, 253-263.

Schilling, R. K. (2010). *Evaluating the salt tolerance of barley expressing the Arabidopsis vacuolar H(+)-PPase (AtAVP1).* (Honours), University of Adelaide, Adelaide.

Schilling, R. K. (2014). *Evaluating the abiotic stress tolerance of transgenic barley expressing an Arabididopsis vacuolar H^+-pyrophosphatase gene (AVP1).* (Doctor of Philosophy), University of Adelaide, Adelaide.

Schilling, R. K., Marschner, P., Shavrukov, Y., Berger, B., Tester, M., Roy, S. J., & Plett, D. C. (2014). Expression of the Arabidopsis vacuolar H(+)-pyrophosphatase gene (AVP1) improves the shoot biomass of transgenic barley and increases grain yield in a saline field. *Plant Biotechnol J, 12*(3), 378-386.

Schubert, D., Lechtenberg, B., Forsbach, A., Gils, M., Bahadur, S., & Schmidt, R. (2004). Silencing in Arabidopsis T-DNA Transformants: The Predominant Role of a Gene-Specific RNA Sensing Mechanism versus Position Effects. *The Plant Cell, 16*(10), 2561-2572.

Seidman, C. E., Struhl, K., Sheen, J., & Jessen, T. (2001). Introduction of Plasmid DNA into Cells *Current Protocols in Molecular Biology*: John Wiley & Sons, Inc.

Shavrukov, Y., Bovill, J., Afzal, I., Hayes, J., Roy, S., Tester, M., & Collins, N. (2013). HVP10 encoding V-PPase is a prime candidate for the barley HvNax3 sodium exclusion gene: evidence from fine mapping and expression analysis. *Planta, 237*(4), 1111-1122.

Shavrukov, Y., Genc, Y., & Hayes, J. (2012). The use of hydroponics in abiotic stress tolerance research. *Hydroponics–a standard methodology for plant biological researches. InTech*, 39-66.

Shearer, M. K. (2013). *Characterisation of AtPQL1, AtPQL2 and AtPQL3 as Candidate Voltage Insensitive Non-Selective Cation Channels (vi-NSCCs)* (Doctor of Philosophy Conventional), University of Adelaide, Adelaide.

Shi, H., Ishitani, M., Kim, C., & Zhu, J. K. (2000). The *Arabidopsis thaliana* salt tolerance gene *SOS1* encodes a putative Na^+/H^+ antiporter. *Proc Natl Acad Sci U S A, 97*(12), 6896-6901.

Shi, H., Lee, B. H., Wu, S. J., & Zhu, J. K. (2003). Overexpression of a plasma membrane Na^+/H^+ antiporter gene improves salt tolerance in *Arabidopsis thaliana*. *Nat Biotechnol, 21*(1), 81-85.

Shi, H., Quintero, F. J., Pardo, J. M., & Zhu, J. K. (2002). The putative plasma membrane Na^+/H^+ antiporter *SOS1* controls long-distance Na^+ transport in plants. *Plant Cell, 14*(2), 465-477.

Shi, H., & Zhu, J. K. (2002). Regulation of expression of the vacuolar Na^+/H^+ antiporter gene *AtNHX1* by salt stress and abscisic acid. *Plant Mol Biol, 50*(3), 543-550.

Sunarpi, Horie, T., Motoda, J., Kubo, M., Yang, H., Yoda, K., . . . Uozumi, N. (2005). Enhanced salt tolerance mediated by *AtHKT1* transporter-induced Na^+ unloading from xylem vessels to xylem parenchyma cells. *Plant J, 44*(6), 928-938.

Sundaresan, V., Springer, P., Volpe, T., Haward, S., Jones, J. D., Dean, C., . . . Martienssen, R. (1995). Patterns of gene action in plant development revealed by enhancer trap and gene trap transposable elements. *Genes Dev, 9*(14), 1797-1810.

Szabolcs, I. (1989). *Salt-affected soils*: CRC Press, Inc.

Takano, J., Tanaka, M., Toyoda, A., Miwa, K., Kasai, K., Fuji, K., . . . Fujiwara, T. (2010). Polar localization and degradation of Arabidopsis boron transporters through distinct trafficking pathways. *Proc Natl Acad Sci U S A, 107*(11), 5220-5225.

Tarczynski, M. C., Jensen, R. G., & Bohnert, H. J. (1992). Expression of a bacterial mtlD gene in transgenic tobacco leads to production and accumulation of mannitol. *Proc Natl Acad Sci U S A, 89*(7), 2600-2604.

Tepass, U., Tanentzapf, G., Ward, R., & Fehon, R. (2001). Epithelial cell polarity and cell junctions in Drosophila. *Annu Rev Genet, 35*, 747-784.

Tester, M., & Davenport, R. (2003). Na^+ tolerance and Na^+ transport in higher plants. *Ann Bot, 91*(5), 503-527.

Tester, M., & Leigh, R. A. (2001). Partitioning of nutrient transport processes in roots. *Journal of Experimental Botany, 52*(Spec Issue), 445-457.

Timms, S. (2012). ThermoHID Temperature Measurement Software. Retrieved 12-6-2012, 2012, from http://www.thermohid.co.uk/

Uozumi, N., Kim, E. J., Rubio, F., Yamaguchi, T., Muto, S., Tsuboi, A., . . . Schroeder, J. I. (2000). The Arabidopsis HKT1 gene homolog mediates inward Na(+) currents in xenopus laevis oocytes and Na(+) uptake in Saccharomyces cerevisiae. *Plant Physiol, 122*(4), 1249-1259.

Valvekens, D., Montagu, M. V., & Van Lijsebettens, M. (1988). Agrobacterium tumefaciens-mediated transformation of Arabidopsis thaliana root explants by using kanamycin selection. *Proc Natl Acad Sci U S A, 85*(15), 5536-5540.

van Leeuwen, W., Ruttink, T., Borst-Vrenssen, A. W. M., van der Plas, L. H. W., & van der Krol, A. R. (2001). Characterization of position-induced spatial and temporal regulation of transgene promoter activity in plants. *Journal of Experimental Botany, 52*(358), 949-959.

Vercruyssen, L., Gonzalez, N., Werner, T., Schmulling, T., & Inze, D. (2011). Combining enhanced root and shoot growth reveals cross talk between pathways that control plant organ size in Arabidopsis. *Plant Physiol, 155*(3), 1339-1352.

Wegner, L. H., Sattelmacher, B., Lauchli, A., & Zimmermann, U. (1999). Trans-root potential, xylem pressure, and root cortical membrane potential of 'low-salt' maize plants as influenced by nitrate and ammonium. *Plant Cell and Environment, 22*(12), 1549-1558.

Weigel, D., & Glazebrook, J. (2002). *Arabidopsis: A Laboratory Manual*. Cold Spring Habour, NY: Cold Spring Habour Laboratory Press.

Weigel, D., & Glazebrook, J. (2006). Glufosinate ammonium selection of transformed Arabidopsis. *CSH Protoc, 2006*(7).

Weijers, D., van Hamburg, J.-P., van Rijn, E., Hooykaas, P. J. J., & Offringa, R. (2003). Diphtheria Toxin-Mediated Cell Ablation Reveals Interregional Communication during Arabidopsis Seed Development. *Plant Physiology, 133*(4), 1882-1892.

White, P. J., & Broadley, M. R. (2001). Chloride in Soils and its Uptake and Movement within the Plant: A Review. *Annals of Botany, 88*, 967-988.

Wu, S. J., Ding, L., & Zhu, J. K. (1996). SOS1, a Genetic Locus Essential for Salt Tolerance and Potassium Acquisition. *Plant Cell, 8*(4), 617-627.

Xue, Z.-Y., Zhi, D.-Y., Xue, G.-P., Zhang, H., Zhao, Y.-X., & Xia, G.-M. (2004). Enhanced salt tolerance of transgenic wheat (*Tritivum aestivum L.*) expressing a vacuolar Na^+/H^+ antiporter gene with improved grain yields in saline soils in the field and a reduced level of leaf Na^+. *Plant Science, 167*(4), 849-859.

Yamamoto, Y. Y., & Obokata, J. (2008). ppdb: a plant promoter database. *Nucleic Acids Res, 36*(Database issue), D977-981.

Yang, H., Knapp, J., Koirala, P., Rajagopal, D., Peer, W. A., Silbart, L. K., . . . Gaxiola, R. A. (2007). Enhanced phosphorus nutrition in monocots and dicots over-expressing a phosphorus-responsive type I H+-pyrophosphatase. *Plant Biotechnol J, 5*(6), 735-745.

Yeo, A. R., Yeo, M. E., & Flowers, T. J. (1987). The Contribution of an Apoplastic Pathway to Sodium Uptake by Rice Roots in Saline Conditions. *Journal of Experimental Botany, 38*(7), 1141-1153.

Yew, M. (2011). *Honours Thesis* (Honours), University of Adelaide, Adelaide.

Zhang, H. X., & Blumwald, E. (2001). Transgenic salt-tolerant tomato plants accumulate salt in foliage but not in fruit. *Nature Biotechnology, 19*(8), 765-768.

Zhao, F.-Y., Zhang, X.-J., Li, P.-H., Zhao, Y.-X., & Zhang, H. (2006). Co-expression of the *Suaeda salsa SsNHX1* and Arabidopsis *AVP1* confer greater salt tolerance to transgenic rice than the single *SsNHX1*. *Molecular Breeding, 17*(4), 341-353.